University of Strathclyde

Department of Pure and Applied Chemistry
Centre for Forensic Science

Developing a reliable systematic analysis for arc fault mapping

by

Nicholas John Carey

A thesis presented in fulfilment of the requirements for the degree of Doctor of Philosophy

Volume 1

2009

This thesis is the result of the author's original research. It has been composed by the author and has not been previously submitted for examination which has led to the award of degree.

Signed: **Date:**

This thesis is dedicated to my mother Dawn Elizabeth Carey-Sheill for all of her incredible support and encouragement throughout this entire research project.

Abstract

Establishing a compartment fire's area of origin when it has been burning at post-flashover conditions is a difficult process. Burn patterns traditionally used by fire investigators following post-flashover fires can be erroneous.

This research has looked into the reliability of using the electrical wiring in a building to establish the origin of a fire. Sixty five fully furnished experimental compartment fires were used and the resultant artefacts analysed with various types of microscopy.

Nine separate categories of localised metallic "arcing damage" were identified following the experiments. The surface elemental characteristics of the artefacts were analysed and an association was established between the electrical copper conductors and the materials used to fix the electrical wiring to a surface.

This research has demonstrated the importance of a clear demarcation area between the localised metallic damage of the conductors and the undamaged area, to determine whether or not localised melting of electrical conductors is due to electrical arcing damage.

Correlations were found within the data collected from the experiments that linked the time to arcing events, the approximate temperature at which these events occurred and the circuit protection device operation sequence. No other correlations were revealed.

The analysis of the three-dimensional data has indicated that there is a high probability of arcing damage to electrical conductors occurring close to a fire's area of origin. The series of experimental fires with repeated scenarios has validated the reliability of the arc fault mapping methodology.

Acknowledgements

University of Strathclyde – Centre for Forensic Science

I am indebted to Dr Niamh Nic Daeid for her incredible support and direction. She has always made herself available to me whenever requested. In addition, for her constant evaluation of the research project with frequent meetings and invaluable guidance. I am also indebted to Dr Nic Daeid for her confidence with me to undertake this research project and her ability to suggest solutions that overcome the various obstacles that have presented themselves over the last six years. I am also grateful to Professor Jim Fraser who has been very supportive whilst I have been undertaking this research project. I am grateful to Ainsley Dominic for her experience and guidance with university protocol and for her time reviewing various documents.

Without the £8,000 research grant from the University of Strathclyde awarded in 2004 this research would not have been possible. This enabled the purchase of specialist electrical equipment and materials that was essential to undertake the experiments.

I'm grateful to Mr Stan Ames who has reviewed documents, suggested some very useful practical research methods and his overall guidance that has been invaluable.

Gardiner Associates:

Without the agreement of Gardiner Associates the experiments would not have been possible. I am especially indebted to Mick Gardiner, he has been extremely generous throughout this project. This generosity is not to providing the experiment scenes but also for providing local accommodation during my time at Wethersfield – I'm extremely grateful. My thanks also go to the rest of the incredible and enthusiastic team comprising of: Mike Kelter, Paul England, Clive Gregory, Mick Cloonan, Nick Stuart, Bob Smith, Alan Munford, and Jack Deans. I'm indebted to all of you for allowing me to install the wiring into their scenes and I guess, take over a bit! They were all very patient when I frequently delayed the start of the fires – making the days somewhat longer!

London Fire Brigade

My thanks go to: Peter Mansi, John Galvin, Stuart McMillan, Dave Robinson, Jerry Thomas, Gary Gates, Rick Hunt, John Tindell, Steve Whitmore, Derek Thorpe, Paul Willis, Gary Millington, Mark Ross, Steve Cracknell and Dennis Burke. I'm very grateful to you all for

your support and assistance. Stuart McMillan kindly released me to undertake the experiments between 2005 and 2006. I'm also grateful for the practical help from my colleagues during some of the experiments - assisting with installing the wiring and recovering exhibits.

University of Strathclyde – Department of Physics

I am indebted to Dr Paul Edwards and Professor Robert Martin for all of their assistance and guidance with the Scanning Electron Microscope part of this project.

University of Maryland – Department of Fire Protection Engineering

I'm very grateful to Professor James G. Quintiere who suggested some invaluable methods to analyse and evaluate the three-dimensional data from the experiments.

Forensic Science Society

I am very grateful to the Forensic Science Society for awarding me the annual research grant of £3,000 in 2006. The funds enabled the Scanning Electron Microscope work to be completed.

Olympus Microscopes UK Ltd.

I would like to thank Dr Anya Hunt and Mrs Jackie Roberts from Olympus Microscopes UK Ltd for their assistance and training to use the Olympus LEXT Confocal Laser Scanning Microscope.

Libraries

The reading rooms of the British Library have been an invaluable resource for this project. I frequently used the reading rooms to source material during the literature review and the facilities provided a unique atmosphere to encourage writing.

I would like to also thank Gail Parlaine from the London Fire Brigade library for work with obtaining obscure electrical and fire papers that were used in the literature review. Other librarians have kindly assisted me with sourcing material: Jen Bakewell from the Fire Service College Library and Sally Walsh from Dr JH Burgoyne & Partners LLP library.

Svare Professional Engineering (Isanti, Minnesota, USA)

To Dr. Robert Svare, Mr. Mark Svare and Mr. Matthew Dubbin - for their enormous technical support and encouragement. They reviewed the suggested supply transformer design and their assistance reviewing the specification for the associated equipment. Their generous financial assistance in the summer of 2005 provided funding that met the repair costs of the fire damaged 60kVA generator at Wethersfield this enabled the research project to continue.

Their incredible enthusiasm & encouragement throughout this research project has been both motivating and an inspiration to me.

Friends and family

To all of my friends and family who have been very understanding with my reduced contact throughout this project. Two people in particular have helped me to finish this protracted project:

To Peter Mansi, you have been an incredible rock of support. For your numerous suggestions and advice - thanks matey!

To my partner Sarah Trowbridge. You have been incredibly supportive with this research project. In particular, with the exhibit analysis and the write-up stage over the last two years. I appear to have been somewhat physically and mentally absent from normal life! You've been very patient and understanding.

Contents

Volume 1

Chapter 1 Introduction

Volume 2

Details and summary of the experiments

List of symbols

Quantity	Symbol	Unit name	Unit symbol
Current	**I**	Ampere	**A**
Electromotive Force	**E**	Volt	**V**
Energy	**W**	Joule	**J**
Frequency	***F***	Hertz	**Hz**
Impedance	**Z**	Ohm	**Ω**
Potential Difference	**V**	Volt	**V**
Power	**P**	Watt	**W**
Resistance	**R**	Ohm	**Ω**

List of figures

List of tables

Presentations and publications relating to the research

Arc Fault mapping – a technique to assist in identifying a fire's area of origin.
NJ Carey, MJ Svare and N.Nic Daéid, *IAAI International conference*, Denver 2006

The metallic damage to electrical conductors at fire scenes.
N.J. Carey and N. Nic Daéid, *Interflam* 2007

Arc Fault mapping – an update on current research.
NJ Carey, MJ Svare and N.Nic Daéid, *IAAI International conference*, Denver 2008

The metallic damage to electrical conductors at fire scenes.
NJ Carey and N.Nic Daéid, *Forensic Science Society conference*, 2008

Forensic use of the Olympus LEXT confocal laser scanning microscope,
NJ Carey and N.Nic Daéid, *Olympus LEXT product launch*, Hamburg 2009

Glossary

Accelerant: A fuel or oxidiser used to initiate a fire or to increase the speed of development (often ignitable liquids are used).

Ampacity: The electric current (Amperes) that a conductor/cable can carry continuously in normal use without exceeding its temperature rating.

Amps/Amperes: The unit of electrical current that is equivalent to a flow of one coulomb per second (or 6.24×10^{18} electrons per second), represented by the symbol (I) or (A).

Apparatus: The machines, equipment and fittings in which conductors are used but not the conductors themselves.

Arc/Arcing: A high temperature luminous electric discharge across a gap or through a medium such as charred insulation.

Arcing through char: Arcing associated with a matrix of charred material (often charred conductor/cable insulation) that acts as a semi-conductive medium.

Bead: A rounded globule of re-solidified metal on the surface of an electrical conductor that was caused by arcing. It is characterised by a sharp line/area of demarcation between the melted and un-melted conductor surfaces.

Bonded: The connection of metallic items to ensure that a common electrical potential exists.

Busbar:	Large lengths of copper or aluminum strips that conduct electricity within service risers, trunking, distribution boards, transformer sub-stations, or other electrical apparatus.
Cable:	One or more conductors provided with insulation.
Ceiling layer:	A buoyant layer of hot gases and smoke produced by a fire in a compartment.
Char:	Carbonaceous material that has been burned and has a blackened appearance.
Circuit:	The path taken by electric current to supply electrical equipment or to allow leakage current to return.
Circuit Breaker:	A mechanical device designed to open or close a circuit under normal or abnormal conditions.
Conductor:	The conducting parts of a cable, busbar or functioning part of metalwork that carries electric current.
Connector:	A device used for connecting together flexible cords and cable.
Consumer Unit:	A combined distribution board and main switch controlling and protecting the electrical installation's final circuits in a residential building. Such units may contain Residual Current Devices for protection against electric shock.

Current:	A flow of electric charge, represented by the symbol (I) or (A).
Design current:	The current intended to be carried by a circuit in normal service.
Distribution board:	A group of excess current protective devices in an enclosure, with the purpose of protecting final circuits.
Earth fault loop impedance:	The total opposition to current flow, starting and ending at the point of fault.
Earth leakage current:	A current that flows to earth.
Earthing conductor:	A protective conductor that connects a main earthing terminal to an earth electrode or other means of earthing.
Earthing terminal:	The main earth connection point at the intake position.
Electrical Appliance:	Any device that is designed to use electricity for a particular purpose, excluding a light fitting or independent motor.
Electrical installation:	A group of electrical apparatus and equipment to fulfil a specific purpose within building.
Final circuit:	A circuit connected directly to current using equipment through outlet points.

Fire: A rapid oxidation process that is a chemical reaction resulting in the evolution of light and heat in various intensities.

Fire cause: The circumstances, conditions, or agencies that bring together a fuel, ignition source and oxidiser (air/oxygen) resulting in a fire.

Fire investigation: The process of determining the origin, cause and development of a fire.

Fire patterns: The visible physical effects that remain following a fire.

Flashover: A transition phase in the development of a compartment fire in which surfaces exposed to thermal radiation reach ignition temperature more or less simultaneously and fire spreads rapidly throughout the compartment/space, resulting in full room involvement of the compartment / space.

Frequency (Hz): The number of cycles per second of an AC cycle. In the UK frequency of AC current is 50Hz.

Fuse: A device for opening a circuit by melting a wire-element in a short circuit or overloading fault condition.

Ground: The conductive mass of earth whose electrical potential is taken as zero.

Heat: A form of energy characterised by vibration of molecules and capable of initiating and supporting chemical changes of state.

Heat flux: The measurement of the rate of heat transfer to a surface expressed in kilowatts/meter^2 (kW/m^2).

Impedance: The ratio of voltage and current in RMS terms for AC quantities. In general, impedance extends the concept of resistance to AC circuits. The symbol for impedance is "Z".

Insulation: A suitable non-conducting material enclosing, surrounding and supporting a conductor.

Isolation: The cutting off of a circuit or circuits from the source of electrical energy. An Isolator is a device used for this purpose.

Live: A conductor or object is said to be live when a potential difference exists between it and earth.

MiniTab Minitab Inc. State College, PA. USA: version 15 of a statistical software package designed to run statistical tests including descriptive statistics, hypothesis tests, confidence intervals and normality tests.

Ohm: The unit of electrical resistance between two points of a conductor represented by the symbol (R) or (Ω).

Overcurrent: A current exceeding the rated value for the circuit design. It may occur in a circuit that is electrically sound.

Power: The electrical energy in a circuit, represented by the symbol (P).

Protective conductor: A conductor used for some measure of protection against electric shock.

Potential difference: The voltage or electrical pressure between one point and another point of an electrical circuit.

Rectifier: A device for converting alternating current (AC) into direct current (DC) by allowing the passage of current to flow in one direction.

Residual Current Device (RCD): A device intended to cause the opening of contacts when its trip mechanism attains a given value.

Resistance heating: The localised heating effects at any point in a circuit where there is a high resistance fault. This effect often occurs at conductor connection points and switch contacts.

Ring final circuit: A final circuit arranged in the form of a ring and connected to a single point of the supply.

Short Circuit: An abnormal connection of low resistance between normal circuit conductors where the resistance is normally much greater. This is a gross overcurrent situation.

Spark: A small incandescent particles created by some arcs.

SPSS	SPSS Inc. Chicago, IL. US - version 17 of a statistical software package "Statistical Package for Social Sciences". This software is designed to undertake statistical tests from data displayed in spreadsheets or tables.
Switch:	A mechanical device for making and breaking a circuit.
Switchgear:	Apparatus for controlling the distribution of electrical energy.
Transformer:	A static device in which electrical power is transferred from one winding (or windings) by means of electromagnetic induction, usually to achieve a change of voltage.
Venting:	The escape of smoke and heat through openings in a building.
Ventilation effects:	The patterns of damage created by radiant heat in the areas that a fire is venting from a compartment. These ventilation effects can mask the patterns created during the origin and initial growth of a fire.
Volt:	The unit of electrical pressure (electromotive force), represented by the modern SI symbol "E" or often by the traditional symbol "V".
Watt:	A unit of power equal to one joule per second. Or the rate of work represented by a current of one ampere under the potential of one volt, represented by the symbol (W).

Chapter 1 - Introduction

1.1 Electricity

1.1.1 Electrical energy and electron flow

Electricity is an energy source capable of producing heat, light and motion. It has been harnessed and controlled within the last 180 years. The source of electricity is the movement (or flow) of electrons that surround the nucleus of an atom. Electrons are easily released in some materials which are known as conductors. Metals such as copper and silver are examples of good conductors. Materials where the electrons are tightly bound to the atoms are known as insulators. Insulators can be either natural or synthetic materials, for example: glass, rubber, dry wood, PVC and other plastics.

Electricity is generated by inducing electron flow (electrical current) in a conductor. This is achieved by a magnetic field moving next to a conductor thereby inducing electron flow in that adjacent conductor.

Electrical generators are constructed with either permanent magnets, or coils of wire that create a magnetic field. These resultant magnetic fields are moved by a mechanical force, such as a combustion engine, and the magnetic fields induce electron flow in the adjacent coils that are at the start of an electrical circuit.

Current is the rate of flow of electrons (negatively charged particles) through a conductor. These electrons flow because there is a difference in potential between two places in an electric circuit. A potential difference (PD) is required to produce the electric current and is also described as electrical pressure or voltage (V).

Resistance is the opposition that a conductor (or other device) has to the flow of electrons in an electrical circuit.

The three components of voltage (V), current (I) and resistance (R) are related by Ohm's Law which states that "the ratio of potential difference between the ends of a conductor and the current flowing in the conductor is constant. This ratio is termed the resistance of the conductor". For the law to be obeyed, the temperature of a conductor must not change. It can then be stated that "the current flowing in a circuit is directly proportional to the potential difference, and inversely proportional to the current" [1].

The voltage (V) drives an electric current (I), through a resistance (R). The three components of Ohms law are shown in the circuit diagram and are expressed in equation 1:

$$\mathbf{V = IR} \qquad \text{Equation 1}$$

Where:
V is Volts
I is Amps
R is resistance

Power is the rate of doing work in an electrical circuit. The unit of measurement is the Watt (P). One watt of power is generated in a circuit that has one Amp of current pushed by one Volt of pressure.

Appliances with a resistive load (a heating element or light bulb for example) are rated in watts (100W lamp or a 3,000W water heater). Power can be expressed in equations 2 and 3:

$$P = VI$$ Equation 2

or

$$P = I^2R$$ Equation 3

Where:
P is Power (Watts)

The consumption of electricity is internationally measured by the amount of power which is used within a period of time. The electricity suppliers use the kW/hour as a unit of electrical energy for billing consumers.

1.1.2 Alternating Current (AC)

When a magnetic field moves in both directions past a conductor the flow of current in the conductor will change direction as often as the movement of the magnetic field changes direction. Several devices generating electricity operate on this principle, producing an oscillating form of current called alternating current (AC). In the UK, AC changes direction (reverses) 50 times a second (50 Hertz or cycles per second).

The most important practical characteristic of alternating current is that the voltage or the current may be efficiently increased or decreased using an electromagnetic device called a transformer. AC is predominantly used as the electrical supply in buildings.

1.1.3 Direct Current (DC)

Direct Current (DC) is the constant flow of electrons in one direction from a low potential to a high potential. Many electronic devices will only work with direct current. They are often battery powered or if plugged into an alternating current (AC)

source the AC supply needs to be rectified from alternating current into direct current.

1.1.4 Transformers

A transformer is a piece of electrical equipment that will only operate on AC. It takes in power at one voltage and delivers it at a higher or lower voltage.

Transformers operate using electromagnetic induction. When an alternating current passes through a coil/winding of wire, the magnetic field about the coil expands, then collapses, then expands in a field of opposite polarity, and then collapses again. If another conductor (for example a second winding) is placed within this magnetic field, the changes of the magnetic field induce an alternating current in this second conductor. If the second conductor is a winding with a larger number of turns than the first, the voltage induced in the second coil will be larger than the voltage in the first, because the field is acting on a larger number of individual conductors. The reverse also occurs if the number of turns in the second coil is smaller. In this example the induced voltage (known as secondary voltage) will be smaller than the primary voltage.

The economic transmission of electricity throughout the country via the "National Electricity Grid" is possible with the use of transformers. The electrical transmission efficiency is improved by increasing the voltage using a step-up transformer. This reduces the current flowing in the conductors, while keeping the power transmitted nearly equal to the power input. The voltage is reduced locally with transformers to the required value thus ensuring that reliable voltage values are consistently provided to consumers throughout the transmission network.

1.1.5 Three-phase supplies

The electricity generator in a power station is constructed with three sets of windings. Each winding occupies one third of the generator's circumference (120°) as detailed in figure 1. As the rotor is spun (e.g. by a turbine engine) it passes each

winding separately and induces current in the winding by magnetic induction. Each circuit is a separate phase that has current induced for one third of the time in a cycle. This is more commonly known as a three-phase supply.

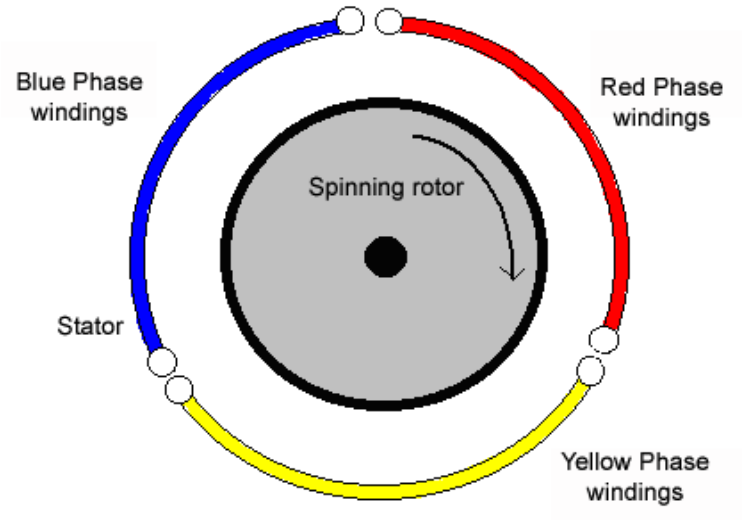

Figure 1 - Simplified circuit diagram of a 3-phase generator windings [2]

The main reason for using three phases is that it removes the need for a neutral or return path due to the way the generator and transformer windings are configured. Three-phases also suit the generator design as it allows for the optimum spacing and sizes of conductors within the interior components of the generator.

The electricity is transmitted through the distribution system (its voltage is stepped up and down) until it reaches the local sub-station transformer. Figure 2 is a circuit diagram that shows the three-phase distribution of electricity from the local sub-station transformer to industrial buildings and the single-phase electrical distribution to residential buildings.

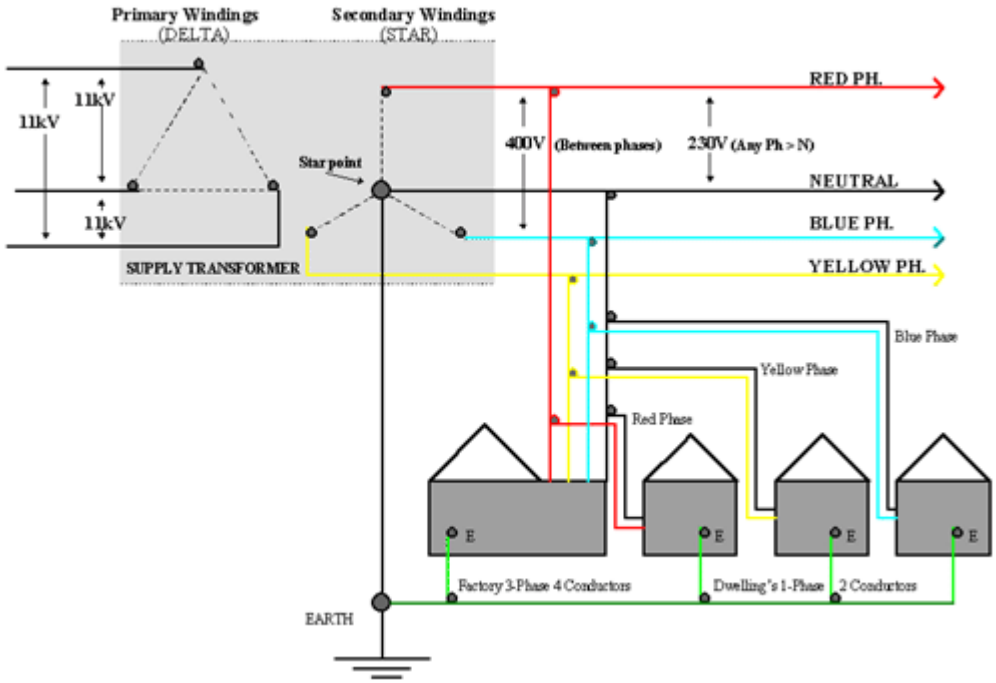

Figure 2 – Electrical distribution from a local sub-station transformer to consumers [2]

1.2 Electrical wiring systems

1.2.1 Introduction to wiring systems

The designer of an electrical installation is expected to consider the environment and use of the installation. For example, in a factory it may be reasonable to fix surface mounted steel conduit to the walls, in a residential property surface mounted steel conduit would be both un-economical and visually unacceptable.

Some common types of wiring systems in use in the UK are:

- PVC - insulated PVC - sheathed cables (known as “Twin and Earth” cable)
- PVC - insulated steel wire armoured PVC - sheathed cables (known as “Steel Wired Armour” or “SWA” cable)
- Mineral-insulated copper clad cables (known as MICCS or “Pyro”)
- Metal and plastic conduit systems
- Skirting or dado trunking systems with internal busbars (solid distribution conductors).

1.3.2 Polyvinyl chloride – insulated, polyvinyl chloride – sheathed cables.

The most widely used wiring system in use in the UK today is polyvinylchloride (PVC) insulated with PVC sheathed cable, known as “twin and earth” cables. Such cables are generally used in domestic and light commercial installations. PVC insulated and sheathed cable is often used in a 'flush' electrical installation where they are installed below the plaster finish of walls. Figure 3 details twin and earth cable with the protective sheath removed.

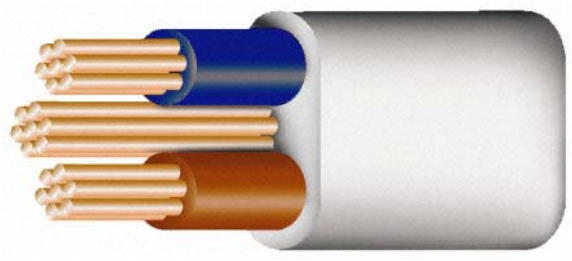

Figure 3 - Twin and earth cable with the PVC sheath removed [3]

Common sizes of twin and earth cable and their rating in Amps are detailed in the current edition of Institute of Electrical Engineers (IEE) wiring regulations [4].

10 mm²	43A to 63A.
6 mm²	32A to 46A.
2.5 mm²	18.5A to 27A.
1.5 mm²	14A to 19.5A.
1.0 mm²	11A.

The lowest current value of the cable ratings represents the cable being installed within building components. The highest value of the cable ratings is for cable clipped to surfaces in free air. The cables are buried in the wall with additional mechanical protection in the form of plastic or metal capping. The capping is installed to physically protect the cables from the plastering process and other construction work. Cables are also installed through holes in floors and roof voids. In shops and offices they are often installed above false ceilings.

Twin and earth cable can also be used for surface wiring where it is clipped directly to the surface of a wall, secured to a cable tray (metal sheet sections installed to run a loom of cables), or installed in plastic and metal trunking if additional mechanical protection is required. The PVC insulation used in twin and earth cable ages well and does not decompose under normal atmospheric conditions. Pure PVC resin has a tensile strength of 10 – 15 N/mm^2. PVC wiring insulation has a very high insulation property at 2 x 10^{11} Ohms/m at 20 degrees C [5]. The dielectric strength of PVC insulation used in this type of cable is 13.8 – 19.7 kV/mm [6].

There are disadvantages with the use of PVC as it has a maximum operating temperature dependant on its design of 70 - 90°C [5], this is the maximum temperature before it starts to soften. It degrades and loses its plasticisers at high temperatures or UV light.

The literature suggests that there are some known inherent problems with PVC electrical wiring insulation. Babrauskas evaluated a number of research publications and reported that PVC wiring insulation is made up of 52-63% PVC resin, 25-29% plasticizers and approximately 16% $CaCO_3$ filler [7]. The thermal degradation of PVC occurs in two stages. The first stage is dehydrochlorination where HCl molecules are released. Testing of pure PVC has shown that measurable amounts of HCl are released at temperatures as low as 100ºC [8]. The second stage is pyrolysis process that occurs at 350 - 500ºC with a cross-linked charred residue remaining [7].

PVC electrical wiring normally contains $CaCO_3$ as a filler. Under dry conditions but at increased temperatures this filler can induce surface wetting that can lead to carbon tracking [7]. Tests on PVC plugs that used this filler by Ohtani [9] showed that if heated to 110-120ºC for 10 days and then cooled to room temperature the insulation resistance can drop considerably over a number of days. This drop in resistance value can eventually lead to current flow across the insulation resulting in ignition of the PVC insulation. It was found that this potential ignition process only occurred when $CaCO_3$ was used as a filler in the PVC electrical insulation.

1.3.3 Steel-wire armoured cables

Steel-wire armoured (SWA) cables as detailed in figure 4 are widely used in commercial and industrial buildings. They are also used in distribution circuits by electricity suppliers to buildings.

Figure 4 - Steel Wired Armour cable [3]

The cable is made up of galvanised steel wire secured between PVC bedding and a tough PVC outer sheath. The PVC or Polyethylene (XPLE) insulated copper conductors are located within the PVC bedding. UK wiring regulations [4] allow the steel wire section of the cable to be used as the circuit protective (earthing) conductor. The cables are often clipped to a wall or ceiling, fixed to cable tray or run in a trench in the ground. The cable is terminated in a metal enclosure with a specially designed gland.

1.2.4 Electrical circuits in UK residential buildings

Circuits are either ring-main for socket outlets, or radial circuits for lighting and individual electrical equipment or appliances.

Most socket outlets are run on a ring main circuit using 2.5mm² PVC twin and earth cable. The ring circuit is started from a fuse or circuit breaker (rated at 30/32A) within the distribution board. The cable is routed to each socket outlet in a ‘daisy chain’ method. The cable then returns to the same fuse or circuit breaker forming the complete ring. This circuit has a high power capacity compared to other circuit designs. The number of sockets outlets allowed to be wired into in a ring circuit is unlimited, however but the maximum floor area for this type of circuit is restricted to a maximum of 100m² [4].

To protect extension cables or electrical appliances that are plugged into the ring circuit against overload and short circuit faults, a cartridge fuse is installed in the plug. The cartridge fuse size varies from 3A to 13A. The design of ring circuits to supply socket outlets originated from the Institution of Electrical Engineers (IEE) meetings from 1942 to 1944 where a lot of thought was put into the improving the circuit design and safety. It was established at the time that the change to ring circuits would save 25% of materials compared to pre-war circuit designs [10]. Figure 5 is a wiring diagram of a ring circuit showing the consumer unit and a connected electrical appliance.

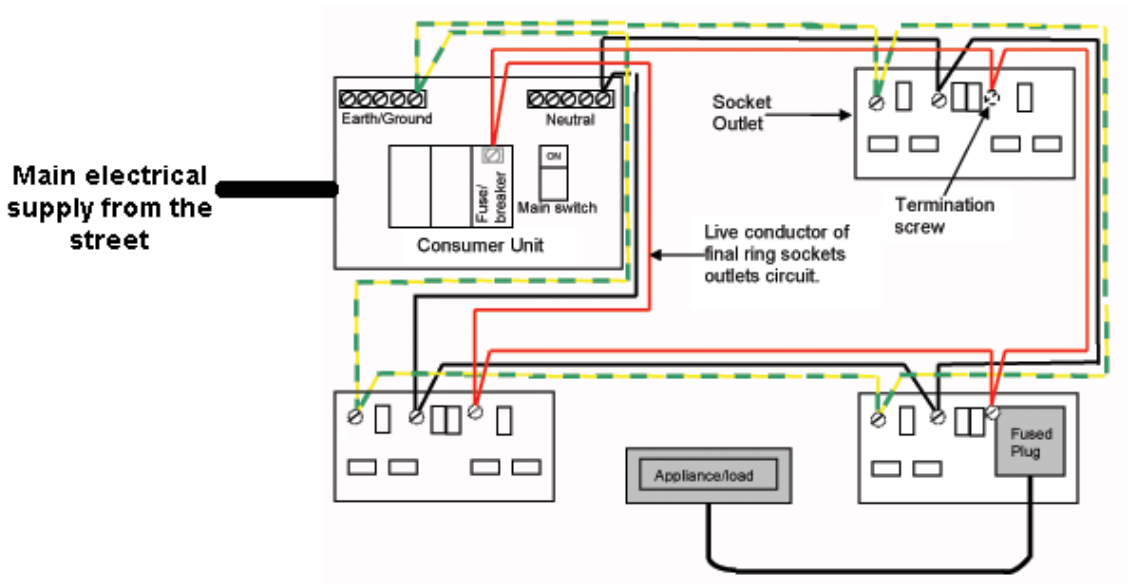

Figure 5 - Diagram of a ring circuit used to supply socket outlets. [2]

Lighting circuits are designed and installed in a radial (single-ended) method. There must be at least one separate lighting circuit for each floor in a building. Each circuit should not exceed ten light fittings, each with a maximum rating of 100W. The circuit is wired generally with 1mm^2 cable with a current carrying capacity of up to 11 Amps [4] and is therefore protected using a 5A fuse or 6A circuit breaker.

Other types of radial single-ended circuits are specified in the current wiring regulations [11] and include water heaters (15A or 16A), shower (30-45A) and cooker circuits (30-45A).

1.3 Protection of electrical circuits

1.3.1 Introduction to circuit protection

Electrical circuits are normally protected against faults that include a short circuit and an overload; they may also be protected against an earth leakage.

A short circuit (sometimes referred to as a "short") is a fault that allows electron flow along a different path than from the one intended. The current flow is often very high and determined by the maximum prospective short circuit current. The maximum prospective short circuit current is the maximum electrical current that can flow in an electrical circuit under short circuit fault conditions. This is determined by the supply system's voltage and impedance (impedance, in general, extends the concept of DC resistance to AC circuits).

In residential single-phase electrical installations in the UK with a 100A supply, the maximum short circuit (fault) current may be up to 16kA (16,000A). In industrial buildings with a three-phase 200-630A supply the prospective short circuit fault current may be up to 25kA [12].

An overload is defined as a circuit carrying more current than its designed use. To protect circuits against an overload condition conductors need to be correctly sized for the current carrying capacity of the load and a weak link in the form of a protection device needs to be inserted into the circuit.

1.3.2 Fuses

A fuse has a main component in the form of a metal wire or strip that will melt when heated by a pre-determined electric current. It is designed to protect an electrical circuit using the heat effect of excessive current flow. This will open the circuit that it is protecting.

Older fuses were of the 're-wireable' type and were constructed with a porcelain casing. When they were removed from the distribution board the fuse wire or strip was exposed and could be replaced. There are still many re-wireable fuses protecting

electrical circuits in the UK although it is unusual to find them in modern electrical installations.

Cartridge fuses constructed with a ceramic body are very common in commercial or industrial electrical installations and are found in every UK 13 Amp plug, as shown in figure 6. Small cartridge fuses constructed with a glass body are also used to protect electronic circuits. There are many different types of design that include silica sand within the body to quench large arcs created during the rupturing of the fuse and a bead soldered onto the fuse wire (known as a Metcalf bead or “M-Bead”) that is designed to lower the melting temperature of the fuse wire [13]. An example of a cartridge fuse and holder is shown by figure 7.

Figure 6 – 5 A cartridge fuse from a UK plug [14]

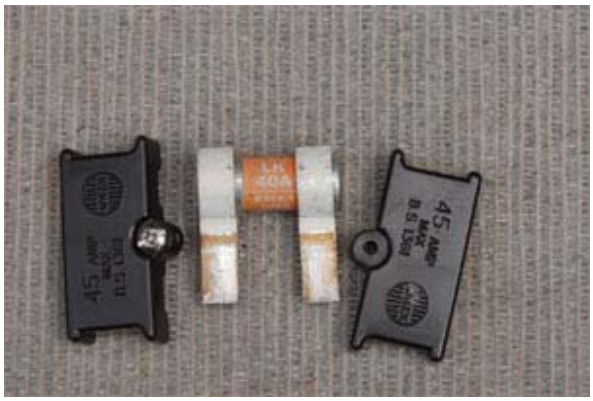

Figure 7 – 40 Amp cartridge fuse and holder designed for use in a distribution board [15]

Industrial cartridge fuses have a high fault current breaking capacity and so the design prevents them from exploding when operating during short circuit faults of up to 25kA. They provide accurate over-current protection, they tend not to degenerate with age, and fuse carriers may be designed to only carry a specified fuse. The level of over-current is determined by the time-current characteristics of the protection device. Figure 8 is a graph produced by a fuse manufacturer to indicate the speed of fuse operation at different levels of current flowing through the fuse.

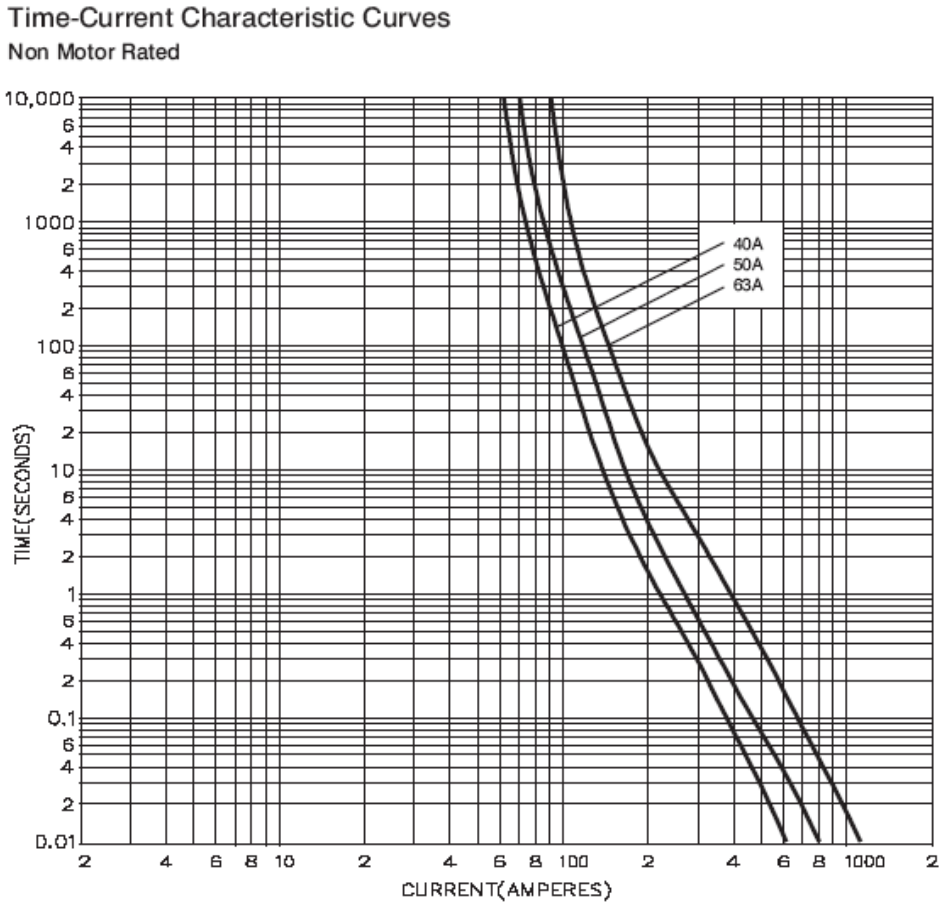

Figure 8 – Time current characteristics of 3 different ratings of BS88 cartridge fuse [16].

Some types of fuses are able to carry one and a half of their designed rating for a long period of time. The safe current carrying capacity of a PVC insulated cable is often twice its specified rating. Contact with wall or roofing insulation will restrict the heat loss of the cable in overload conditions accelerating the damage to the cable [17, 18].

1.3.3 Circuit Breakers

A circuit breaker is an electro-mechanical device that is designed to automatically protect electrical circuits from damage caused by overload or short circuit faults. A circuit breaker can be reset to resume normal operation once the fault is rectified. Circuit breakers are made in varying sizes, from small devices that protect individual circuits in residential buildings up to large switchgear designed to protect high voltage circuits that are a part of the National Grid. Miniature Circuit Breakers (MCBs) are sized to fit into conventional European distribution boards, other larger

circuit breakers are generally fitted into switchgear found in larger industrial installations. An example of the different types of miniature circuit breaker that are available is detailed in figure 9. Typical time/current curves for miniature circuit breakers are detailed in figure 10.

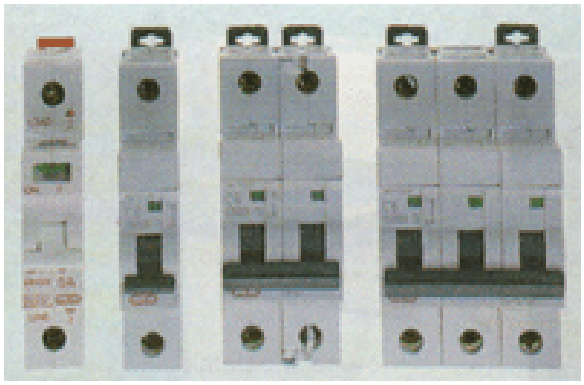

Figure 9 – Some examples of European miniature circuit breakers [19].

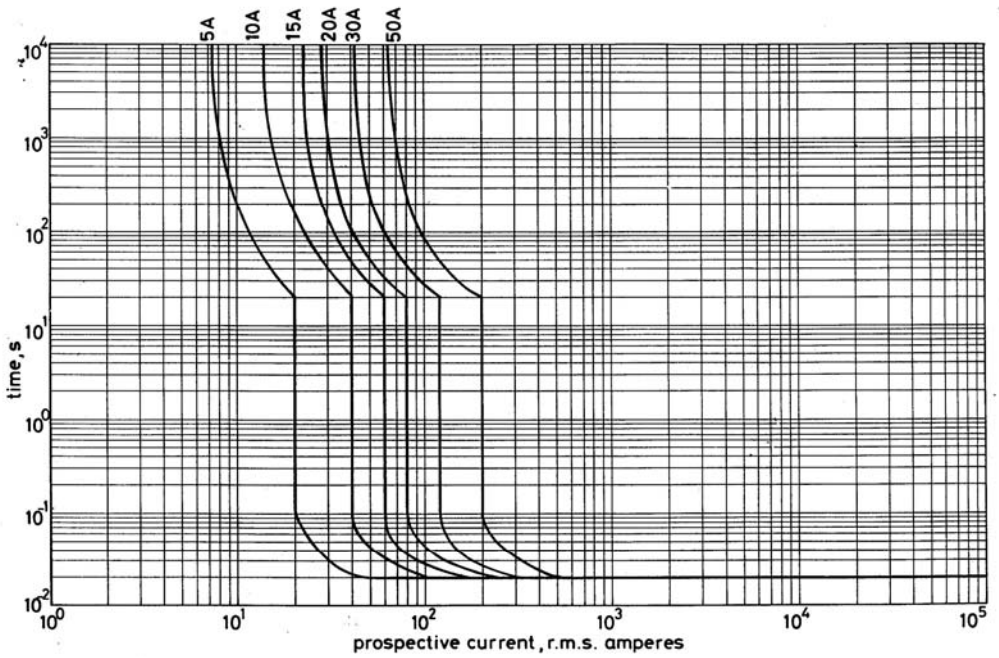

Figure 10 – Time / current curves for miniature circuits breakers [20]

Circuit breakers have many advantages over fuses. They are generally sealed tamperproof units, the 'OFF' indication is visible, they operate very rapidly in short circuit conditions (0.1 seconds for European designed breakers), and they are easy to reset after a fault [21].

1.4.4 Residual Current Devices

Residual Current Devices are generally known as an RCD and have been used in the UK for the last 50 years. Following the implementation of the 17th edition of the UK wiring regulations in July 2008 [4] it became mandatory to install an RCD to protect circuit(s) where cables are buried within 50mm of the finished surface of a room compartment. RCD's are also required by the regulations to be installed in certain high-risk areas, for example, circuits supplying equipment outside the property.

An RCD detects a leakage of electrical current to Earth, for example a person receiving an electric shock, or a fault within an installation or appliance, and thus allowing the current flow to go to Earth. The trip rating or size of an RCD is specified in milli-amps (stated on the casing) and this dictates its primary use. The most common size of RCD in the UK is 30mA. Figure 11 details a typical RCD designed to be installed in a distribution board.

Figure 11 – Typical RCD found in residential and commercial electrical installations [19].

The main component within an RCD is a core balance transformer. A core balance transformer is an iron ring that has several electrical windings wound around it. It acts in a similar way to a conventional transformer except that it does not increase or decrease the voltage but it does create magnetic fields both in normal operation and in fault conditions.

Figure 12 details the circuit diagram of an RCD and it illustrates how the live and neutral conductors pass through a core balance transformer from the electrical supply

to the load. The core-balance transformer has an additional search coil connected to a trip actuator.

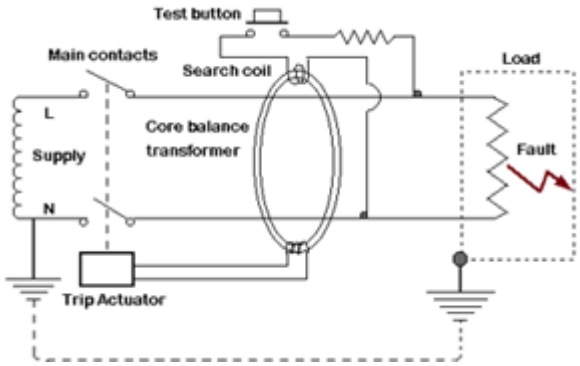

Figure 12 – Circuit diagram of an RCD [19]

When the circuit is healthy and the main switch closed, current will create a magnetic flux in the live and neutral sides of the core-balance transformer. The magnetic flux is normally equal and opposite so that the core-balance transformer will be balanced. If there is a leakage to earth from either the live or neutral conductor to Earth, the imbalance creates a magnetic flux in the core-balance transformer windings and a voltage is induced in the search coil. If the voltage in the search coil is sufficient the trip actuator will operate.

The RCD can be tested via a test button that simulates an earth fault by inserting a resistor in the circuit. The test circuit is designed to ensure the electro-mechanical operation of the RCD and not the time to operate or the accurate size of the trip current. It is not uncommon for an old RCD to fail to operate when tested with a dedicated meter [19].

1.4 Electrical causes of fire

1.4.1 Introduction

An electrical ignition source is defined as a fault, damage or malfunction of an electrical system that creates unwanted heat to ignite susceptible fuels [22]. It may also be as a result of tampering, experimentation or an incendiary device construction. An electrical cause of fire is not the mishandling or careless use of an electrical heat source such as a heater left next to combustible material or an oil pan left on an electric cooker.

The Institution of Engineering and Technology (IET), previously called the Institute of Electrical Engineers (IEE) publishes the "Requirements for Electrical Installations BS/EN 7671 (17^{th} edition)" [23] which is the guidance for electrical installations in the UK. The document was first published in 1882 titled "Rules and Regulations for the Prevention of Fire Risks Arising from Electric Lighting" and illustrates that as far back as 1882 the problem of the risk of fire from electrical installations was recognised [24]. In the chapter "Objects and Effects" of the current wiring regulations [11] fire, as well as electric shock, burns and injury from mechanical movement of electrically operated equipment, are defined as the main risks that the regulations are designed to protect against.

Since 1882 the IEE (now IET) regulations have been expanded and developed to meet the changes and advancements in materials and technology. The early circuit protection was very crude compared to modern circuit protection devices (MCBs and RCDs). The early wiring and control equipment was also constructed with material that was easy to ignite. For example switches and sockets were constructed of timber and wiring was constructed with rubber and cloth insulation. Current wiring regulations state that wiring and equipment must be fire resistant [11]. All connections (recognised in the regulations as the weak points in an electrical circuit) must be contained within fire resistant enclosures, for example, thermosetting plastic junction boxes etc. and wiring is mainly constructed from PVC insulation that has a good inherent resistance to fire spread from small ignition sources. If electrical

installations in the UK are constructed in accordance with the regulations, the risk of the electrical installation being a cause of a fire is substantially reduced.

There is a large problem internationally with electricity being incorrectly attributed as the cause of fires [25-28]. The most recently published fire statistics from the Government Department of Local Communities for the UK were for the year 2005 and this was published in March 2007 [29]. The data shows that there were a total of 68,500 accidental fires in dwellings and other buildings in 2005. Of these, 16,900 were listed as being of electrical origin, (5,500 fires originating within the electrical distribution system and 11,400 in other electrical appliances). This accounts for 24.67% of the accidental fires in buildings. The data also covers the same categories for each year from 1995 and the percentage of electrical origin fires in UK buildings is similar for each year over the last decade.

Experience of the author within the London Fire Brigade suggest that the fire officers in attendance at a fire scene rapidly determine that a fire is of electrical origin if there are any electrical appliances present in the fire damaged compartment. This initial suggested electrical cause for the fire is frequently found to be incorrect. This data is used to compile the national fire statistics. Several scientists and engineers in the literature have addressed this problem. Butler and Orr analysed the 1987 UK fire statistics and published a paper in 1993 which concluded that electrical heat sources such as cookers were being categorised as electrical causes of fire incorrectly. Of the 38,077 electrical origin fires reported in 1987 some 18,591 were cooking related fires where the cooker was in fact the heat source that ignited food [27].

Twibell reported that approximately 25% of all accidental fires over a 5 year period determined by the Fire Service were recorded as ‘electrical’ in origin [20]. He undertook a survey of fatal fire examinations conducted by the Forensic Science Service laboratory in Huntington, Cambridgeshire over a 5 year period from 1990 to 1994. Electrical cause of fire accounted for only 6% of the fires examined by the laboratory scientists [28]. This is a significant contrast from the national fire statistics.

Beland [26, 30-34] and Ettling [35-37] in North America have also come to similar findings. The main point they make is that fire officers in the UK and US complete reports that include the cause of the fire. In the UK it is listed on the Fire Damage Report – FDR1 [38] as the 'supposed cause of fire'. There is an ongoing problem with a lack of fire investigation training for these Fire Service officers completing the FDR1 forms unless they are assigned the role as a fire investigator either full or part-time [39].

In the US the national fire statistics affected the National Electrical Code [40]. In 2002 the code was amended to make it mandatory to install Arc Fault Circuit Interrupters (AFCI's) [41] to circuits supplying socket outlets in bedrooms. This was because the fire statistics revealed that the main cause of fires in bedrooms in the US were faults in the electrical wiring. AFCI's are not available in the UK and enquiries made with the IEE [42] suggest that there are no plans for them to be introduced in the UK in the near future.

1.4.2 Scene examination – initial considerations

Investigators that suspect an electrical origin fire must establish that the building's electrical installation was energised at the time of the fire. There must be evidence of a potential electrical fault that is capable of igniting the initial fuel package. The remains of wiring, and if applicable, the electrical appliance(s) capable of generating sufficient heat need to be located at the fire's area of origin.

An electrical expert may be used to undertake a detailed electrical examination of the wiring and equipment at the fire scene. It should not be carried out in isolation and a full fire scene examination and excavation also needs to be undertaken, as the electrical examination results need to be considered in context with all of the other fire scene data to ensure that the electrical evidence is not misinterpreted.

1.4.3 Categories of electrical causes of fire

In general an electrical fault is the unintended flow of electrical current within an electrical circuit or to Earth thus completing the electrical path through another route. The recognised electrical faults that have the potential to be an ignition source are:

- A short circuit.
- A current overload.
- A voltage overload.
- Resistance heating.
- An arc (including in-line arcing).
- Carbon tracking.

1.4.4 A short circuit

When a short circuit occurs in the wiring of a domestic or commercial electrical installation it is generally a highly energetic event. It occurs when a live conductor comes into contact with the neutral conductor or either an earthed conductor or an earthed conductive component. In the case of a three-phase installation, a short circuit will also occur if two of the phase (live) conductors contact each other.

When a short circuit occurs in a correctly designed electrical installation there will be an immediate rise of electrical current to a high value. This will result in a rapid rise in temperature if the fault is not de-energised very quickly. Circumstances that limit the amount of electrical current that will flow in the circuit in a short circuit condition are the size of the supply transformer (sub-station), the impedance of the circuit from the point of the fault back to that supply transformer, and the resistance at the point of the short circuit. In the case of a short circuit between a live conductor and either an earthing conductor or an earthed conductive component this is known as the “earth fault loop impedance”. The variables that limit the time a short circuit has the capacity to generate heat are the rating and type of circuit protective devices that have been used in the circuit. The time-current characteristics of the protective device influence the time it takes for the protective device to detect a short circuit and to operate (breaking the flow of current).

A common misconception is that the size/rating (i.e. Amperage) of the protective device will limit the amount of current that will flow in a short circuit condition. If a fault occurs in a circuit the maximum current capable of flowing in that circuit is only limited by the resistance of the wiring from the electricity supplier sub-station transformer to the fault. This high fault current will flow throughout the entire circuit until a circuit protection device detects the fault and operates, opening the circuit. Figure 13 details the circuit diagram of a sub-station supply transformer to a final circuit in a property.

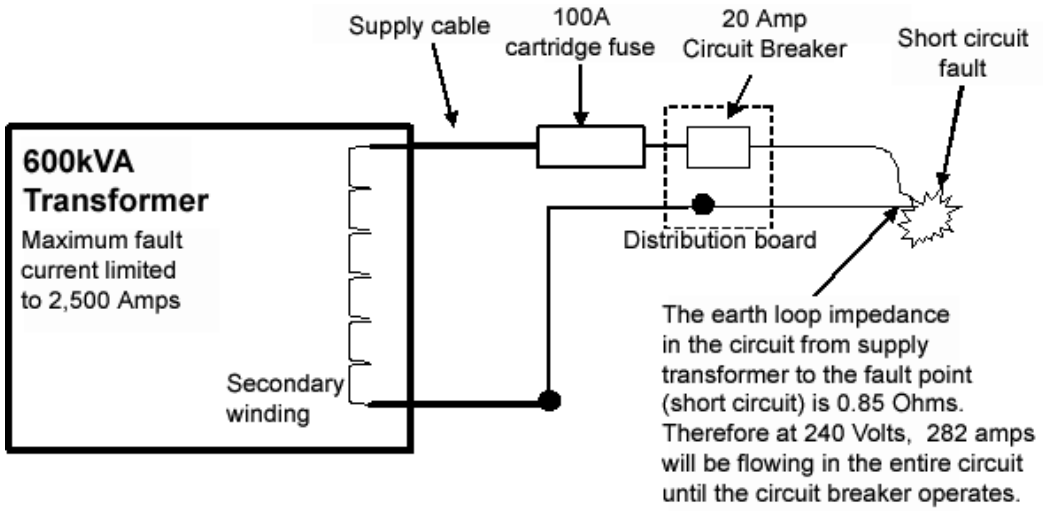

Figure 13 – A circuit detailing the electricity supplier's (sub-station) transformer to a point in a final circuit with a short circuit fault.

The supply transformer's output capacity is 2,500A. The calculation illustrated in equation 4 below assumes a negligible resistance at the point of the fault (where live and neutral conductors are in contact with each other). The total resistance in the circuit from the fault to the transformer secondary winding is 0.85Ω and the voltage is 240V.

$$I = \frac{V}{R}$$ Equation 4

$$I = \frac{240}{0.85}$$

$$I = 282.35 \text{ Amps}$$

This fault current of 282A will therefore flow in the wiring until the circuit breaker operates and de-energises the circuit. The fault current is just over 10 times the maximum rating for the final circuit cable which is a maximum of 27A for 2.5mm^2 twin and earth PVC insulated cable at 60 degrees C [11]. If the fault is not cleared quickly, there will be a very rapid increase in temperature in the cable. A correctly operating circuit breaker would be expected to operate within 0.1 seconds although the fault current is very high, the length of time that it flows in the circuit is very short, therefore the heating effect in the cable will be minimal.

In a correctly designed circuit, with a low earth fault loop impedance a short circuit should result in the rapid operation of the protective device. If the protective device is a fuse the element wire within the fuse will melt within approximately 0.2 – 0.4 of a second. The fuse wire element will generally vaporise and turn into small globules of metal within the fuse. Visual examination of a re-wireable fuse is generally sufficient to observe the globules. If a cartridge fuse is subjected to an x-ray examination following the fire, the presence of the globules on the x-ray image will indicate a fuse which has operated as a result of a short circuit fault. Twibell [13] undertook a series of tests creating faults in circuits protected by cartridge fuses followed by x-ray analysis. He published the reliability of this physical evidence in fuses that is created by short circuit faults. Figure 14 is an example of fuse x-rays with overloading and short circuit faults affecting the fuses.

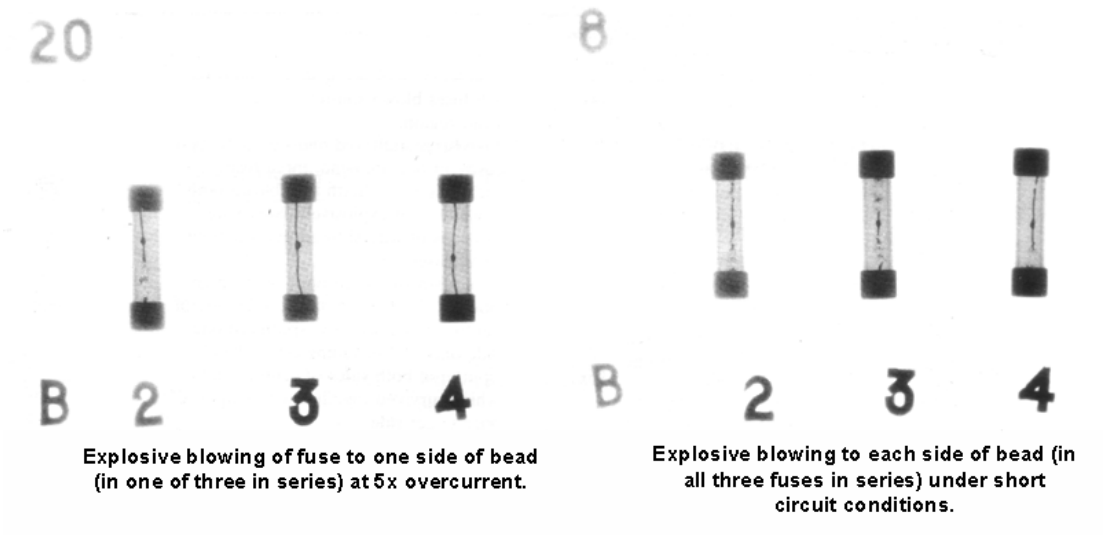

Figure 14 – overload and short circuit evidence revealed with x-ray images [13].

Short circuits are generally caused by a breakdown of electrical insulation (UV light, chemical action), mechanical damage (tools, rodents, abrasion), or thermal effects (contact with hot surfaces etc.).

The most common cause of post-fire short circuit damage that the fire investigator is likely to observe is the damage of the wiring insulation due to flame impingement on the cable allowing the energised conductors to touch each other. It is important for the fire investigator to understand this as evidence of a short circuit post-fire is not evidence that a short circuit was the cause of the fire.

1.4.5 An overload of current

An overload of current occurs when excessive current is flowing in a circuit for a given conductor size. The resistance of the conductor generates excessive heat in this condition. Fuses and circuit breakers are circuit protection devices that are designed to react and operate when a circuit suffers from an overcurrent fault.

An overload of current is often caused by connecting too many appliances or pieces of equipment to a circuit. Unless there is substantial structural collapse of a building it is generally possible to establish what was connected to a circuit at the time of a fire. By calculating the current ratings of the appliances it is possible to determine the

total current flowing in the circuit. For example, houses converted into a large number of bed-sits may experience overloaded circuits where the electrical installation is not upgraded. Following a number of circuit protection device operations, the by-passing of the protection device with a section of conductor, nail etc. may result in the chronic overloading of a circuit.

Physical evidence of an overloaded circuit will be the internal heating effects of the conductor damaging the insulation material. Cooke and Ide [43] documented a "sleeving" of the insulation where the internal heating of the conductor shrinks the plastic insulation away from it creating a loose fit. Ettling [35] in 1980 reported that during his experiments of overloading cables he observed that the PVC insulation softens and sags away from the conductors, but in contrast PVC insulation that is heated up from the outside due to a fire will char and burn and will often stay in contact with the conductors. Ettling appeared to be observing similar sleeving effects during his research abeit described it in a different way.

Experiments and demonstrations of gross overloading of conductors undertaken by the author on a number of occasions have frequently shown the sagging away and softening of the PVC insulation [44]. If the overloading of the cable is continued then it begins to char, blister and produce volatile gaseous products where it is in contact or close to the overloaded conductors as shown in figure 15. The physical evidence described will affect the entire circuit from the point of the fault to the distribution board. The identification of the circuit and a careful examination following the route of the cable from the area of the fire back to the distribution board, should reveal the consistent overloading damage to the cable in areas that have not been affected by the fire (for example, within floors, walls, separate compartments, and service cupboards). Figures 15 and 16 are photographs of overloading damage to conductors created during demonstrations.

Figure 15 – Current overloaded PVC insulated cable [45].

Figure 16 – Overloaded drum of cable with two heaters connected to the circuit [45].

Coiled cable can also accelerate the overloading effect. If an extension cable is left rolled on to a drum used to transport it, the build-up of heat from current that would normally be within the capacity of the cable (if unwound from the drum) can overload the cable and damage it to the point of ignition of the insulation. Figure 16 is a demonstration of this effect with a drum of rubber insulated cable supplying a load of two electric heaters.

1.4.6 A voltage overload

A voltage overload is an excessive voltage that is applied to a circuit. This has the potential to damage electrical equipment and appliances connected to the affected circuits and to increase temperature of the conductors. A natural and extreme form of voltage overload is lightning where there may be thousands of volts affecting circuits in the path of the lightning strike.

Another cause of a voltage overload is a “lost neutral”, also known as a “floating neutral”, in a three-phase system electrical installation. In the UK the voltage in a three-phase system between the phases is 400 or 415 Volts. The voltage between a

single phase and either neutral or earth is 230 volts. Due to the configuration of the sub-station supply transformers, if the neutral is disconnected at either the intake of a three-phase distribution board or at the sub-station transformer, the voltage will rise on one phase and drop on the other two phases. The effect of this is an increase from the normal 230 volts up to 400 volts on one phase. This additional voltage can seriously affect electrical components such as capacitors and cause them to ignite.

Other electrical items such as transformer windings can overheat as a result of the increased voltage. Conventional circuit protection devices such as fuses and circuit breakers are not able to detect voltage overload faults as they only react to excessive current flowing in the circuit that they are protecting.

1.4.7 Resistance heating

The weak link in any electrical circuit is the connections of the conductors and associated equipment in the circuit. Electrical installation design dictates that the minimum resistance within a circuit is achieved to make it as efficient and reliable as possible [21]. A circuit may expect to contain connections between lengths of cable and connections with equipment such as switches, sockets, appliances, etc. A good connection or joint is essential to ensure reliability and to minimise the potential for a localised build up of heat at the connection. Figure 17 details the resistance heating at a nylon plastic terminal connector in progress.

Figure 17 – Resistance heating of a terminal connection [45].

Connections can be affected by movement or vibration, worn push connections, insecure connections and corrosion (or oxidation) between the components of the connection. Figures 18 details localised overheating on a printed circuit board and figure 19 details a poor solder connection on a circuit board.

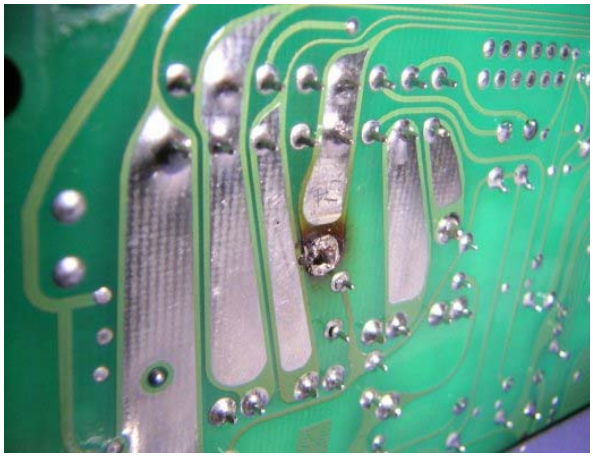

Figure 18 – Example of a dry solder joint with localised overheating to the printed circuit board [46].

Figure 19 – The solder is dull in colour indicating a dry brittle solder connection [47].

In the case of soldered connections dry joints can occur if the original soldering operation was not completed correctly. This can occur if the connection is moved while the solder was still a liquid or if the connection was cooled to quickly. Other causes of dry joints are insufficient solder being applied to the connection or a lack of resin flux due to prolonged heating at the connection using the soldering iron.

Localised heat can build up in the areas of poor connection and these are termed "resistance heating" or "glowing connections" [48-51]. This has been researched in the US by Meese [49, 52] who reported on a substantial amount of experimental research work between 1975 and 1977 relating to the problems of electrical connections in residential wiring systems. A recent research and development report published by the Norwegian Fire Research Laboratory details the problem that exists in Norway where resistance heating was noted as a main electrical cause of fire [53]. The report suggests that some 70 residential fires annually are due to resistance heating faults within electrical socket outlets [54]. This corroborates the author's experience of undertaking electrical examinations at fire scenes and diagnosing faults

in electrical installations. In general it is the enclosure of the connection and the fuel package of combustible material which dictates whether or not resistance heating at a connection will lead to a fire.

1.4.8 An arc (including in-line arcing)

The definition of arcing is the electron flow across a gap and was discovered by Sir Humphrey Davy [55] in 1812 when he connected 2,000 liquid cells together at the Royal Institution. During experimental work when he pulled apart two electrodes with carbon tips which were connected to the cells a sustained arc was created. Arcing and the arcing phenomena are described in more detail in section 1.5.

Below 375V [56, 57], the arc created by shorting electrical wires together lasts only 8 ms (0.008 second) and generates a limited amount of heat energy, therefore making it a poor ignition source for most combustible materials [31, 58]. Arcs created in the 230 volt electrical system found in residences and commercial buildings are also poor sources of ignition [44]. Figure 20 shows an arc being created by the short circuit between live and neutral conductors at 240 volts.

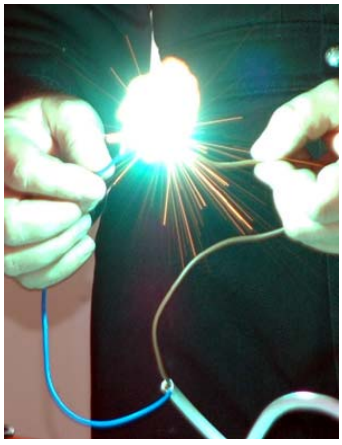

Figure 20 – The author demonstrating an arc [59].

With respect to an electrical fault, arcs often result from a short circuit. This may occur as the conductors approach each other before the short takes place (although below 350V AC, an arc will not jump an air gap greater than 0.5 x 10^{-4} mm in

normal air [57]), or as the conductors move apart immediately after the short circuit event. The 50 Hz AC cycle means that after a maximum of 0.04 second the applied voltage passes through zero at which point the arc is quenched.

Evidence of arcing is often visible at a fire scene without magnification, though in some cases magnification is required. This evidence is in the form of localised melting of the conductors. This often results in various metallic melting patterns that may include one or more of the following: the welding of the conductors together, beading, notching or severing of the conductors. There may also be a spatter of molten or even vaporised metal immediately around the area of the arcing; this may affect adjacent conductors or the surfaces of other items close by [30, 36, 60, 61]. Figures 21 – 23 are microscopic images (x6.4 – x50 magnification), that are examples of arcing damage to electrical conductors at fire scenes.

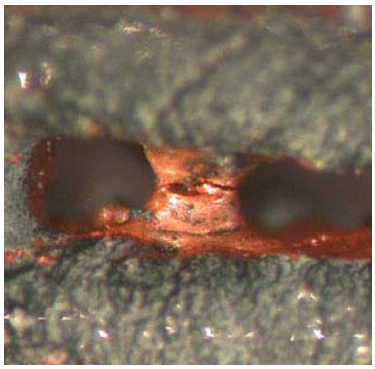

Figure 21 – Conductors welded together at 20x magnification.

Figure 22 – Bead and notch on a conductor at 20x magnification

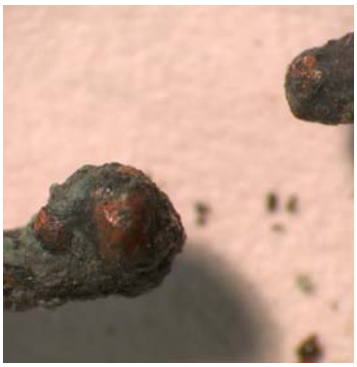

Figure 23 – A severed conductor at 20x magnification.

Arcing can occur in a circuit “in-line”. This means that the arcing fault is occurring in series in a circuit, for example, where a conductor is broken and the current flow is starting and stopping at the break in the circuit due to mechanical movement or vibration. When in-line arcing occurs, the current flow in the circuit is slightly reduced and so the conventional over current circuit protection device will not operate [25].

1.4.9 Carbon Tracking

It is possible for arcing to occur across a carbonised conductive path and this is termed “carbon tracking” or “arcing through char”. Two methods exist for the creation of a carbonised path: a high voltage or the effects of contaminated moisture [25]. Contaminated moisture is a particular problem with cables using polymeric insulation and PVC insulation [62-64]. In 1978 Noto and Kawamura [63] described the tracking and ignition phenomena of PVC insulated cables used in the wiring of buildings. Figure 24 shows carbon tracking in its early development, the timber substrate ignited and a cross-section of the damaged timber substrate.

Figure 24 – demonstration of arcing through char [65].

Evidence of carbon tracking at a scene is very difficult to identify unless the fire is suppressed shortly after its ignition. The reason for this is that evidence of the carbonised pathway becomes destroyed during the early stages of the fire’s development.

1.4.10 Examination of the electrical system in detail

The systematic and thorough examination of the electrical installation [66] is needed to either confirm or eliminate an electrical cause of fire.

It is good practice to work from the electrical intake in the building towards the area of the fire when carrying out an electrical examination. NFPA 921 [67] gives some guidelines that are useful to the investigator relating to this examination.

It is essential before commencing an electrical examination that the electrical supply has been de-energised. It is recommended that electrical test equipment is used to ensure that the supply is isolated [68].

The examination needs to cover the type and operation of circuit protection devices and the distribution board(s). It also needs to cover the thorough documentation of the electrical circuits in the building establishing the wiring's routes, connection points, and the equipment or appliances that they are supplying. All points and types of electrical faults need to be identified and documented. Fire investigators often ignore the electrical examination of a fire scene especially if the cause of the fire is considered to be deliberate [69]. Frequently the defence of a person accused of arson will cite the potential of an electrical cause of fire [70]. The electrical system is potentially able to provide useful data that can be used to confirm or refute a fire's area of origin and it is the validation of this potential that this research work is aimed at.

1.5 Arcing phenomena and the history of arcing

1.5.1 The history of arcing

Sir Humphrey Davy undertook a substantial amount of early research into electricity. A lot of this scientific research was termed "chemical philosophy" in the early 19th century and an example of this early work associated with static electricity was detailed in the publication the Elements of Chemical Philosophy [55] in the section titled "Of electrical attraction and repulsion, and their relations to chemical changes" where he wrote:

"1. If a piece of dry silk be briskly rubbed against a warm plate of polished flint glass, it will be found to have acquired the property of adhering to it, which it will retain for several seconds…. "

Davy is acknowledged as the person to discover arcing. A large amount of his research was published in 1840 in a series of volumes [71]. A description of his discovery of arcing in 1812 explains how 2,000 wet chemical cells were connected together to provide enough power for sustained arcing between two electrodes to

occur. Figure 25 is a reproduction of a diagram of some of the equipment used in this experiment in 1812.

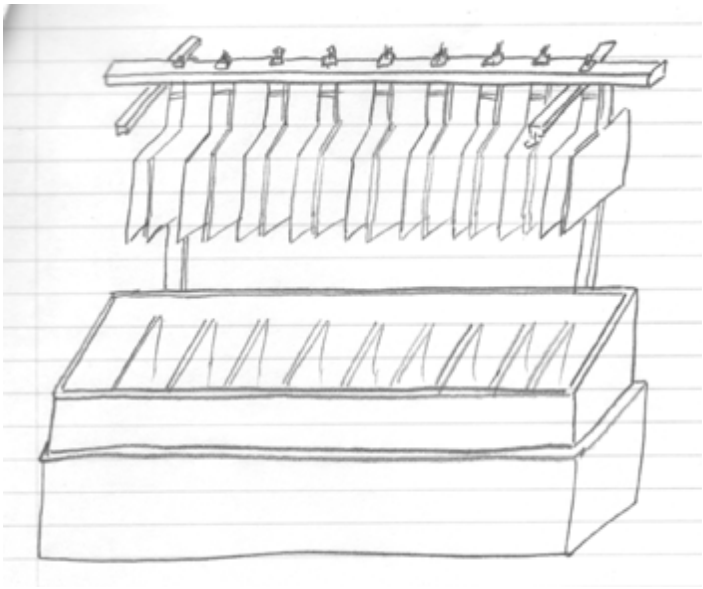

Figure 25 – A reproduced diagram of one of Davy's wet chemical cells *"A porcelain trough with plates of zinc and copper that are removable to form cells"* [72].

Davy describes the experiments as follows:

"The most powerful combination that exists in which number of alternatives is combined with extent of surface, is that constructed by the subscription of a few zealous culminators and patrons of science, in the laboratory of the Royal Institution. It consists of two hundred instruments, connected together in regular order, each compound of a few double plates arranged in cells of porcelain, and containing in each plate 32 square inches, so that the whole number of double plates is 2,000 and the whole surface is 128,000 square inches.

This battery when the cells were filled with 60 parts of water with one part of Nitric acid and one part of Sulphuric acid, afforded a series of brilliant and impressive effects. When pieces of charcoal about an inch long and one-sixth of an inch in diameter, were brought near each other (within the 13^{th} or 14^{th} part of an inch), a bright spark was produced, and more than half the volume of the charcoal became ignited to the whiteness and by withdrawing the points from each other a constant discharge took place through the heated air, in a space equal to at least four inches,

producing a most brilliant ascending arch of light, broad, and conical in form in the middle".

Davy discovered that a piece of carbon at the end of the electrode enhanced the effect and duration of the arc. Figure 26 is a reproduction of the diagram of this experiment in Davy's work. The "arch of light" was later renamed by Davy as an electric arc. Much research work was undertaken by many 19th century scientists and engineers to enhance this arcing effect in order to use it as a reliable light source.

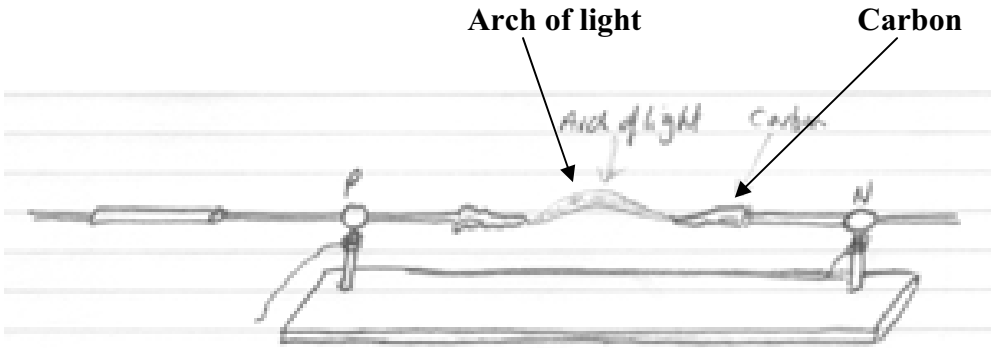

Figure 26 – A reproduced diagram of the "arch of light" observed by Davy when the cells were connected [73].

Hertha Ayrton [74-77] undertook a considerable body of research on arcing at the end of the 19th Century and she devised a way of encapsulating the electrodes of an arc lamp in an inert gas to prevent the "hissing" sound of the arcing. The elimination of the sound also increased the reliability of the arc lamp and considerably increased the lamp life. Ayrton presented a paper on her research minimising the problem of the hissing of the arc lamp to the Institution of Electrical Engineers in 1899 [77]. In their publication, (Electrical Review), the paper was described as *"of very great interest and novelty, and marks a decided step toward the solution of a long-standing difficult and important problem".* [1]

[1] Three months later in a historic move she was elected as the first female member of the Institution. It was almost 30 years before another woman became a member of the Institution and Ayrton's election was a significant recognition of her contribution to the field.

All of Ayrton's work on arcing was published in 1902 [74] and became the standard reference work on the subject. Ayrton was referenced by Windred [57] in 1940 in his book on 'Electrical Contacts' and its description of the reduction of damage to switchgear as a result of arcing.

Maier, Hepworth and Zeilder [78-80] continued the work into the construction of arc lamps with additional developments and design recommendations for the manufacturers of these lamps which revolutionised the artificial illumination of commercial and domestic properties as well as streets towards the end of the 19th century. In the 20th century research has continued with the improvement of electrical lighting and low energy fluorescent, sodium (SON), high pressure mercury (HQL) and Metal Halide (HQI) discharge lamps that are all associated with the arc have undergone significant developments in the last 30 years [21].

It is interesting to note that the latest generation of lighting is now moving away from the electric arc with the introduction and rapidly developing use of Light Emitting Diodes (LEDs) technology for lighting in buildings. LED lamps have the advantage of a very high lumen (light output) per watt and also run with a negligible temperature loss.

1.5.2 Arcing phenomena

Arcing is a type of continuous electric discharge (electron flow) between two electrodes in a gas at low pressure or in open air, emitting intense light and heat. The discharge is carried largely by electrons travelling from the negative to the positive electrode, but also in part by positive ions travelling in the opposite direction. The impact of the ions produces great heat in the electrodes and in an arc in air at normal pressure, the arc centre reaches a temperature of around 10,000K (9726° C) [81]. The temperature of the electrodes is limited by the boiling temperature of the electrode material, for copper this is 2562° C [82, 83].

The conductivity or dielectric strength of air is 1.4kV/mm [84] however the electrical breakdown across an air gap can occur at lower values if the air is ionised by either a

previous arc or by flames [25]. Arcing events in electrical distribution equipment can escalate rapidly following the initial arc fault and cause the total destruction of electrical distribution switchgear and services. The modelling and prevention of these arcing events have been researched by various engineers [85-89]. Gammon and Mathews [86, 87, 90] have published a number of papers describing the development mathematical models to predict the arc currents that were first described in 1960 by Kaufman and Page [91]. The purpose of modelling arc faults that may occur in electrical distribution equipment is to improve the detection and isolation of the circuit involved to reduce or even to prevent permanent damage to the wiring and equipment.

1.6 Arc characteristics and metallurgy

1.6.1 Introduction to copper metal

Copper metal is frequently used as an electrical conductor as it has a higher inherent conductivity of electricity and heat than any other material, with the exception of silver [92]. Alexander and Street [93] describe how the pure copper metal is very ductile and can be rolled into strips that are under 0.25mm thick or drawn into wires that are less than 0.02mm in diameter. It can be pressed or spun into various shapes without cracking. It is possible to alloy copper with other metals but this generally affects its electrical conductivity. For example the addition of 10% aluminium doubles the copper's physical strength but reduces the electrical conductivity to approximately one sixth [93].

A continuous casting and rolling process currently produces virtually all copper rod that is used to make electrical wiring [93]. This process enables a segregation of impurities, reduction of copper oxide particles on the surface, and the elimination of welded connections that connected sections of copper metal (essential for production prior to the 1960's).

Oxygen is added to copper in the production process to scavenge for dissolved hydrogen and sulphur. If the oxygen content is kept under control, microscopic bubbles form that offset the normal shrinkage of 4% in volume during the liquid to

solid transformation. The pores are then generally eliminated during the hot rolling process.

In a paper for the Copper Development Association, Pops [94] described the electrical nature of copper used in the electrical industry. He explains that it exhibits high conductivity as its conducting electrons show relatively little resistance to movement under an electric field. Copper's outermost electrons have an atomic spacing (mean free path) of 100 between collisions. The electrical resistivity is inversely related to this mean free path and thus is very low. The spacing between copper atoms is about 2.3×10^{-10} m (0.23 nm) [95].

1.6.2 The effects of arcing damage to the copper metal

Copper wire is a polycrystalline structure [60] (many crystals bonded together). The crystals are known as grains and they are elongated in shape by the manufacturing process of drawing the wire. If a structure contains only the elongated copper grains this is an indication that it is a high purity copper.

Levinson [60] described how the grain structure in copper changes when copper wire melts. The original elongated structure is replaced by a dendritic (tree-like) structure. He explaind that the presence of copper oxide in the spaces between the copper dendrites indicates that oxygen was absorbed by the molten copper. A small amount of porosity in the copper may also be present. Levinson's paper indicates that in the location of an electrical arcing event affecting the copper wire grain structure, copper oxide should be present in the area of localised melting found during the arcing event.

Levinson [60] and Gray [96] both report a porosity effect of "hollows" or "swiss cheese" effect on the surface of localised copper wire melting due to arcing occurrences. Levinson suggested that this effect would be found if the wire was melted by the fire, the resistance effect of a gross over-current or by arcing. He explains this porosity as a result of partial entrapment of gas pockets liberated from the copper wire. Gray also observed this effect on some of his test samples that

consisted of 5A rated two-conductor flexible copper cable when examined with a Scanning Electron Microscope (SEM).

Typical melting effects from conductors that have arcing damage are shown in figures 27 to 36. These magnified photographs taken through a microscope are of conductor damage from the practical experiments of this research project.

Figure 27 – Two conductors welded together.

Figure 28 – Severed conductor with a bead on one end and a notch at the other conductor end.

Figure 29 – Arcing between two conductors. One severed with beading at each end. The other conductor is notched.

Figure 30 – All three conductors of this cable are affected. The arcing has occurred at a fixing screw. All are notched with beading on the notch edges.

Figure 31 – A severed conductor with a "bull-nose" bead. The demarcation between melted and unmelted conductor is visible.

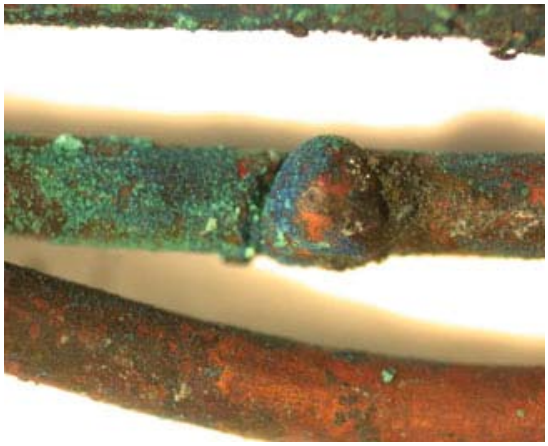

Figure 32 – A bead within a notch on the conductor. The demarcation between melted and unmelted conductor metal is visible.

Figure 33 – Gross beading affecting all three conductors of this cable. The conductors are also welded together.

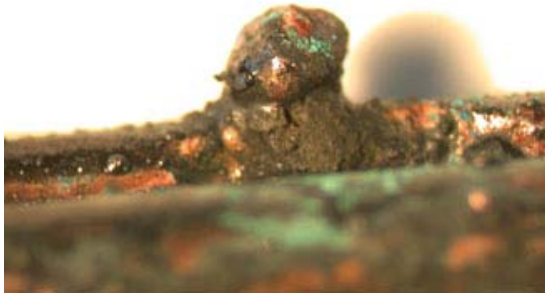

Figure 34 – A raised bead on a conductor that is visible at the fire scene without magnification.

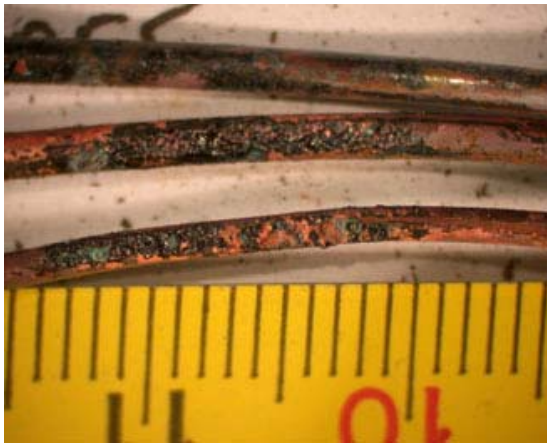

Figure 35 – Arcing through char affecting two conductors over a length of 14mm. The scale in the image is in mm.

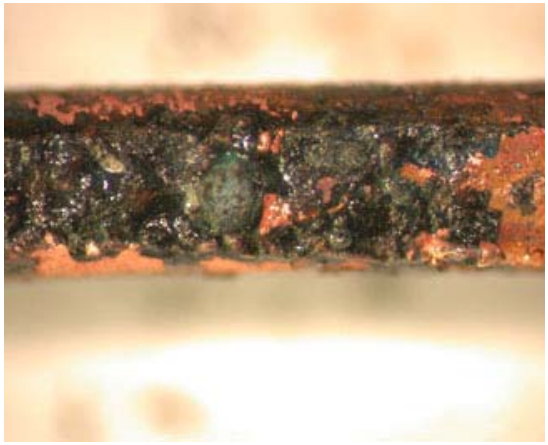

Figure 36 – A close-up of a section of figure 35 showing the arcing through carbonised cable insulation in more detail.

1.7 How arcing can assist the fire scene investigator

1.7.1 Introduction to the methodology of arc mapping

The arcing damage to electrical conductors that is often found at a post-fire scene where the electrical installation was energised during the early development of the fire can be useful to the investigation as it can provide reliable data to establish a fire's area of origin [97]. This data can be vital when the fire in a compartment(s) has reached flashover conditions whereby the conventional burn patterns that fire investigators often rely on have been overwritten by the flashover and ventilation effect patterns.

The melting temperature of pure copper is 1084º C [98] and commercially available electrical conductors are generally 99.999% copper [92]. Compartment fire temperatures vary depending upon the fuel packages and the ventilation that are available in the fire. Tests have shown that these compartment fire temperatures do not often exceed 900º C at ceiling level [99-102].

As the fires in the compartment interact with the energised cables, the fire burns through the cable and electron flow occurs between the conductors due to either the conductors coming into contact with each other, or through the carbonised plastic cable insulation that has become conductive due to the effects of the heat. When electron flow is established between the energised conductors an arcing event often takes place. The localised melting of copper conductors during an arcing event survives the fire and may be observed by an investigator who undertakes a careful examination of the electrical installation during the fire investigation process.

The majority of arcing damage observed at a fire scene is as a result of the fire rather than the cause of the fire. The arcing damage to electrical conductors can provide important information about the location of the origin and the sequence of the fire's spread. A comparison of the position of the metallic damage to conductors with the layout of the electrical system can help to establish the area where the fire first attacked the energised electrical installation. This is achieved by locating the points

of arcing damage on a cable that is furthest away from the source of the electricity (distribution board); this indicates the point of the first attack by fire on that circuit. Multiple cables can be used to locate the area of origin of a fire in a compartment by detailing the arcing locations on the cables on to a diagram of the electrical system in that compartment. This was first used by Svare in the late 1970's [103], and the methodology was first published by Deplace and Vos in 1983 [97].

A more detailed description of the scene examination process was described by Rothchild in 1986 [104]. Svare detailed the use of this methodology whilst presenting at a conference in China in 1988 [105], in course handouts for the Federal Bureau of Alcohol Tobacco and Firearms in 1998 [61], and in the UK for the first time in 1999 [106]. Compartment fire tests undertaken in the US using UK wiring by the author and Svare in 1999 [107, 108] showed that this methodology could be applied successfully to UK wiring and circuit protection devices. More recently others have published this methodology [100, 109-112] and some additional compartment fire tests have been undertaken in the US using fixed electrical wiring, extension cables, and appliance cables [100, 101].

1.7.2 Arc mapping as part of a scene examination

The majority of fire scenes generally encountered are those in which arc mapping can be applied. They will often include domestic properties, retail units, industrial buildings, and factories. The fixed electrical installations, extension flexible cables, and electrical appliance flexible cables should all be examined closely where they have interacted with the fire. Each circuit needs to be identified and traced from the electrical distribution board(s) housing the circuit protection devices for each of the circuits involved in the fire. A diagram of the electrical circuits should be overlaid on to the plan of the compartment(s) involved in the building.

A careful and methodical examination of the conductors will often identify arcing damage where the fire first attacked the wiring insulation. Disposable gloves over hands are normally what are required to feel the beads, notches, welded points etc. that suggests evidence of an arcing event. Care needs to be taken not to misidentify

other conductor damage in the form of alloying (eutectic melting), thermal damage, or mechanical damage that may appear to be electrical arcing damage [102, 108].

Churchward's [113] description of the conductor examination is a detailed and accurate explanation of the care that is needed to achieve this type of electrical examination at a fire scene.

1.8 Arcing - the cause or a consequence of a fire

A considerable amount of research work has been published explaining various analytical techniques that have been applied to conductor exhibits recovered from fire scenes [118 – 125]. The purpose of this was to determine whether the arcing damage was the cause of the fire or a consequence of the fire externally attacking the electrical wiring during the fire's development and spread. The general rationale for this research is in the importance that a successful analytical technique would have on some fire investigation cases. For example, millions of UK pounds and US dollars in fire loss claims against liable insurance companies, manufacturers, or contractors could be recovered if it can be proved that arcing damage found during a scene examination was the cause of a fire.

Two comprehensive reviews have been undertaken to date examining the literature relating to the application and development of analytical techniques to determine if arcing damage found on electrical conductors during fire scene examinations is the cause or the consequence of the fire. In 1993 Jonson [114] from Sweden reviewed the published material for the previous 15 years that detailed the methods used to examine fire damaged electrical conductors. These methods included optical microscopy, Raman spectroscopy, scanning electron microscopy, energy dispersive X-ray analysis, and Auger electron spectroscopy.

In 2003 Babrauskas [82] [115] published a very comprehensive review of the literature published to date on 'cause' or 'consequence' arcing beads by physical or chemical testing. He reviewed all of the published research work that had been

carried out by scientists and engineers in the US, UK, India, and Japan to reliably categorise arcing beads found at fire scenes. Babrauskas also correlated the six different methods that the researchers had established as reliable indicators:

"1. 'Cause' beads have square or rectangular pock marks, while 'victim' beads lack these structures.

2. Victim' beads show small surface-deposited particles, while 'cause' beads do not have these.

3. 'Cause' beads have small voids, while 'victim' beads have large ones;

4. The number of voids or their total cross-sectional area is different in 'cause' beads than in 'victim' beads.

5. 'Cause' beads have a small dendrite-arm spacing, while 'victim' beads have a large spacing.

6. Based on examining long segments of wire and not just beads, if long segments are uniformly re-crystallized, the wire suffered gross electrical overheating; this does not directly establish cause/victim status, but may be of help in assessing the sequence of events that transpired."

The abilities and usefulness of Raman spectroscopy and Auger electron spectroscopy for this analysis was questioned by Babrauskas [82]. The use of Raman spectroscopy to analyse the crystal structure the carbon residue of PVC insulation was published by Lee et al in 2002 [116]. The "cause" beads contain both graphitized carbon and amorphous carbon while the "consequence" beads (due to fire attack) only contain amorphous carbon. Babrauskas [115] thought that it was not clear how the carbon migrates into the copper metal as the reported work stated that the temperatures are only 110-250 °C when the PVC insulation is being charred. In addition, there was a low probability (27-60%) of successfully identifying a cause bead with this method. The conclusion of Babrauskas' review was that he thought that it was unlikely that any of the six methods that he reviewed could be developed in the future to become robust and reliable for this purpose [82].

The Auger electron spectroscopy analytical method is used to detect the oxygen content on the conductor surface. This methodology suggests that if the oxygen level is high the arc was created pre-fire, whereas if the oxygen level was low, the arc was created during the fire when the fire is consuming oxygen during the combustion chemical reaction. The Auger electron spectroscopy analytical method to establish the content of oxygen of the surface of a conductor was patented in the US in 1980 [117] and published by Anderson [118]. This analytical method was seen as a significant breakthrough as an analytical method to determine if an arc bead was the cause of a fire or the consequence of a fire. Anderson used this method for a number of significant fire cases and gave evidence in court relating to his analysis of arc beads using Auger electron spectroscopy.

The use of Auger electron spectroscopy was brought into doubt by Howitt [119] as he was unable to reproduce it with his own exhibits of known origin. In 2004 Beland [120] published a blind test that was undertaken in association with Anderson where Beland created arcing damage to conductors in his laboratory that were either a cause or generated as a result of a fire. The resultant conductor exhibits were sent via a third party to be encoded prior to analysis. Anderson used auger electron spectroscopic analysis that he had been using for case work to establish whether the damage was a cause or victim. The results indicated a 40% success rate for correct interpretation of the samples. The results of Beland's blind test appear to substantially undermine the reliability of this analytical method.

In 2005 Beland [121] described the problems of investigators who claimed that their field experience, relating to the electrical causes and consequences of fires, should not be challenged even if their theories contradict physical evidence. He evaluated the different types of conductor damage characteristics and concluded that generally the damage to electrical conductors, devices, and installations that are often recovered from fire scenes are the normal consequential effects of external attack by fire. He also concluded that there is not a way currently to determine whether that type of evidence is the cause or consequence of a fire with a reasonable degree of scientific certainty.

1.9 Summary of literature review

The literature review undertaken in this chapter covers a number of separate subjects relating to the electrical causes of fires, arcing phenomena, the history of arcing, the arcing effects of copper and its metallurgy, and whether arc mapping can assist a fire investigator.

The discovery of arcing goes back to the infancy of electrical engineering. The published literature explains a lot of the physical characteristics of arcing following the research by scientists and engineers in laboratories. Beland [26, 30-34, 120-134] has published a significant number of papers on electrical causes of fire and the problems with fire investigators readily blaming electrical installations and equipment as the cause of fires, due the incidence of arcing damage often being easily observed during fire scene examinations. Babrauskas [25, 82, 115, 135] has undertaken very detailed reviews of published work on electrical causes of fire and arcing damage to conductors and concluded that there is a very limited amount of previous research work relating to electrical causes of fire (outside of Japan). This would seem to be surprising considering the amount of fires with their inevitable financial losses that are determined as electrical in origin.

A considerable amount of research has been undertaken in the last 30 years on establishing whether physical or chemical analysis of arcing damage to electrical conductors can be used to establish whether the evidence subjected to analysis is the cause or the consequence of a fire. Independent testing of known arcing damage to conductors has established that there is not currently a scientifically reliable method to answer this question and it appears that a reliable analytical method for determining the cause or consequence is not predicted in the near future.

This literature review has also established that there has not been any published work for a protracted series of practical tests involving the installation of electrical wiring into fully furnished compartment fires prior to the experiments undertaken for this research during 2004 to 2006.

1.10 Aims and objectives of the work

No work has been previously undertaken involving controlled tests which repeat the arcing process that occurs on cables within fully furnished compartment fires or to investigate the metallic damage to conductors from arcing that has occurred in real fire conditions.

Data from the analysis of electrical conductors with arcing damage can reliably indicate a fire's area of origin within a compartment fire. Previous work has focused on either the physical appearance of arcing damaged exhibits, their location, or their cause. Not all of these aspects have been previously combined together and this work addresses this issue.

The aims and objectives of this research are:

1. **Aim:** To explore the potential and reliability of the "arc mapping" methodology for estimating the origin of compartment fires.
   Objective: To undertake a series of full-scale experimental compartment fires and evaluate the three-dimensional locations of the fire's origin compared to the arcing locations.

2. **Aim:** To compare pre-fire arcing patterns to the arcing patterns resultant from fully developed compartment fires.
   Objective: To prepare pre-fire arcing exhibits and physically compare the metallic patterns of the pre-fire exhibits with the arcing exhibits recovered from the full-scale tests.

3. **Aim:** To identify a series of arcing damage patterns from the experimental exhibits.
   Objective: Review all of the experimental fire exhibits, fully document and categorise them on the basis of their physical and microscopic properties.

4. **Aim:** Establish whether any surface elemental characteristics within the experimental exhibits that would indicate the mechanism by which they were produced.

   Objective: Undertake a series of SEM analysis techniques on a random number of arcing exhibits to produce elemental maps to identify the presence of copper, aluminium, zinc, iron, carbon and oxygen.

5. **Aim:** Examine the potential of an alternate examination technique that would address the short comings of optical microscopy (depth of field) and SEM analysis (complexity and cost).

   Objective: Use a confocal laser scanning microscope on a selected number of exhibits already examined with an SEM.

6. **Aim:** Establish whether any correlations exist between any of the variables that might affect the reliability of arc mapping.

   Objective: Use a statistical software package to undertake a series of correlation tests.

1.11 Summary of the thesis

This thesis describes practical experiments carried out between 2004 and 2006 and analytical examinations of the generated exhibits from these experiments undertaken from 2006 to 2009. The evaluation of the experiment data has validated the reliability of arc mapping.

The experimental set up for the compartment fire tests is described and presented in chapter 2. Initial tests were used to refine the experimental site conditions and considerable upgrading of the electrical supply system was required to generate the appropriate arc faulting conditions required. The chapter details the means by which the data was recorded for the 39 full scale tests used in the study. Repeat scenarios and layouts were used for these tests. 15 tests were carried out in mobile homes and 24 tests were carried out in concrete block buildings. A summary of the data

produced for one test is presented. Similar data for all 39 tests are presented in volume two.

The physical examination of the conductors is described in chapter 3. In total 141 exhibits were recovered. This chapter describes the initial clean up and low power microscopy carried out on the exhibits. The arcs were grouped into 9 categories according to their morphology. Statistical analysis of the arcing categories based on factors such as approximate ceiling temperature of the compartment at the time of arcing, time since ignition of the arcing, room configuration and room construction were carried out using SPSS software version 17 (SPSS Inc. Chicago, IL. USA). No correlations were found which confirmed the random nature of the arcing category observed.

Chapter 4 describes in depth the further microscopy work carried out on the recovered exhibits. Both scanning electron microscopy (SEM) and confocal laser scanning microscopy were carried out and comparisons made. SEM analysis also facilitated elemental mapping of the arc surface. The value of using a scanning electron microscope and Confocal laser scanning microscope when evaluating localised melting to conductors to establish whether the evidence is electrical activity or other thermal damage was established.

Chapter 5 describes the investigation of the application of arc fault mapping to the experimental tests. A simple mathematical model is presented to indicate the presence of arcing on cables as a function of their distance form the known point of origin of the fire. Three blind tests were used to validate the model.

Conclusions and further work are presented and suggested in chapter 6.

Chapter 2 – Experimental methodology for the practical burn tests.

2.1. Summary

This chapter provides details of the electrical circuit arrangements used in all of the field tests. Examples of photographs taken during the tests, the specification of the equipment and materials used to construct the experiments, the electrical and temperature data that was collected during these tests, and the problems encountered along with their solutions are presented. A total of 39 full-scale experiments are detailed in table 1. The number of times the full-scale experimental scenarios were repeated ranged from 3 to 4 for scenario E and F respectively, to eight repeats for scenarios A to D. The compartments were arranged and furnished in approximately the same configuration within each scenario and the point and means of ignition was the same within each scenario. Repeating the tests within the different scenarios allowed the investigation of arcing within and between room configurations to be investigated as part of the study.

Table 1 – Scenario type and dates for the 39 experiments

	10 March 2005	14 April 2005	8 September 2005	29 September 2005	23 March 2006	20 April 2006	11 May 2006	22 June 2006	7 September 2006	28 September 2006
Scenario A	☒	☒			☒	☒	☒	☒	☒	☒
Scenario B	☒			☒	☒	☒	☒	☒	☒	☒
Scenario C		☒	☒		☒	☒	☒	☒	☒	☒
Scenario D			☒	☒	☒	☒	☒	☒	☒	☒
Scenario E	☒	☒	☒	☒						
Scenario F	☒	☒	☒							

The red line indicates the date after which all experiments were completed within concrete block buildings dry-lined with plasterboard.

2.2 Description of the experiment site

The live burn tests used in this research were made available by Gardiner Associates Limited, a fire investigation training provider. The training site was located within the Ministry of Defense Police and Guarding Agency Headquarters and Training Centre at Wethersfield, Essex, UK. The fire ground area was made up of twelve compartments and an overview of the testing ground is presented in figures 46 and 47. Four compartments were located in mobile homes that were reinforced and dry lined with plasterboard. The other eight compartments were arranged in two terraced units constructed with concrete blocks with internal walls finished with plasterboard.

During the fire investigation practical training courses six compartments were used. The test compartments were fully refurbished and furnished into six different scene scenarios for each training burn. Each scene scenario was arranged in the same configuration for each training course to ensure consistency. Each of the fire scenes are repeated up to seven times annually. For this research, electrical circuits were installed into a number of these scenes on a repetitive basis prior to ignition. This facilitated the reproducibility of test conditions across a number of different physical layouts for the scene scenarios used. Figure 37 details a plan of the Wethersfield site and figure 38 is a view of the generator and buildings.

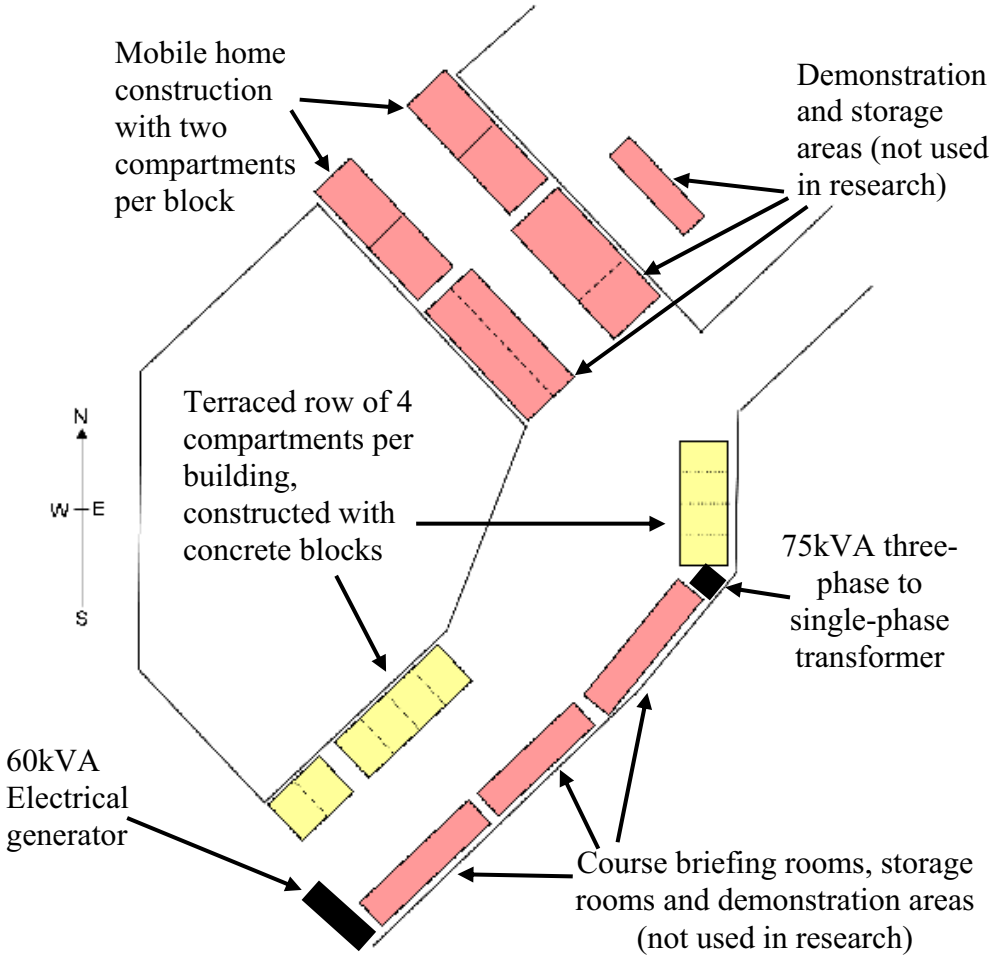

Figure 37 – Overview of the Wethersfield site [136].

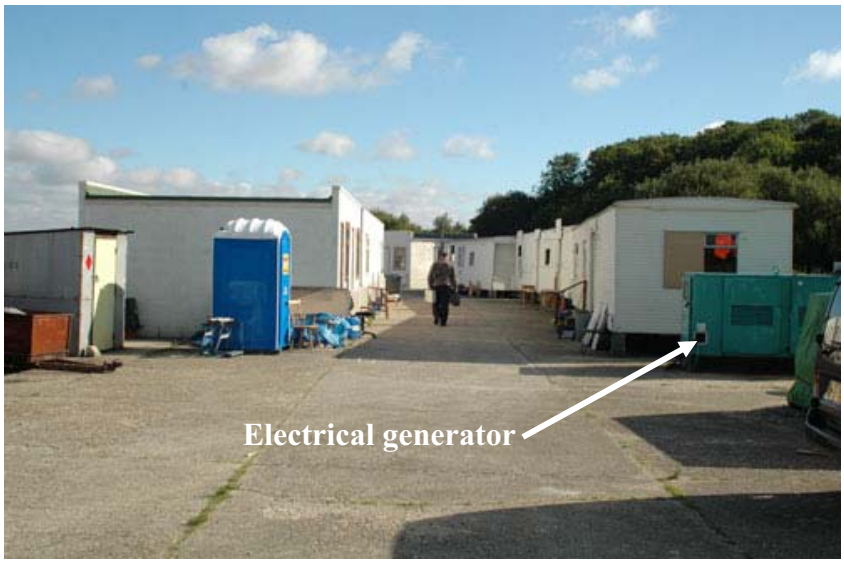

Figure 38 – View taken from the south-west end of the Wethersfield site.

2.3 Developing the circuit design and electrical installation

2.3.1 The three-phase generator

The generator available at the experimental site was manufactured by Stamford AC Generators (Newage International Ltd.). PO Box 17, Barnack Road, Stamford, Lincolnshire. PE9 2NB, UK. Figures 39-40 show the generator installed on site and table 2 gives the general specifications of the generator.

Figure 39 – The 60 kVA three-phase generator on site.

Figure 40 – The generator controls.

Figure 41 – The electrical output of the generator is displayed with voltage, current and frequency meters that are built into the control panel.

Table 2 – Specification of the generator

Manufactured: 05/95	Stator winding: 311
Serial number: CO55882/02	Stator configuration: Star
Type: UG.1224F1	Enclosure: IP22
AVR: SX460	Insulation class: H
Power factor: 0.8	BS 5000
Volts: 415	NEMA MG1-22
Rating: Cont. (continuous)	IEC 34-1
Excitation volts: 40, Amps 2.00	Ambient Temp: 40 degrees C
KVA: 60	Hertz: 50
RPM: 1500	Phase: 3
Amps: 83.5	

The following electrical measurements were taken at the generator:

Phase (live) to neutral voltage = 238V.

Phase to phase voltage = 411V.

The measurements were made with the following electrical loading on each of the generator's phases; red phase = 25A, yellow phase = 45-50A and blue phase = 25A.

2.3.2 Circuit design

The electrical circuit installation chosen for each test consisted of one power ring circuit, one power radial circuit, and two radial lighting circuits. This configuration of circuits was chosen as it best represented the types and variety of circuits

commonly found in domestic premises in the UK. Each circuit was installed in each test compartment. Figure 42 shows the circuit layout in a typical compartment. Circuit 1 is ring configuration designed for socket outlets that used 2.5mm^2 conductors. Circuit 2 is a radial power circuit designed for one or two socket outlets that also used 2.5mm^2 conductors. Circuit 3 and 4 are radial circuits designed for lighting that used smaller sized 1mm^2 conductors.

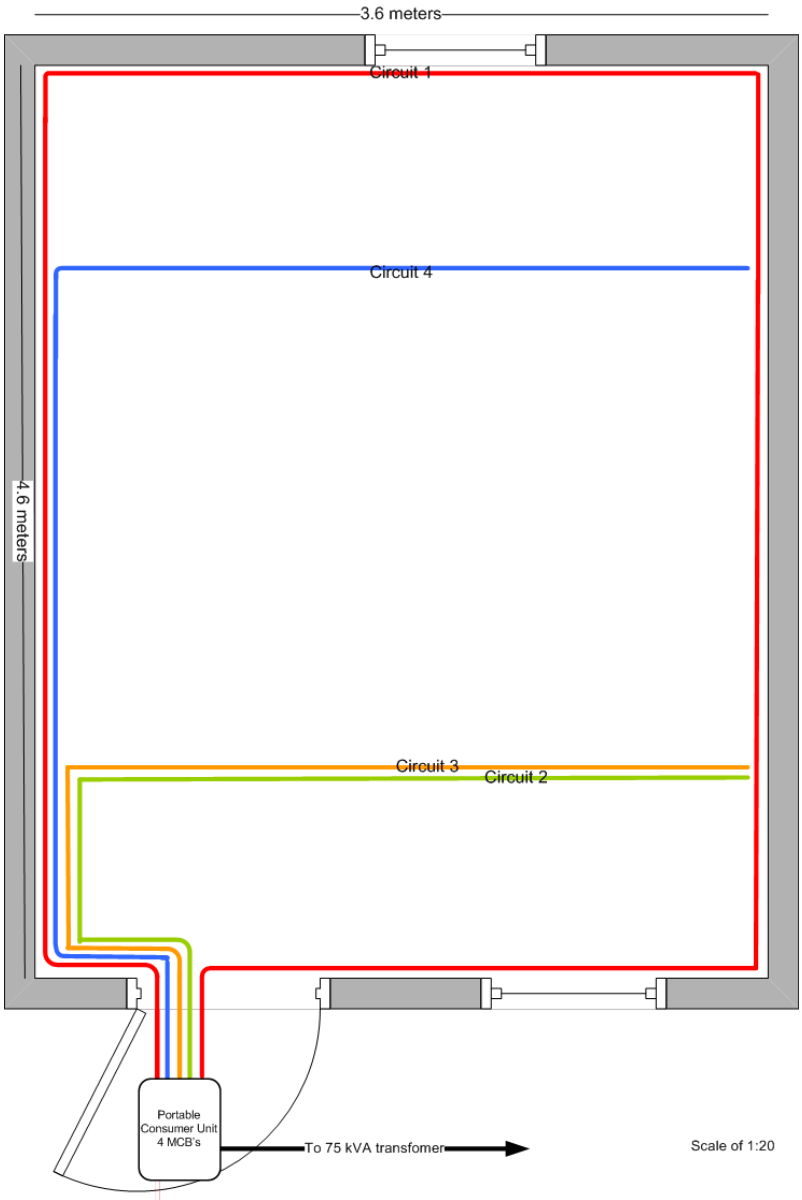

Figure 42 – The typical routes of the electrical circuits installed within the compartments fires used in the research.

The cables used in the compartments were two different sizes dependant upon the circuit type. Circuit number 1 (a ring main circuit) was wired from the portable

consumer unit located outside the compartment with 2.5mm^2 PVC insulated and PVC sheathed cable. The cable was certified by the British Approvals Service for Cables (BASEC) with a certificate number of 078/01 that was detailed on the cable drums. The cable had a maximum operating temperature of 60 degrees C and was constructed to comply with British Standard 6004 [137] and this standard number was stamped into the plastic cable sheath at intervals.

Circuit number 2 was wired in a radial (single ended) configuration from the portable consumer unit. The cable was also the same 2.5mm^2 PVC insulated and PVC sheathed cable used in circuit 1 and the specification has already been detailed.

Circuit number 3 and 4 were wired in a radial configuration to replicate lighting circuits. The cable was 1.0mm^2 PVC insulated and PVC sheathed cable. The cable was certified by the British Approvals Service for Cables (BASEC) with a certificate number of 078/01 that was detailed on the cable drums. The cable had a maximum operating temperature of 60 degrees C and was constructed to comply with British Standard 6004 [137], this information was stamped into the plastic cable sheath at intervals.

2.3.3 Cable installation

A number of initial experiments (23 in total) were undertaken in order to optimise both the cable installation and the electrical supply to the compartments.

For the optimisation experiments, the cables were fixed to the walls and ceiling of the compartment using 75mm long, number 8 size, zinc plated steel “pozi-drive” self-tapping screws (part number T3738353, manufactured by Thornsman). PVC plastic cable-ties were used to secure the cable to the screws. However, during the burn tests it was noticed that the cables tended to prematurely drop from the ceiling in the early stages of the fire. This appeared to be occurring because the PVC plastic cable ties were melting during the fire when the ceiling temperatures exceeded their melting temperature. To overcome this problem extra screws were used to construct

a “cross” shape to hold the cables in place for the experimental tests. Figures 43 and 44 detail the cable supporting methods.

Figure 43 – Cables fixed with screws and cable ties above and to the side of the compartment’s entrance doorway.

Figure 44 – The method of crossing two screws into an ‘X’ shape to support the cables during the fire and its suppression by fire crews.

The cable fixing method for the last 4 experiment fires used small blocks of timber 100mm by 25mm in size with 16mm diameter holes for the cables to pass through and 4mm diameter holes to allow the pozi-drive screws to fix the timber blocks to the ceiling. The purpose of these timber blocks was to determine if there was a difference with the physical evidence found on the cables after the fire when there were no steel screws used to fix the cables. Figure 45 shows the timber block cable supporting method.

Figure 45 –Timber blocks simulating floor joists used to support the cables.

2.3.4 Low fault current issues

Circuit breakers were used to protect the wiring during the fault conditions that would occur as the fire attacked the insulation of the cables. The circuit breakers protecting the wiring in the optimisation experiments (23 in total) operated as predicted during the fire. This indicated that electrical faults had occurred on the installed cables due to fire attacking the cable insulation. However, when all of the wiring was examined post-fire, no localised melting damage consistent with arcing was observed on any of the conductors.

During the optimisation experiments the electrical power was supplied to the test compartments using a three-phase generator available at the fire testing ground site. An evaluation of the electrical data collected from the initial tests suggested that the fault current, when the cables failed, was too low to produce localised thermal damage to the solid conductors used in the experiments. An examination of flexible cables and extension cables used within the compartments as part of the training

scene scenarios indicated that they were experiencing localised melting and arcing to the fine copper strands of these cables. It was determined that a lower fault current was creating this arcing damage to the flexible cables and therefore the fault current from the one phase of the generator supplying the research wiring was insufficient to replicate a residential electrical supply. The reason behind the low fault current appeared to be the generator's exciter coils magnetic field collapsing in a fault condition thus limiting the output of the generator [138].

Different variations to the electrical installation supplied by the three-phase generator were tried unsuccessfully to rectify this problem. These included: upgrading the conductor size of the cable linking the generator to the portable consumer unit attached to each compartment, loading the generator on each of its phases with cooking appliances, and loading the final circuits just before they enter the compartments with portable heating appliances.

The final solution to resolve the low fault current problem was to use transformers to increase the voltage at the generator's output utilising two or three of the available phases and then to reduce the voltage where it was required to minimize the losses of distributing the electrical current across the site. The transformer option was the most favourable as it would also produce an electrical buffer between the electrical faults and the generator. In addition, calculations showed that if the transformers could be sized sufficiently it would be possible to obtain a constant output of 200 - 300A at 250V thereby maximising the total potential of the generator.

2.3.5 Transformer design

The initial design was for two transformers to be used. The first would be located next to the generator with the primary winding connected to two of the three available phases. The secondary winding of the transformer would output 1000V. A second transformer would reduce the voltage from 1000V to 250V. Both transformers would be rated at 70kVA (or 70,000W) to ensure that there was no

restriction of the fault current through the transformers between the supply generator and the loads. Figure 46 details the two transformer design.

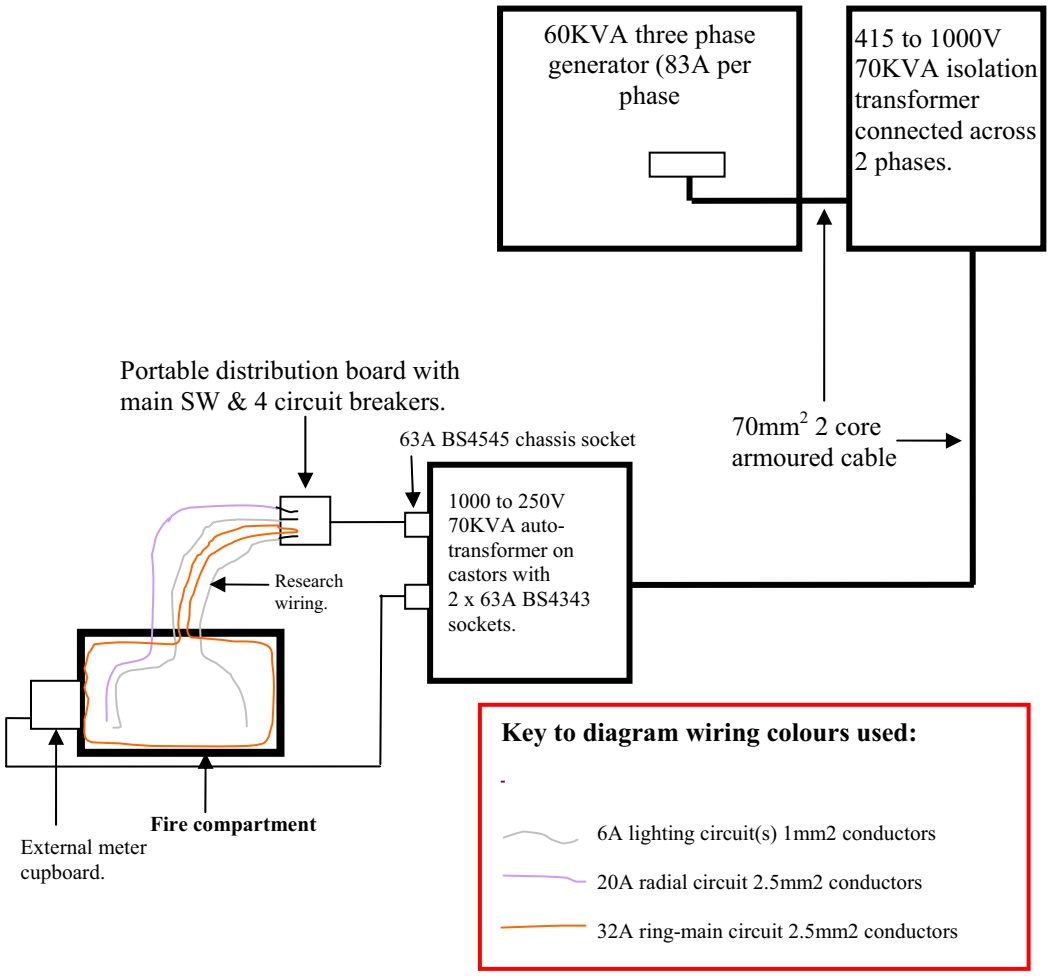

Figure 46 –Initial experimental design using two transformers with 1000V between them.

There were going to be some considerable practical problems moving the smaller step-down transformer from scene to scene as it weighed some 250kgs. In addition, there were concerns about the possible electrical safety risks and it was determined that stepping the voltage up to 1000V would add little advantage in reducing electrical losses from the generator to the fire compartments.

The final agreed design was to use a 75kVA three-phase to single-phase transformer located in the centre of the site and connected via a 95mm² armoured cable to the

60kVA three-phase generator. This design would enable a continuous output of 300 Amps at 250 Volts. Figure 47 details the final design of electrical distribution from the generator to the compartments using one three-phase to single-phase transformer.

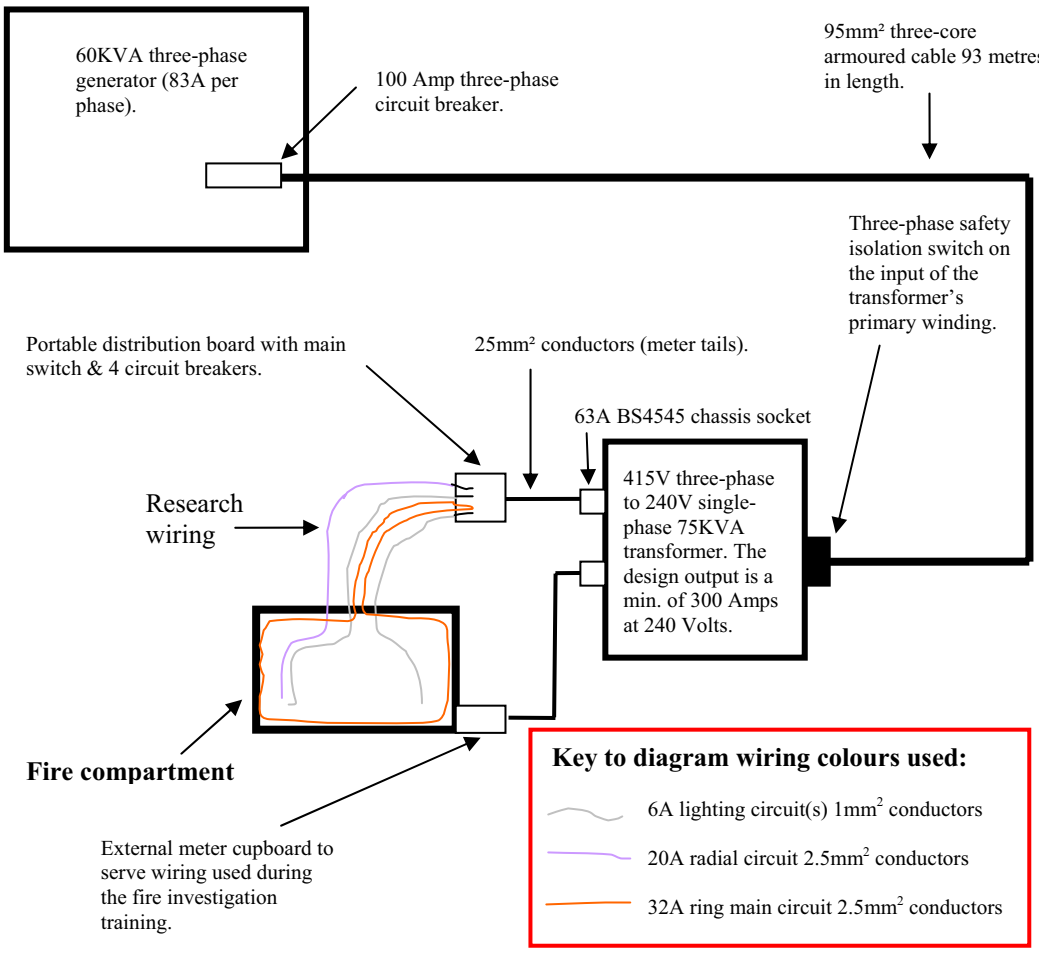

Diagram 47 – Revised transformer design.

The transformer was located in the middle of the site to limit the length of the connecting cable that linked the transformer to the portable distribution boards connected to each fire compartment. The transformer was delivered bolted to a timber pallet. A forklift was used to raise the transformer from the pallet and to install the supplied wheels that were bolted to the base framework. The 100 metre length of 95mm^2 four-core armoured cable was rolled off the 2 meter diameter drum that it was supplied on and connected to the generator and the transformer. Figure 48

shows the transformer in position at the site with the 95mm^2 armoured cable connected.

Figure 48– The 75kVA transformer installed on-site.

The transformer was manufactured by Carroll and Meynell Limited, Guisley Way, Durham Lane, Industrial Park, Eaglescliffe, Stockton-On-Tees, TS16 0RF. The connection at the generator and the transformer were made with glands designed for that particular cable size. These glands ensured the safe and secure fixing of the cable to the equipment casings. The conductor connections were made using special eye-bolts that were crimped onto the conductors using a hydraulic crimping machine with dyes specific for that conductor size. Particular care was made to ensure that all of the terminated conductors were of the correct length and that they were also routed to ensure that any vibration created by the generator end of the circuit would not cause mechanical damage to the conductor insulation. Figures 49 and 50 show the interior of the transformer enclosure and the connection unit on the side of the transformer used for the input armoured cable.

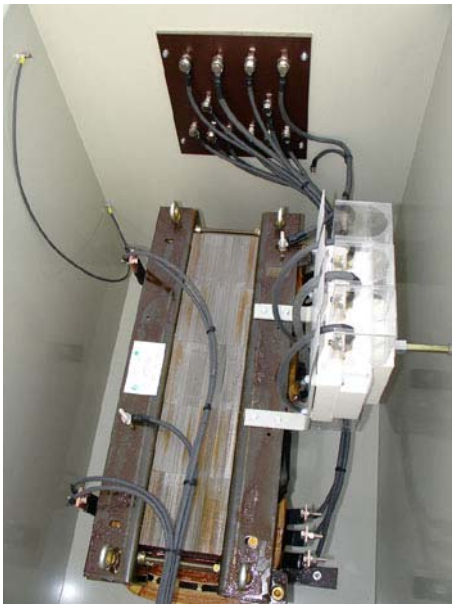

Figure 49 – The interior of the transformer.

Figure 50 – The alternate tapping connections in the cable intake enclosure to enable adjustment of the secondary winding voltage of +/- 5% of the design.

Testing on completion of the installation revealed a high insulation resistance test of 999 Mega Ohms. The voltage was measured at the generator end of the circuit once it was energised and readings of 409V to 411V phase to phase were obtained. Similar readings were obtained at the transformer input connection (with no transformer load). The earth loop impedance readings at the input terminals of the transformer were 0.23 Ohms. The insulation resistance test and the earth fault loop impedance test results were all well within the minimum requirements specified by the UK Institution of Electrical Engineers Requirements for Electrical Installations BS/EN 7671 [139].

Two connecting cables were constructed using 25mm^2 double PVC insulated single conductors and a 16mm^2 protective earth bonding single conductor. One cable was 12 metres in length and the second cable was 20 metres in length. These cables were wired to BS/EN 4343, 240V rated, waterproof plugs and sockets. These cables linked the output of the step-down transformer to the input of the portable distribution board located outside each compartment for the experiments. For testing purposes a short circuit fault was created on some final circuit conductors that were connected to the

portable distribution board that was in-turn plugged into to the secondary output of the step-down transformer. The resultant localised melting conductor damage was comparable to the damage observed at a conventional electrical installation.

2.3.6 Circuit protection

A six-way portable consumer unit enclosure manufactured by Hager was used to house the 4 circuit breakers that were required to provide overcurrent and short circuit protection to the circuits in the compartment fires used in the experiments. The enclosure was manufactured with fire retardant thermoplastic to a water ingress protection standard of IP55. A two-pole main switch was used within the enclosure rated at 100A and manufactured to the specification detailed in British/European Standard 60947-3 [140]. The purpose of the main two-pole switch was to replicate the conventional switching arrangements found in a domestic or light-commercial consumer unit and to allow the quick and safe isolation of the circuits in the experiments in the event of a problem. Figure 51 shows the portable consumer unit connected to the wiring for one of the experiments and table 3 details the protection devices used in the experimental set up.

Figure 51 – The portable distribution board constructed to IP 55 ingress protection.

Table 3 - detailing the circuit protection devices used in the experiments

Circuit number	Overcurrent rating	Type	Maximum fault current device can clear.	Voltage	BS/EN number
Circuit 1	32A	C	10,000A	230/400V	60898
Circuit 2	20A	C	10,000A	230/400V	60898
Circuit 3	6A	C	10,000A	230/400V	60898
Circuit 4	6A	C	10,000A	230/400V	60898

2.4 Data collection

2.4.1 Introduction

Data was collected from each test as follows:

- Photograph and video images were recorded for each compartment fire.
- The sequence and time of each circuit breaker's operation was documented.
- Data loggers were used to record the voltage, current and temperature within the compartments during the tests.
- Time/temperature data was collected for each compartment fire.

2.4.2 Circuit breaker operation

Each electrical circuit was numbered in a consistent manner for every test. The circuit breakers were also numbered and it was ensured that the correct circuit was connected to the correctly numbered circuit breaker in each case.

The data was collected with the assistance of the time keeper during the fires. The time keeper called out the time at 1 minute intervals throughout the fire development. This was to record the time in minutes from the ignition of the fire on to the sound track of the video used to record each test. The circuit operation time coincided with the observed flame impingement on the area of the circuits in the fire's early development. In the initial experiments the circuit breaker sequence established

which circuit faulted during the fire's development as the fire degraded and burnt through the cable's PVC plastic insulation.

2.4.3 Temperature data from the compartment fires

Thermocouples were placed at three levels within each fire compartment. The thermocouples are the solid stainless steel sheathed rod 'Type K' specification, with a diameter of 2mm and a rod length of 600mm, capable of reading temperatures between -60º to +1370ºC. The thermocouple rods were installed from the outside through holes in a side wall at floor, ceiling and midway between the floor and ceiling. The exact location on the wall varied depending upon the configuration of the furniture in the compartment and in order to expose the end tips of the thermocouples to the hot gases in the compartment.

The solid rod thermocouples were connected via thermocouple interconnecting cables to an 8 channel data logger model number TC-08, with an input of ±70mV (Pico Technology Limited). The data logger was connected to a laptop computer via a RS232 specification serial cable using the manufacturer's "PicoLog" data acquisition software. Figure 52 shows the type of data logger used to acquire the thermocouple data

Figure 52 – The Pico Technology TC-08 temperature data logger [141].

The acquired temperature data was imported into an Excel spreadsheet as raw comma-separated data. The spreadsheet was used to define the data labels and to

produce graphs displaying the temperatures at time intervals in seconds throughout the fire's development from ignition to suppression. It was possible by visually analyzing the time temperature graph to determine when the compartment reached flashover conditions which, for these experiments, was taken as the point when the mid-position and floor temperatures sharply increase to reach the ceiling temperature.

Figure 53 is an example of the time temperature graphs produced for each experiment. The sharp decline in all three temperatures at 240 seconds indicates the time that the fire crew were committed to suppress the fire.

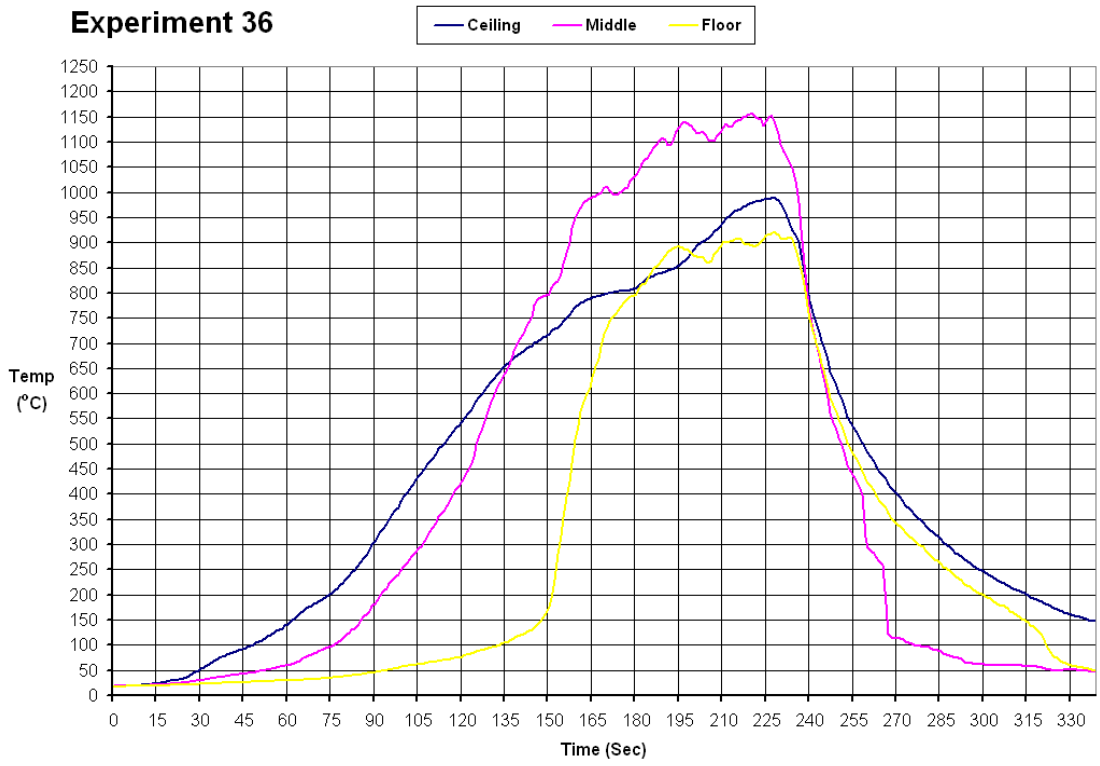

Figure 53 – Example of a time temperature graph from experiment 36 [142].

The time temperature graphs for each compartment fire experiment have been presented in volume 2.

2.4.4 Voltage and Current data collection

Two electrical data loggers were used during the practical experiments. These were a RMS Clamp-on Ammeter, model number CL600 and a RMS Voltage module, model number L260. Both data loggers are manufactured by Chauvin Arnoux Incorporated and distributed in the US by AMEC Instruments. The units were sourced in the US and shipped to the UK as the L260 logger was not available to purchase in the UK.

The CL600 clamp-on ammeter as shown in figure 63 has an appearance similar to a conventional clamp-on current reading meter, with the exception of a read-out display showing the amperage. The meter is clamped around either the live or the neutral conductor in the circuit where the electrical current is measured. For each of the experiment fires the logger was clamped around the live conductor at the point it enters the portable consumer unit. This ensured that the current flow was recorded for all of the four circuits in each experiment. It was therefore usually possible to acquire the fault current peak from the time of a fault until the circuit breaker detected the fault and operated to clear the fault. This time period was approximately 0.1 seconds.

The data was transferred via an RS232 serial cable to the Simple Logger software version 6.11 supplied with the data loggers. The dedicated data logger software produced graphs to insert into other software applications. The data was also capable of being imported into spreadsheet software for manipulation if required. The CL600 logger records the electrical current data at one second intervals with a range of 0 to 600A.

A limitation of this equipment was that it recorded at a sample rate on 1 second unless it detected an event. A review of the clamp meter data collected during the experiments suggests that it not record the peak fault current. The graphs in experiments 1 to 5 detail a fall in current at the point of the arcing events. These experiments had loads connected to the circuits and so the graphs detail the drop in current as the circuit breakers operate. The remaining experiments did not have loads connected to the circuits. Figure 54 details the clamp-on ammeter data logger.

Figure 54 – AMEC CL600 Clamp-on ammeter data logger [143].

The L260 voltage logger as indicated in figure 55 had a capability to measure voltages in the range of 0 to 600V RMS with a resolution of 4V when recording at its maximum capacity. The unit is a grey box 73 x 59 x 41mm in size and weighs 140g. It has two 4mm recessed individual sockets for the connection of specific live and neutral leads to the circuit. The logger recorded the voltage across the live and neutral conductors. The connection leads were directly wired into the portable consumer unit across the live and neutral terminals of the main switch. This method of connecting the L260 data logger was found to be a reliable method of connecting it to all of the circuits at once during the experiment burns days.

Figure 55 – AMEX L260 AC voltage data logger module [144].

The data was transferred from the unit's internal memory to a computer via "Simple Logger" software version 6.11 [145] provided by the manufacturer. Graphs were produced directly by the software and it was possible to annotate the graphs and modify the time limits of the data to produce additional graphs enabling a close-up view of a particular event. Figure 56 shows the voltage and current data loggers in use during an experiment.

Figure 56 – The voltage and current loggers connected to the research circuits.

2.5 Recovery of exhibits

2.5.1 Description of the method

All of the wiring was initially examined in-situ within each experimental compartment. Each circuit was examined individually starting with circuit one and finishing with circuit four. Gloved fingers were carefully run over the conductors to feel for any localised melting damage to the copper conductors in the form of molten copper beads, notches, conductors welded together, and localised areas of roughness to the conductors surface. Figure 57 shows the examination of the conductors following an experiment.

Figure 57 – Examination of the copper conductors post-compartment fire [146].

During this examination process when localised metallic damage was located, coloured cable-ties were fixed to the conductors either side of the damage. This procedure enabled the effective identification of the conductor damage whilst it was being documented. Figure 58 illustrates cable ties being used to identify arcing damage prior to packaging. The damaged conductor areas were indicated on the diagram drawn for each compartment fire. The distances of the arcing damage to other physical features of the compartment were measured and documented (for example the distance from the arcing to the nearest wall).

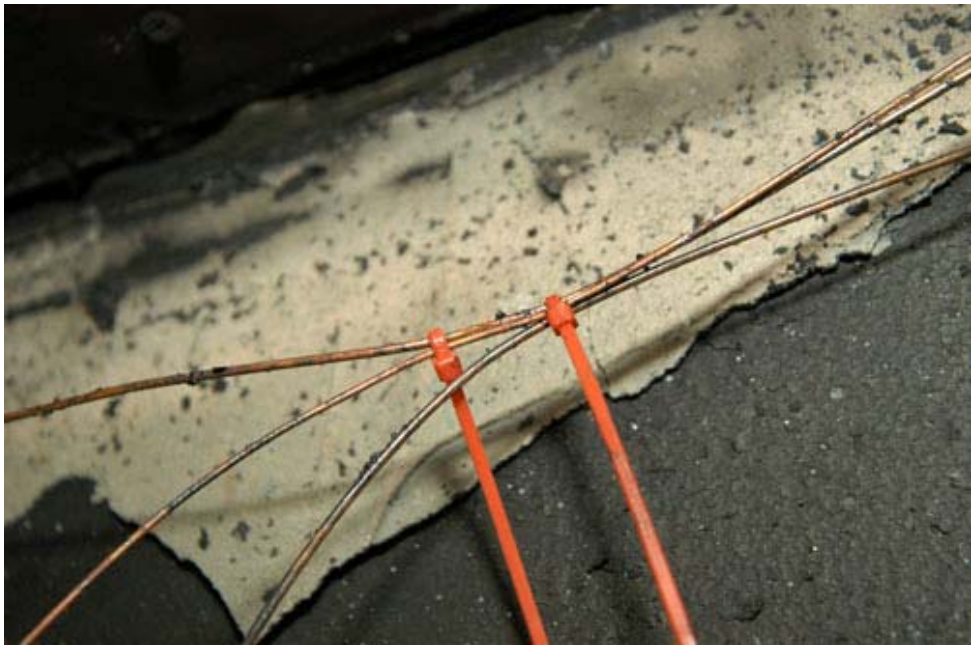

Figure 58 – Cable-ties used to identify arcing damage.

2.5.2 Packaging and numbering protocol

Once all of the documentation of arcing damage in relation to the circuits and the compartment was completed, the conductors were cut either side of the cable-ties with a standard side-cutter hand tool. The exhibit was immediately packaged into re-sealable polythene bags. Figure 58 shows a packaged exhibit from an experiment.

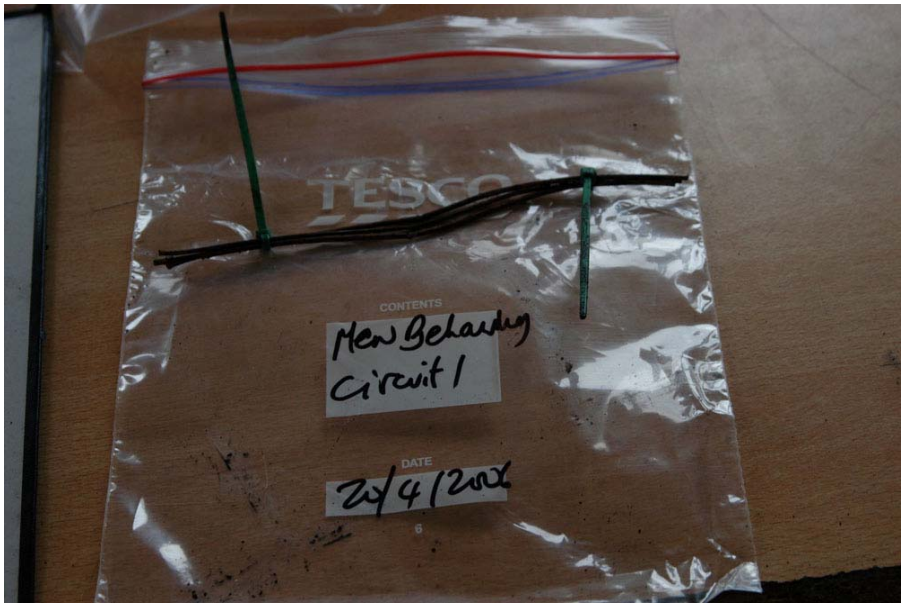

Figure 59 – A clear re-sealable polythene bag containing an exhibit.

Each compartment scenario name, date of the fire, and circuit number was marked on the bag with a permanent marker. The scenario names were later adjusted to letters (A-F). The exhibits from each compartment were put together into a larger clear polythene plastic bag to keep them together during their transportation. The exhibits were later numbered during the optical microscope examination process.

2.6 Example of an experiment

The large number of photographic images that were collected during the 39 experiments and the subsequent exhibit analysis has necessitated a separate volume to be produced for this thesis (Volume 2). This second volume describes all of the 39 experiments in detail, describing the experiment and displaying pre-fire, post-fire images from the experiment and images taken during the exhibit analysis.

Experiment 33 has been selected to include in volume 1 of this thesis as an example of the data collected for each test carried out.

Experiment 33

Figure 60 - “Scenario B”, 7 September 2006 [147]

Table 4 – MCB operation data

Circuit number	MCB operating time from ignition
4	1:31 minutes
1	1:47 minutes
3	1:26 minutes
2	1:26 minutes

The fire in experiment 33 (scenario B) originated in a refuse bin located in the rear left corner of the compartment. The compartment fire developed to flashover conditions within 5 minutes from the ignition time. The ceiling temperature reached 975° C with the floor thermocouple recording 725° C at this time.

Arcing was located on circuit 1 – 1350mm from the left wall and adjacent to the rear wall.
Arcing was located on circuits 2 & 3 – 1690mm from the left wall on the ceiling and 1000mm from the front wall.
Arcing was located on circuit 4 – 100mm from the left wall and 1000mm from the rear wall.

Figure 61 - The refuse bin alight [147].

Figure 62 - Early fire development taken from the doorway[147].

Pre-fire and post-fire photographs of experiment 33

Figure 63 - Pre-fire over-view photograph of experiment 33. The dashed white circle indicates the fire's area of origin, a refuse bin in the rear left corner of the compartment [147].

Figure 64 - Close-up view of the fire's area of origin – the green refuse bin located between the vacuum cleaner and the table [147].

Figure 65 - Post fire overview of the compartment [147].

Figure 66 - Post-fire view of the area of origin for this fire [147].

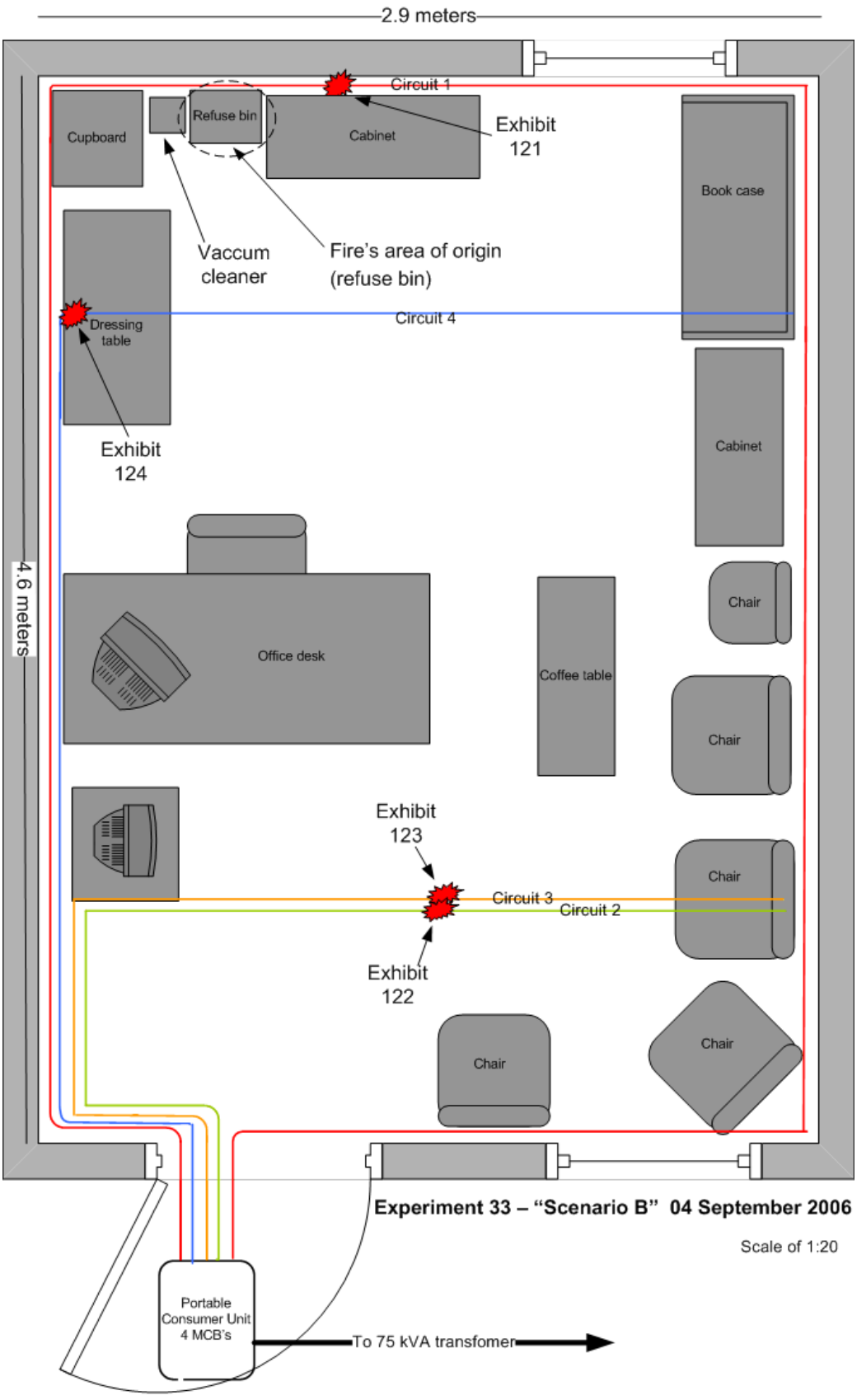

Figure 67 – plan of experiment 33 detailing the compartment layout and electrical circuit routes.

Microscope images for exhibit 121 – arcing category D (experiment 33)

Figure 68 - Microscope image of exhibit 121 (DSCN3177). The two 2.5mm^2 conductors (live & neutral) each have a notch with a bead within the notch.

Figure 69 - 20x magnification image of the bottom conductor displaying the notch (DSCN3179)

Figure 70 - 20x magnification image of the top conductor with its large bead above the conductor surface (DSCN3183).

Figure 71 - This is a view 180 degrees from the view to the left of this large example of a bead (DSCN3184).

Microscope images for exhibit 122 – arcing category D (experiment 33)

Figure 72 - One of the three conductors had arcing damage in the pattern of a notch. This circuit (2) may have faulted with circuit 3

Figure 73 - 15x magnification of the notch with a small bead at the notch left edge.

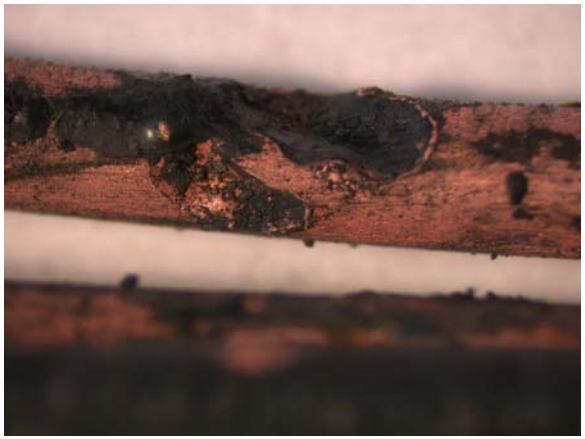

Figure 74 - An alternative view of the image top right of this page.

Figure 75 - 20x magnification. The image highlights the demarcation at the edge of the notch and what appeared to be a copper ridge at the edge.

Microscope and SEM images for exhibit 123 – arcing category B (experiment 33)

Figure 76 - Microscope image of exhibit 123. Two conductors had arcing damage. The lower conductor has a bead with a large hole.

Figure 77 - SEM image of the lower conductor. The demarcation is clearly defined at the notch edge.

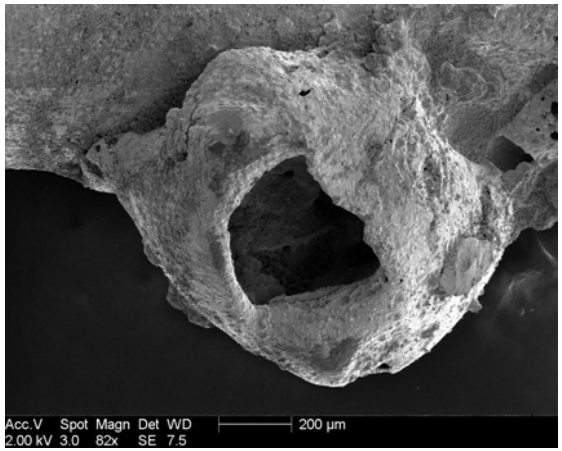

Figure 78 - SEM image at 82x magnification of the bead of the lower conductor.

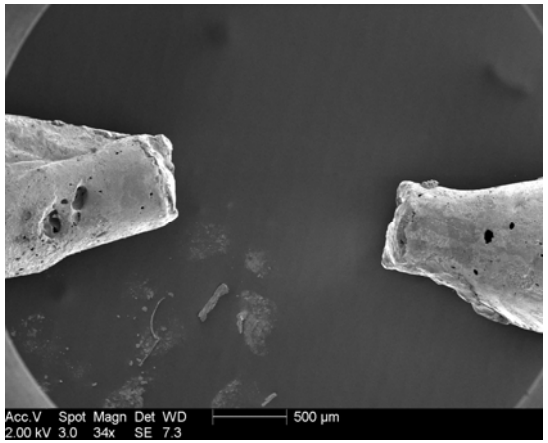

Figure 79 - SEM overview image of the severed ends of the upper conductor.

Confocal laser scanning microscope images for exhibit 123 – arcing category B (experiment 33)

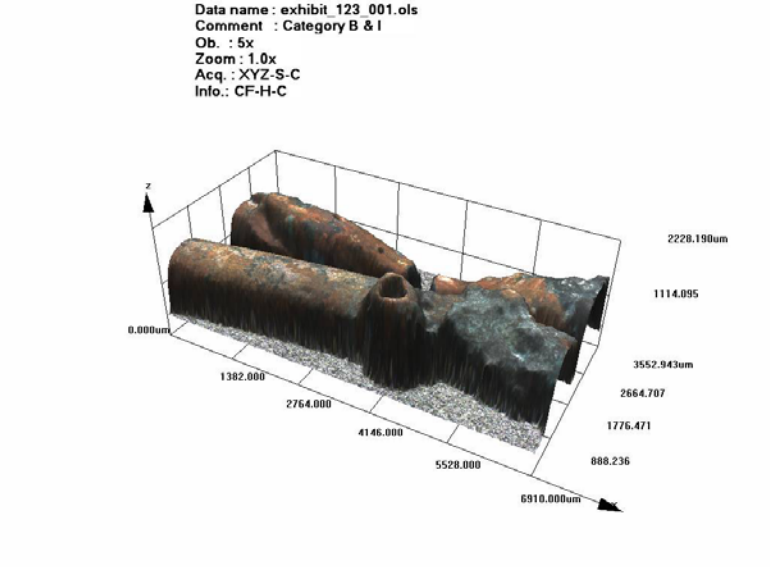

Figure 80 - LEXT image of exhibit 123 in real colour rendering mode. The scan has enabled the entire exhibit to be documented.

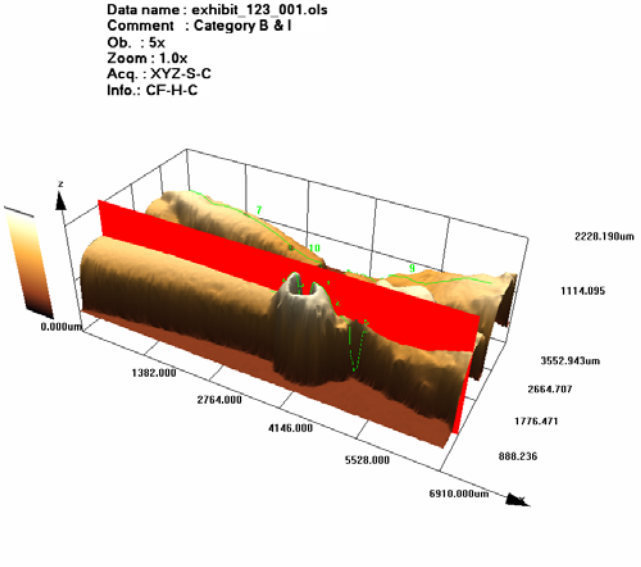

Figure 81 - A brown rendered view using the "slice tool" in the LEXT software to create a profile of the bead.

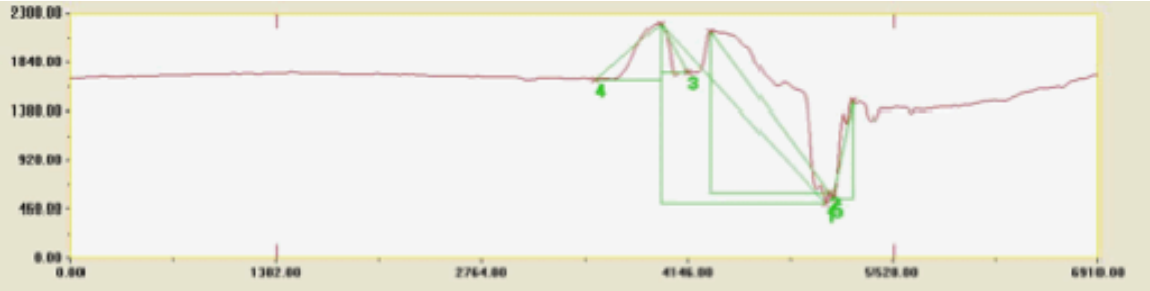

Figure 82 - Profile of the notch and bead using the "slice tool" as displayed in the image to the upper right (microns).

Microscope and SEM images for exhibit 124 – arcing category G (experiment 33)

Figure 83 - Microscope image of exhibit 124. The middle conductor has a notch with a large bead on the edge. The lower conductor has severed ends with a bead at the right severed end.

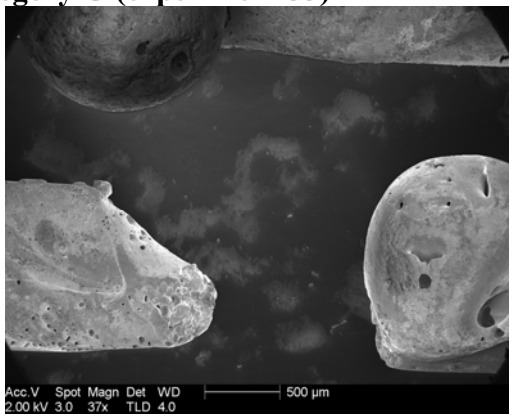

Figure 84 - SEM image of the lower conductor's severed ends.

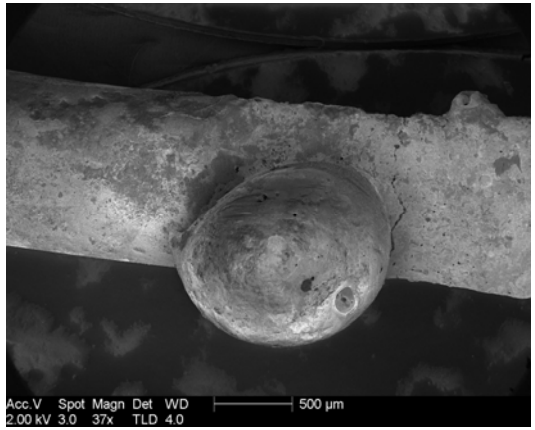

Figure 85 - SEM image of the notch with a bead on the surface. There was a crack in the conductor surface to the right of the bead.

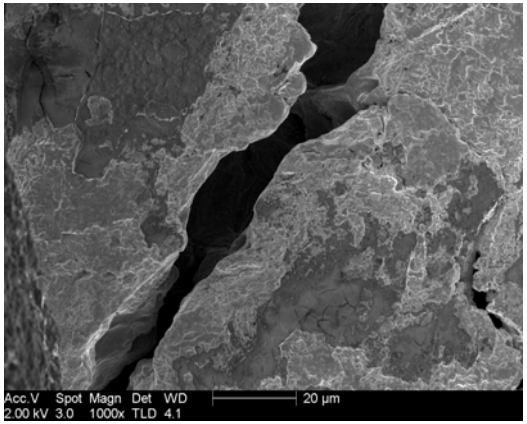

Figure 86 - SEM image at 1000x magnification documenting the crack in the conductor surface.

Confocal laser scanning microscope image for exhibit 124 – arcing category G (experiment 33)

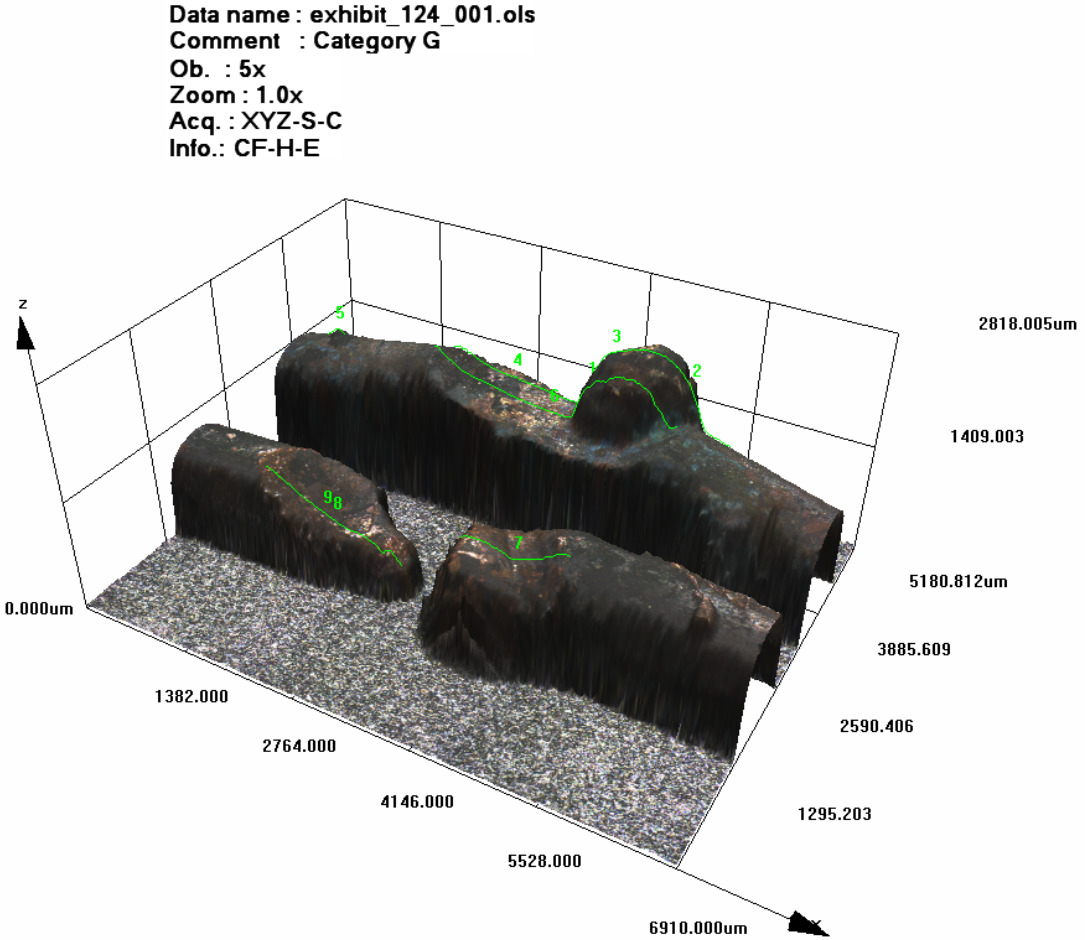

Figure 87 - LEXT image for exhibit 124. This equipment enabled the entire to be documented in detail (exhibit_124_with_measurements.jpg)

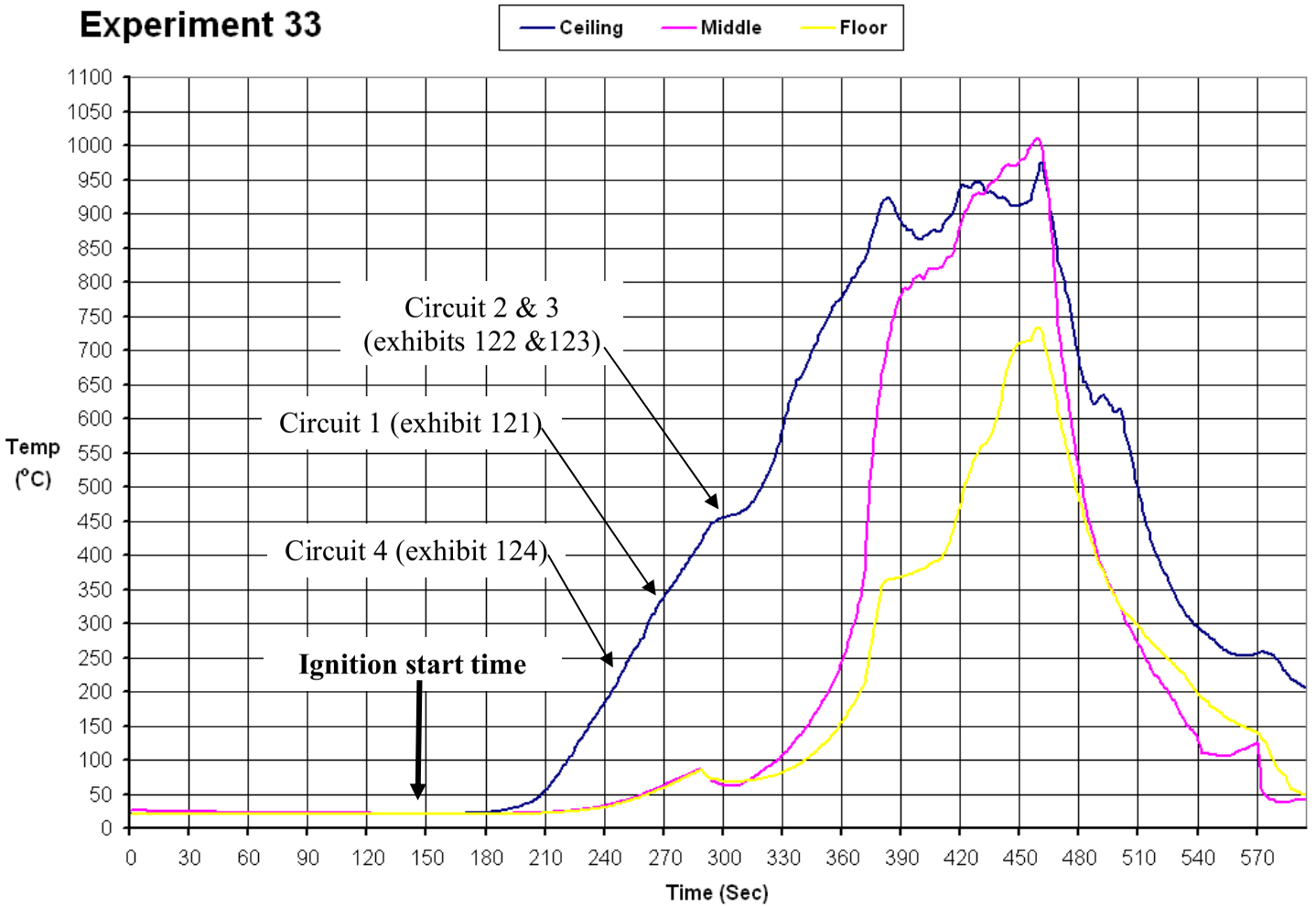

Figure 88 - Time temperature graph for experiment 33 (ignition start time adjusted following examination of video recording)

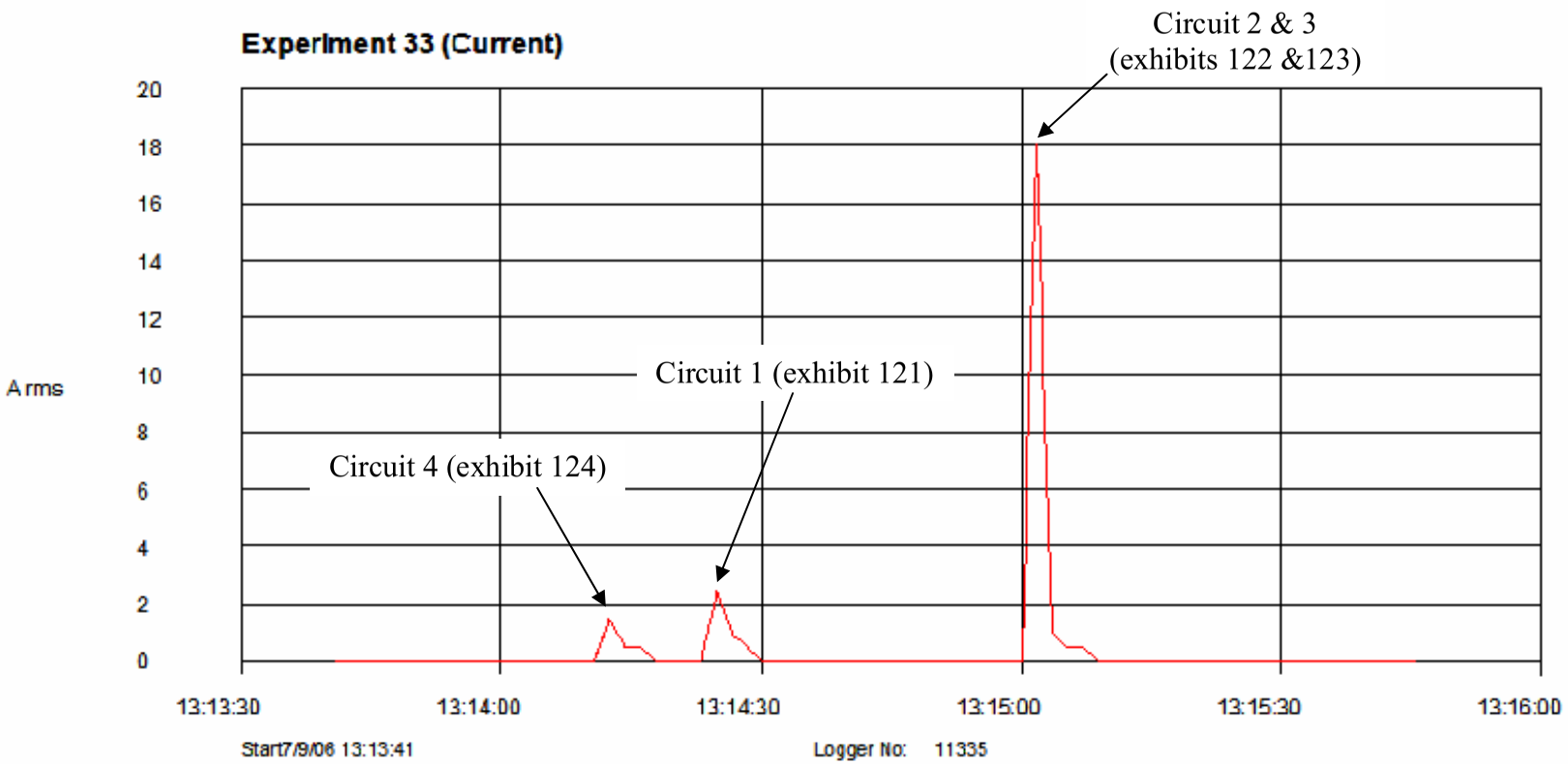

Figure 89 - Current (Amps) graph for experiment 33 detailing the operation of the circuit breakers and the fault current

Chapter 3 – Physical examination and categorisation of the electrical arcs derived from the practical fire experiments

3.1 Introduction

The exhibits recovered from the practical fire experiments were analysed in several stages. Cable ties were fixed to the conductors and the exhibit number was written on the cable tie to reduce the risk of mis-identification of the exhibits in the future.

Initially all of the exhibits were cleaned with a nylon brush and then examined with a low power optical microscope, documented with notes and photography. This examination allowed the arcing damage to be categorised based upon its morphology. Further analysis was undertaken on a reduced sample set of the exhibits within each category. This additional analysis was undertaken using a Scanning Electron Microscope (SEM), an additional SEM with wavelength dispersive spectroscopy (WDS) to generate element maps and a confocal laser scanning microscope. The results of these analyses are presented and discussed in chapter 4.

A three-dimensional analysis comparing the arcing locations to the fire's point of origin was also undertaken and this work is detailed in chapter 5.

3.1.1 Exhibit documentation

All of the localised metallic (arcing) damage to the conductor exhibits recovered from the experiments were examined and documented with a Nikon trinocular microscope model SMZ-10. A digital camera (Nikon Coolpix D995) was also attached to the microscope using a dedicated microscope coupler.

The camera settings were adjusted to enable the best possible image to be recorded. A total of 1763 images using the microscope were recorded. The images were recorded at the highest resolution possible for this model of camera (2048 by 1536

pixels at 300dpi dots per inch). One of the main problems encountered when using the digital camera attachment was a limited depth of field. The depth and height areas of the localised melting to the surface of the copper conductors was often quite pronounced and it was often not possible to get the entire area of interest into focus. Other microscopy techniques detailed in chapter 4 resolved these issues. Figure 90 is an image of the Nikon optical microscope used.

Figure 90 – Nikon microscope in use to document the exhibits.

A halogen desk lamp was found to be a very effective light source to illuminate the images while being examined with the microscope. In some cases where PVC insulation material remained fused to the conductors the light was reflected by the PVC causing the images to be overexposed when photographed. However this did not affect the categorisation of the arc damage.

3.1.2 Record keeping

During the examination process, each exhibit was carefully cleaned with a nylon brush to ensure that as much of the remaining burnt PVC plastic debris was removed to enable the copper metal conductor to be observed clearly. Care was taken to ensure that no damage occurred to the exhibit as a result of the cleaning process.

Each exhibit was given a unique reference number. The type of damage was documented for each conductor along with any unusual features and if appropriate, a recommendation for further analysis. The digital image file numbers created by the digital camera were also recorded for each exhibit. A fine tip pen was used to add the exhibit number to the microscope sample base to assist with the identification of the exhibits from the electronic images.

3.2 Categorisation of the arcing damage to the conductors

3.2.1 Methodology of the categorisation

A total of 141 exhibits were recovered from the experimental fires and it was not possible to analyse all of them using an SEM due to the availability of the equipment and funding constraints for the equipment time. It was therefore necessary to select a sub sample of the exhibits upon which to undertake the SEM analysis. In order to undertake this it was decided to categorise the types of localised metallic (arcing) damage.

All of the microscope images were reviewed at the end of the optical microscope examination process and a category was assigned to each exhibit. Several exhibits had localised melting patterns that fell into two separate categories. The dominant features were used to assign the main category for each exhibit and where appropriate a sub-category was also assigned. In total 9 categories of arcing were identified. The number of exhibits that fell within each of the individual categories varied and is presented in table 5. Categories A and G occurred least with each containing a total of 9 exhibits. The categories with the largest numbers of exhibits were B (38 exhibits) and D (45 exhibits).

A number of pre-fire arcs were also generated by connecting the live and neutral conductors of an energised system together. These samples were analysed as control pre-fire acing exemplars.

Table 5 - exhibit categories

Assigned category	Description	Exhibit identification numbers	Total
A	Arcing through charred plastic insulation "arcing through char"	001, 002, 007, 013, 043, 055, 088, 140, 142	9
B	Severed ends	003, 005, 011, 015, 024, 027, 029, 030, 031, 035, 043, 044, 049, 050, 061, 62a, 064, 065, 067, 067a, 076, 077, 082, 085, 089, 090, 091, 093, 096, 097, 104, 105, 106, 123, 130, 132, 134, 139a	38
C	Bead and notch	008, 020, 033, 037, 039, 056, 057, 066, 070, 071, 084, 094, 109	13
D	Bead within notch(s)	004, 018, 019, 021, 036, 038, 041, 042, 046, 048, 051, 054, 060, 062, 068, 078, 079, 082, 083, 086, 087, 092, 098, 100, 101, 102, 104, 105, 112, 115, 119, 121, 122, 123, 127, 128, 129, 131, 133, 136, 137, 138, 143, 144, 145	45
E	Two notches	009, 023, 025, 026, 032, 034, 040, 045, 058, 066, 072, 073, 081, 107, 110, 114, 125	17
F	One notch	006, 010, 022, 028, 035, 049, 052, 057a, 063, 064, 074, 095, 099, 103, 113, 120, 126	17
G	Bead(s) at conductor end	003, 012, 016, 024, 030, 061, 096, 111, 124	9
H	Conductors welded together	054, 058a, 069, 075, 090, 117, 118, 134, 135, 141	10
I	Bead on conductor surface.	053, 059, 077, 080, 081, 083, 099, 117, 120a, 139, 143	11
Pre-fire	Arcing created using the same equipment and conductors as used in the experiments	1, 2, 3, 4, 5, 6, 7, 8, 9, 10, 11, 12, 13, 14, 15, 16, 17	17

Five exhibit numbers (014, 017, 047, 108 and 116) had been allocated to exhibits where no localised melting damage was observed using the subsequent microscopic examination. It appeared that PVC debris attached to the conductors gave the appearance of localised melting during the scene examination following the experiments.

A subset of samples from each arcing category was chosen at random for subsequent SEM and Confocal Laser microscopy examination. The samples chosen were representative of each arcing category.

3.2.2 Explanation of each category and their variations

There were up to 5 individual conductor sections per exhibit, however, the majority of exhibits consisted of 1 or 2 conductors. All but one of the categorised localised metallic (arcing) damage were very similar to diagrams previously published and documented in fire investigation course handouts [61], photographs and diagrams published in NFPA 921 Guide to Fire and Explosion Investigation 2008 edition [68]. The microscopic images detailed in figures 91 to 100 are examples of each category.

Energised electrical conductors affected by a fire often create chaotic arcing damage due to the rapid localised melting and cooling of the copper metal at the site of the arcing. Variations of metallic damage to the conductors within each category have been observed in this series of experiments. A comparison of figures 95 and 96 illustrate the variation in notch size and shape. The molten copper bead on a conductor surface indicated in figure 99 is significantly smaller that bead on the surface shown in figure 100.

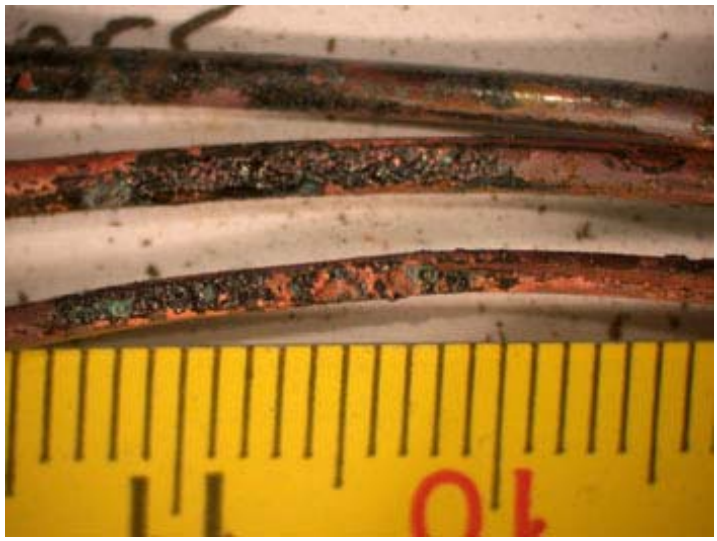

Figure 91 – Category A: Arcing through charred plastic PVC insulation (exhibit 055). The metallic damage is very shallow and there are numerous small beads and notches over a wide lateral area of the conductor surface.

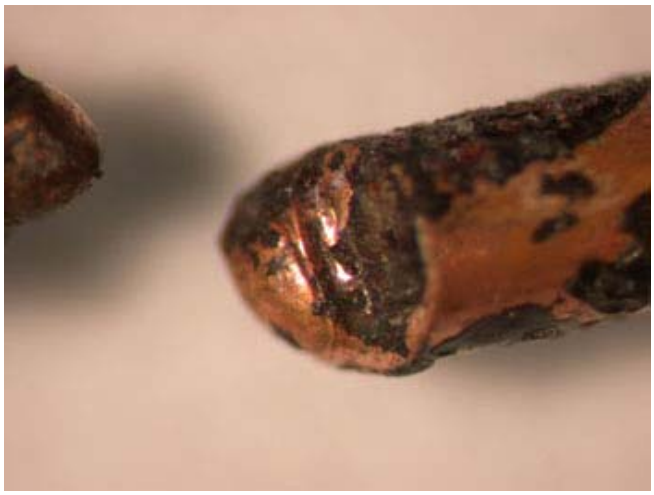

Figure 92 – Category B: Severed conductor ends (exhibit 067). The conductors were severed during the arcing event. Localised damage observed at each end often had a clear demarcation line between the localised metallic damage and un-damaged conductor.

Figure 93 - Category C: Bead and notch conductor damage (exhibit 066). A large notch and a smaller bead were found on the same conductor. Often the bead was located at the edge of the notch. The metallic damage is very localised with clear demarcation between damaged and undamaged conductor.

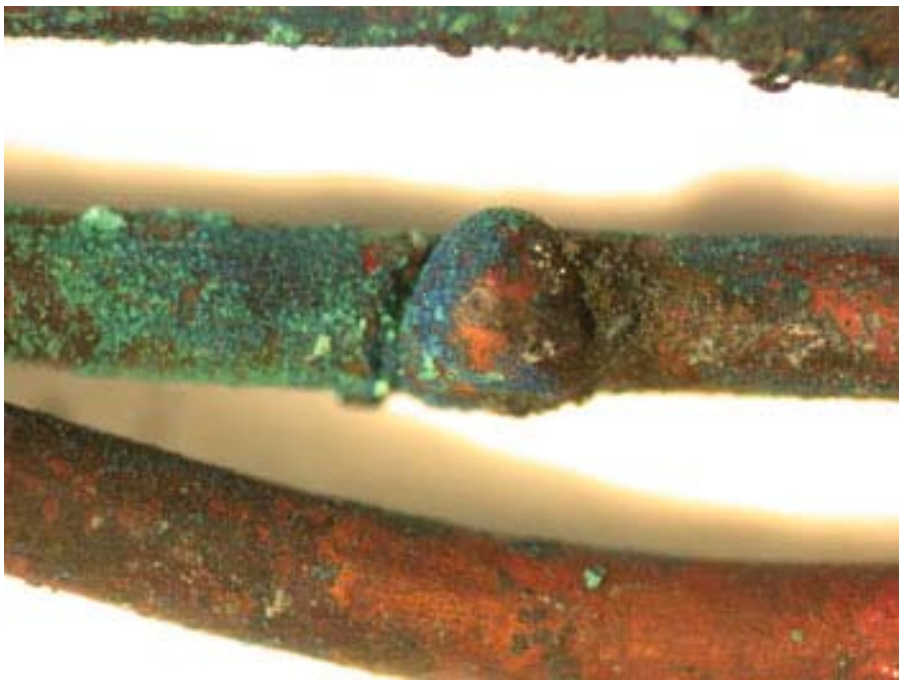

Figure 94 – Category D: Bead within notch (exhibit 068). A large bead was located within the notch on the conductor. The metallic damage is localised with a clear demarcation area at the edge of the notch and the undamaged conductor.

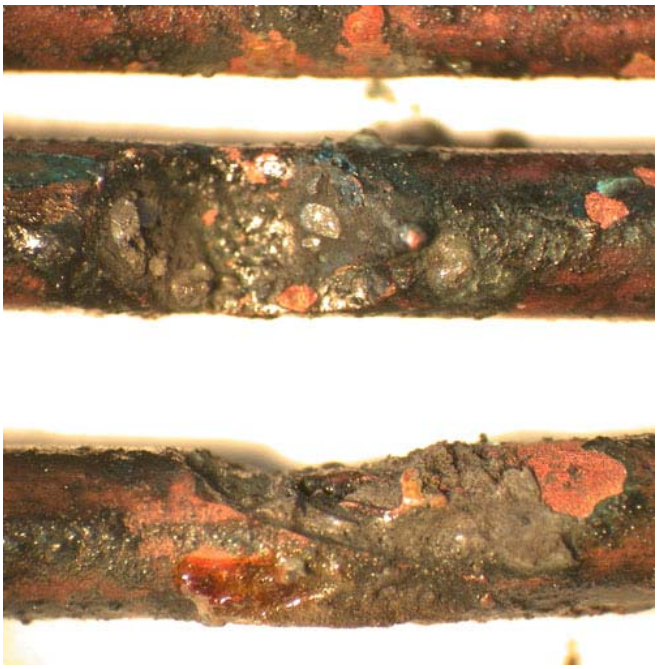

Figure 95 – Category E: Two notches (exhibit 009). A notch was found on each adjacent conductor of this exhibit that have faulted together. There was a clear demarcation area between the damaged and undamaged conductor with the metallic damage very localised.

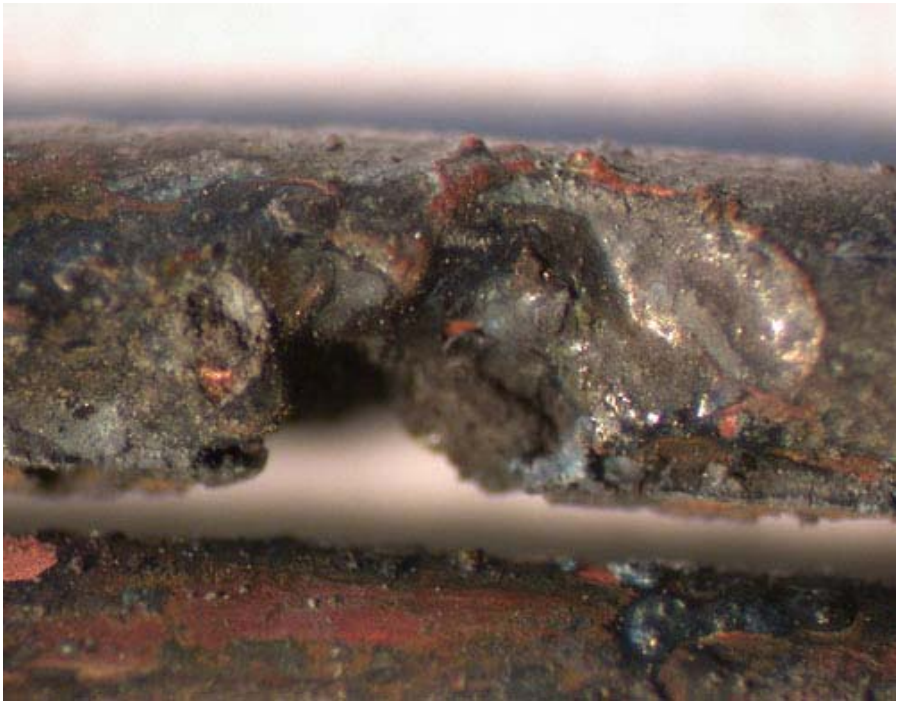

Figure 96 – Category F: One notch (exhibit 063). The damage on this exhibit was in the form of a large notch affecting only one conductor in the cable. This suggests that electron flow was established through another route (possibly via a fixing screw and an adjacent circuit).

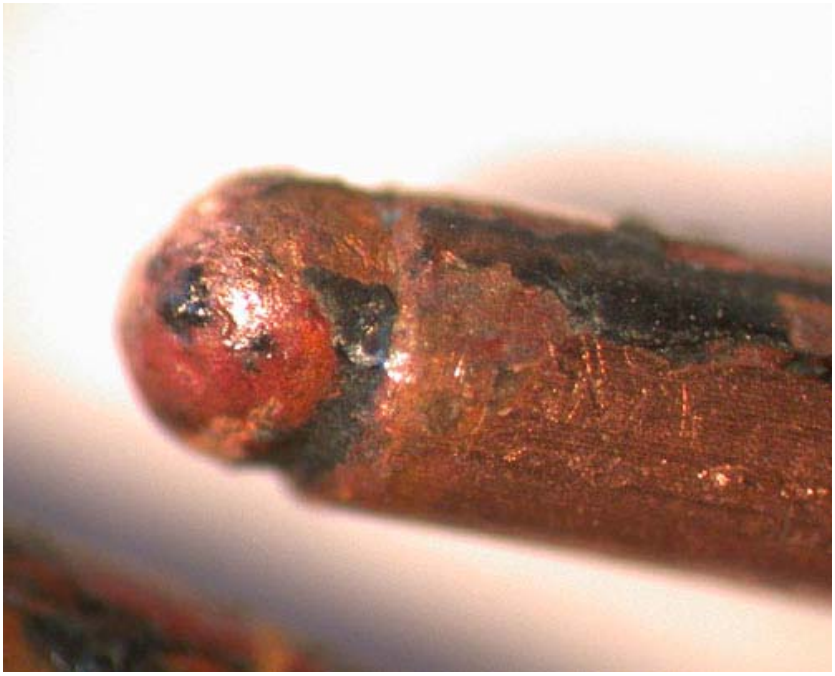

Figure 97 – Category G: Bead(s) at the conductor end (exhibit 012). This example was a bead at the end of a severed conductor with a clear demarcation area between the localised metallic damage and the undamaged conductor.

Figure 98 – Category H: Two conductors welded together (exhibit 054). In this example the conductors have welded themselves together during the arcing event in the short period of time that the copper metal was molten. The damage was localised and copper splatter from the arcing event was often observed adjacent to the weld.

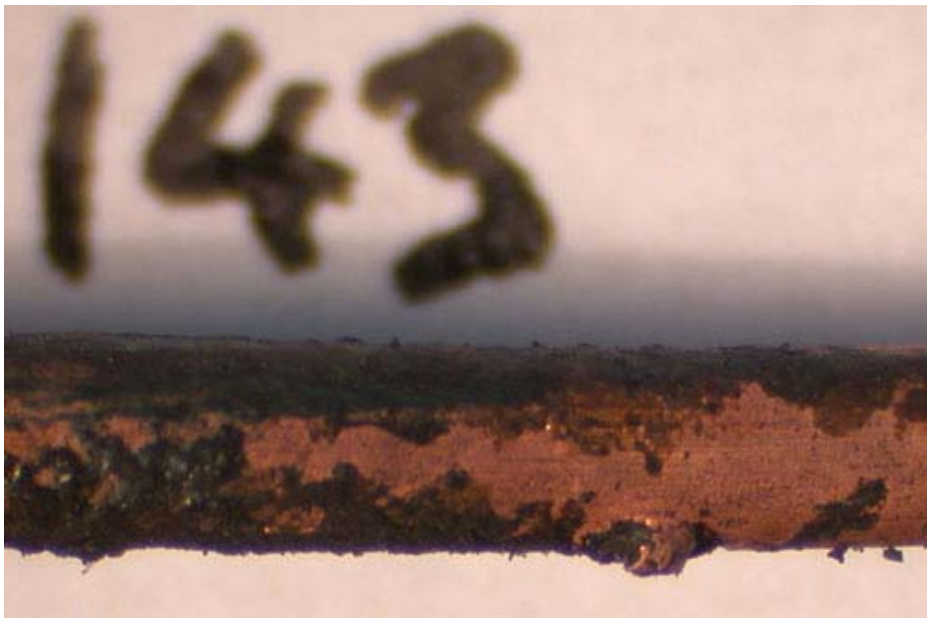

Figure 99 – Category I: Bead on conductor surface (exhibit 143). This example was the smallest surface bead observed in the series of experiments. The example of this category detailed in figure 109 is a bead that was substantially larger.

Figure 100 – A second example of Category I (exhibit 125) bead on conductor surface.

3.2.3 General observations

The metallic damage to the conductors in the form of localised melting (arcing) in the experiments was very varied. Four different methods of electrical conduction between the conductors appeared to be possible:

1. The softening of the PVC insulation allowing the energised conductors to touch each other.
2. The carbonised PVC insulation matrix allowing current flow between energised and non-energised conductors followed by the bare copper conductors to touch each other.
3. The heat conducting through the metal fixing screws softening the PVC insulation and enabling the conductors to come into contact with the metal fixing screw to enable faulting.
4. The pyrolysis of the PVC insulation causing a reduction in its insulation properties allowing current flow until it becomes a carbonised semi-conducting material.

The different categories of arcing damage revealed by microscopic examination illustrated the variety of arcs previously presented in the literature apart from category A. Exhibits with arcing damage that were located away from any cable fixings suggesting that either the conductors had come together as a result of the PVC insulation softening in the early stages of the experimental fires and the conductors coming into contact, or the carbonised PVC insulation detaching from the cable allowing the conductors to come into contact, or electron flow between the conductors through the carbonised PVC matrix had occurred.

A number of localised melting events occurred at the position of fixing screws that were used to support the wiring and to fix it to the compartment internal lining surface. The screws were fixed at 300 to 400mm spaces along the length of the circuit. The heat of the fire conducted through the steel screws and this appeared to melt the PVC plastic insulation more rapidly in the location of the screws. This appears to have allowed the exposed copper conductors to electrically fault allowing electron flow between them at the point of the fixing screw. This often resulted in the

copper conductors becoming welded to each other, welded to the screw, or severed at the point of the fixing screw. A high number of the element analysis undertaken revealed iron and zinc residues in the arcing damage suggesting that the cable fixing screws were playing a significant role by interacting with the conductors. Full contact arcing between the conductors either directly or via the cable fixing screws appeared to increase the probability of welding or severing of the conductors.

The fault current recorded during the experiments was very varied and ranged from 0.5 to 67 Amps. On occasions the recorded fault current was below the rating of the circuit breaker protecting a circuit. Assuming that the fault current recorded by the clamp ammeter data logger is fully representative of the total current flow per event (P= VI) proportional to the conductors contact area that was often approximately 1mm^2. For example, a fault current of 10 Amps at 240 volts with produce 2,400 Watts of energy at the arcing area. This large amount of energy through a small area would expect very high temperatures capable of melting the artefacts. A limitation of the clamp ammeter data logger was that it recorded at 1 second intervals unless it detected activity. Considering the short duration of the arcing events it is likely that the fault currents in the circuits during the arcing events were considerably higher than recorded with the data logger.

3.3 The visible differences of 'short circuit' and 'arcing through char' (category A) localised melting

3.3.1 Introduction

In the early stages of the experimental work, patterns of localised melting (Category A) were located on several circuits that did not conform to the arcing damage patterns documented in the literature [31, 32, 36, 60, 68, 82, 96, 100, 102, 109, 120, 122, 124]. These different patterns of localised melting were compared to other collected exhibits and it was discovered that localised melting appeared to be examples of "arcing through char". This effect appears to occur when there has been electron flow through the carbonised PVC insulation during the fire's development. This type of arcing event is repeated due to a limited fault current, resulting from the

resistance properties of the charred PVC cable sheath and conductor insulation. This electrical resistance effect delays the operation of the circuit breaker leading to metallic patterns on the surface of the conductor over a much larger lateral surface area than normal.

An extensive literature review revealed that this arcing pattern had not been illustrated or documented in any of the texts reviewed [13, 20, 30-32, 35-37, 49, 56, 60, 61, 68, 96, 101, 102, 104, 106, 109, 112, 121, 122, 125, 130, 135, 148-152]. As such this category of arc will be discussed in detail in this section and compared with more common arcing damage observed in the practical tests and discussed in the relevant literature.

3.3.2 Observed physical differences

The category A "arcing through char" localised metallic (arcing) damage was very shallow below the surface of the conductor. It also had a wide lateral area of damage along the length of the conductor. In some cases the measured damage extended over a width of 14mm although the conductor diameter was 1mm. Figure 101 illustrates this type of shallow surface damage to the conductor. The physical appearance consists of multiple indentations and small beads on the conductor surface.

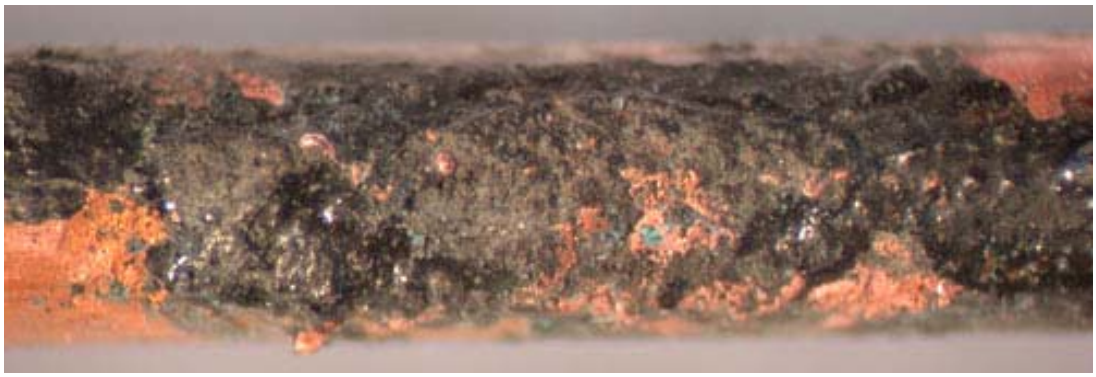

Figure 101 – An optical microscope image of arcing through char conductor damage (exhibit 088).

Figure 102 – An optical microscope image detailing the ‘short circuit’ fault at a fixing screw location (exhibit 081 – arcing category E).

The comparison of figures 101 and 102 details the significant difference between the lateral conductor surface areas and the size of the beading observed within the two categories. It was observed that the surface depth of the conductor damage of the category A exhibits was considerably less than the majority of the other exhibits recovered from the experiments.

Experiments 36 to 39 were wired with ceiling fixings that consisted of separate timber blocks rather than fixed directly with fixing screws. In these cases two 25mm diameter holes were drilled through each timber block to support the cables. The timber blocks were fixed to the ceilings with appropriate screws and the cable was pulled through the blocks, in a similar method to installing cables in timber floor joists. A total of 13 exhibits were recovered from these four experiment scenes. Three of the exhibits displayed similar localised metallic damage to the example presented in figure 101. Since the cables had not been fixed to the ceiling with screws, the potential influence of electrical conduction through the metallic screws can be discounted as the cause of this type of damage. This corroborates the previous hypothesis that the wide and shallow lateral localised melting damage observed occurs as a result of arcing through the carbonised PVC cable insulation whilst being attacked by fire.

The PVC plastic changes its electrical properties when it changes its physical state to carbon in a fire. It becomes a semi-conductor with an increased electrical resistance. This increased electrical resistance limits the current flow between the energised conductors. This effect appears to have delayed the operation of the circuit breaker protecting the circuits. Electrical arcing occurred when a sufficient fault current flowed in the circuit, or the conductors physically touched each other as the charred PVC insulation matrix deteriorated in the fire.

3.4 The features of arcing and gross melting damage to conductors

The gross melting effects experienced by copper conductors that are exposed to temperatures exceeding the melting temperature of copper (1083º C [98]) is detailed by Ettling [35]. He described the flow and distortion of the metal experiencing these high temperatures that are not frequently encountered in compartment fires where the ceiling temperature does not generally exceed 900ºC [100, 153]. Figure 103 details gross melting damage to copper conductors that was detailed by Ettling. DeHaan also presents similar images to describe gross melting damage to conductors [154]. Figure 104 also details gross melting to a conductor that features strands fused together over a large area and large beads with smooth flowing patterns at the bead edge.

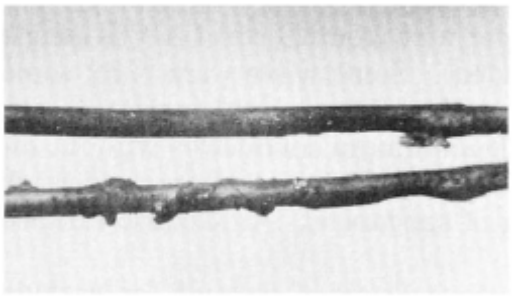

Figure 103 – Gross melting damage to electrical conductors caused by exposure to high overall temperatures [35]

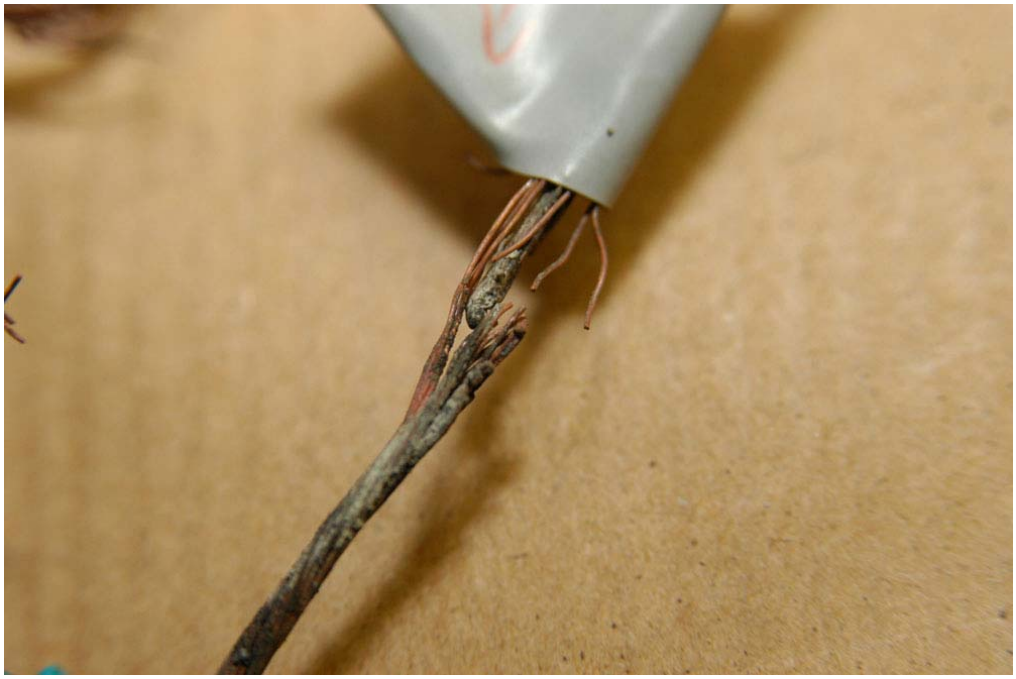

Figure 104 – Gross melting to electrical conductors caused by exposure to high overall temperatures [155]

Electrical arcing damage is formed following a discharge carried largely by electrons travelling from the negative to the positive electrode, but also in part by positive ions travelling in the opposite direction. The impact of the ions produces significant localised heat in the electrodes and in an arc in air at normal pressure, the arc centre reaches a temperature of around 10,000K (9726° C) [81]. The temperature of the electrodes is limited by the boiling temperature of the electrode material, for copper this is 2562° C [82, 83]. The temperatures are sufficiently high for the plasma gas to be electrically conductive away from the luminous region [156].

The very high localised heating effect generates a clear demarcation area between the localised melting and the undamaged conductor surface. Figure 105 details the demarcation areas on the two conductors of exhibit 112. A separate indicator that is observable with an optical microscope is the localised melting of the arcing damage interrupting the striation marks that are created when the conductor was originally manufactured.

Figure 105 – microscope image of exhibit 112 that details the demarcation area between the highly localised arcing damage and the undamaged conductor

3.5 Statistical analysis of the experimental data

3.5.1 Introduction to the data analysis

Potential correlations between the variables within the experimental tests carried out were explored using the software SPSS (Statistical Package for Social Sciences version 17.0 - SPSS Inc. Chicago, IL. USA). The statistical exploration of the data was carried out to investigate whether the type of scenario had any correlation with the category of arcing damage observed and what, if any, correlations existed between the arcing category and the other measured variables (temperature, current, distance from the point(s) of origin, time since ignition and circuit fault sequence).

The data collected during the experiments was initially entered into a spreadsheet software package (Microsoft Excel 2003). The exhibit number and arcing category data were also added to the spreadsheet following the exhibit categorisation process. A summary of all of the data recorded for each exhibit is presented in table 6. In

addition to the data presented in this table 13 of the 39 experiments were accelerated with an ignitable liquid (experiments number: 2, 5, 12, 14, 18-21, 25, 28, 32, 36). A visual evaluation of the data suggested that the majority of arcing occurred between 200 and 600 °C.

Table 6 - Data collected from experiments 1 - 39

Experiment description	Circuit number	Exhibit number	Arcing category	Distance probability	Temperature °C	Current (Amps)	MCB sequence	Time from ignition (s)
Experiment 1 – Scenario A	1	001	A	0.99	440	25	1	130
Cable fixing: Metal screws	2	002	A	1	600	28	4	203
Building type: Portocabin	3	003	B	1	420		3	170
Flashover: Yes	4	004	D	0.78	450	24.5	2	140
Experiment 2 – Scenario B	1				300	9	1	105
Cable fixing: Metal screws	2				325		3	120
Building type: Portocabin	3				300	9	1	105
Flashover: Yes	4				275	67	2	95
Experiment 3 – Scenario F	1	006	F		325	33	2	210
Cable fixing: Metal screws	2	007	A		575	8	4	251
Building type: Portocabin	3				450	14	3	230
Flashover: Yes	4	008	C		280	30	1	200
Experiment 4 – Scenario E	1	005	B		460	8	2	140
Cable fixing: Metal screws	2				510	9	3	153
Building type: Portocabin	3				350	27	1	100
Flashover: Yes	4				510	8	3	153
Experiment 5 – Scenario F	1	009	E		180	25	1	240
Cable fixing: Metal screws	2	010	F		190	8	2	642
Building type: Portocabin	3	011	B		190	8	2	642
Flashover: No	4	012	G		330	14	3	693
Experiment 6 – Scenario E	1	013	A		625	25	2	110
Cable fixing: Metal screws	2	014			675	12	3	134
Building type: Portocabin	3	015	B		575	26	1	105
Flashover: Yes	4	016	G		625	25	2	110

Table 6 - Data collected from experiments 1 – 39 continued

Experiment description	Circuit number	Exhibit number	Arcing category	Distance probability	Temperature °C	Current (Amps)	MCB sequence	Time from ignition (s)
Experiment 7 – Scenario C	1	017		0.80	175	27	1	240
Cable fixing: Metal screws	2	018	D	0.97	450	2	3	360
Building type: Portocabin	3	019	D	0.97	475	26	4	368
Flashover: No	4	020	C	0.99	210	9	2	258
Experiment 8 – Scenario A	1	021	D	0.98	125	25	1	128
Cable fixing: Metal screws	2	022	F	0.98	450	24	4	223
Building type: Portocabin	3	023	E	1	450	3	3	221
Flashover: No	4	024	B	0.99	250	8	2	155
Experiment 9 – Scenario D	1	025	E		150	6	1	69
Cable fixing: Metal screws	2	026	E		200	3	2	79
Building type: Concrete block	3	027	B		240	28	3	85
Flashover: Yes	4	028	F		390	4	4	99
Experiment 10 – Scenario C	1	029	B	0.94	165	37.5	2	173
Cable fixing: Metal screws	2				370	14	3	251
Building type: Portocabin	3	030	B	0.96	380	3	4	258
Flashover: No	4	031	B	0.88	165	30	1	162
Experiment 11 – Scenario E	1	032	E		460	2.5	3	118
Cable fixing: Metal screws	2	033	C		380	3	2	109
Building type: Portocabin	3	034	E		225	2.5	1	77
Flashover: Yes	4	035	F		530	16	4	133
Experiment 12 – Scenario F	1	036	D		95	27	1	73
Cable fixing: Metal screws	2	037	C		425	46	2	170
Building type: Portocabin	3	038	D		425	46	3	171
Flashover: Yes	4	039	C		95	27	1	73

Table 6 - Data collected from experiments 1 – 39 continued

Experiment description	Circuit number	Exhibit number	Arcing category	Distance probability	Temperature ºC	Current (Amps)	MCB sequence	Time from ignition (s)
Experiment 13 – Scenario E	1	040	E		330	9	1	144
Cable fixing: Metal screws	2	041	D		450	0.5	4	190
Building type: Portocabin	3	042	D		430	0.5	3	183
Flashover: No	4	043	A		400	0.5	2	168
Experiment 14 – Scenario D	1	044	B		260	0.5	1	62
Cable fixing: Metal screws	2	045	E		580	1	3	90
Building type: Concrete block	3	046	D		400	0.5	2	77
Flashover: Yes	4	047			690	2	4	98
Experiment 15 – Scenario B	1				350	1	3	275
Cable fixing: Metal screws	2	048	D		260	1	2	255
Building type: Concrete block	3	049	B		190	0.5	1	240
Flashover: Yes	4	050	B		190	0.5	1	240
Experiment 16 – Scenario C	1	051	D	0.97	280	27	2	210
Cable fixing: Metal screws	2	052	F	1	310	2	4	233
Building type: Concrete block	3	053	I	1	310	2	3	230
Flashover: Yes	4	054	H	1	200	2	1	150
Experiment 17 – Scenario A	1	055	A	1	440	1	2	140
Cable fixing: Metal screws	2	056	C	1	450	3	3	150
Building type: Concrete block	3	057	C					
Flashover: Yes	3	057A	F	0.97	450	3	4	151
	4	058	E					
	4	058A	H	0.98	400	5	1	128

Table 6 - Data collected from experiments 1 – 39 continued

Experiment description	Circuit number	Exhibit number	Arcing category	Distance probability	Temperature ºC	Current (Amps)	MCB sequence	Time from ignition (s)
Experiment 18 – Scenario D	1	059	I		300	1.5	2	63
Cable fixing: Metal screws	2	060	D		520	1	3	71
Building type: Concrete block	3	061	B		550	4	4	76
Flashover: Yes	4	062	D					
	4	062A	B		235	17.5	1	54
Experiment 19 – Scenario B	1				720	4	2	322
Cable fixing: Metal screws	2	063	F		720	4	2	322
Building type: Concrete block	3	064	B		720	4	2	322
Flashover: Yes	4	065	B		280	1.5	1	288
Experiment 20 – Scenario D	1	066	E		325	46	2	133
Cable fixing: Metal screws	2				590	25	4	180
Building type: Concrete block	3	067	B					
Flashover: Yes	3	067A	B		350	3	3	156
	4	068	D		250	2	1	92
Experiment 21 – Scenario B	1	069	H	0.92	320	19.5	2	599
Cable fixing: Metal screws	2	070	C	0.91	475	1.5	4	624
Building type: Concrete block	3	071	C	0.97	450	1.5	3	615
Flashover: Yes	4	072	E	0.97	230	19.5	1	585
Experiment 22 – Scenario A	1	073	E	0.98	420	1	1	180
Cable fixing: Metal screws	2	074	F					
Building type: Concrete block	2	075	H	0.96	500	1	3	230
Flashover: Yes	3	076	B	0.96	545	3.5	2	210
	4	077	B	1	420	1	1	180

Table 6 - Data collected from experiments 1 – 39 continued

Experiment description	Circuit number	Exhibit number	Arcing category	Distance probability	Temperature °C	Current (Amps)	MCB sequence	Time from ignition (s)
Experiment 23 – Scenario C	1	078	D	1	350	1.5	2	215
Cable fixing: Metal screws	2	079	D	1	410	1	3	240
Building type: Concrete block	3	080	I	0.98	425	4	4	249
Flashover: Yes	4	081	E	1	150	1.5	1	155
Experiment 24 – Scenario B	1	082	B	1	220	7	2	297
Cable fixing: Metal screws	2	083	D					
Building type: Concrete block	2	084	C	0.94	390	7	4	334
Flashover: Yes	3	085	B					
	3	086	D	0.94	390	7	3	332
	4	087	D	0.93	144	1	1	278
Experiment 25 – Scenario D	1	088	A		380	21	2	74
Cable fixing: Metal screws	2	089	B		400	3.8	3	80
Building type: Concrete block	3	090	H		380	21	2	74
Flashover: Yes	4	091	B		350	1.5	1	58
Experiment 26 – Scenario A	1	092	D	0.94	80	3	1	93
Cable fixing: Metal screws	2				500	21	4	122
Building type: Concrete block	3	093	B	0.77	480	8.5	3	120
Flashover: Yes	4	094	C	0.96	230	1	2	100
Experiment 27 – Scenario C	1				460	1.5	4	358
Cable fixing: Metal screws	2	095	F	1	460	9	3	355
Building type: Concrete block	3	096	B	1	380	2	2	339
Flashover: Yes	4	097	B	1	280	23	1	316
Experiment 28 – Scenario D	1	098	D		170	1.5	2	73
Cable fixing: Metal screws	2	099	F		250	1	4	128
Building type: Concrete block	3	100	D		240	1	3	120
Flashover: Yes	4	101	D		130	1.5	1	67

Table 6 - Data collected from experiments 1 – 39 continued								
Experiment description	**Circuit number**	**Exhibit number**	**Arcing category**	**Distance probability**	**Temperature °C**	**Current (Amps)**	**MCB sequence**	**Time from ignition (s)**
Experiment 29 – Scenario B	1	102	D	0.96	270	35	2	549
Cable fixing: Metal screws	2	103	F	1	475	4	4	577
Building type: Concrete block	3	104	B					
Flashover: Yes	3	105	B	0.98	475	4	3	576
	4	106	B	0.98	200	3	1	488
Experiment 30 – Scenario C	1	107	E	0.95	480	13.5	2	246
Cable fixing: Metal screws	2	108						
Building type: Concrete block	2	109	C	0.99	700	2	4	266
Flashover: No	3	110	E	0.99	520	15	3	255
	4	111	G	0.95	220	2	1	204
Experiment 31 – Scenario A	1	112	D	0.96	390	5	1	97
Cable fixing: Metal screws	2	113	F	1	625	2.5	3	112
Building type: Concrete block	3	114	E					
Flashover: Yes	3	115	D	1	625	2.5	3	112
	4	116		1	390	5	2	98
Experiment 32 – Scenario D	1	117	H		340	2	3	80
Cable fixing: Metal screws	2	118	H		325	6.5	2	76
Building type: Concrete block	3	119	D		325	6.5	2	76
Flashover: Yes	4	120	F					
	4	120A	I	0.97	250	1.5	1	60
Experiment 33 – Scenario B	1	121	D	0.95	320	2.5	2	107
Cable fixing: Metal screws	2	122	D	097	460	18	3	146
Building type: Concrete block	3	123	B	0.97	460	18	3	146
Flashover: Yes	4	124	G	0.95	225	1.75	1	91

Table 6 - Data collected from experiments 1 – 39 continued

Experiment description	Circuit number	Exhibit number	Arcing category	Distance probability	Temperature °C	Current (Amps)	MCB sequence	Time from ignition (s)
Experiment 34 – Scenario A	1	125	E	0.99	650	2.5	2	129
Cable fixing: Metal screws	2	126	F	0.99	680	2	3	140
Building type: Concrete block	3	127	D	1	680	2	3	140
Flashover: Yes	4	128	D	0.92	575	1.5	1	120
Experiment 35 – Scenario C	1				350	8	2	257
Cable fixing: Metal screws	2	129	D	0.96	380	1	3	263
Building type: Concrete block	3	130	B	0.99	350	8	2	257
Flashover: No	4	131	D					
	4	132	B	0.98	150	1.5	1	230
Experiment 36 – Scenario D	1	133	D		250	0.4	2	84
Cable fixing: Wood blocks	2				475	1	3	111
Building type: Concrete block	3	134	B		475	1	3	111
Flashover: Yes	4	135	H		200	1	1	73
Experiment 37 – Scenario B	1	136	D	0.80	400	5	2	156
Cable fixing: Wood blocks	2				540	30	3	174
Building type: Concrete block	3	137	D	1	540	30	4	175
Flashover: Yes	4	138	D	0.99	370	3	1	145
Experiment 38 – Scenario A	1	139	I	0.66	450	1.5	2	118
Cable fixing: Wood blocks	4	139A	B	0.66	450	1.5	2	118
Building type: Concrete block	2	140	A	0.96	460	2	4	176
Flashover: No	3				520	1.5	3	136
	4	141	H	1	440	3	1	116
Experiment 39 – Scenario C	1	142	A	0.84	270	1.5	2	307
Cable fixing: Wood blocks	2	143	D	0.97	340	4	4	465
Building type: Concrete block	3	144	D	0.98	350	1.5	3	450
Flashover: Yes	4	145	D	0.93	250	1.5	1	297

The maximum normal operating temperature of PVC/PVC cable insulation is specified in BS/EN6004:2000 as 70 °C [157]. BS/EN6004:2000 also specifies that the cable must be able to withstand temperatures of up to 160 °C for 5 seconds without deteriorating [157]. The auto-ignition temperature of PVC cable is varied in the literature and detailed as between 263 and 454 °C [7].

The data displayed in Table 6 confirms that the PVC/PVC insulation did not electrically breakdown until it was above the operating temperature. The arcing damage occurred within the auto-ignition temperature range. This suggests that the arcing events generally occurred in the temperature range between the PVC plastic thermally deteriorating (with the transition into carbon char) and its auto-ignition temperature.

The distance to the fire's area of origin represented by the distance probability was calculated for the exhibits recovered from the scenes with single areas of origin only or scenes with multiple areas of origin but where the fire development was dominated by one area within the scene. This is further discussed in chapter 5.

3.5.2 Testing for correlation between the variables within the practical experimental tests

The strength of the relationship between two variables (if one exists) can be measured in various ways using statistical tests. The calculation of a correlation coefficient is used to reflect the degree to which selected variables are related. There are a number of statistical tests available to determine the correlation coefficient of a set of data.

The Pearson correlation coefficient is a measure of the strength and direction of the linear relationship between two variables, describing the direction and degree to which one variable is linearly related to another. Pearson's correlation is most usually used on data that is normally distributed [158].

Spearman's rho is a non-parametric measure of the correlation relationship between variables, without making any assumptions about the frequency distribution of the variables.

Kendall tau is also a non-parametric correlation coefficient. The Kendall tau correlation coefficient is considered to be equivalent to the Spearman correlation coefficient but requires the data to be symmetrical.

The data set generated contains data that is both categorical, (i.e. the classification of the arcs) and numerical. Since there are different numbers of exhibits within each arcing category and tests scenario the data can be considered unsymmetrical and as such Spearman's rho is the most appropriate non-parametric test to use to interrogate the data for correlations between the variables.

The experimental data was imported from the spreadsheet software into the statistical analysis package SPSS version 17.0 (SPSS Inc. Chicago, IL. USA). The following variables were examination for correlations using Spearman's rho correlation:

- Scenario type
- Circuit number.
- Circuit Breaker (MCB) sequence number.
- Temperatures of the arcing events.
- Fault current during the arcing events.
- Arcing category (coded into a numerical).
- The distance from the fire's area of origin*.
- The time from ignition for each of the arcing events.

* The distance from the fire's area of origin was calculated using an algorithm discussed in chapter 5

The full data matrix of all samples was initially analysed using SPSS. Table 8 details the results of the correlation tests. These suggest that there was a significant correlation (0.583) between the "temperature of the arcing events" and the "circuit

breaker operation sequence". The literature describes that correlations above 0.6 demonstrate a strong correlation [159] and as such the relationship between these two variables was investigated further. The data revealed a general trend in the circuit breaker operation sequence with the circuit breakers generally operating on circuits 1, 2, 3 and 4 in that order as the ceiling temperature of the compartment increased. This is illustrated in figure 106.

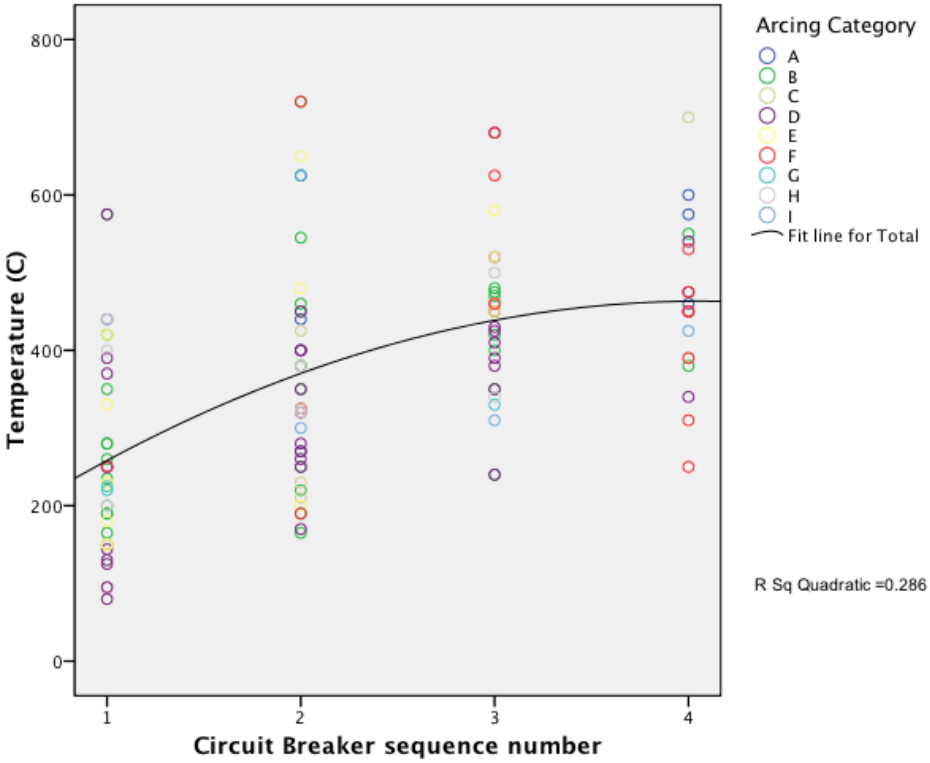

Figure 106 – Linear scatter plot chart detailing the trend between the temperature at the time of the arcing event and circuit breaker sequence.

The uniformity of the ceiling temperatures throughout the experimental fire compartments was questioned once the correlation of the temperature and the circuit breaker operation was discovered. The fire compartment had one temperature sensing thermocouple installed in the centre of the room for each of the experimental fires. The concern was that if the fire started at one end of the room and the thermocouple was located two metres away there may be a significant lag in detecting the temperature at the arcing event site.

The European Network of Forensic Science Institutes (ENSFI) conducted six experimental fires in 2001 at the Building Research Establishment site at Cardington,

Bedfordshire, UK [160, 161]. The compartments were uniform in size with a similar length and height to the compartments used in this research. However, the compartment width was one metre less that the Wethersfield compartments. The ENSFI tests were furnished with a similar fuel load throughout the tests. Two thermocouple trees were used in each compartment. One thermocouple tree was located adjacent to the fire's area of origin and designated the "hot tree". The second thermocouple tree was located at the opposite end of the compartment and was designated the "cold tree".

An evaluation of the temperature data in the ENSFI tests established that in some cases there was a slight lag in the time between the thermocouple trees in the compartment as the fire developed during the experiments. However, this was not consistent across all of the tests and was more evident in the fires accelerated with ignitable liquid. The temperature data is presented in table 6.

DeHaan conducted two separate series of fire tests in San Jose, California (1996) and Moses Lake, Washington (1998) with a total of 10 compartment fires [162]. Thermocouples were installed at ceiling and floor height on either side of each compartment and the temperatures documented for each fire throughout the series of tests. A short time lag was observed between the ceiling thermocouples as each fire developed.

The evaluation of the ENSFI and DeHaan data indicates that there is an established time lag equivalent temperatures at ceiling level 2 to 3 metres apart in the order of 15-20 seconds and there is a temperature difference of less than 100 º C between the two sites.

Table 7 – Temperature data from the ENSFI fire tests [160]

	Time from ignition (mins)	Hot thermocouple tree	Cold thermocouple tree
Test 1 Deliberate ignition using petrol ignitable liquid applied to sofa and carpet. Distance between thermocouple trees – approximately 2 metres.	3.5	150	75
	4	350	200
	4.5	850	520
Test 2 Deliberate ignition using petrol ignitable liquid applied to the sofa and carpet. Distance between thermocouple trees – approximately 2 metres.	4	220	190
	4.25	450	420
	4.5	750	875
Test 3 Accidental cause - a waste paper bin as the initial fuel package. Distance between thermocouple trees – approximately 1.8 metres.	2	50	75
	2.5	130	160
	3	150	175
	3.5	175	300
	4	550	770
Test 4 Accidental cause – an overheated electrical heater. Distance between thermocouple trees – approximately 1.3 metres.	10	50	50
	11	50	50
	12	75	75
	13	110	105
	14	180	185
	15	300	330
	15.5	875	740
Test 5 Accidental cause – a cigarette ignition of the sofa (assisted with firelighters for the purposes of the test). Distance between thermocouple trees – approximately 3 metres.	2	80	90
	3	130	140
	4	160	160
	5	100	220
	6	50	220
	7	75	70
	8	100	50
Test 6 Deliberate ignition with petrol ignitable liquid applied to the carpet. Distance between thermocouple trees – approximately 3.3 metres.	2	210	150
	2.5	900	575
	3	800	800

The Spearman's rho correlation also suggested that there was a correlation (0.251) between the "time from ignition" and the "circuit breaker operation sequence". The variables were graphed to demonstrate the extent of this relationship (figure 107) and no strong linear relationship is indicated.

There were no other correlations observed within the data. The data matrix was sub divided by category of arc, scenario and type of building (mobile home and block build buildings) and reanalysed using the Spearman's rho correlation. No correlations other than those already exposed in the full data set were revealed. This demonstrated that the type of arcing damage observed was not related to the configuration or construction of the compartment within which the fire occurred. On the contrary, the arcing damage observed in some situations was related specifically to the microenvironment of the conductor itself and was influenced by the fixing methods (screws or wooden fixtures) evidenced through microscopic and SEM elemental analysis (presented in chapter 4).

Table 8 – Nonparametric correlations (Spearman's Rho test)

			Temperature (C)	Arcing Category (Number)	Current (Amps)	Distance from fire's area origin probability	Circuit Breaker sequence number	Time from ignition (seconds)	Circuit Number
Spearman's rho	Temperature (C)	Correlation Coefficient	1.000	-.057	.040	.166	.583**	.093	-.102
		Sig. (2-tailed)	.	.510	.621	.163	.000	.248	.200
		N	159	135	156	72	156	158	159
	Arcing Category (Number)	Correlation Coefficient	-.057	1.000	-.052	.083	.024	-.104	-.036
		Sig. (2-tailed)	.510	.	.551	.477	.780	.232	.664
		N	135	145	134	75	133	135	145
	Current (Amps)	Correlation Coefficient	.040	-.052	1.000	-.063	-.008	.073	-.098
		Sig. (2-tailed)	.621	.551	.	.604	.923	.362	.223
		N	156	134	156	70	154	156	156
	Distance from fire's area origin probability	Correlation Coefficient	.166	.083	-.063	1.000	.182	.007	.140
		Sig. (2-tailed)	.163	.477	.604	.	.129	.953	.221
		N	72	75	70	78	71	71	78
	Circuit Breaker sequence number	Correlation Coefficient	.583**	.024	-.008	.182	1.000	.251**	-.156
		Sig. (2-tailed)	.000	.780	.923	.129	.	.002	.051
		N	156	133	154	71	156	156	156
	Time from ignition (seconds)	Correlation Coefficient	.093	-.104	.073	.007	.251**	1.000	-.048
		Sig. (2-tailed)	.248	.232	.362	.953	.002	.	.553
		N	158	135	156	71	156	158	158
	Circuit Number	Correlation Coefficient	-.102	-.036	-.098	.140	-.156	-.048	1.000
		Sig. (2-tailed)	.200	.664	.223	.221	.051	.553	.
		N	159	145	156	78	156	158	169

**. Correlation is significant at the 0.01 level (2-tailed).

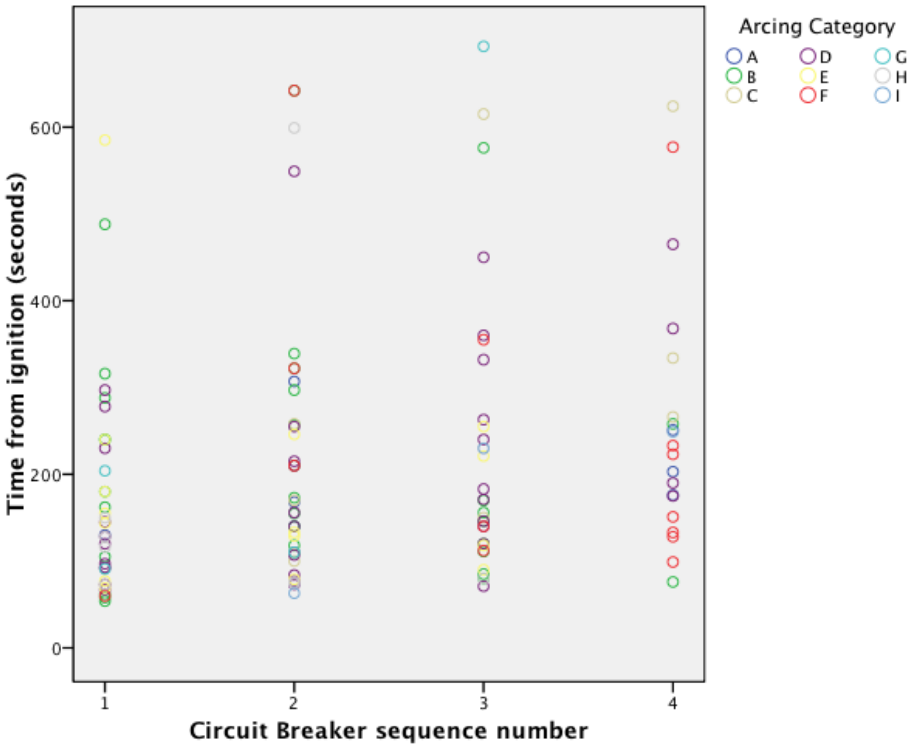

Figure 107 - Linear scatter plot chart detailing the correlation between the time from ignition and "circuit breaker sequence.

Two and three-dimensional scatter plots were created for various sets of variables in the data to illustrate the relationships between the category of arcing observed and other variables. The variables chosen for comparison were: the distance of the arc from the point of origin of the fire, the temperature at which the arc occurred and the fault current. These are considered to be the most defining characteristics in terms of the environment of the arc.

The relationship between the arcing category, the temperature of the arcing events and the fault current are illustrated in figures 108 and 109. Arcing categories B, D, E and F were observed in the largest number of exhibits. Arcing categories A, G and I were observed in the least number of exhibits in these experiments. The chart details a cluster of exhibits in the temperature axis between 200 and 600 °C with the majority occurring in the 250 to 350 °C range. The data illustrates that each of the categories of arc occurs over a range of temperatures.

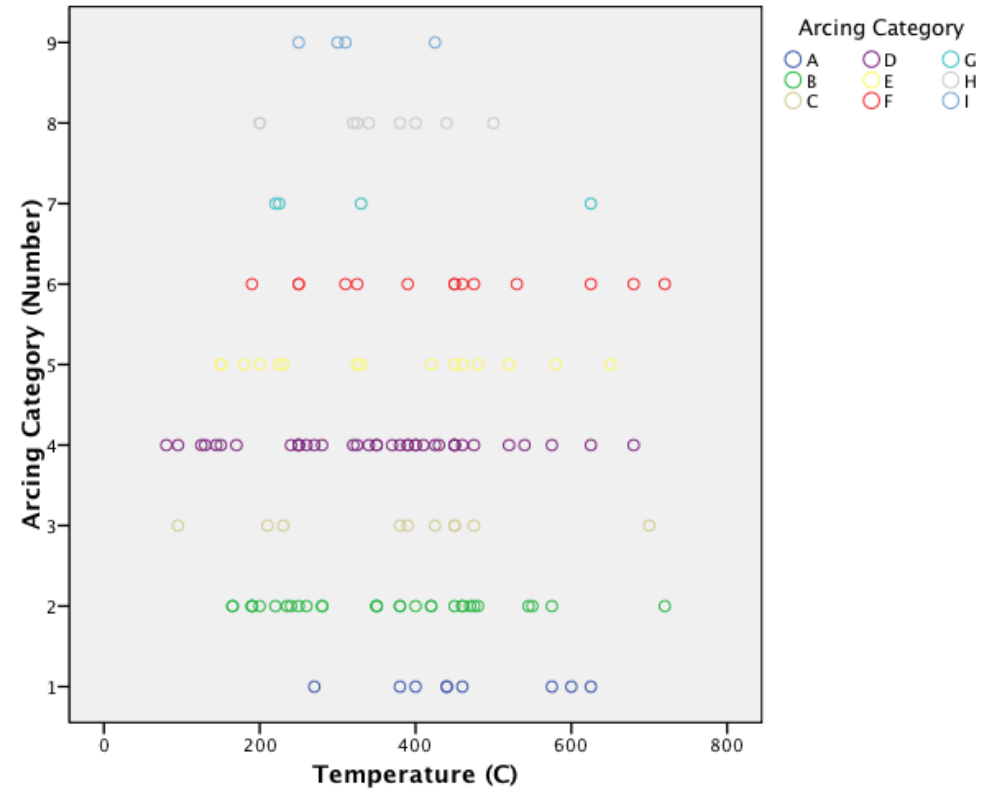

Figure 108 – Comparison of the temperature and arcing categories

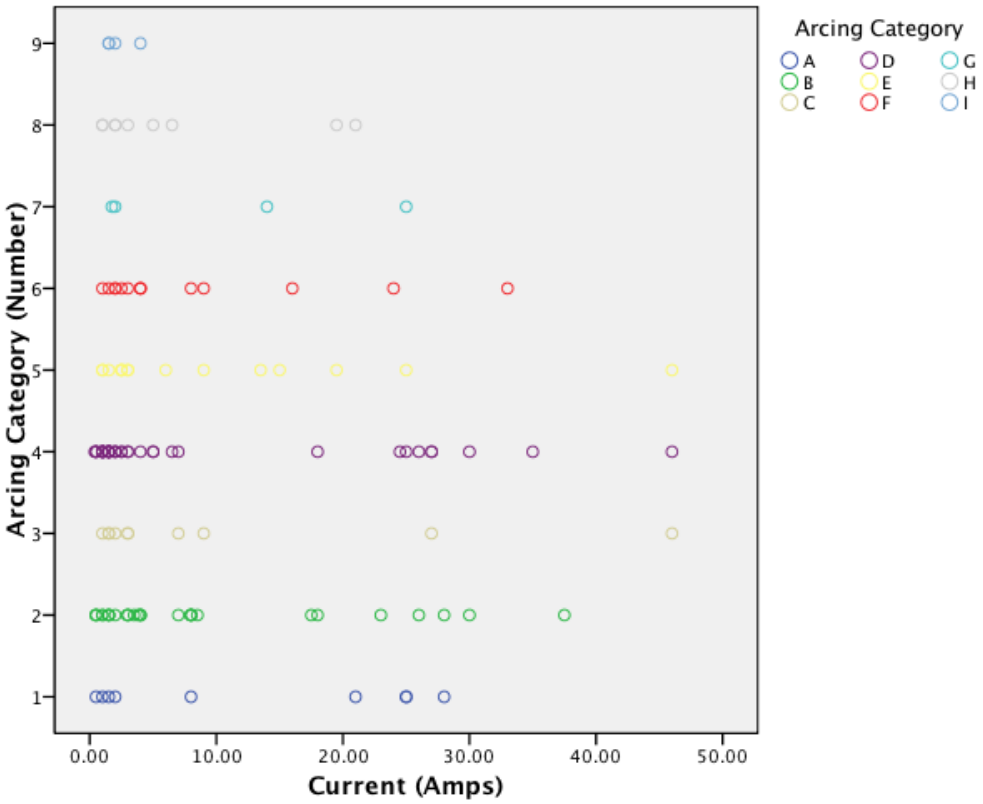

Figure 109 – Comparison of the current and arcing categories

The scatter plot clustered the fault current data predominantly in the 0 to 20 Amps range of the axis. This suggests that the majority of the recorded fault current that was flowing at the point of the arcing events during the experiments was below the 20 Amps value.

Figure 110 illustrates the relationships between the arcing category, temperature of the arcing events and the fault current.

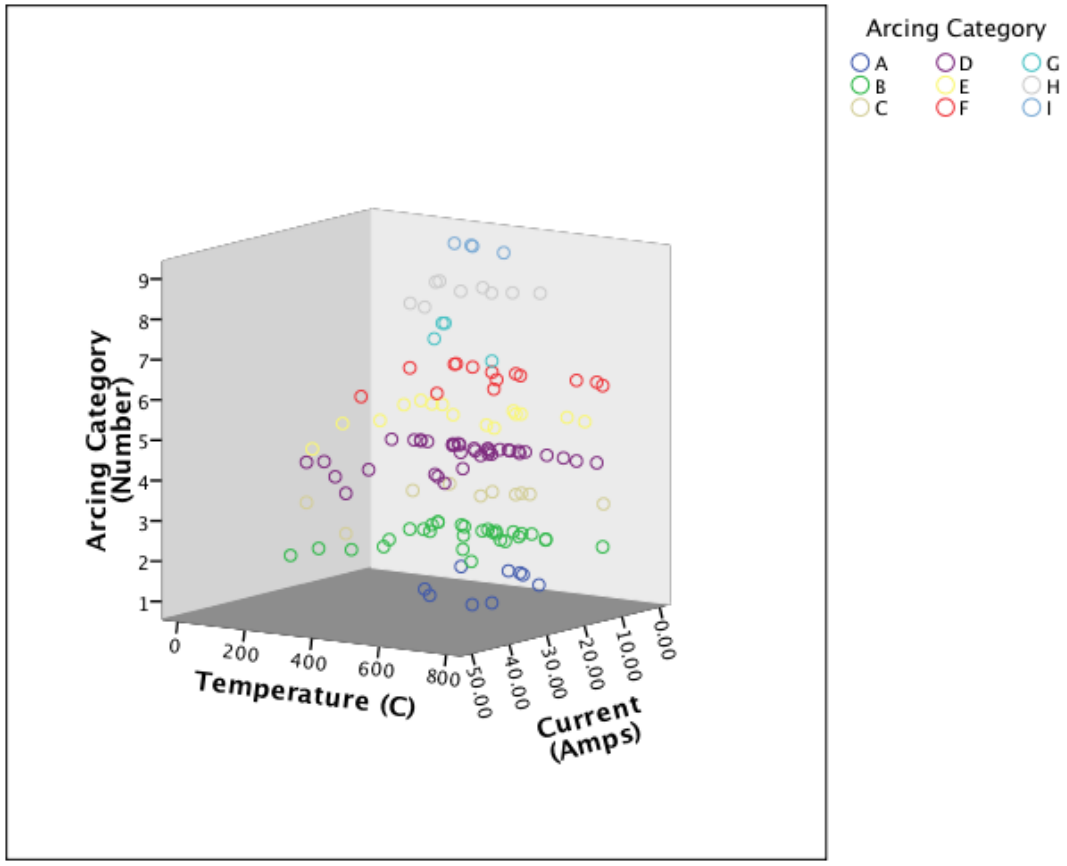

Figure 110 – Three-dimensional scatter plot comparing the arcing category type, temperature and the fault current during the arcing event.

The relationship between the arcing category and the distance from the fire's area of origin is illustrated in figure 111. The majority of arcs, regardless of category, cluster towards the area of origin providing a basis for the potential of arc fault mapping. This is further discussed in chapter 5.

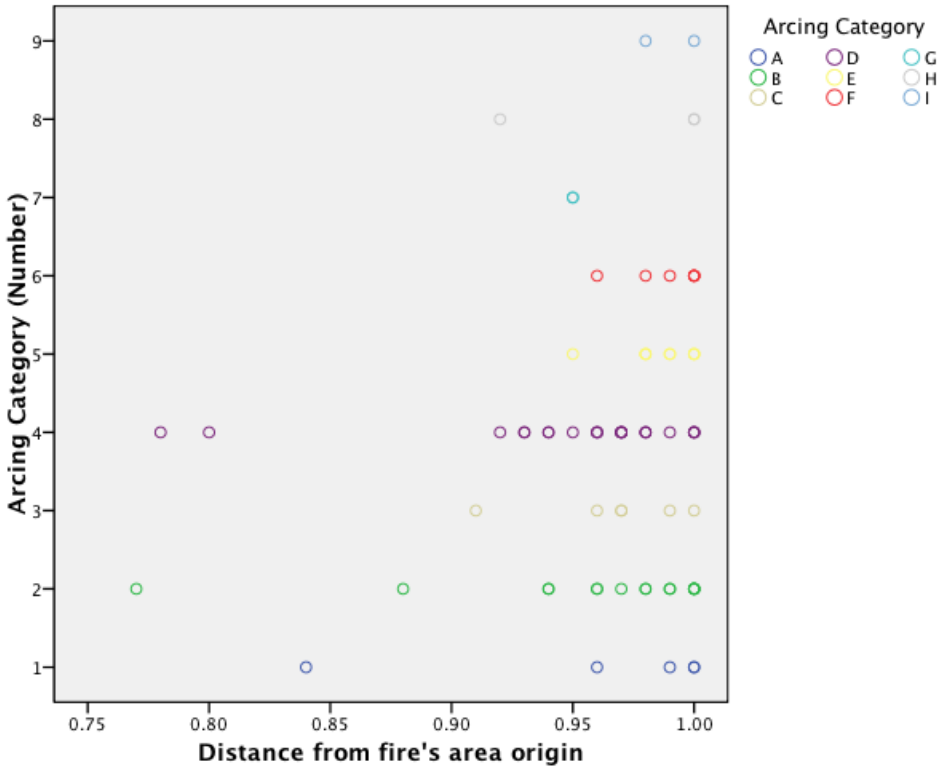

Figure 111 – Comparison of the arcing category and the distance from the fire's area of origin.

Figure 112 further illustrates the comparison between the arcing category, the temperature of the arcing events and the distance from the fire's area of origin. The three-dimensional scatter plot detailed a cluster of data points between 200 and 600 °C on the temperature axis. The cluster was also skewed towards the 0.85 and 1.00 area of the distance from the area of origin axis indicating that the arcing occurred on the conductors in close proximity to the point of origin in all cases.

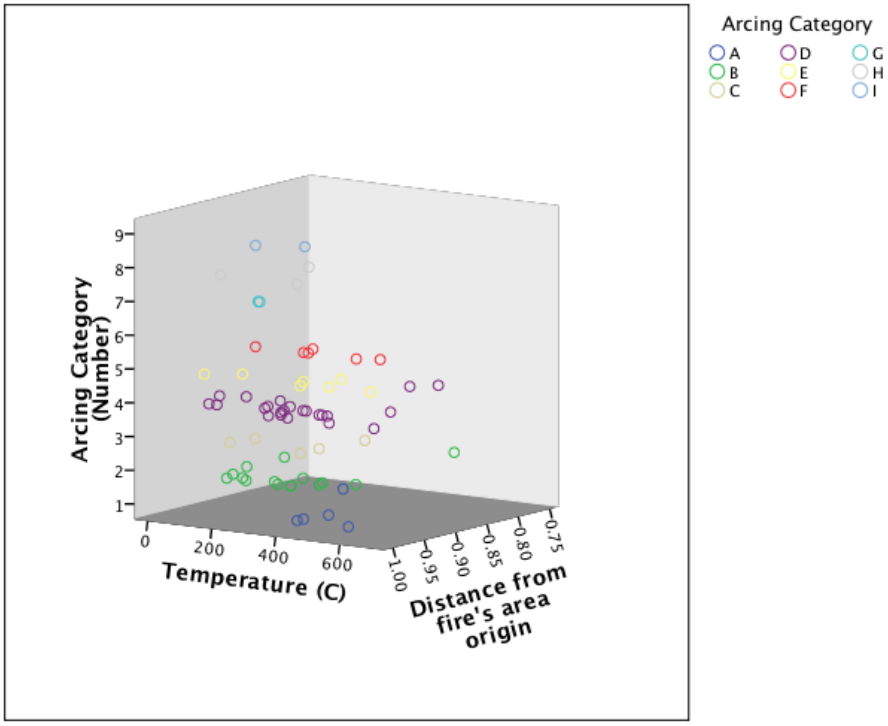

Figure 112 – Three-dimensional scatter plot detailing the relationship of the arcing category, the temperature and the distance from the fire's area of origin.

3.5.3 Conclusions of the statistical analysis

The volume of data collected during the experiments and the number of exhibits recovered from the experiments prevented the easy manual evaluation of the data. Inputting the data into a spreadsheet package enabled the correlation of the various measured variables using SPSS version 17 software. The full data set and various sub sets of the data were analysed using the Spearman's rho correlation coefficient calculations. The tests have shown that the majority of variables in the experiments were not correlated with each other.

A significant correlation between the temperature at the time of the arcing event and the circuit breaker sequence was revealed. This is a logical result as the circuit breakers protecting the circuits located close to the fire's area of origin operated first as the temperature increased.

A correlation was also revealed between the time from ignition (seconds) and the circuit breaker operation sequence. This result is also logical as the circuit breakers

operated in sequence as the fire developed over time. The majority of the experimental fires developed from ignition to flame spread across the ceiling surface within 3 to 4 minutes.

The lack of correlation between arcing pattern types (categories) and the other variables is a useful contribution to the fire investigation community. The arcing categories are reproducible but are independent of other environmental conditions within the compartment fire. When the data for each arcing category and for each repeated scenario were analysed, no correlations other than those already described were revealed. This again emphasises the fact that the type of arc produced during the arcing event is unpredictable.

Chapter 4 Microscopy

4.1 Scanning Electron Microscopy (SEM)

Scanning electron microscopy (SEM) analysis is an established microscopic method that has been used in the metallurgy industry to identify metallic damage to structural components. The Transmission Electron Microscope (TEM) was invented and introduced in 1931 by Max Knoll and Ernst Ruska (Ernst Ruska was awarded the Nobel Prize for Physics in 1986 for this invention [163]) and their electron Microscope is illustrated in Figure 113

Figure 113 – the original electron microscope [164].

In a TEM, electrons are speeded up in a vacuum until their wavelength is extremely short, only one hundred-thousandth of that of white light. Beams of these fast-moving electrons are focused on a sample and are absorbed or scattered by the sample's parts so as to form an image on an electron-sensitive photographic plate [164].

In a scanning electron microscope (SEM), electrons are accelerated in a vacuum to energies of typically a few keV. The resultant beam of electrons is focused using magnetic lenses, and scanned across the sample in a raster pattern. At each point in the scan, a signal is measured from the sample which is used to build up an image pixel by pixel. Commonly used signals include the measurement of secondary and backscattered electrons emitted from the sample. Backscattered electrons are electrons from the beam which interact with the nuclei of the target atoms, and are thus sensitive to the atomic number of the element probed. Secondary electrons are lower energy electrons ejected by the target atoms themselves, and this signal is largely dependent on the surface topography of the sample.

As the wavelength of the high energy electrons used in the SEM is many orders of magnitude shorter than that of visible light, the resolution of this technique is far higher than that of optical microscopy. The other advantage of SEM in this application is the significantly increased depth of focus achievable.

A 1978 court case in the US described the "use of the SEM is particularly valuable in the study of metallurgical failure, for example, in which examination of a fractured surface is sought." [165]. In the fire investigation industry a metallurgist is occasionally retained to provide expert opinion in cases involving electrical items and in particular to determine if a conductor(s) with localised melting is the result of electrical arcing damage or another form of melting damage [166].

4.2 Preparing the exhibits

The copper conductor exhibits still had a quantity of PVC carbon residue attached to them. This carbon residue would mask the localised melting patterns of the arcing events if they were not removed. The amount of carbon residue and the strength of adhesion to the copper surface varied considerably between the exhibits. Levinson described the use of acetone when cleaning copper conductors with arcing damage [60]. However, an optimum cleaning process for copper electrical conductors was not found during the literature review. Acids and other similar metal cleaning chemicals could not be used as other elements would be transferred on to the copper

conductor surface and this would affect the surface element analysis. In addition, the localised melting was often very subtle and delicate and so was important that these patterns did not change as a result of the required cleaning process. The copper conductor sections could not exceed 50mm in length, as they had to be mounted on to an aluminium alloy stub for the SEM analysis. The exhibits were individually cut to size and placed into a small glass vial. The glass vial and its plastic lid were marked with the exhibit number to prevent the loss or incorrect identification of the exhibit identity numbers. The glass vial was filled with acetone and sealed. The glass vials containing the exhibits were sonicated in an ultrasonic bath for 1.5 hours. Figure 114 details the cleaned exhibits within the sealed glass vials. A flow chart summarising the cleaning process from exhibit recovery to SEM analysis is detailed in figure 115.

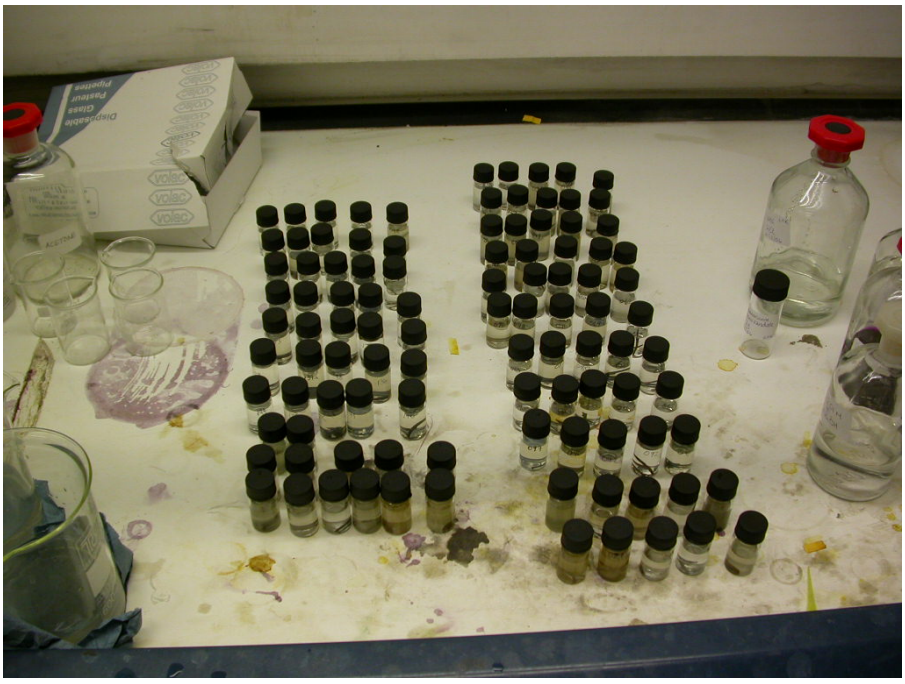

Figure 114 – Glass vials with individual exhibits and acetone in the fume cupboard at in University of Strathclyde laboratory [167].

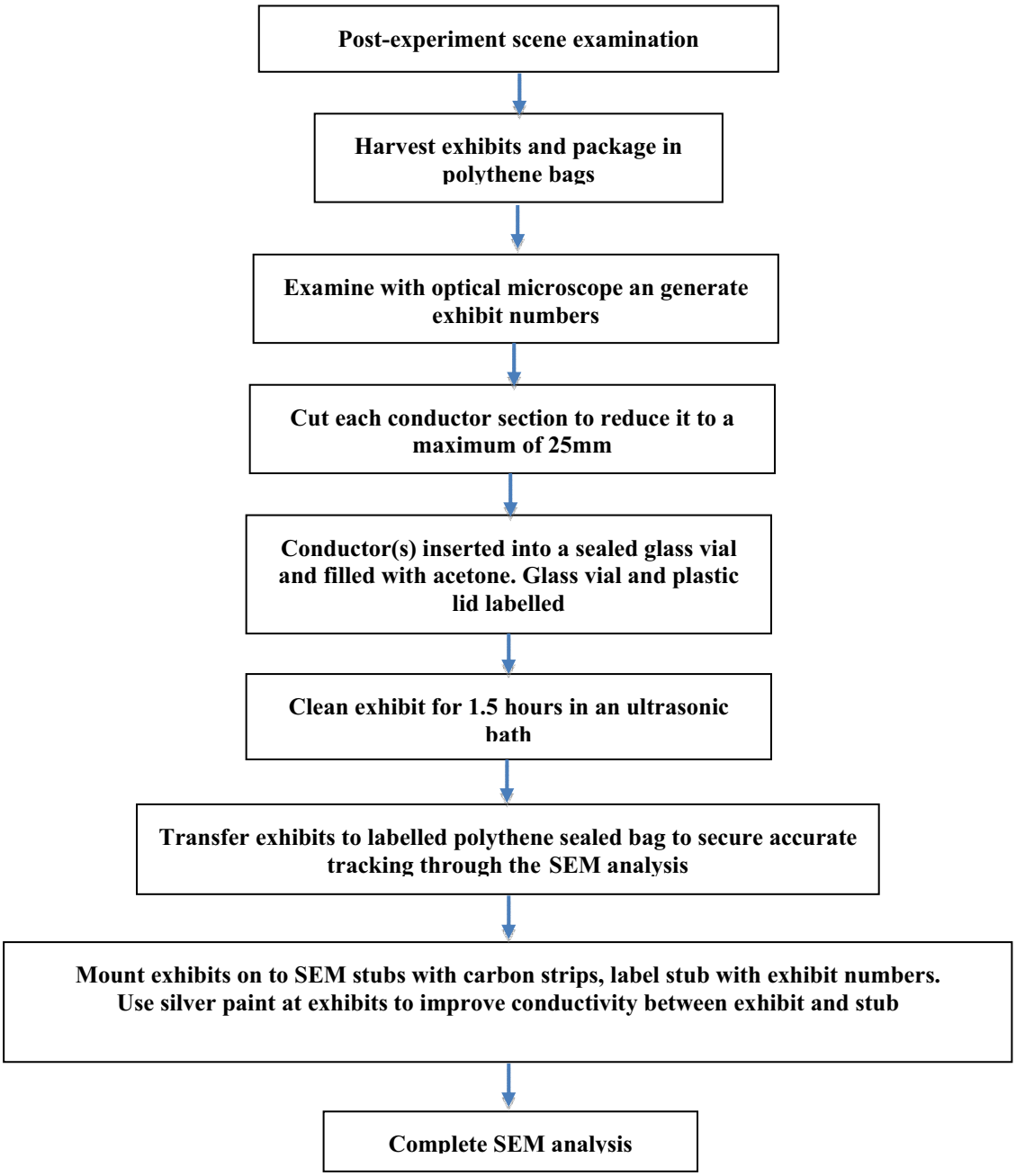

Figure 115 - Flow chart detailing the exhibit identification and cleaning process

4.2.1 Preparation of pre fire exhibits

Twenty cables were prepared with conductors separated and the ends stripped of insulation. Each cable was connected to a portable consumer unit that was connected to the 75kVA supply transformer. The live and neutral conductors were touched

together to create a short circuit fault with the resultant localised melting (arcing) damage to the conductors.

The purpose of creating the pre-fire arcing damage was to produce control samples that were not fire damaged to compare the arcing damage patterns and the elemental components of the conductor surface.

The voltage and current was monitored and recorded with data loggers. The voltage was constant at 240 volts and immediately reduced to 0 volts when the circuit breaker operated. The fault current recorded during the first 10 pre-fire arcing events varied between 2 and 23 Amps. All of the fault currents recorded during the pre-fire arcing events were varied.

A sub sample of the 141 recovered exhibits were analysed using SEM. The total numbers of exhibits that could be analysed with an SEM was restricted by funding and time limitations. A minimum of 8 exhibits per category were analysed. Where there were large numbers of exhibits in any one category, 8 examples were selected randomly throughout the category to obtain the required number of exhibits per arcing category. For example, from a total of 40 exhibits in the arcing category and 8 were required therefore every fifth exhibit in that category was selected for SEM analysis. The exhibits examined using an SEM are listed in table 9.

Table 9 – Details of the exhibits analysed with the SEM

Arcing category	Exhibit numbers	Total
A	002, 007, 013, 043, 055, 088, 140, 142	8
B	011, 62a, 067, 090, 093, 123, 130, 132, 139a	9
C	008, 020, 033, 037, 039, 056, 066, 071, 084	9
D	054, 062, 068, 078, 112, 128, 129, 133, 136, 138, 144, 145	12
E	009, 032, 045, 058, 073, 107, 110, 114, 125	9
F	006, 028, 049, 052, 063, 064, 120, 126	8
G	003, 012, 016, 024, 030, 061, 111, 124	8
H	054, 058a, 069, 117, 118, 134, 135141	8
I	053, 077, 080, 081, 083, 099, 117, 139, 142, 143	10
Pre-fire	001, 002, 003, 004, 005, 006, 007, 008, 009, 010, 011, 012, 013, 014, 015, 016, 017	17

4.3 Cameca SX100 SEM equipment description

A Cameca SX 100 Electron Probe Micro-Analyser (EPMA) was selected as the most appropriate equipment for this work as it could generate high resolution images and undertake a surface elemental analysis. An EPMA is SEM-derived instrument designed especially for X-ray microanalysis, and has Wavelength Dispersive Spectroscopy (WDS) units integrated into its design. The Cameca SX 100 was first manufactured and released in 1994. It is a fully digitized instrument with integrated electronics and automation, enabling the unattended analysis once the samples are mounted and the software is programmed with the required analysis locations [168].

Electron Probe Micro Analysis (EPMA) bombards a micro-volume of the sample with a focused electron beam (typical energy of 5-30 keV) and collects the X-ray photons induced and emitted by the various elemental species. The wavelengths of these X-rays are characteristic of the emitting material. Therefore, the sample composition can be identified by recording the WDS spectra. WDS spectrometers are based on Bragg's law [169] and use various moveable, shaped monocrystals as monochromators [170]. Figure 116 details an overview of the Cameca SX100.

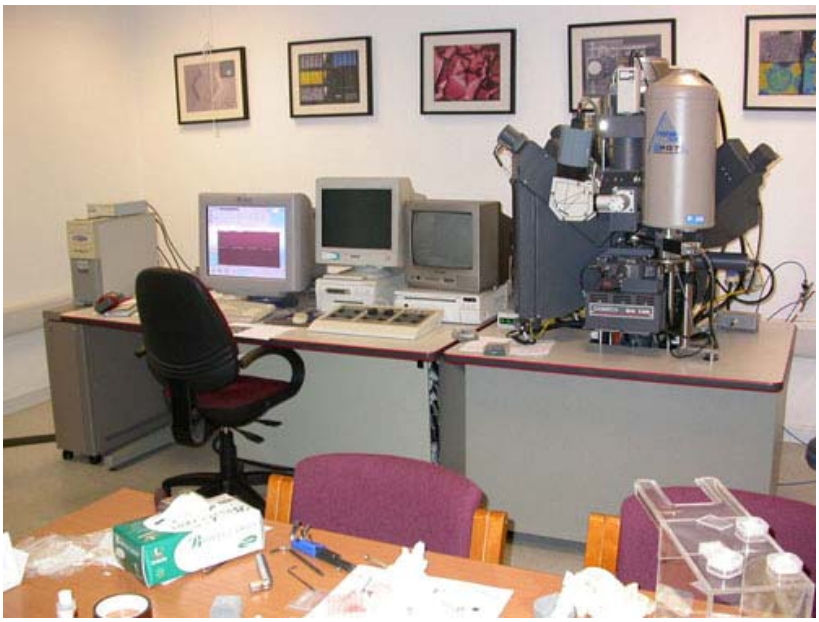

Figure 116 – Image of the Cameca SX100 SEM [171]

4.3.1 Cameca SX 100 equipment operation

The Cameca SX100 was a complex piece of equipment to operate and programme. The dedicated UNIX based software operated the motorised stage mechanism, the SEM settings and the image capture. The UNIX operating system used a number of text commands similar to the Microsoft DOS operating system used in the majority of Personal Computers in the early 1990's. Figure 117 is an example of the SEM images produced by the Cameca SX100.

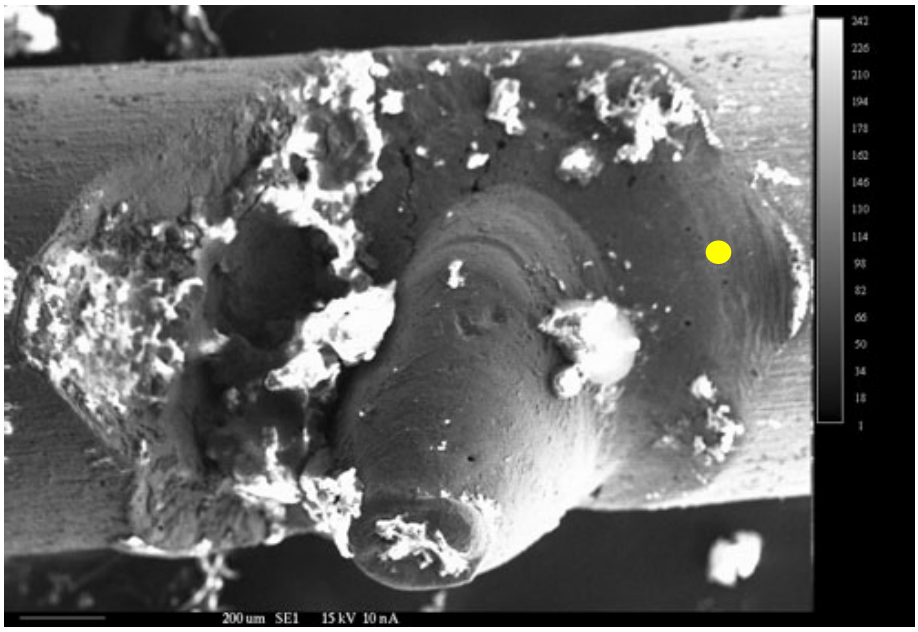

Figure 117 – SEM image of exhibit 144 using the Cameca SX100. The yellow spot is the location of the element scan detailed in figure 127.

4.3.2 Element scans of the conductor surface

It was possible to select an area of the conductor surface and retrieve a scan of elements present that surface at any particular point. This was undertaken on a number of exhibits with similar results. The Cameca SX100 software produced element spectra that displayed large amounts of particular elements. These elements were present on the conductor surface in the area of the localised melting. Copper, Carbon, Oxygen, Zinc, Chlorine and Iron were detected in large quantities in all cases. Carbon produced a peak that exceeded the height of the scale. Some unusual

elements were also detected which included Magnesium, Lithium, Silicon, Chlorine, Potassium, Calcium and Sulphur, but these appeared to be associated with the PVC debris. Figure 118 is the spectrum graph for a point on the surface of the localised melting to exhibit 144 illustrated in figure 117.

An element scan of the pre-fire exhibits displayed a significant quantity of chlorine. It appears that the copper metal absorbs some of the chlorine from the PVC insulation material that it is in contact with following manufacturing of the cable.

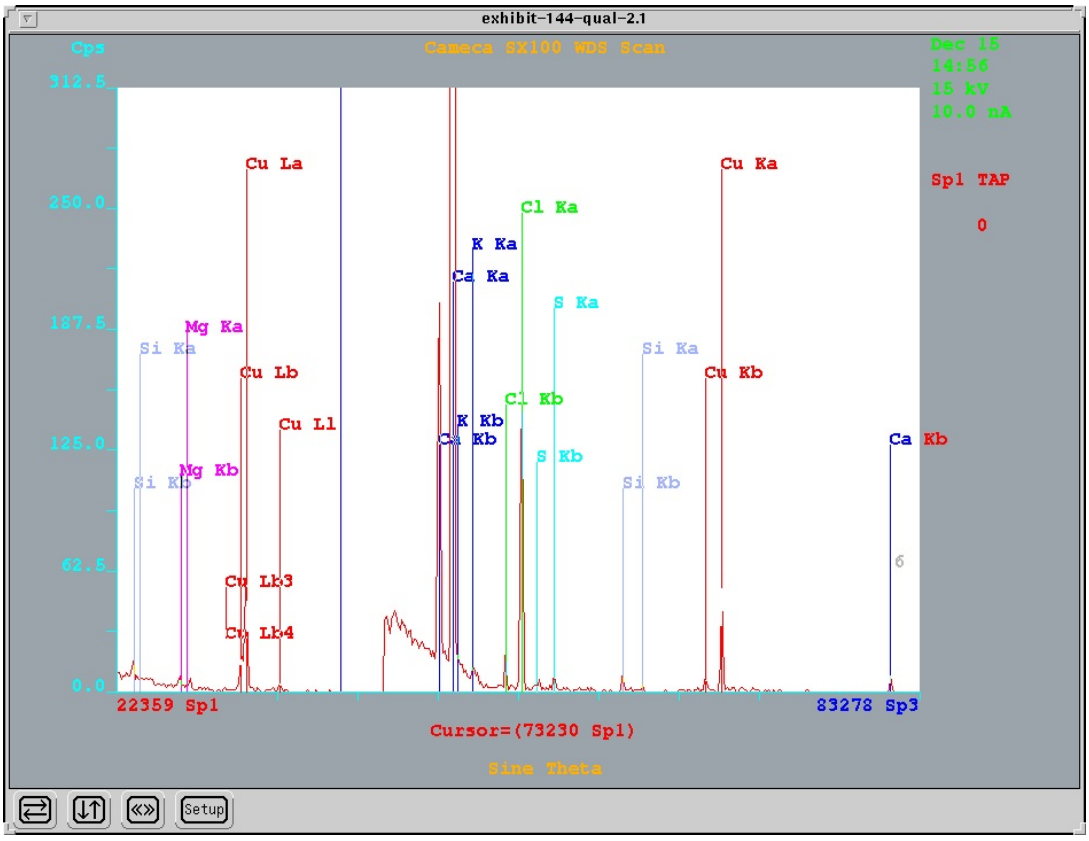

Figure 118 – Element spectrum for a point on exhibit 144

4.3.3 Element maps

The Cameca SX 100 SEM had the capability to scan a defined area and document the X Y co-ordinates of up to 6 selected elements. These co-ordinates were then processed in the software to produce individual image maps of the defined area for each of the elements. A number of image maps were programmed for randomly

selected exhibits but were very time consuming as the scans were undertaken by the SEM one pixel at a time.

The element maps were outputted as “IMG” files. This file format is not compatible with generally available image manipulation software (Adobe Photoshop etc.) however they can be manipulated using a bespoke software program called “Cathodoluminescence Hyperspectral Imaging and Manipulation Program” or “Chimp” designed to run on a computer with a Microsoft Windows operating system and the “.NET Framework” installed. Using the be-spoke Chimp software it was possible to alter the image intensity output from greyscale to a rainbow colour pattern. The greyscale option was found to produce the clearest image to analyse the experiment exhibits.

The Chimp software could also output TIFF or JPEG file formats to use in other software applications. The element maps were useful to undertake and evaluate for this research. The large amounts of carbon and copper elements were anticipated. The absence of the aluminium element is consistent with the limited aluminium in the proximity of the electrical conductors in the fire compartments.

The localised areas of iron and zinc were related directly to the areas of localised melting during the arcing events when other materials interacted with the electrical conductors during the arcing events. Element maps have not been reported in the literature for examination of electrical conductors with localised melting (arcing) damage prior to this research [172].

Figures 119 to 125 detail one SEM scan for exhibit 133 and the 6 elements map scans. A scale links the brightness to the quality of the element. Figure 120 details no aluminium detected. Figure 121 details a large amount of carbon. Figure 122 details a large amount of copper. Figure 123 details that there is a small amount of zinc on the bead area. Figure 124 details a large amount of oxygen present over the entire area scanned. Figure 125 a large amount of Iron on the bead area of the arcing

damage. The iron appears to be from a fixing screw and this suggests that the conductor faulted against a screw.

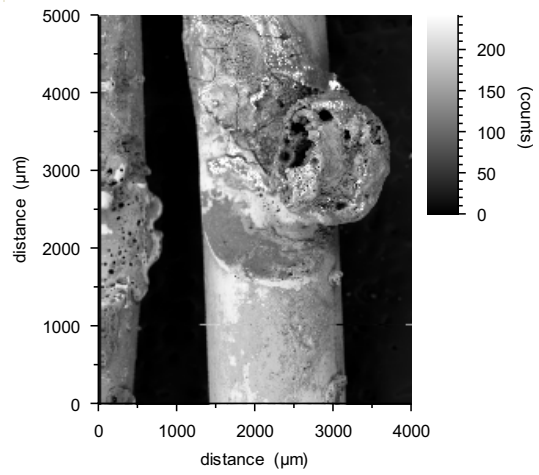

Figure 119 - Exhibit 133 Back Scatter Electron scan

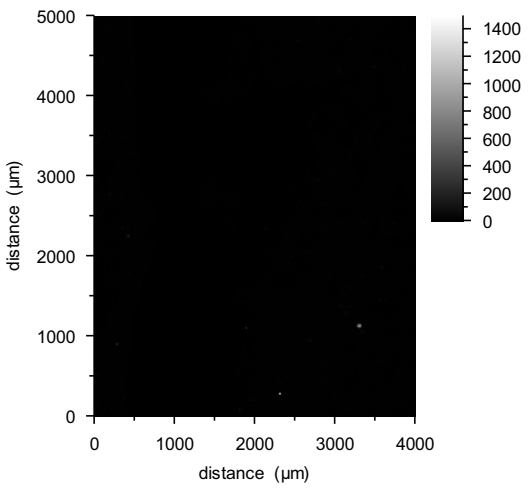

Figure 120 – Exhibit 133 Aluminium element scan

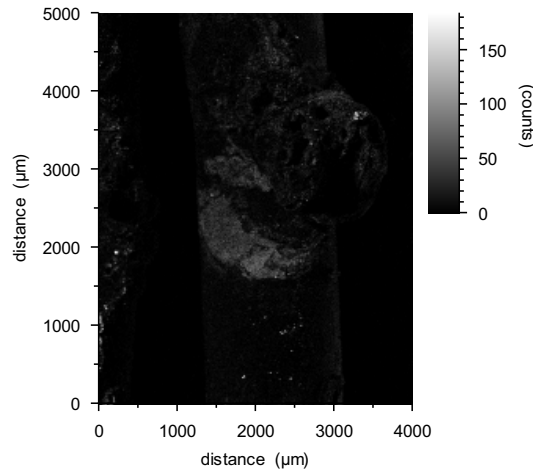

Figure 121 – Exhibit 133 Carbon element scan

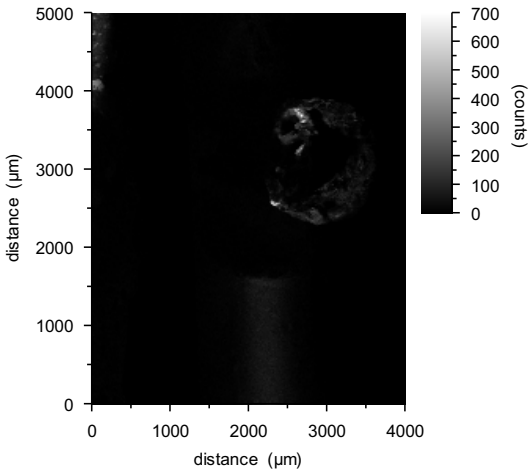

Figure 122 – Exhibit 133 – Copper element scan

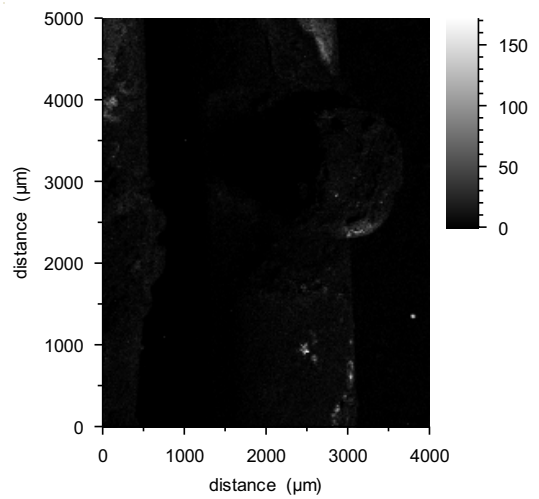

Figure 123 – Exhibit 133 – Zinc element scan

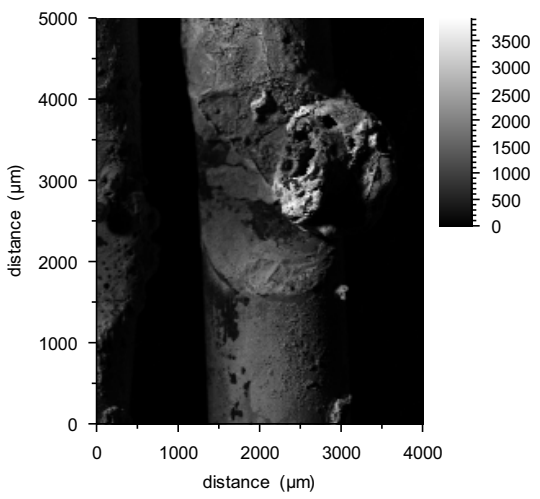

Figure 124 – Exhibit 133 Oxygen element scan

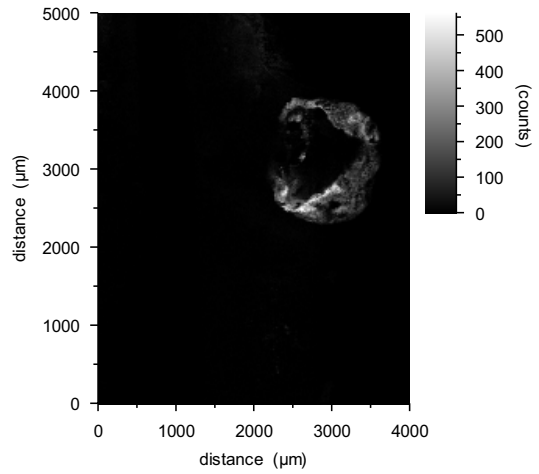

Figure 125 – Exhibit 133 Iron element scan

Exhibit 133 was recovered from experiment 36. The notes for this experiment describe this exhibit as a two conductors that have faulted across a fixing screw.

Table 10 details the exhibits used to create element image maps. It also details which elements were detected and the arcing category.

Table 10 – List of exhibits used to create element image maps

Exhibit number	Arcing category	Cable fixing method	Al	C	Cu	Zn	O	Fe
007	A	Metal screws	☒	☒	☒	☒	☒	☒
012	G	Metal screws	☒	☒	☒	☒	☒	☒
016	G	Metal screws		☒	☒	☒	☒	☒
032	E	Metal screws		☒	☒	☒	☒	☒
039	C	Metal screws	☒	☒	☒	☒	☒	☒
049	B	Metal screws		☒	☒	☒	☒	☒
058a	H	Metal screws		☒	☒		☒	
062a	B	Metal screws	☒	☒	☒	☒	☒	☒
071	C	Metal screws	☒	☒	☒	☒	☒	☒
077	B	Metal screws		☒	☒	☒	☒	☒
114	E	Metal screws		☒	☒	☒	☒	
123	B	Metal screws		☒	☒	☒	☒	☒
126	F	Metal screws		☒	☒	N/A	N/A	N/A
128	D	Metal screws	☒	☒	☒	☒	☒	☒
129	D	Metal screws	☒	☒	☒	☒	☒	☒
133	D	Metal screws		☒	☒	☒	☒	☒
135	H	Wood blocks		☒	☒	☒	☒	☒
140	A	Wood blocks		☒	☒	☒	☒	☒
144	D	Wood blocks	☒	☒	☒	☒	☒	☒
145	D	Wood blocks	☒	N/A	☒	☒	N/A	N/A
Pre-fire 1		Not applicable		☒	☒	☒	☒	

4.4 FEI Sirion 200 SEM equipment description

The FEI Sirion 200 model was a Field Emission Scanning Electron Microscope that was used to capture the majority of the SEM images for this research. The software that operated the equipment and captured the high quality images was Microsoft Windows based. The equipment captured images immediately and the manual stage

controller was logical to operate. Figure 126 is a photograph of the FEI Sirion 200 in the Department of Physics dedicated SEM laboratory.

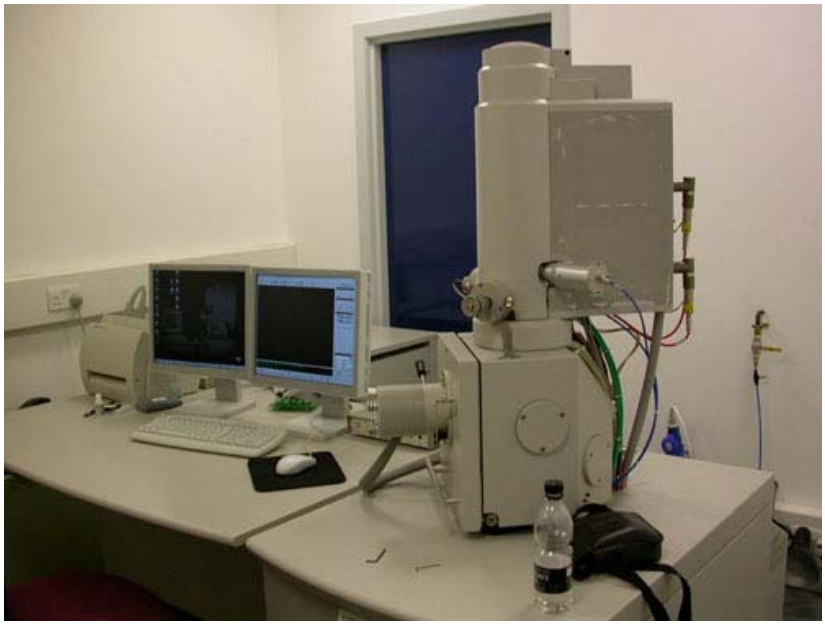

Figure 126 – Image of the FEI Sirion 200 SEM installed at the University of Strathclyde – Department of Physics [173].

Figure 127 details the stage area exposed when the SEM has been vented. Figure 128 details an aluminium alloy stub with exhibits attached prior to being inserted into the SEM stage assembly.

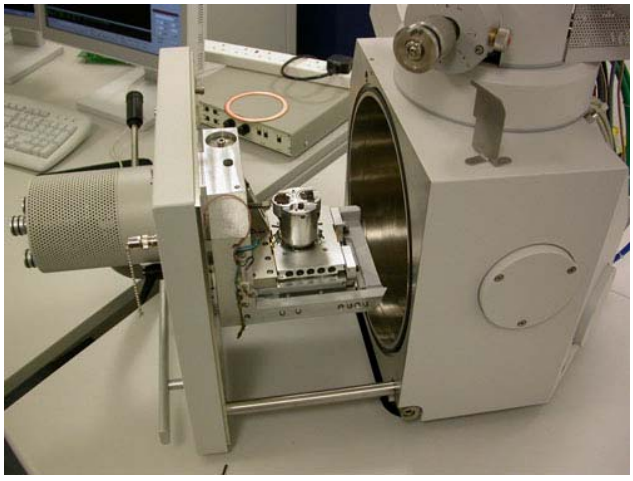

Figure 127 – A stub mounted onto the SEM stage of the FEI Sirion 200 [174]

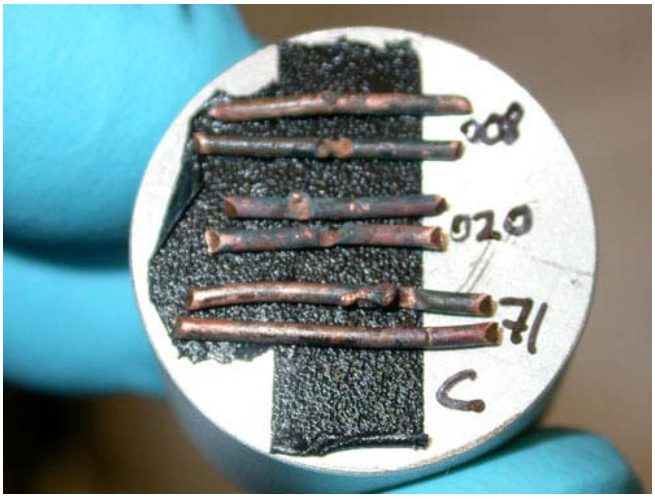

Figure 128 - Exhibits mounted on to the SEM stub [175]

4.5 Image output

The images for both the Cameca SX100 and the FEI Sirion 200 were outputted in high resolution Tagged Image Format Files (TIFF) format without any image compression applied during the output process. Copies of the original images were converted into Joint Photographic Experts Group (JPG) to use in word processing software. The conversion process was undertaken using a batch macro in Adobe Photoshop (version 7) software, to ensure the optimum image quality available.

4.6 Results

There was a difference in the specification of the two SEM instruments. The image output of the Cameca SX100 had a definition of 0.92 million pixels (1172 x 787 pixels). The FEI Sirion had a resolution of 1.35 million pixels (1290 by 1044 pixels). The FEI Sirion image output also appeared to be more defined when compared to the image output of the Cameca SX100.

The image quality and definition was found to be useful when analysing the arcing damage patterns on the exhibits. The edge of the pattern is described as the demarcation area between the area of localised melting on the conductor surface and the adjacent undamaged area of the conductor. This work has confirmed that the demarcation area is one of the most important features of electrical arcing damage compared to other effects of localised melting (thermal effects etc.). A conventional

optical microscope can detail the demarcation area of the localised melting with good results, however, the SEM was a considerable improvement for this type of surface analysis. Figure 129 details an example of the image output for the Cameca SX100 SEM. Figure 130 details an example the image output for the FEI Sirion 200 SEM.

One issue identified whilst undertaking the SEM work was that if the area of localised melting on the conductor surface was wide (for example "Category A" of arcing damage) several SEM scans were required to document the affected area. Separate images needed to be stitched together manually in a different image manipulation software application to detail the entire damaged surface area. Figure 131 details five SEM images stitched together to display the entire area of arcing damage to a conductor with "Category A" localised melting.

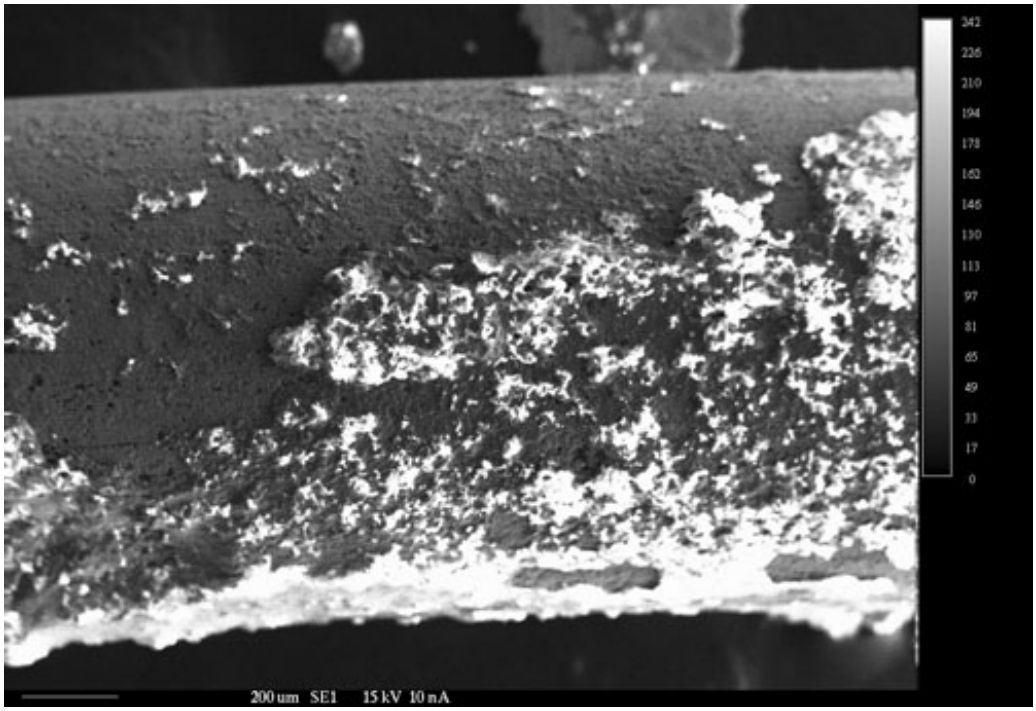

Figure 129 – Cameca SX100 SEM image of exhibit 145

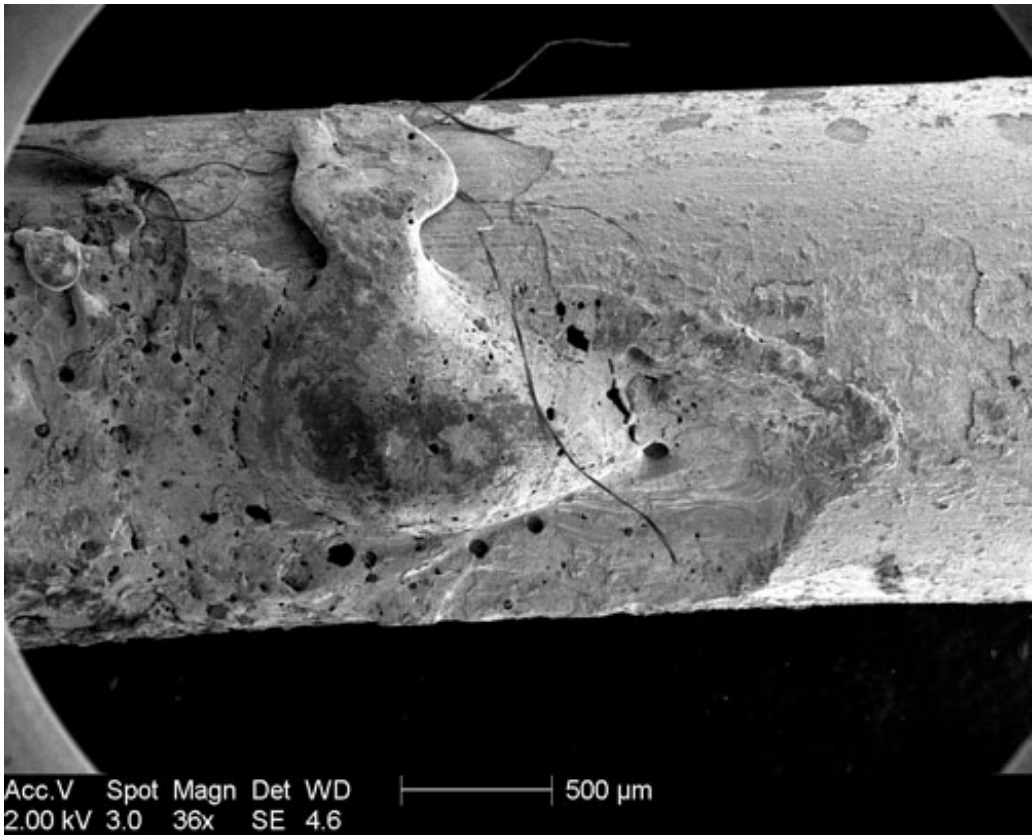

Figure 130 – FEI Sirion 200 SEM image of exhibit 002.

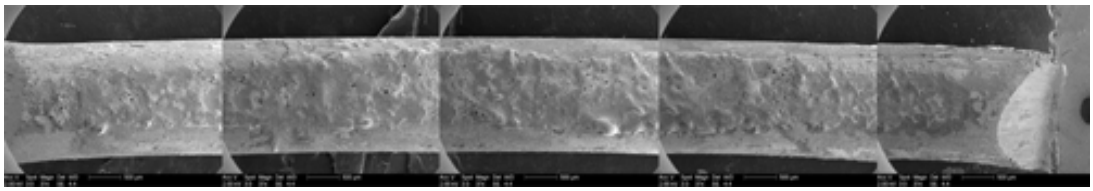
Figure 131 – Five SEM images stitched together (category A arcing damage)

4.7 Pre-fire localised melting (arcing) damage to conductors

There was a significant difference in the localised melting patterns between the pre-fire and post-fire arcing damage. The pre-fire arcing generally affected a much large area of conductor surface than the post-fire arcing recovered from the experiments. An explanation for this difference could be the matrix of surviving charred PVC insulation covering the conductors for the exhibits recovered from the full-scale experimental fires. Figures 132 – 135 detail SEM images of the localised metallic damage to pre-fire exhibits.

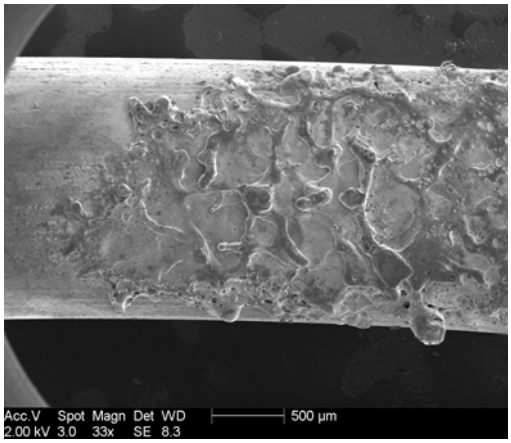

Figure 132 – left side of pre-fire exhibit (pre-fire 9 neutral)

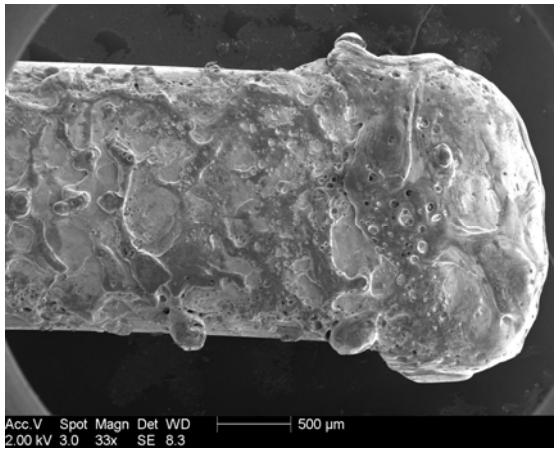

Figure 133 – right side of pre-fire exhibit (pre-fire 9 neutral)

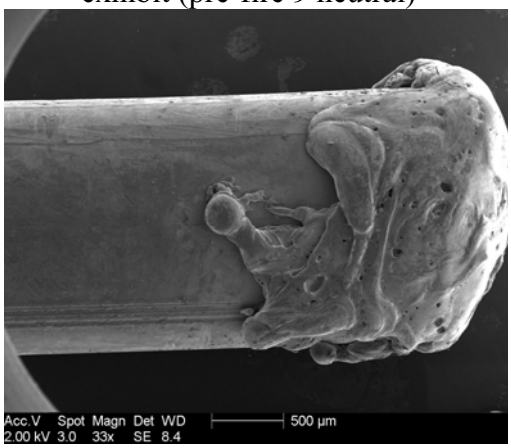

Figure 134 – pre-fire exhibit 13 neutral conductor

Figure 135 – pre-fire exhibit 1

4.8 Confocal Laser Scanning Microscope

4.8.1 Equipment description

The Olympus LEXT OLS 3100 is a confocal laser scanning microscope capable of a 0.12µm resolution three-dimensional measurement. It has a magnification from 120x to 14,400x and it combines a 408nm laser with optics to operate at this wavelength [176]. The software captures the images and stitches them together to create a three-dimensional view that can be navigated. The selected view can be captured as an image. Figure 136 details the typical equipment set-up and figure 137 details the microscope and the exhibit mounting stage.

Figure 136 – Olympus LEXT OLS 3100 confocal laser scanning microscope [177]

Figure 137 – The Confocal laser scanning microscope with a motorised stage [177]

The Olympus LEXT OLS3000 user manual describes the principle of laser scanning microscopes as follows:

"A laser scanning microscope aims laser beam at a small spot with objective lens and scans over the specimen in X-Y directions. It then captures a light from specimen with detector and outputs the image of specimen on to a computer monitor. In confocal optics, the pinhole is placed at a position that is optically joined together with focusing position (confocal plane) to repel light that comes from place other

than focusing position. As the result, the part where light was repelled is truly darkened in the image and; it is possible to slice optically the specimen of shouldered shape. Contrary to it, in ordinary microscope, the light that comes from place other than focusing position is overlapped with image forming light at focusing position and whole image turns blurry." [178]

The optical system was designed to be used with a 408-nm laser light (violet opt system). The optical system is intended to prevent the occurrence of aberrations associated with the use of a short-wavelength light source [178]. Figure 138 is a diagram that details the light sources and the optical system. Figure 139 details the light path for the violet opt system.

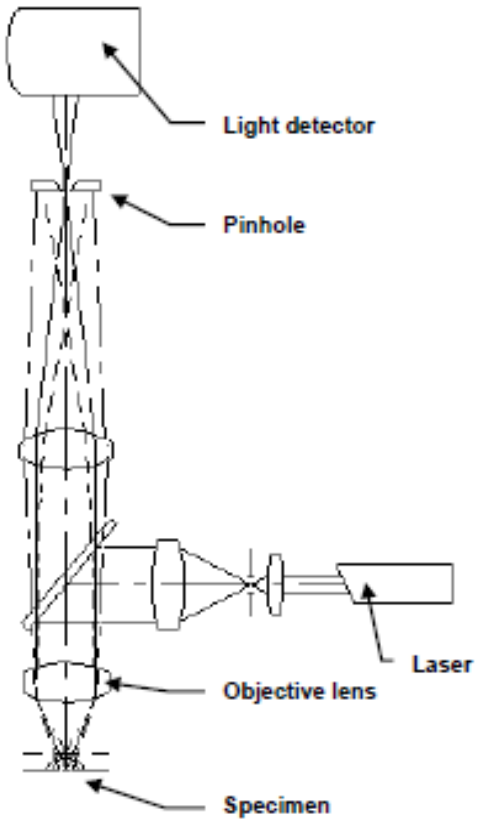

Figure 138 – Confocal laser scanning microscope optical system [178]

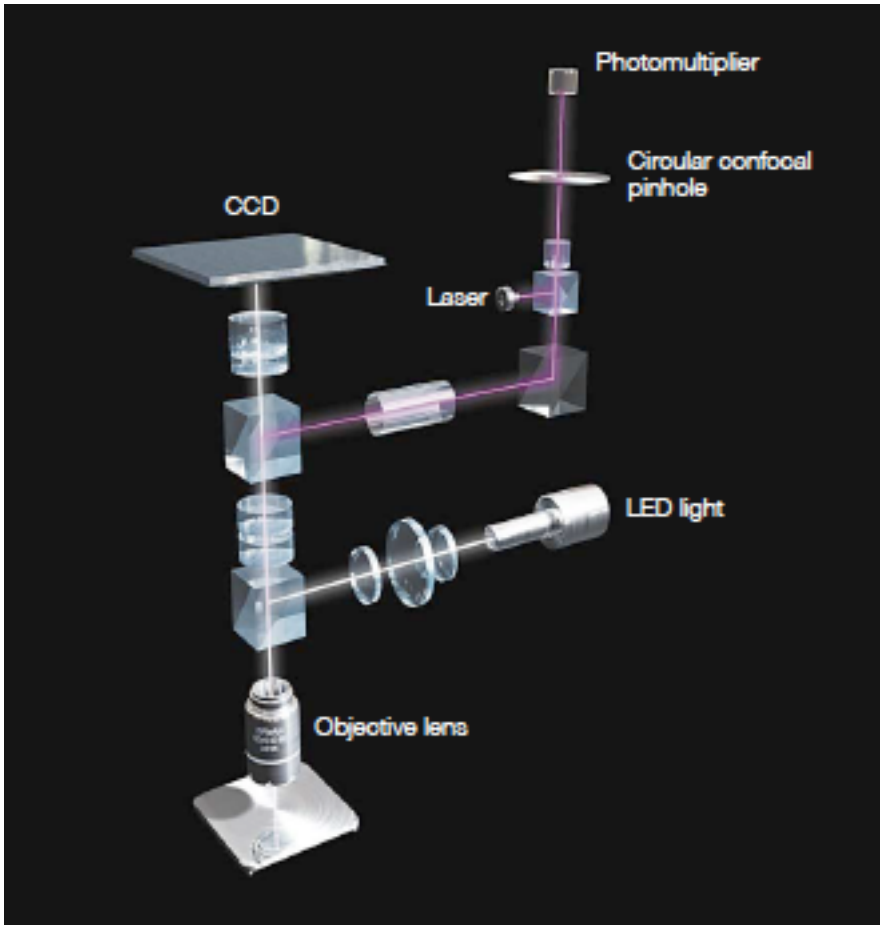

Figure 139 - Basic concept of a light path in the violet opt system [177]

Exhibits from each arcing category that had been previously analysed with SEM were selected for analysis with a LEXT OLS 3100 confocal laser scanning microscope unit set up at the Kroto Research Campus at the University of Sheffield. Table 11 details the exhibit numbers and arcing category that were analysed with the LEXT.

Table 11 – Details of the exhibits analysed with the confocal laser scanning microscope

Arcing category	Exhibit numbers	Total
A	002, 013, 055, 140, 142	5
B	011, 62a, 090, 093, 123, 130, 132, 139	8
C	008, 020, 033, 037, 056, 071, 084	7
D	062, 078, 112, 128, 129, 133, 136, 138, 144, 145	10
E	032, 045, 058, 073, 107, 110, 125	7
F	006, 028, 049, 052, 063, 064, 120, 126	8
G	012, 016, 111, 118, 124	5
H	054, 058a, 117, 141	4
I	053, 077, 080, 139, 143	5
Pre-fire	001	1

4.8.2 LEXT operation

The exhibit was placed onto the stage and the parameters of the software were checked. A file name was inputted for the exhibit to be scanned. The "live TV" option enabled the optical system to be focused. The magnification level was set and the intensity of the Non-Confocal image was adjusted.

The Confocal intensity was set to approximately 10 steps above the non-confocal image. The surface of the exhibit was viewed to check that the general intensity did not exceed the suggested range.

The X, Y and Z area of the exhibit to be scanned was selected and the scan commenced. The scan commenced repeating in steps from the top surface area to the bottom of the exhibit.

Once the scan was completed a three-dimensional image was obtained that could be navigated in the software. Measurements from selected points could be made and these were stored. A Rich Text Format (RTF) report could be created that detailed the scanned images and the measurements. All of the original scanned images were stored on the hard drive of the attached computer.

The "enhanced mode" and "real colour" options improved the quality and rendering of the final output.

4.8.3 Benefits of confocal laser scanning microscope

The equipment created a large number of useful images during the automated scanning process. The profile view and measurements embedded on to the scale are not available with other microscopic equipment and the automatic stitching of the scanned images enables an entire exhibit to be captured in one process.

4.8.4 Issues with a confocal laser scanning microscope

It was not possible to scan shapes with an angle that exceed 70 degrees and the instrument could not scan copper metal exhibits mounted on to aluminium. It was found that the image became jagged if the "enhanced" mode was not selected. The software also appeared to have a recurrent fault when generating the automatic RTF reports and would often crash whilst undertaking this function.

4.8.5 Comparison of SEM and LEXT images

The capturing of the entire exhibit surface when using the confocal laser scanning microscope with its ability to compile the stitched scans was found to be useful when evaluating metallic damage over a wide surface area of an electrical conductor. Arcing category A was found to be the most difficult arcing category to analyse when using the SEM compared to the LEXT. Figure 140 and figure 141 detail this difference with the five SEM scans stitched together separately with image manipulation software and the confocal laser scanning microscope capturing the same exhibit with a three-dimensional image with sufficient detail.

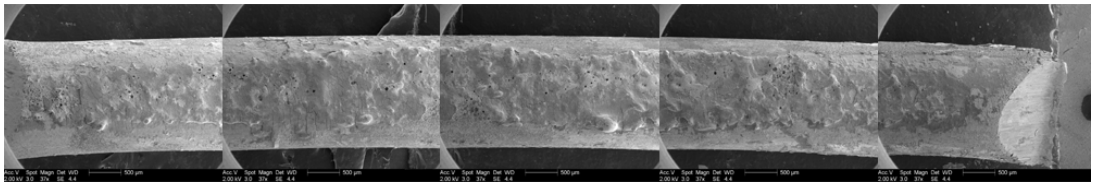

Figure 140 – Five SEM images stitched together to detail the extent of the arcing through char damage, exhibit 055 – arcing category A

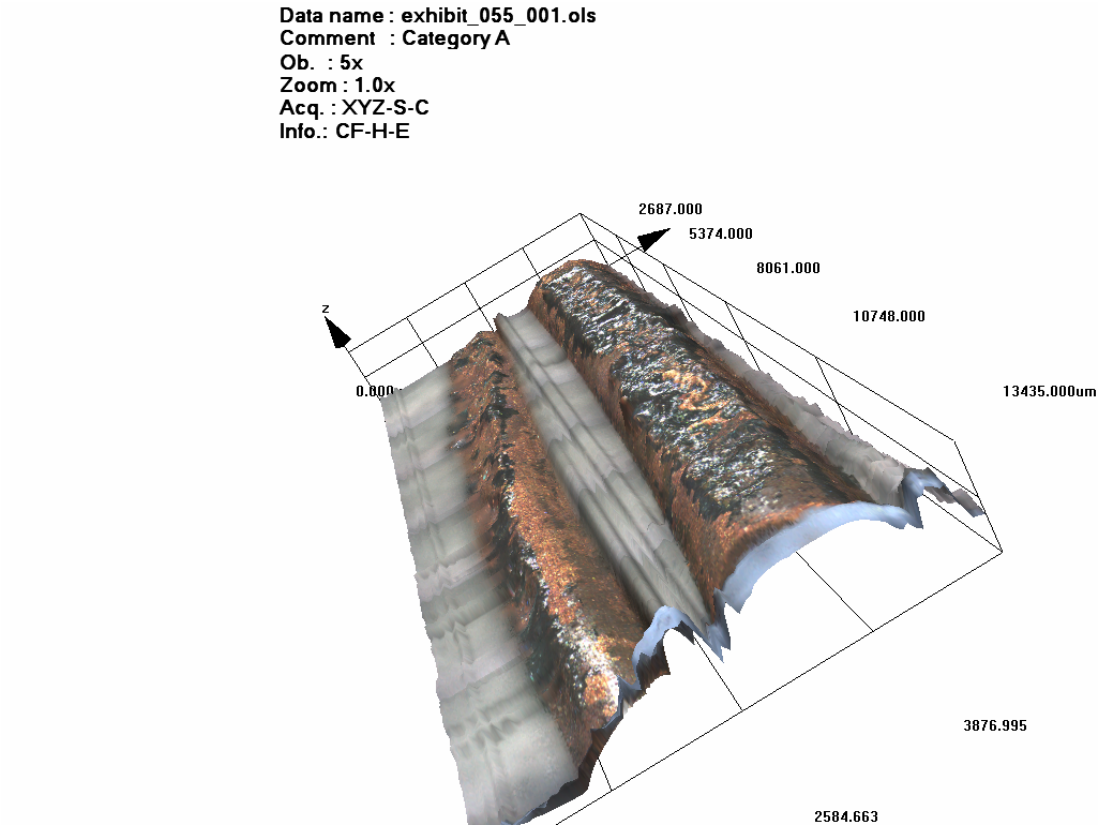

Figure 141 - A capture from the confocal laser scanning microscope of exhibit 055 – arcing category A.

The images captured for each arc using both the SEM and LEXT instruments are presented in volume two.

4.9 Microscopy conclusions

Several types of microscopy were used to analyse the exhibits recovered from the full-scale experimental fires. Overall the SEM produced the most detailed high-resolution images of the exhibits. However, the SEM was both time consuming to prepare the exhibits and to use the equipment. The Confocal laser scanning microscope produced versatile three-dimensional images with limited exhibit preparation time.

The element image maps were found to be of limited use to determine the type of localised metallic damage to an exhibit. However the elemental surface analysis highlighted a large number of elements that were present on the surface of the exhibits from the large-scale experimental fires. Six elements were explored in detail

and the results obtained indicated that the elemental profile of the arcs reflected the microenvironment within which they were formed. Evidence was found of element transfer between the cable fixing screws and the conductors.

The SEM and Confocal laser scanning microscope analysis techniques were found to be useful when analysing the demarcation area between the localised metallic damage to conductors and the undamaged area of the conductors. Both techniques could easily distinguish between pre-fire and post-fire arcing.

Chapter 5 Arc mapping

5.1 Introduction

The methodology of arc mapping was detailed earlier in this thesis: chapter 1, section 1.7. The literature review indicated that prior to this research the reliability of arc mapping had not been established with a series of full-scale experimental fires where different compartment scenarios were repeated.

One of the challenges of this research was evaluating the three-dimensional data that was collected during the full-scale experimental fires. Figure 142 details the relationship between the x, y, z co-ordinates of the fire's area of origin (x_o, y_o, z_o) and the x, y, z co-ordinates of the arcing damage for one of the four circuits (x_j, y_j, z_j).

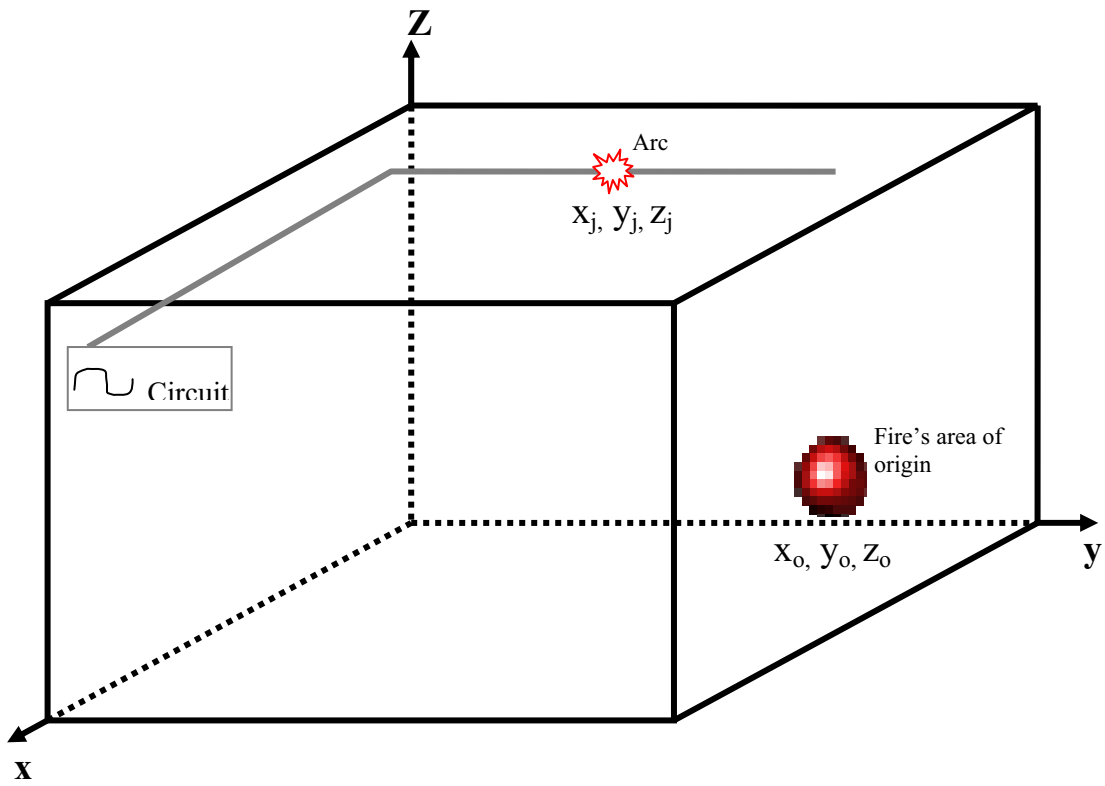

Figure 142 – Three-dimensional diagram showing the relationship between the fire's area of origin and the arcing damage on one circuit.

5.1.1 The data collection

Data relating to the fires area of origin (which was known in all of the 39 test experiments) was collected prior to the experiments commencing by measuring and recording x, y, z co-ordinates. Following the experimental fire the x, y, z co-ordinates of the arcing damage to the circuits was measured and recorded. The measurements were transferred into the compartment scale diagrams created with drawing package Microsoft Visio version 2003 software.

5.1.2 Calculations to undertake a probability analysis

A mathematical method was used to establish the relationship between the fire's area of origin and the arcing damage locations for the experimental fires [179]. The x, y and z co-ordinates were used for the fire's area of origin and the arcing damage for each separate electrical circuit in the compartment.

Fire's area of origin : (x_o, y_o, z_o)

Arc in circuit: (x_j, y_j, z_j)

The spatial relationship between the fire and the arcing damage can be represented by equation 9.

$$R_o = R_{oj} + R_j \qquad \text{equation 9}$$

Where:

R_o is the area of origin location

R_{oj} is the distance between the fire's area of origin and the arcing damage

R_j is the arcing damage location

The three-dimensional comparison between the arcing damage location and another three-dimensional point in the compartment using x, y and z co-ordinates is given by equation 10.

$$R_{oj} = \sqrt{(x_o - x_j)^2 + (y_o - y_j)^2 + (z_o - z_j)^2} \qquad \text{equation 10}$$

Figure 143 details a cross-sectional view of a compartment with the fire's area of origin, the actual arcing location and the minimum distance between the circuit and the fire's area of origin. R_{oj} is the distance between the fire's area of origin and the arcing damage on a circuit in the experimental fires and R_{min} is the minimum distance between the fire's area of origin location and the circuit that sustained the arc fault.

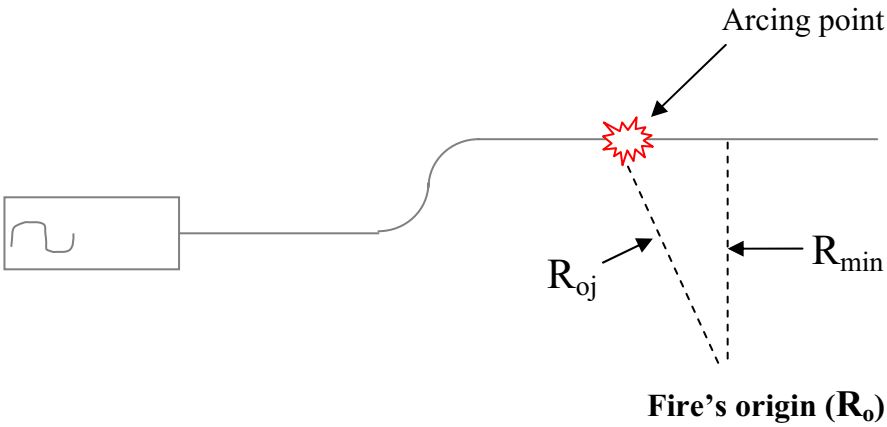

Figure 143 – A cross sectional view showing the two different distances from the fire's area of origin to the circuit's arcing point and the minimum possible distance.

The results were expressed as a probability value which gave a measure of the proximity of the arc to the point on the circuit closest to the fire's area of origin where a value of 1 means that they coincide.

5.1.3 Using spreadsheet software to automate the calculations

The data for R_{oj} and R_{min} with each circuit and experiment was inputted into a Microsoft Excel spreadsheet using the x, y, z coordinates for all of the experimental fires area of origin locations, the actual arc locations on the circuit, and the closest possible arcing locations from the fire's area of origin and the circuit. For the purposes of the calculations only fires which were set with one area of origin were included. As a consequence the total number of 39 practical experiments was reduced to 22.

The formulas to calculate R_{min} / R_{oj} (the minimum distance between the fire's area of origin and the arc, divided by the actual distance of the two locations) were inputted into the same spreadsheet.

The master spreadsheet of data was copied and collated so that there was a separate sheet for each experimental fire scenario. The data was analysed for each scenario and separate histograms created for the repeat tests. The three-dimensional location of the arcing damage for each circuit was compared to the closest point on that circuit to the fire's area of origin in each case.

5.1.4 Importing the data into a statistical package

The Excel spreadsheet data was imported and analysed with the statistical software package MiniTab version 15 (Minitab Inc. State College, PA. USA) and the results are detailed in figure 144. This statistical package was able to display all four separate circuit results on one histogram chart.

Statistical analysis suggests that the majority of the arcing events occurred on the electrical circuits within a short distance or adjacent to the closest possible points on the circuit to the fire's area of origin. The majority of the probability results were in the 0.85 to 1.0 range. A reduced probability for circuit 1 was observed for almost all of the experiments. The location of the cable for circuit 1 (the power ring circuit) was consistent throughout all of the experimental fires. The cable was located at the junction of the top of the walls and the ceiling. The fire dynamics appear to have slightly delayed the exposure of the PVC insulation to the heat flux in the fire's early development resulting in arcing damage occurring further away from the area of origin in some cases and resulting in a greater spread of results. Figure 144 details the results of all four circuits' results on to a single histogram.

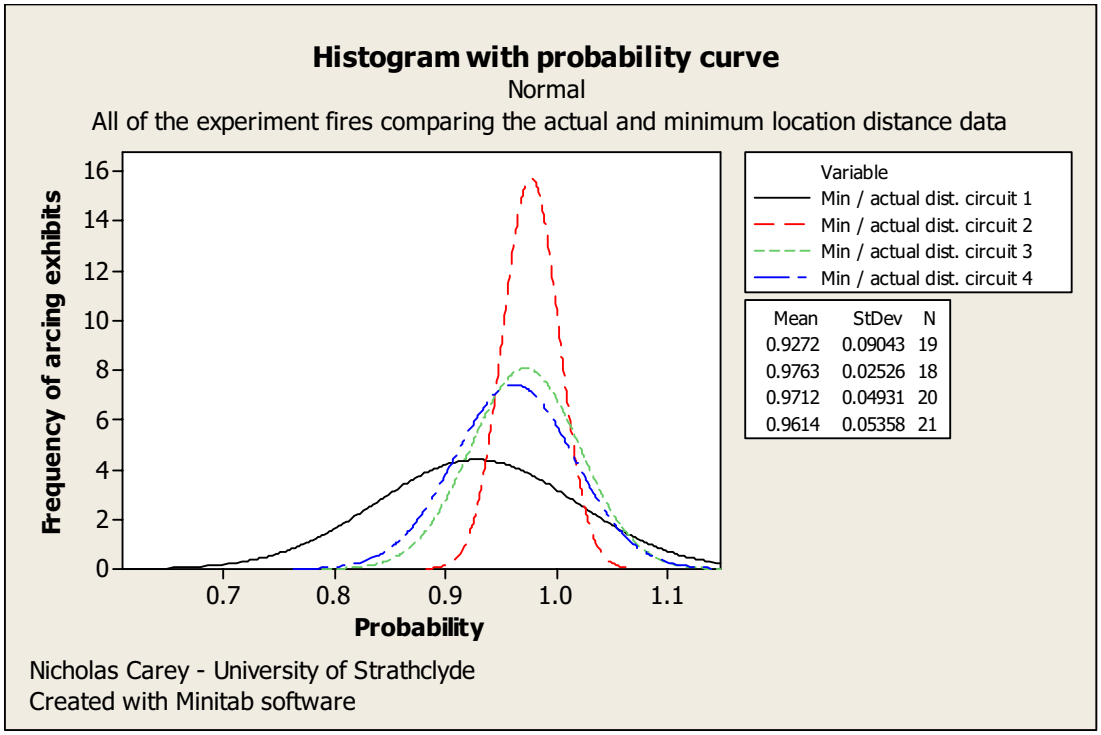

Figure 144 – Histogram detailing the probability of the arcing damage compared to the closest point on a circuit.

5.2 Arcing in more than one location on the same circuit

The effect of two separate points of arcing damage located on the same circuit was observed on 9 of the 156 circuits installed into the series of 39 experimental fires. The interpretation of this evidence is that an insufficient fault current flowed during the first arcing event on the circuit preventing the circuit breaker from operating on that occasion.

An example of this phenomenon is occurred in experiment 38 (scenario A). The post-fire examination revealed that the conductors for circuit 4 had electrically faulted creating arcing damage in two separate locations. Exhibit 141 from circuit 4 was located furthest from the electrical source, 0.5 meters of the fire's area of origin. Circuit 4 had then further faulted through circuit 1 (exhibits 139 and 139a) at a location 1.8 meters from the fire's area of origin. The effect of arcing in two separate locations on the same electrical circuit is illustrated in figure 145.

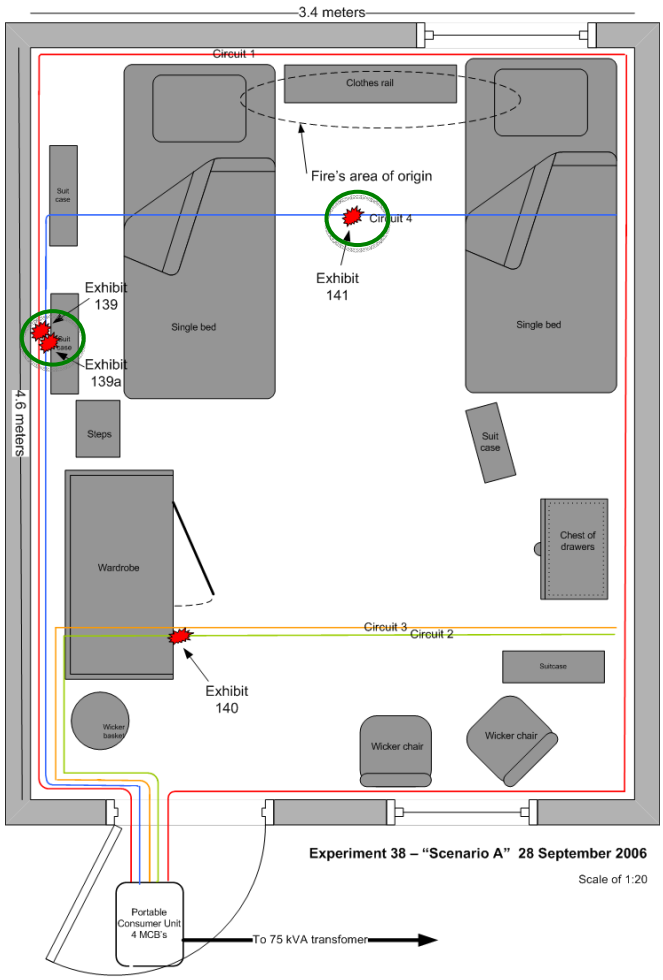

Figure 145 – Diagram of experiment 38 detailing two separate areas of localised metallic (arcing) damage on circuit 4.

In North America, arcing in more than one location on an electrical circuit exposed to a fire is frequently encountered [180]. Testing by the author and Svare in 1999 using US and European circuit breakers to protect wiring exposed to compartment fires suggested that European circuit breakers were more sensitive than North American circuit breakers in fault conditions [107].

Experience of the author whilst examining electrical wiring at fire scenes is that arcing damage at multiple points on an electrical circuit is not often observed in UK residential circuits. The difference in the circuit breaker design suggests that European circuit breakers de-energise circuits in fire conditions faster than the North American versions during arcing events. Experience of American investigators

indicates that residential circuits protected by 15 or 20 Amp circuit breakers will often demonstrate multiple arcing locations on a circuit [181].

5.3 Blind tests

A series of three blind test experimental fires was undertaken using different compartment fires with scenarios that were unknown. Four electrical circuits were installed into empty compartments in the same configuration as the previous 39 experiments. The compartments were furnished and then ignited. No observations were made of the interior of the three compartments until each of the fires were extinguished. The scenarios were laid out as a domestic lounge, a bedroom and a travel agents office. The conductors placed within the three scenarios were examined and the arcing locations were identified and documented.

5.3.1 Blind test 1

Blind test 1 was configured as a domestic lounge. The furniture layout was different to any of the six scenarios repeated in the previous experimental fires. A three-seat settee was located on the left wall. An armchair was located on the left wall in the rear left corner of the room. The room layout and position of arcing damage is illustrated in figure 146.

Arcing was observed on all four circuits. Circuit 4 had arcing damage 1 metre from the rear wall and 1.2 metres from the left wall. Circuits 1 and 4 had arcing damage between them adjacent to the left wall and 2.51 metres from the rear wall. Circuits 2 and 3 had arcing damage 1 metre from the front wall and 1.62 metres from the left wall.

The locations of the arcing damage suggested that the fire's area of origin was the armchair in the rear left corner of the room. The fire's actual area of origin was a refuse bin located between the armchair and the three-seat settee.

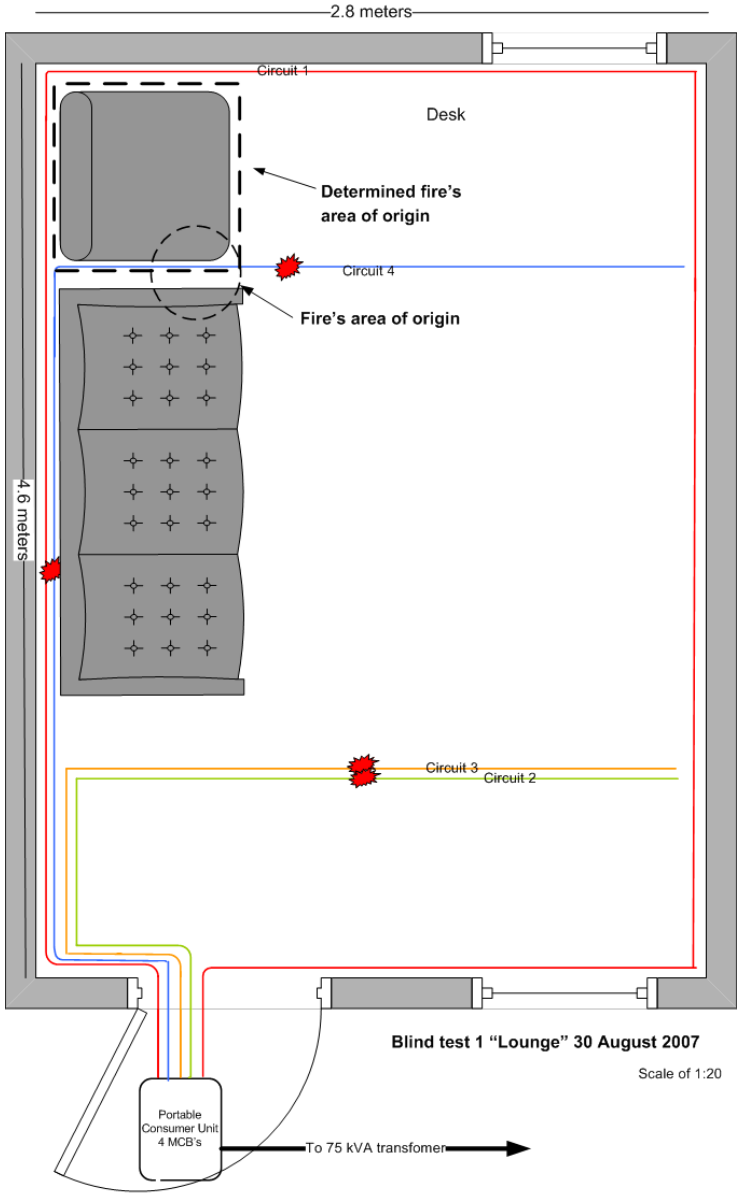

Figure 146 – Room plan for blind test 1 (furniture mainly omitted for clarity)

5.3.2 Blind test 2

Blind test 2 was configured as a travel agents office. The furniture layout was different to any of the six scenarios repeated in the previous experimental fires. The room was furnished with a desk and other items of furniture generally found in an office location. The room layout and position of arcing damage is illustrated in figure 147.

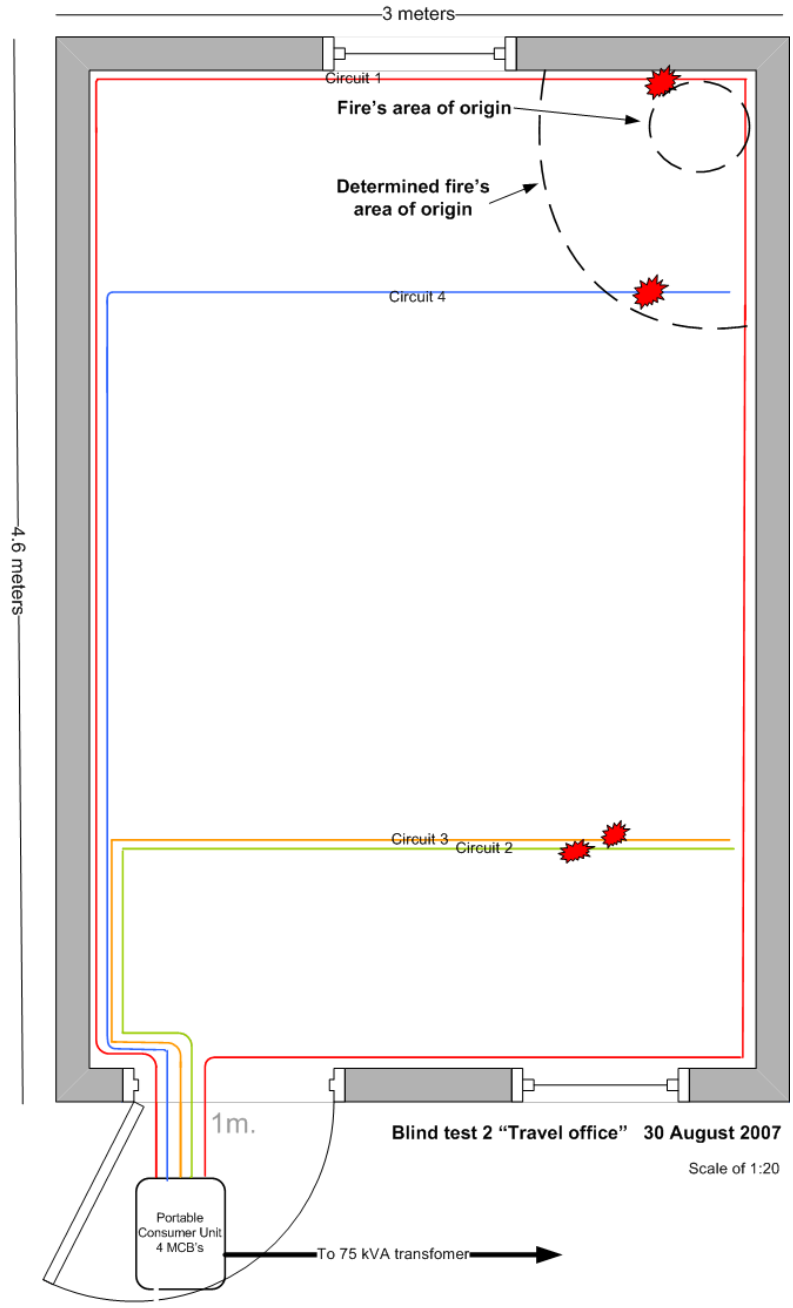

Figure 147 – Room plan for blind test 2 (furniture mainly omitted for clarity)

Arcing was observed on all four circuits. Arcing damage was located in two separate areas close to each other in the rear right corner of the compartment. Circuit 1 had arcing damage 0.4 metres from the right wall and adjacent to the rear wall. Circuit 4 had arcing damage 1 metre from the rear wall and 0.56 metres from the right wall. Circuits 2 and 3 had arcing damage 1 metre from the front wall and 0.84 and 0.65 metres respectively from the right wall. The locations of the arcing damage

suggested that the fire's area of origin was located in the rear right corner of the room. The fire's area of origin was located in a refuse bin in the rear right corner of the compartment.

5.3.3 Blind test 3

Blind test 3 was configured as a bedroom. The furniture layout was different to any of the six scenarios repeated in the previous experimental fires. The room was furnished with beds, a wardrobe and an armchair and is illustrated in figure 148.

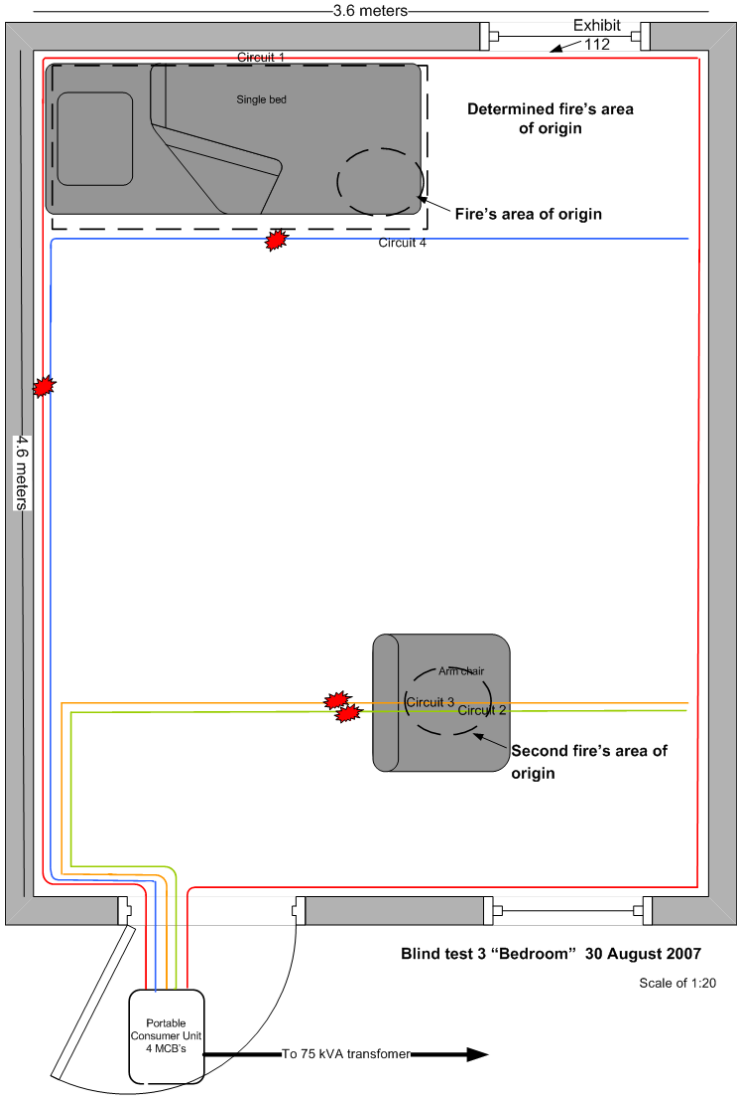

Figure 148 – Room plan for blind test 3 (furniture mainly omitted for clarity)

Arcing damage was located on all circuits. Arcing damage was located on circuit 1 adjacent to the left wall and 2.2 metres from the rear wall. Arcing damage was

located on circuit 4 one metre from the rear wall and 1.23 metres from the left wall. Arcing damage on circuits 2 and 3 were in the same location in the compartment, 1 metre from the front wall and 1.6 metres from the left wall.

The locations of the arcing damage suggested that the fire's area of origin was the single bed located in the rear left corner of the room. In this case the fire had two separate areas of origin. One was the end of the single bed located in the rear left corner of the room. The second area of origin was the armchair underneath and adjacent to the arcing locations of circuits 2 and 3.

5.4 Blind test x, y, z co-ordinates data analysis

The x, y, z co-ordinates for the three blind tests were analysed and illustrated similar probabilities as the experimental data. This demonstrated that the locations of the arcing damage on each electrical circuit when compared to the closest possible location to the fire's area of origin was a reliable indicator or the fire's area of origin. The exception was circuit 1, the ring main circuit, routed at the junction of the wall and ceiling in the compartments. The fire dynamics would add a lag to the exposure of the cable in this location when compared to the flow of the hot gases at ceiling level in the early development of the fire. This was also observed for circuit 1 in the experimental fires and suggests that arc mapping may be more indicative when located on cables which are not in corner configurations. Figure 149 details the probability of the x, y, z co-ordinates for the three blind tests.

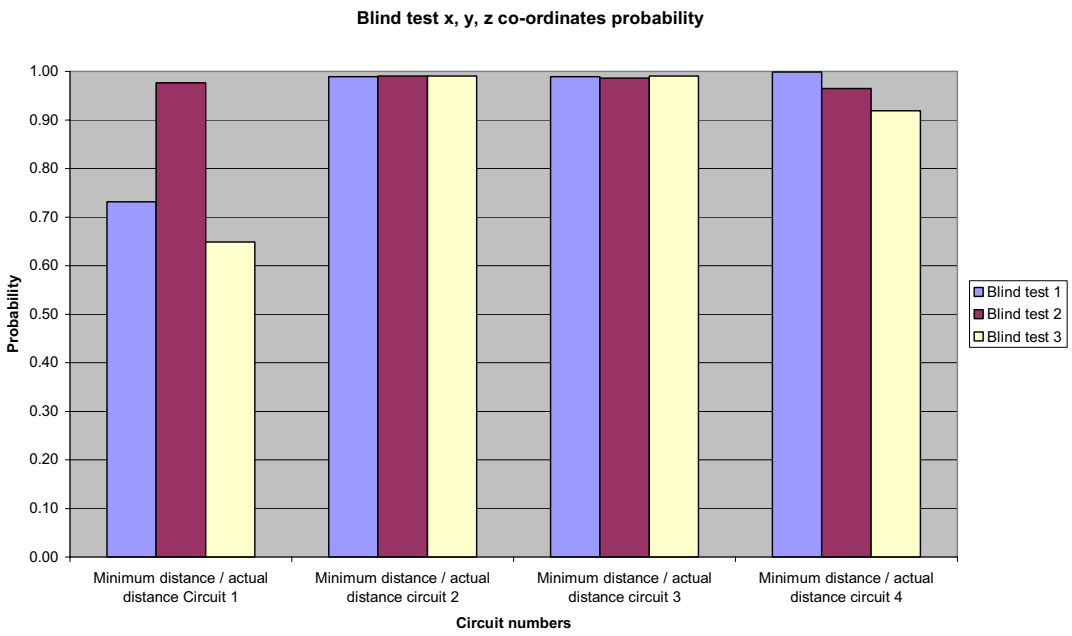

Figure 149 – Chart detailing the co-ordinates data analysis (series 1 represents blind test 1 etc.). The closer the value is to 1 the closer proximity of the arc to the part of the conductor which was closest to the fire's area of origin.

5.5 Arc mapping conclusions

Analysis of the three-dimensional data recorded during the experiments and the arcing events has indicated that there is a high probability of arcing damage occurring to electrical conductors located close to the fire's area of origin. The series of full-scale experimental fires with repeated scenarios mathematically validated the reliability of the arc mapping methodology. Blind testing where the arcing damage was used to suggest an area of origin of the fire was successful in all tests and illustrates its value in scene investigation.

Chapter 6 Conclusions and future work

6.1 Conclusions

6.1.1 Experiments

This work represents the first time that a systematic series of practical experiments has been undertaken involving the installation of fixed electrical wiring into fully furnished compartment fires that are repeated. The research involved a total of 62 compartments over a three-year period between 2004 and 2006 with 39 experiments using suitable electrical supply equipment.

The practical experiments involved fires in fully-furnished compartments. The furniture layout and compartment dimensions were repeated as scenarios. The fire's area of origin for each experimental scenario was kept as constant as possible within the parameters set by the fire investigation training provider hosting the fire scenes.

The optical microscope examination and documentation, established that these experiments produced a series of nine categories of arcing damage and that these arcing categories were repeated many times throughout the experiments with some small variations within each category. Microscopic examination also established that the chaotic event of electrical arcing produces evidence that while slightly different in size and shape, can still be categorised into one of the nine types.

The research involved fully-furnished compartment fires where the pre-fire layout and the fixing of the cables was known and documented. The fire's area of origin and its development in the compartment was also documented and observed.

6.1.2 Arcing through char

The research has demonstrated that "arcing through char" (a phenomenon documented in text books) is a metallic pattern that can be visually identified at a fire scene and discriminated from other metallic damage patterns. This type of arcing

appears to result as a consequence of the charring and degradation of the PVC insulation material sheathing the conductor.

6.1.3 SEM and Confocal laser scanning work

SEM and Confocal laser scanning microscope analysis were found to be useful when analysing the demarcation area between the localised metallic damage to conductors and the undamaged area of the conductors. The SEM has the advantage of facilitating the elemental analysis of the arc damage. It was demonstrated that the microenvironment of the arc had an effect on the elemental composition which could be contaminated by adjacent metals such as fixing screws. This suggests that elemental mapping of arc damage must be considered and contextualised to the immediate environment of the arc on the conductor. Microscopic analysis also indicated a clear distinction between pre and post fire arcing damage.

6.1.4 Statistical analysis of the data

The full data set and various sub sets of the data were analysed using the Spearman's rho correlation coefficient calculations. The tests have shown that the majority of variables in the experiments were not correlated with each other.

A significant correlation between the temperature at the time of the arcing event and the circuit breaker sequence was revealed. A correlation was also revealed between the time from ignition (seconds) and the circuit breaker operation sequence.

The lack of correlation between arcing pattern types (categories) and the other variables is a useful contribution to the fire investigation community. The analysis of each arcing category and repeated scenario revealed no correlations. This suggests that the type of metallic pattern produced during an arcing event is unpredictable.

6.1.5 Arc mapping

The series of full-scale experimental fires discovered that an arcing event can occasionally occur in more than one location on a circuit.

The analysis of the three-dimensional data has indicated that there is a high probability of arcing damage to electrical conductors occurring close to the fire's area of origin. The series of full-scale experimental fires with repeated scenarios has validated the reliability of the arc mapping methodology.

6.2 Future work

The installation of thermocouple trees into a number of fire compartments at Wethersfield to validate the ENSFI test fire temperature results is recommended. The thermocouple tree locations should be uniform to detect the temperature levels at ceiling height throughout the compartment.

Additional metallurgy analysis should be undertaken in the future to examine the internal grain structure of arcing damage to copper metal. The grain structure could then be categorised and compared to the data collected in the experiments to test for correlations in the dataset.

A research project should be planned to explore the creation of a zone model software package. The purpose of this software would be to predict the probability a fire's area of origin location within a compartment/building fire when the x, y, z co-ordinates of arcing events and the location of the electrical source are inputted.

References and bibliography

1. Lewis, M., *Electrical Installation Technology 2: Science and Calculations*. 1988. p. 27-30.
2. Carey, N.J., *Electricity handout 2 : Generation and distribution to buildings.* 2000.
3. RS Components, L. 2007 [cited 2007 26 February 2007]; Cable diagrams]. Available from: http://rswww.com.
4. *Requirements for Electrical Installations BS/EN 7671*. 17th ed. 2008: The Institution of Electrical Engineers, London.
5. BICC Cables, *Materials used in cables*, in *Electric Cables Handbook*, G.F. Moore, Editor. 2002, Blackwell Science Ltd. p. 49-50.
6. *Dielectric strength of solids*, in *CRC Handbook of Chemistry and Physics 1998-1999 17th Edition*, D. Lide, Editor. 1998, The Chemical Rubber Publishing Company. p. 15-33.
7. Babrauskas, V., *Mechanisms and Modes for Ignition of Low-Voltage PVC Wires, Cables, and Cords*, in *Fire & Materials 2005,*. 2005, Interscience Communications Ltd.,: London. p. 291-309.
8. Salovey R. and Bair H.E., *Degradation of Poly(vinyl chloride).* Journal of Applied Polymer Science, 1970. **14**: p. 713-721.
9. Otani H. and Kawamura K., *An experimental study on thermal deterioration of electric insulation of a PVC attachment plug.* Journal of Japan Society for Safety Engineering, 2003. **42**(4): p. 216-221.
10. Mullins, M., *The origin of the BS 1363 Plug and Socket Outlet System.* IEE Wiring Matters, 2006. **18**(Spring 2006).
11. BSI - British Standards, *Requirements for Electrical Installations BS/EN 7671* 2008, The Institution of Engineering and Technology.
12. E-ON Central Networks PLC. *Information for electrical contractors*. 2009 [cited 2009 12/04/2009]; Prospective short circuit currents and earth loop impedance measurements at single and three-phase electrical supplies in buildings.]. Available from: http://www.eon-uk.com/distribution/605.aspx.
13. Twibell, J.D. and C.C. Christie, *The forensic examination of fuses.* Science and Justice, 1995. **35**: p. 141-149.
14. Carey N. J., *5 Amp plug-top fuse*, DSC_1002.jpg, Editor. 2009.
15. Carey N. J., *40 Amp cartridgefuse designed for use in a distribution board*, DSC_9120.jpg, Editor. 2007.
16. Bussman. *BS88, IEC269 Industrial HRC Fuse Links*. 2007 [cited 7 March 2007]; Available from: http://www.bussmann.co.uk/images/Data%20Sheets/BS88/BD.pdf.
17. Prusaczyk, J.E. and R.M. Boardway, *The Effect of Thermal Insulation on the Fire Hazards of Electrical Wiring.* Fire Technology, 1982. **18**(2): p. 162-173.
18. Theriault, M. and A. Theriault, *Effects of Mineral Wool Insulation on Electrical Cables in Buildings.* Fire Technology, 1992. **28**(3): p. 228-239.
19. Carey, N.J., *Electricity handout 3 : Circuit Protection Systems.*. 2000.
20. Twibell, J., *Fire Investigation*, N. Nic Daeid, Editor. 2004, CRC Press. p. 77-78, 87-88, 98.

21. Lewis, M., *Electrical Installation Technology 1: Theory and Regulations*. 1992, Stanley Thornes (Publishers) Ltd. p. 79-85.
22. National Fire Protection Association - 921 Technical Committee, *Definitions*, in *National Fire Protection Association 921 Guide to Fire and Explosion Investigations.* . 2008, NFPA, Quincy, MA, USA. p. 15.
23. *Requirements for Electrical Installations BS/EN 7671 inc. amendment 1, 1994*. 1994, The Institution of Electrical Engineers, London. p. vi.
24. Tricker R, *Wiring Regulations in Brief: A Complete Guide to the Requirements of the 16th Edition of the IEE Wiring Regulations, BS 7671 and Part P of the Building Regulations*. 2007: Butterworth-Heinemann. 640.
25. Babrauskas, V. *How do electrical wiring faults lead to structure ignitions?* in *7th Fire & Materials Conference*. 2001. San Francisco, USA.
26. Beland, B., *Reflections on the cause and origin.* Fire and Arson Investigator Magazine, 1997. **48**(1): p. 8-9.
27. Butler, J. and T. Orr, *Following the wrong leads.* Fire Prevention, 1993(264): p. 26-27.
28. Twibell, J., *Reporting of electrical fires hides true picture.* Fire Prevention, 1995(282): p. 13-15.
29. *Department for Communities and Local Government - Fire Statistics, United Kingdom, 2005*. March 2007. p. 71.
30. Beland, B., *Examination of electrical conductors following a fire.* Fire Technology, 1980. **16**(4): p. 252 - 258.
31. Beland, B., *Considerations on arcing as a fire cause.* Fire Technology, 1982. **18**(2): p. 188-202.
32. Beland, B., *Electrical damages - cause or consequence?* Journal of Forensic Sciences, JFSCA, 1984. **29**(3): p. 747-761.
33. Beland, B., *Apparent electrical fires.* Fire and Arson Investigator Magazine, 1996. **47**(2): p. 19-21.
34. Beland, B., *Comments on Fire Investigation Procedures.* Journal of Forensic Sciences, JFSCA, 1984. **29**(1): p. 190-197.
35. Ettling, B., *Electrical wiring in building fires.* Fire Technology, 1980.
36. Ettling, B., *Arc marks and gouges in wires and heating at gouges.* Fire Technology, 1981. **17**(1): p. 61 - 68.
37. Ettling, B., *A Guide to Interpreting Damage to Electrical Wires.* Fire & Arson Investigator Magazine, 1986. **37**(2): p. 46-47.
38. UK Government - Department for Communities and Local Government, *Fire Statistics, United Kingdom, 2006*, Communities and Local Government, Editor. 2008, Communities and Local Government Publications,. p. 11 - 19.
39. Gardiner M., *Fire investigation training in the UK*. 2008.
40. NFPA, *National Electrical Code® 2005 Edition (NFPA 70)* 2005. 792.
41. Lee, D., A. Trotta, and W. King, *New Technology for Preventing Residential Electrical Fires: Arc-Fault Circuit Interrupters (AFCIs).* Fire Technology, 2000. **36**(3): p. 145-162.
42. IEE, *Request for information from the IEE in 2005*.
43. Cooke, R. and R. Ide, *Principles of Fire Investigation*. 1985, Institution of Fire Engineers. p. 279-280, 285-289.

44. Carey, N.J., *Practical electrical demonstrations*. 1998 - 2009, London Fire Brigade Training Centre and Gardiner Associates facilities (Wethersfield, Essex): London.
45. Twibell, J.D. and N.J. Carey, *Images taken from electrical demonstrations undertaken at Cambridge F&RS HQ*. 2001.
46. Till, I. *The Vauxhall Owners Network*. 2007 [cited 06/08/2007]; Available from: http://www.cavweb-forums.co.uk/showthread.php?t=39987.
47. Univeristy College Dublin. *The Siemens RoboRugby Autonomous Robot design competition*. 2007 [cited 06/08/2007]; Available from: www.roborugby.org/images/solder/dryjoint.jpg.
48. Ettling, B., *Glowing connections.* . Fire Technology, 1982. **18**(4): p. 344 - 349.
49. Meese, W. and R. Beausoliel, *Exploratory Study of Glowing Electrical Connections.* 1977, National Bureau of Standards. p. 29.
50. Sletbak, J., et al., *Glowing Contact Areas in Loose Copper Wire Connections.* IEEE Transactions on Components, Hybrids and manufacturing Technology, 1992. **15**(3): p. 322-327.
51. Aronstein, J. *Evaluation of Receptacle Connections and Contacts.* in *Proceedings of 39th IEEE Holm Conference on Electrical Contacts.* 1993: IEEE.
52. Meese, W. and R. Cilimberg, *Analysis of Current Technology on Electrical Connections in Residential Branch Circuit Wiring.* 1975, National Bureau of Standards. p. 23.
53. Stensaas, J., *Fires due to Electrical Installation Material.* 2006, SINTEF NBS - Norwegian Fire Research Laboratory. p. 65.
54. SINTEF-NBL. *Fire caused by electrical installations*. 2007 [cited 2007 17/04/2007]; Available from: http://www.sintef.no/content/page1____13533.aspx.
55. Davy, H.L., *Elements of Chemical Philosophy*. Vol. Part1 Volume 1. 1812.
56. Dunki-Jacobs, J.R., *The escalating arcing ground-fault phenomenon.* IEEE Transactions on Industry Applications, 1986. **IA-22**(6): p. 1156-1161.
57. Windred, G., *Electrical Contacts*. 1st ed. 1940: Macmillan and Co. Limited, London. 205-206, 240-242.
58. Ettling, B., *Electrical fire causes: some comments and cautions.* Speaking of fire - International Fire Service Training Association, (IFSTA), Oklahoma State University, 1985(Spring 1985).
59. Marquart, M., *Image of an arc being created by Nick Carey during a demonstration of a short circuit.* 2006, Gardiner Associates, Wethersfield, Essex.
60. Levinson, D., *Copper Metallurgy as a diagnostic tool for analysis of the origin of building fires.* Fire Technology, 1977. **13**(3): p. 211-222.
61. Svare, R., *Using the electrical system to help reconstruct the fire scene.* . 1998, Svare Professional Engineering.: Isanti, MN. p. 113-116.
62. Billings, M.J., A. Smith, and R. Wilkins, *Tracking in Polymeric Insulation.* IEEE Transactions on Electrical Insulation, 1967. **EI-2**(3): p. 131-137.
63. Noto, F. and K. Kawamura, *Tracking and Ignition Phenomena of Polyvinyl Chloride Resin Under Wet Polluted Conditions.* IEEE Transactions on Electrical Insulation, 1978. **EI-13**(6): p. 418-425.

64. Rajini, V., et al., *Comparison of Surface Tracking in Polymeric Insulating Materials.*, in *Powercon 2004 (2004 International Conference on Power System Technology)*. 2004, IEEE: Singapore.
65. Malooly, J., *Photograph of arcing through char demonstration*. 2007.
66. Munday, J.W., *Electrical Fire Causes and Diagnostics*, in *Fire Investigation Course Handout.* 2001. p. 4-6.
67. NFPA 921 Technical Committee, *Interpreting Damage to Electrical Systems.*, in *NFPA 921 Guide to Fire and Explosion Investigations*. 2004, NFPA, Quincy, MA, USA. p. 71-76.
68. National Fire Protection Association - 921 Technical Committee, *Electricity and fire*. 2008. 81-85.
69. Mansi P.M., *Observations at fire scene examinations*. 2008.
70. Andrews S., *Potential electrical causes of fire raised in court by the defence team*. 2008.
71. Davy, H., *The collected works of Sir Humphrey Davy*, J. Davy, Editor. 1840.
72. Davy, H.L., *Elements of Chemical Philosophy*. 1812, J. Johnson & Co.: London. p. Figure 17 of Plate III "A porcelain trough with plates of zinc and copper that are removable to form cells".
73. Davy, H.L., *Elements of Chemical Philosophy*. 1812, J. Johnson & Co.: London. p. Page 152 Figure 18 of Plate III "Two pieces of charcol about 1 inch long were brought near each other and a bright spark was produced.....a constant discharge took place through the heated air equal to at least 4 inches, producing a most brilliant ascending arch of light".
74. Ayrton, H., *The Electric Arc*. 1903, The Electrician Printing and Publishing Co.: London.
75. Barnard, S., *Beautiful Genius: Hertha Ayrton and the Electric Arc.* Proceedings of the IEEE, 2000. **88**(10): p. 1677-1679.
76. Sharp, E., *Hertha Ayrton 1854 – 1923*. 1926, London: Edward Arnold & Co.
77. Ayrton, H. *The Hissing of the Electric Arc*. in *Journal of the proceedings of the Institution of Electrical Engineers*. 1899.
78. Zeilder, J., *Electric arc lamps: Their principles, construction and working*. 1908.
79. Hepworth, C.M., *The Electric Arc Light for Lantern Projection ... With a description of the Ross-Hepworth Arc Lamps, and the new patent Eccentrical Carbons, etc*. 1897: pp. 23. Ross & Co.: London. 8º.
80. Maier, J., *Arc and glowlamps. A practical handbook on electric lighting*. The specialist series 1885.
81. Takikawa, H., et al., *Measurement of the radial temperature distribution in the central part of an arc burning through a polyethylene tube.* Electrical Engineering in Japan, 1993. **113**(1): p. 1-9.
82. Babrauskas, V., *Ignition Handbook*. 2003, Fire Science Publishers: Issaquah, WA, USA. p. 542-543, .
83. Ushio, M., *Arc discharge and electrode phenomena.* Pure and Applied Chemistry, 1988. **60**(5): p. 809-814.
84. *Dielectric strength of gases*, in *CRC Handbook of Chemistry and Physics 1998-1999 17th Edition*, D. Lide, Editor. 1998, The Chemical Rubber Publishing Company. p. 15 - 31.

85. Crnko, T., *Arcing fault hazards and safety suggestions for design and maintenance.* IEE Industry Applications Magazine, 2001. **7**(3): p. 23-32.
86. Gammon, T. and J. Matthews, *Historical evolution of arcing-fault models for low voltage systems.* Conference record of industrial and commercial power systems technical conference 2000, 1999: p. 1-6.
87. Gammon, T. and J. Matthews, *The application of current-dependant arc model to arcing at a main distribution panel, a sub-panel and a branch circuit.* Conference proceedings - IEEE Southeast + Con., 2001: p. 72-78.
88. Lee, R., *The other electrical hazard: Electrical arc blast burns.* IEEE transactions on industrial applications., 1982. **IA-18**: p. 246-251.
89. Pfeiffer, J., *Arc flash calculations.* Fire & Arson Investigator Magazine, 2005: p. 18-20.
90. Gammon, T. and J. Matthews, *Conventional and Recommended Arc Power and Energy Calculations and Arc Damage Assessment.* IEEE Transactions on Industry Applications, 2003. **39**(3): p. 594-599.
91. Kaufmann, R.H. and J.C. Page, *Arcing fault protection for low-voltage power distribution systems - Nature of the problem.* IEEE Transactions on Power and Apparatus, 1960: p. 160-167.
92. *The Elements*, in *CRC Handbook of Chemistry and Physics 1998-1999 17th Edition*, D. Lide, Editor. 1998, The chemical Rubber Publishing Company. p. 4-9.
93. Alexander, W. and A. Street, *Metals in the Service of Man.* 8th ed. 1982: Pelican.
94. Pops, H. *The Metallurgy of Copper Wire*. Innovations - On-line Journal of the Copper Development Association 1997 December 1997 [cited 28/03/2007].
95. University of Alabama. *Atomic spacing*. 2007 [cited 06/08/2007]; Available from: http://bama.ua.edu/~stjones/AtomSpacing.htm.
96. Gray, D., *Investigation of electrical fires.* MSC Thesis in Fire Engineering - University of Edinburgh., 1982.
97. Deplace, M. and E. Vos, *Electric short circuits help the investigator determine where the fire started.* Fire Technology, 1983. **19**(3): p. 185-191.
98. *Thermal and physical properties of pure metals*, in *CRC Handbook of Chemistry and Physics 1998-1999 17th Edition*, D. Lide, Editor. 1998, The Chemical Rubber Publishing Company. p. 12-191.
99. Carey, N., M.J. Svare, and M. Dubbin. *Arc fault mapping - a technique to assist in identifying a fire's area of origin.* in *International Association of Arson Investigators Annual General Meeting*. 2006. Denver, USA.
100. Churchward, D., R. Cox, and D. Reiter, *Arc surveys as a means to determine fire origin in residential structures.*, in *International symposium on Fire Investigation, Science & Technology (2004),* . 2004: Fire Service College, UK.
101. Johnson, W. and L. Rich. *Arc Fault Analysis: Post flashover studies of the power cord.* in *Fire and Material Conference, 2007*. 2007. San Francisco, USA.
102. Svare, M.J., M. Dubbin, and N.J. Carey. *Reconstructing the fire scene using the electrical system*. in *International Association of Arson Investigators, ATC*. 2006. Denver, USA.
103. Svare, R., *Arc Mapping*. 1999.

104. Rothchild, L., *Some fundamental electrical concepts in locating the cause and origin of a fire.* . National Association of Forensic Engineers (NAFE) Journal, 1986. **175A**: p. 37-44.
105. Svare, R., *Determining Fire Point-of-Origin and Progression by Examination of Damage in the Single Phase, Alternating Current Electrical System.* Journal of People to People, International Arson Investigation Delegation to the People's republic of China and Hong Kong, 1988.
106. Svare, R. *Arc Mapping*. in *Live, Learn, Pass It On*. 1999. Brunel University, Uxbridge, London.
107. Carey, N., *Comparison of behaviour during a fire: UK & US electrical wiring systems*. 1999, London Fire Brigade. p. 10.
108. Carey, N., *Powerful Techniques - Arc Fault Mapping*. Fire Engineers Journal, 2002: p. 47-50.
109. DeHaan, J.D., *Kirk's Fire Investigation - Sixth Edition*. 2006, Pearson - Prentice Hall: Upper Saddle River, NJ. p. 415-418.
110. Hoffman, D.J., *Arc mapping to determine Fire 'Point-of-Origin'*. 2002, SEL report, (Safety Engineering Laboratories Inc., Michigan, USA).
111. Icove, D. and J.D. DeHaan, *Forensic fire scene reconstruction*. 2004, Prentice Hall, Upper Saddle River, NJ. p. 137-138.
112. Sanderson, J., *Arc Mapping - special report.* Fire Findings 2005. **13**(2): p. 7-11.
113. Churchward, D., R. Cox, and D. Reiter, *Arc surveys as a means to determine fire origin in residential structures.* Fire & Arson investigation conference proceedings, Fire Service College (UK) and NFPA 921 committee, June 2004, 2004.
114. Jonson, S., *Electrical causes of fire with special emphasis on primary and secondary damages: A review of the literature.* 1993, SKL - National Laboratory of Forensic Science, Sweden.
115. Babrauskas, V. *Fires due to electrical arcing: Can 'Cause' beads be distinguished from 'Victim' beads by physical or chemical testing?* in *Fire and Materials 2003*. 2003: Interscience Communications Ltd., London.
116. Lee, E.-P., et al., *Study on discrimination between primary and secondary molten marks using carbon residue.* Fire and Safety Journal, 2002. **37**: p. 353-368.
117. *Methods for use in fire investigation*. 1980: USA. p. 10.
118. Anderson, R.N., *Surface analysis of electrical arc residues in fire investigation.* Journal of Forensic Sciences, JFSCA, 1989. **34**(3): p. 633-637.
119. Howitt, D.G., *The Surface Analysis of Copper Arc Beads - A Critical Review.* Journal of Forensic Science, 1997. **42**: p. 608-609.
120. Beland, B., *Examination of arc beads by Auger Spectroscopy.* Fire and Arson Investigator Magazine, 2004(April): p. 41-42.
121. Beland, B., *Some criteria to distinguish between: Electrical causes and consequences of fires.* Fire & Arson Investigator Magazine, 2005: p. 12-14.
122. Beland, B., *Arcing phenomenon as related to fire investigation.* Fire Technology, 1981. **17**(3): p. 189 - 201.
123. Beland, B., *The overloaded conductor.* Fire & Arson Investigator Magazine, 1981: p. 56-59.

124. Beland, B., *Heating of damaged conductors.* Fire Technology, 1982. **18**(3): p. 229 - 236.
125. Beland, B., *Arc Tracking in Relation to Fire Investigation.* Fire & Arson Investigator Magazine, 1995: p. 27-29.
126. Beland, B., *Short circuit current for the fire investigator.* Fire and Arson Investigator Magazine, 1996. **46**(4): p. 19-21.
127. Beland, B., *Rating and Insulation of Electrical Devices.* Fire & Arson Investigator Magazine, 1996. **47**(1): p. 21-23.
128. Beland, B., *Theory, Tests and Field Experience.* Fire & Arson Investigator Magazine, 1996. **46**(4): p. 1.
129. Beland, B., *Inrush Current.* Fire & Arson Investigator Magazine, 1996. **46**(3): p. 36-37.
130. Beland, B., *Mechanical behaviour of copper conductors in relation to fire investigation.* Fire and Arson Investigator Magazine, 1997. **47**(4).
131. Beland, B., *Reflections on the Cause and Origin.* Fire & Arson Investigator Magazine, 1997. **48**(1): p. 8-9.
132. Beland, B., *Small Fires Can Be Difficult To Investigate.* Fire & Arson Investigator Magazine, 1997. **47**(4): p. 20.
133. Beland, B., *An Unusual Explosion.* Fire & Arson Investigator Magazine, 2006. **57**(2): p. 40-42.
134. Beland, B., C. Roy, and M. Tremblay, *Copper-Aluminium interaction in fire environments.* Fire Technology, 1983. **19**(1): p. 22 - 30.
135. Babrauskas, V., *Electrical discharges through air : What voltage is required to cause arcs and sparks?* Fire Findings, 2004. **12**(1): p. 1-4.
136. Kelter, M., *Wethersfield Site*, in *Microsoft Publisher*, Idea_for_proposed_new_block_plan.pub, Editor. 2006, Gardiner Associates Ltd.
137. BSI - British Standards, *BS 6004:2000 Electric cables - PVC insulated, non-armoured cables for voltages up to and including 450/750 V, for electric power, lighting and internal wiring*. 2000. p. 14.
138. Svare, M., *Three-phase generator limitations*. 2004.
139. *Requirements for Electrical Installations BS/EN 7671 inc. amendment 1, 1994*. 16th ed. 1994: The Institution of Electrical Engineers, London. 279.
140. BSI - British Standards, *BS EN 60947-3:1999 Low-voltage switchgear and controlgear - Part 3: Switches, disconnectors, switch-disconectors and fuse-combination units*. 1999.
141. Pico Technology. *TC-08 Thermocouple Data Logger* 2007 [cited 17/04/2007]; Available from: http://www.picotech.com/thermocouple.html.
142. Stuart, N., *Graph produced from the time temperature data acquisition at Wethersfield site.* 2006, Gardiner Associates Limited.
143. AMEC. *CL600 Clamp-On AC Loggers* 2004 [cited 18/04/2007]; Available from: http://www.aemc.com/products/html/moreinfo.asp?id=3010801&dbname=products.
144. AMEC. *L260 RMS Voltage Module*. 2004 [cited 18/04/2007]; Available from: http://www.aemc.com/products/html/moreinfo.asp?id=3010602&dbname=products.

145. Chauvin Arnoux Inc., *Simple Logger Software version 6.11*. 2002, Chauvin Arnoux Inc.,.
146. Marquart, M. and D. Heenan, *Photograph of the post-fire electrical examination.* 2006, Gardiner Associates, Wethersfield, Essex.
147. Marquart, M. and D. Heenan, *Series of images taken at Wethersfield, Essex*. 2006, US Bureau of Alcohol, Tobacco, Firearms & Explosives: Wethersfield, Essex.
148. Barrow, D., *Chemistry of electric fuse arcing.* IEE Proceedings, part A: Physical science, measurement & instrumentation, Management & Education, Reviews., 1991. **138**(1): p. 83-88.
149. Gray, D.A., D.D. Drysdale, and F.A.S. Lewis, *Identification of electrical sources of ignition in fires.* Fire Safety Journal, 1983. **Vol 6**(2): p. 147-150.
150. Hoffman, J., ., and . *Electrical power cord damage from radiant heat and fire exposure.* Fire Technology, 2001. **37**: p. 129-141.
151. Lentini, J., *Scientific Protocols for Fire Investigation*. 2005, CRC - Taylor & Francis. p. 88-89, 238-239, 337-338.
152. Yereance, R., *Electrical Fire Analysis*. 1995, Charles C. Thomas Publishers. p. 202-205.
153. Carey N. J. and Nic Daeid N., *The metallic damage to electrical conductors at fire scenes*, in *Interflam 2007*. 2007, Interscience Communications: University of London, Royal Holloway College, Egham, Surrey.
154. DeHaan, J.D., *Kirk's Fire Investigation - Sixth Edition*. 2006, Pearson - Prentice Hall: Upper Saddle River, NJ. p. 346.
155. Carey, N.J., *Gross melting to electrical conductor*, DSC_6555.jpg, Editor. 2008: London.
156. Weaver P.M. and J.W. McBride. *Conductive measurements in the investigation of short circuit arcs in miniature circuit breakers*. in *41st IEEE Holm conference on Electrical Contacts*. 1995.
157. BSI - British Standards, *Electric cables — PVC insulated, non-armoured cables for voltages up to and including 450/750 V, for electric power, lighting and internal wiring* 2000, British Standards Institute: London.
158. Aitken C and Taroni T, *Multivariate Normal and correlation*, in *Statistics and the Evaluation of Evidence for Forensic Scientists*. 2004, John Wiley & Sons, Ltd: Chichester. p. 64-67.
159. Deborah Rumsey, *Quantifying the Relationship: Correlations and Other Measures*, in *Statistics for Dummies*, M. Hacker, Editor. 2003, Wiley Publishing Inc.: Hoboken, New Jersey. p. 287-296.
160. Nic Daeid, N., *Fire and Explosion Investigation Working Group Live Burn project - Cardington 2001*. 2002, European Network of Forensic Science Institutes: Glasgow. p. 72.
161. Nic Daeid, N., *The ENSFI fire and explosion investigation working group and the European live burn tests at Cardington.* Science and Justice, 2003. **43**(1): p. 49-54.
162. DeHaan, J.D., *Full-scale Compartment Fire Tests.* News of the California Association of Criminalists, 2001. **2nd Quarter 2001**: p. 14-21.
163. Ernst Ruska, *Nobel Lectures.* Physics 1981-1990, 1993.

164. Mary Bellis. *History of the Microscope - Electron Microscope*. 1997 [cited; Available from: http://inventors.about.com/od/mstartinventions/a/microscope_2.htm.
165. *Structural Probe Inc. v. Franklin Institute*, in *450F*. 1978.
166. Crane (Crane Engineering), *The role of a metallurgist - analysis of electrical conductors recovered from fire scenes using an SEM*. 2003: Minneapolis.
167. Carey, N.J., *Image of the exhibits cleaning process at the Centre for Forensic Science laboratory*. 2006.
168. Cameca. *Cameca SX100 Electron Probe Micro Analyzer - Synopsis*. 2009 [cited 2009 24/06/2009]; Diagram of the SX100]. Available from: http://www.cameca.com/doc_en_pdf/SX100_synoptic_web.pdf.
169. Schields P.J. *Bragg's Law and Diffraction: How waves reveal the atomic structure of crystals*. 2007 [cited 2009 24/06/2009]; Explanation of Bragg's Law with a Java applet to use the calculus]. Available from: http://www.eserc.stonybrook.edu/ProjectJava/Bragg/.
170. Cameca - France. *EPMA - Analysis techniques*. 2009 [cited 2009 24/06/2009]; Available from: http://www.cameca.com/html/epma_technique.html.
171. Carey, N.J., *Image of Cameca SX100 SEM at University of Strathclyde - Dept. of Physics (DSCN3773.jpg)*. 2006.
172. Edwards P., *The use of element maps on electrical conductors with arcing damage*, N.J. Carey, Editor. 2006: Glasgow.
173. Carey, N.J., *Image of FEI Sirion 200 at University of Strathclyde - Dept. of Physics (DSCN3768.jpg)*. 2006.
174. Carey, N.J., *Image of the SEI Sirion 200 with the stage exposed (DSCN3777.jpg)*. 2006.
175. Carey, N.J., *Image of the exhibits mounted onto the SEM aluminium alloy stub (DSCN3785.jpg)*. 2006.
176. Olympus Corporation, *Microscope general catalogue for industrial use*. 2008.
177. Olympus Corporation, *Confocal Laser Scanning Microscope LEXT OLS3100.* 2008.
178. Olympus Corporation, *Olympus Confocal Laser Scanning Microscope LEXT OLS 3000 Users Manual*. 2005.
179. Quintiere J, *Calculations to undertake a probability analysis of three dimensional points*. 2007: Kuala Lumpur.
180. Svare, R., *Arcing in more than one location on a circuit in the US*. 2008: Minneapolis, USA.
181. Svare, M.J., *Multiple areas of arcing on electrical circuits in North America.* 2003: MN.

University of Strathclyde

Department of Pure and Applied Chemistry
Centre for Forensic Science

Developing a reliable systematic analysis for arc fault mapping

by

Nicholas John Carey

A thesis presented in fulfilment of the requirements for the degree of Doctor of Philosophy

Volume 2

2009

This thesis is the result of the author's original research. It has been composed by the author and has not been previously submitted for examination which has led to the award of degree.

Signed: **Date:**

Contents

Introduction

The large scale tests were all undertaken at a fire investigation training facility located at the Ministry of Defense Police Headquarters and Training Centre, located at Wethersfield, Essex, United Kingdom. This facility allowed for the test scenarios to be carried out under realistic conditions, which would normally be encountered during the development of a compartment fire from its ignition to flashover conditions. A total of 39 experiments were conducted between March 2005 and September 2006.

The facility was located within a large ex-military airfield complex. The fire ground area was made up of twelve compartments. Four of these were located in mobile homes that were structurally reinforced with timber and dry lined with plasterboard. The other eight compartments were arranged in two terraced blocks. They were constructed with concrete blocks with internal timber-framed walls that divided each building into four separate compartments. The compartments were internally dry lined with plasterboard and a skim of plaster with a finish that was consistent with conventional residential and light commercial construction. Each compartment was fitted with an external door and either one or two single glazed windows.

The facility had a dedicated electrical supply consisting of a diesel powered 65kVA three-phase 415 volt generator. A custom-built 75kVA three-phase to single phase transformer was designed, built and installed at the facility for the purposes of this research project. A four-core armoured cable ($95mm^2$) was also specified and installed to link the generator and the transformer with minimum electrical losses. The electrical supply configuration was required at this remote location to replicate a typical electrical intake within a residential or light commercial building. The electrical supply configuration was consistent throughout the series of experiments. Figure 1 is a site plan detailing the buildings, the generator and the transformer.

A dedicated cable set was constructed to link the transformer output to a portable electrical distribution board. The distribution board was positioned directly outside

each compartment prior to the experiment. Four separate final electrical circuits were installed into the compartments and connected to the portable distribution board. The cables were fixed to the ceiling and routed to replicate typical electrical circuits used in the UK.

Circuit 1 was wired with 2.5mm^2 PVC/PVC cable in a "ring" circuit configuration with 32A circuit protection, replicating a power circuit. Circuit 2 was wired with 2.5mm^2 PVC/PVC cable in a "radial" circuit configuration with 16A circuit protection, replicating a dedicated electrical appliance circuit. Circuits 3 and circuit 4 were wired with 1.0mm^2 PVC/PVC cable in radial configurations with 6A circuit protection, replicating lighting circuits.

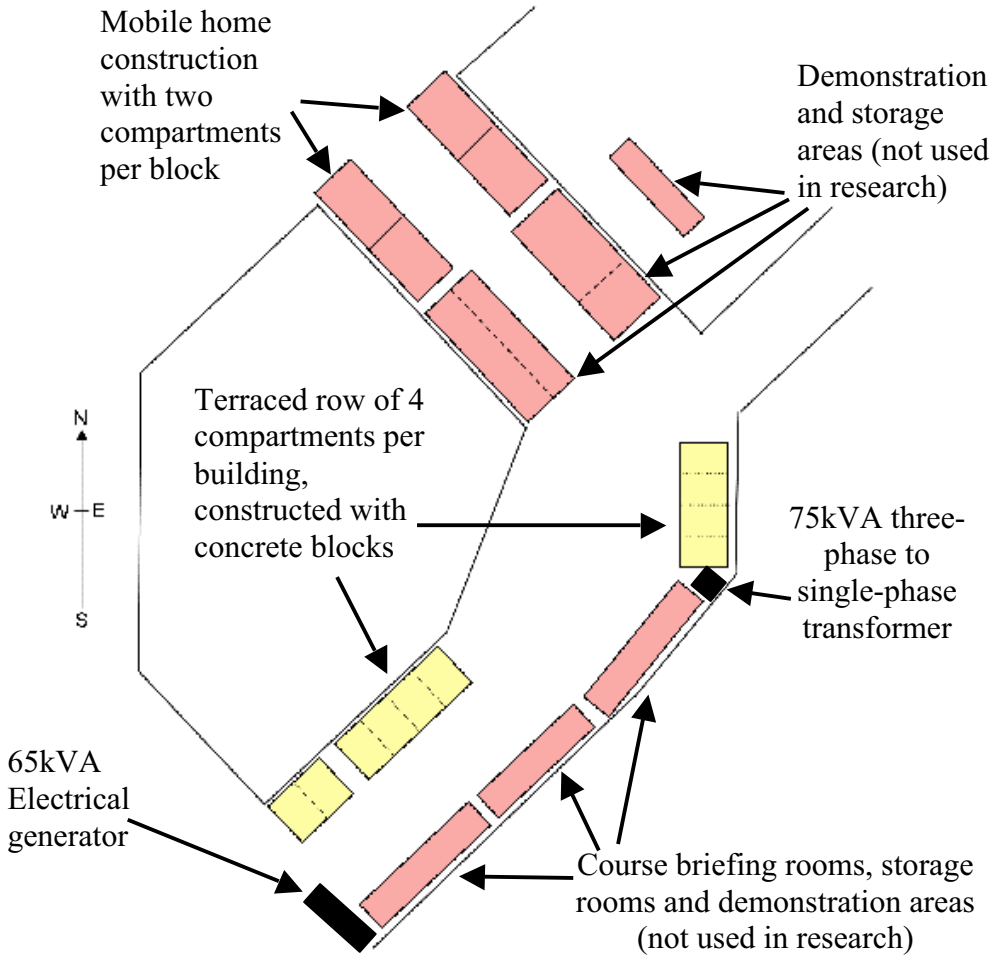

Figure 1 – Overview of the facility used for the experiments

A number of fire scene scenarios were used for training purposes. These provided the test scenarios within which the electrical conductors related to this research were placed and facilitated the reproducibility of the experimental scenarios. The data collected during each experiment has been summarised in this volume. A diagram of each experiment details the cable routes and the location of the localised metallic (arcing) damage. Pre-fire and post-fire photographs have been selected to document the experiments. Several experiments include additional photographs to detail the fire development at different stages.

Microscopic photographs of each exhibit have been used to detail the localised metallic (arcing) damage to the electrical conductors recovered from the experiments. Scanning Electron Microscope (SEM) and Confocal Laser Scanning Microscope (Olympus LEXT) images are included for the selected exhibits subjected to this additional analysis.

Table 1 – Scenario type and dates for the 39 experiments.

	10 March 2005	14 April 2005	8 September 2005	29 September 2005	23 March 2006	20 April 2006	11 May 2006	22 June 2006	7 September 2006	28 September 2006
Scenario A	☒	☒			☒	☒	☒	☒	☒	☒
Scenario B	☒			☒	☒	☒	☒	☒	☒	☒
Scenario C		☒	☒		☒	☒	☒	☒	☒	☒
Scenario D			☒	☒	☒	☒	☒	☒	☒	☒
Scenario E	☒	☒	☒	☒						
Scenario F	☒	☒	☒							

The red line indicates the date after which all experiments were completed within concrete block buildings dry-lined with plasterboard.

Experiment 1

Figure 2 - “Scenario A” 10 March 2005

Circuit number	MCB operating time from ignition
1	2:10 minutes
4	2:20 minutes
3	2:50 minutes
2	3:23 minutes

Table 2 – circuit breaker data

The fire in experiment 1 (scenario A) originated in clothing hung on a clothes rail located between two single beds at one end of the compartment. .

The fire developed rapidly and the ceiling and middle thermocouples recorded a maximum temperature of 950 degrees and 1000° C respectively within 5 minutes from ignition. The floor thermocouple recorded a temperature of 300° C at 5 minutes. The external observations of the fire development and post-fire burn patterns suggest that the compartment reached flashover conditions. Arcing damage on the conductors of all four circuits was visually observed.

Arcing damage was located on circuit 1 – 1.22m from left wall and adjacent to the rear wall.

Arcing damage was located on circuit 2 – 2.6m from rear wall and adjacent to the right wall.

Arcing damage was located on circuit 3 – 2.6m from rear wall, adjacent to the right wall and 100mm from below the ceiling.

Arcing damage was located on circuit 4 – 1.7m from the rear wall and adjacent to the right wall.

Pre-fire and post-fire photographs of experiment 1

Figure 3 - Pre-fire photograph, view from the doorway. The black oval indicates the fire's area of origin.

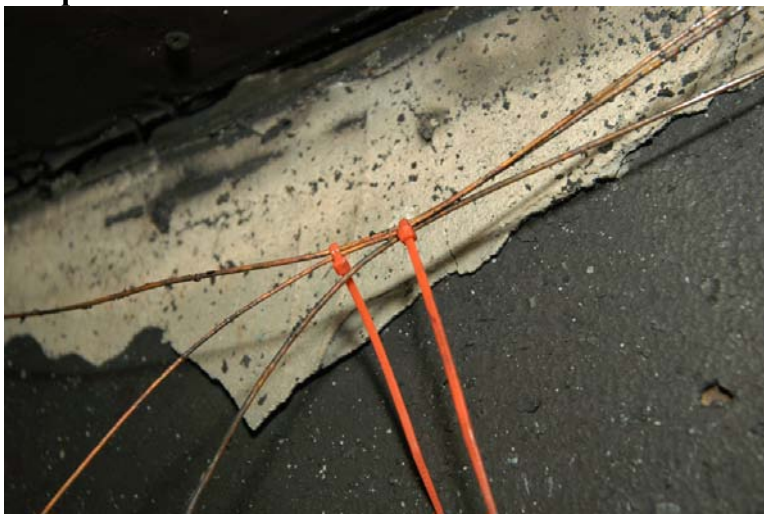

Figure 4 - A close-up photograph detailing exhibit 001 in-situ prior to recovery.

Figure 5 - Post-fire photograph. The white oval indicates the fire's area of origin. The white arrow indicates location of exhibit 001.

Figure 6 - Post-fire photograph indicating the arcing damage to circuit 3 above the doorway.

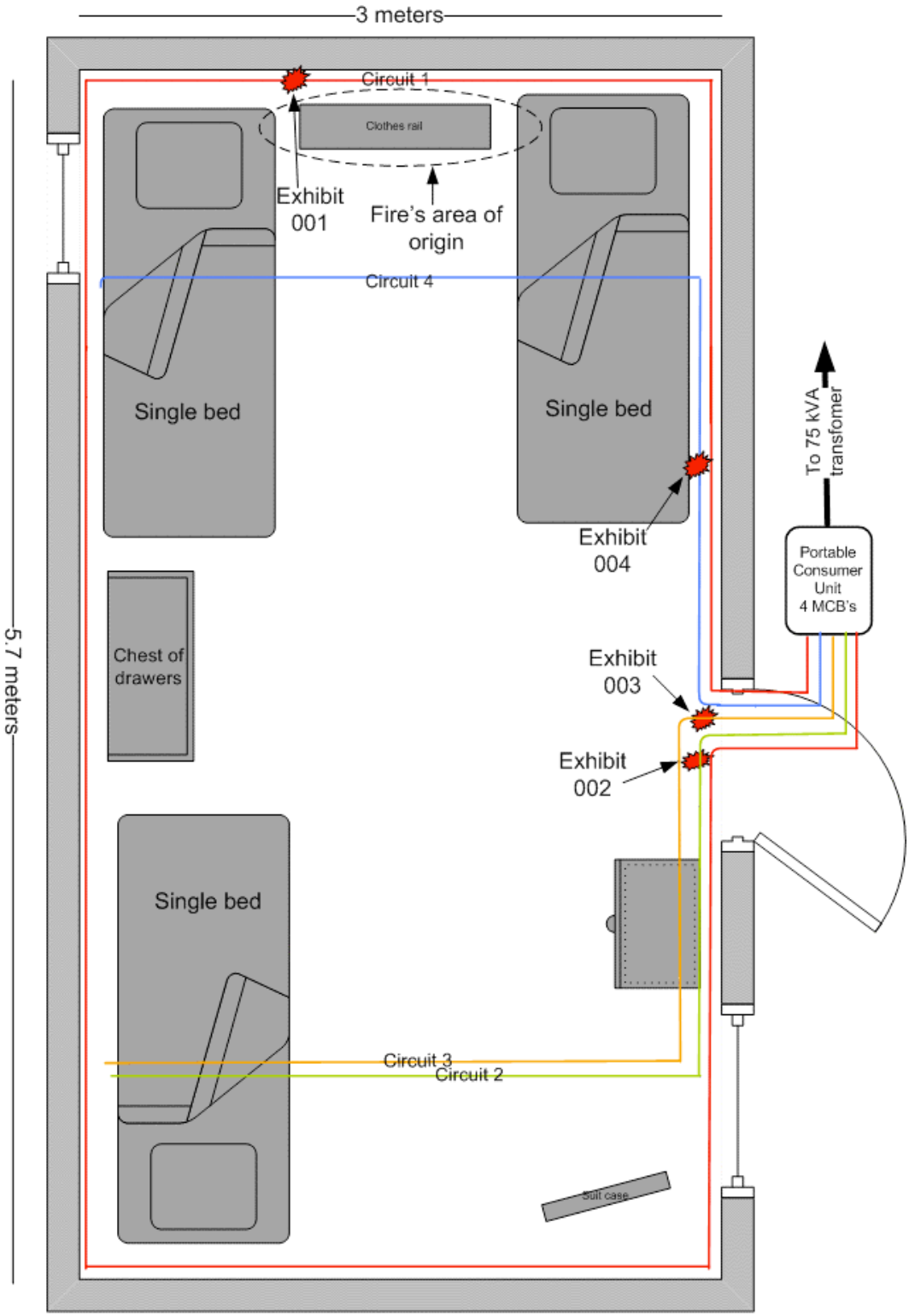

Figure 7 - **Experiment 1 – "Scenario A" 10 March 2005**

Scale of 1:25

Microscope images for exhibit 001 – arcing category A (experiment 1)

Figure 8 - Microscope image of exhibit 001 with localised metallic damage affecting two of the three conductors

Figure 9 - Microscope image of exhibit 001 at 20x magnification, detailing the wide area of lateral metallic damage.

Microscope and SEM images for exhibit 002 – arcing category A (experiment 1)

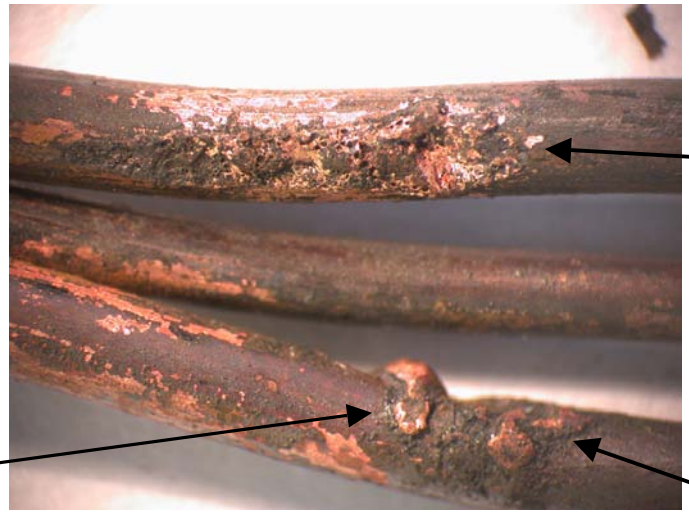

Figure 10 – Microscope image of exhibit 002.

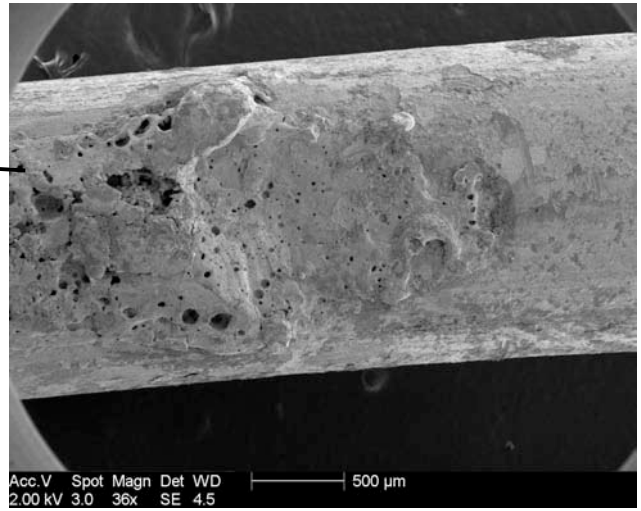

Figure 11 - SEM image of the top conductor.

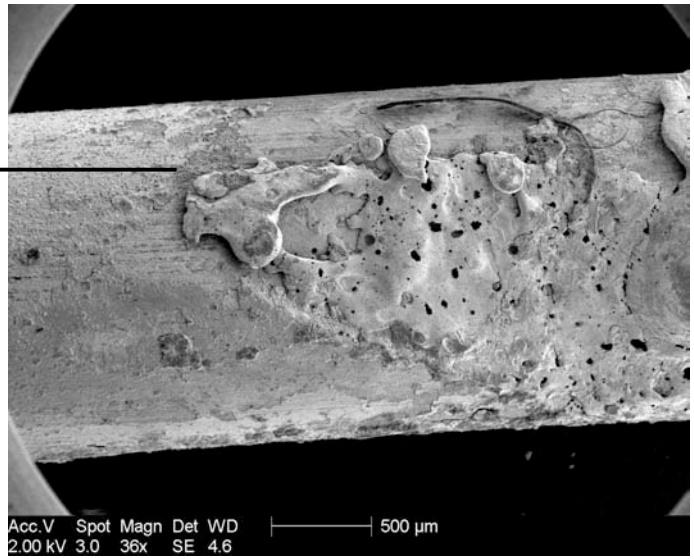

Figure 12 - SEM image of the bottom conductor.

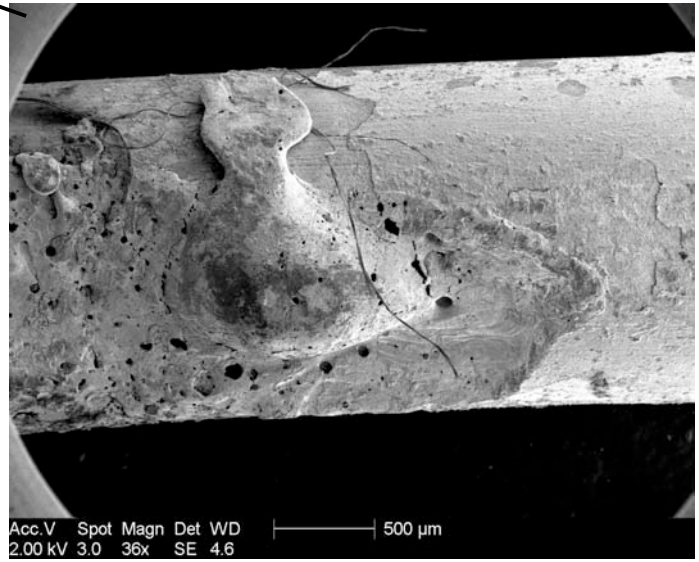

Figure 13 - SEM image of the bottom conductor.

Confocal laser scanning microscope images of exhibit 002 - arcing category A (experiment 1)

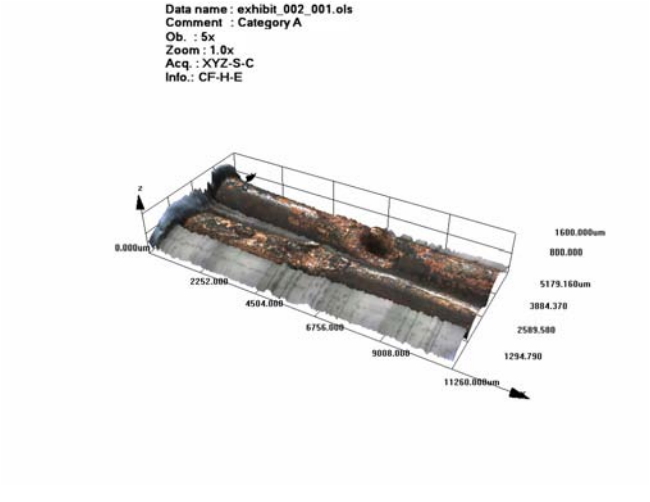

Figure 14 - LEXT overview image of exhibit 002. The entire exhibit is displayed in detail

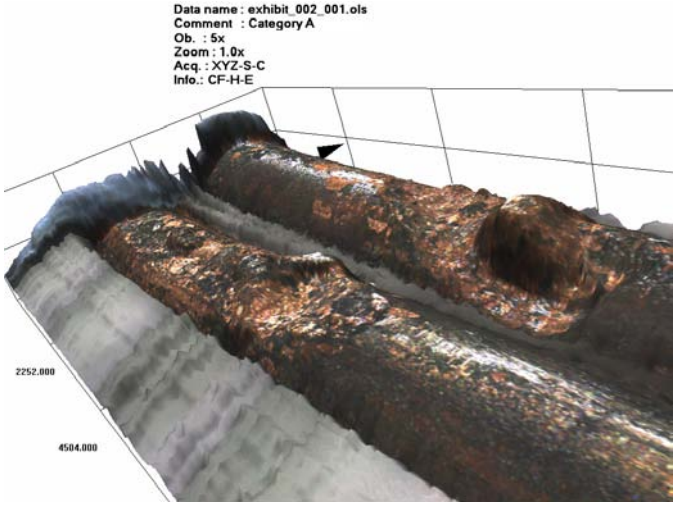

Figure 15 – exhibit rotated in the 3-D software.

Figure 16 – Close-up image of figure 14 with the 3-D software.

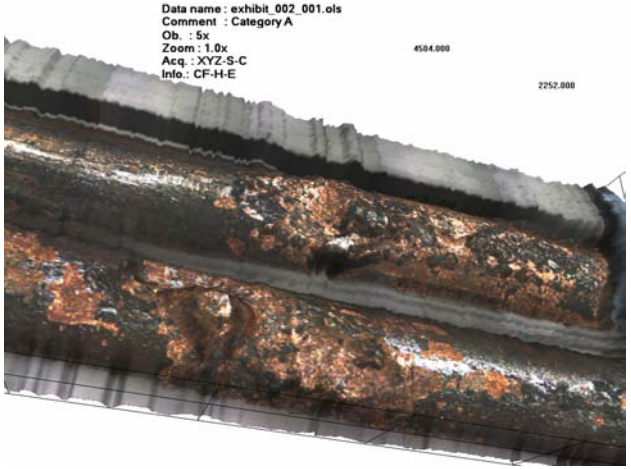

Figure 17 - LEXT image captured in the 3-D software.

Microscope and SEM images for exhibit 003 – arcing category B (experiment 1)

Figure 18 - Microscope image of exhibit 003 detailing two severed ends.

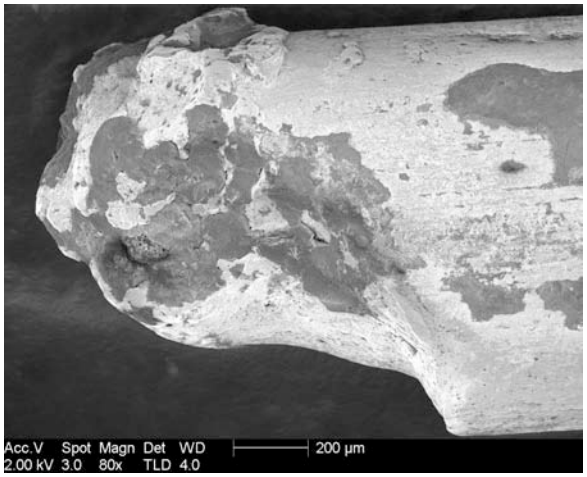

Figure 19 - SEM image of right severed end.

Figure 20 - SEM image of left severed conductor end.

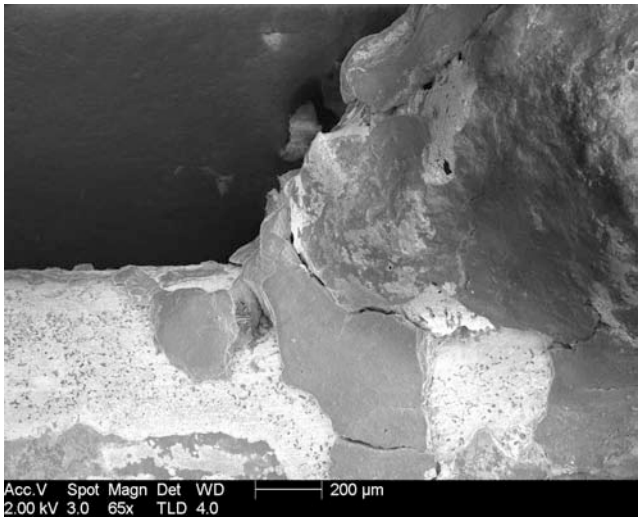

Figure 21 - SEM image at 65x magnification of the demarcation area between the bead and the conductor.

Microscope images for exhibit 004 – arcing category D (experiment 1)

Figure 22 - Microscope image of exhibit 004. One conductor has a bead on the surface.

Figure 23 - Microscope image at 20x magnification.

Figure 24 - Microscope image at 20x magnification.

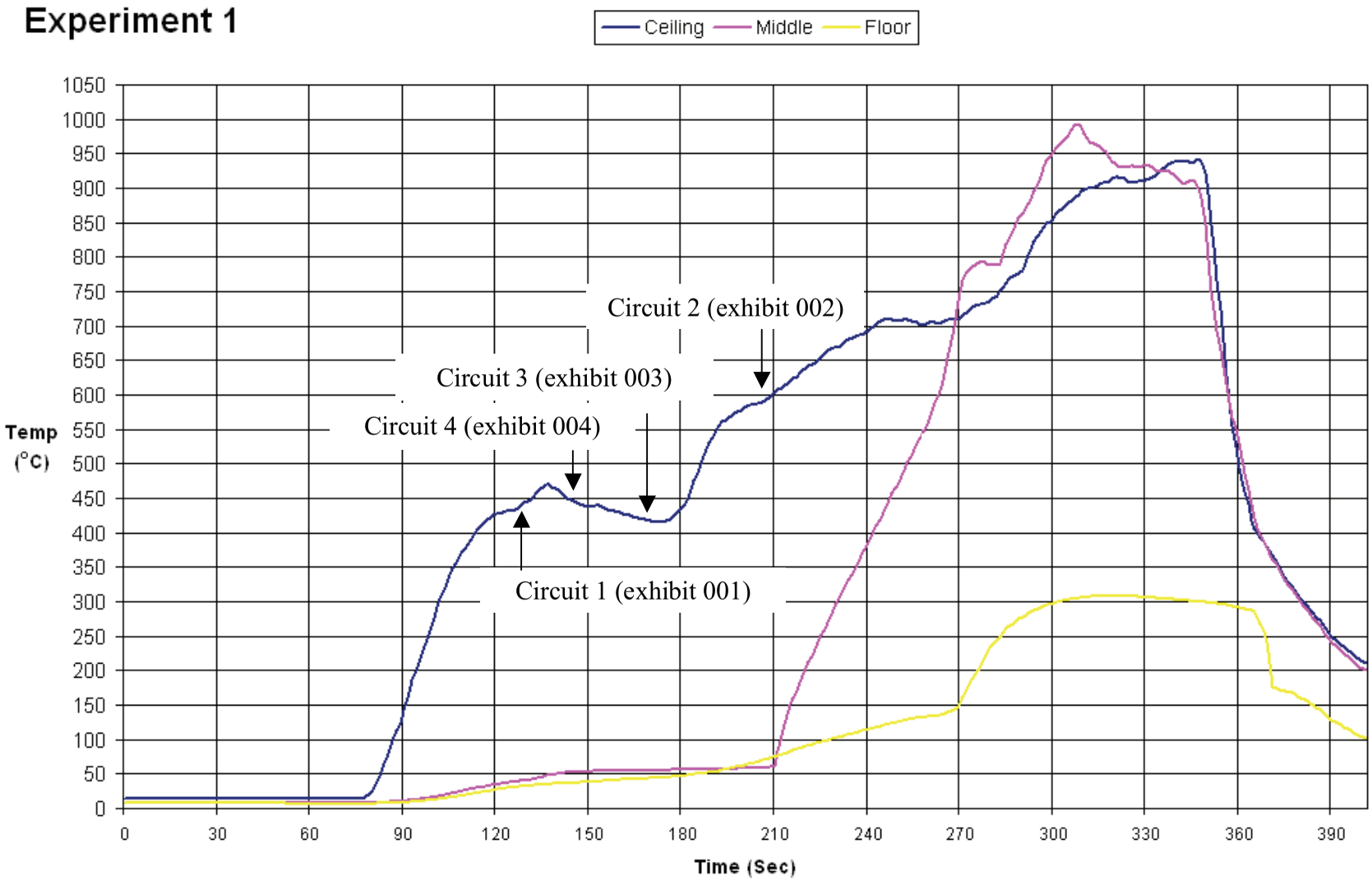

Figure 25 - Time temperature graph for experiment 1

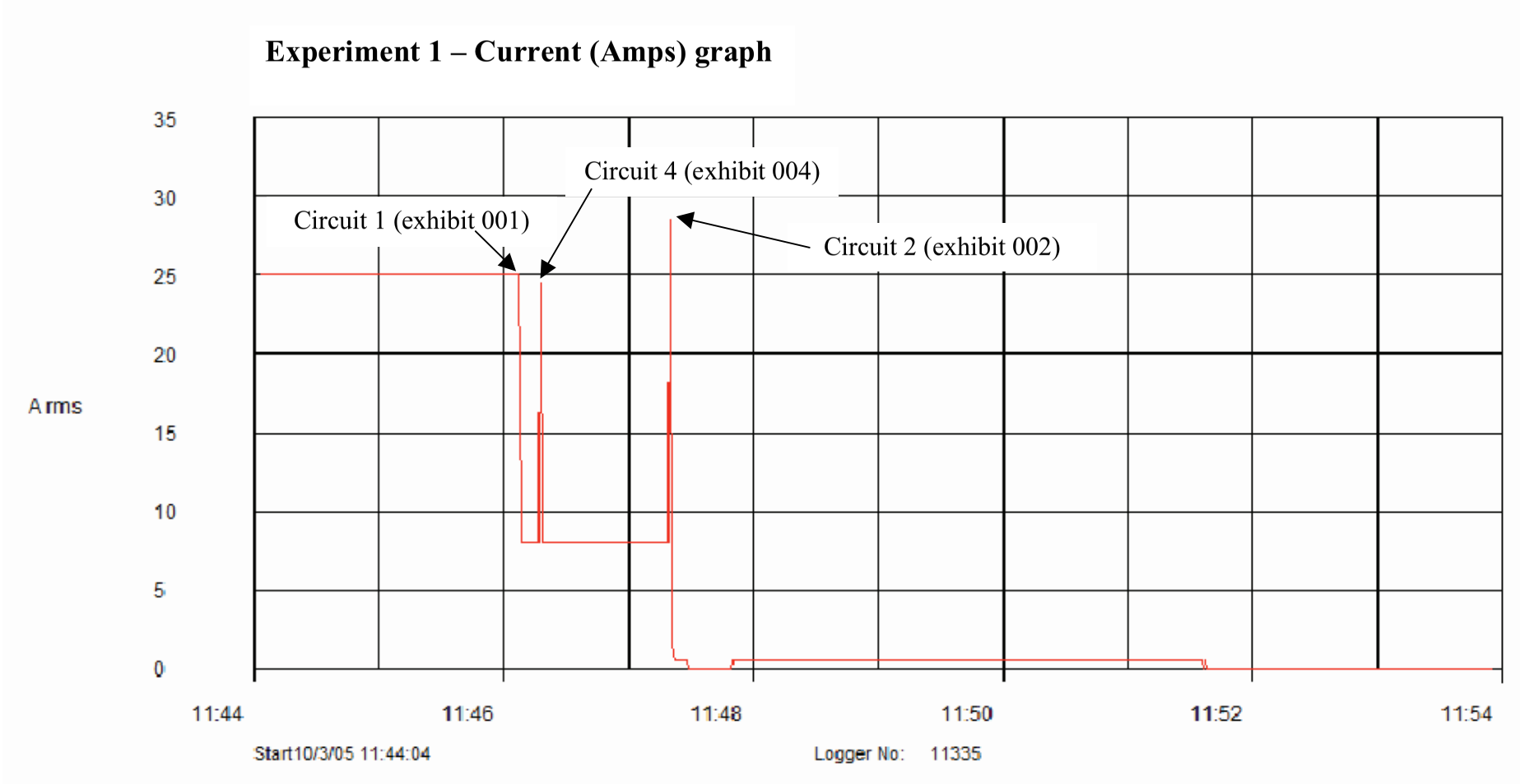

Figure 26 - Current (Amps) graph for experiment 1 detailing the operation of the circuit breakers and the fault current

Experiment 2

Figure 27 - "Scenario B" 10 March 2005

Circuit number	MCB operating time from ignition
4	1:35 minutes
1	1:45 minutes
3	1:45 minutes
2	2:00 minutes

Table 3 – circuit breaker data

The fire in experiment 2 (scenario B) was accelerated with an ignitable liquid poured throughout approximately 50% of the compartment.

The ceiling thermocouple recorded a temperature of 800° C. The middle thermocouple recorded 900° C 5 minutes from ignition the floor thermocouple recorded 450 degrees. External observations of the fire and post-fire burn patterns suggest that this compartment reached flashover conditions.

The final circuit cable length for this experiment was 30m between the compartment and the portable distribution board. This introduced a high resistance and subsequently limited the fault current. The circuit breakers operated correctly and the current data logger recorded the highest fault current for the entire series of experiments at 67 Amps.

No visible arcing damage was located during the post-fire scene examination.

Pre-fire and post-fire photographs of experiment 2

Figure 28 - Pre-fire photograph, showing the majority of the room. The black line indicates the fire's area of origin.

Figure 29 - A close-up photograph detailing the cables installed for the experiment.)

Figure 30 - Post-fire photograph. A considerable amount of ceiling plasterboard fell down during the experiment.

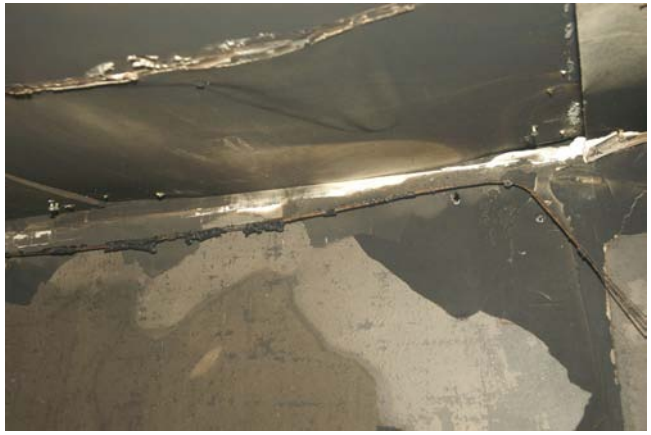

Figure 31 - Post-fire photograph detailing post fire damage to the cables.

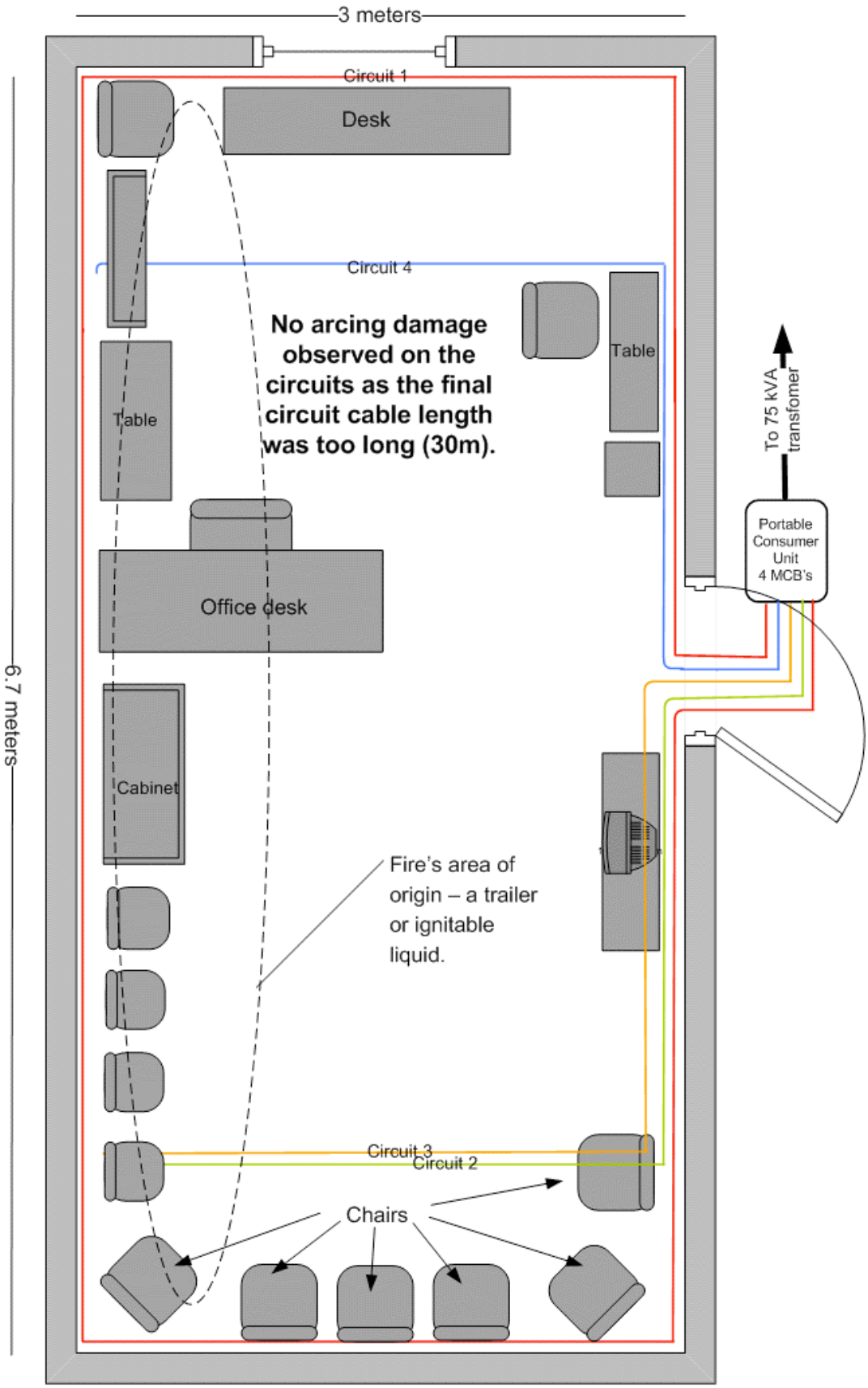

Figure 32 **Experiment 2 – "Scenario B" 14 April 2005** Scale of 1:25

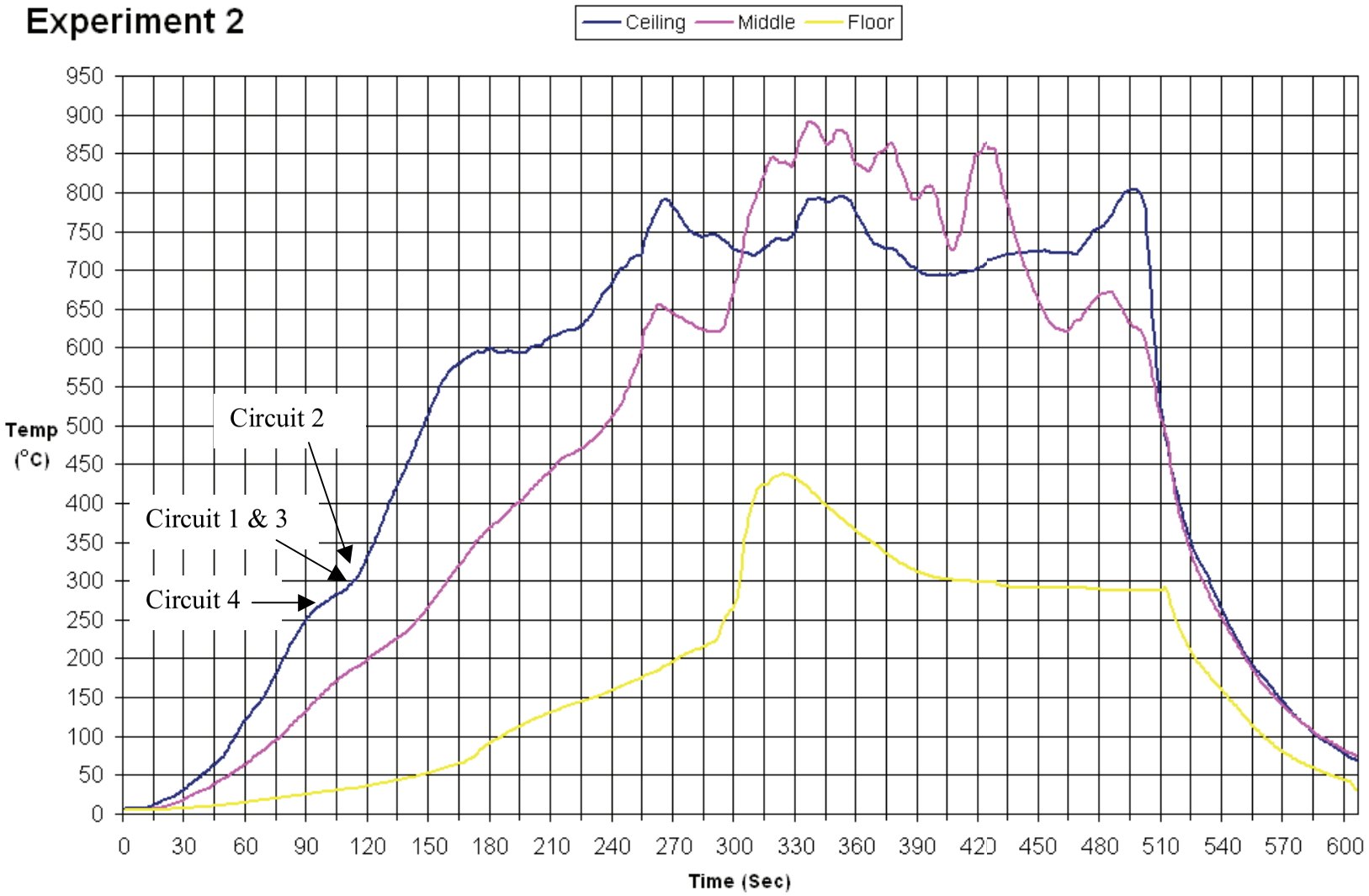

Figure 33 - Time temperature graph for experiment 2

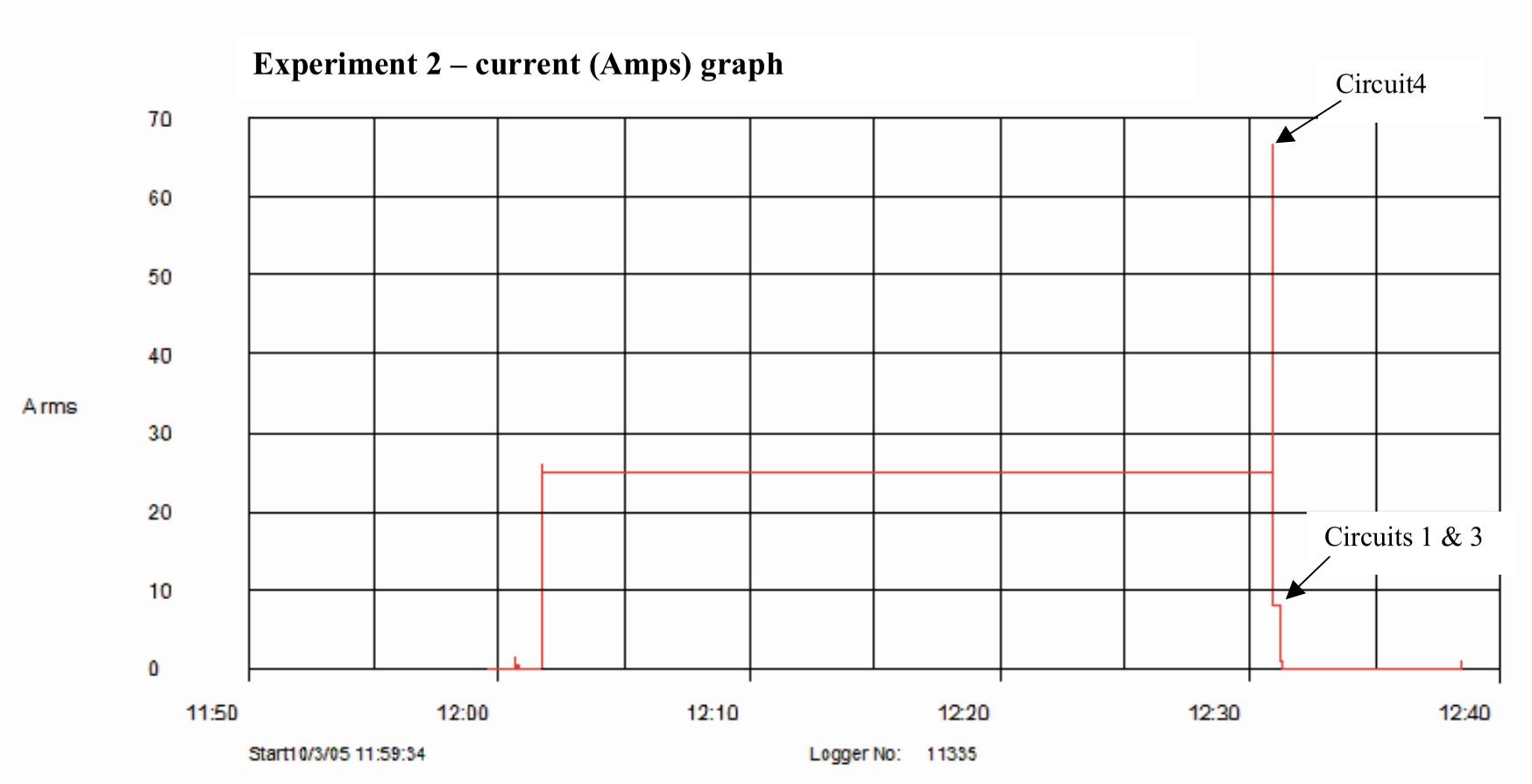

Figure 34 - Current (Amps) graph for experiment 2 detailing the operation of the circuit breakers and the fault current

Experiment 3

Figure 35 - “Scenario F” 10 March 2005

Circuit number	MCB operating time from ignition
4	3:20 minutes
1	3:30 minutes
3	3:50 minutes
2	4:11 minutes

Table 4 – circuit breaker data

The fire in experiment 3 (scenario F) originated in two separate areas, at curtains and a small basket near the door of the compartment and on a three-seat settee located near the middle of the compartment.

The fire was ignited as part of the training exercise in a specific sequence as follows:
1: ignition of the curtains
2: ignition of the sofa
3: ignition of a small basket by the door

The fire developed rapidly with the ceiling, middle and floor thermocouples recording temperatures in the region of 950° C 5 minutes from ignition. The compartment reached flashover conditions at this point.

Arcing damage was located on circuit 1 – 1.32m from rear wall and adjacent to the left wall.

Arcing damage was located on circuit 2 – 3.8m from rear wall, adjacent to the right wall and 300mm from the ceiling.

No arcing damage was located on circuit 3 conductors.

Arcing damage was located on circuit 4 – 2.4m from the rear wall and adjacent to the right wall.

Pre-fire and post-fire photographs of experiment 3

Figure 36 - Pre-fire photograph, view from the doorway. The black ovals indicate the fire's areas of origin.

Figure 37 - Pre-fire photograph taken from the TV end of the room. The black oval indicates the 3rd area of origin.

Figure 38 - Post-fire photograph of view above. The white ovals indicate the fire's area of origin.

Figure 39 - Post-fire photograph of the view above. The black oval indicates the 3rd area of origin.

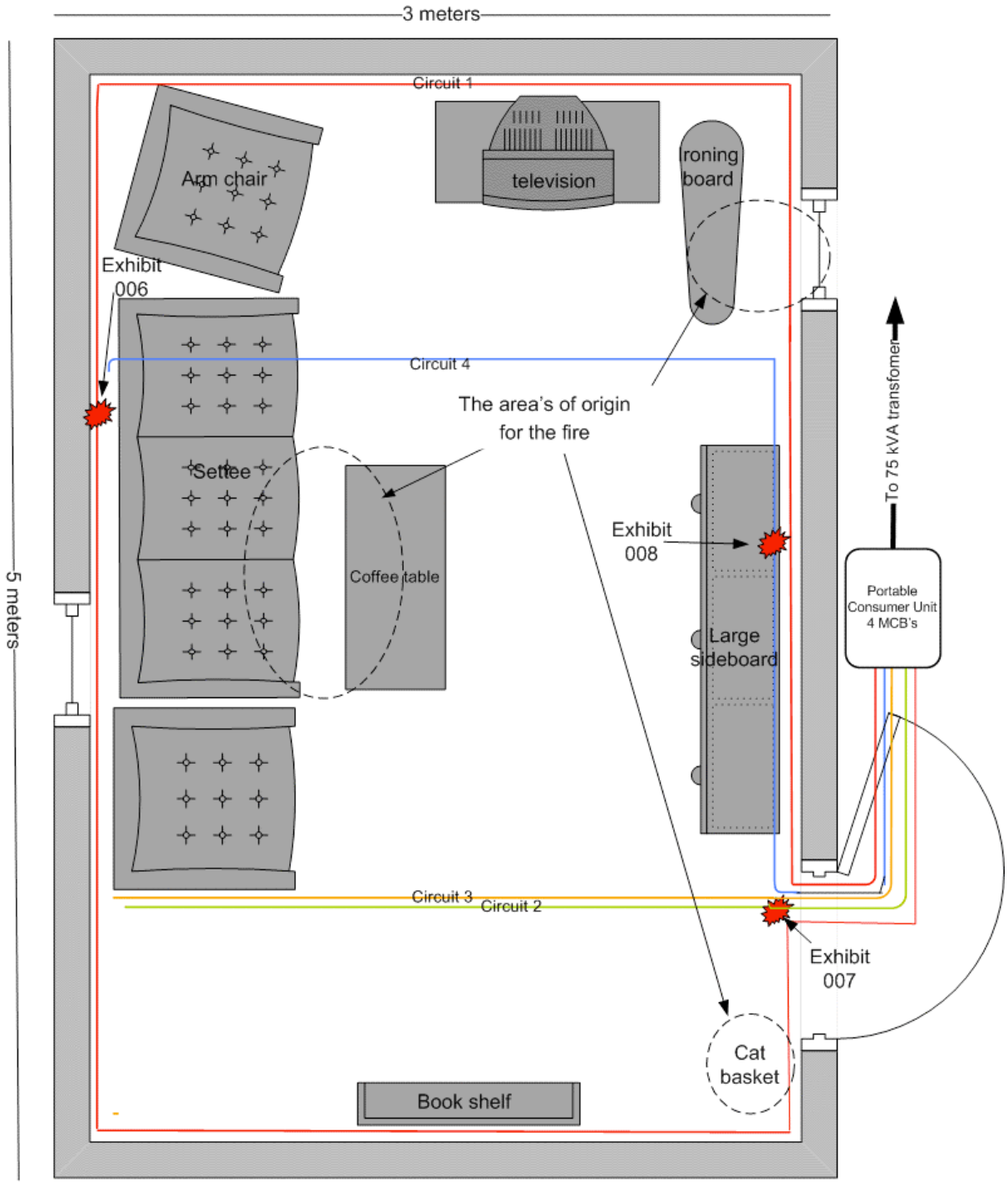

Figure 40 -
Experiment 3 – "Scenario F" 10 March 2005

Scale of 1:20

Microscope and SEM images of exhibit 006 – arcing category F (experiment 3)

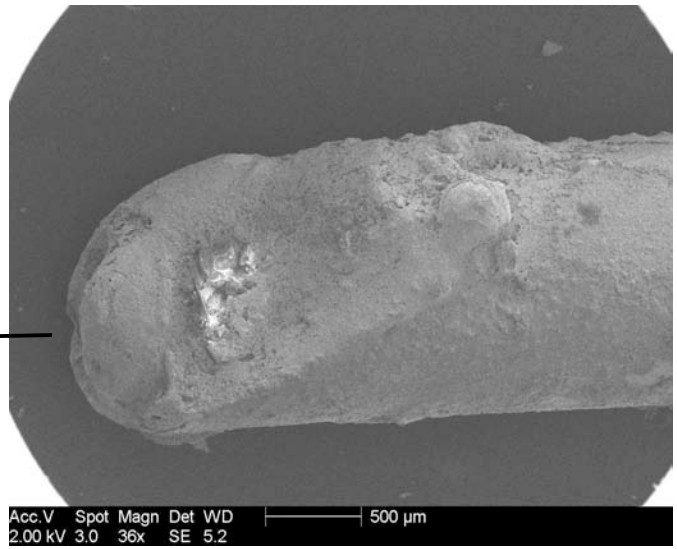

Figure 41 - SEM image of exhibit 006 severed ends.

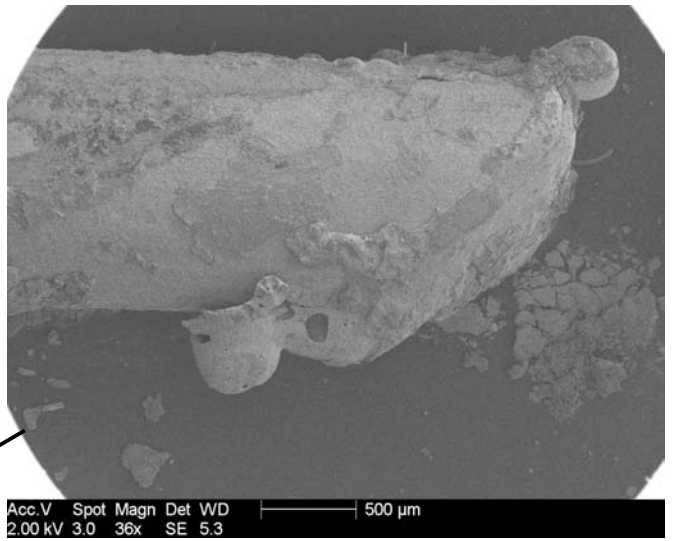

Figure 42 - SEM image of severed end.

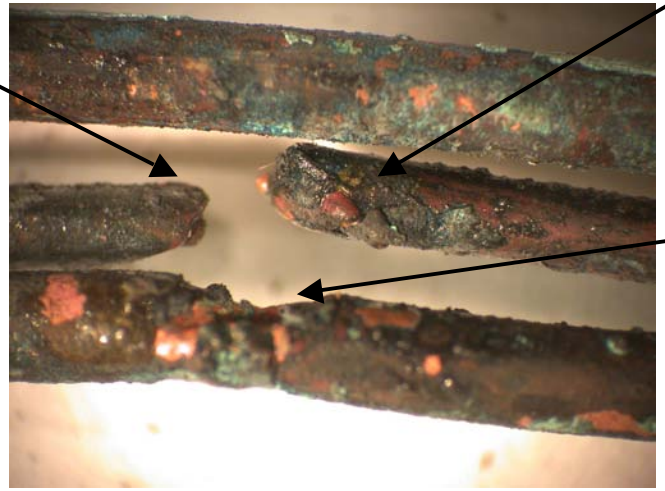

Figure 43 - Microscope image of exhibit 006.

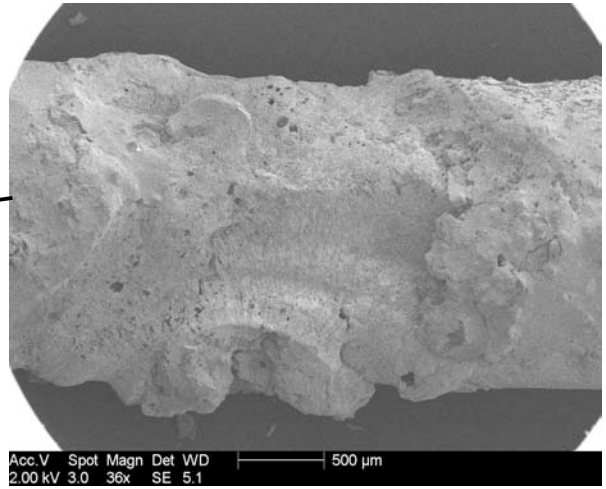

Figure 44 - SEM image of bottom conductor.

Confocal laser scanning microscope images of exhibit 006 – arcing category F (experiment 3)

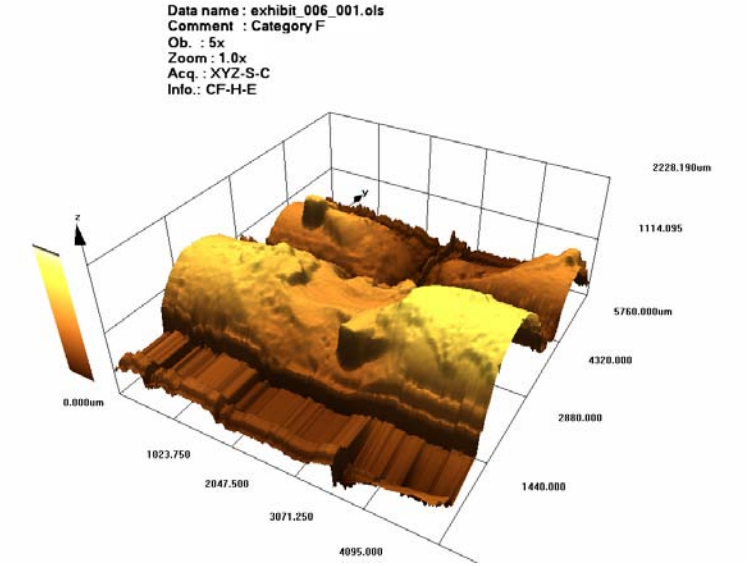

Figure 45 - LEXT overview image. The brown colour rendering was used initially with the Confocal laser scanning microscope during the initial scans to find the preferred settings. The brown render was found to be less effective than the "real colour" setting.

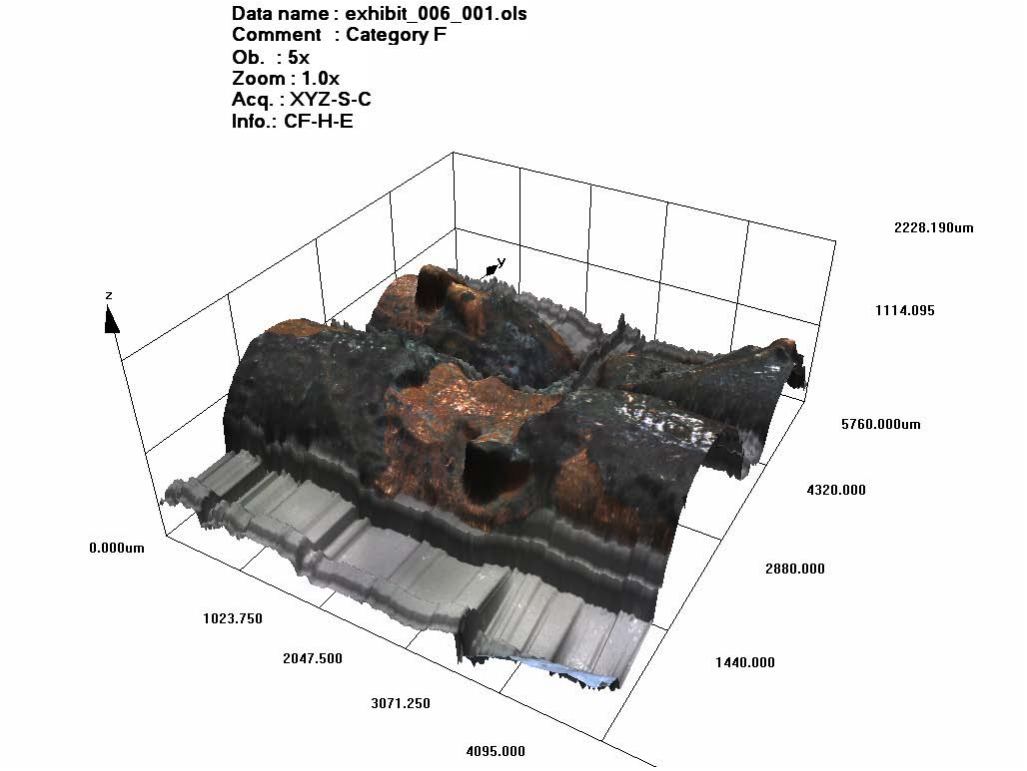

Figure 46 - LEXT image in the "real colour" setting. The entire exhibit is displayed in detail.

Microscope and SEM images of exhibit 007 – arcing category A (experiment 3)

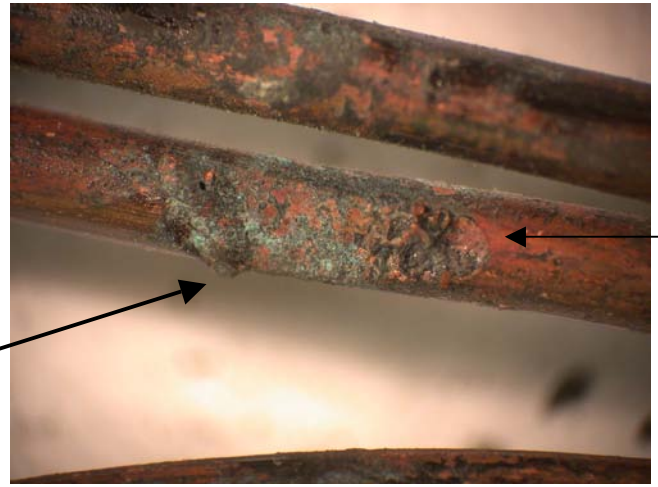

Figure 47 - Microscope image of exhibit 006.

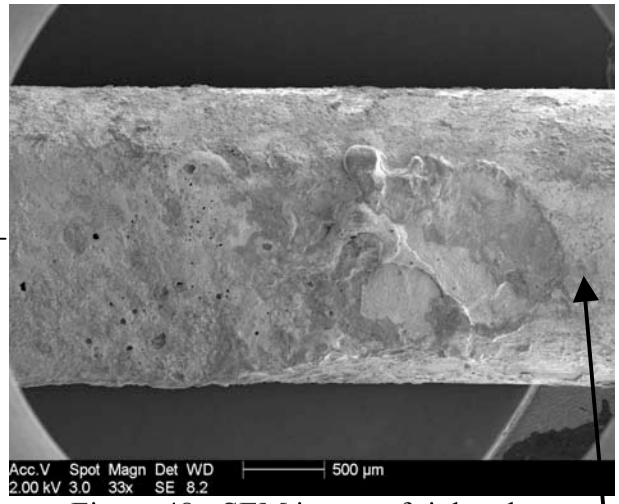

Figure 48 - SEM image of right edge.

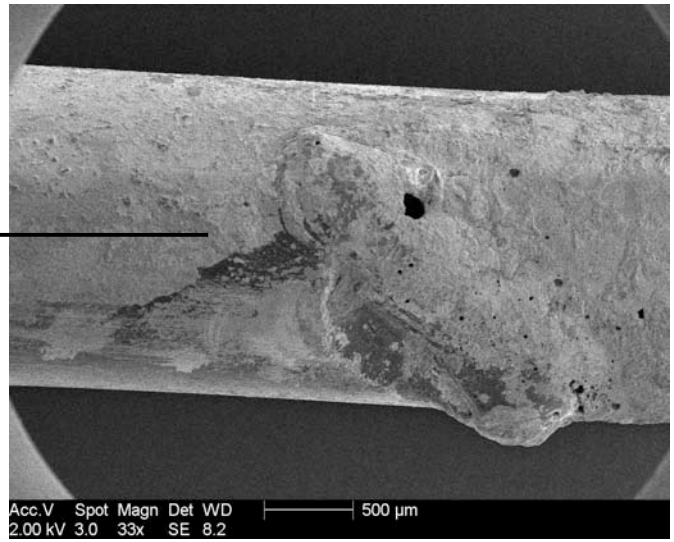

Figure 49 - SEM image of left edge.

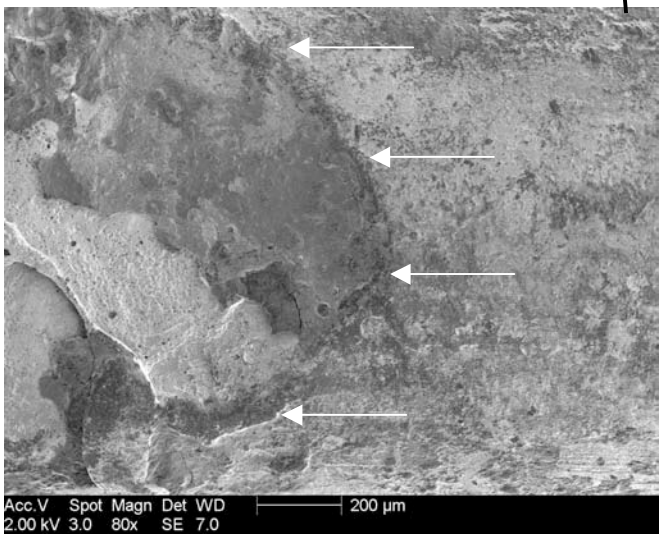

Figure 50 - SEM image of right edge detailing the demarcation at the edge of the notch indicated by arrows.

Microscope and SEM images for exhibit 008 – arcing category C (experiment 3)

Figure 51 - Microscope image of exhibit 008.

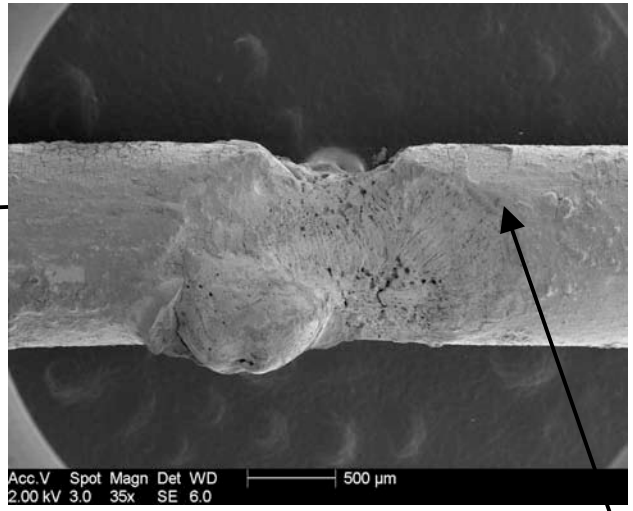

Figure 52 - SEM image of the top conductor.

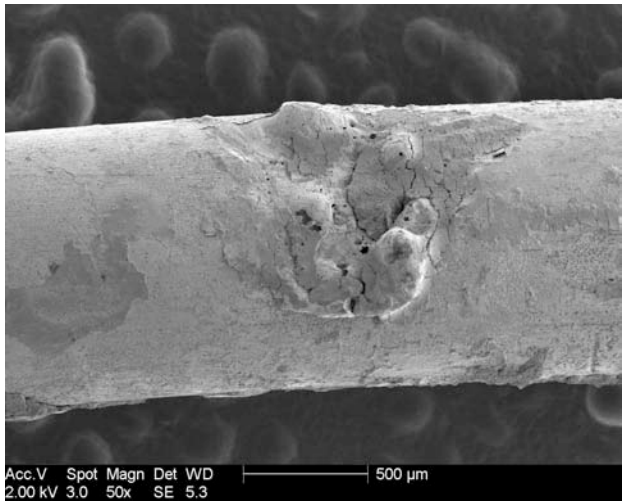

Figure 53 - SEM image of the small notch on the bottom conductor.

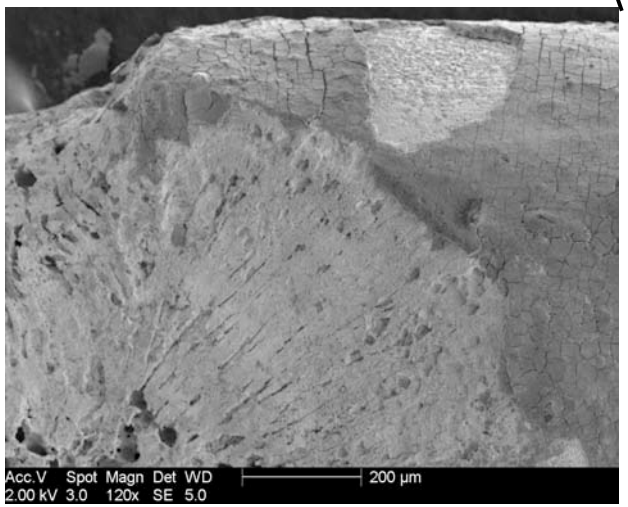

Figure 54 - SEM image at 120x magnification detailing the demarcation area at the edge of the notch.

Confocal laser scanning microscope images of exhibit 008 (experiment 3)

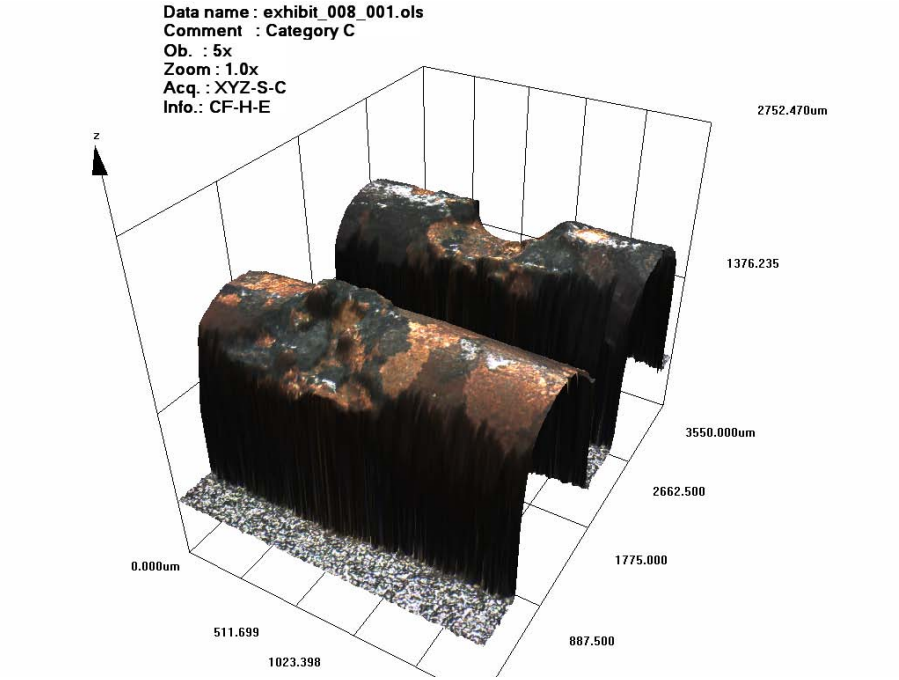

Figure 55 - LEXT overview image of exhibit 008.

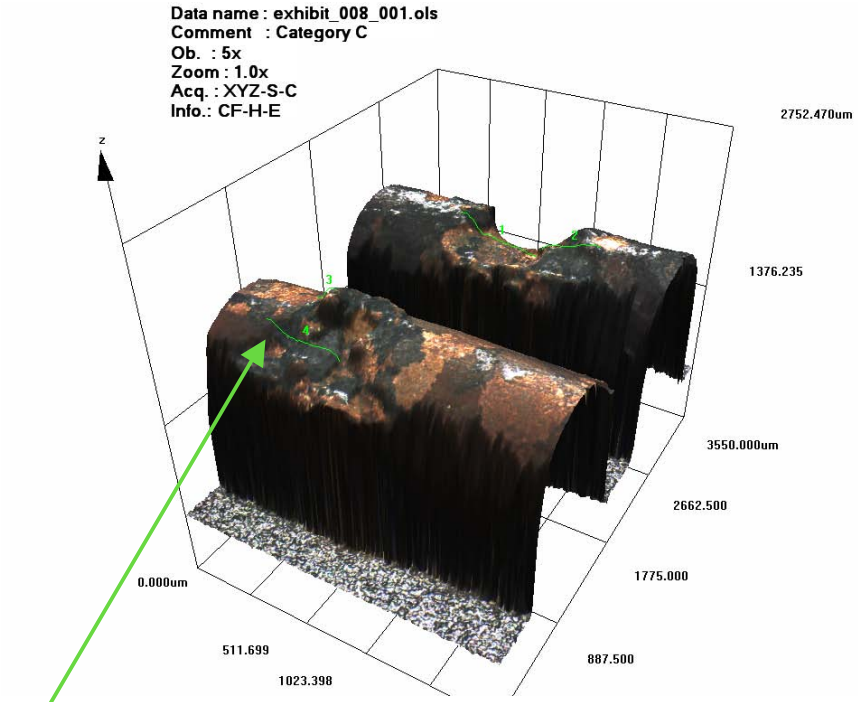

Figure 56 – LEXT image with measurement locations.

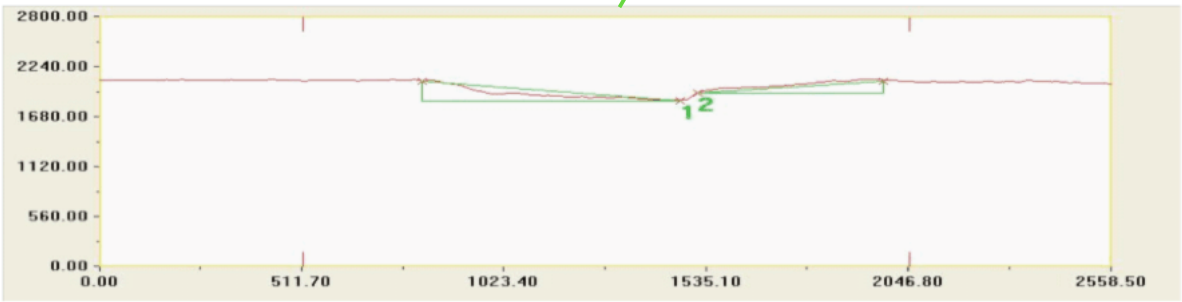

Figure 57 – Profile of the notch created using the LEXT software “slice tool”

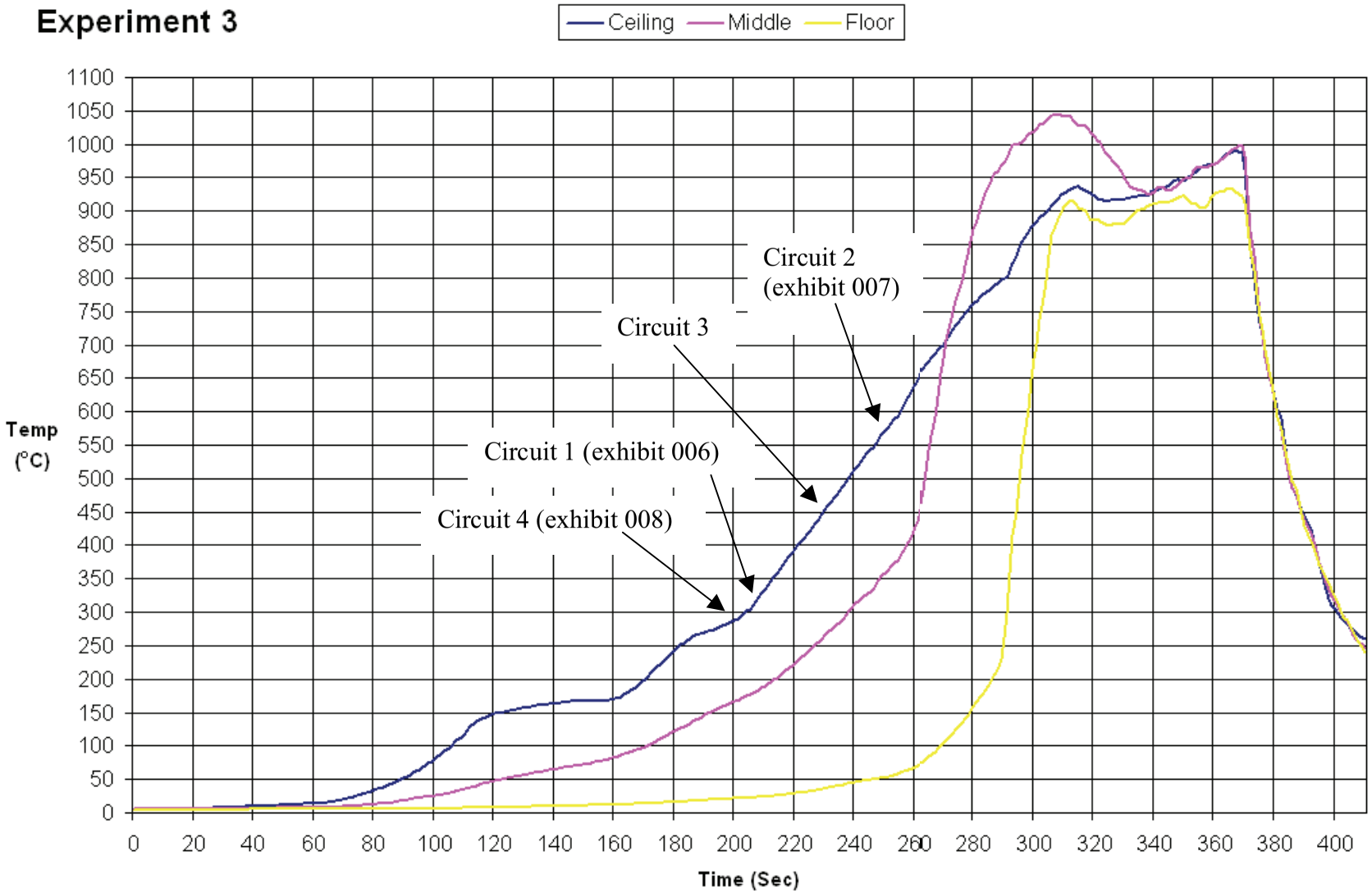

Figure 58 - Time temperature graph for experiment 3

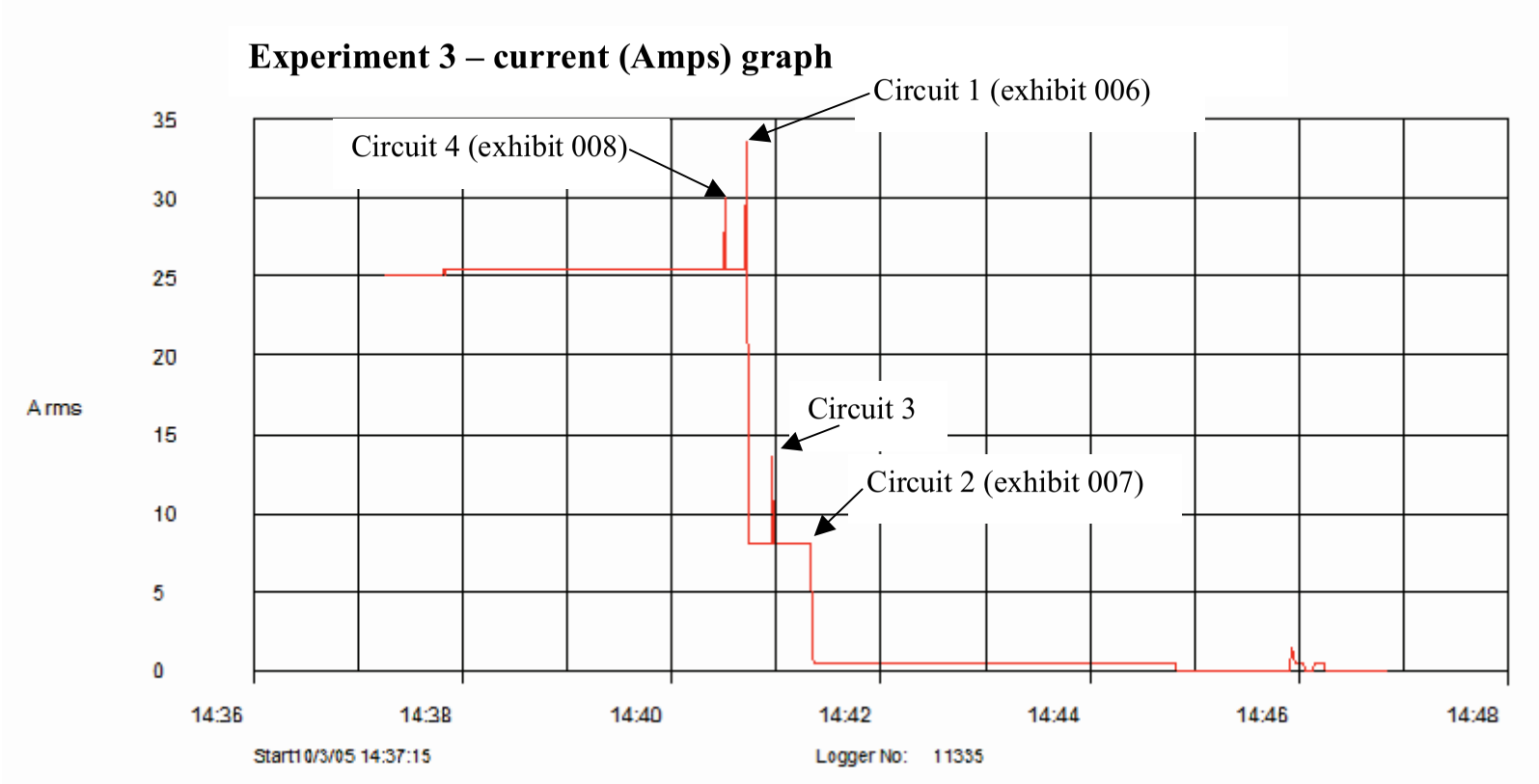

Figure 59 - Current (Amps) graph for experiment 3 detailing the operation of the circuit breakers and the fault current

Experiment 4

Figure 60 – “Scenario E” 10 March 2005

Circuit number	MCB operating time from ignition
3	1:40 minutes
1	2:20 minutes
2	2:33 minutes
4	2:33 minutes

Table 5 – circuit breaker data

The fire in experiment 4 (scenario E) originated in three separate areas. These were within a wardrobe opposite the door, on a bed to the right hand side of the door and on combustible materials at floor level between the wardrobe and bed. The wardrobe was the dominant fire plume.

The ceiling thermocouple recorded a temperature of 800° C 4.5 minutes from ignition. The middle thermocouple recorded 750° C with the floor thermocouple recording 400° C. The compartment reached flashover conditions at this time.

The wiring/cables in this test quickly fell from the ceiling to the floor as the plastic cable ties used to fix the cables to the ceiling failed. Following this experiment the method of mechanical fixing of the cables to the ceiling was changed to ensure that the cables would reliably stay in position throughout the development of the fire.

Arcing damage was only located on circuit 1 – 1.38m from left wall and adjacent to the rear wall (above the armchair).

Pre-fire and post-fire photographs of experiment 4

Figure 61- Pre-fire photograph, view from the doorway. The black ovals indicate the fire's areas of origin.

Figure 62 - Pre-fire photograph, the grey oval indicate the fire's 3rd area of origin within the wardrobe.

Figure 63 - Post-fire photograph of the view above. The white ovals indicate the fire's areas of origin.

Figure 64 - Post-fire photograph detailing the damage to the wardrobe. The white arrow is the location of exhibit 005.

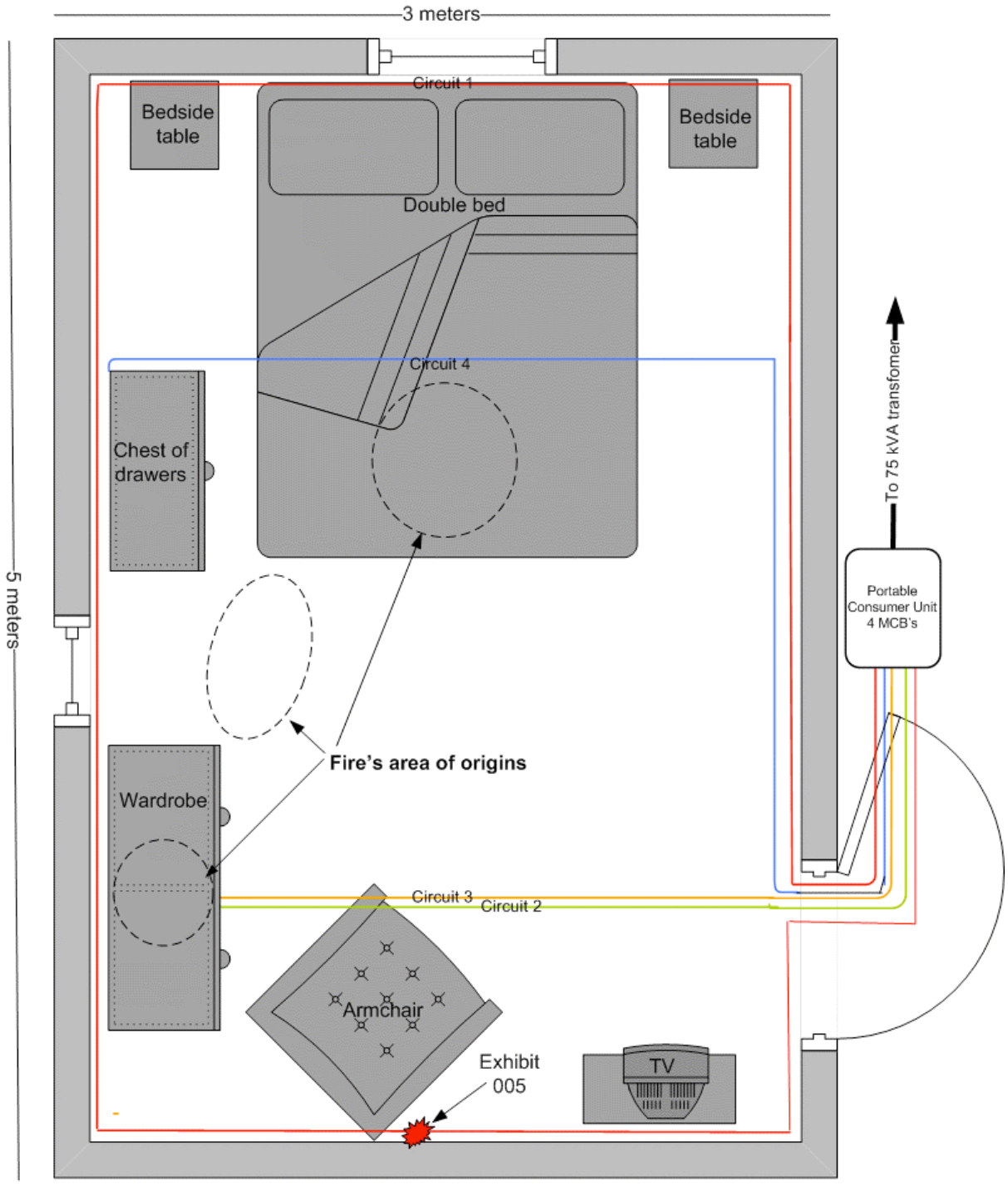

Figure 65 -
Experiment 4 – "Scenario E" 10 March 2005

Scale of 1:20

Microscope images for exhibit 005– arcing category B (experiment 4)

Figure 66 - Microscope image of exhibit 005. Two of the three conductors have localised metallic (arcing) damage.

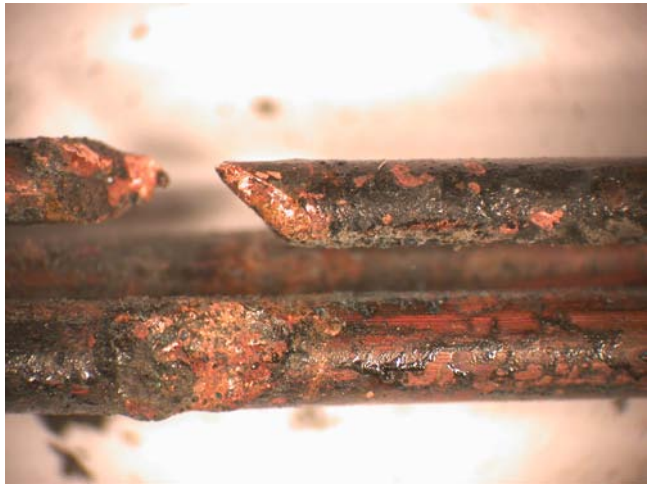

Figure 67 - Microscope image at 20x magnification detailing the bottom conductor notch in figure 66.

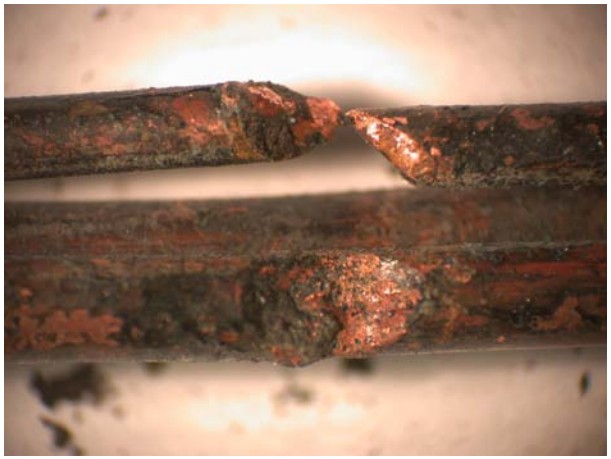

Figure 68 - Microscope image at 20x magnification detailing the severed ends of the top conductor.

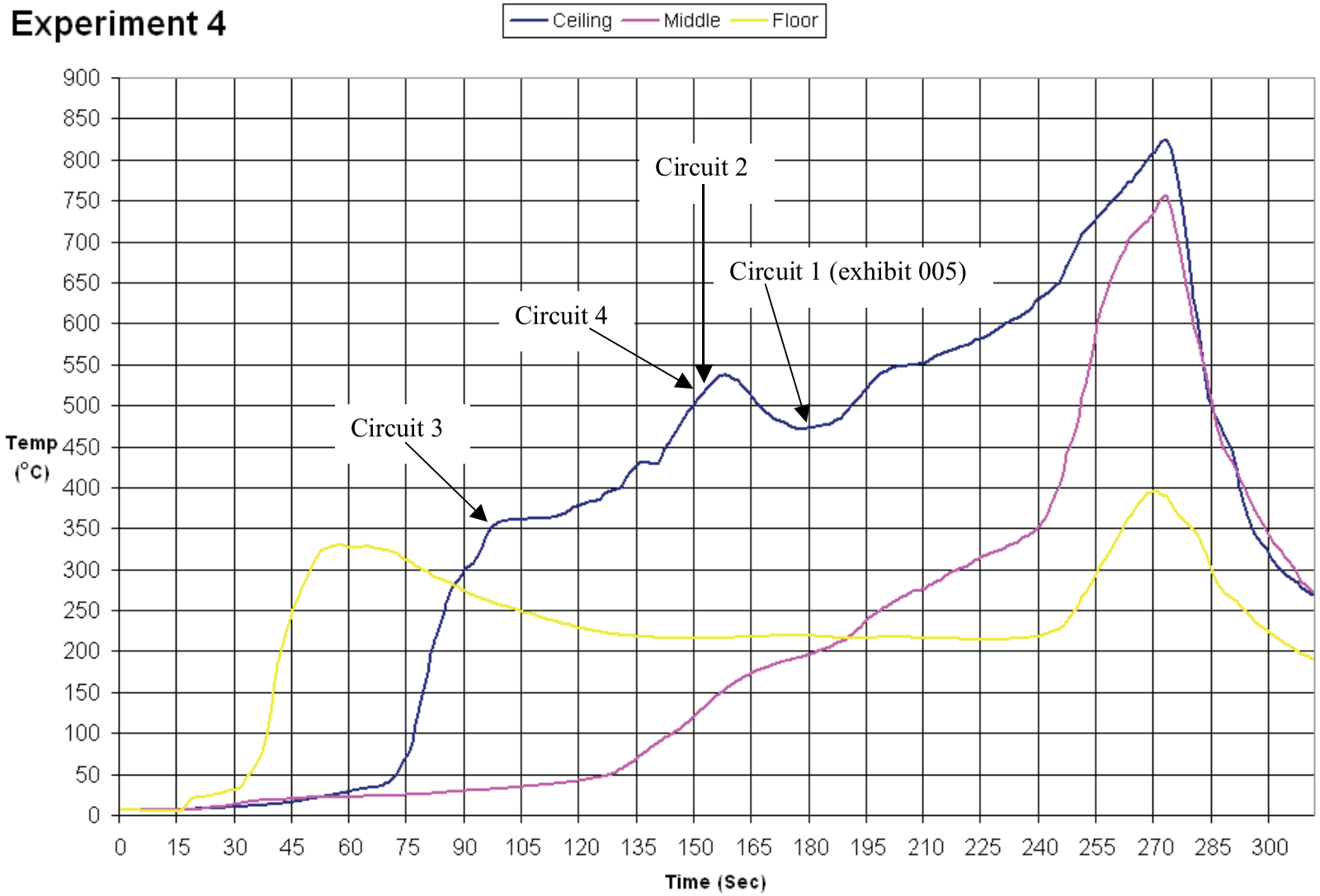

Figure 69 - Time temperature graph for experiment 4

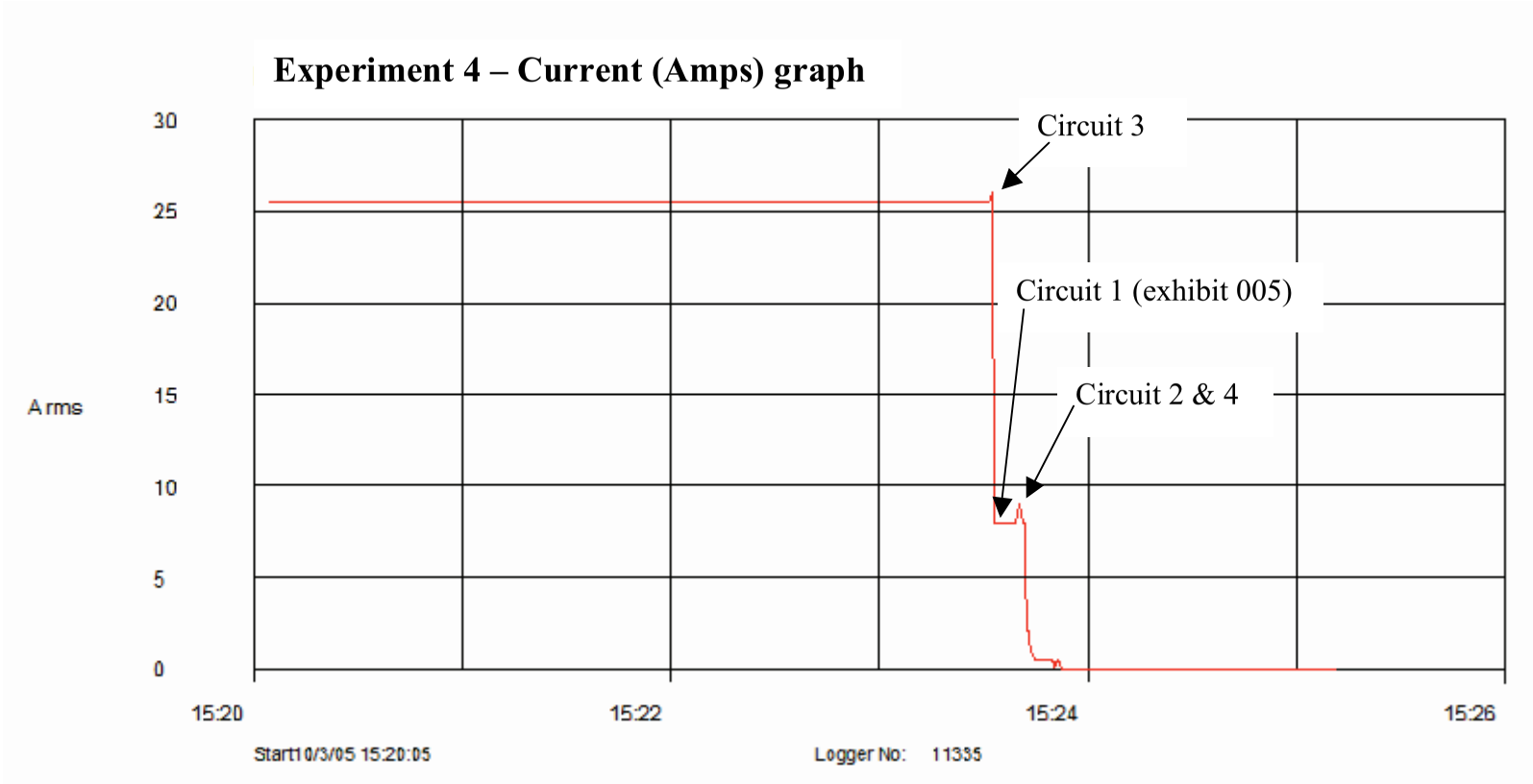

Figure 70 - Current (Amps) graph for experiment 4 detailing the operation of the circuit breakers and the fault current

Experiment 5

Figure 71 - – "Scenario E" 10 March 2005

Circuit number	MCB operating time from ignition
1	1:40 minutes
2	10:42 minutes
3	10:42 minutes
4	11:33 minutes

Table 6 – circuit breaker data

The fire in experiment 5 (scenario E) originated in two separate areas: the armchair in the rear right area of the room and a stool located beside the entrance door. In this case the fire development was slow for the first 7 minutes as the door to the compartment was closed. The fire was ventilation controlled and self-extinguished.

The current (Amperes) data logger was re-set at 3 minutes as it was in the paused mode.

At 9 minutes the right armchair was re-ignited with a blowtorch and to facilitate fire development for the purposes of the training exercise. The right armchair was the dominant fire plume in the compartment.

Arcing damage was located on circuit 1 – 4.46m from rear and adjacent to the right wall.

Arcing damage was located on circuit 2 and 3 – 4.6m from rear wall and 0.2m from left wall.

Arcing damage was located on circuit 4 - 0.7m from the rear wall and 0.07m from the left wall.

Pre-fire and post-fire photographs of experiment 5

Figure 72 - Pre-fire photograph, view from the doorway. The white oval indicates the fire's area of origin.

Figure 73 - Pre-fire close-up photograph of the fire's area of origin.

Figure 74 - Post-fire photograph of the view above showing the area of origin. The arrows indicate arcing damage locations.

Figure 75 - Post-fire photograph detailing the location of exhibit 009 indicated by the white arrow.

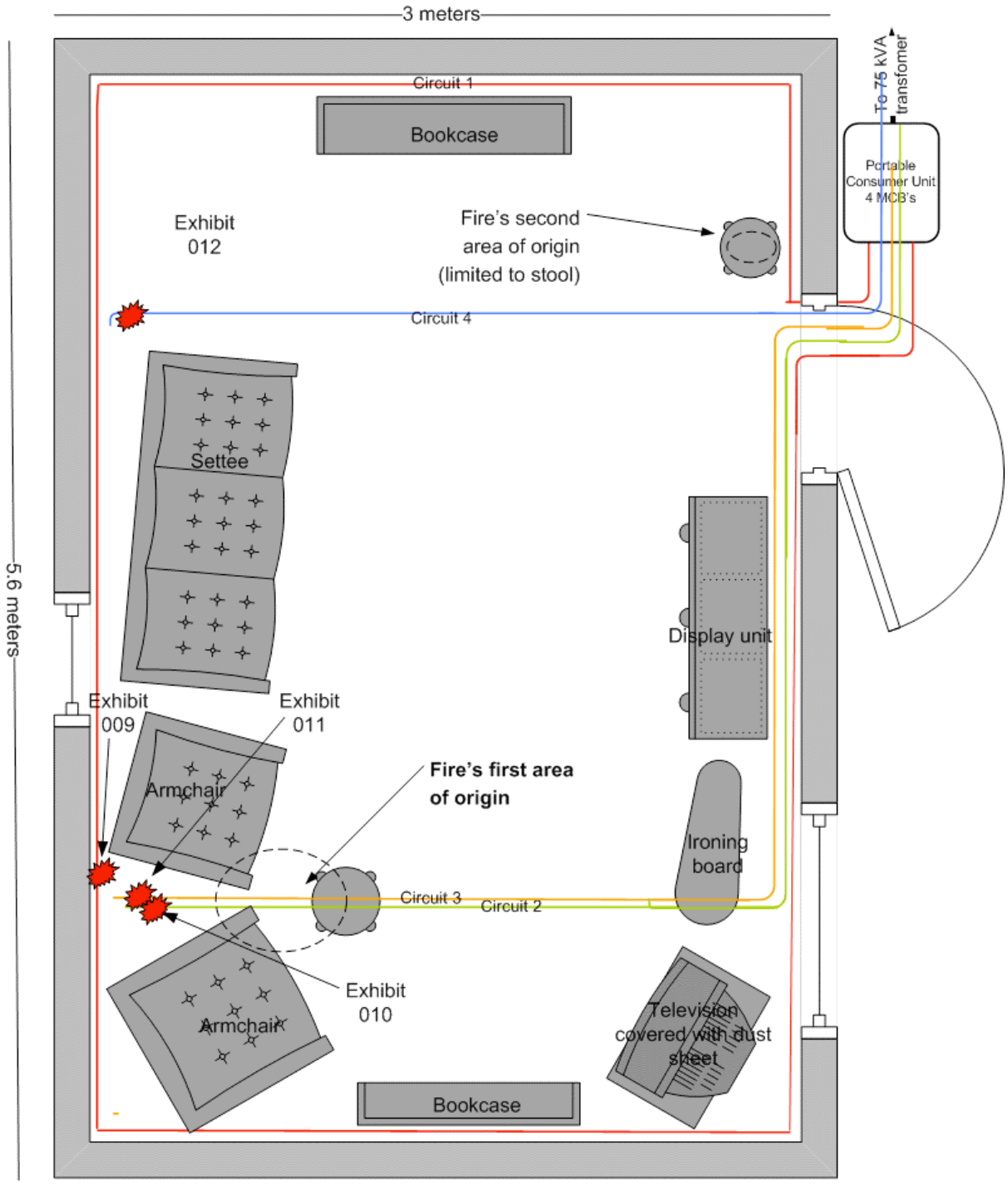

Figure 76 -
Experiment 5 – "Scenario F" 14 April 2005

Scale of 1:20

Microscope and SEM images for exhibit 009 – arcing category E (experiment 5)

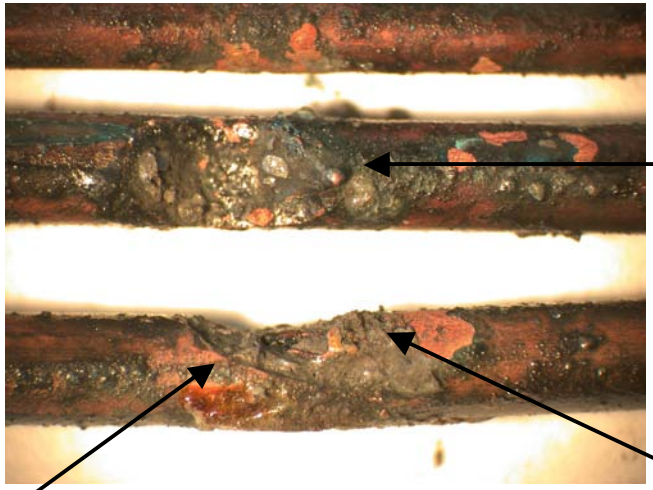

Figure 77 - Microscope image of exhibit 009.

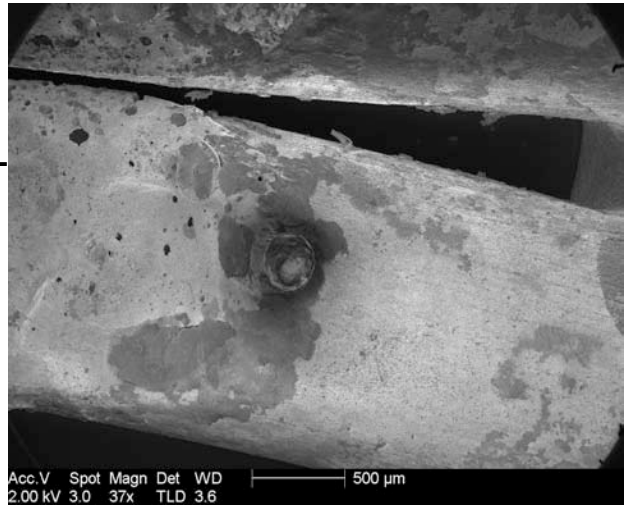

Figure 78 - SEM image of the top conductor.

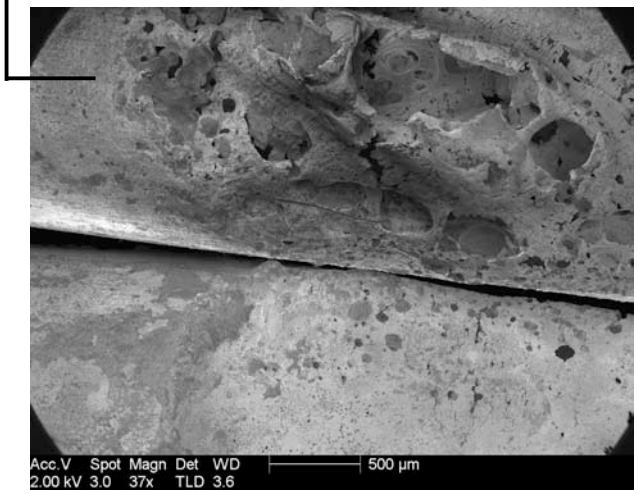

Figure 79 - SEM image detailing the left side of the bottom conductor.

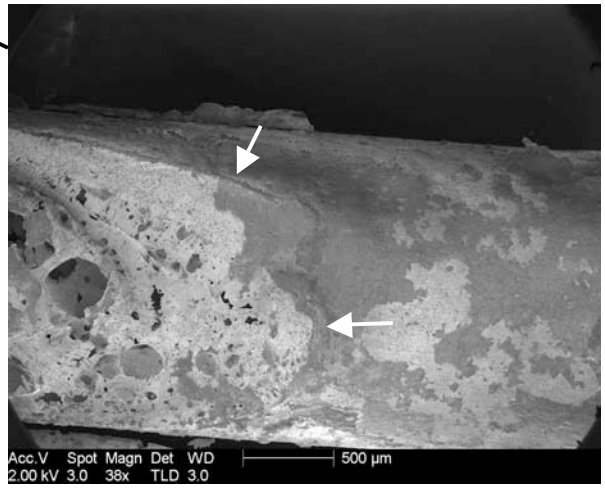

Figure 80 - SEM image of the right edge of the bottom conductor notch. Note the demarcation of the arcing damage when compared to the undamaged conductor area.

Microscope images for exhibit 010– arcing category E (experiment 5)

Figure 81 - Microscope image of exhibit 010. There is a notch affecting one of the three conductors.

Figure 82 – Microscope image detailing the bottom conductor at 20x magnification. The demarcation area at the left edge of the notch is defined.

Microscope and SEM images for exhibit 011 – arcing category E (experiment 5)

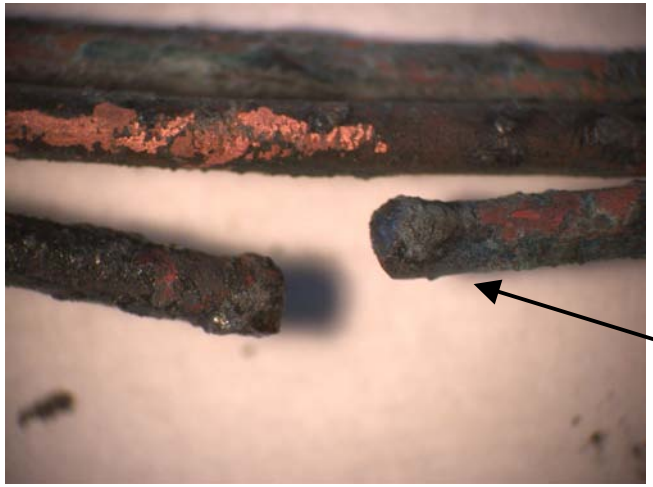

Figure 83 - Microscope image of exhibit 011.

Figure 84 - SEM image detailing the right severed end.

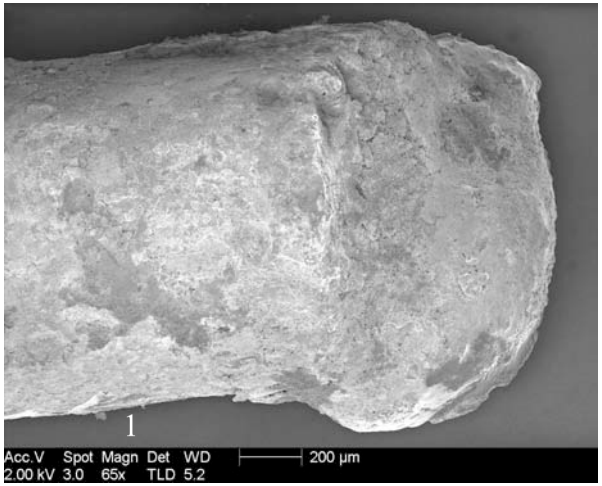

Figure 85 - SEM image detailing the left severed end.

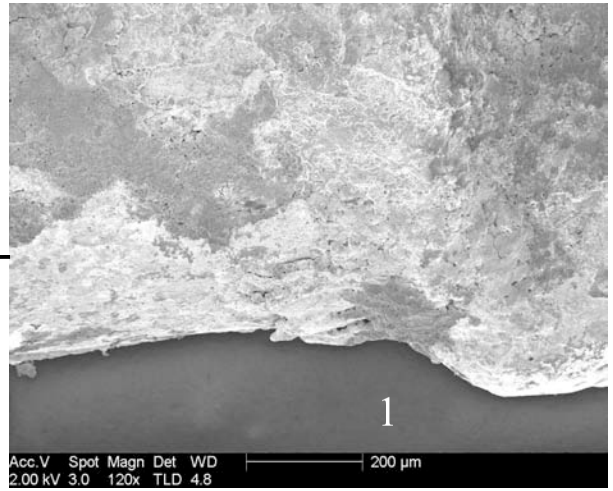

Figure 86 - SEM image at 120x magnification of area “1”.

Confocal laser scanning microscope images of exhibit 011 (experiment 5)

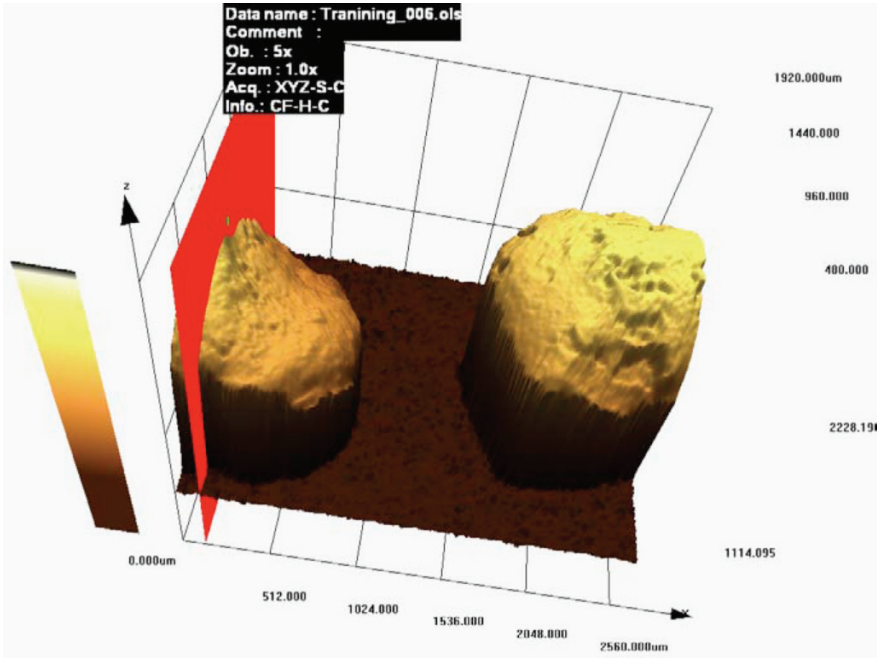

Figure 87 - Overview of the LEXT scan in brown colour mode. The "slice tool" option in the software produced the profile shown below.

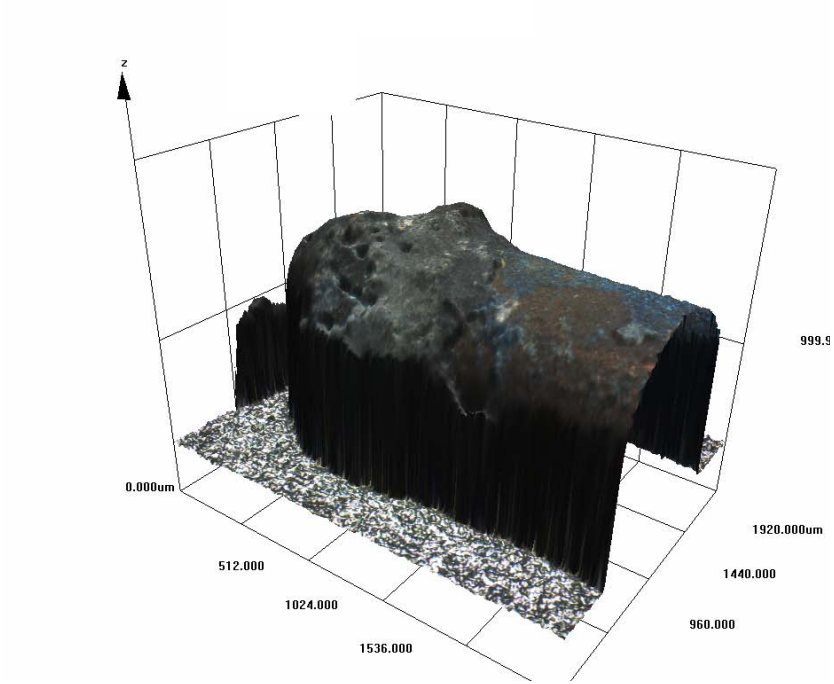

Figure 88 - LEXT 3-D image of one severed end of exhibit 011 in "real colour" mode.

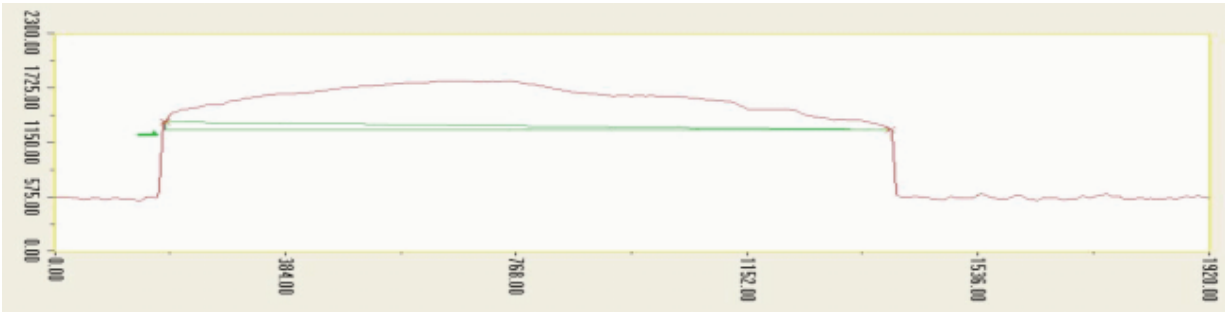

Figure 89 - LEXT profile for exhibit 011 created using the "slice tool" detailed in figure 87 in the LEXT software.

Microscope and SEM images of exhibit 012 (one of three conductors) arcing category E (experiment 5)

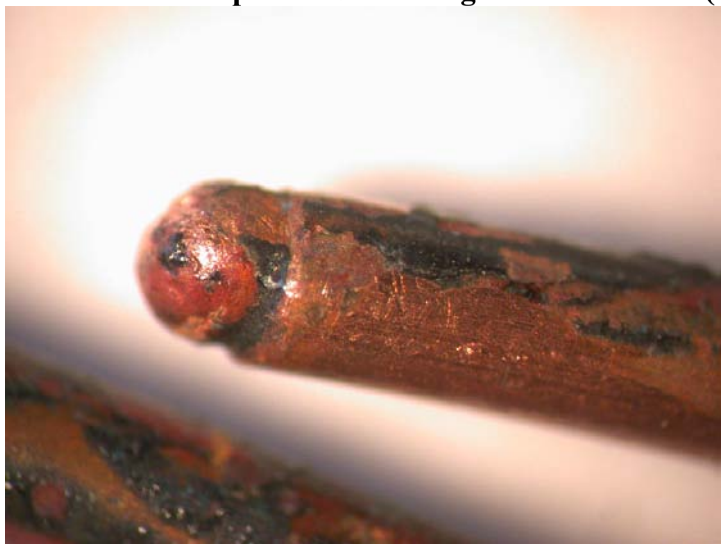

Figure 90 - Microscope image of exhibit 012 - 1 of 3 conductors.

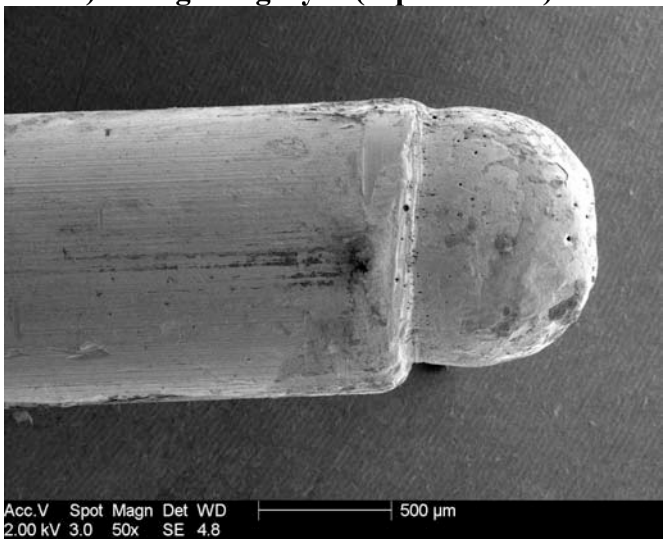

Figure 91 - SEM image of the severed conductor end.

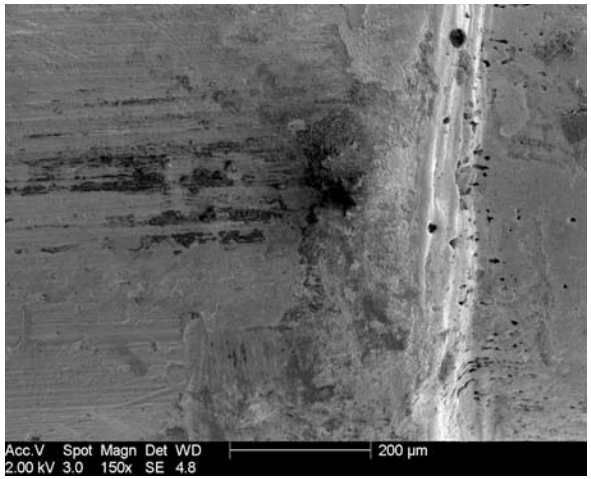

Figure 92 - SEM image of the demarcation area between the bead and the undamaged copper conductor.

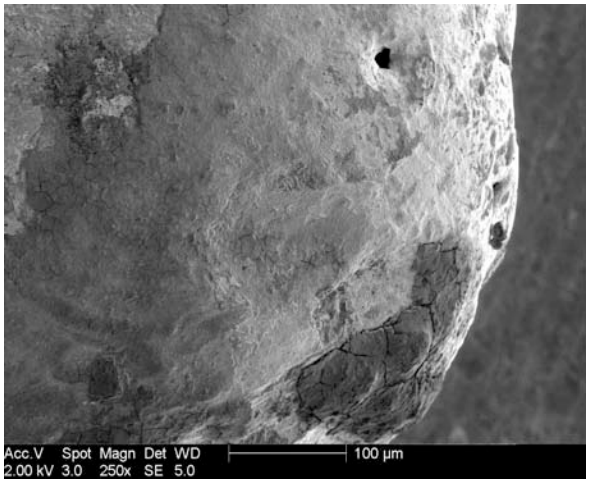

Figure 93 - SEM image at 250x magnification of the bead surface. Note the holes in the melted copper surface resulting from arcing damage.

Microscope and SEM images of exhibit 012 (two of three conductors) arcing category E (experiment 5)

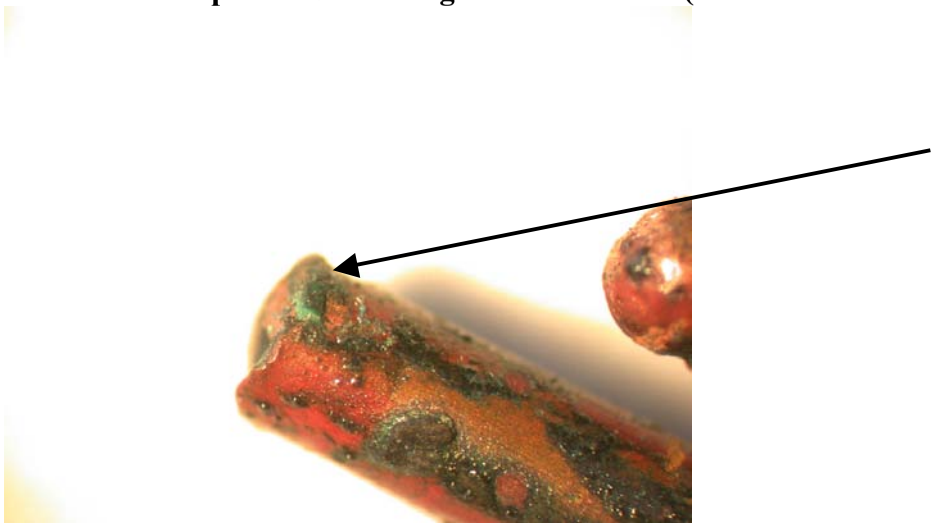

Figure 94 - Microscope image of the middle severed conductor.

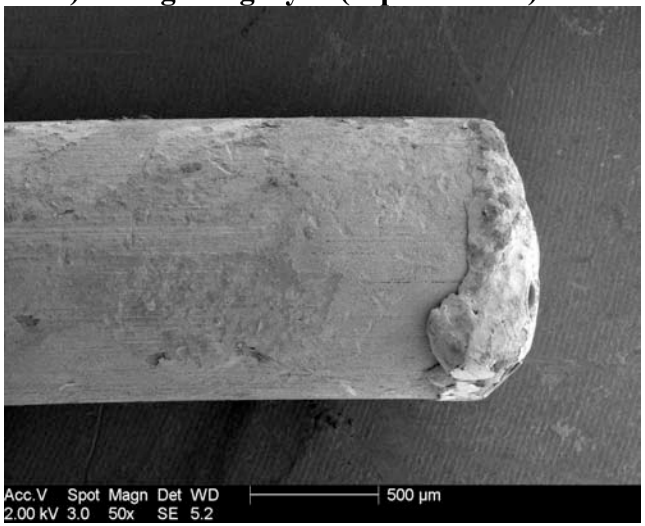

Figure 95 - SEM image of the severed end.

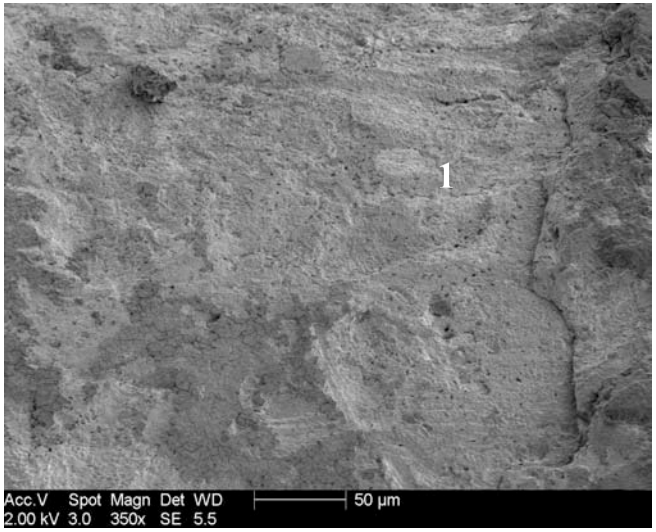

Figure 96 - SEM image of demarcation area at 350x magnification.

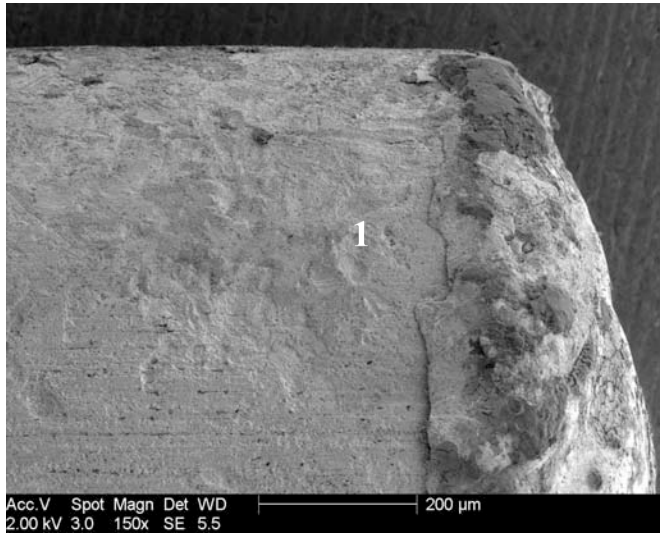

Figure 97 - SEM image at 150x magnification detailed in figures 95 and 96.

Microscope and SEM images of exhibit 012 (three of three conductors involved with this exhibit) arcing category E (experiment 5)

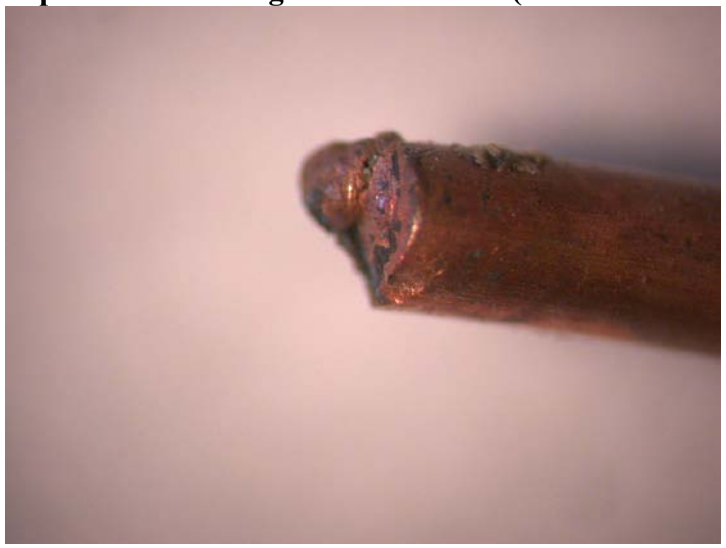

Figure 98 - Microscope image of the bottom severed conductor of exhibit 012

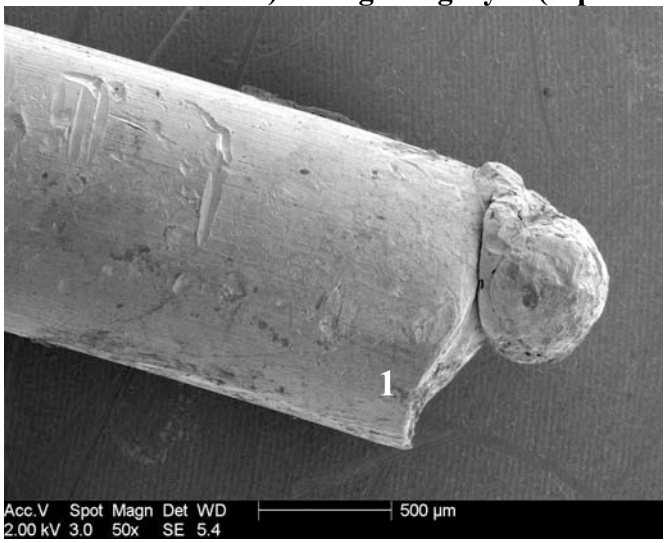

Figure 99 - SEM image of the opposite side of the severed conductor displayed with figure 98.

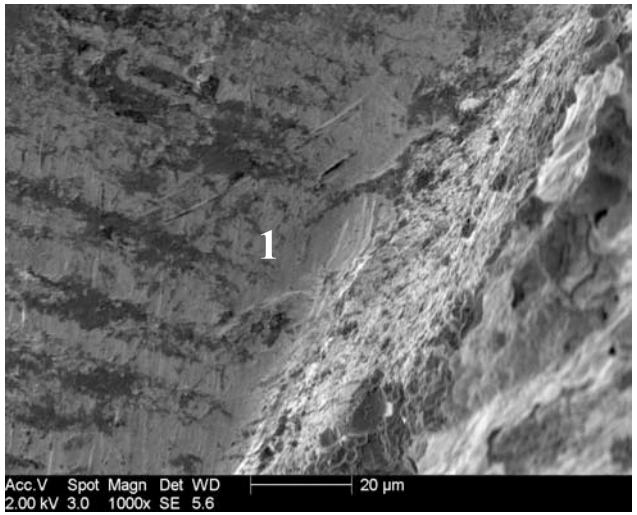

Figure 100 - SEM image of at 1000x magnification of the edge.

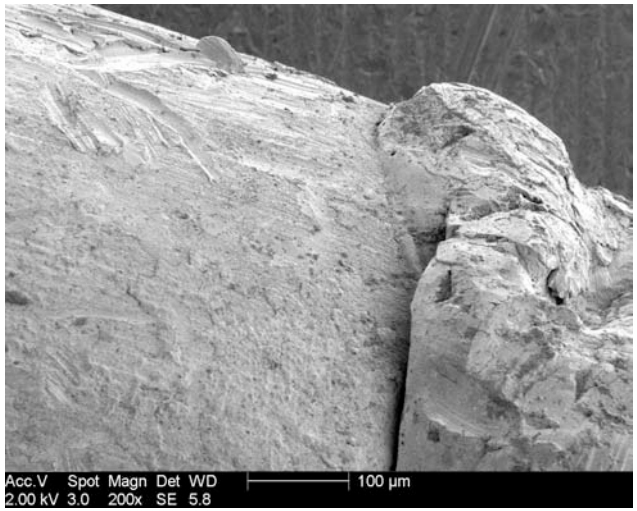

Figure 101 - SEM image of the top edge of fig. 99 at 200x.

Confocal laser scanning microscope images of exhibit 012 (experiment 5)

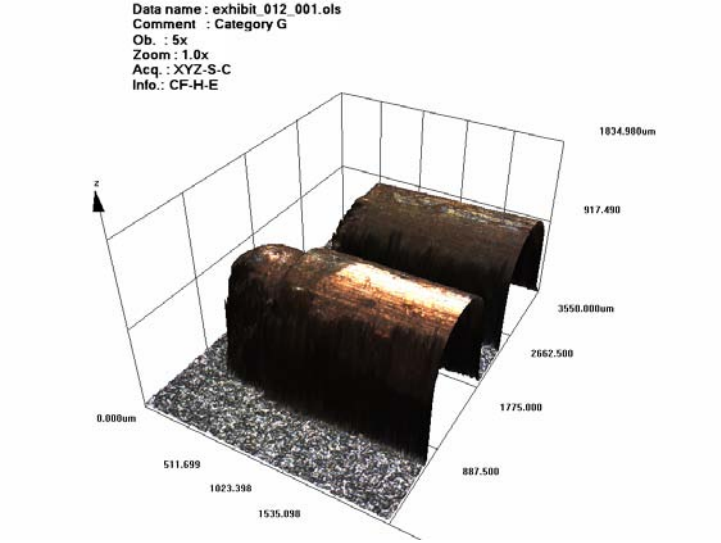

Figure 102 - LEXT image of exhibit 012.

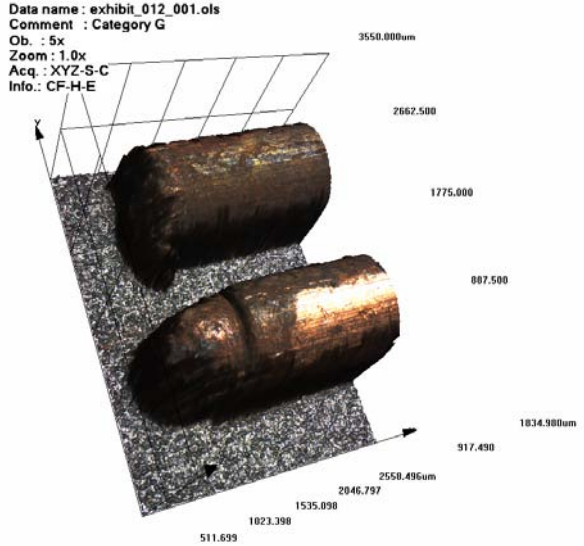

Figure 103 - LEXT image orientated in the software.

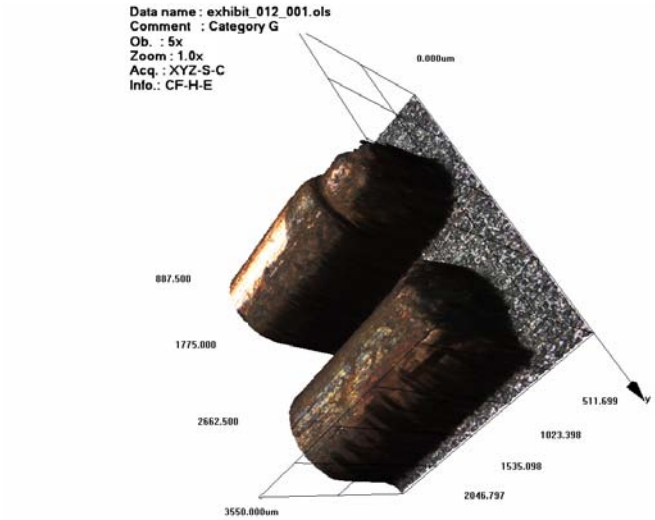

Figure 104 - LEXT image orientated in the LEXT software.

The Confocal laser scanning microscope images of exhibit 012 are limited to two of the three severed conductors of this exhibit. They are detailed figures 91 and figure 95.

The three-dimensional image was orientated within the equipment's dedicated software enabling figures 103 and 104 to be captured.

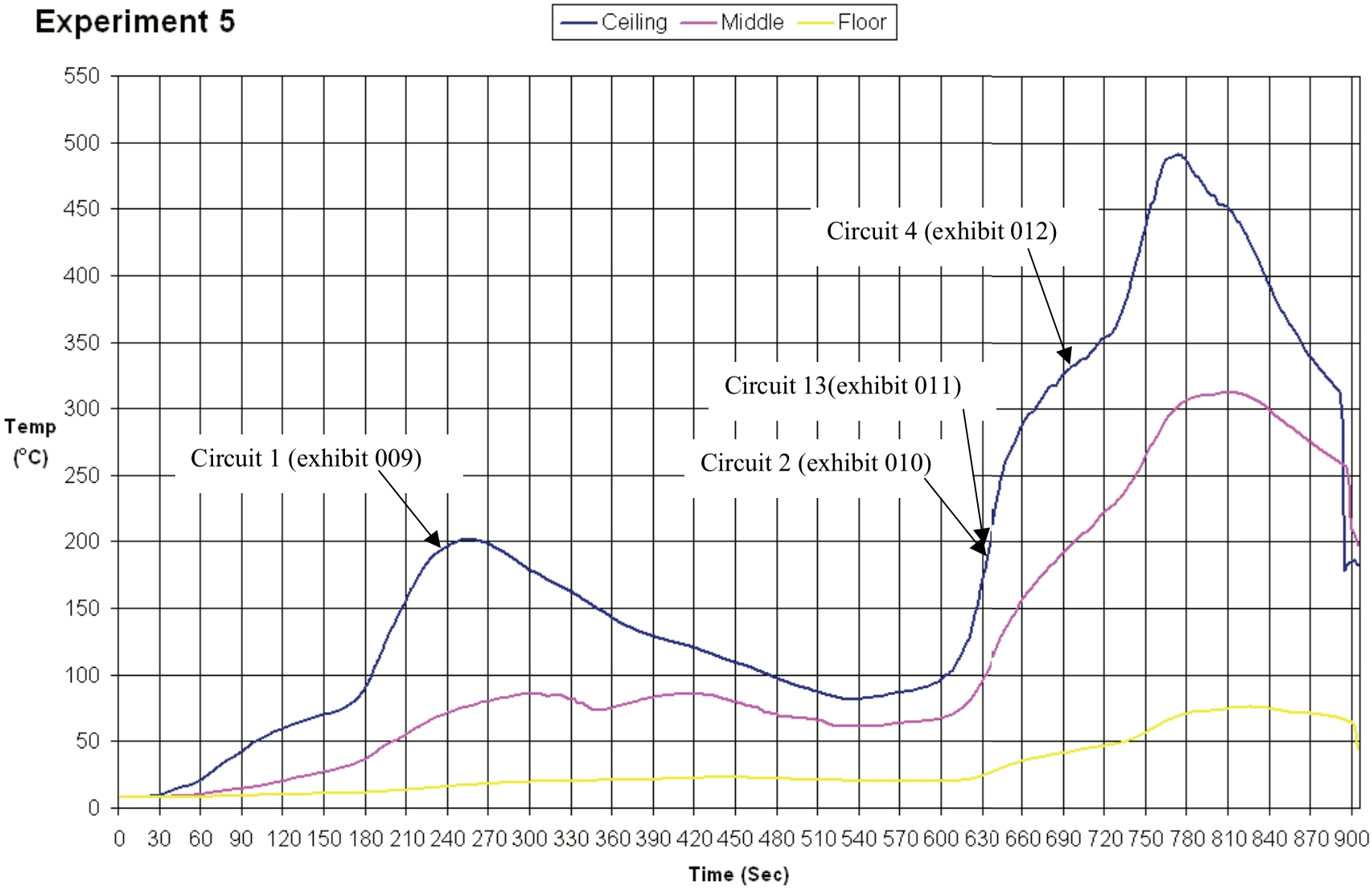

Figure 105 - Temperature graph for experiment 5

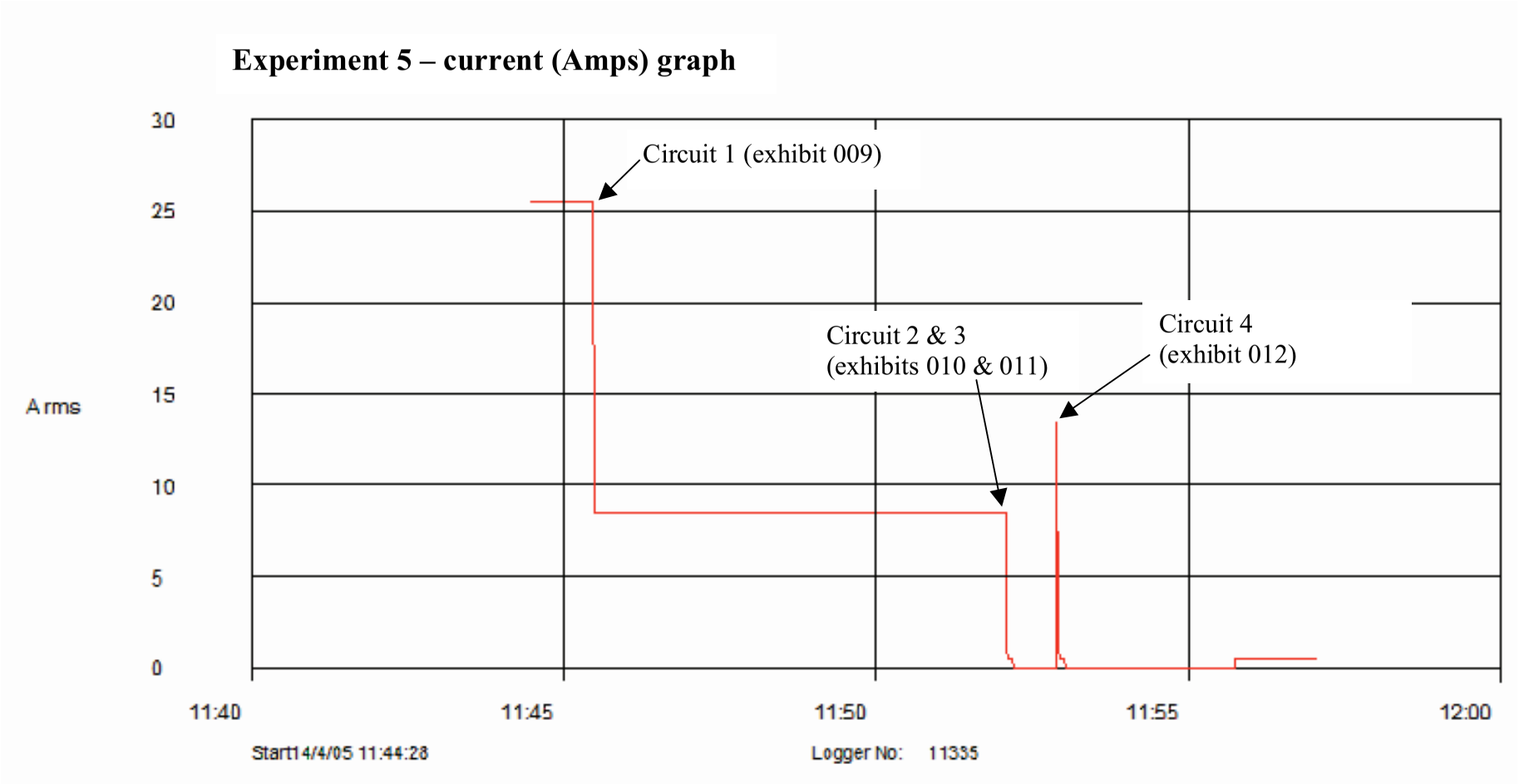

Figure 106 - Current (Amps) graph for experiment 5 detailing the operation of the circuit breakers and the fault current

Experiment 6

Figure 107 “Scenario E” 10 March 2005

Circuit number	MCB operating time from ignition
3	1:45 minutes
1	1:50 minutes
4	1:50 minutes
2	2:14 minutes

Table 7 – circuit breaker operation data

The fire in experiment 6 (scenario E) was laid out in the same way as experiment 4. The fire originated in three separate areas within this compartment. These were inside the wardrobe, a second ignition point a paper trail on the floor, and a third ignition point on the double bed.

The fire developed rapidly with the ceiling thermocouple recording a temperature of 850° C 3.5 minutes from ignition. The floor thermocouple recorded 575° C at this time suggesting that the compartment had reached flashover conditions.

The predominant area of origin for the fire was the wardrobe. The fire spread up and within the wardrobe with flame impingement on the ceiling first observed above the wardrobe.

Arcing damage was located on circuit 1 – 2.93m from left wall above the wardrobe.
Arcing damage was located on circuit 2 – 0.29m from rear wall and 1m from left wall.
Arcing damage was located on circuit 3 - 0.32m from rear wall and 1m from the left wall.
Arcing damage was located on circuit 4 - 0.08m from the rear wall and 1m from the right wall.

Pre and post-fire photographs of experiment 6

Figure 108 - Pre-fire photograph, showing the majority of the room. The black ovals indicate the fire's areas of origin.

Figure 109 - A close-up photograph detailing the ends of circuits 2 and 3.

Figure 110 - Post-fire photograph of the compartment. The white ovals indicate the area of origins. The pre-dominant area was the wardrobe.

Figure 111 - Post-fire photograph detailing with arrows the arcing damage locations of circuits 2 and 3.

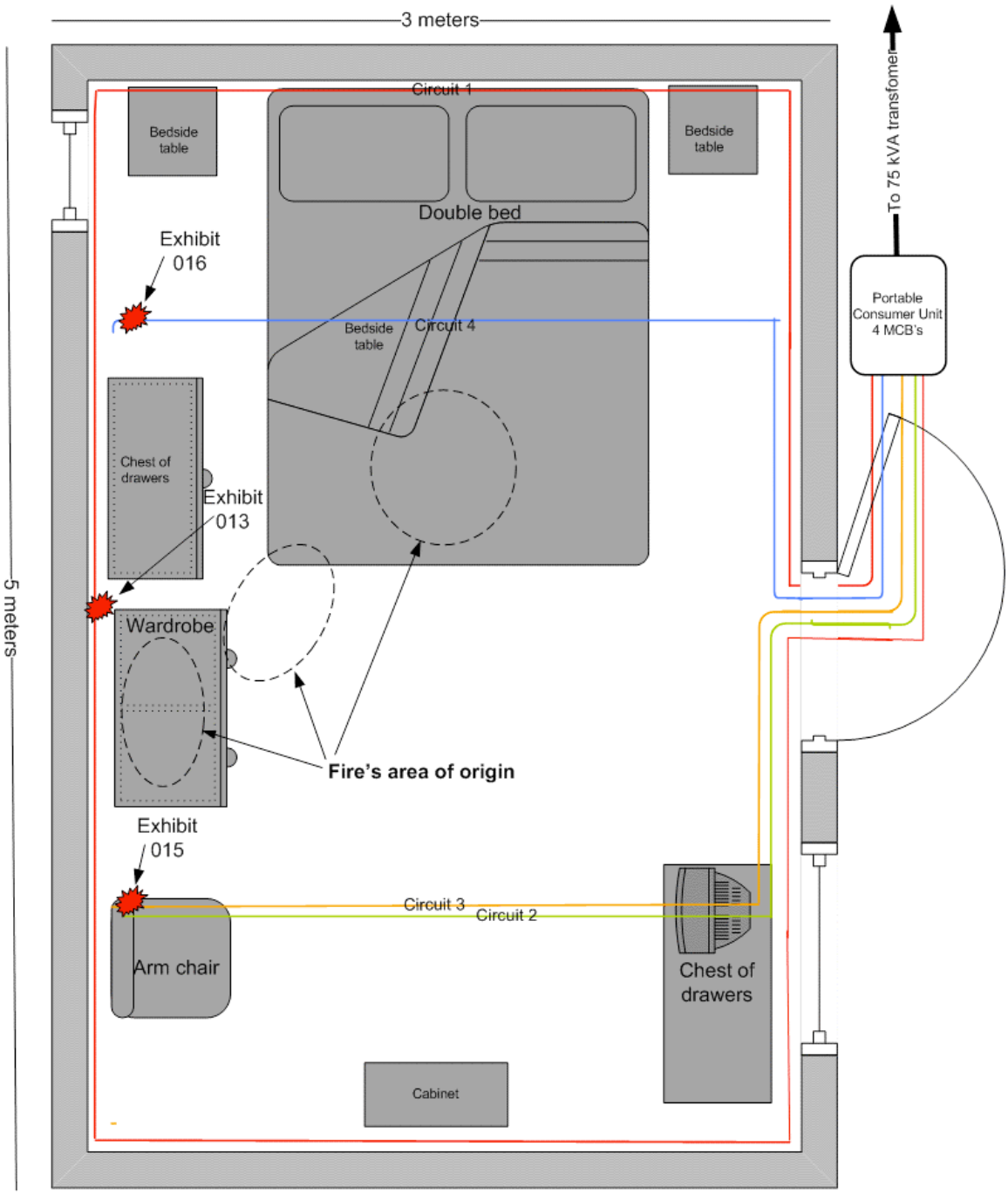

Figure 112 -
Experiment 6 – "Scenario E" 14 April 2005

Scale of 1:20

Microscope and SEM images for exhibit 013 arcing category A – experiment 6

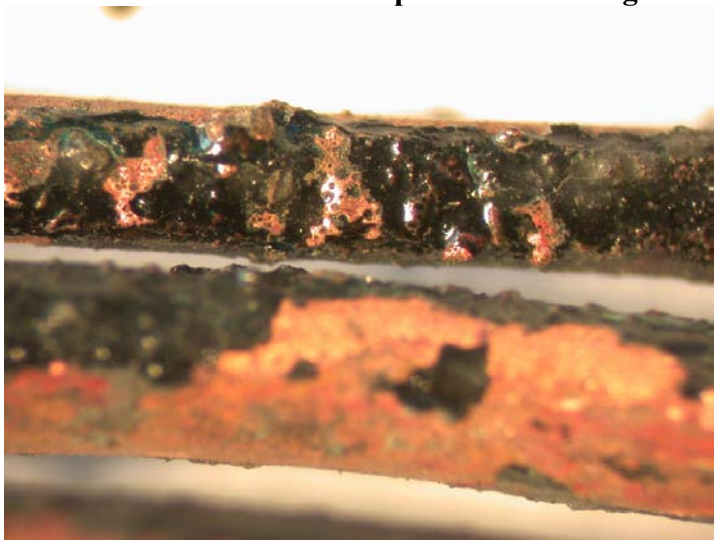

Figure 113 - Microscope image of exhibit 013.

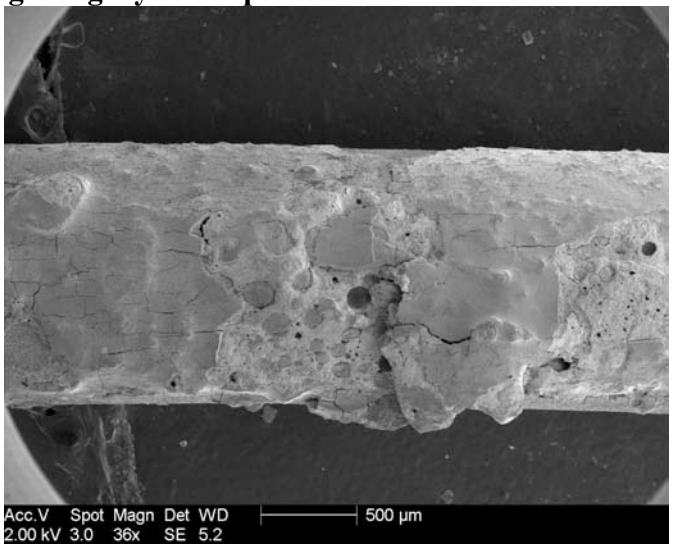

Figure 114 - SEM image of the bottom conductor in fig. 113

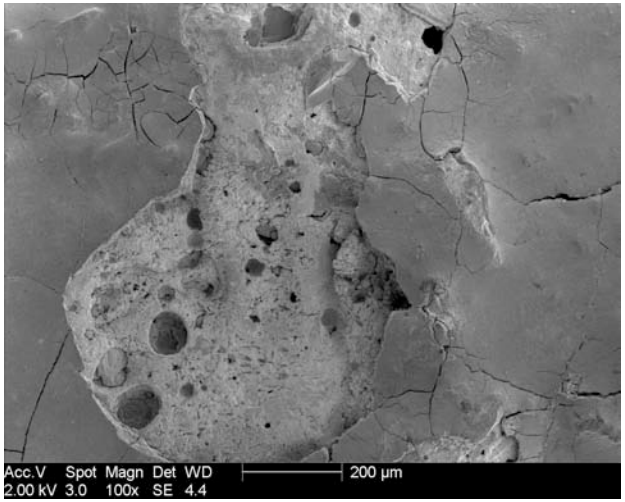

Figure 115 - SEM image of the left edge of the top conductor in figure 113

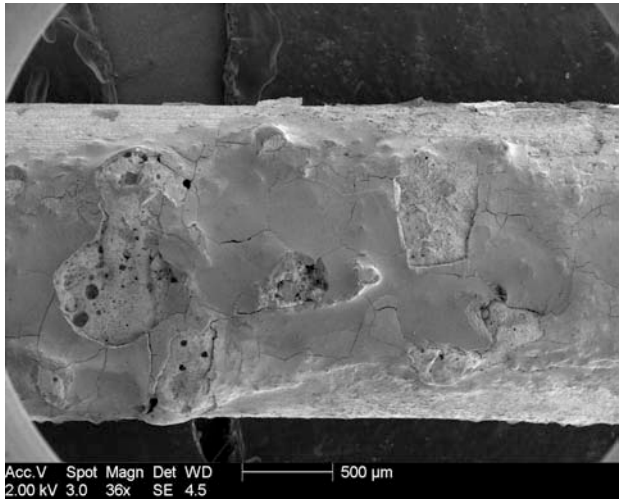

Figure 116 - SEM image of the right edge of the top conductor in figure 113. There is a large amount of PVC debris.

Confocal laser scanning microscope images of exhibit 013 – arcing category A (experiment 6)

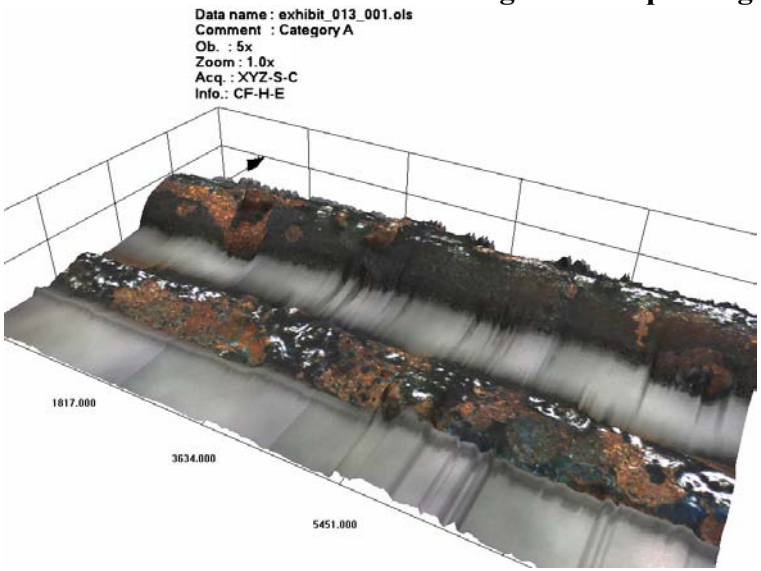

Figure 117 - LEXT image capture of the 3-D scan for exhibit 013.

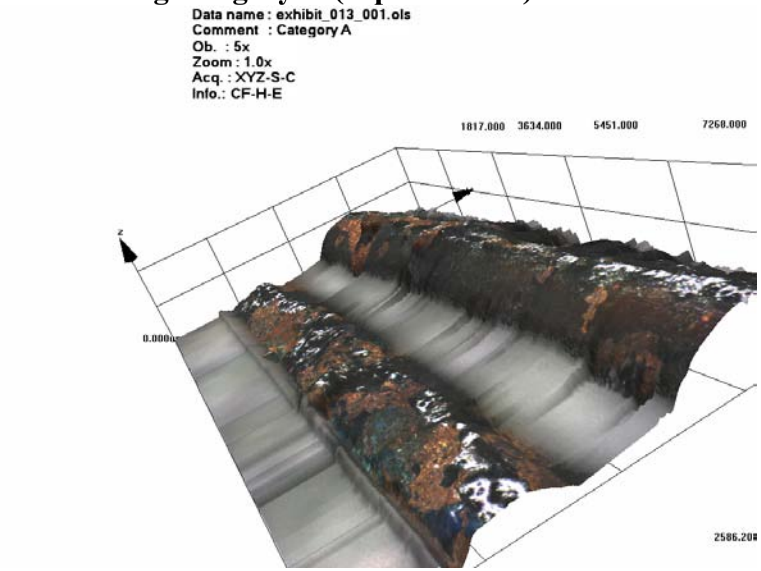

Figure 118- LEXT 3-D scan orientated in the software.

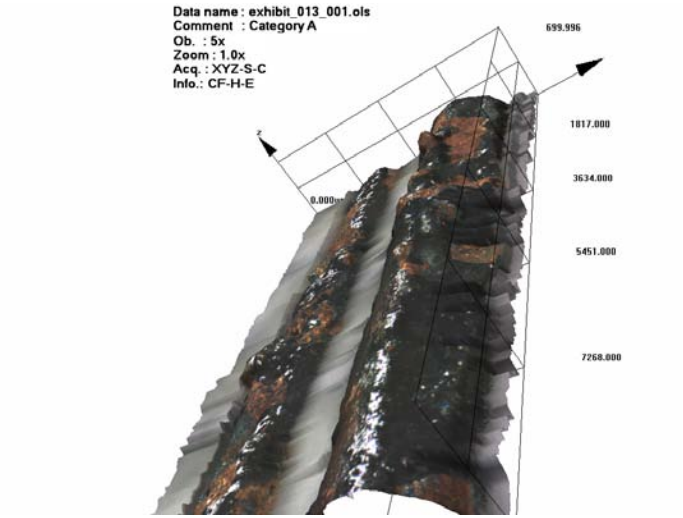

Figure 119 – A capture of the LEXT 3-D scan.

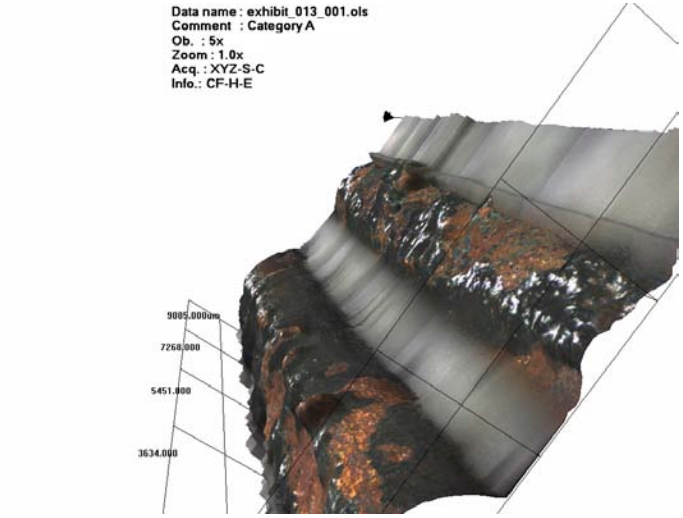

Figure 120 – A capture of the LEXT 3-D scan.

Microscope images for exhibit 015 arcing category B – experiment 6

Figure 121 - Microscope image of exhibit 015.

Figure 122 - Microscope image at 20x magnification of the right severed end.

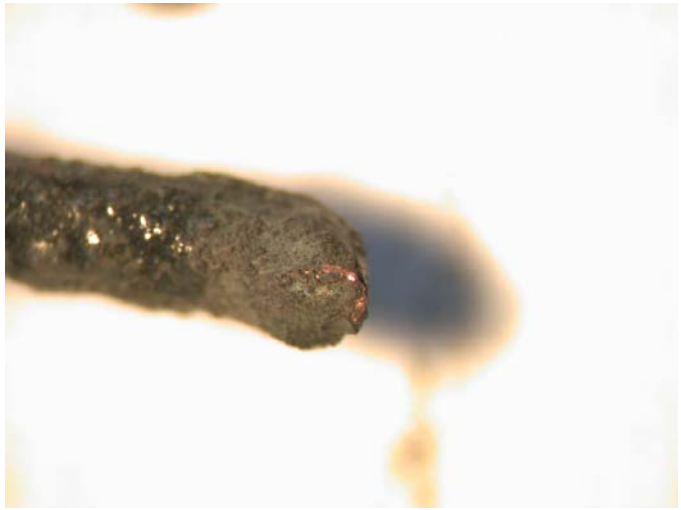

Figure 123 - Microscope image at 20x magnification of the left severed end.

Microscope and SEM images for exhibit 016 arcing category G – experiment 6

Figure 124 - Microscope image of exhibit 016

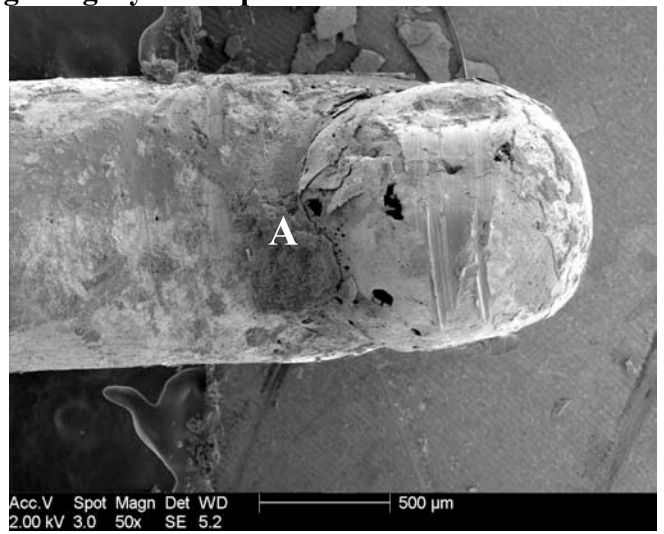

Figure 125 - SEM image of the top conductor in fig. 124

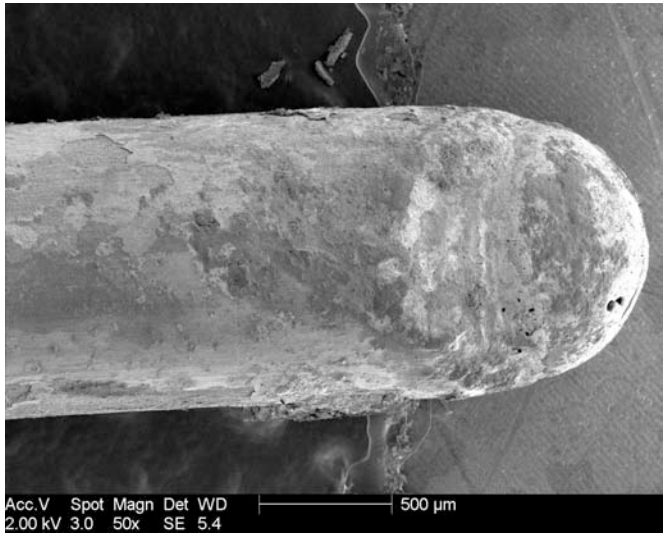

Figure 126 - SEM image of the bottom conductor detailed in fig. 124

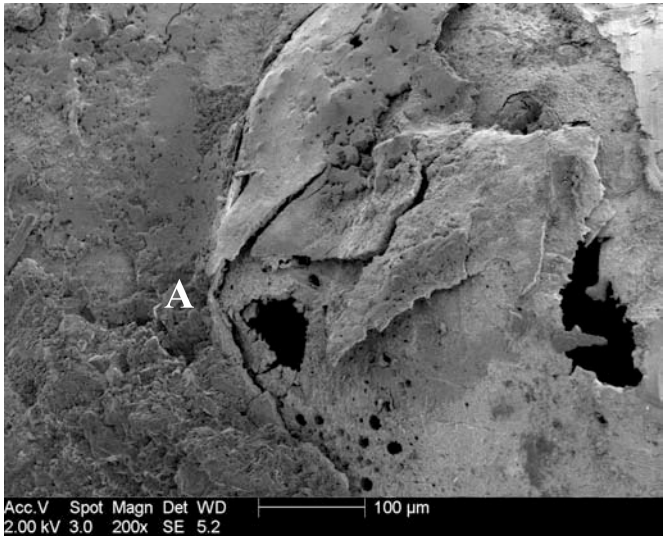

Figure 127 - SEM image at 200x of left area of figure 125

Confocal laser scanning microscope images of exhibit 016 – arcing category G (experiment 6)

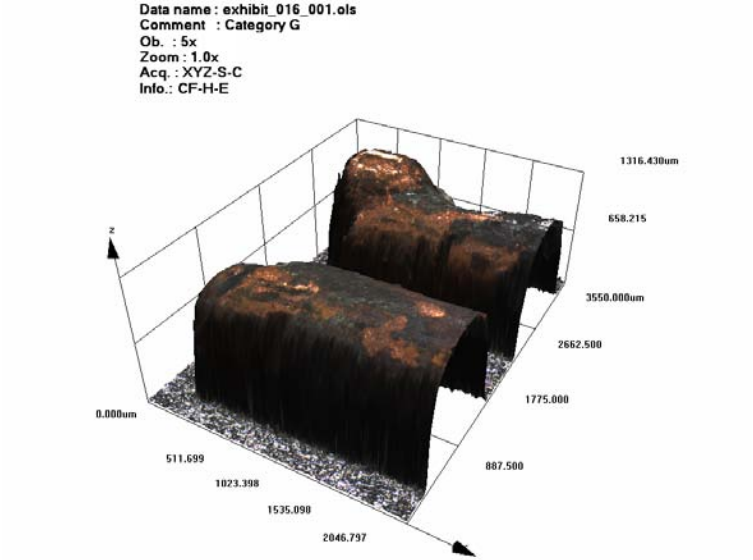

Figure 128 - Image capture of 3-D scan of exhibit 016.

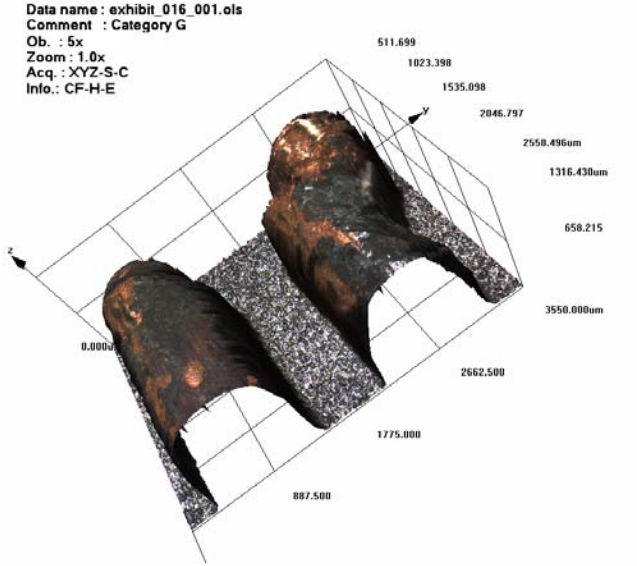

Figure 129 – Capture of the LEXT 3-D scan orientated.

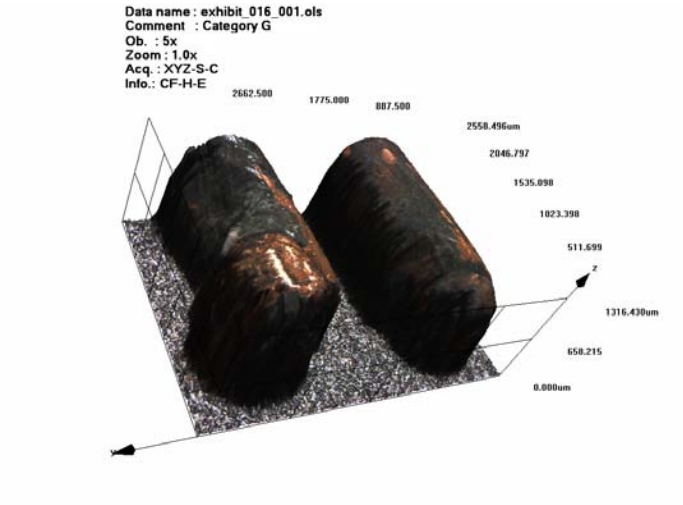

Figure 130 – Capture of the LEXT 3-D scan.

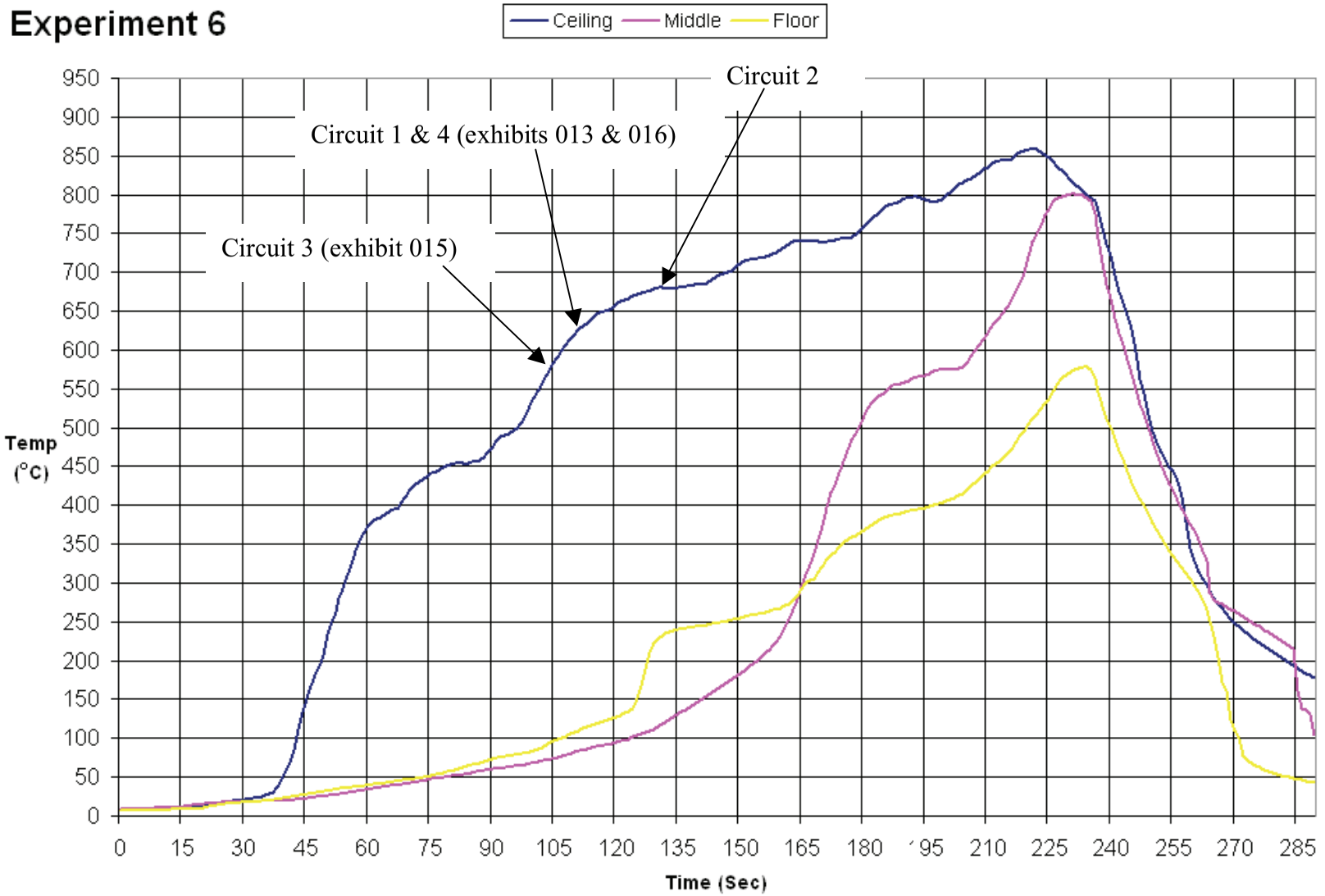

Figure 131 - Temperature graph for experiment 6

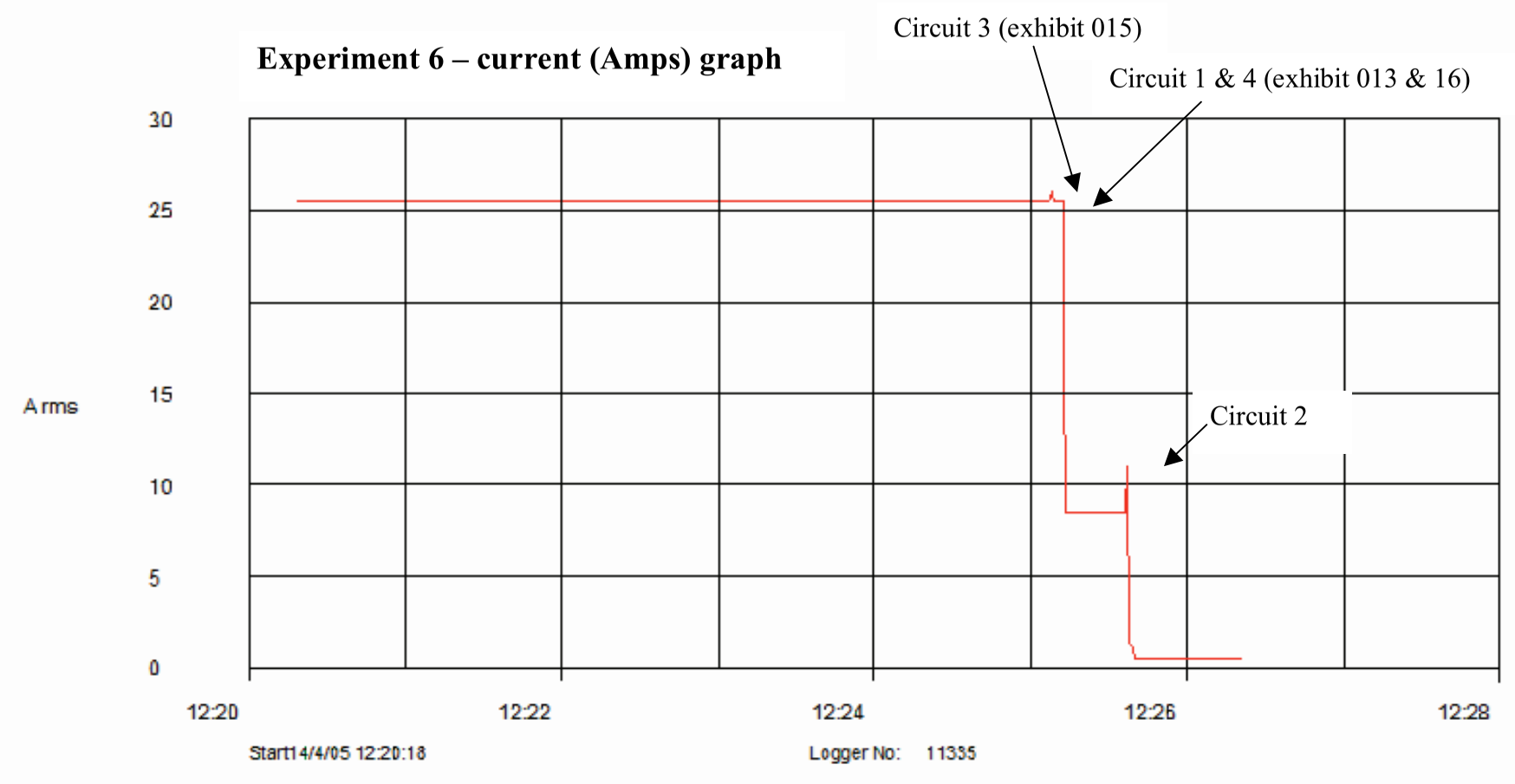

Figure 132 - Current (Amps) graph for experiment 6 detailing the operation of the circuit breakers and the fault current.

Experiment 7

Figure 133 – “Scenario C” 14 April 2005

Circuit number	MCB operating time from ignition
1	4:00 minutes
4	4:18 minutes
2	6:00 minutes
3	6:08 minutes

Table 8 – circuit breaker operation data

The fire in experiment 7 (scenario C) originated in a toy box located between a television and an artificial Christmas tree located at one end of the compartment. The ceiling temperature peaked at 730° C at 7 minutes and 10 seconds. This compartment did not appear to reach flashover conditions prior to the fire being extinguished. This fire was observed to be ventilation controlled as a contributory factor to the fire’s development appeared to be the size of the compartment door until a window within the compartment failed.

Arcing locations in compartment:

Arcing damage was located on circuit 1 – 120mm along front wall (from right wall). This was later determined to be PVC debris and not localised metallic (arcing) damage.
Arcing damage was located on circuit 2 – 220mm from rear wall on the ceiling.
Arcing damage was located on circuit 3 – 180mm from the rear wall on the ceiling.
Arcing damage was located on circuit 4 – 1100mm from front wall on the ceiling

Note: there was no current (Amps) data recorded for this experiment.

Pre-fire and post-fire photographs of experiment 7

Figure 134 - Pre-fire photograph of the compartment.

Figure 135 - Pre-fire photograph of the fire's area of origin indicated with a black oval.

Figure 136 - Post fire photograph of experiment 7, burn patterns show protected areas at low level.

Figure 137 - Post-fire photograph of the area of origin that is indicated with a white oval. Note the TV that fell into this area.

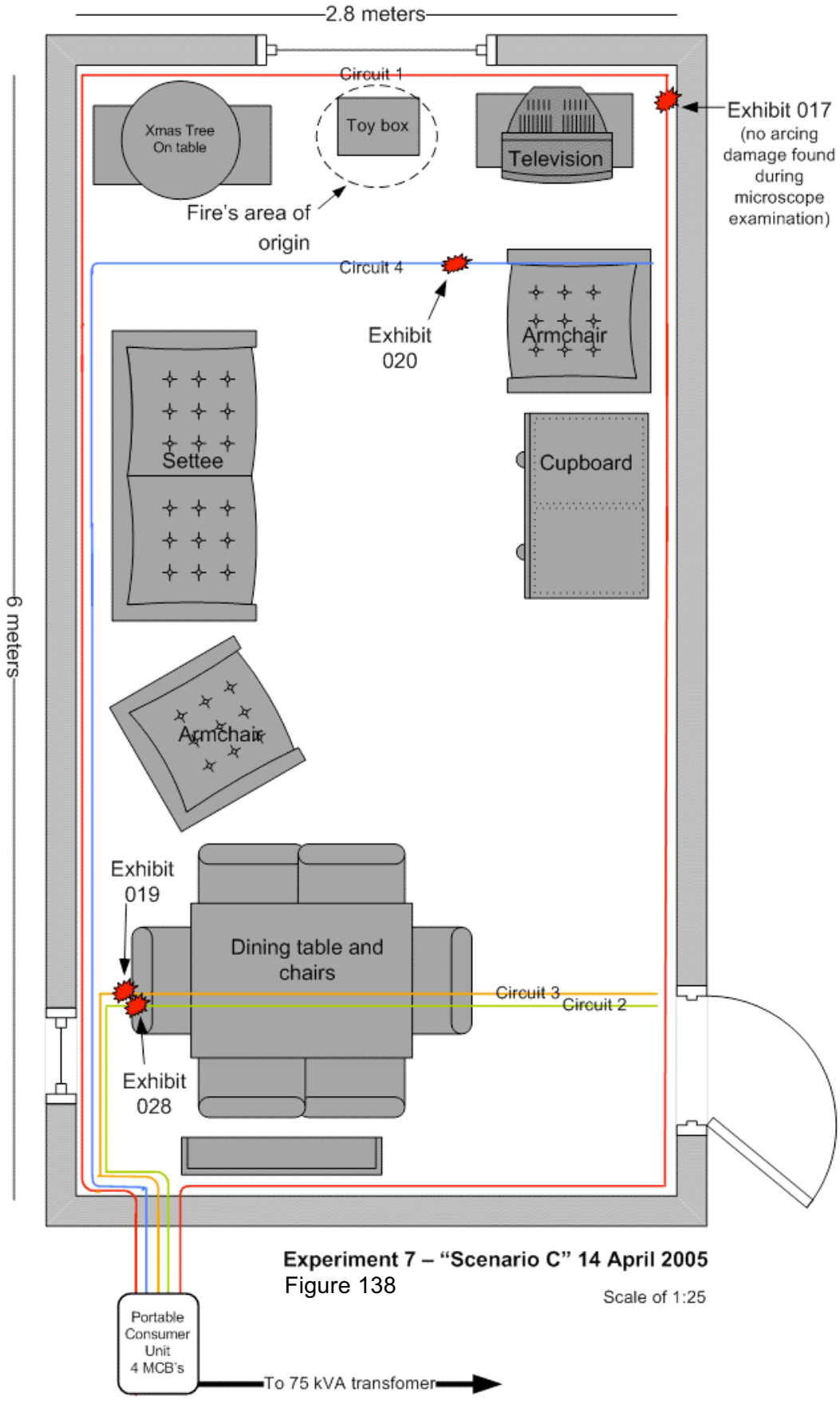

Experiment 7 – "Scenario C" 14 April 2005

Figure 138

Scale of 1:25

Microscope images for exhibit 018 arcing category D – experiment 7

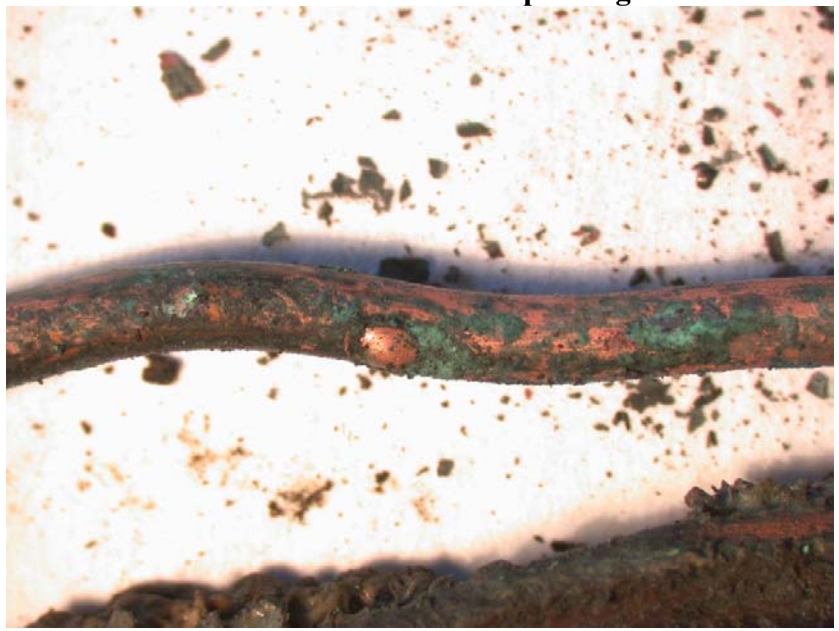

Figure 139 - Microscope image for exhibit 018 detailing the arcing damage to one conductor with a bead located within a notch.

Figure 140 - Microscope image at 20x magnification.

Microscope images for exhibit 019 arcing category D – experiment 7

Figure 141 - Microscope image of exhibit 019 detailing the arcing damage to the bottom conductor.

Figure 142 - Microscope image of at 20 magnification detailing the deep notch and bead within.

Microscope and SEM images for exhibit 020 arcing category C – experiment 7

Figure 143 - Optical microscopic image of exhibit 020, two conductors with localised metallic damage.

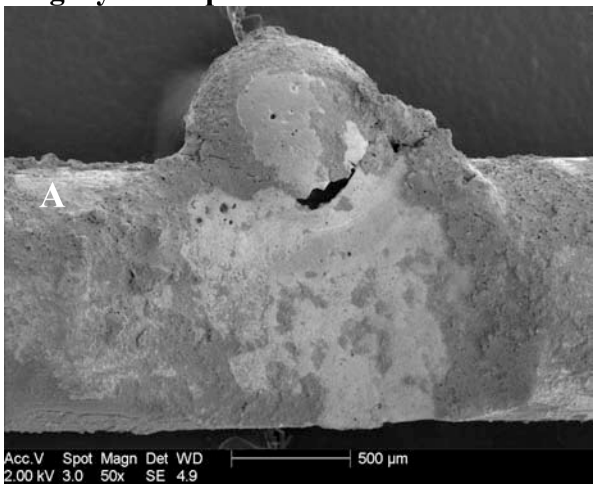

Figure 144 - SEM image of the bottom conductor in figure 143, a notch with a bead on the notch edge.

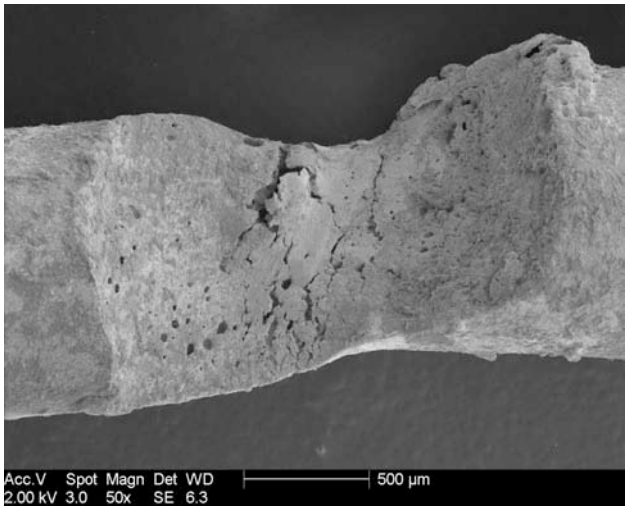

Figure 145 - SEM image of the top conductor in figure 143. This exhibit created a notch with a 2mm diameter.

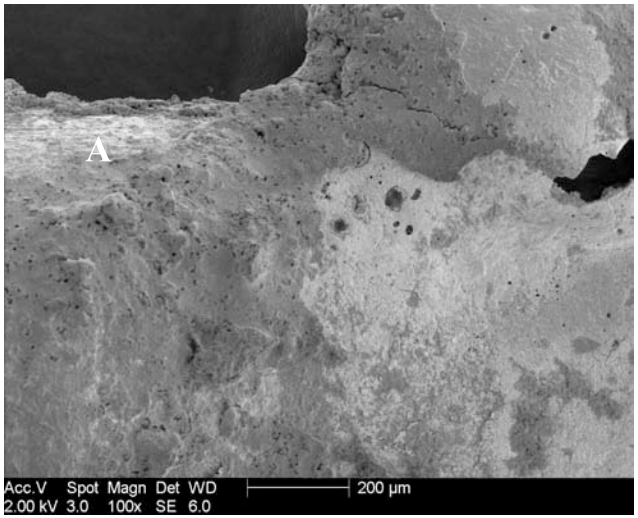

Figure 146 - SEM image at 100x magnification of the area indicted with “A” in figure 144.

Confocal laser scanning microscope images of exhibit 020 – arcing category C (experiment 7)

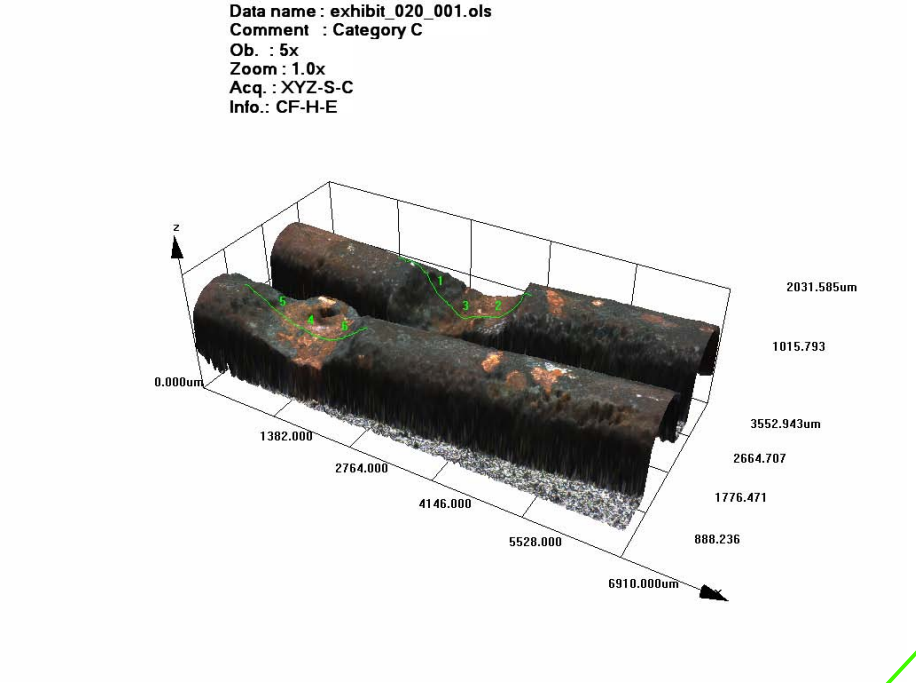

Figure 147 - LEXT image of exhibit 020

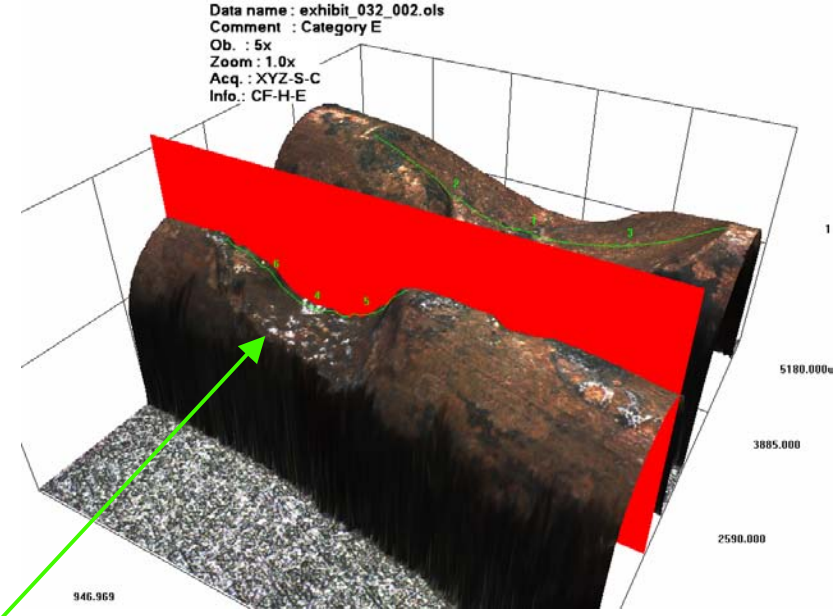

Figure 148 - LEXT image with the software "slice tool" in use

Figure 149 – Profile of notch created with the LEXT software's "slice tool" as detailed in figure 148.

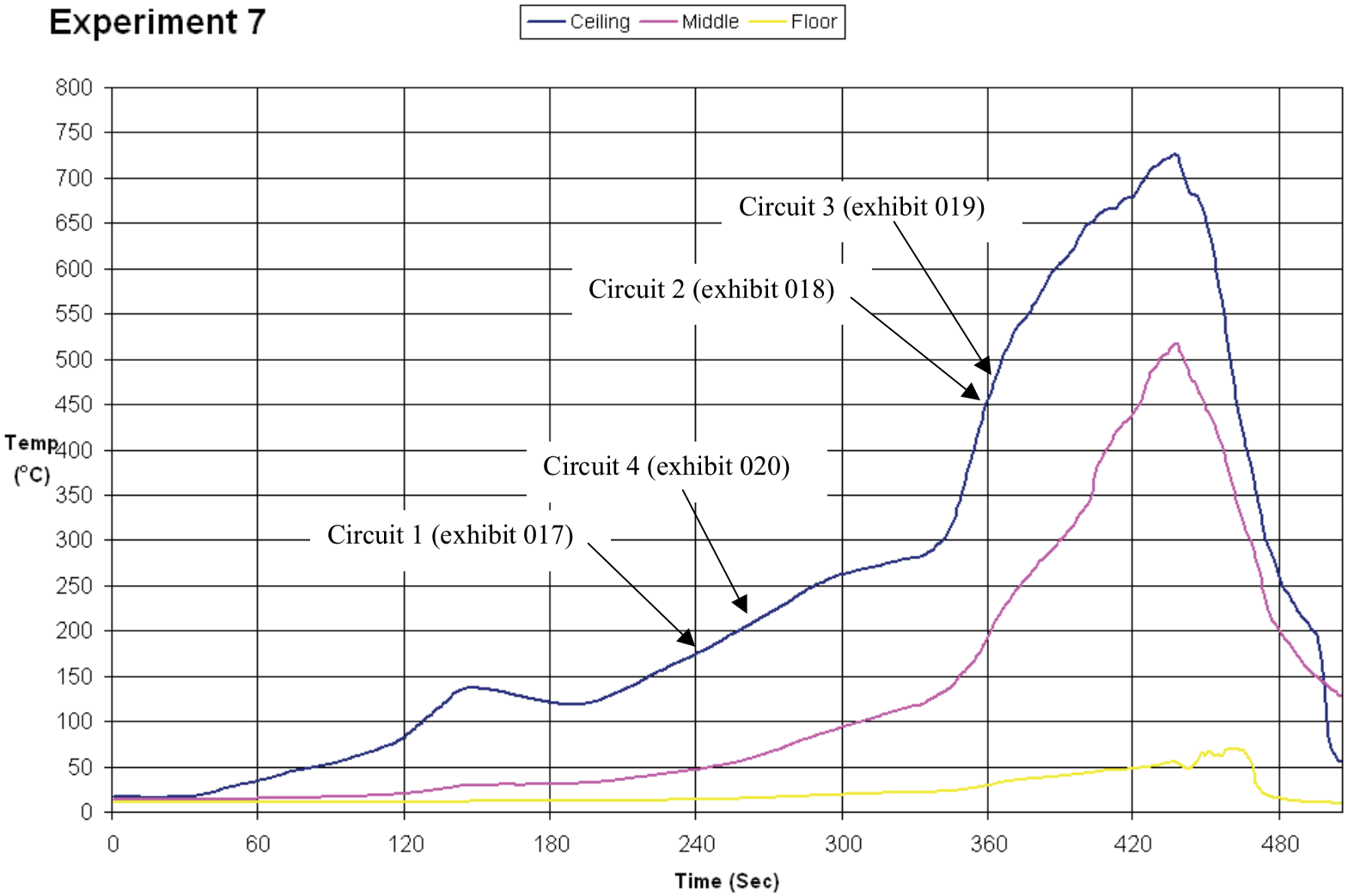

Figure 150 - Time temperature graph of experiment 7

Experiment 8

Experiment 8 – “Scenario A” 14 April 2005

Circuit number	MCB operating time from ignition
1	2:08 minutes
4	2:35 minutes
3	3:41 minutes
2	3:43 minutes

Table 9 – circuit breaker operation data

The fire in experiment 8 (scenario A) originated in clothing located on a clothing rail located between two single beds in the compartment.

The fire was slow to develop with a peak ceiling temperature of 800° C being attained at 8.5 minutes. This fire did not reach flashover conditions, as the floor temperature did not exceed 120° C throughout the fire’s development. The post-fire burn patterns in the compartment also suggest protected areas at low level within the compartment.

Arcing damage locations within the compartment:

Arcing damage was located on circuit 1 – 1140mm from the front wall.

Arcing damage was located on circuit 2 – 230mm from the rear wall and 1000mm from the left wall on the ceiling.

Arcing damage was located on circuit 3 – 1330mm from the rear wall and 1000mm from the left wall on the ceiling.

Arcing damage was located on circuit 4 – 1250mm from the front wall and 1000mm from the right wall on the ceiling.

Pre-fire and post-fire photographs of experiment 8

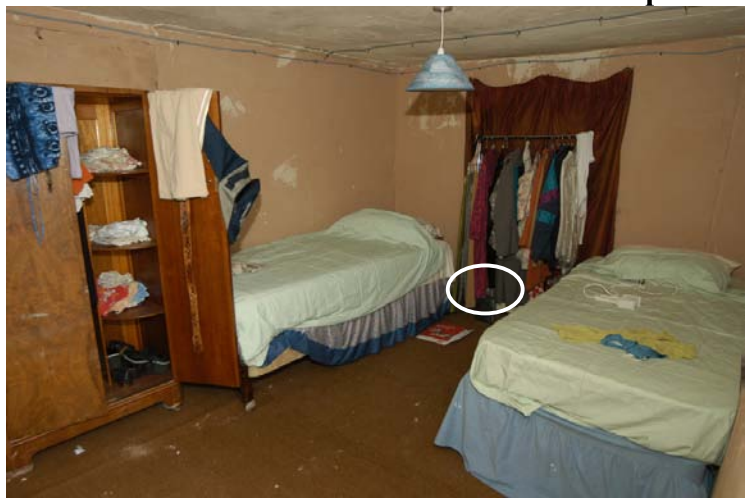

Figure 152 - Pre-fire photograph of experiment 8 detailing the fire's area of origin with the white circle.

Figure 153 - Ignition source (a heater) energised. The photograph details the heating element glowing.

Figure 154 - Post-fire photograph the white oval indicates the fire's area of origin in the compartment.

Figure 155 - The fire developing on the clothes rail approximately 2 minutes after the heater energised.

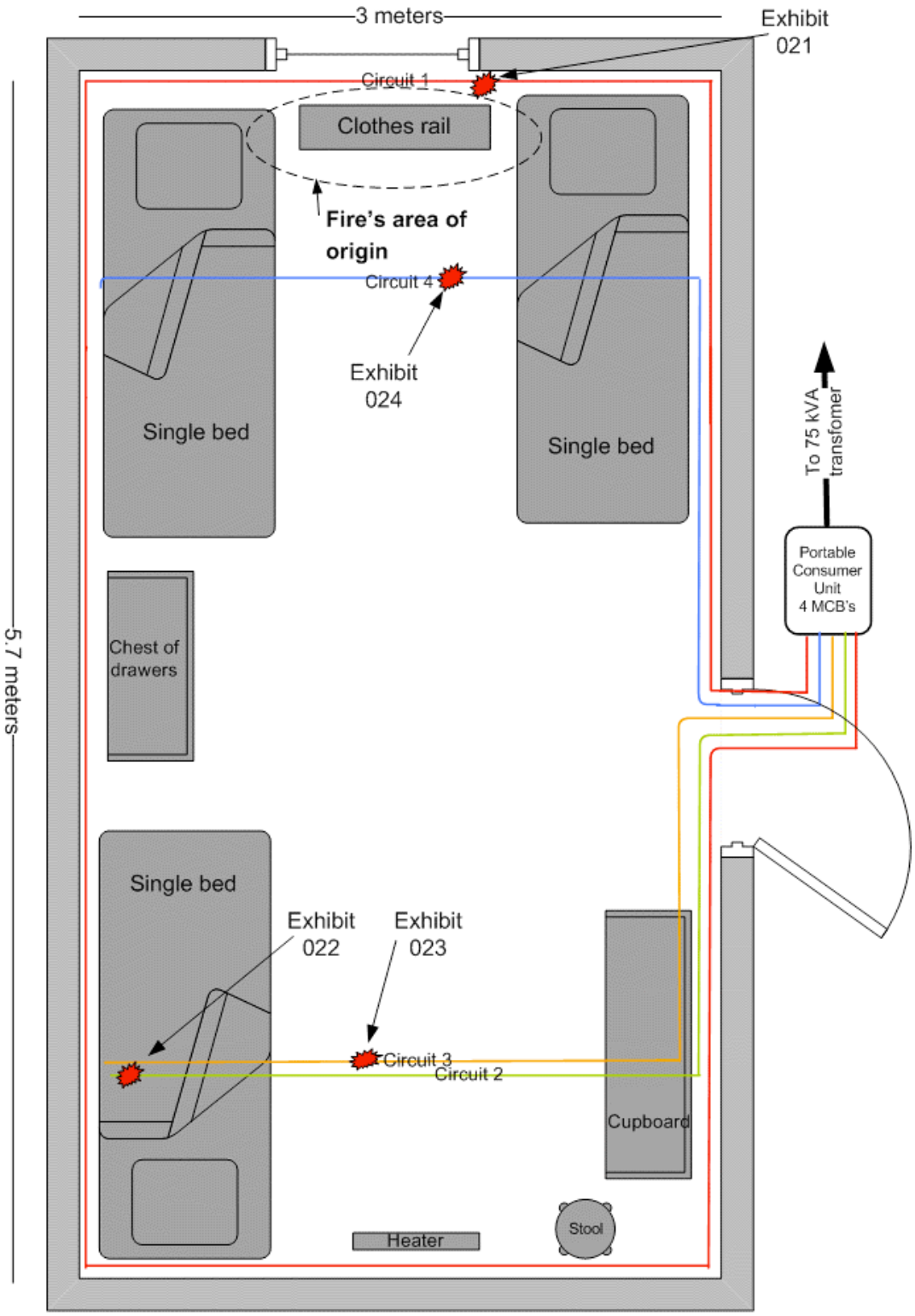

Figure 156 -
Experiment 8 – "Scenario A" 14 April 2005

Scale of 1:25

Microscope images for exhibit 021 arcing category D – experiment 8

Figure 157 - Optical microscope image of exhibit 021

Figure 158 - Close-up image of the lower conductor.

Figure 159 - Close-up image of the top conductor.

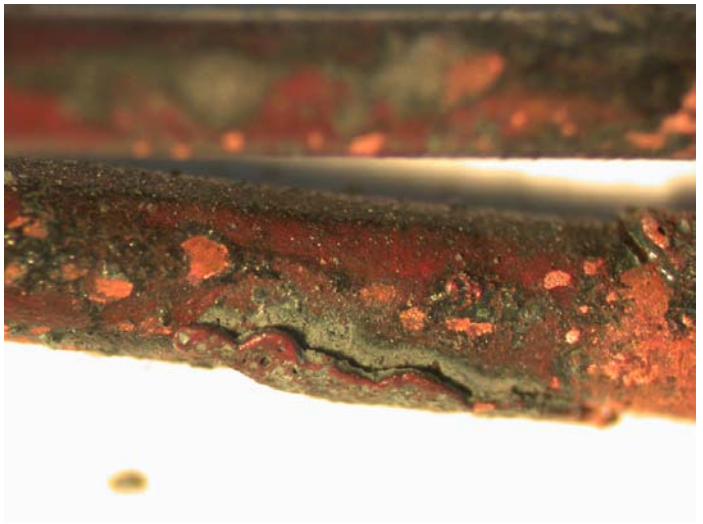

Figure 160 - The opposite view of figure 159.

Microscope images for exhibit 022 arcing category F – experiment 8

Figure 161 - Optical microscope image of exhibit 022

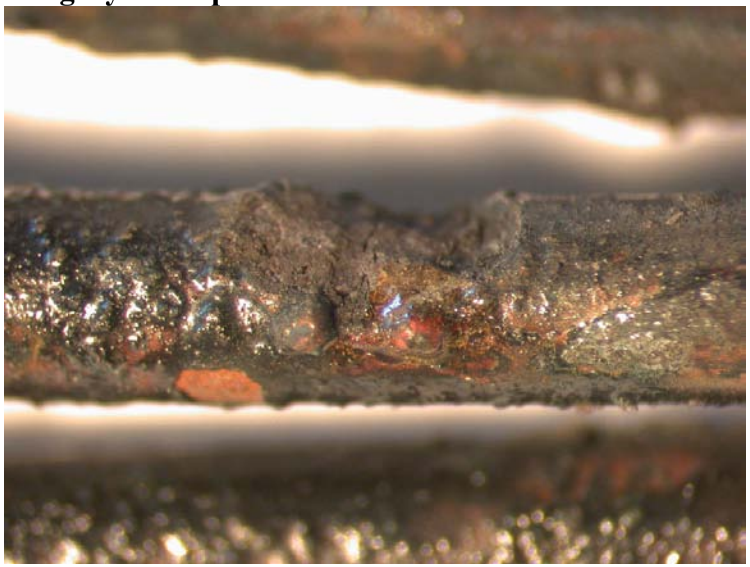

Figure 162 – Right edge of the notch. There was a lot of PVC debris on this exhibit.

Figure 163 - Close-up view of figure 161 at 20x magnification.

Microscope images for exhibit 023 arcing category E – experiment 8

Figure 164 - Overview of exhibit 023 with 2 of 3 conductors involved.

Figure 165 - Close-up image of the two conductors at 15x magnification

Figure 166 - Close-up view of the top conductor detailed in figure 164

Figure 167 - Bead on the underside of the notch detailed in figure 165.

Microscope and SEM images for exhibit 024 arcing category B – experiment 8

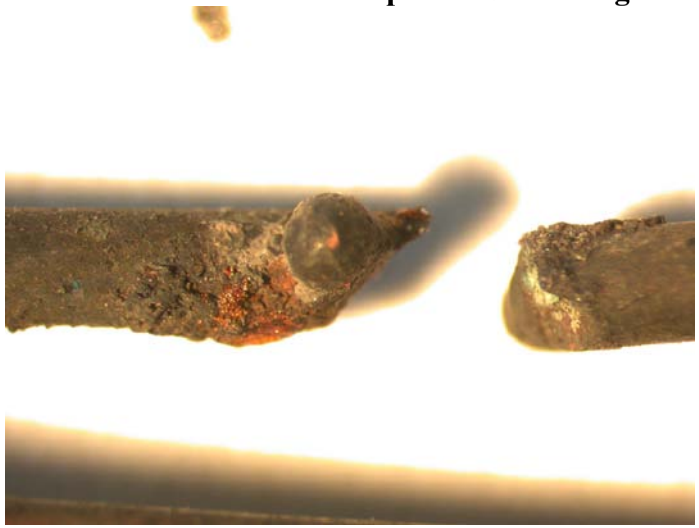

Figure 168 - Optical microscope image of exhibit 024

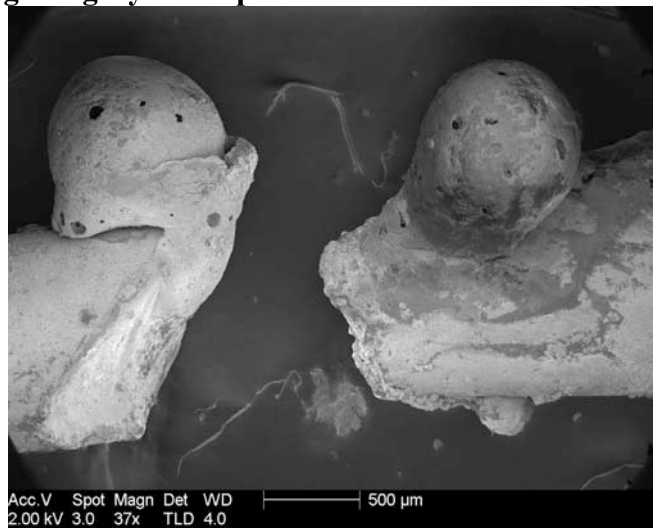

Figure 169 - SEM image of the two severed ends.

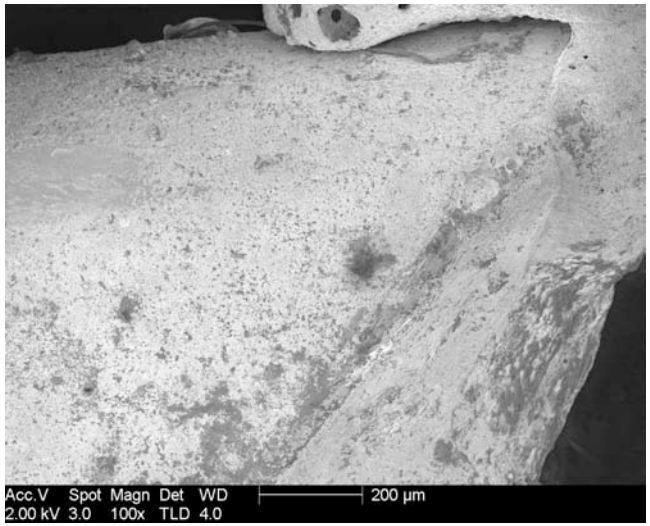

Figure 170 - SEM image of left severed end's demarcation area.

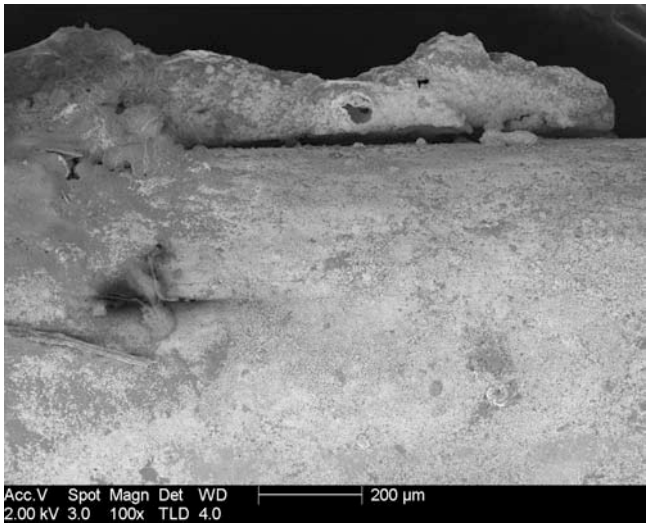

Figure 171 - SEM image at 100x of copper splatter in the demarcation area, out of view in figure 169.

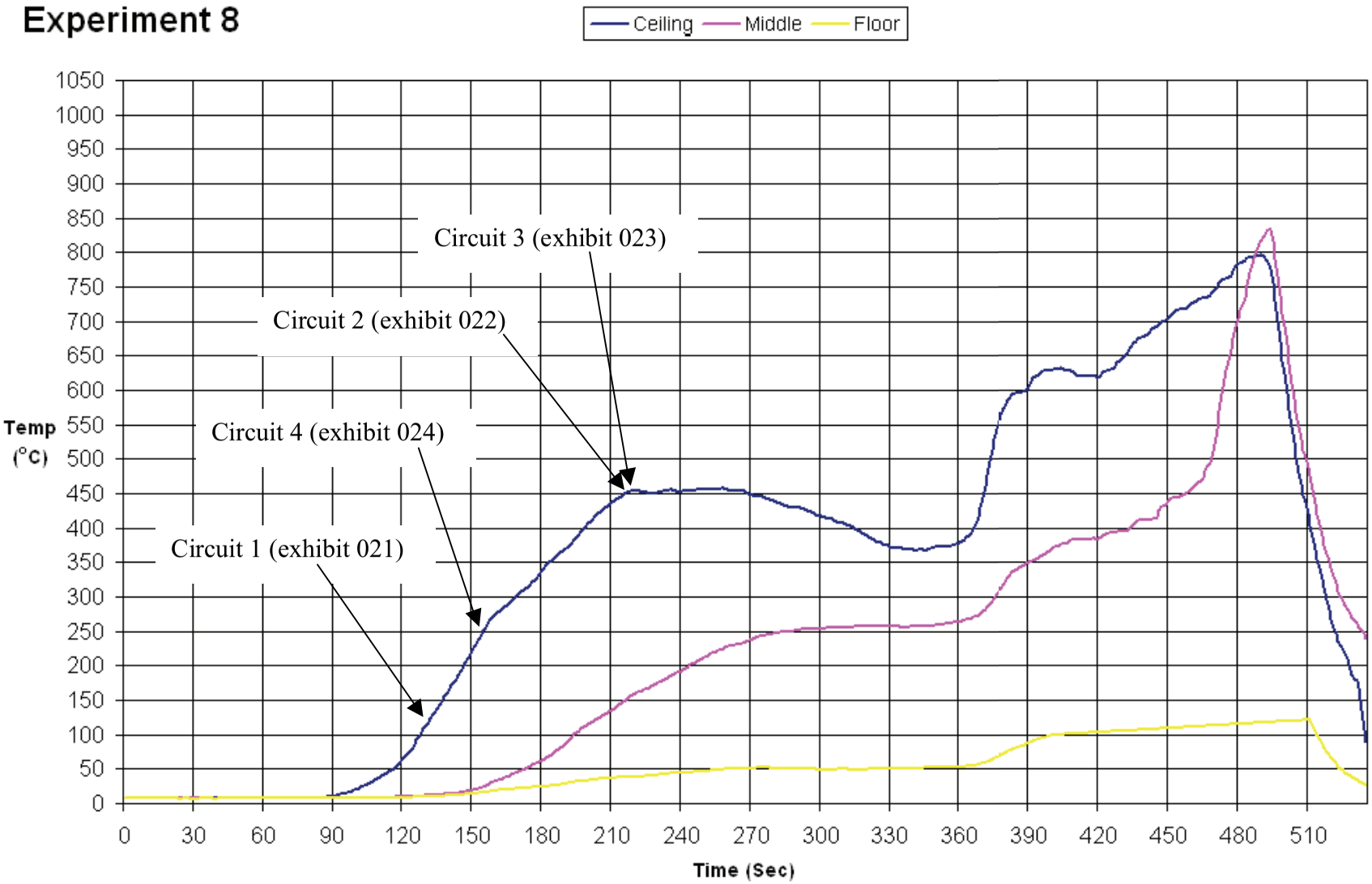

Figure 172 - Time temperature graph for experiment 8

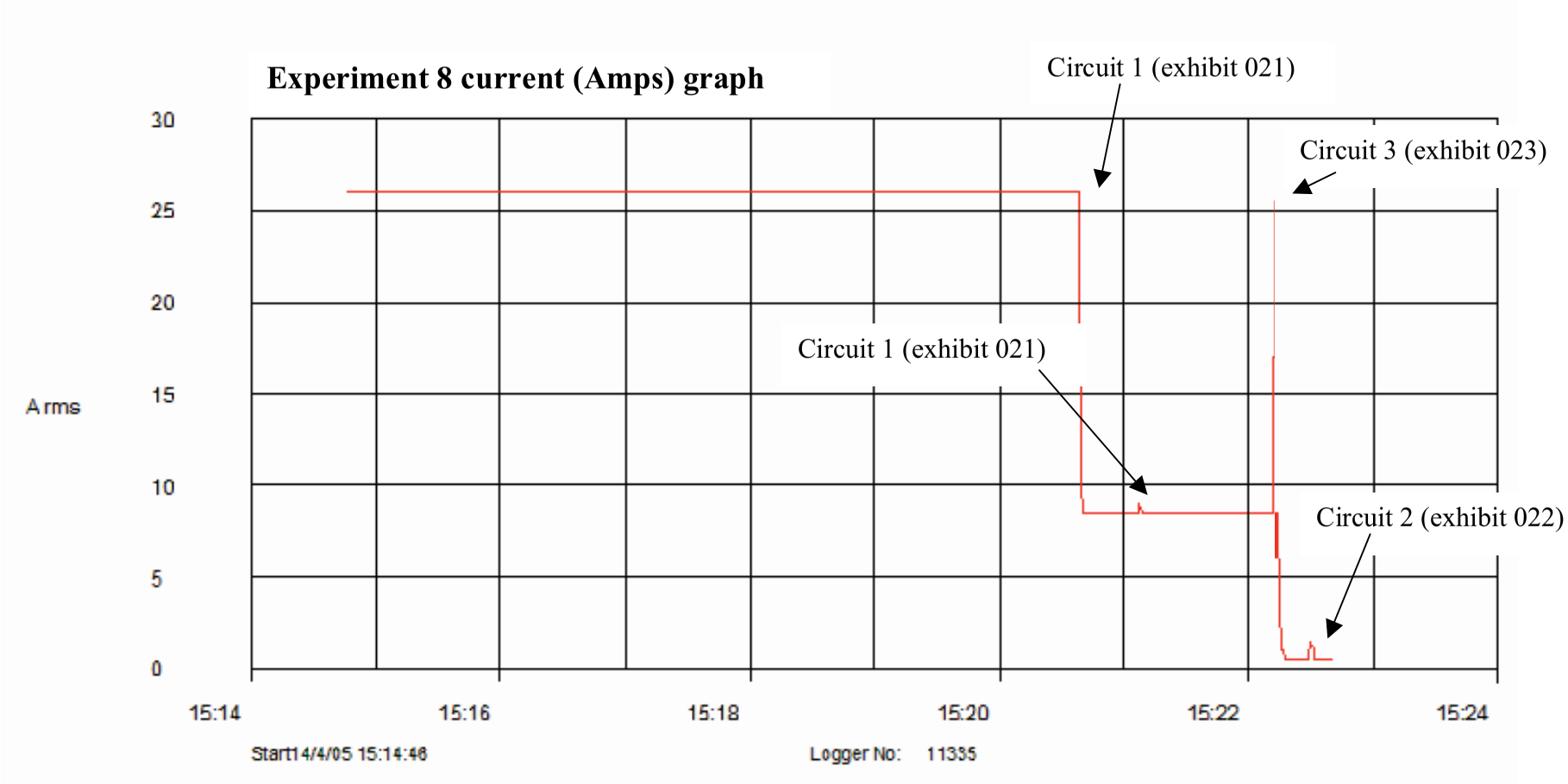

Figure 173 - Current (Amps) graph for experiment 8 detailing the operation of the circuit breakers and the fault current

Experiment 9

Figure 174 – "Scenario D" 8 September 2005

Circuit number	MCB operating time from ignition
1	1:09 minutes
2	1:19 minutes
3	1:25 minutes
4	1:39 minutes

Table 10 – circuit breaker operation data

The fire in experiment 9 (scenario D) originated in two separate areas within the scene. These locations were within two armchairs, one on each side of one end of the compartment. The armchairs were ignited using a mixture of white spirit and diesel fuel.

The fire developed rapidly and flashover conditions were reached in 2.5 minutes. The peak ceiling temperature was 975° C with the middle temperature thermocouple recording just over 1000° C at the point of flashover.

Locations of localised metallic damage to the conductors: Arcing damage was located on circuit 1 – 650mm from the left wall.

Arcing damage was located on circuit 2 – 1400mm from the left wall and 1000mm from the front wall on the ceiling.

Arcing damage was located on circuit 3 – 1400mm from the rear wall and 1000mm from the front wall on the ceiling. (Circuits 2 and 3 appear to have faulted together at the same point).

Arcing damage was located on circuit 4 – 100mm from the left wall and 1000mm from the rear wall on the ceiling.

Pre-fire, fire development and post-fire photographs of experiment 9

Figure 175 - Pre-fire photograph of experiment 9. The white oval indicates the fire's areas of origin.

Figure 176 - Two separate fires involving the two armchairs have just been ignited and are developing.

Figure 177 - Post-fire photograph of the experiment.

Figure 178 - The smoke layer is increasing in size.

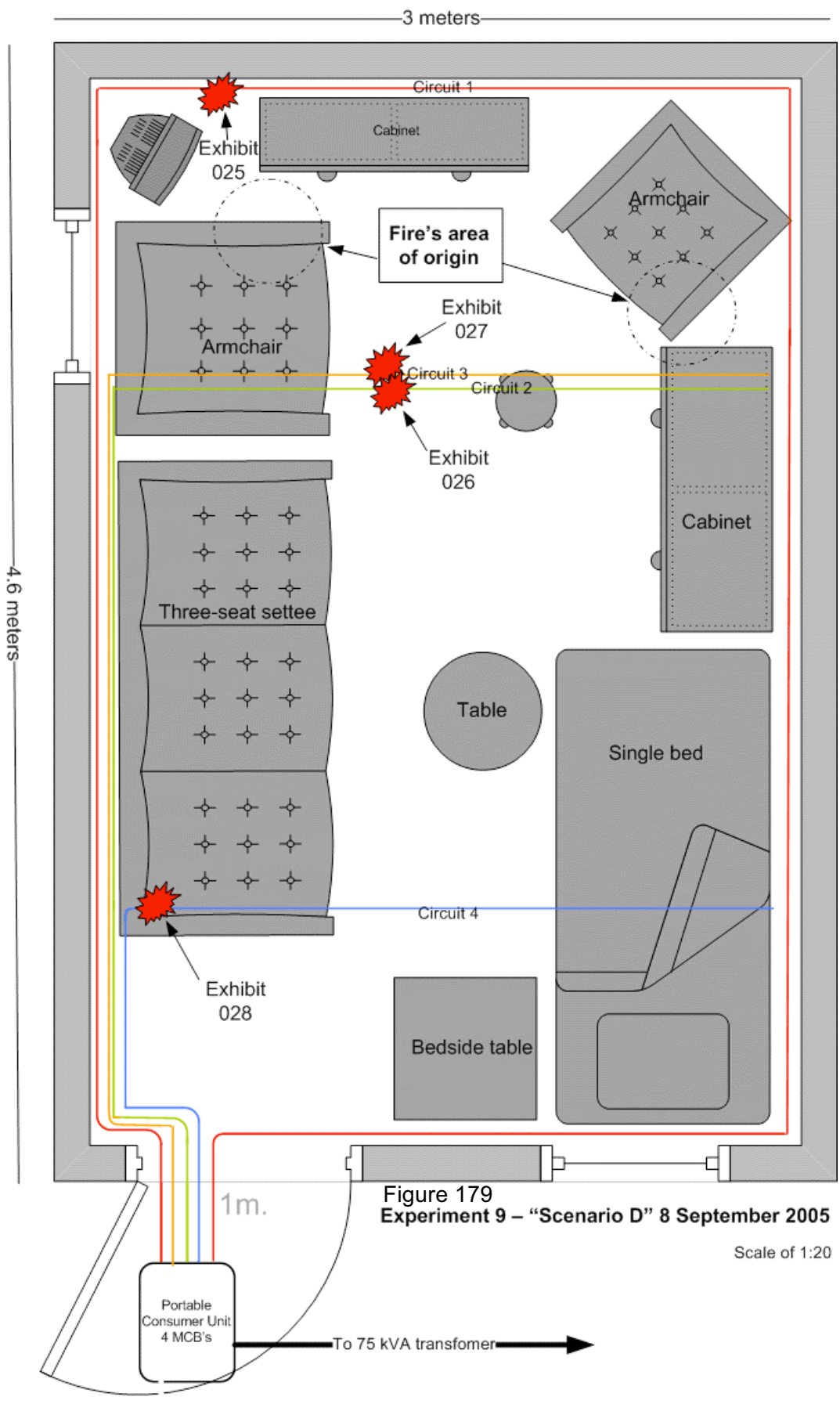

Figure 179
Experiment 9 – "Scenario D" 8 September 2005

Scale of 1:20

Microscope images for exhibit 025 arcing category E – experiment 9

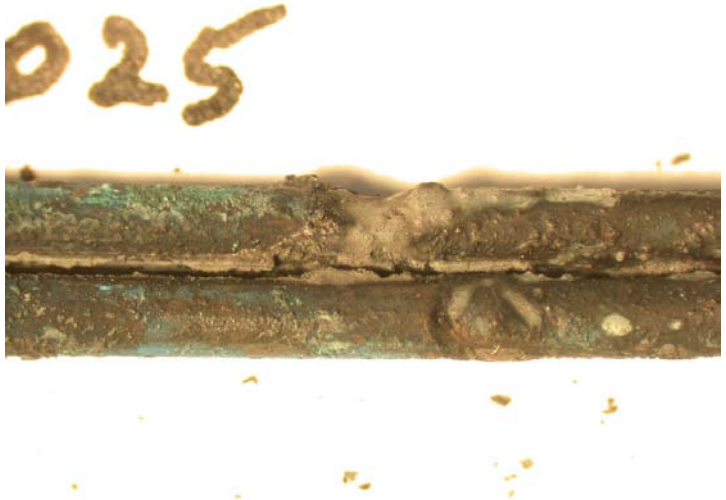

Figure 180 - Microscope image of exhibit 25. The localised melting has affected two conductors each with a notch.

Figure 181 - Microscope image detailing the notch of the bottom conductor.

Figure 182 – Similar view of figure 181 with different lighting.

Microscope images for exhibit 026 arcing category E – experiment 9

Figure 183 - Microscope image of exhibit 026. The bottom conductor had a wide notch.

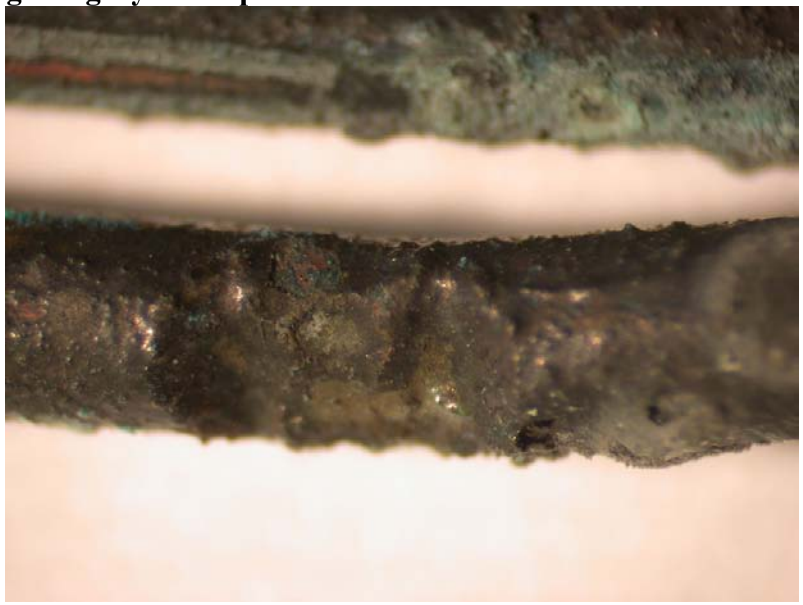

Figure 184 - Microscope image at 20x magnification detailing the notch. The demarcation is clear on the left edge of the notch. There is a lot of PVC debris attached to this exhibit.

Microscope images for exhibit 027 arcing category B – experiment 9

Figure 185 - Microscope image of exhibit 027. This localised metallic damage has severed one of the three conductors.

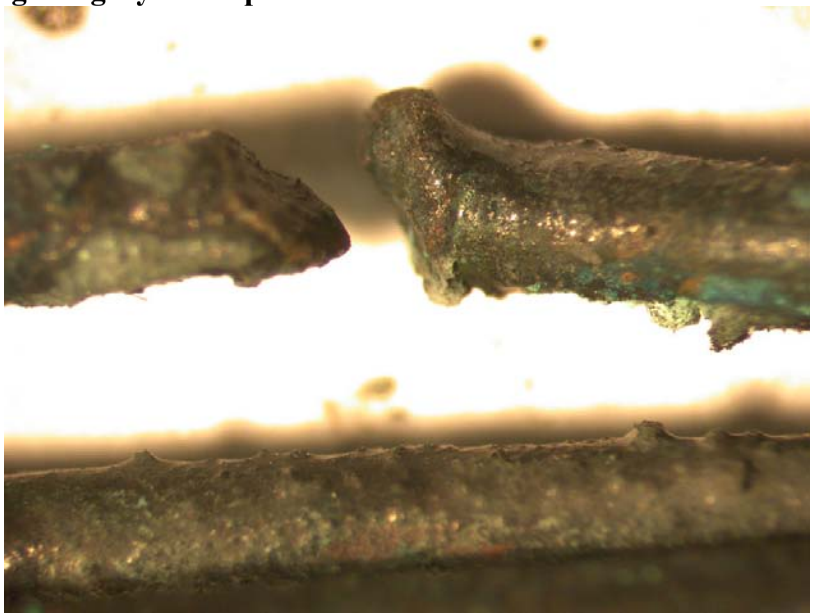

Figure 186 - Microscope image of exhibit of the severed ends at 20x magnification. The depth of field limits the area of the image in focus.

Microscope and SEM images for exhibit 028 arcing category F – experiment 9

Figure 187 - Microscope image of exhibit 028. One of the conductors has a wide notch.

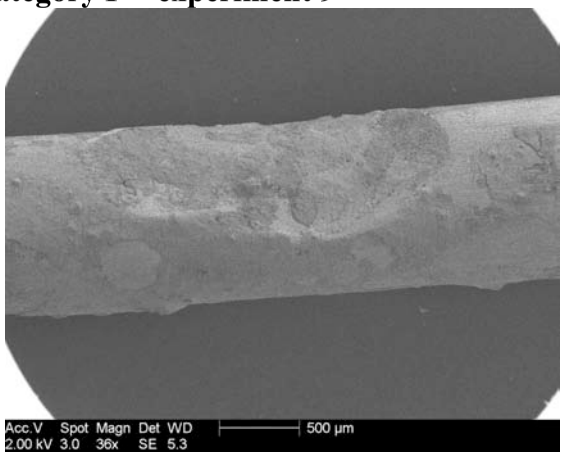

Figure 188 - SEM image of the lower conductor with an overview of the notch. The image quality is an issue due to the operator adjustment of the SEM.

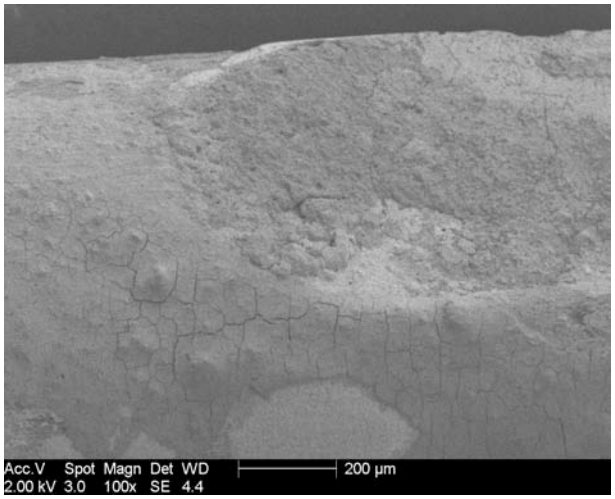

Figure 189 - SEM image of the left side of the notch at 100x magnification.

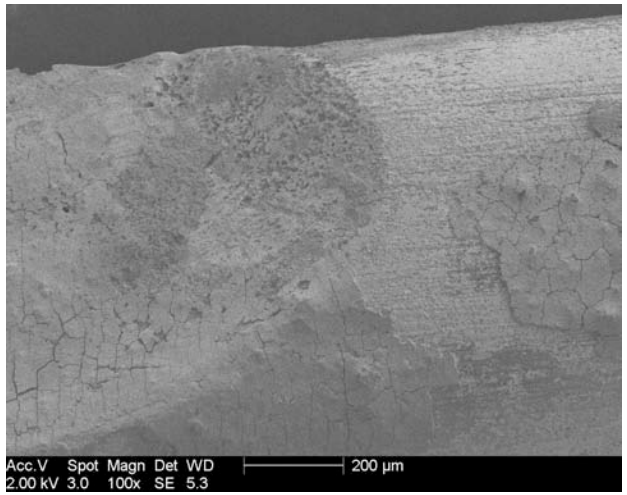

Figure 190 - SEM image of the right side of the notch showing a clear demarcation between the arcing damage and the undamaged area of the conductor.

Confocal laser scanning microscope images of exhibit 028 – arcing category F (experiment 9)

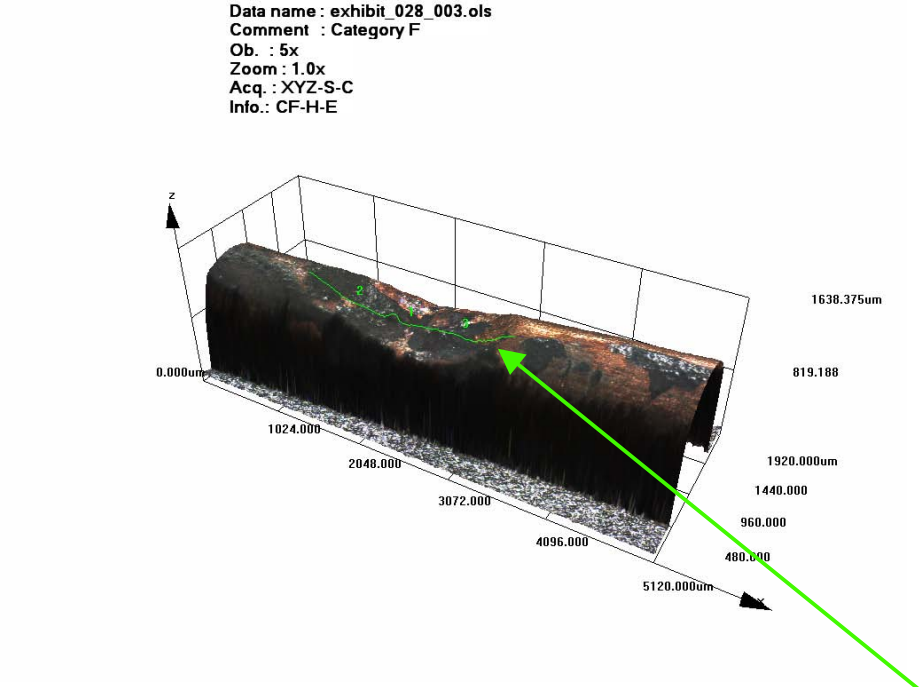

Figure 191 - LEXT image of exhibit 028.

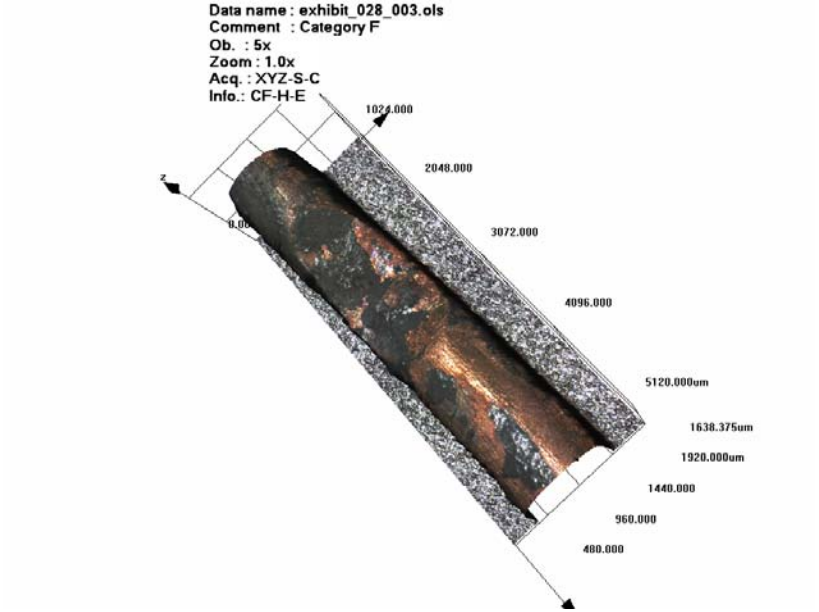

Figure 192 - LEXT 3-D image rotated in the software.

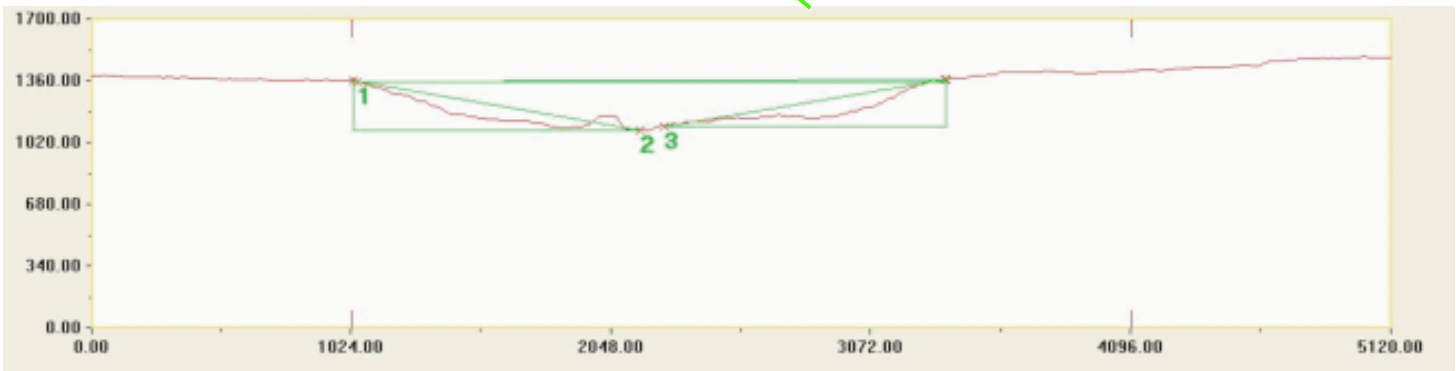

Figure 193 – Profile of the notch captured by using the LEXT software's "slice tool" (scale is detailed in microns).

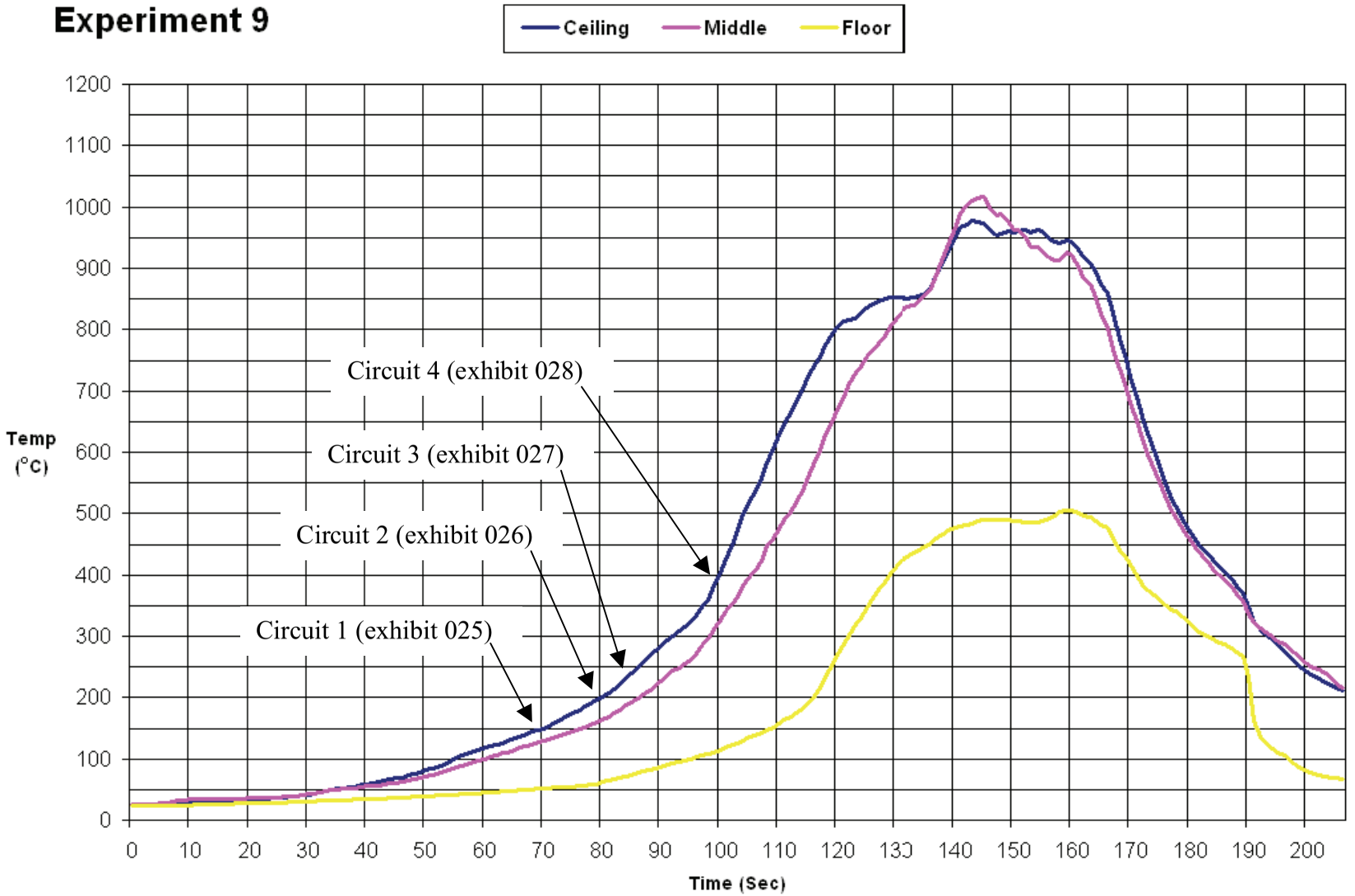

Figure 194 - Time temperature graph for experiment 9

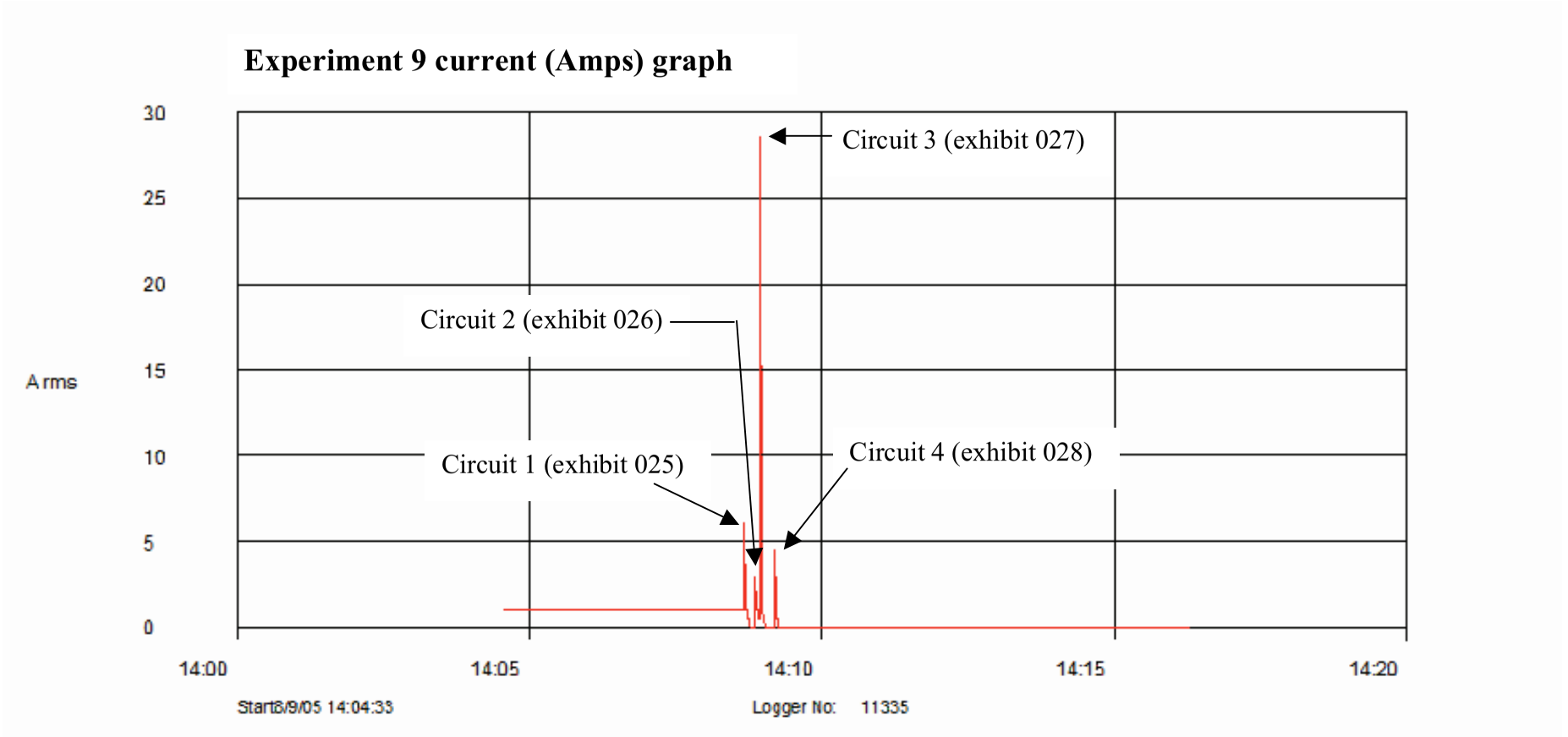

Figure 195 - Current (Amps) graph for experiment 9 detailing the operation of the circuit breakers and the fault current

Experiment 10

Figure 196 – “Scenario C” 8 September 2005

Circuit number	MCB operating time from ignition
4	2:42 minutes
1	2:53 minutes
2	4:11 minutes
3	4:18 minutes

Table 11 – circuit breaker operation data

The fire in experiment 10 (scenario C) originated at a Christmas tree that was located 300mm from the right wall and 1500mm from the rear wall.

The fire was slow to develop with a peak ceiling temperature of 770° C being reached at 9.5 minutes. The floor temperature reached 300° C at this time and post-fire burn patterns suggest that the fire was ventilation controlled and did not quite reach flashover conditions.

The localised metallic damage to the conductors was found at the following locations:

Arcing damage was located on circuit 1 – 950mm from the front wall and 1000mm from the right wall on the ceiling.

No evidence of arcing damage found on circuit 2.

Arcing damage was located on circuit 3 – 2200mm from the rear wall and 1000mm from the left wall on the ceiling.

Arcing damage was located on circuit 4 – 2200mm from the front wall.

Pre-fire and post-fire photographs of experiment 10

Figure 197 - Pre-fire photograph the white oval indicates the fire's area of origin.

Figure 198 - Arcing damage to exhibit 029 on circuit 1.

Figure 199 - Post-fire photograph of the scene.

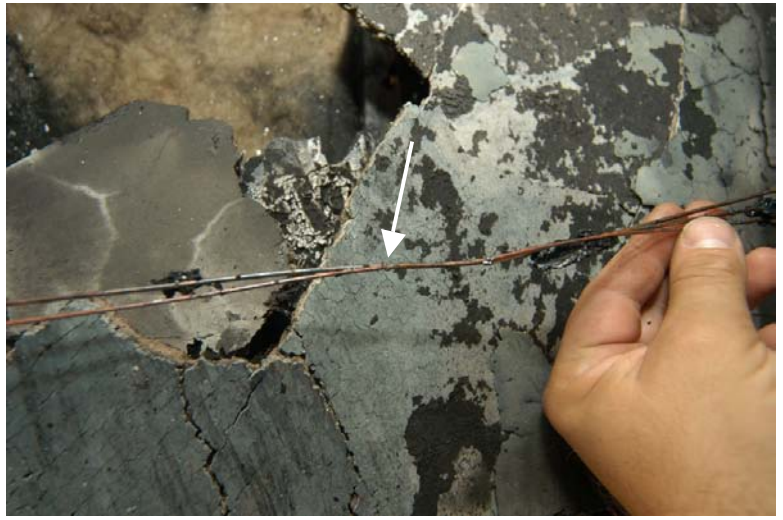

Figure 200 - View of exhibit 029 in-situ at the scene.

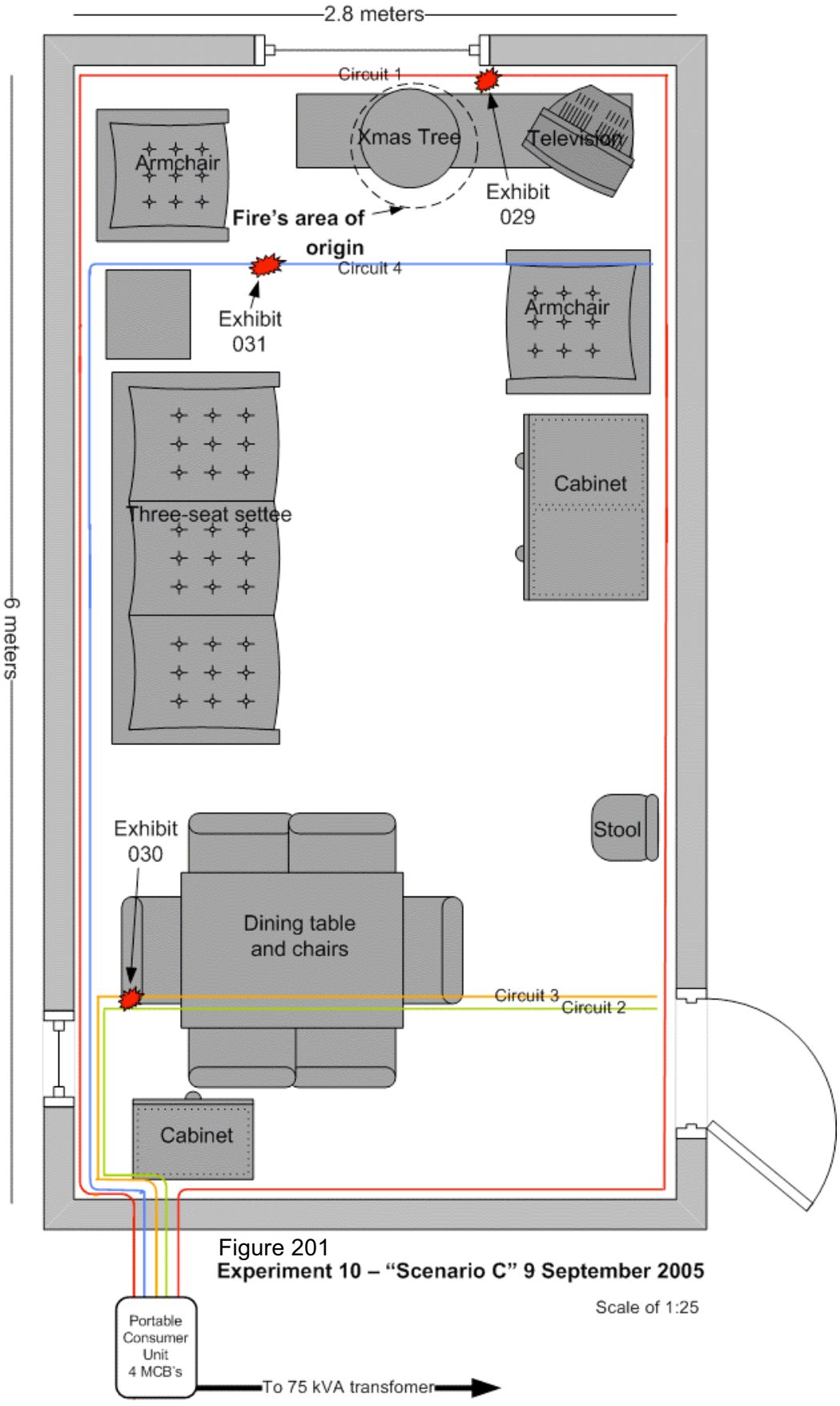

Figure 201
Experiment 10 – "Scenario C" 9 September 2005

Scale of 1:25

Microscope images for exhibit 029 arcing category B – experiment 10

Figure 202 - Overview of exhibit 029.

Figure 203 - Close-up of the top conductor in figure 202.

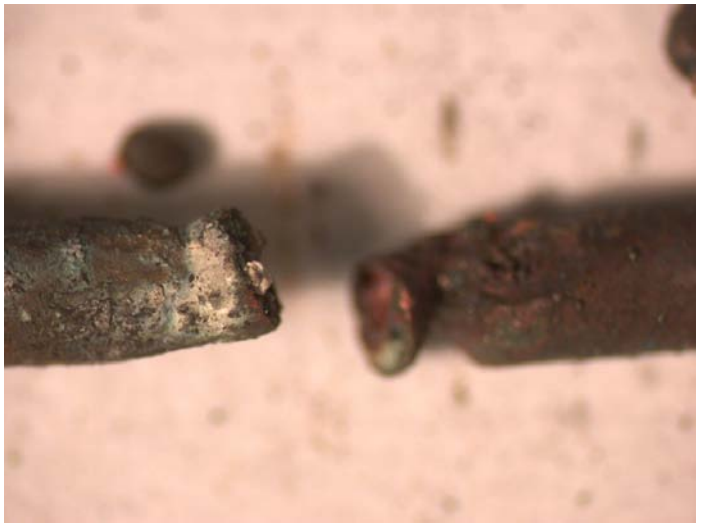

Figure 204 - Close-up view of the bottom severed conductor in figure 202.

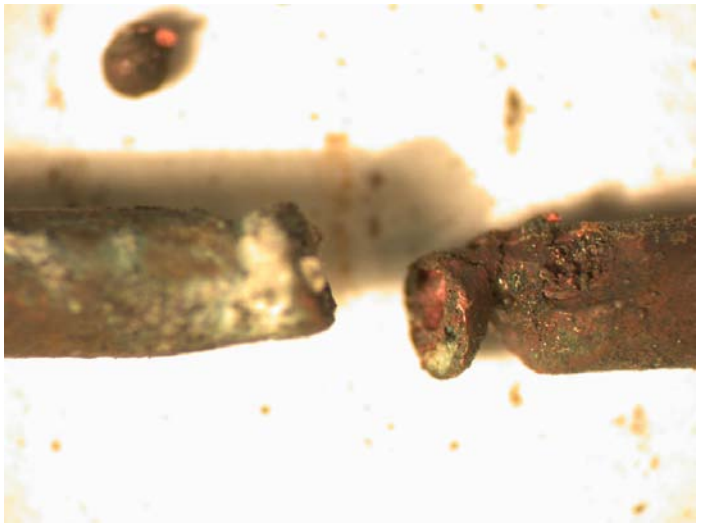

Figure 205 - Similar view to figure 204 with the right severed conductor end in focus.

Microscope and SEM images for exhibit 030 arcing category B – experiment 10

Figure 206 - Microscope image of exhibit 030.

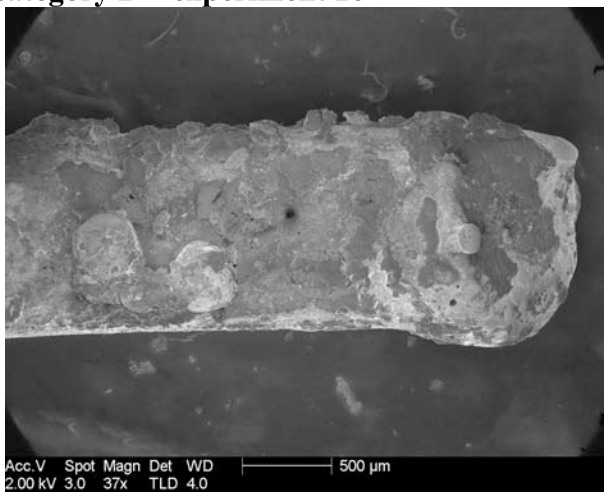

Figure 207 - SEM image of the right conductor in figure 206.

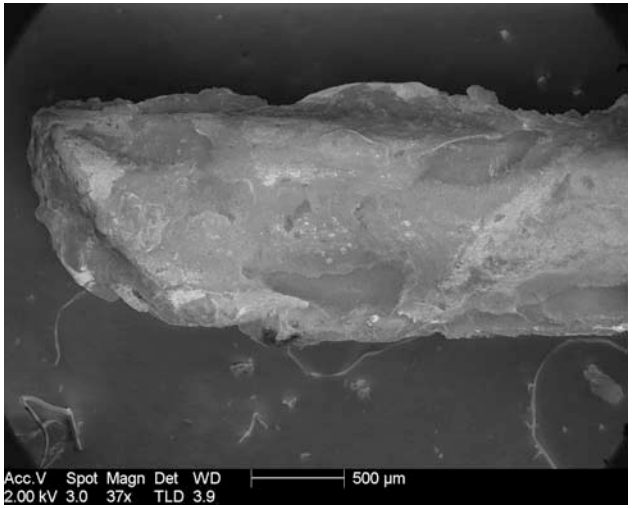

Figure 208 - SEM image of the left severed conductor in figure 206

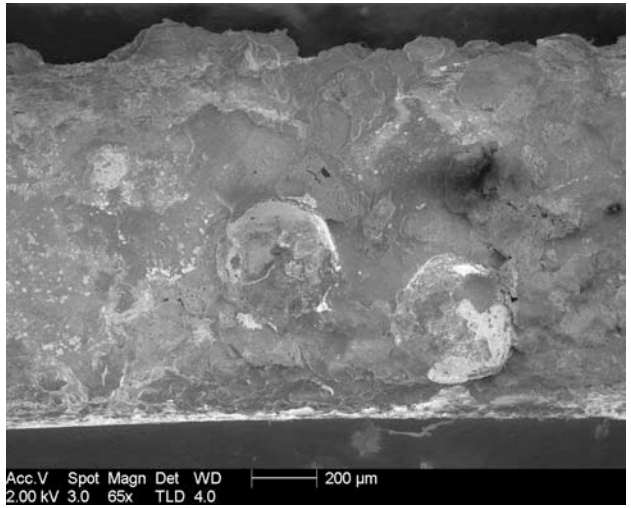

Figure 209 - SEM image at 65x magnification of the demarcation area of the right conductor in figure 207.

Microscope images for exhibit 031 arcing category B – experiment 10

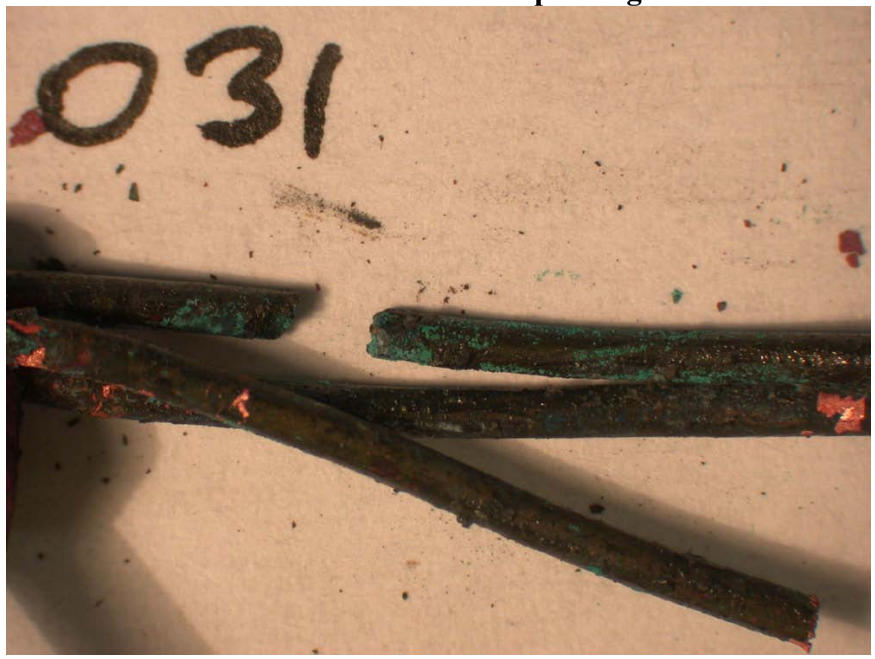

Figure 210 - Optical microscope image of exhibit 032 that involved one of the three conductors with severed ends.

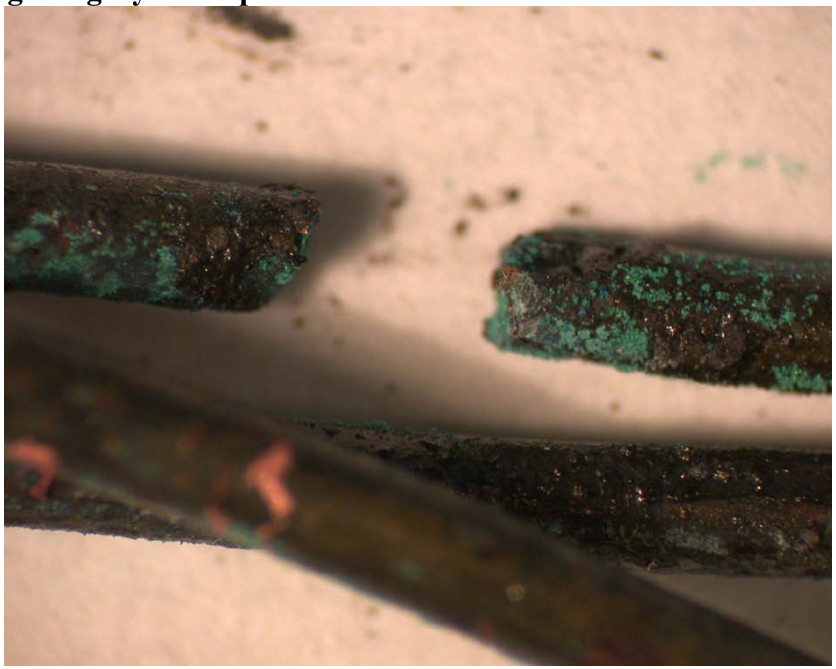

Figure 211 - Close-up image of the severed ends detailed in figure 210. There was a lot of PVC debris still attached to the conductors.

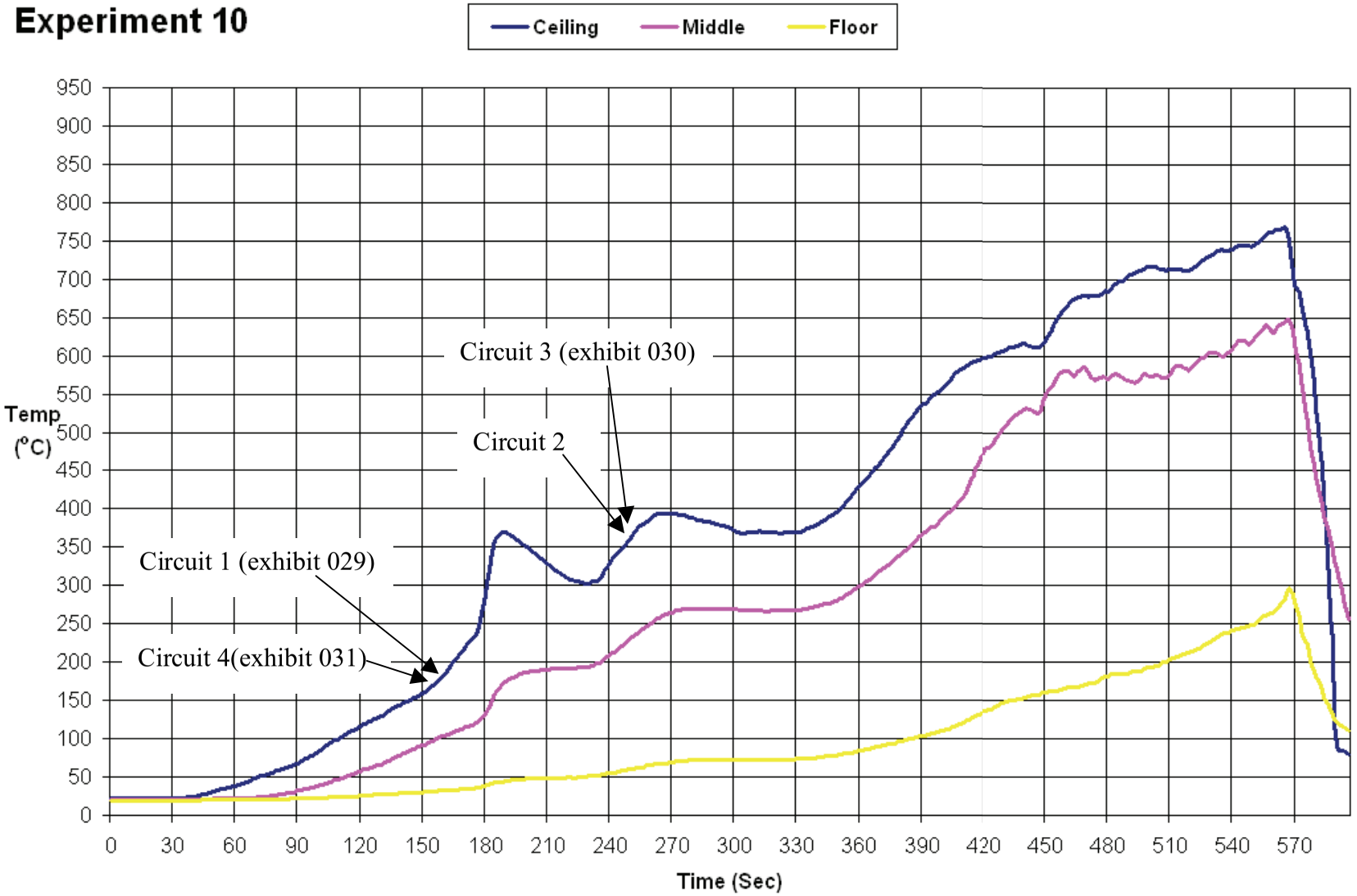

Figure 212 - Time temperature graph for experiment 10

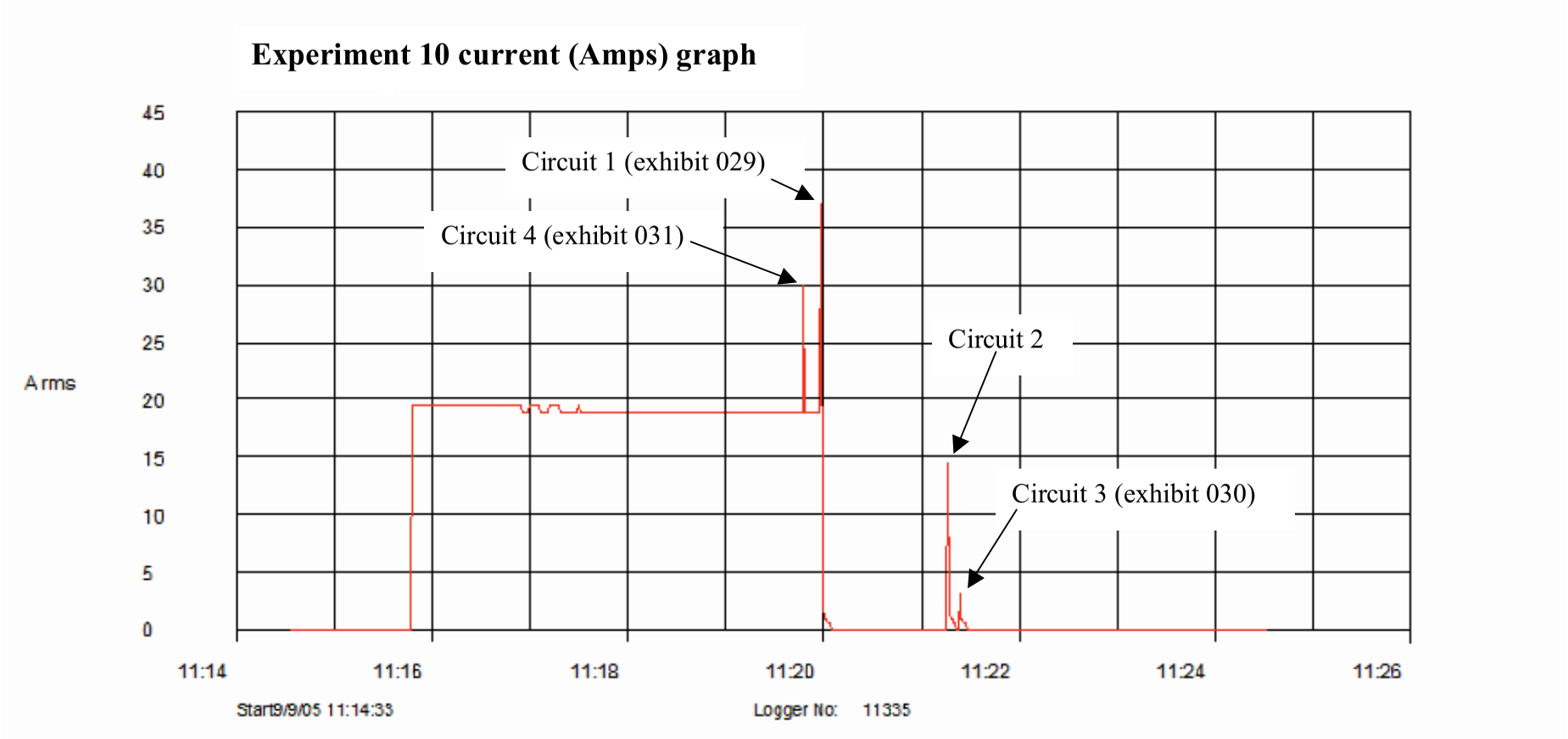

Figure 213 - Current (Amps) graph for experiment 10 detailing the operation of the circuit breakers and the fault current

Experiment 11

Figure 214 – "Scenario E" 8 September 2005

Circuit number	MCB operating time from ignition
3	1:17 minutes
2	1:49 minutes
1	1:58 minutes
4	2:13 minutes

Table 12 – circuit breaker operation data

The fire in experiment 11 (scenario E) originated in three separate areas within the compartment. One was located on the double bed, the second on the floor on a paper trail and the third within a wardrobe.

The fire's development was rapid with a peak ceiling temperature of 675° C being recorded within 3 minutes. The middle and floor thermocouples recorded temperatures of 525° C and the fire appeared to reach flashover conditions until it was extinguished at 4 minutes.

Localised melting damage to conductors was found at the following locations:

Arcing damage was located on circuit 1 – 1570mm from the left wall.

Arcing damage was located on circuit 2 – 2250mm from the front wall and 1000mm from the left wall on the ceiling.

Arcing damage was located on circuit 3 – 1860mm from the front wall.

Arcing damage was located on circuit 4 – 1850mm from the front wall and 1000mm from the right wall at the ceiling level.

Pre-fire and post-fire photographs of experiment 11

Figure 215 - Pre-fire photograph, the black and white ovals indicate the fire's areas of origin.

Figure 216 - Pre-fire photograph of the wardrobe area in the compartment, which in the early development was the dominant fire plume.

Figure 217 - Post-fire photograph the white ovals details detail the area of origin.

Figure 218 - Post-fire photograph of the wardrobe area in the compartment. The arrows indicate areas of arcing.

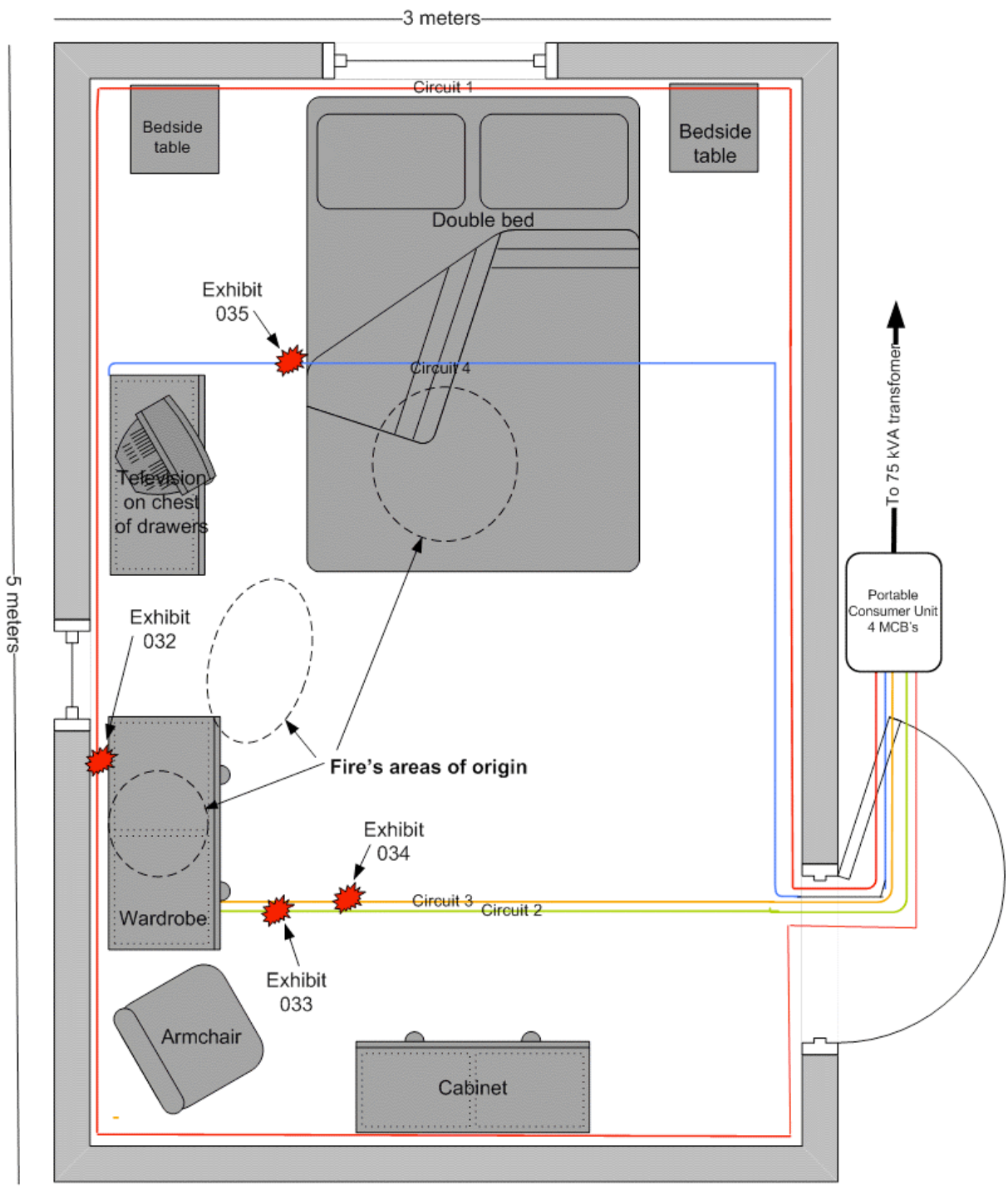

Figure 219 -
Experiment 11 – "Scenario E" 9 September 2005

Scale of 1:20

Microscope and SEM images for exhibit 032 arcing category E – experiment 11

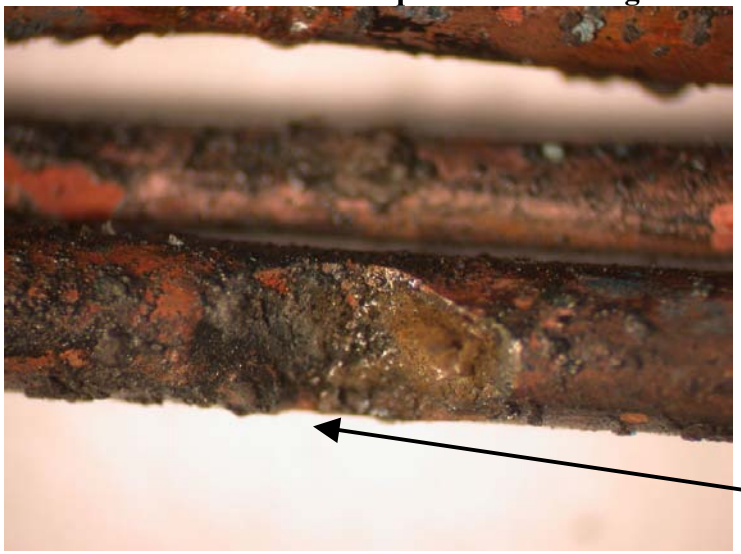

Figure 220 - Microscope image of the notch damage to one conductor.

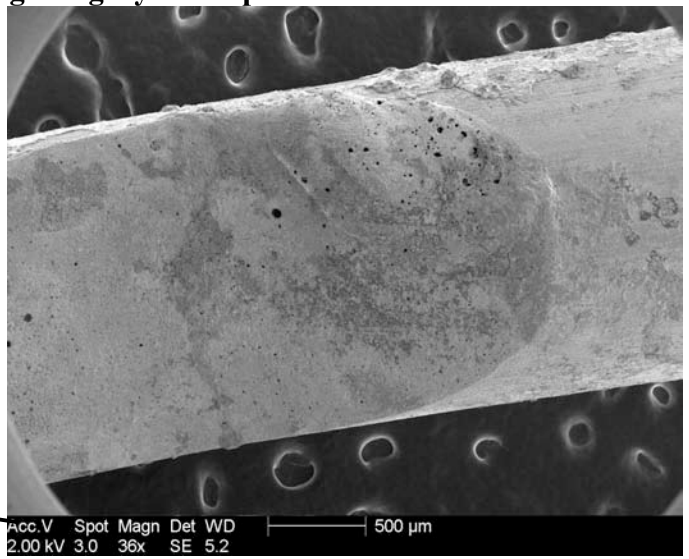

Figure 221 - SEM image of the right edge of the notch.

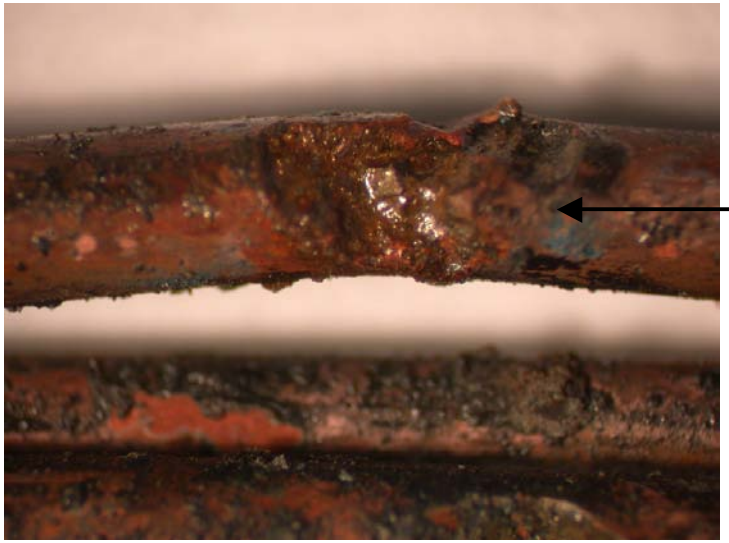

Figure 222 - Microscope image similar to figure 220.

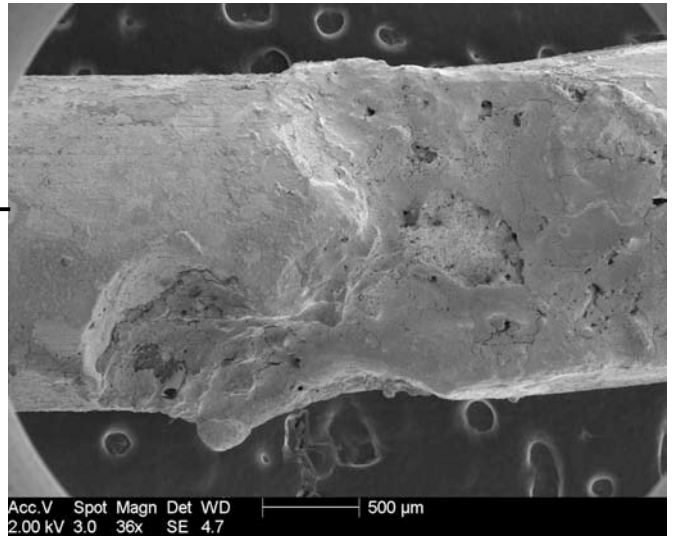

Figure 223 - SEM image of the left edge of the notch.

Confocal laser scanning microscope images of exhibit 032 – arcing category E (experiment 11)

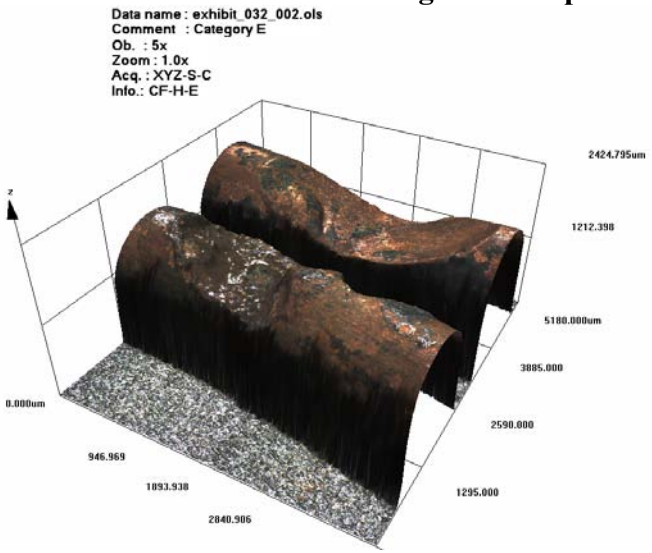

Figure 224 - LEXT image of exhibit 032.

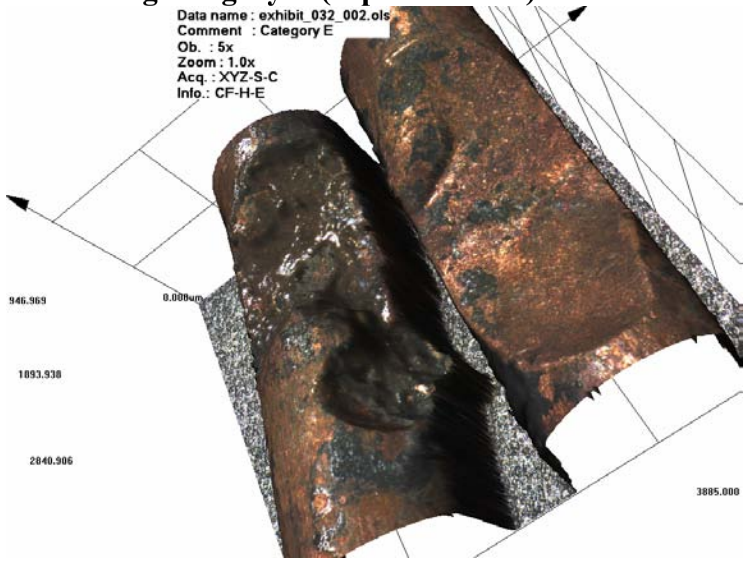

Figure 225 - LEXT image rotated in the 3D software.

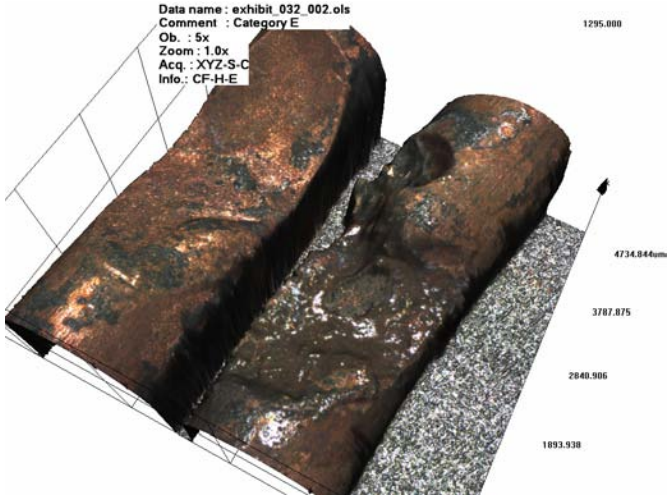

Figure 226 – Image rotated in the software. The demarcation area is clear in this view at the edge of the two notches.

Microscope and SEM images for exhibit 033 arcing category C – experiment 11

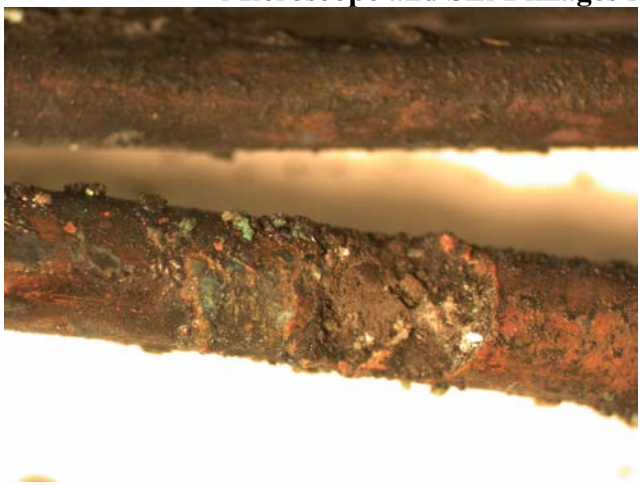

Figure 227 - Microscope image of first conductor (of two) forming exhibit 033. The damage pattern is a notch in the conductor surface.

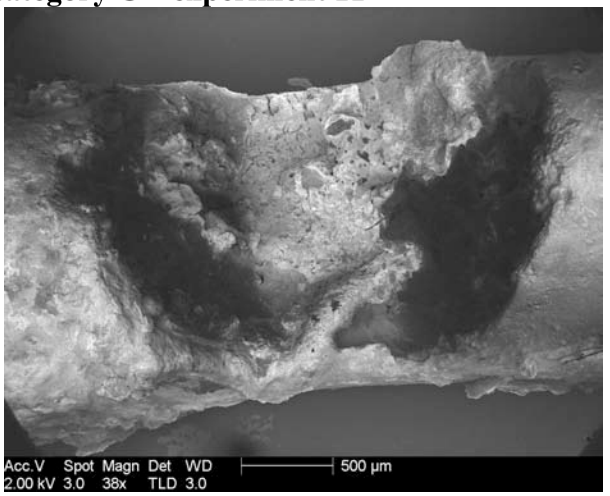

Figure 228 - SEM image of the conductor detailed in figure 227. The demarcation of the right edge is clear.

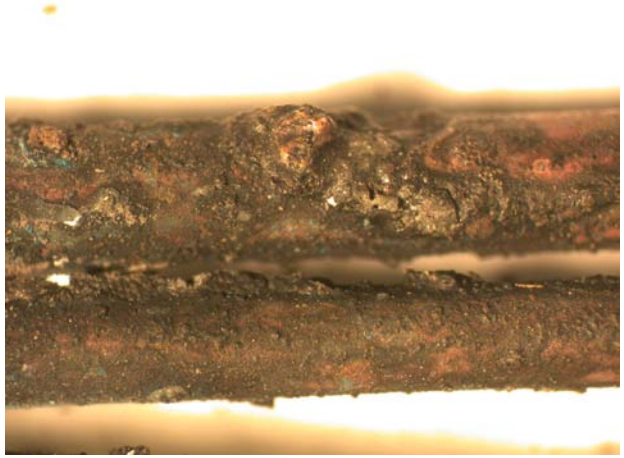

Figure 229 - Microscope image of the second conductor of exhibit 033. The metallic damage is a notch with a bead within it.

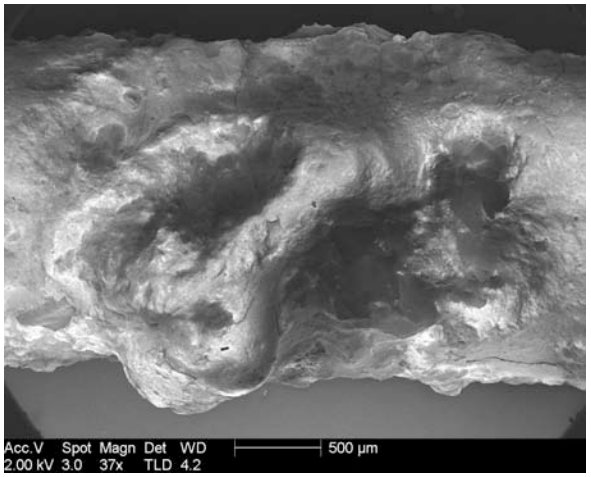

Figure 230 - SEM image of the conductor detailed in figure 229. The cleaning process has removed PVC debris.

Confocal laser scanning microscope images of exhibit 033 – arcing category C (experiment 11)

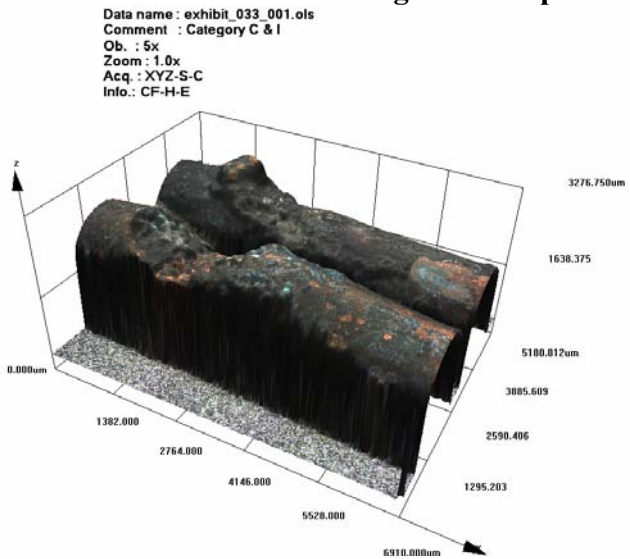

Figure 231 - LEXT image of exhibit 033 in "real colour" mode.

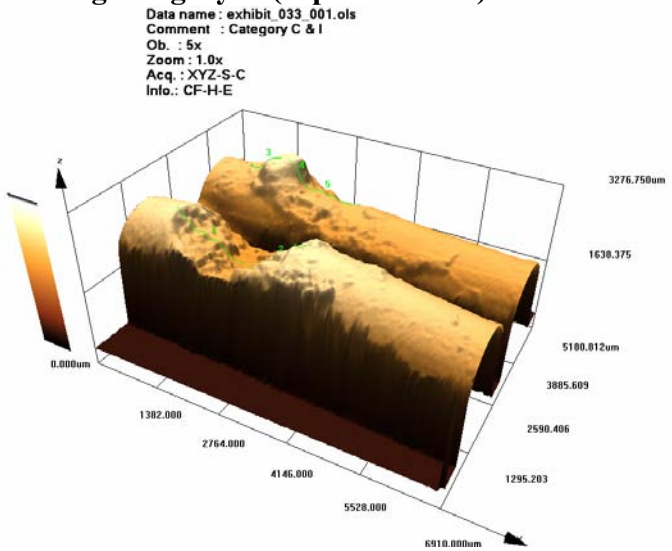

Figure 232 - LEXT image using the brown rendering option.

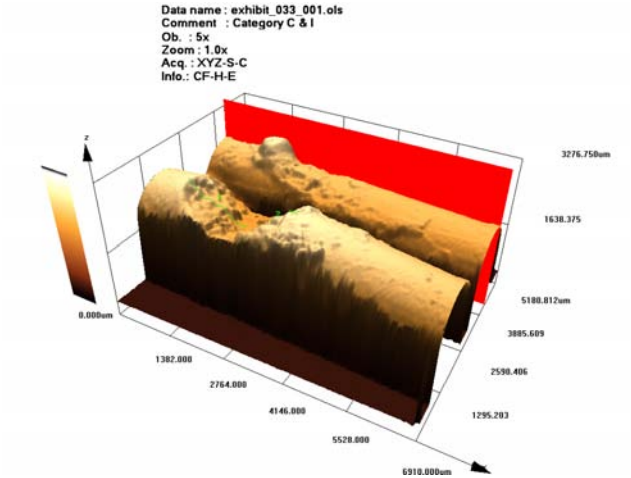

Figure 233 – View of the LEXT software slice tool in use.

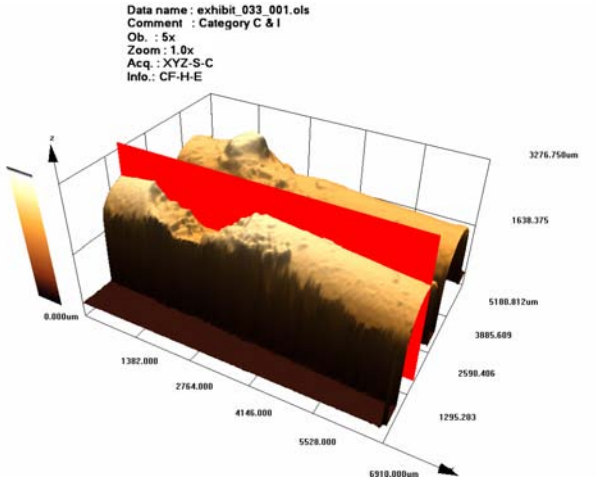

Figure 234 – LEXT "slice tool" being used to create a profile of the notch.

Microscope images for exhibit 034 arcing category E – experiment 11

Figure 235 - Microscope image of exhibit 034. The metallic damage involves two conductors. Each one had a large notch.

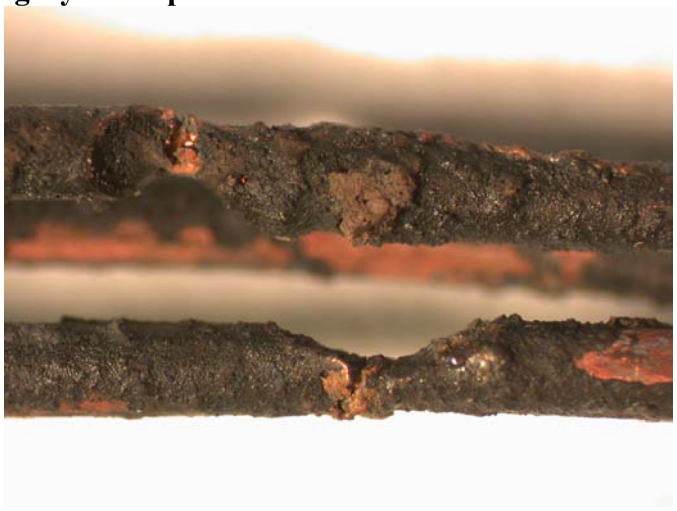

Figure 236 – 20x magnification of the top and bottom conductors detailed in figure 235. Note the cracks in the metal surface below the notches.

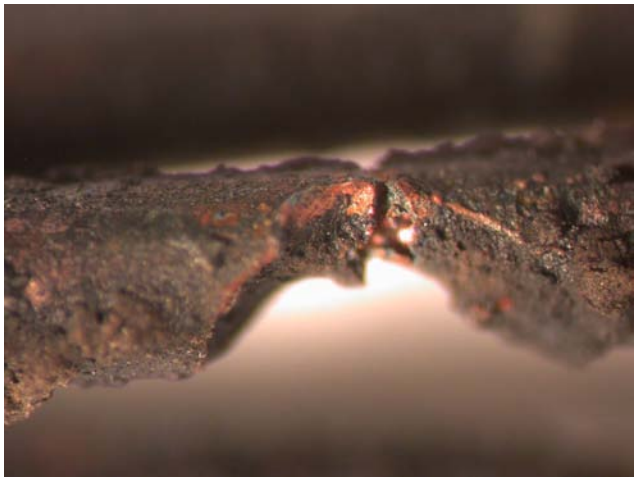

Figure 237 - Microscope image at 40x magnification of the bottom conductor detailed in figures 235 and 236.

Microscope images for exhibit 035 arcing category F – experiment 11

Figure 238 - Microscope image of exhibit 035. The metallic damage has affected two conductors. The top conductor is severed and the bottom conductor has a notch.

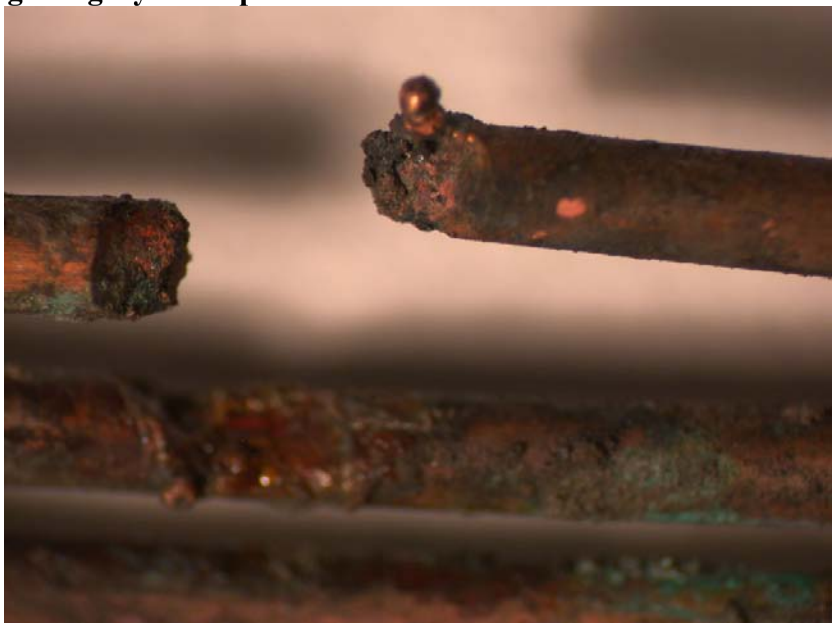

Figure 239 - Microscope image at 20x magnification detailing the severed ends of the top conductor. The demarcation area of the left severed end is very clear.

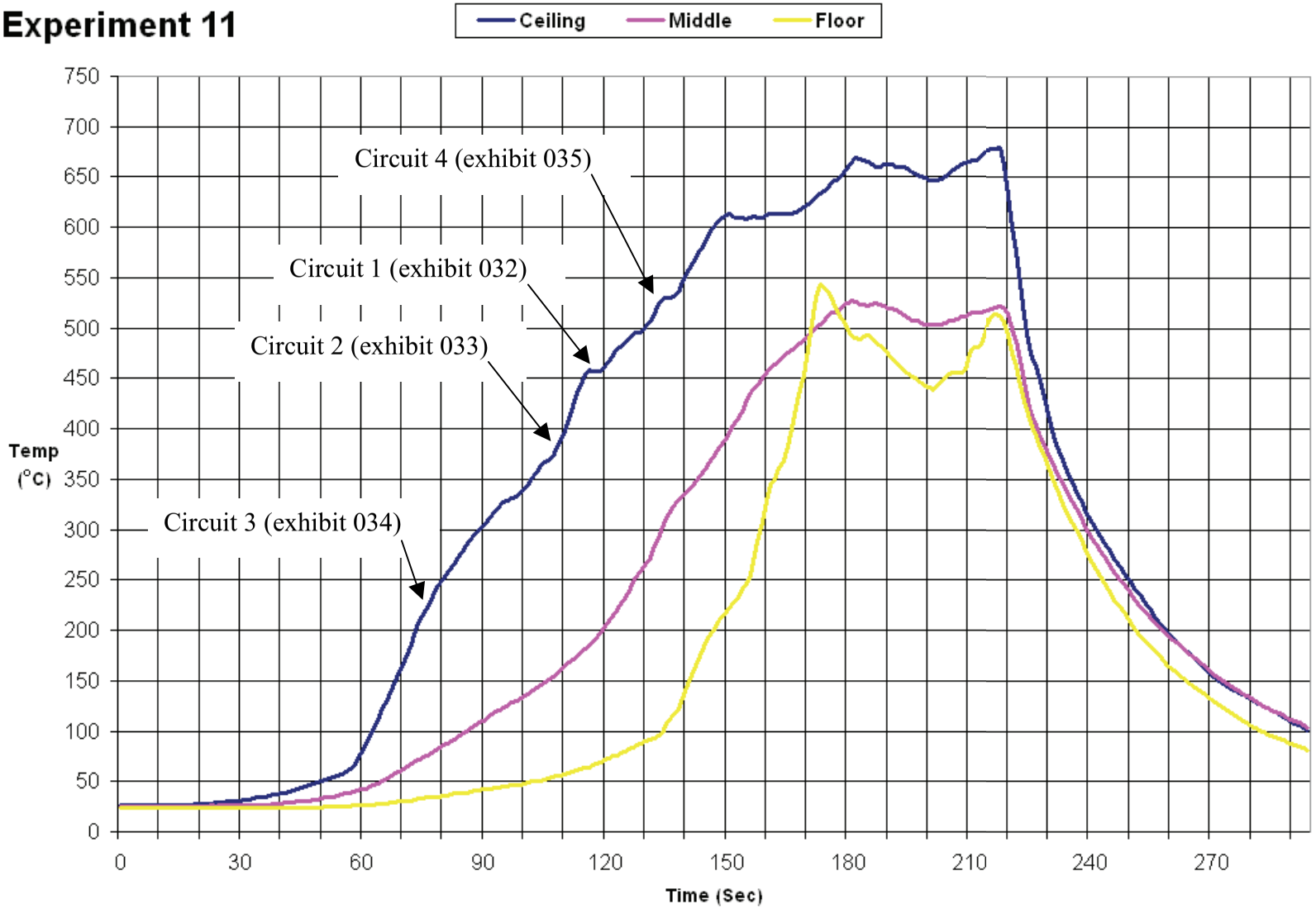

Figure 240 - Time temperature graph for experiment 11

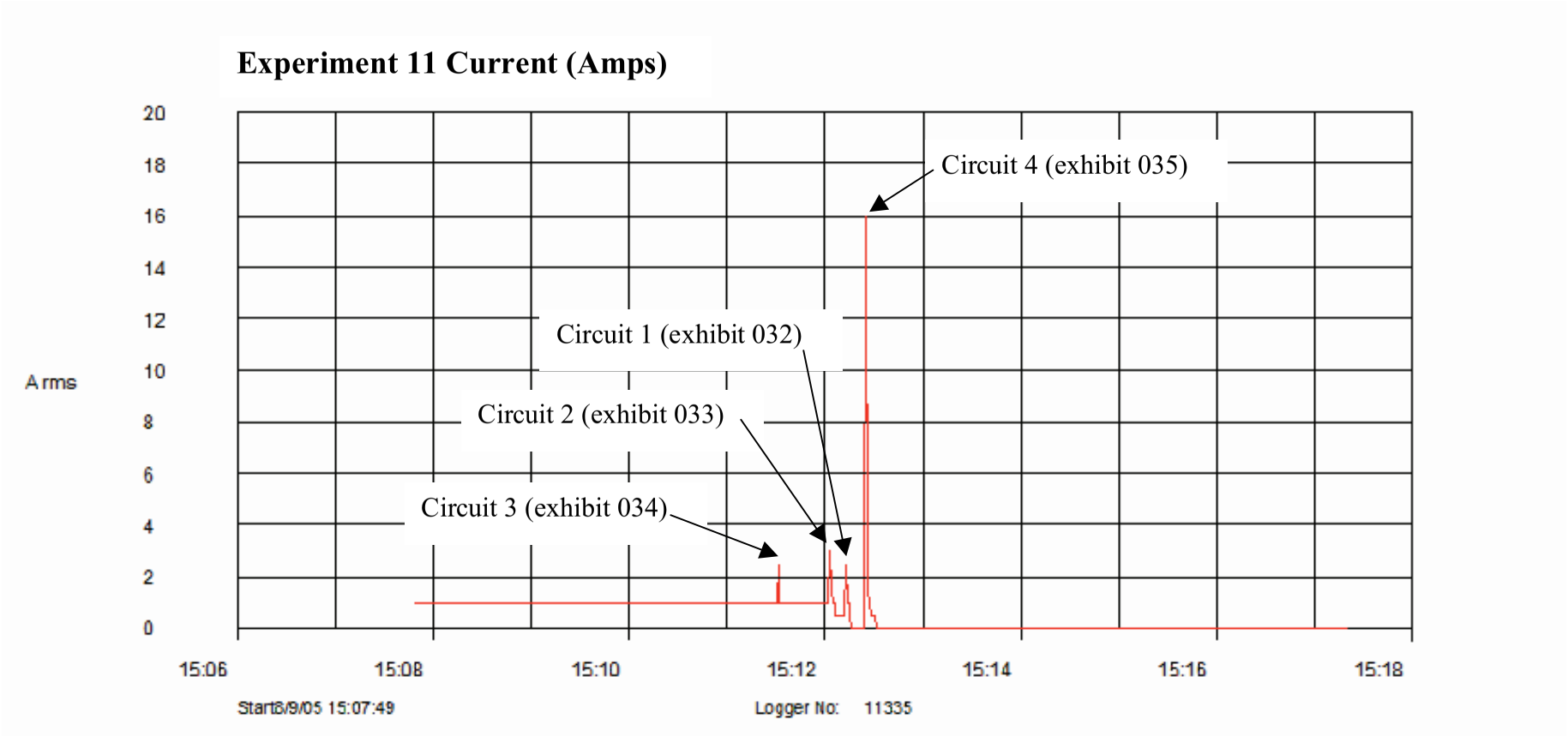

Figure 241 - Current (Amps) graph for experiment 11 detailing the operation of the circuit breakers and the fault current

Experiment 12

Figure 242 – "Scenario F" 9 September 2005

Circuit number	MCB operating time from ignition
1	1:13 minutes
4	1:13 minutes
2	2:50 minutes
3	2:51 minutes

Table 13 – circuit breaker operation data

The fire in experiment 12 (scenario F) originated in three separate areas within the compartment. These were at the curtains, the sofa and a cat basket by the door. The initial flame impingement which affecting the ceiling occurred as a result of the curtain fire.

The fire developed rapidly and was extinguished at 4 minutes and 10 seconds. The middle thermocouple reached almost 900° C at 4 minutes. The ceiling temperature had reached 750° C at this point and the floor temperature reached 400° C. It appears that the compartment had reached flashover conditions just prior to being extinguished.

Arcing damage was located on circuit 1 – 3300mm from the left wall.

Arcing damage was located on circuit 2 – 2370mm from the front wall and 1000mm from the left wall at the ceiling level.

Arcing damage was located on circuit 3 – 3300mm from the left wall and 1000mm from the left wall at the ceiling level.

Arcing damage was located on circuit 4– 3300mm from the left wall. The faulting to circuits 1 and 4 are in the same location.

Pre-fire and post-fire photographs of experiment 12

Figure 243 - Pre-fire photograph of experiment 12. The white ovals indicate the fire's areas of origin.

Figure 244 - Pre-fire photograph of the wiring installed on the ceiling for the experiment.

Figure 245 - Post-fire photograph with the white ovals indicating the fire's areas of origin and the arrows indicating points of arcing to circuits 1 and 4.

Figure 246 – Post-fire photograph of the ceiling with arrows indicating points of arcing at circuits 1 and 4.

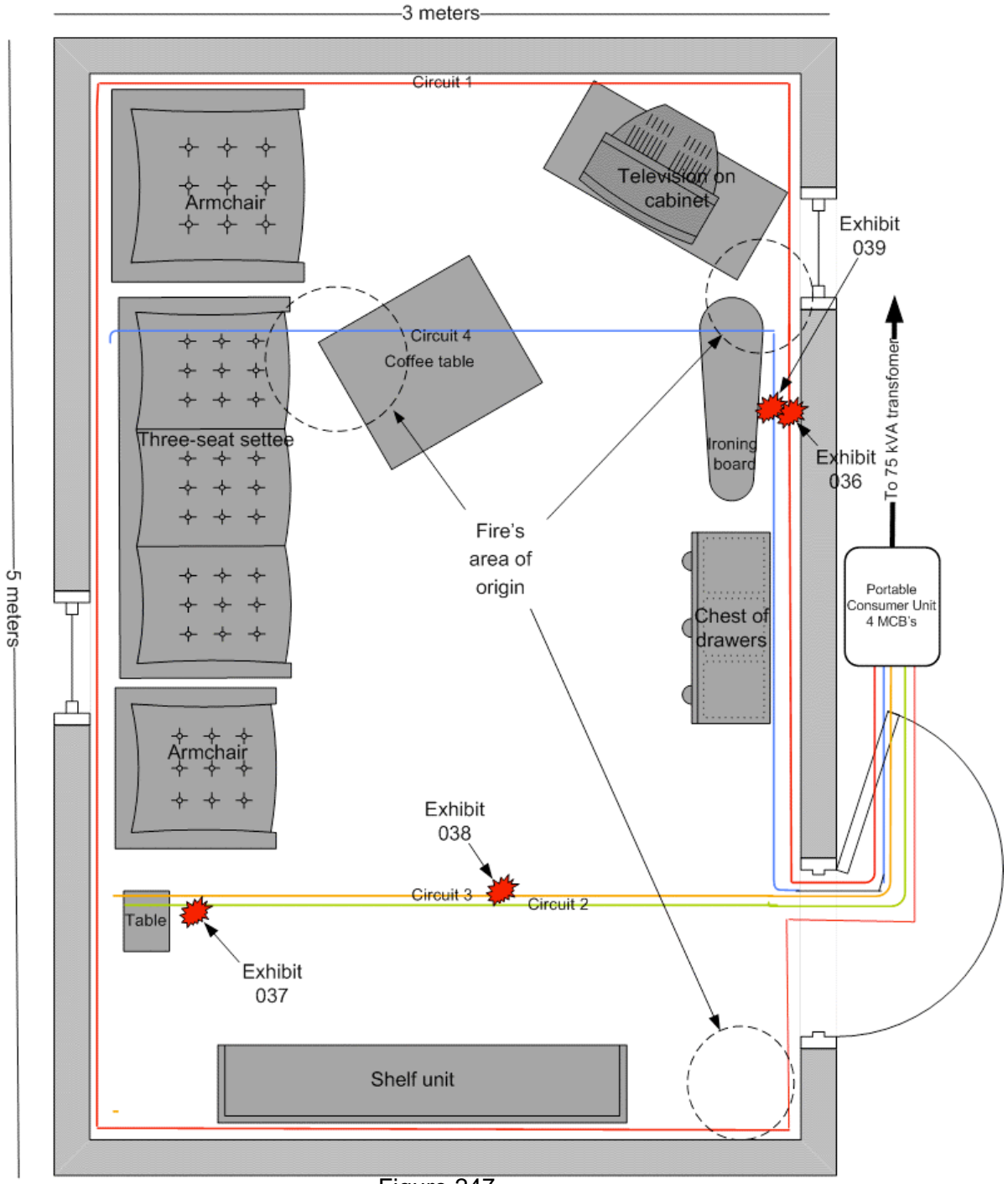

Figure 247 -
Experiment 12 – "Scenario F" 9 September 2005

Scale of 1:20

Microscope images for exhibit 036 arcing category D – experiment 12

Figure 248 - Microscope image of exhibit 036. The localised metallic damage involved two conductors. One with a notch and the other with a bead within a notch.

Figure 249 – Microscope image at 20x magnification detailing the damage to the two conductors.

Figure 250 – A side view taken at 20x magnification of the lower conductor detailed in figure 249.

Microscope and SEM images for exhibit 037 arcing category C – experiment 12

Figure 251 - Microscope image of exhibit 037. The metallic damage was limited to one conductor with a notch and a large bead to side of the notch edge.

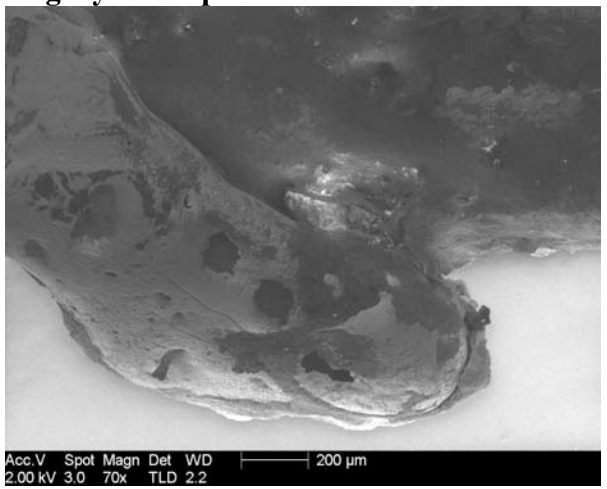

Figure 252 - SEM image of the bead at 70x magnification.

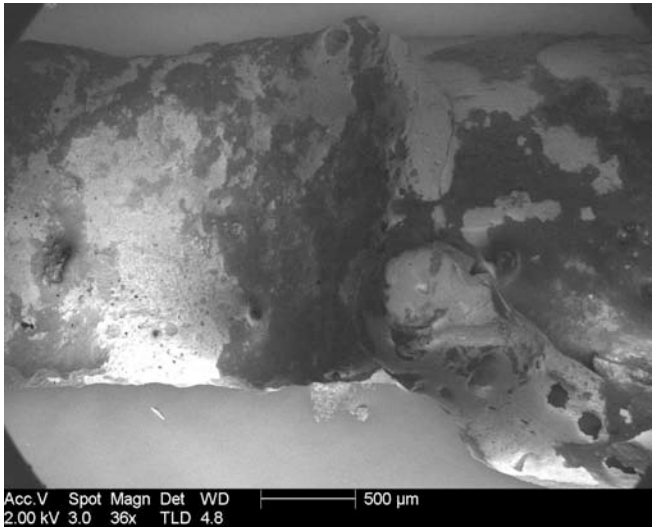

Figure 253 - SEM image detailing the left side of notch.

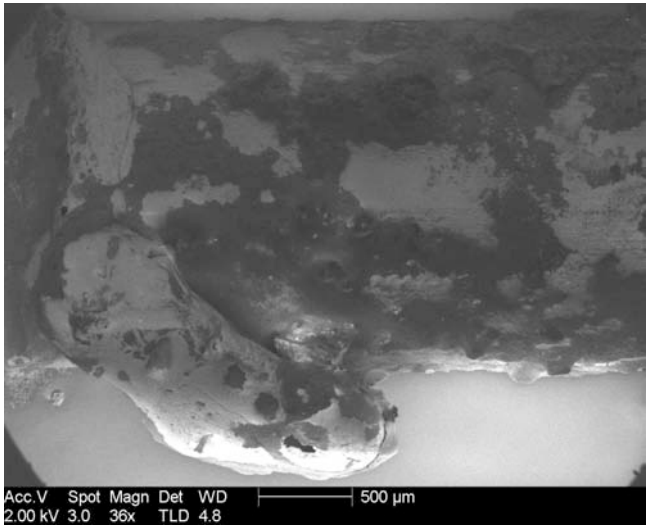

Figure 254 - SEM image detailing the right side of notch.

Confocal laser scanning microscope images of exhibit 037 – arcing category C (experiment 12)

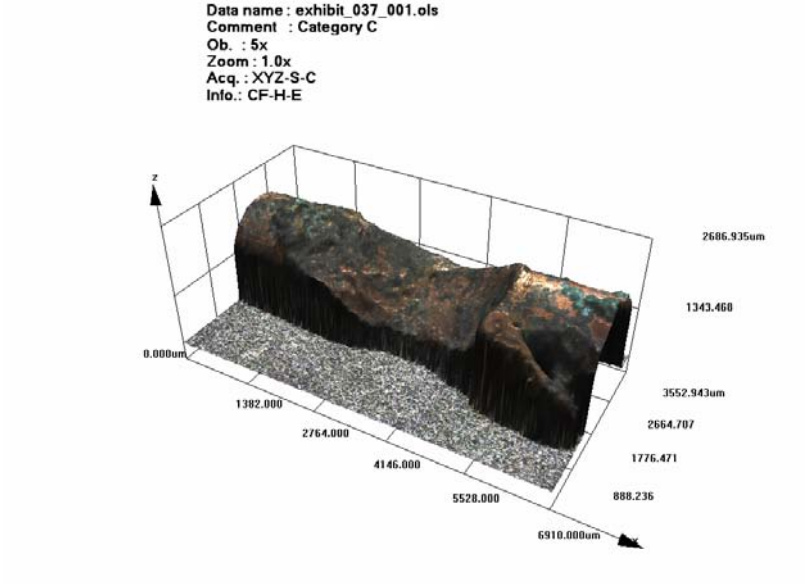

Figure 255 - LEXT image of exhibit 037 in “real colour” mode.

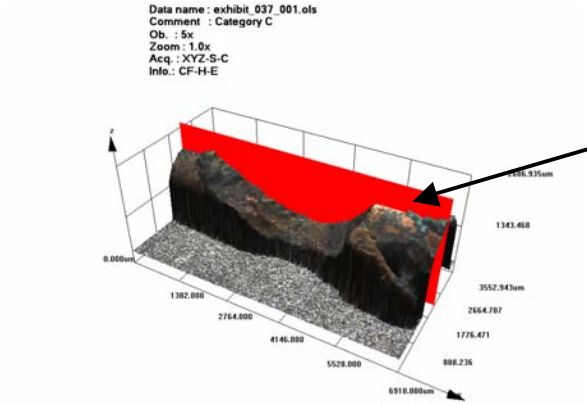

Figure 256 - LEXT image with the “slice tool” in use to create a profile. The profile measurements are detailed in table 14.

Table 14 - LEXT software report with profile measurement details (microns).

#	Judge	Width	Height	Length	Angle	Upper	Lower
1		2830.19	1081.45	3029.77	20.913	897.729	357413.
2		1398.21	958.457	1695.18	34.430	17728.9	87670.4
3		486.334	72.242	491.671	8.449	1265.57	7460.38
Number		3	3	3	3	3	3
Average		1571.58	704.052	1738.87	21.264	6630.74	150848.
Max		2830.19	1081.45	3029.77	34.430	17728.9	357413.
Min		486.334	72.242	491.671	8.449	897.729	7460.38
Range		2343.86	1009.21	2538.10	25.981	16831.1	349953.
Sigma		1181.50	550.609	1269.61	12.994	9613.06	183331.
3*Sigm		3544.52	1651.82	3808.85	38.982	28839.1	549994.

Microscope images for exhibit 038 arcing category D – experiment 12

Figure 257 - Microscope image of exhibit 038. The localised metallic damage has affected one conductor consisting of a notch with a bead within it.

Figure 258 - Microscope image at 20x magnification detailing the bead within a notch. The demarcation between the arcing damage and the undamaged conductor surface is clear to the left and right edges of the notch.

Microscope and SEM images for exhibit 039 arcing category C – experiment 12

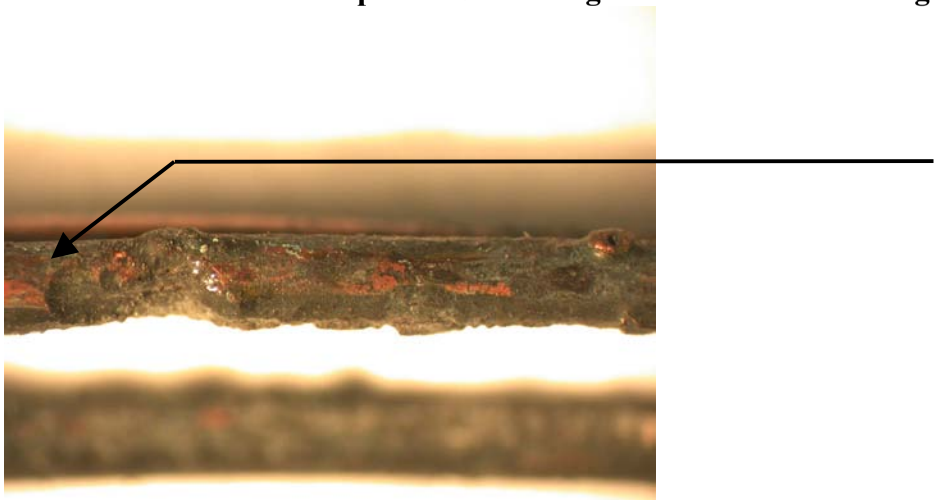

Figure 259 - Microscope image of exhibit 039.The damage is limited to one conductor with a notch.

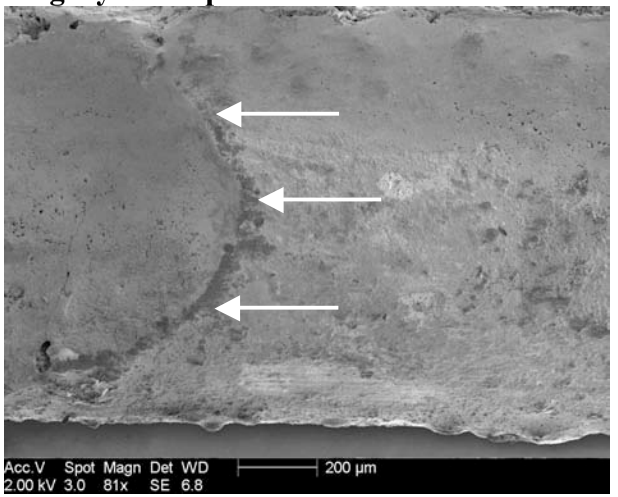

Figure 260 - SEM image of the left notch edge. The white arrows indicate the demarcation between the notch and the undamaged section of conductor.

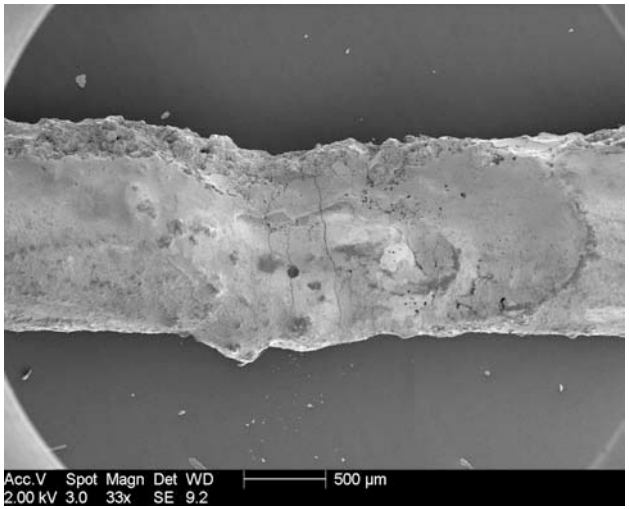

Figure 261 - SEM overview image of the notch damage.

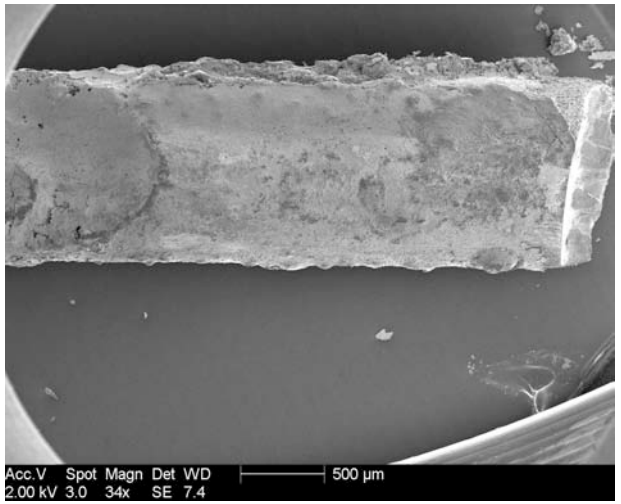

Figure 262 - SEM image of the left side of the notch.

Confocal laser scanning microscope images of exhibit 039 – arcing category C (experiment 11)

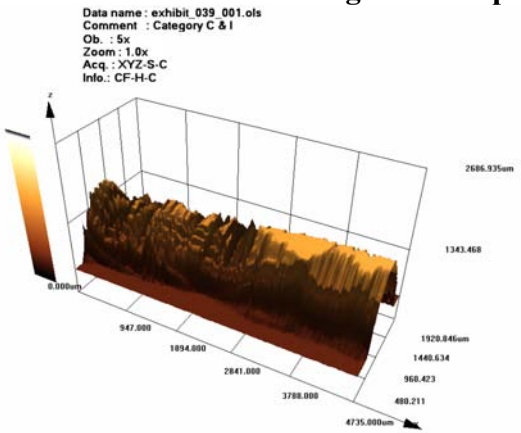

Figure 263 - LEXT image using the "brown" rendering option. This scan detailed the effect of not using the enhance amplifier when scanning.

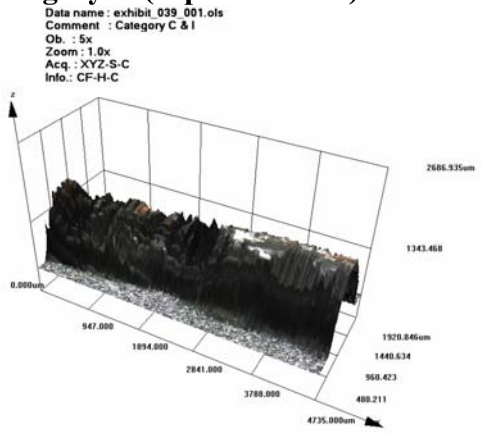

Figure 264 - LEXT image using the "real colour" option. This detailed the effect of not using the enhance amplifier when scanning the exhibit.

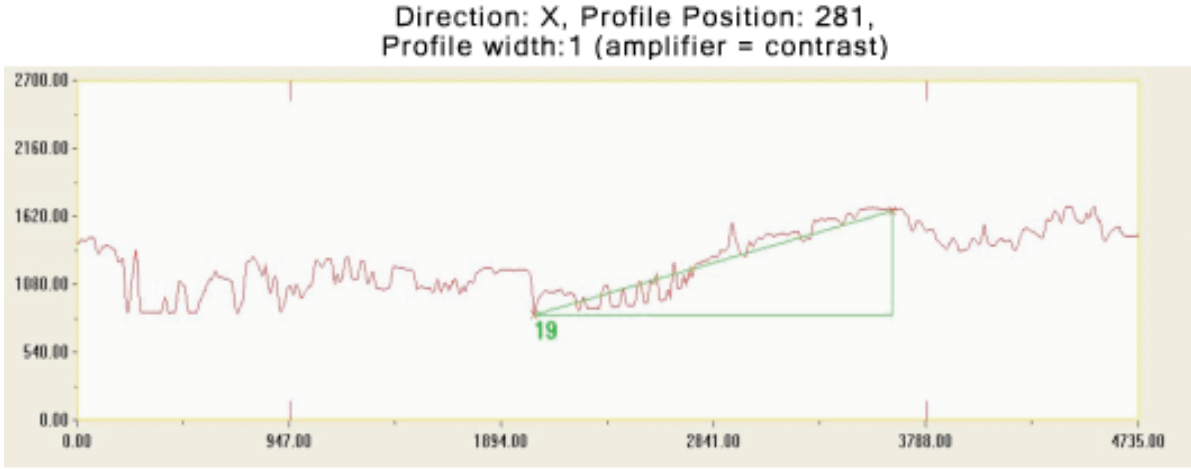

Figure 265 – Profile of the notch created with the LEXT software's "slice tool". Note the poor profile is due to the "contrast" selection.

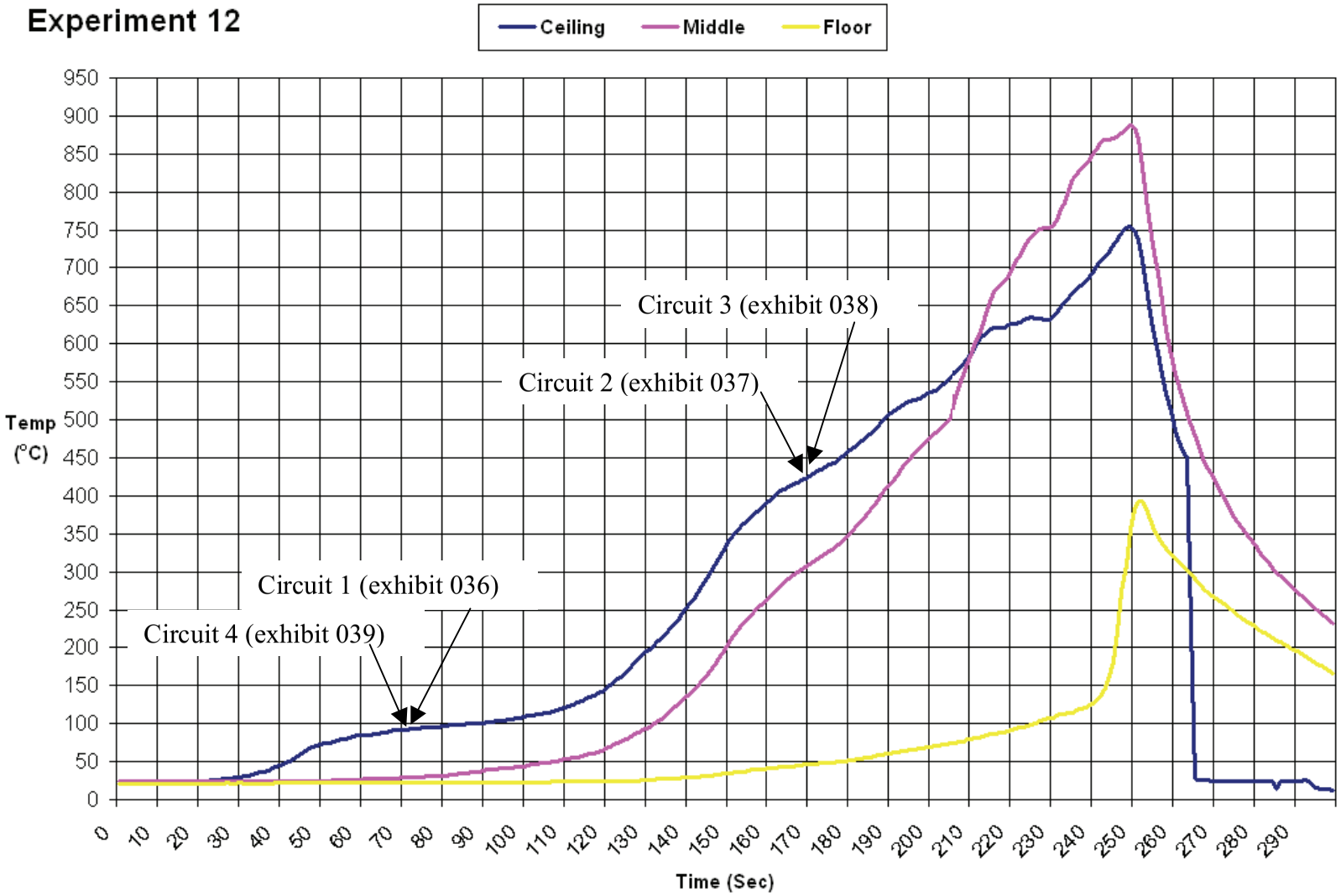

Figure 266 - Time temperature graph for experiment 12

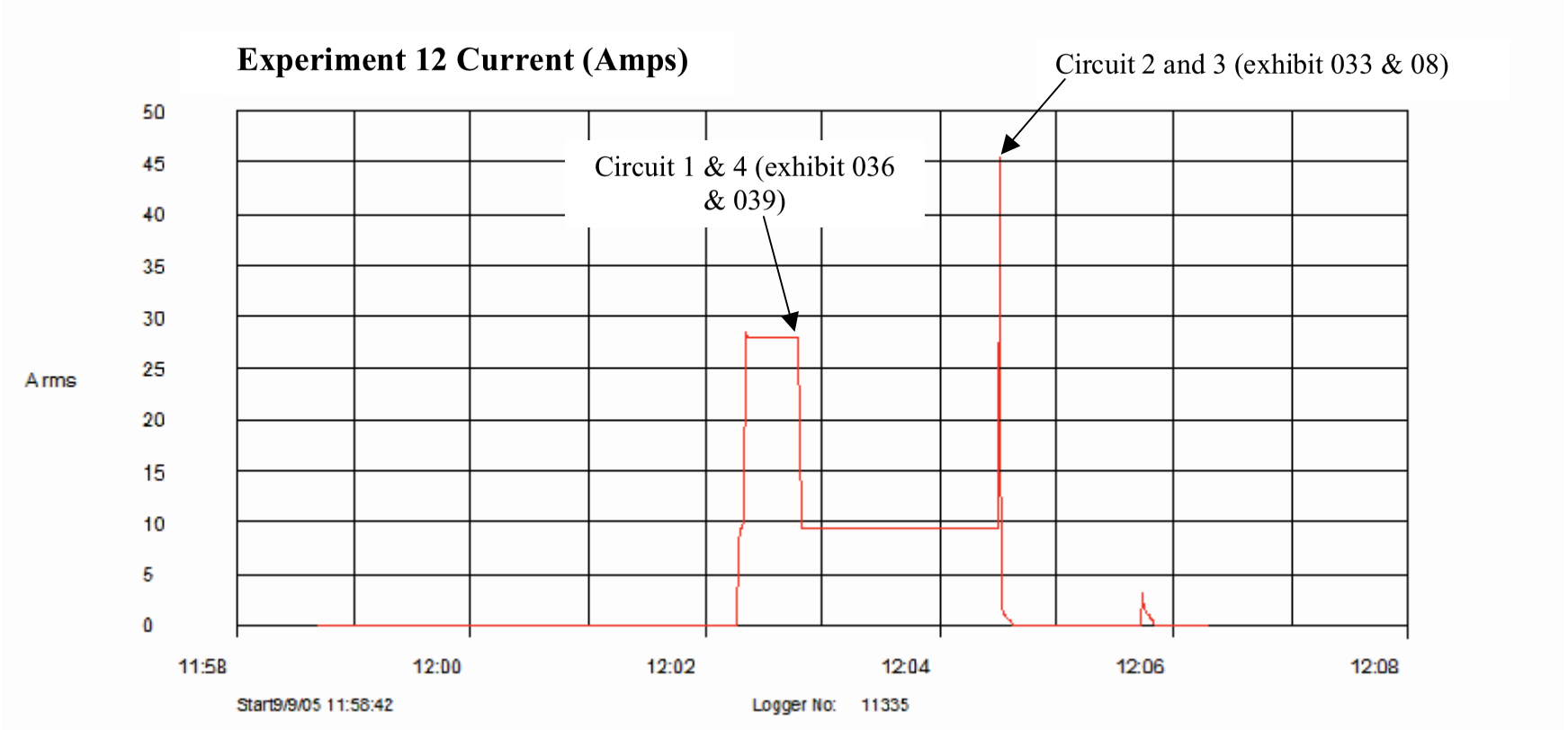

Figure 267 - Current (Amps) graph for experiment 12 detailing the operation of the circuit breakers and the fault current

Experiment 13

Figure 268 – “Scenario E” 29 September 2005

Circuit number	MCB operating time from ignition
1	2:24 minutes
4	2:48 minutes
2	3:10 minutes
3	3:03 minutes

Table 15 – circuit breaker operation data

The fire in experiment 13 (scenario E) originated in three separate areas that were ignited virtually simultaneously. The predominant area of origin was in a wardrobe with flame impingement on the ceiling observed first above the wardrobe.

This fire was ventilation controlled initially and the fire continued to develop with the ceiling temperature reaching 720° C at 5 minutes just prior to the fire being extinguished.

Arcing damage was located on circuit 1 – 1900mm from the left wall.

Arcing damage was located on circuit 2 – 740mm from the front wall and 1000mm from the left wall at the ceiling level.

Arcing damage was located on circuit 3 – 7400mm from the front wall and 1000mm from the left wall at the ceiling level. The faulting to circuits 2 and 3 are in the same location.

Arcing damage was located on circuit 4 – 700mm from the rear wall and 1000mm from the right wall at ceiling level.

Pre-fire and post-fire photographs of experiment 13

Figure 269 - Pre-fire photograph of experiment 13.

Figure 270 - Pre-fire photograph of experiment 13. The white ovals detail the fire's area of origin.

Figure 271 - Post-fire over-view image of experiment 13. Most of the ceiling plaster board fell down shortly after the fire was extinguished.

Figure 272 - Post-fire over-view detailing the fire's area of origin. The arrows detail the arcing damage locations to circuit 1(left of wardrobe) and circuit 4 (above the bed)

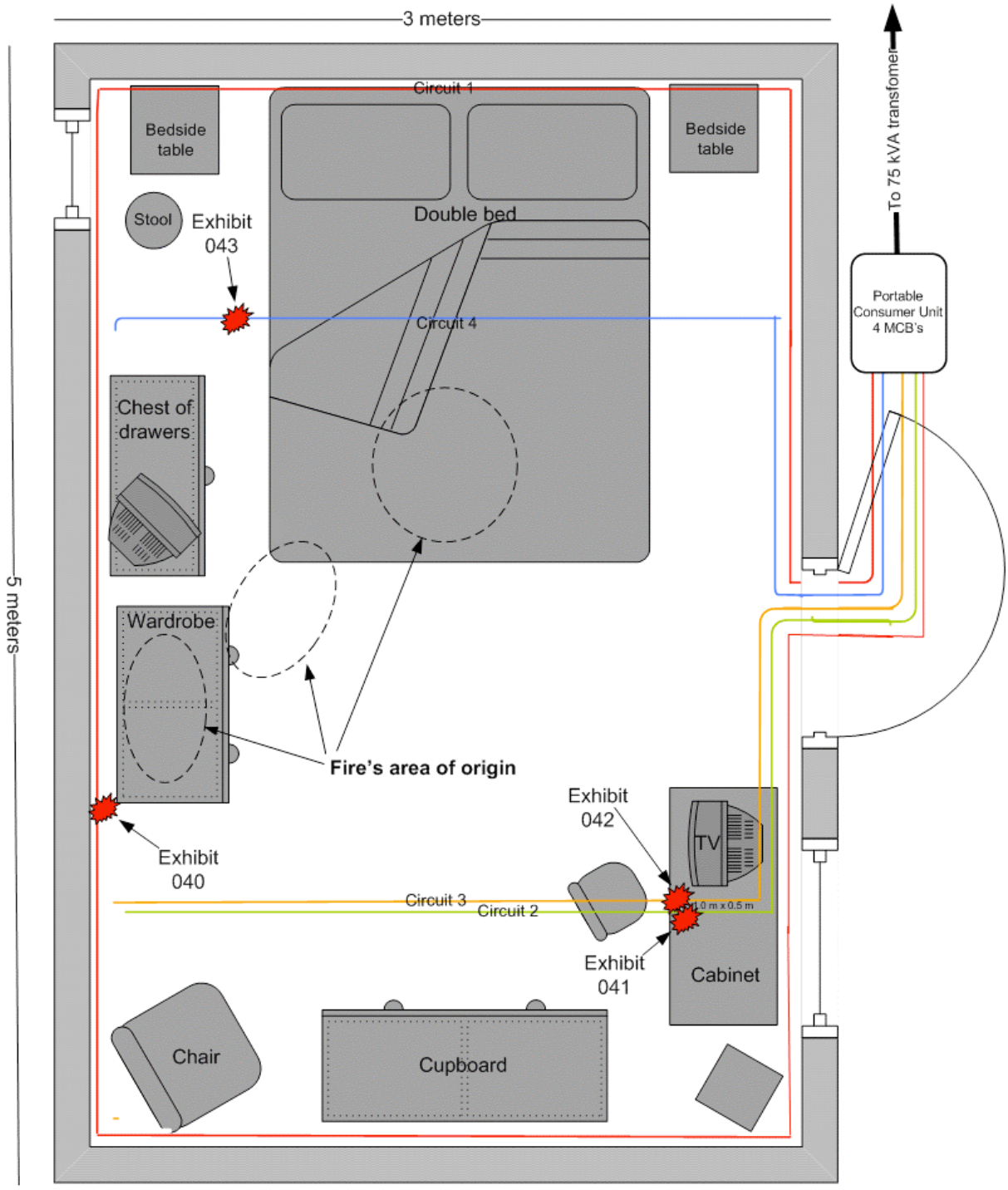

Figure 273 - **Experiment 13 – "Scenario E" 29 September 2005**

Scale of 1:20

Microscope images for exhibit 040 arcing category E – experiment 13

Figure 274 - Microscope image of exhibit 040 at 6x magnification. Two conductors have arcing damage. Each one has a notch.

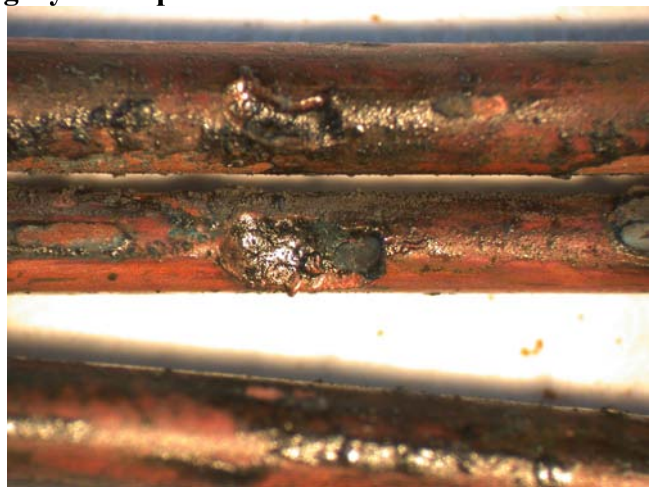

Figure 275 - View of both notches at 20x magnification.

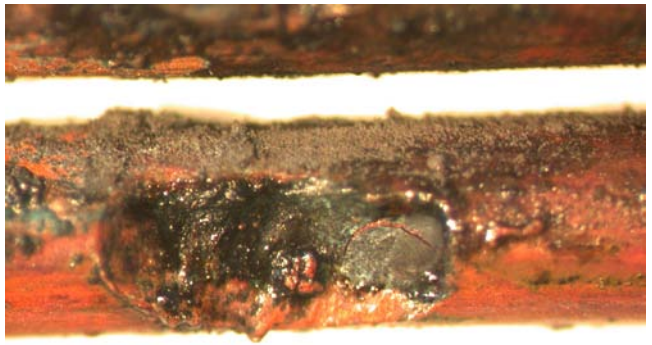

Figure 276 - View of the middle 1.5mm^2 protective earth conductor notch at 40x magnification.

Figure 277 - View of the notch damage to the 2.5mm^2 conductor at 40x magnification.

Microscope images for exhibit 041 arcing category D – experiment 13

Figure 278 - Microscope image of exhibit 041. One of the three conductors has arcing damage that is a notch with a bead within it.

Figure 279 - View at 20x magnification of the bottom conductor damage. Figures 278 – 280 are all over-exposed.

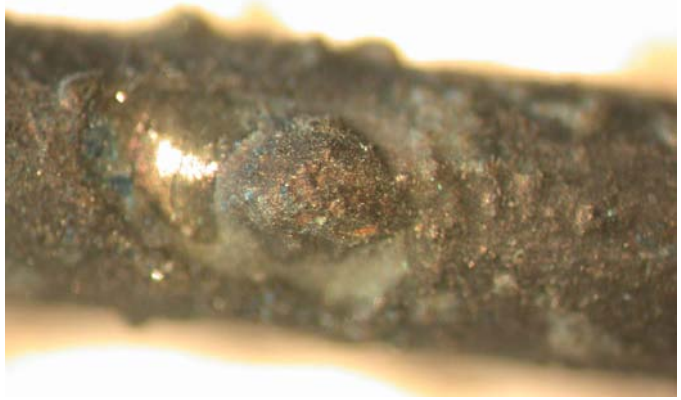

Figure 280 – 40x microscope image of the notch with a bead within.

Microscope images for exhibit 042 arcing category D – experiment 13

Figure 281 - Microscope image of exhibit 042. One conductor has localised metallic damage with a wide notch and a bead at the edge of the notch.

Figure 282 – Microscope image at 20x magnification detailing the arcing damage to the bottom conductor in figure 281.

Microscope and SEM images for exhibit 043 arcing category A – experiment 13

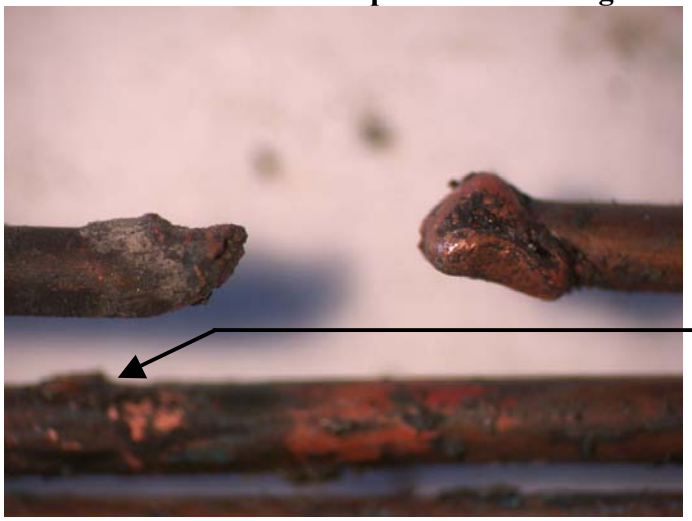

Figure 283 - Microscope image of exhibit 043 with damage to two conductors. The bottom conductor is out of focus.

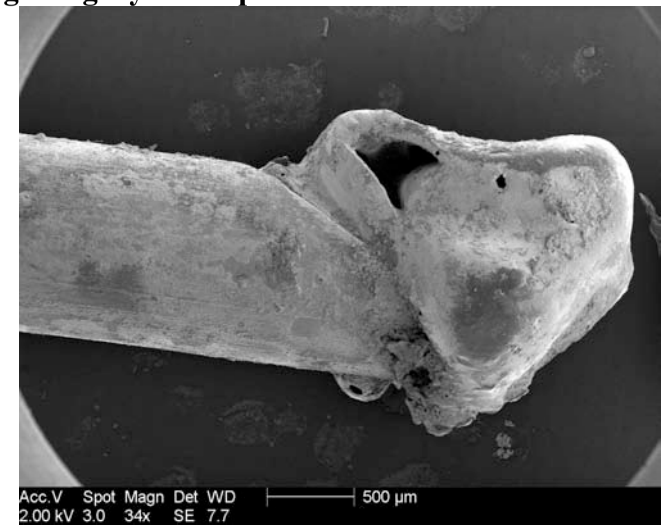

Figure 284 - SEM image of the right severed end detailed in figure 283, with an unusual shaped bead at the end.

Figure 285 - SEM image of the left severed end in figure 283 at 38x magnification.

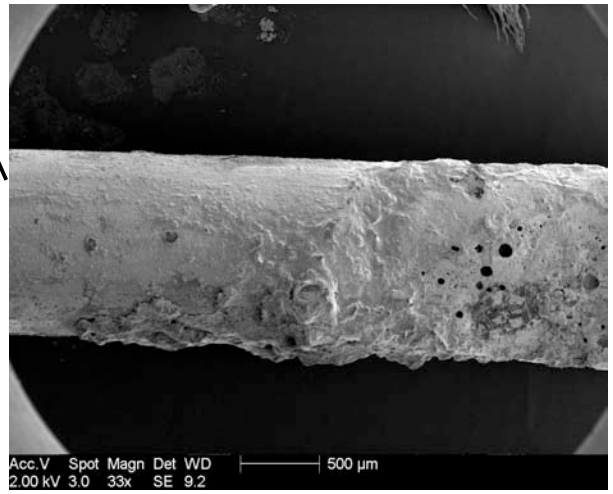

Figure 286 - SEM image of the notch damage to the bottom conductor in figure 283.

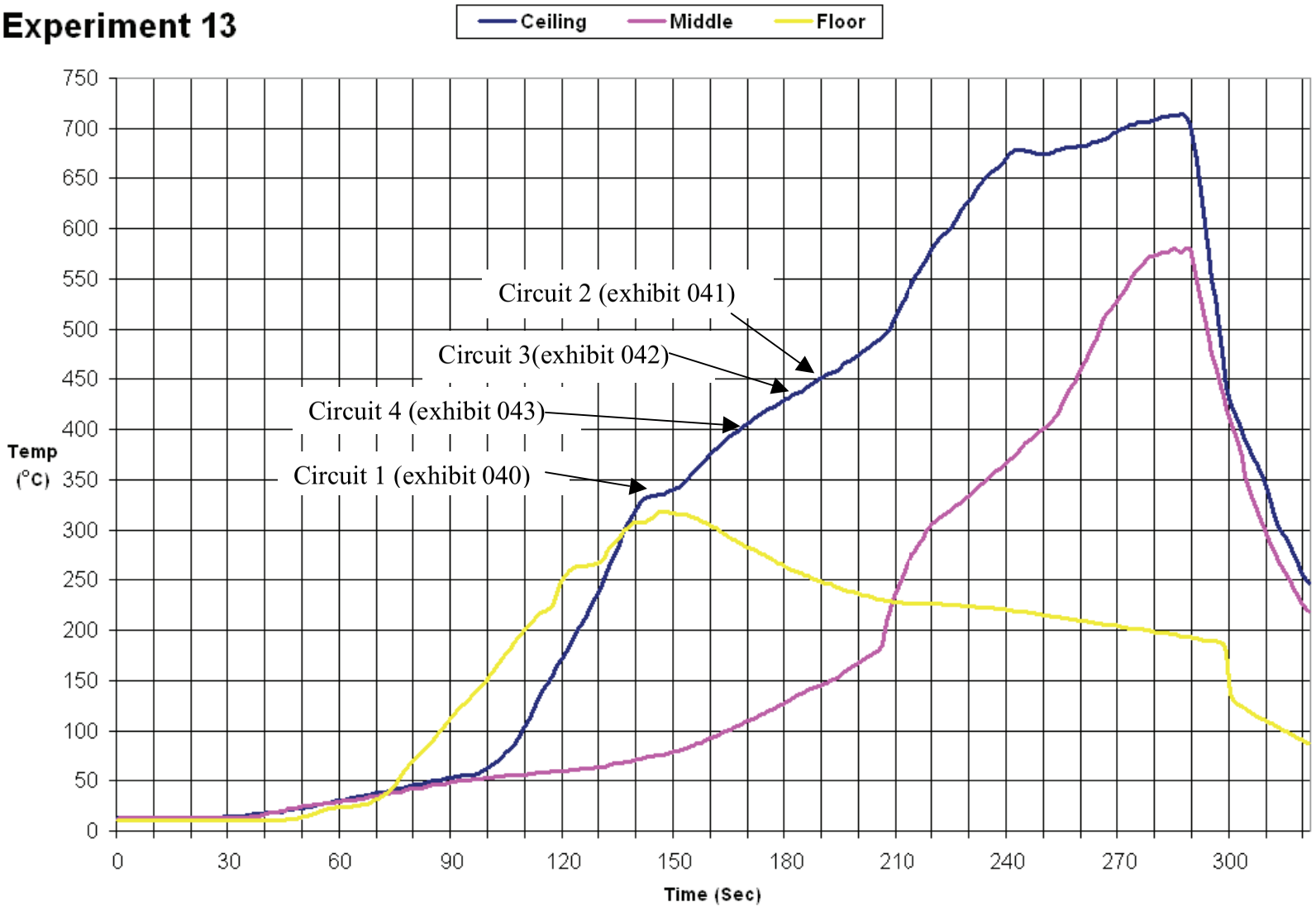

Figure 287 - Time temperature graph for experiment 13

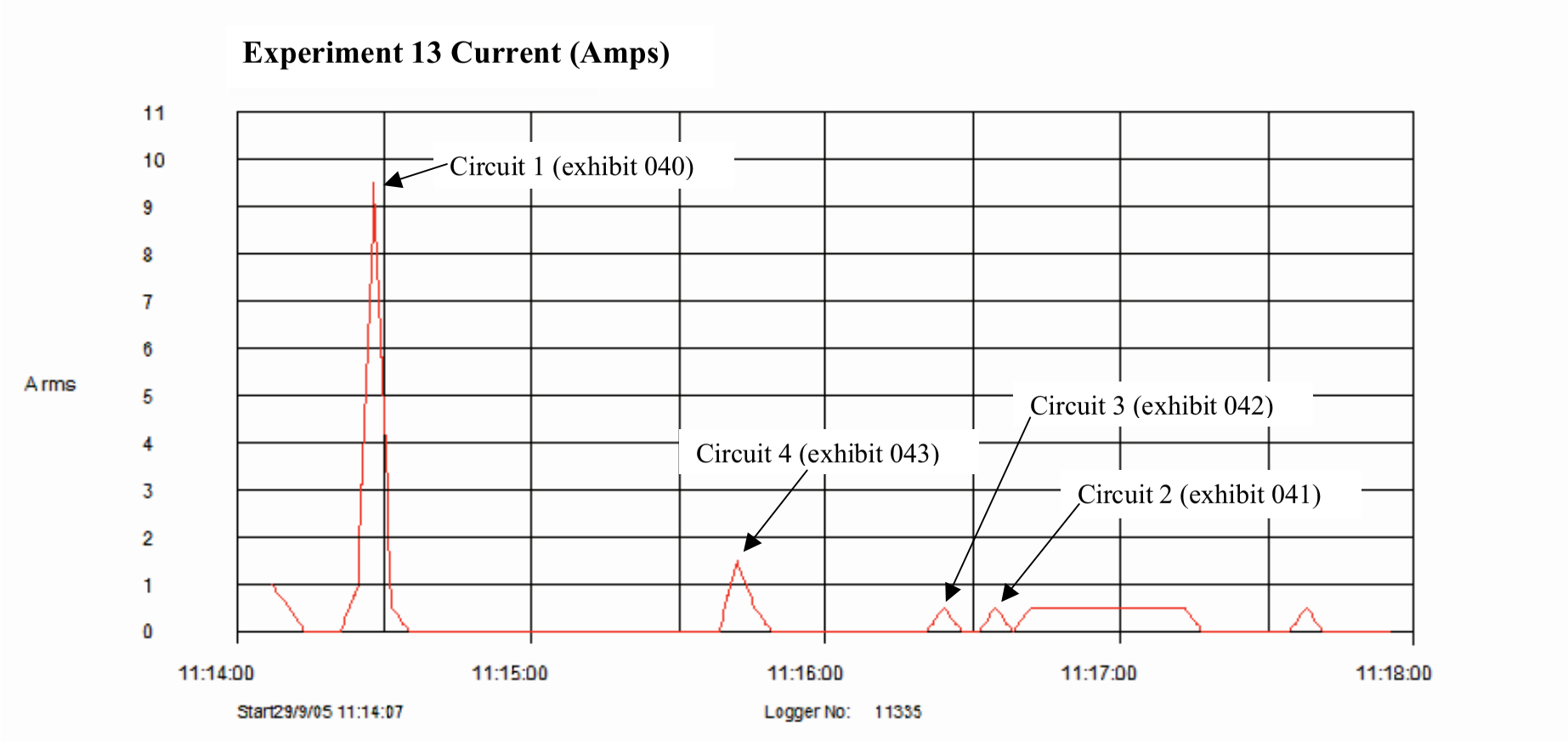

Figure 288 - Current (Amps) graph for experiment 13 detailing the operation of the circuit breakers and the fault current

Experiment 14

Figure 289 - "Scenario D" 29 September 2005

Circuit number	MCB operating time from ignition
1	1:02 minutes
3	1:17 minutes
2	1:30 minutes
4	1:38 minutes

Table 16 – circuit breaker operation data

The fire in experiment 14 (scenario D) originated in two separate areas. They were located on each of the armchairs at the far end of the room.

This was a rapidly developing fire with the ceiling temperature exceeding 1100° C in just over 3 minutes.

Localised melting (arcing) damage was locate at the following points in the compartment:

Arcing damage was located on circuit 1 – 1000mm from the rear wall and adjacent to the right wall.

Arcing damage was located on circuit 2 – 100mm from the right wall and 1000mm from the rear wall at ceiling level.

Arcing damage was located on circuit 3 – 100mm from the right wall and 1000mm from the rear wall at the ceiling level.

Arcing damage was located on circuit 4 – 600mm from the right wall and 1000mm from the front wall at the ceiling level. The faulting to circuits 2 and 3 are in the same location.

Pre-fire and post-fire photographs of experiment 14

Figure 290 - Pre-fire photograph of experiment 14. The white ovals detail the fire's two areas of origin.

Figure 291 - Pre-fire photograph taken from an area of origin with the entrance door in the background.

Figure 292 - Post-fire photograph of experiment 14. The white ovals detail the fire's two areas of origin. The white arrows indicate the arcing damage locations to circuits 1 (right), 2 (left) and 3 (centre).

Figure 293 - Post-fire image of the compartment viewing the entrance door.

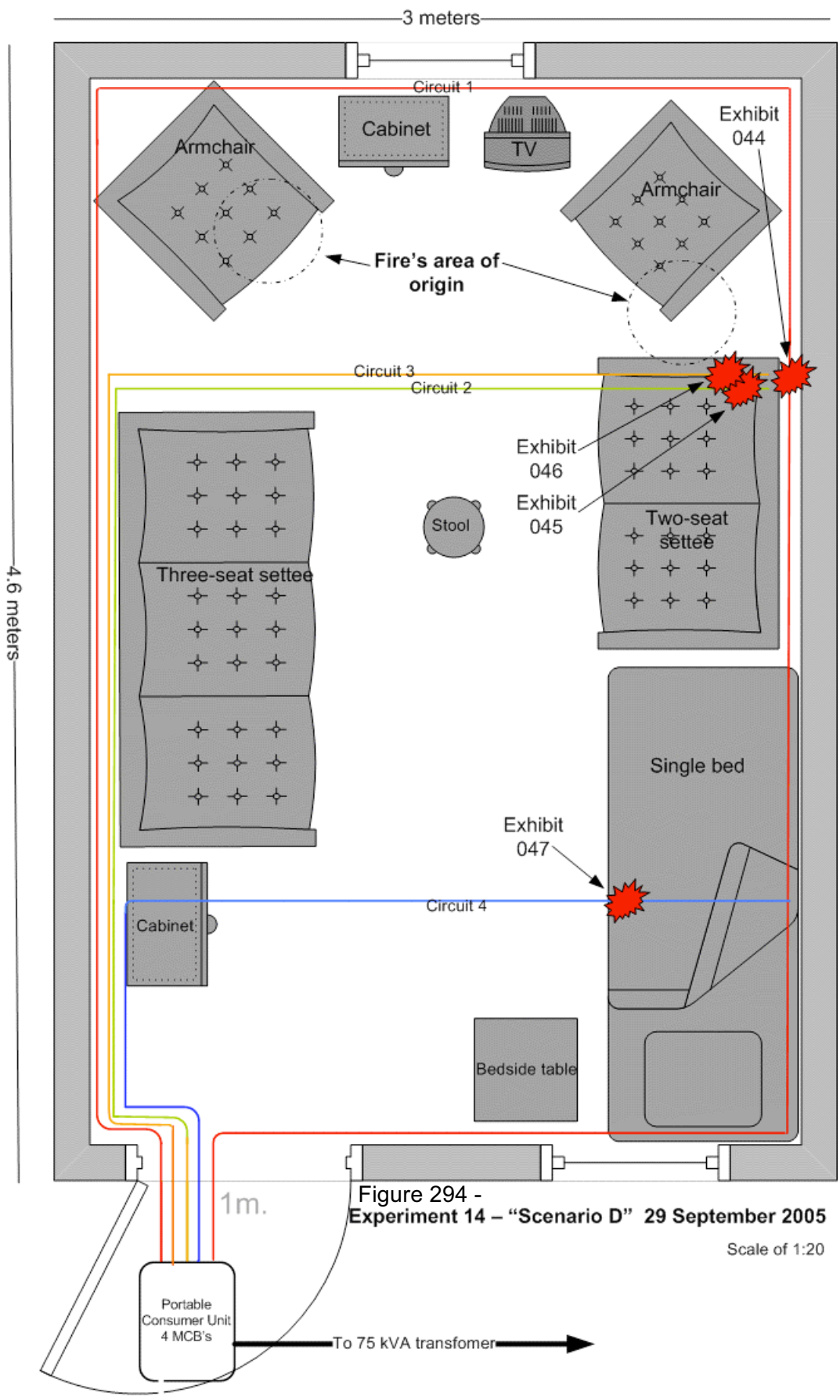

Figure 294 -
Experiment 14 – "Scenario D" 29 September 2005

Scale of 1:20

Microscope images for exhibit 044 arcing category B – experiment 14

Figure 295 - Microscope image of exhibit 044. The localised metallic has affected two conductors and each one has a notch.

Figure 296 - Microscope image at 20x magnification detailing the centre conductor notch as displayed in figure 295.

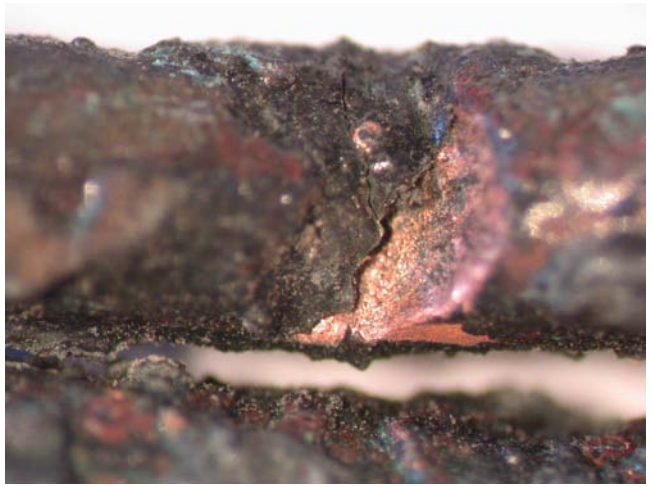

Figure 297 - Microscope image at 40x magnification of the notch detailed in figures 296 and 296. Depth of field issues renders a large area of the image as out of focus.

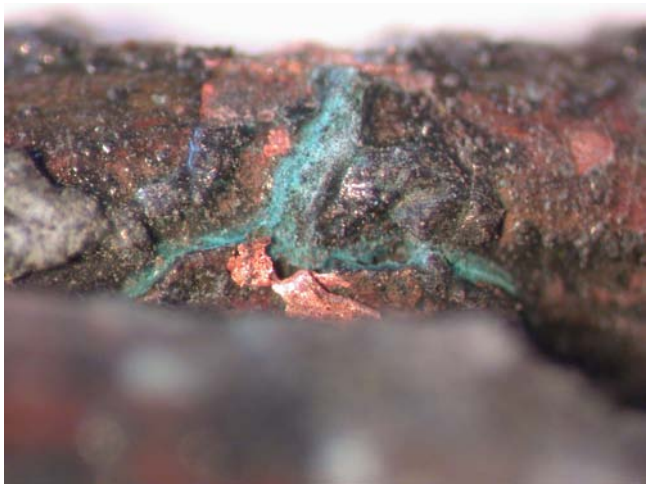

Figure 298 - 40x magnification of the bottom conductor damage detailed in figure 295.

Microscope and SEM images for exhibit 045 arcing category E – experiment 14

Figure 299 - Microscope image of exhibit 045, two of the conductors have notch damage.

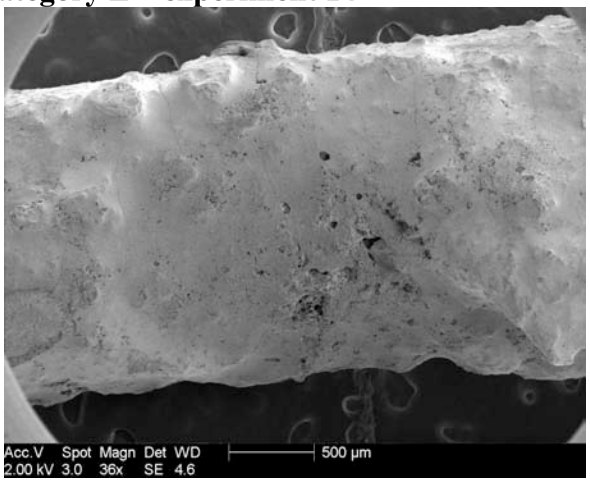

Figure 300 - SEM image of the top conductor notch detailed in figure 299.

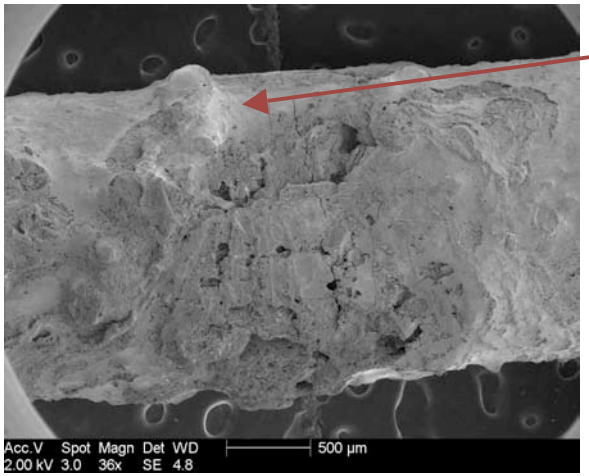

Figure 301 - SEM image at 36x magnification of the bottom notch detailed in figure 299.

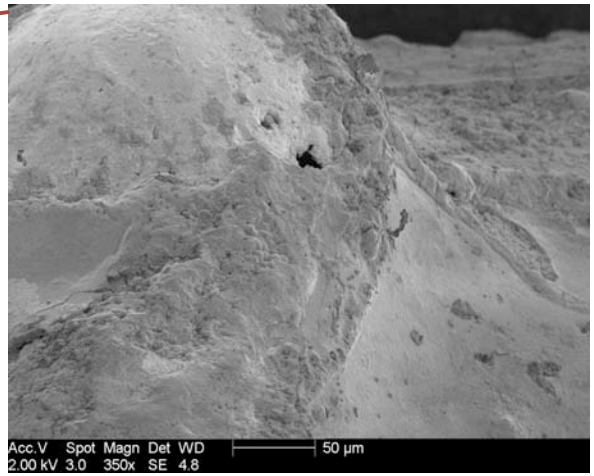

Figure 302 - SEM image at 350x magnification detailing the demarcation area between the arcing damage and the un-damaged conductor detailed in figure 301.

Confocal laser scanning microscope images of exhibit 045 – arcing category E (experiment 14)

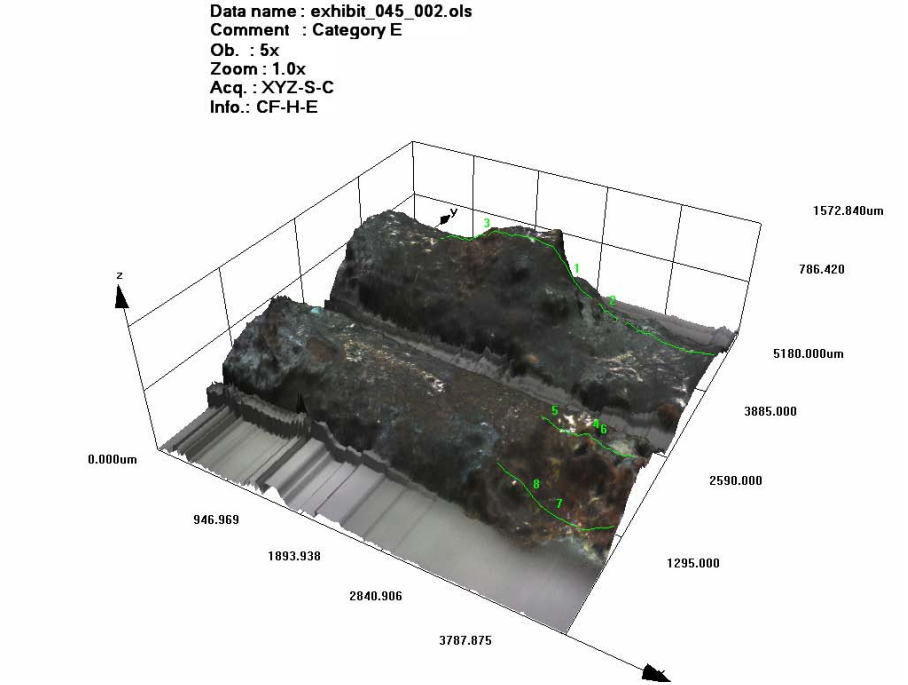

Figure 303 - LEXT image of exhibit 045.

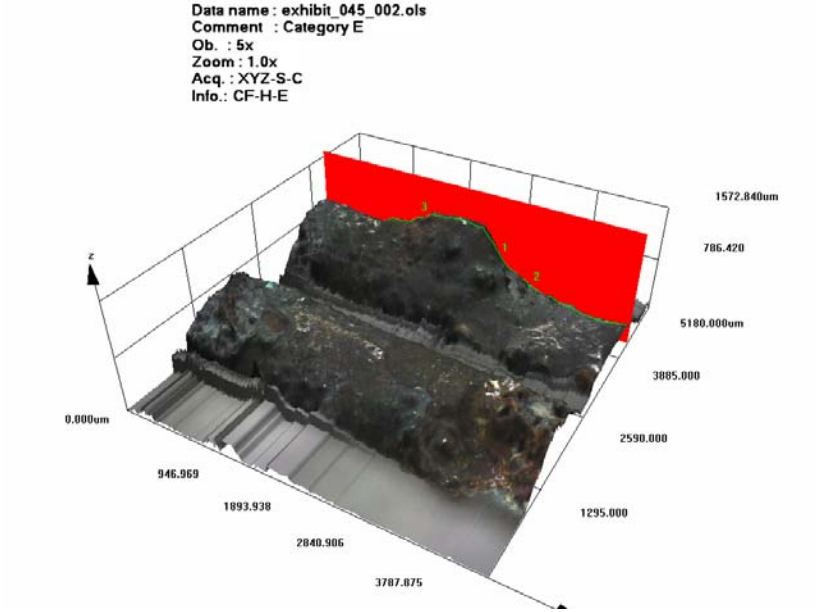

LEXT image with the “slice tool” in use on the top conductor to create a profile.

Microscope images for exhibit 046 arcing category D – experiment 14

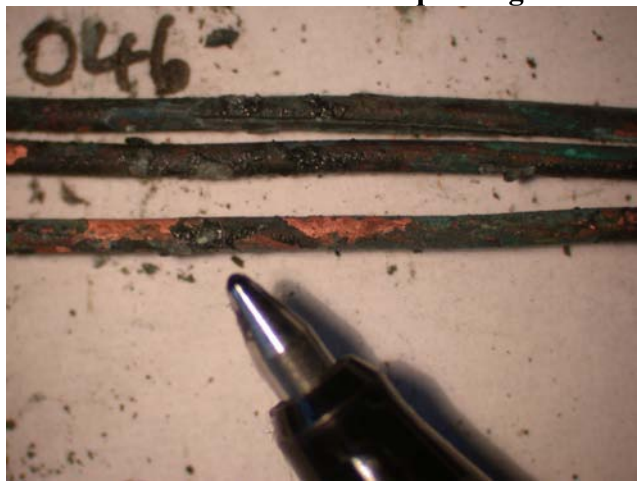

Figure 305 - Microscope image of exhibit 046 at 6x magnification with the arcing damage indicated with the pen ballpoint tip.

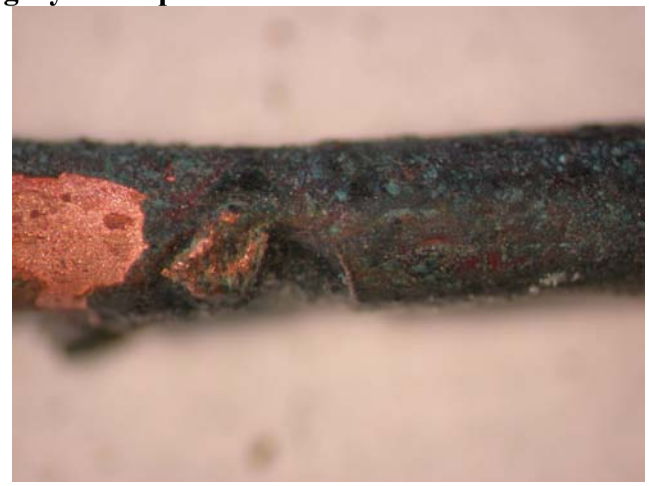

Figure 306 - Microscope image of the notched area of the conductor indicated in figure 305 at 40x magnification.

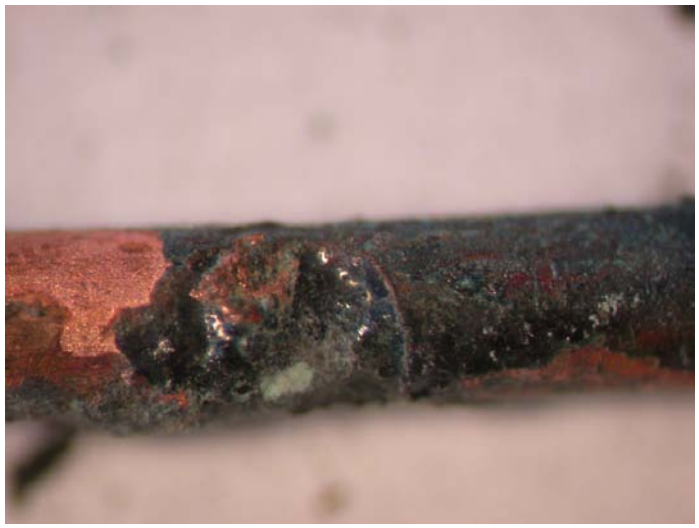

Figure 307 - Microscope image at 40x magnification of the notch re-orientated. The right notch edge has a clear demarcation area.

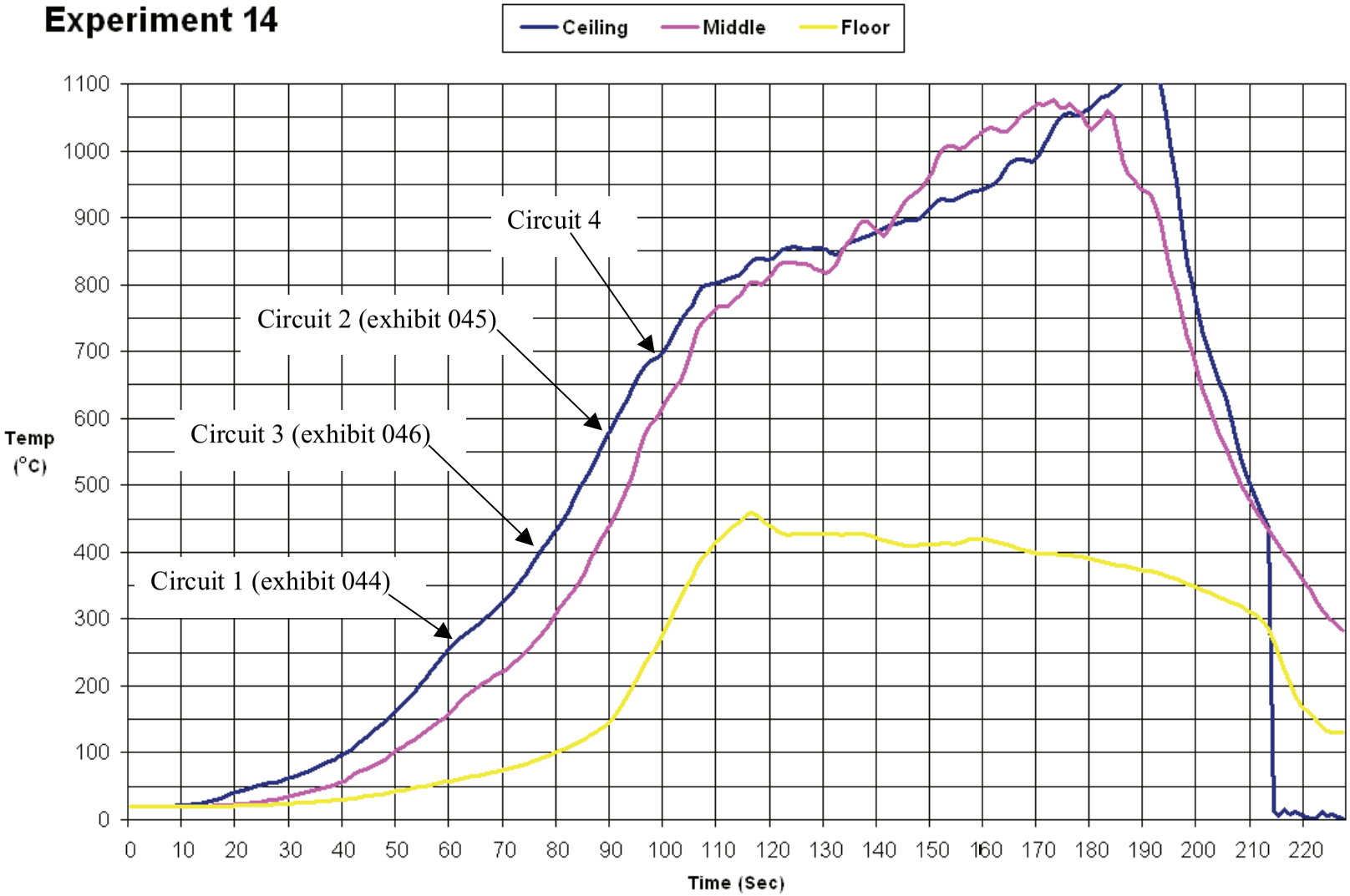

Figure 308 - Time temperature graph for experiment 14

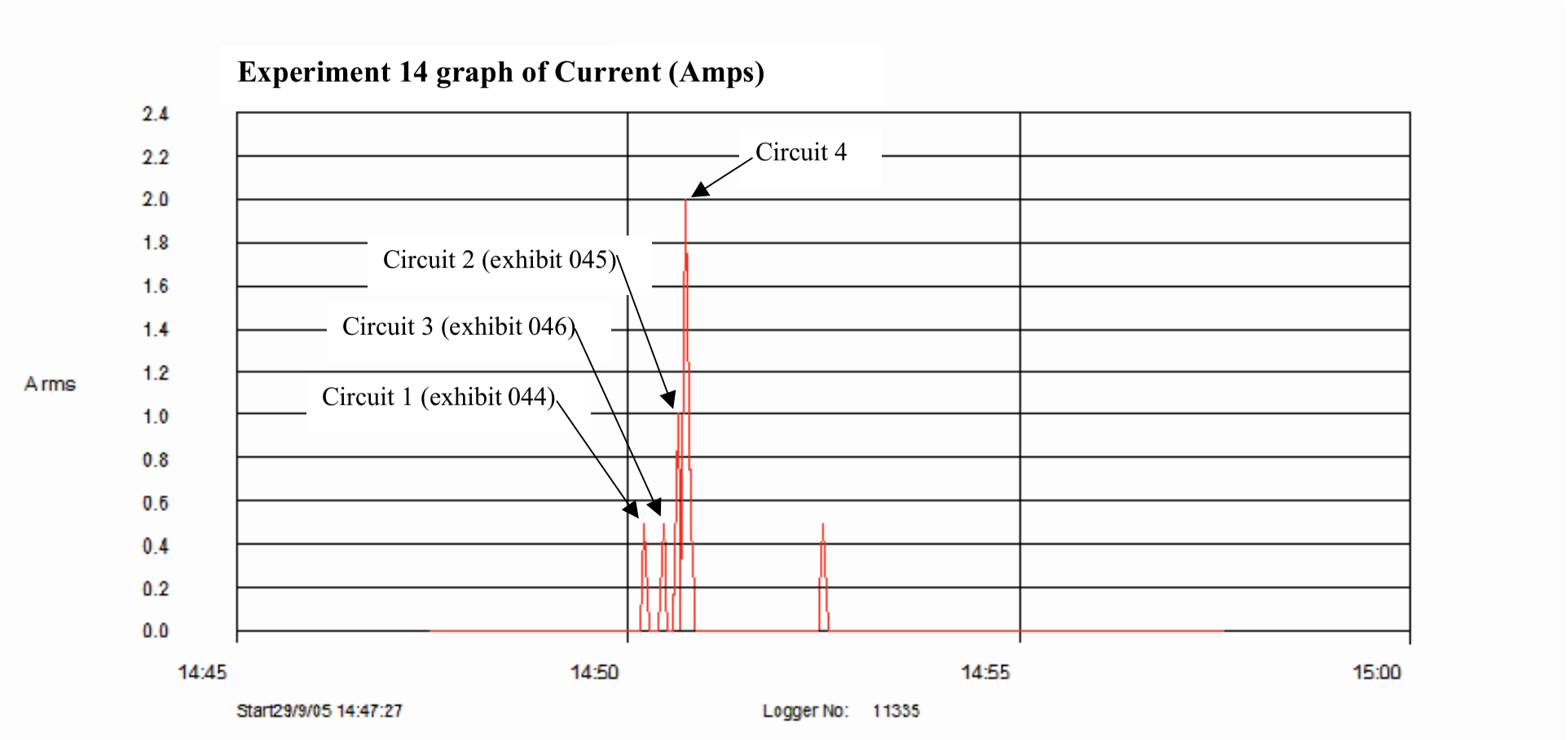

Figure 309 - Current (Amps) graph for experiment 14 detailing the operation of the circuit breakers and the fault current

Experiment 15

Figure 310 – “Scenario B” 29 September 2005

Circuit number	MCB operating time from ignition
3	4:00 minutes
4	4:00 minutes
2	4:15 minutes
1	4:35 minutes

Table 17 – circuit breaker operation data

The voltage measurement at the portable consumer unit = 267 Volts.

The fire in experiment 15 (scenario B) originated in three separate areas as a result of using a white spirit and diesel mixture of fuel poured onto strips of polyurethane foam. This has provided a trailer with an approximate delay fuse of 10 minutes.

The three resultant areas of origin for the fire were located under a desk, within a refuse bin in the left rear corner of the room and on a shelving unit in the right rear corner of the room. The shelving unit was the predominant origin of the fire with the first flame impingement being observed on the ceiling in this area. The compartment went to flashover at 5 minutes with peak ceiling, middle and floor temperatures of 850° C.

No arcing damage located on circuit 1 during the scene examination.

Arcing damage was located on circuit 2 – 1800mm from the left wall and 1000mm from the rear wall at ceiling level.

Arcing damage was located on circuit 3 – 1800mm from the left wall and 1000mm from the rear wall at ceiling level. Circuits 2 and 3 appear to have faulted between the circuits.

Arcing damage was located on circuit 4 – 750mm from the right wall and 1000mm from the front wall.

Pre-fire and post-fire photographs of experiment 15

Figure 311 - Pre-fire view of experiment 15 taken from the door.

Figure 312 - Pre-fire view of wiring installed on the ceiling.

Figure 313 - Post-fire view of the compartment with white ovals indicating the location of the two areas of origin.

Figure 314 - Post-fire view of the fire damaged wiring above the dominant area of origin, the shelf unit. The arrows indicate the arcing damage to circuits 2 and 3.

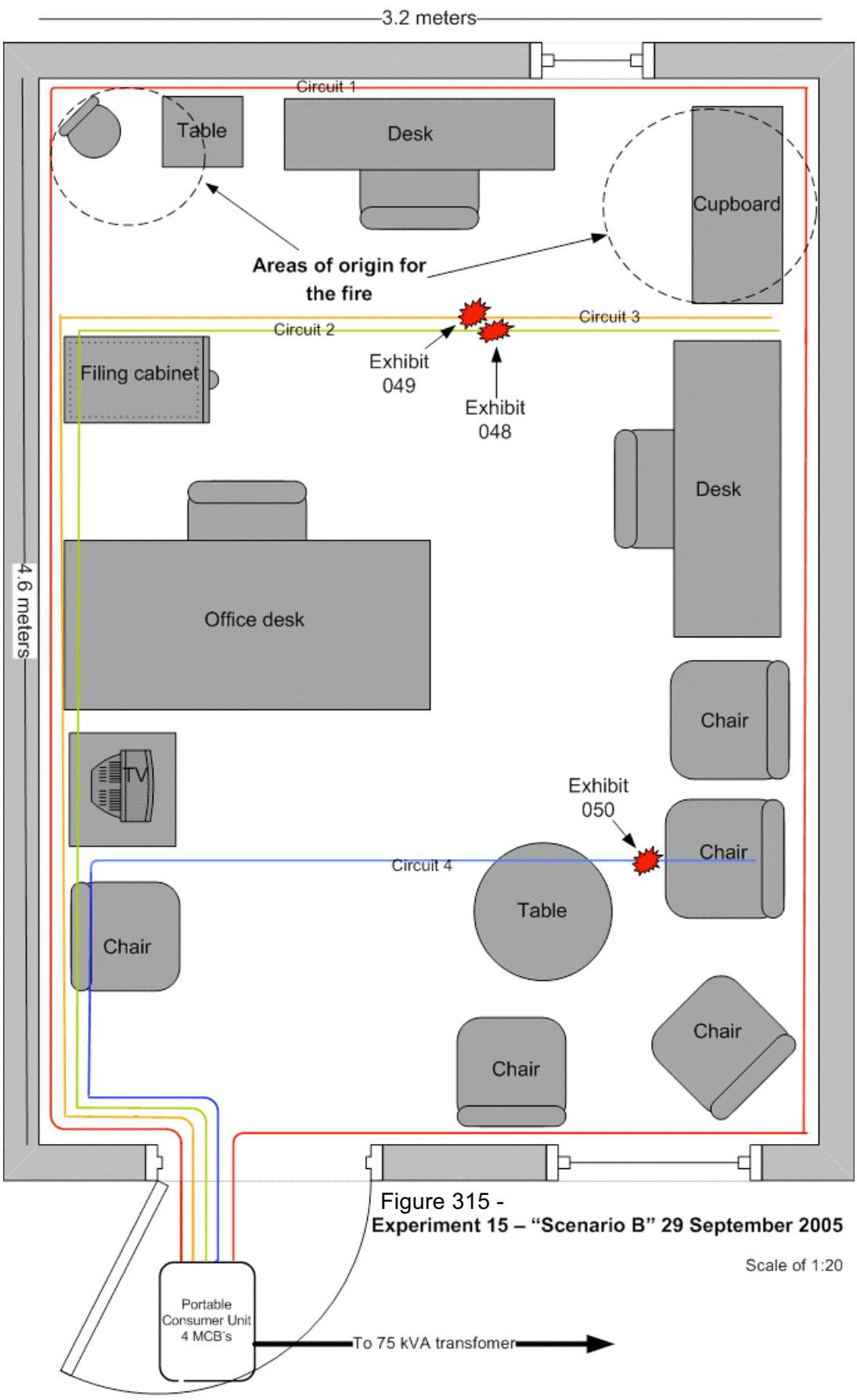

Figure 315 -
Experiment 15 – "Scenario B" 29 September 2005

Scale of 1:20

Microscope images for exhibit 048 arcing category D – experiment 15

Figure 316 - Microscope image of exhibit 048 at 6x magnification. Two of the conductors were damaged with notches and beads.

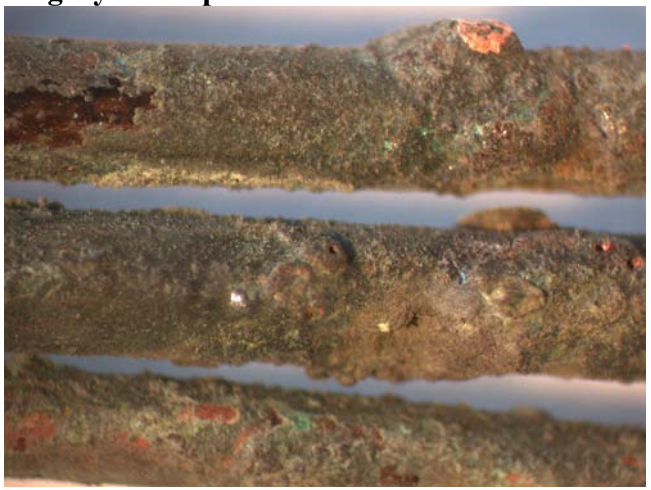

Figure 317 - Microscope image of the two conductors at 20x magnification.

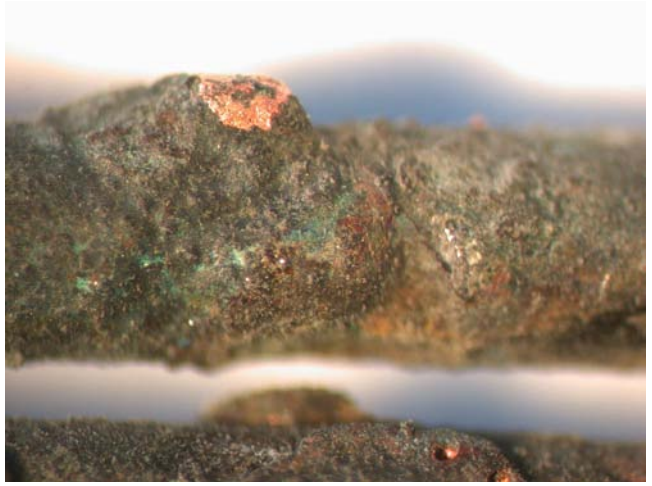

Figure 318 - Microscope image at 40x magnification of the top conductor notch and bead as detailed in figure 317.

Microscope and SEM images for exhibit 049 arcing category B – experiment 15

Figure 319 - Microscope image of exhibit 049. Two conductors were involved. One with severed ends and the top one with a notch.

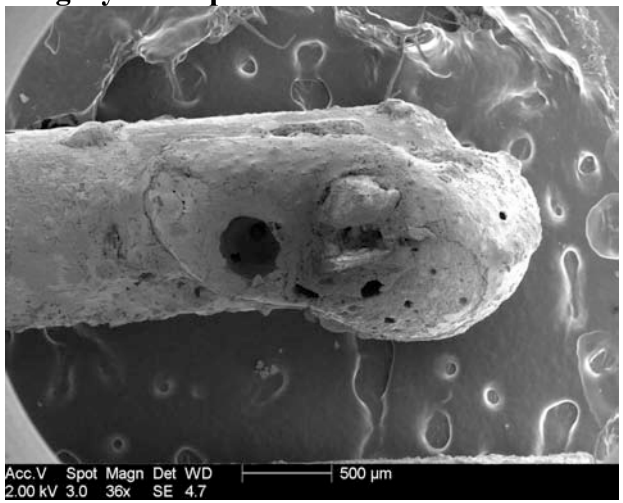

Figure 320 - SEM image at 36x magnification of the right severed end as detailed in figure 319.

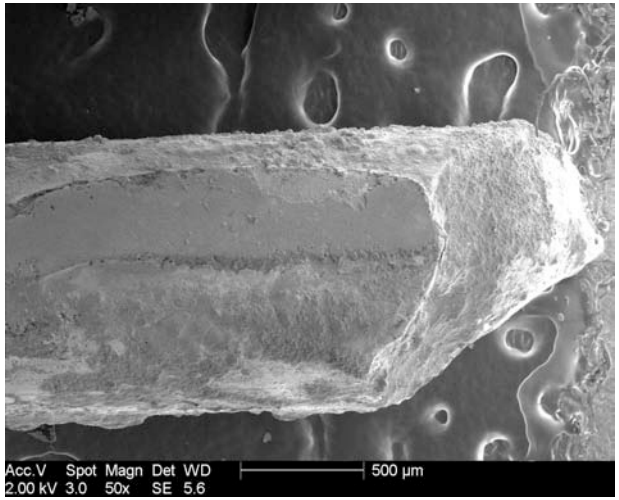

Figure 321 - SEM image of the left severed end as detailed in figure 319 above.

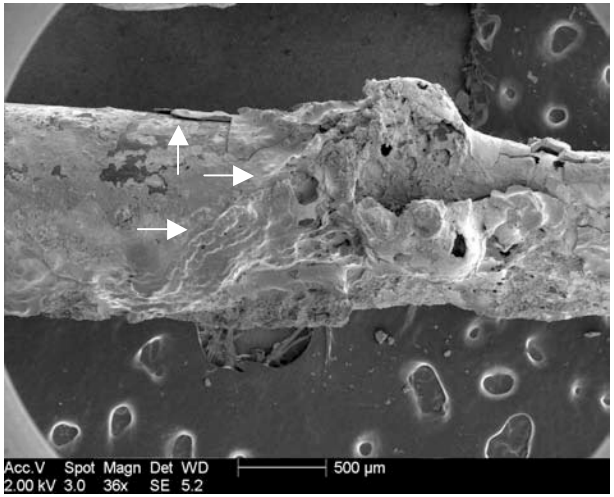

Figure 322 - SEM image indicating the clear demarcation between the notch and undamaged conductor.

Confocal laser scanning microscope images of exhibit 049 – arcing category B (experiment 15)

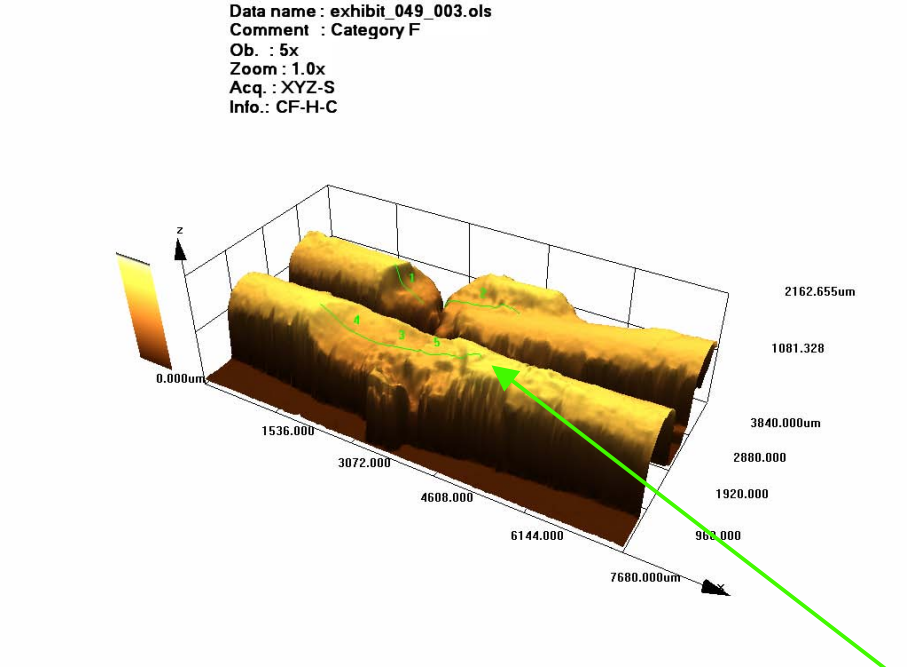

Figure 323 - LEXT image of exhibit 049 in the brown colour render.

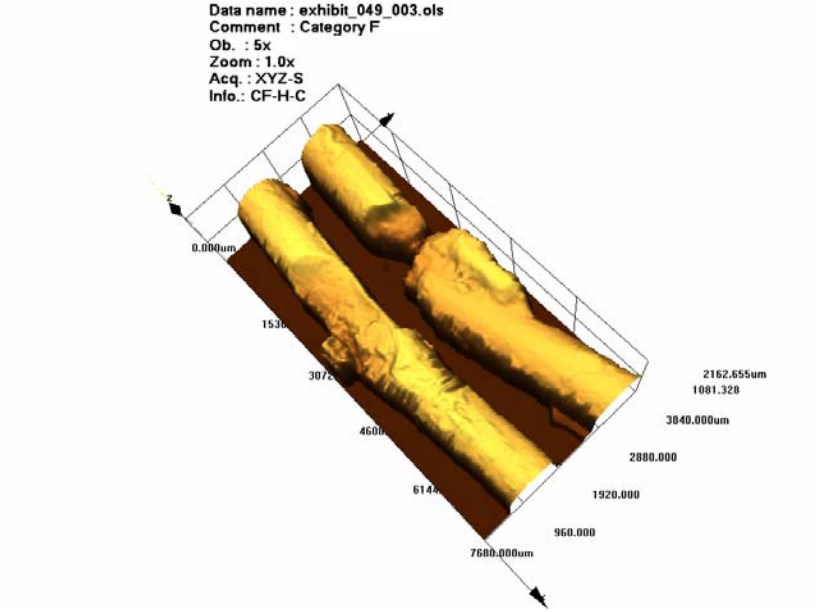

Figure 324 - LEXT image orientated in the software.

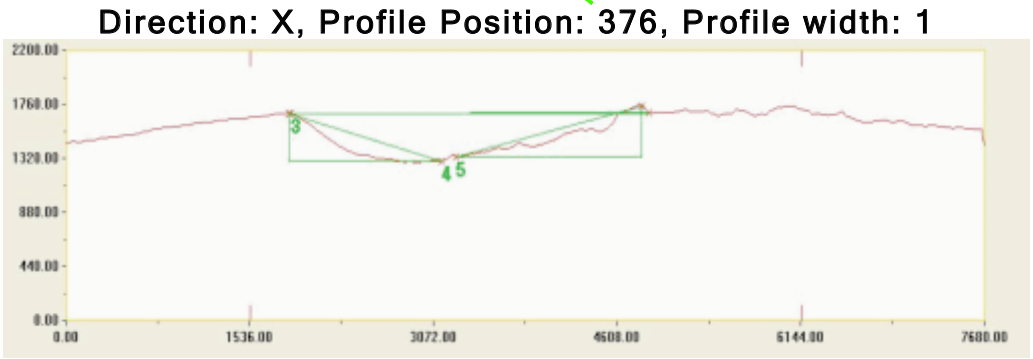

Figure 325 – Profile of the localised melting captured with the LEXT software's "slice tool".

Microscope images for exhibit 050 arcing category B – experiment 15

Figure 326 - Microscope image of exhibit 050. Two conductors were involved. One with severed ends and the adjacent with a notch.

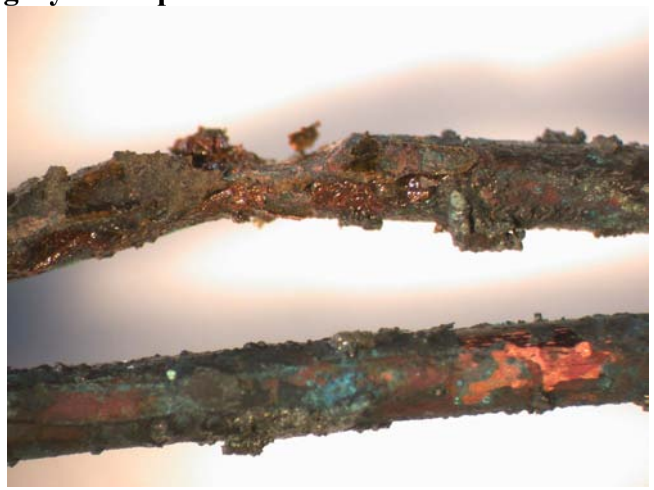

Figure 327 – 20x magnification image of the middle conductor with a notch detailed in figure 326.

Figure 328 - The right severed conductor at 40x magnification.

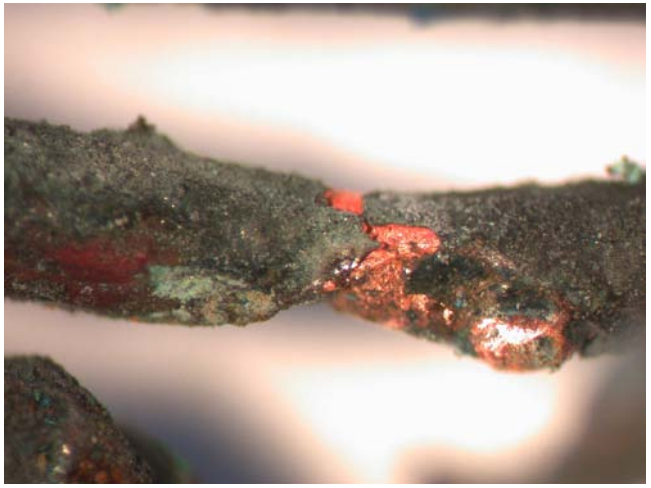

Figure 329 - Alternative view of the notch in figure 327.

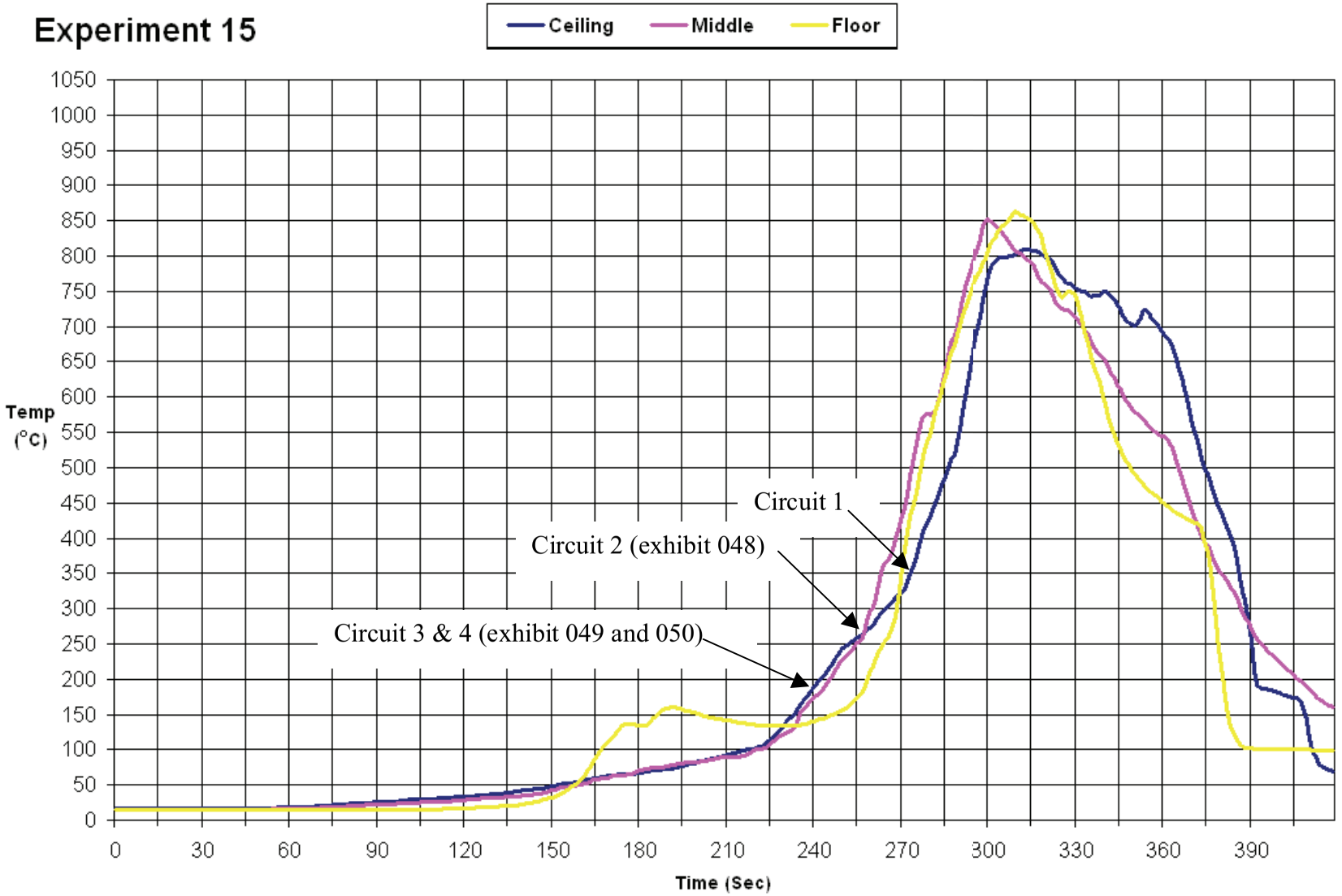

Figure 330 - Time temperature graph for experiment 15

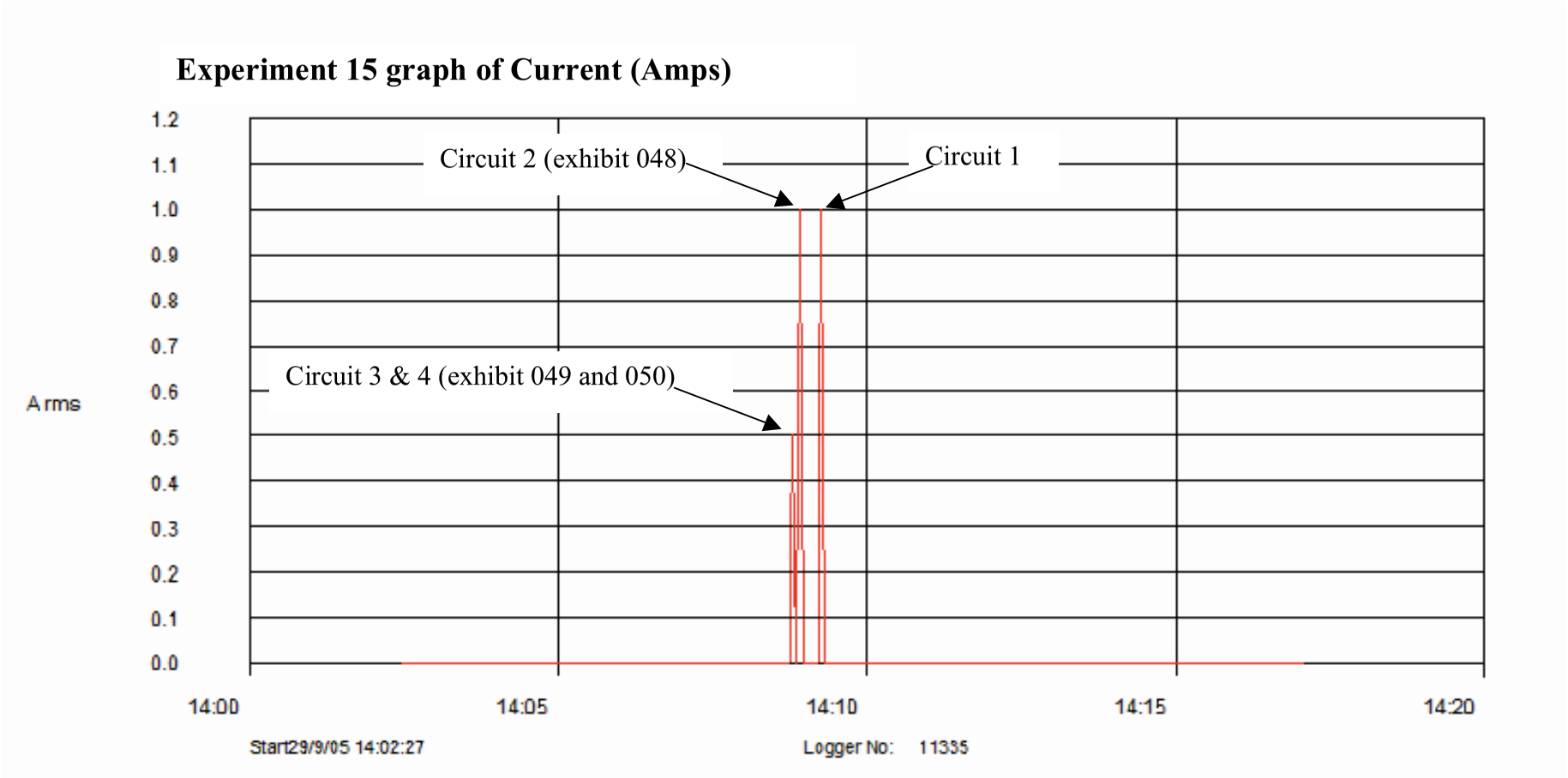

Figure 331 - Current (Amps) graph for experiment 15 detailing the operation of the circuit breakers and the fault current

Experiment 16

Figure 332 – "Scenario C" 23 March 2006

Circuit number	MCB operating time from ignition
4	2:30 minutes
1	3:30 minutes
3	3:55 minutes
2	3:58 minutes

Table 18 – circuit breaker operation data

The fire in experiment 16 (scenario C) originated in a toy box located 1300mm from the left wall and 800mm from the rear wall.

The peak ceiling temperature recorded was 1025° C at 6.5 minutes with the middle thermocouple temperature recording 1110° C. The floor temperature reached 410° C at this time and the compartment reached flashover conditions. Collecting the MCB data for this experiment was difficult due to smoke logging of the area in front of the compartment as detailed in figure 332.

Localised metallic damage to the conductors was located in the following areas:

Arcing damage was located on circuit 1 – against the rear wall and 1850mm from the left wall at ceiling level.

Arcing damage was located on circuits 2 and 3 - 1550mm from the left wall and 1000mm from the front wall at the ceiling level. The conductors of circuits 2 and 3 appear to have faulted between each circuit.

Arcing damage was located on circuit 4 – 1240mm from the left wall and 1000mm from the rear wall.

Pre-fire and post-fire photographs of experiment 16

Figure 333 - Pre-fire photograph of experiment 16. The white oval indicates the fire's area of origin (a toy box).

Figure 334 - Pre-fire photograph of experiment 16 taken from the fire's area of origin with the entrance in the background.

Figure 335 - Pre-fire photograph of experiment 16. The white oval indicates the fire's area of origin. The white arrows indicate arcing damage to circuit 4 (left) and circuit 1 (right).

Figure 336 - Post-fire photograph of the view shown above in figure 334.

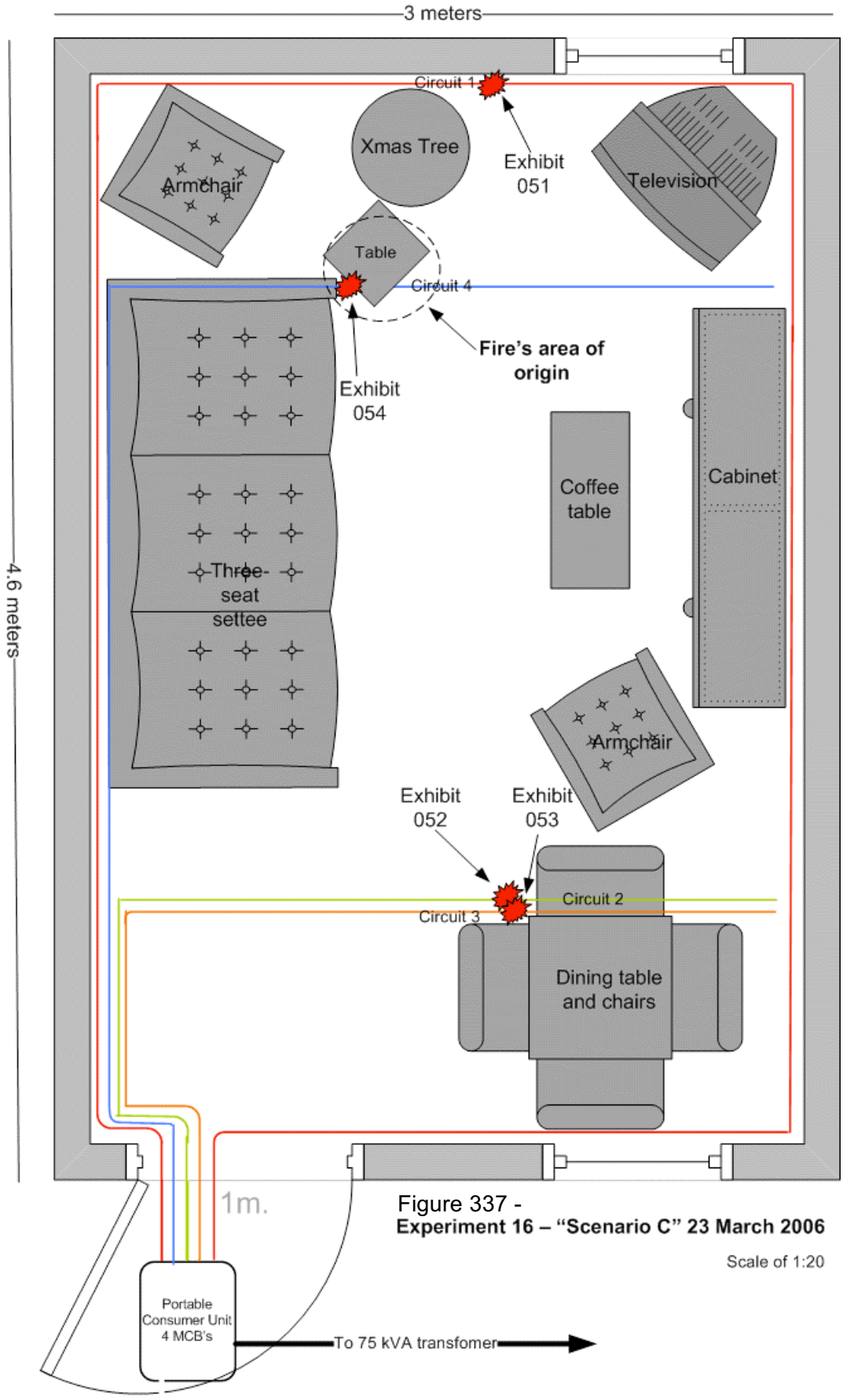

Figure 337 -
Experiment 16 – "Scenario C" 23 March 2006

Scale of 1:20

Microscope images for exhibit 051 - arcing category D (experiment 16)

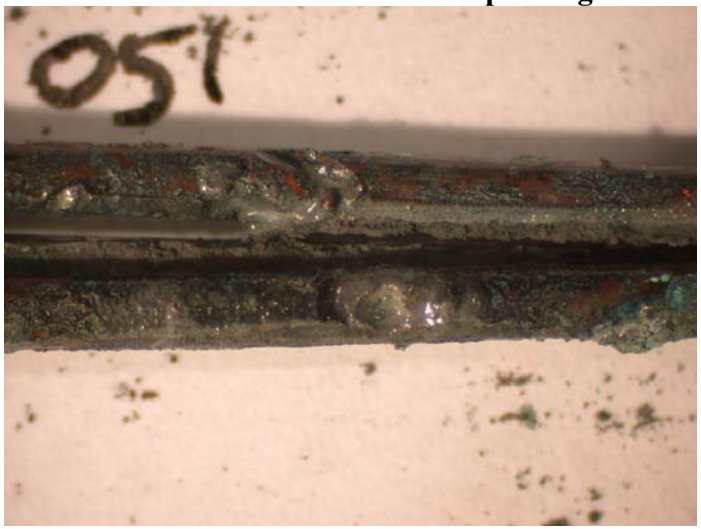

Figure 338 - Microscope image of exhibit. This exhibit involves two conductors. Each one has a notch with a bead within the notch.

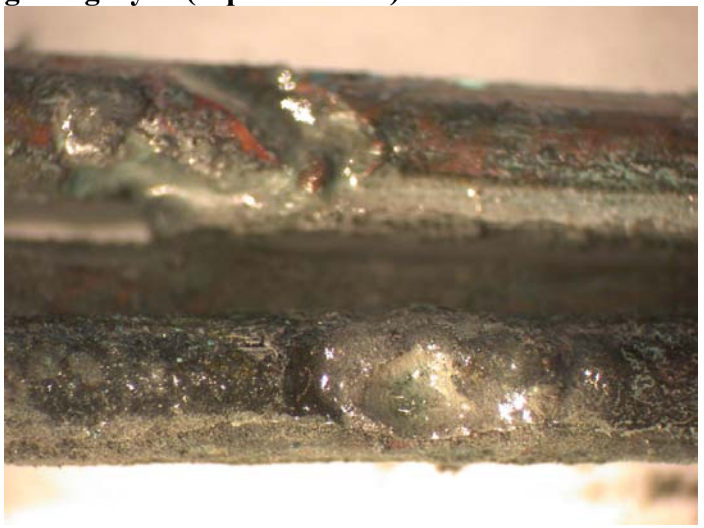

Figure 339 - 20x magnification of arcing damage of the two notches.

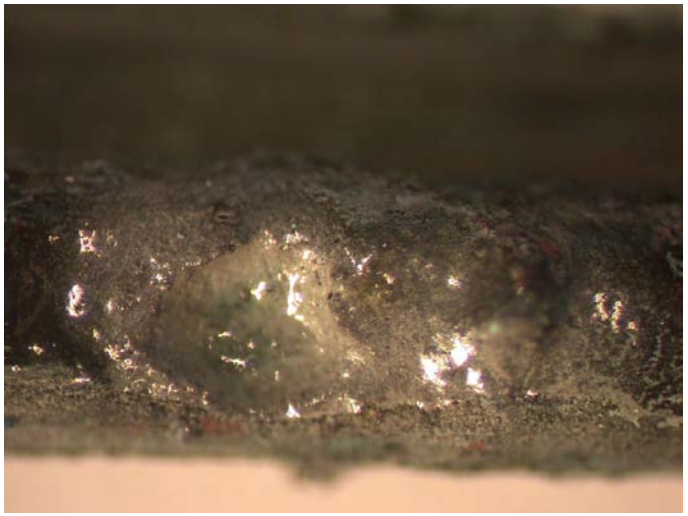

Figure 340 - 40x magnification of lower conductor notch.

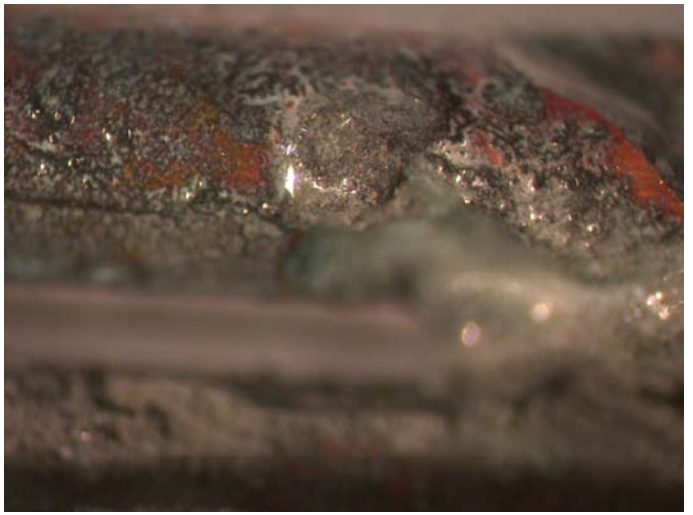

Figure 341 - 40x magnification of upper conductor notch.

Microscope and SEM images for exhibit 052 - arcing category F (experiment 16)

Figure 342 - Microscope image of exhibit 052. This has involved one conductor with a wide notch.

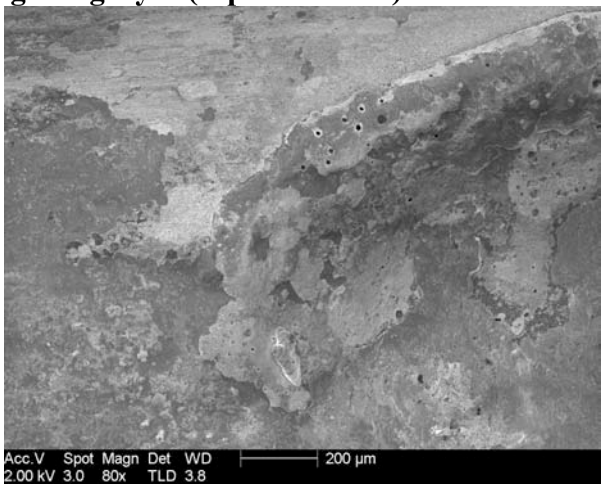

Figure 343 - SEM image at 80x magnification of the notch's left edge.

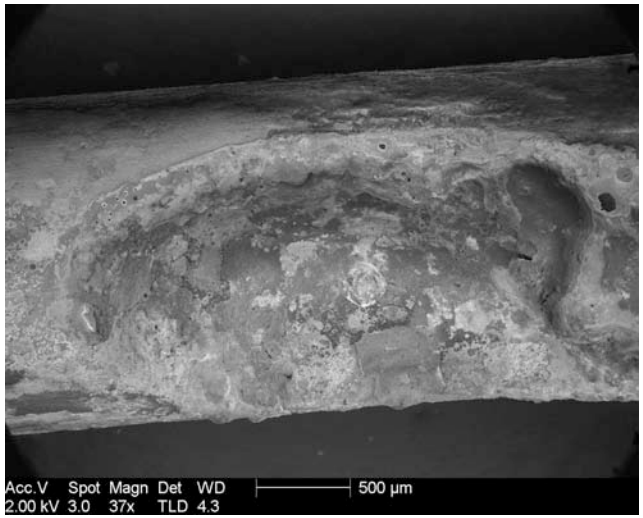

Figure 344 - SEM image showing the demarcation between the notch and the undamaged conductor.

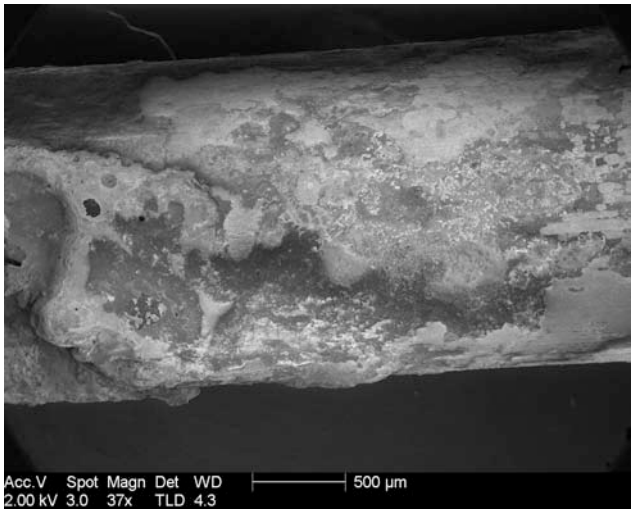

Figure 345 - SEM image of the right edge of the notch.

Microscope and SEM images for exhibit 053 - arcing category I (experiment 16)

Figure 346 - Microscope image of exhibit 053. Two conductors have localised melting (arcing) damage.

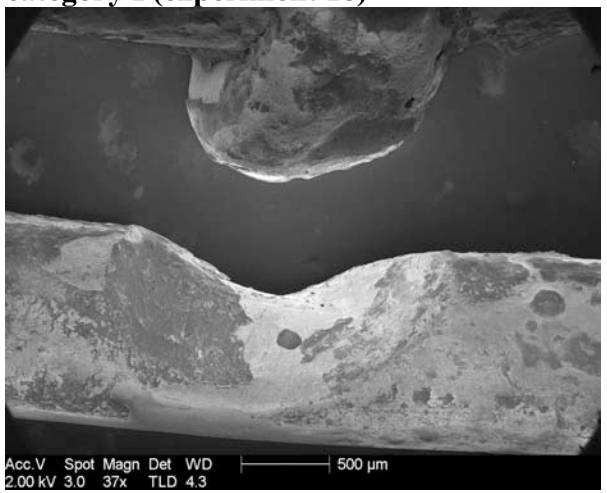

Figure 347 - SEM image of both conductors. The bead and the notch were adjacent to each other at the scene.

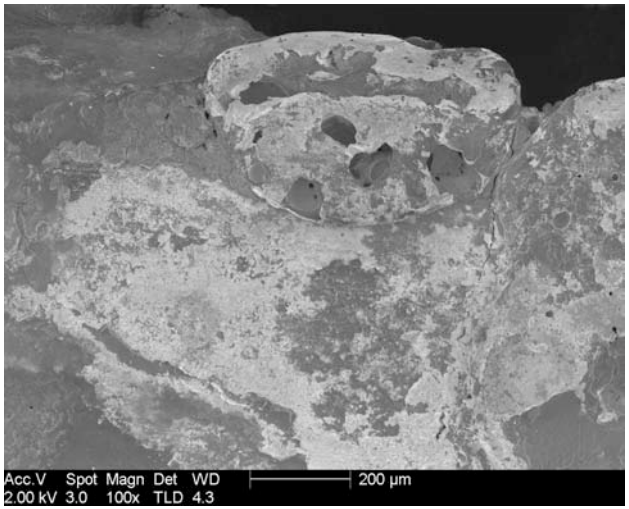

Figure 348 - SEM image of the demarcation at the edge of the notch.

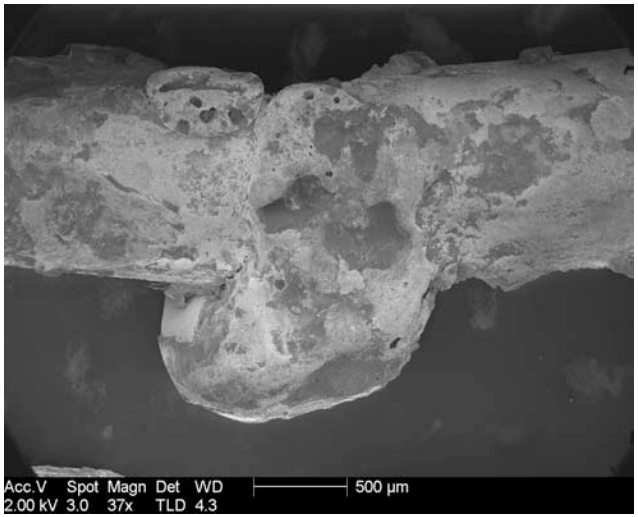

Figure 349 - SEM image of the bead.

Confocal laser scanning microscope images of exhibit 053 – arcing category I (experiment 16)

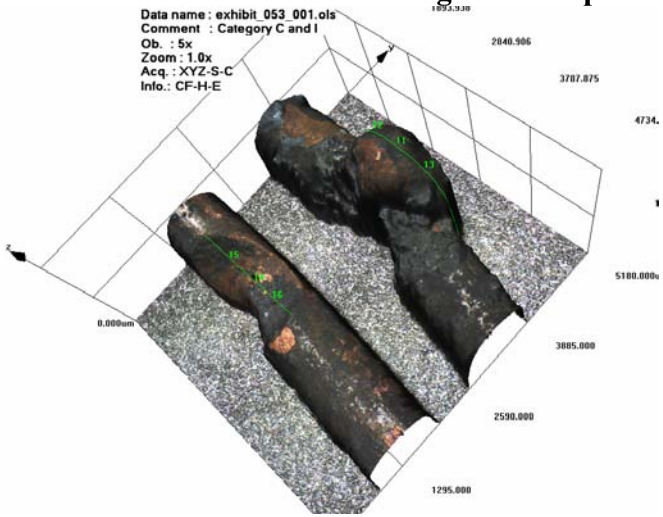

Figure 350 - LEXT image of exhibit 053. The scan has documented the two conductors side-by-side.

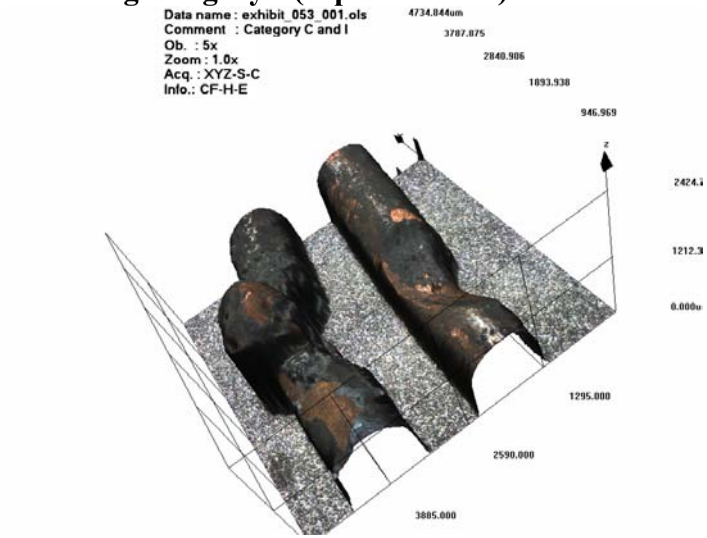

Figure 351 - LEXT image orientated in the 3-D software.

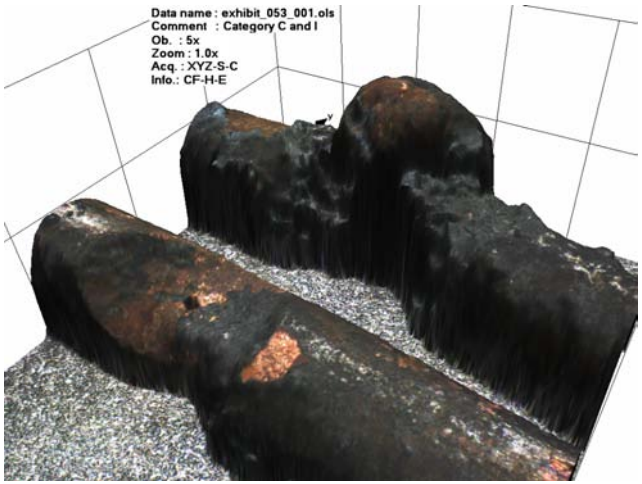

Figure 352 - LEXT software used to zoom into the areas of interest.

Microscope and SEM images for exhibit 054 - arcing category H (experiment 16)

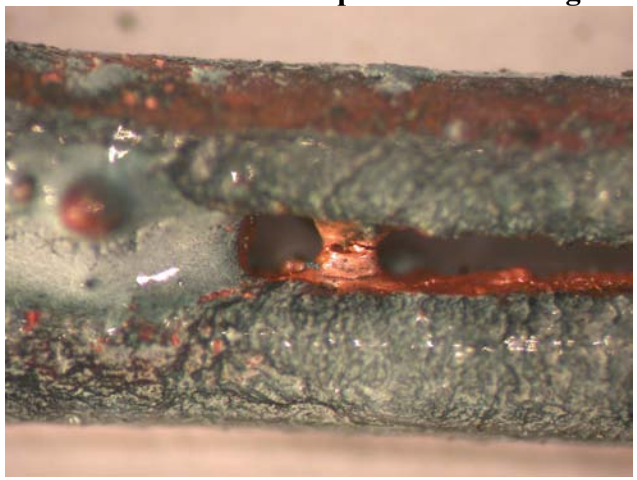

Figure 353 - Microscope photograph prior to cleaning with acetone solvent using an ultrasonic bath.

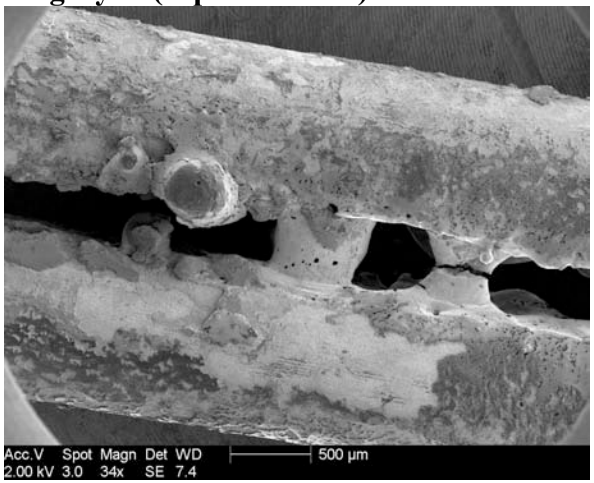

Figure 354 - SEM image of the two welded area of the conductors.

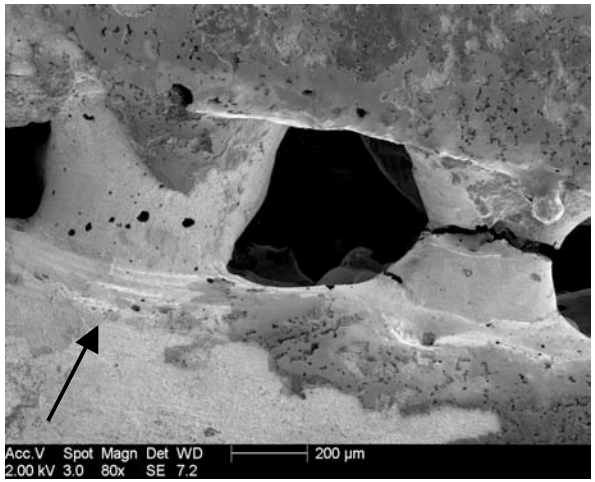

Figure 355 - 80x magnification of the welded conductors detailed in figures 353 & 354. Note the rib lines at the bottom of the weld. This is a possible effect of alternating current.

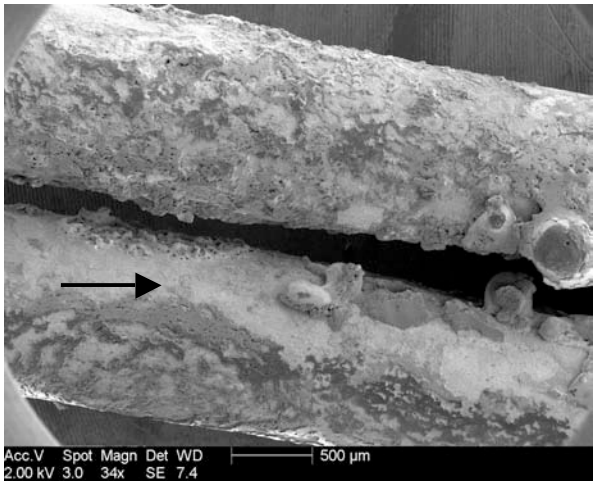

Figure 356 - The left edge of the lower conductor's arcing damage – a notch with a clear demarcation area.

Confocal laser scanning microscope images of exhibit 054 – arcing category H (experiment 16)

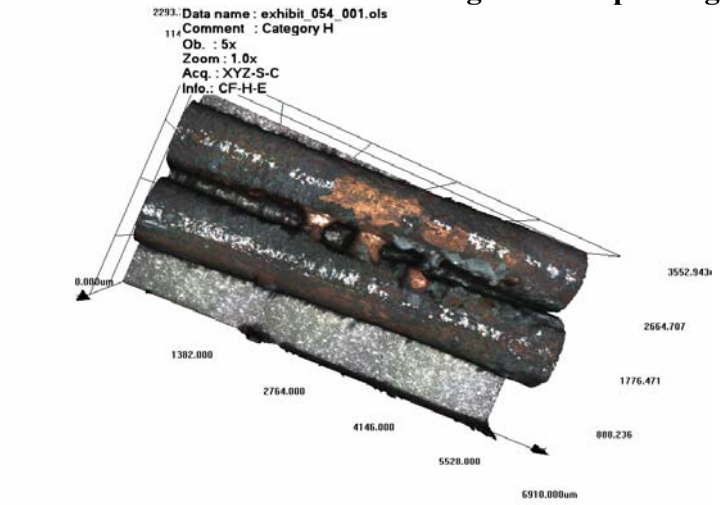

Figure 357 - LEXT overview image of exhibit 054 detailing the entire exhibit.

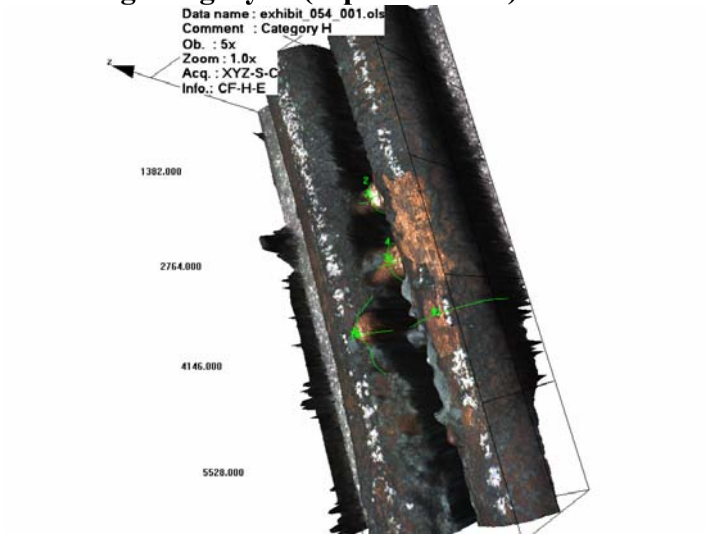

Figure 358 - LEXT image captured while orientating the 3-D scan in the software.

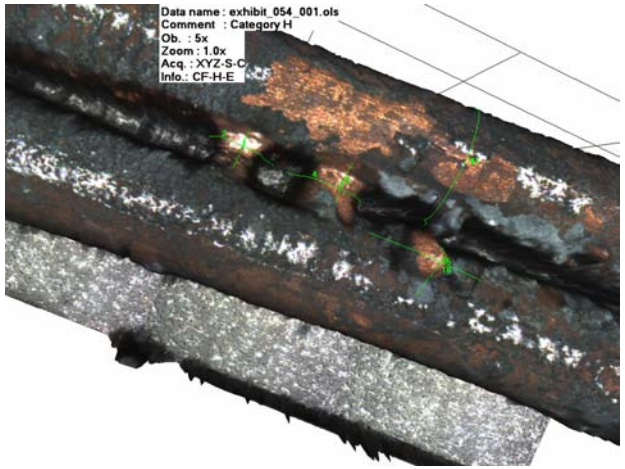

Figure 359 - LEXT image captured while zooming into the 3-D scan in the software.

Category A – arcing through insulation char. This LEXT scan comprised of 18 separate scans that were automatically stitched together in the LEXT software package.

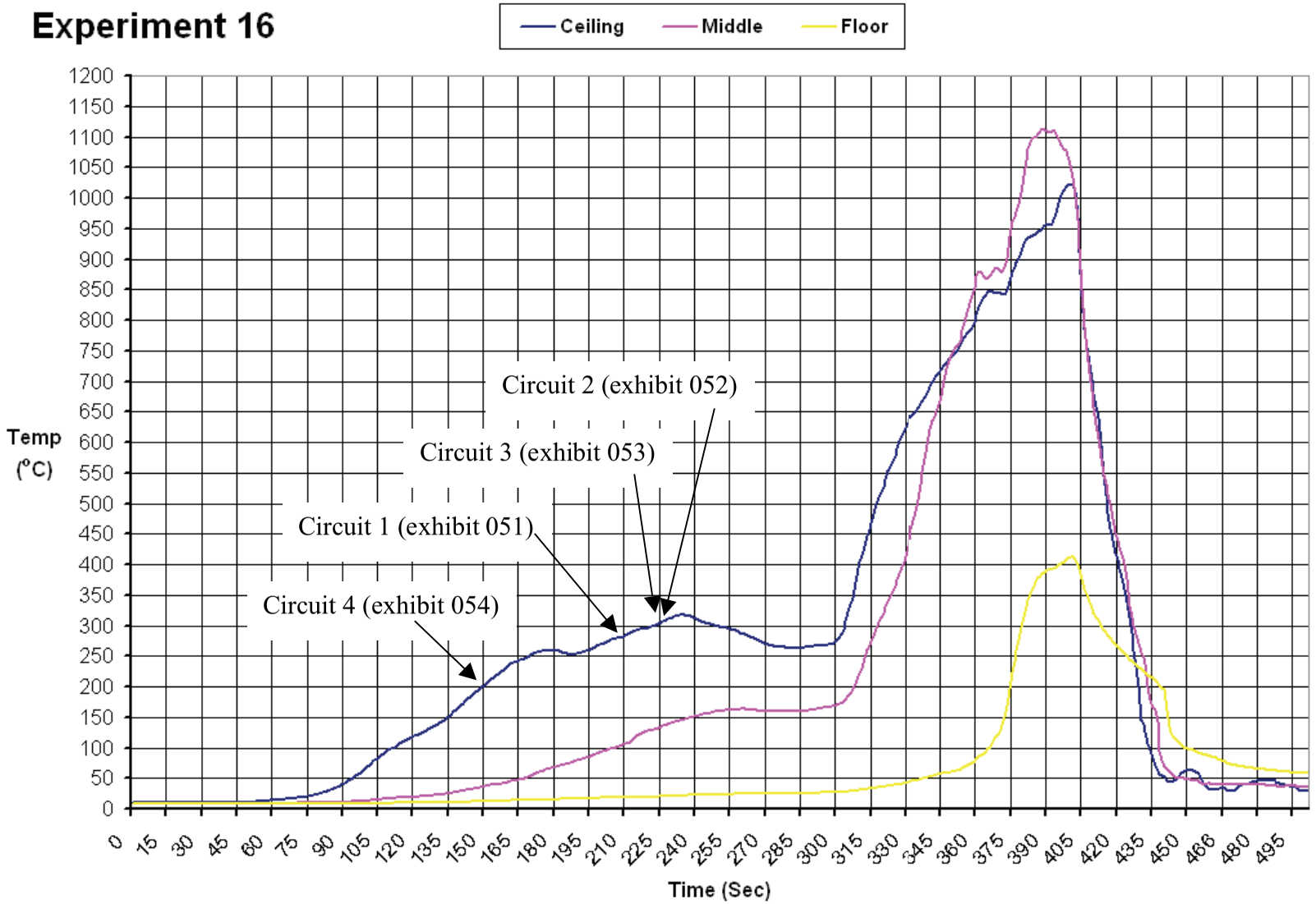

Figure 360 - Time temperature graph for experiment 16

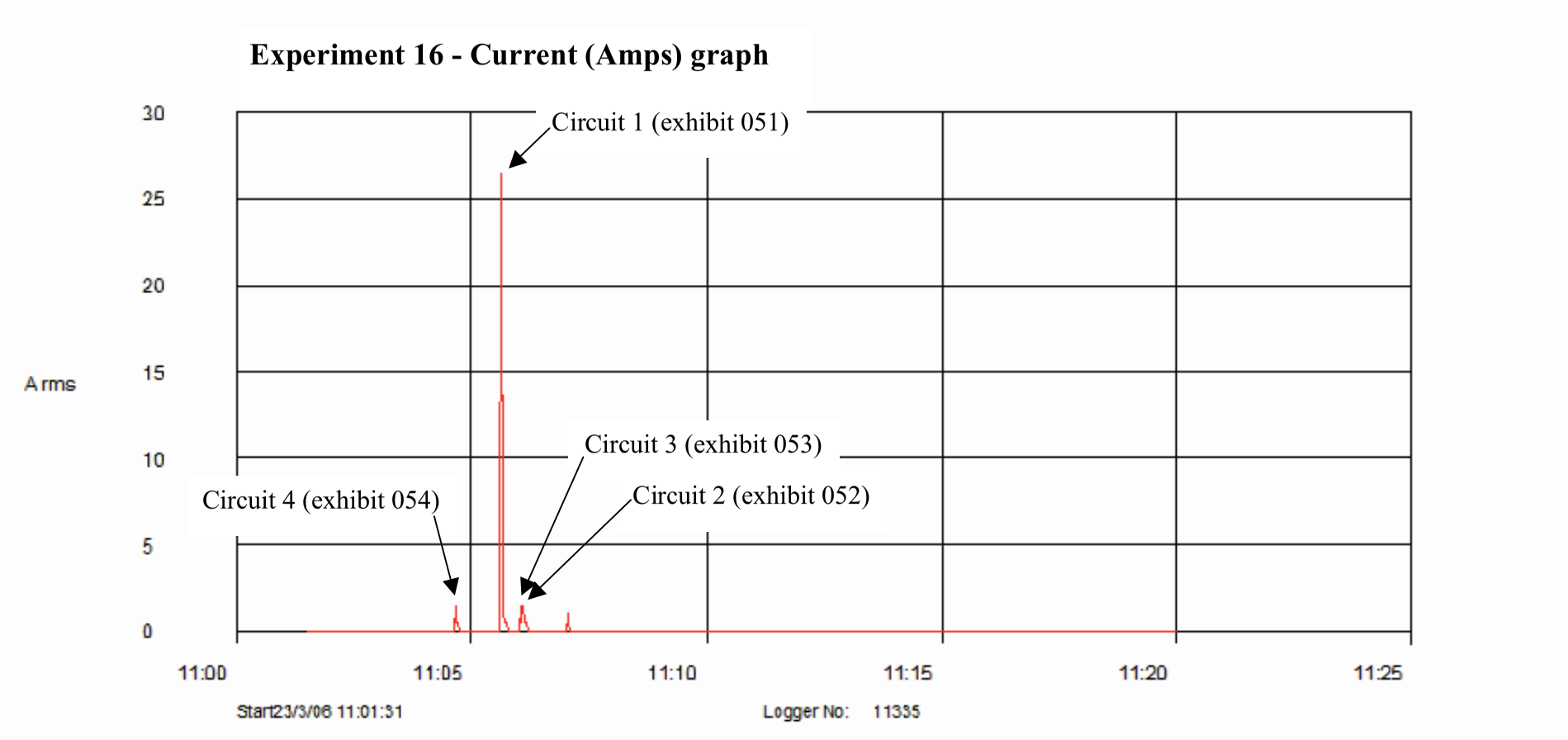

Figure 361 - Current (Amps) graph for experiment 16 detailing the operation of the circuit breakers and the fault current

Experiment 17

Figure 362 – “Scenario B” 23 March 2006

Circuit number	MCB operating time from ignition
4	2:08 minutes
1	2:20 minutes
2	2:31 minutes
3	2:31 minutes

Table 19 – circuit breaker operation data

The fire in experiment 17 (scenario B) originated in a clothes rail that was 700mm wide and 400mm deep. The rail was located adjacent to the rear wall. The centre of the clothes rail was 1800mm from the left wall.

The fire developed rapidly with the ceiling, middle and floor temperatures peaking at 4 minutes. The ceiling temperature reached 800° C and the floor temperature was recorded at a peak of 600° C. The fire was at flashover conditions at this point.

Arcing damage was located on circuit 1 – 1830mm from the left wall and some odd marks also recovered 2.2m from the left wall.

Arcing damage was located on circuit 2 – 1360mm from the left wall and 1000mm from the front wall at the ceiling level.

Arcing damage was located on circuit 3 – 1360mm from the left wall (same location as circuit 2) and 2630mm from the left wall. The faulting to circuits 2 and 3 are in the same location indicating that they have faulted between the two circuits.

Arcing damage was located on circuit 4 in two locations – 1800 and 2400mm from the left wall (600mm distance between the two arcing locations). Both were 1000mm from the rear wall.

Pre-fire and post-fire photographs of experiment 17

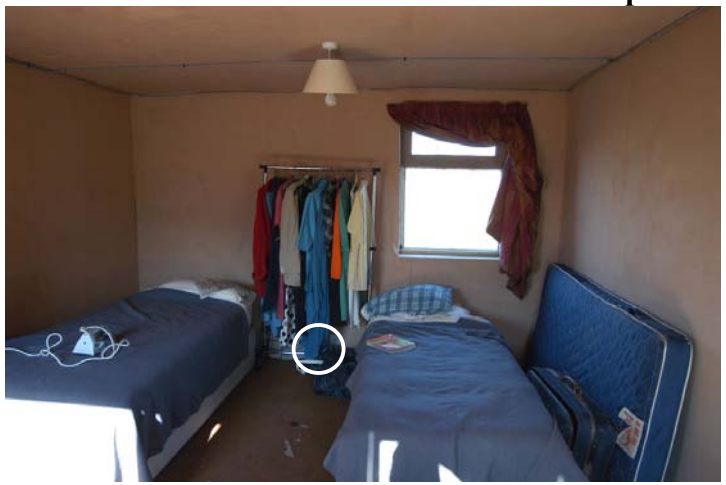

Figure 363 - Pre-fire photograph of experiment 17. The area of origin is indicated by the white circle

Figure 364 - Pre-fire photograph taken from the back wall of the compartment detailing the wiring.

Figure 365 - Post-fire photograph with a white circle indicating the area of origin. Te left arrow is the arcing damage to circuit 1. The middle and right arrows are the arcing damage to circuit 4.

Figure 366 - Post-fire photograph the ceiling area of the front of the compartment. This details circuits 1 (wall edge), 2 and 3 (routed across the ceiling).

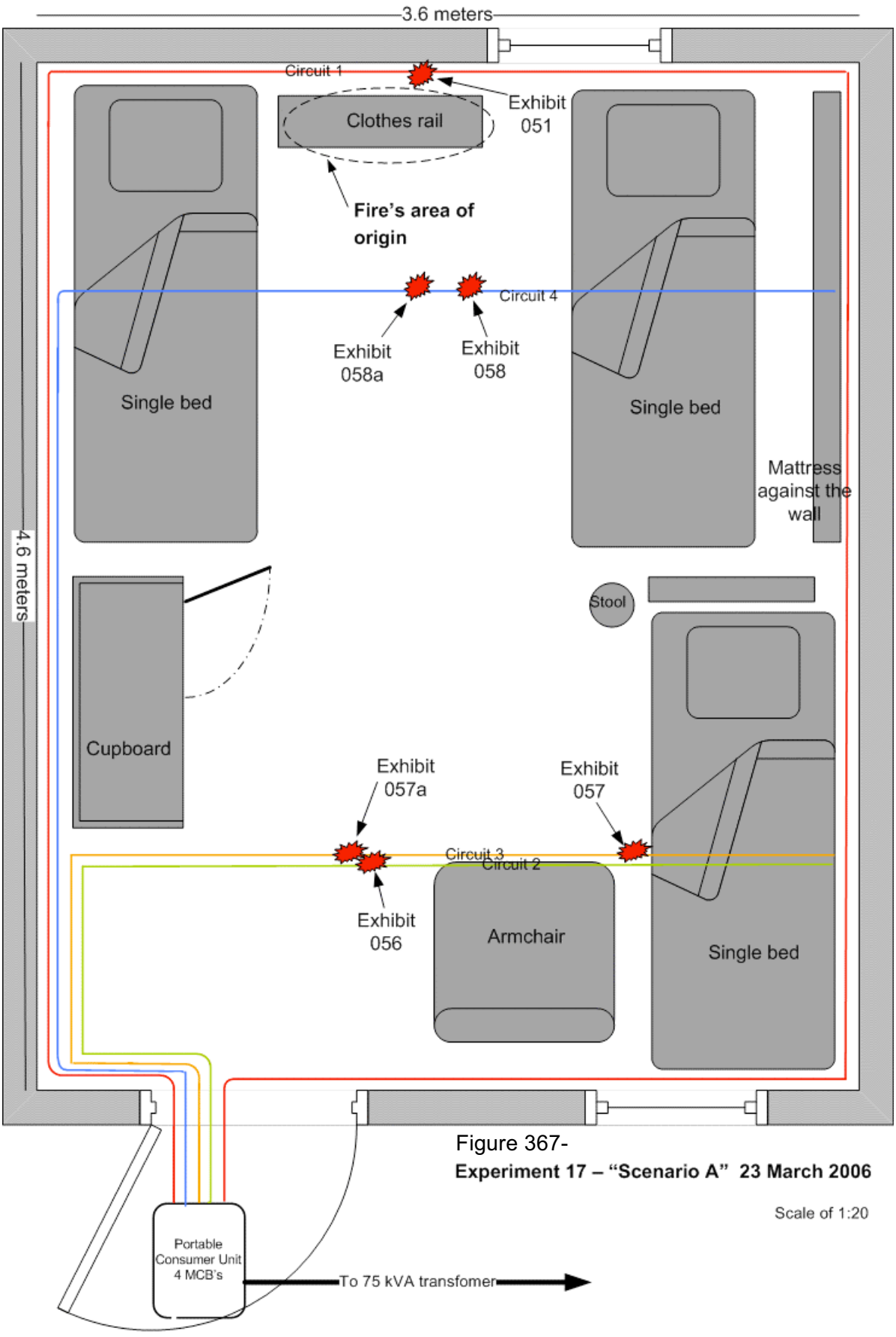

Figure 367-
Experiment 17 – "Scenario A" 23 March 2006

Scale of 1:20

Microscope and SEM images for exhibit 055 - Arcing category H (experiment 17)

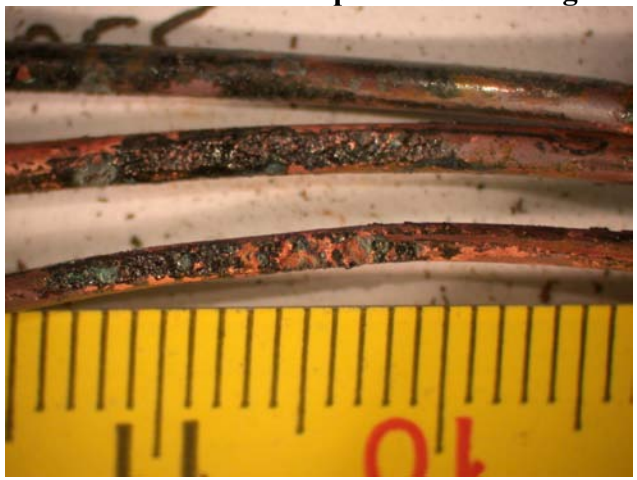

Figure 368 - Microscope image of exhibit 55 – arcing through charred insulation. The scale is in millimetres. The surface of the conductor affected with arcing is similar to glass paper.

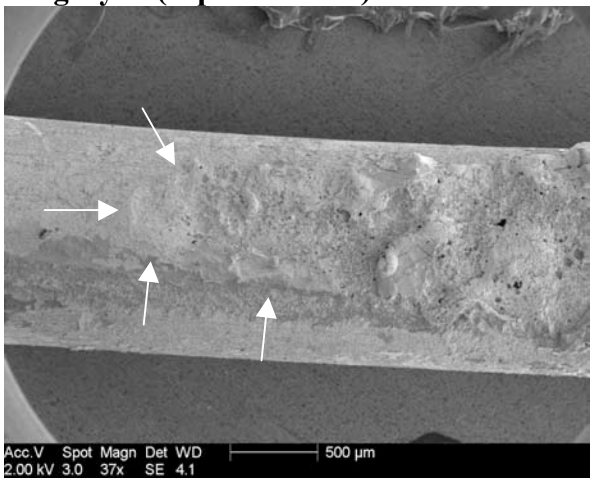

Figure 369 - SEM image of the left side of the bottom conductor. Detailing the demarcation between the arcing damaged surface and the undamaged metallic surface.

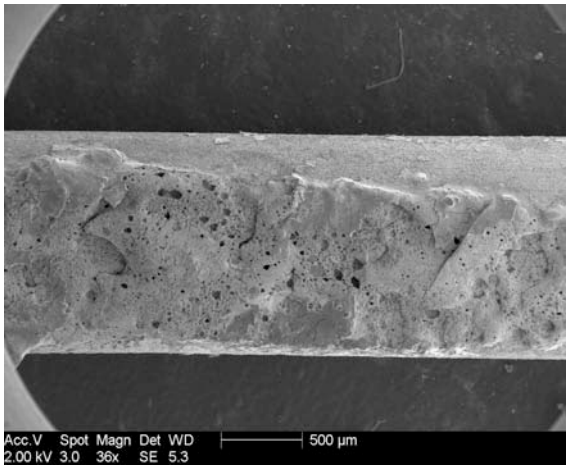

Figure 370 - SEM image detailing the central area of the arcing damage to the bottom conductor.

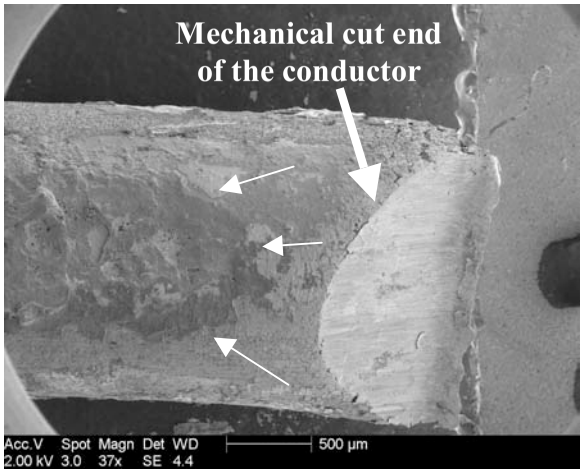

Figure 371 - SEM image of the right edge of the arcing damage to the top conductor. A mechanical cut edge of the conductor is also detailed with this image.

Confocal laser scanning microscope images of exhibit 055 – arcing category A (experiment 17)

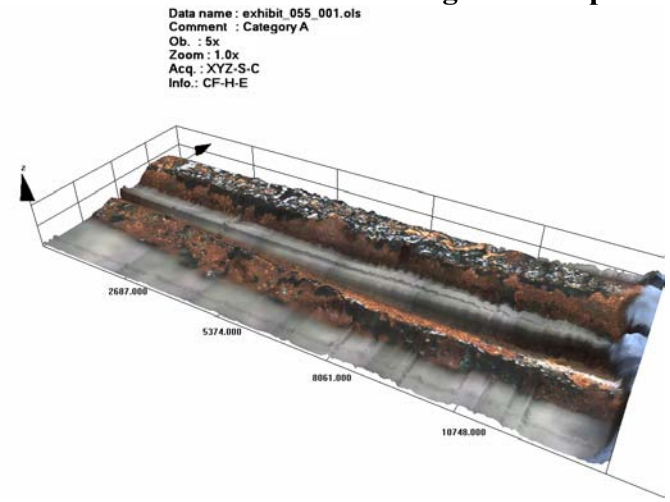

Figure 372 - LEXT image of exhibit 055. The depth of this scan was limited due to the category. The silver/grey effect is due to the limited scan depth.

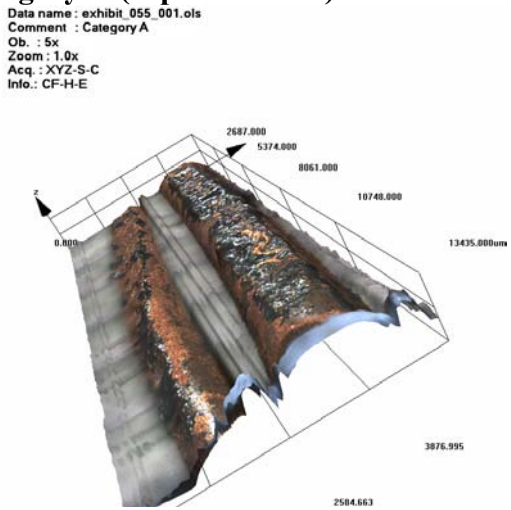

Figure 373 - LEXT image of an end profile detailing the shallow depth of the scans forming this image.

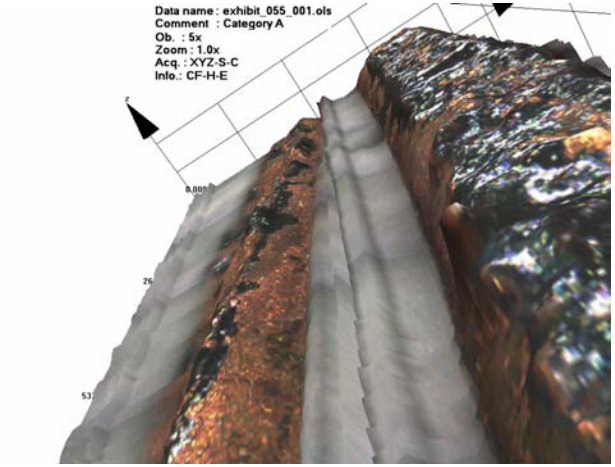

Figure 374 - LEXT image capture of a close-up view in the software, highlighting the surface detail of the conductor damage.

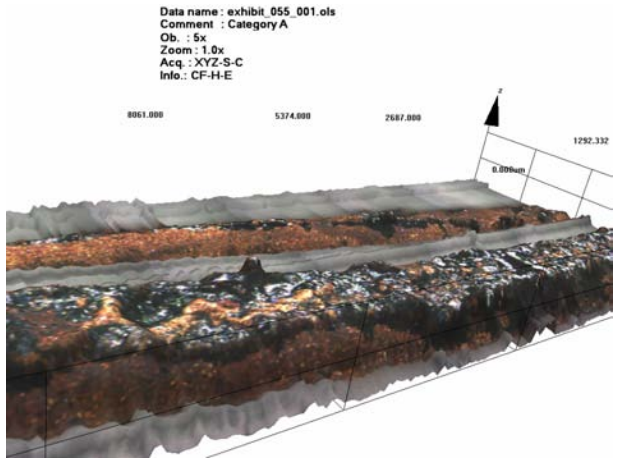

Figure 375 - LEXT image capture of a close-up view in the software. See figure 376 for a full-size image.

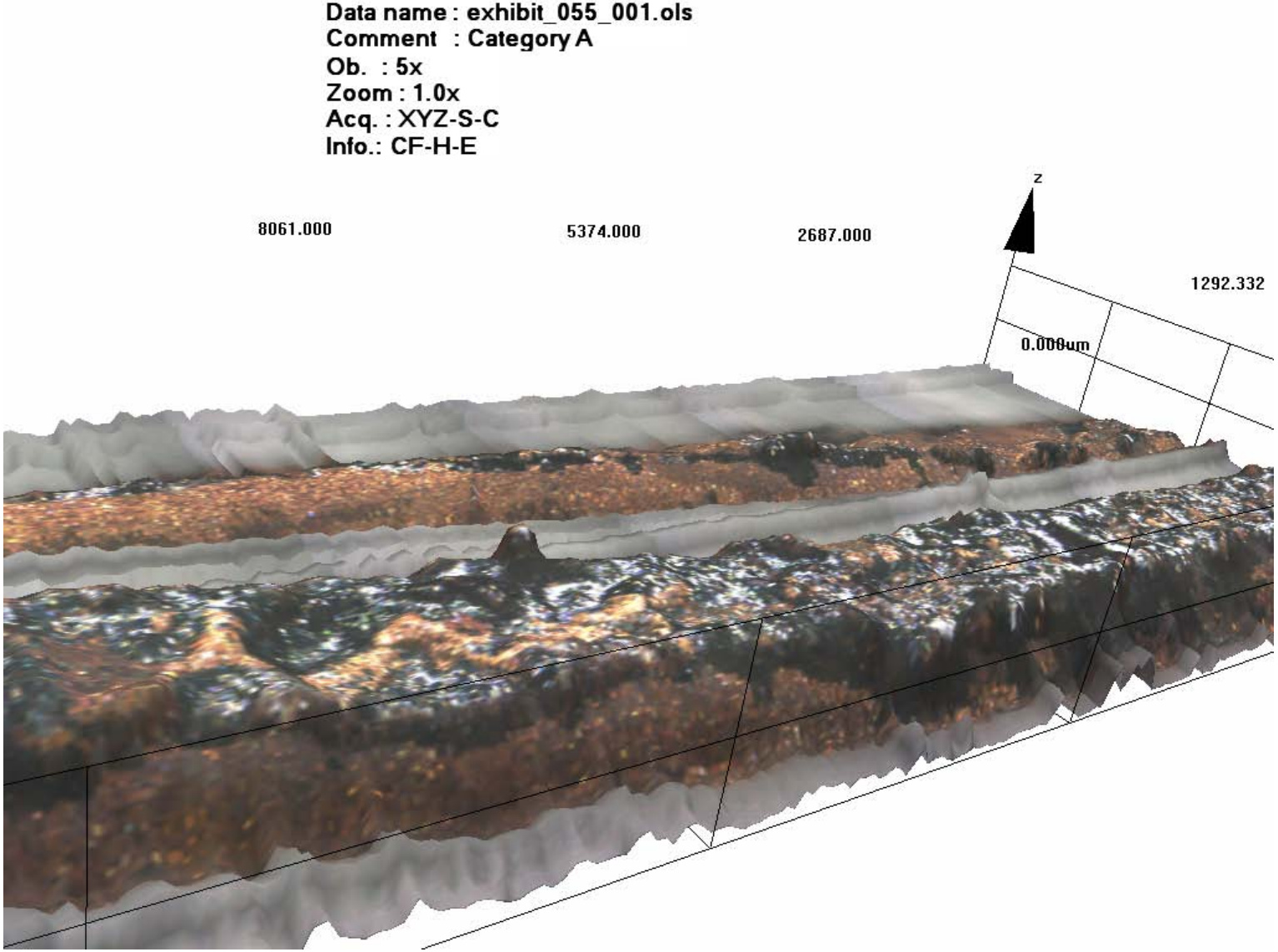

Figure 376 - A full-size view of figure 375 (exhibit 055)

Microscope and SEM images for exhibit 056 - arcing category C (experiment 17)

Figure 377 – A microscope image of exhibit 56. The arcing damage is limited to the top conductor.

Figure 378 - A notch on one conductor with a bead to the side.

Figure 379 – 40x magnification of the bead at the side of the notch. The depth of field limitations with an optical microscope render the notched area is out of focus.

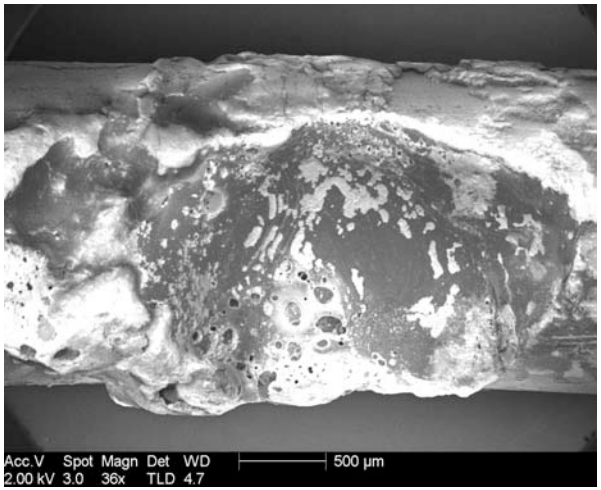

Figure 380 - SEM image detailing the notch area. The entire image is in focus, a major advantage when comparing optical and SEM microscopes for this type of analysis.

Confocal laser scanning microscope images of exhibit 056 – arcing category C (experiment 17)

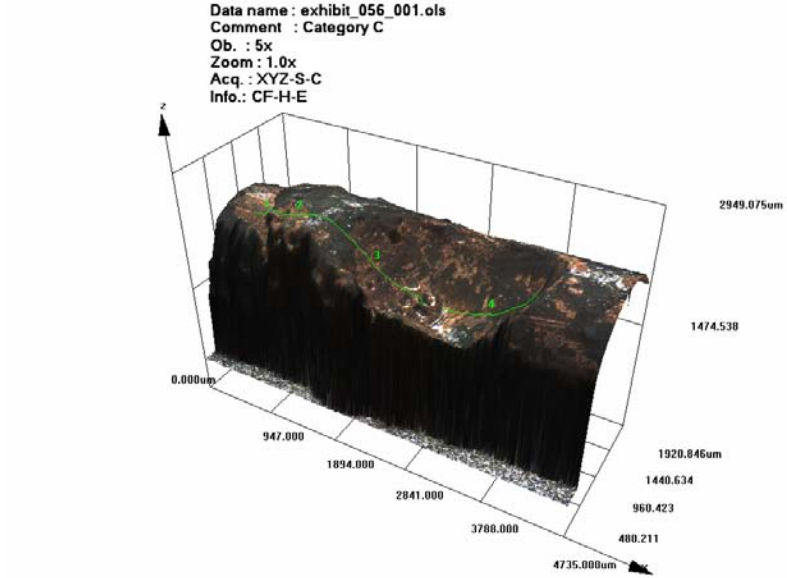

Figure 381 - LEXT image of exhibit 056.

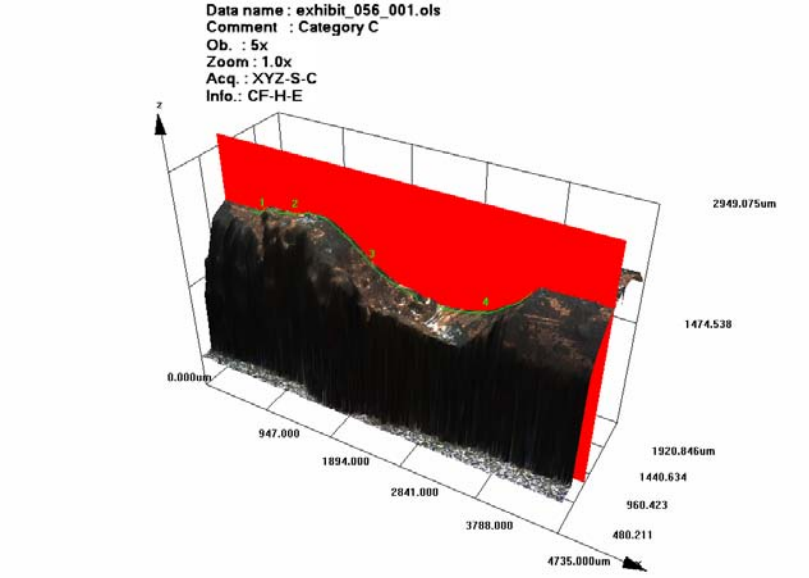

Figure 382 - LEXT image detailing the profile slice tool used in the software to obtain the measurements in table 20.

Table 20 Measurement data

#		Width	Height	Length	Angle	Upper	Lower
1		245.313	121.005	273.534	26.256	450.779	4282.76
2		624.853	92.250	631.626	8.398	1309.41	10102.3
3		1295.99	705.510	1475.58	28.563	14367.6	35339.4
4		1032.16	537.255	1163.61	27.498	0.000	121194.

Microscope images for exhibit 057 - arcing category C, and exhibit 057a arcing category F (experiment 17)

Figure 383 - Microscope image of exhibit 57. This was furthest from the electrical source and closer to the origin of the fire than exhibit 57a (below). This metallic damage did not operate the circuit breaker

Figure 384 - 20x magnification of the exhibit detailing the bead on one conductor and the notch on the other conductor.

Figure 385 - Microscope image of exhibit 57a on circuit 3. This arcing event operated the circuit breaker. This is the second area of arcing on the same circuit

Figure 386 – 20x magnification of figure 385. This exhibit may be linked to exhibit 056 as they were adjacent to each other and the circuit breakers for both circuits operated almost simultaneously

Microscope images for exhibit 058 - arcing category E (experiment 17)

Figure 387 - Microscope image of exhibit 058 with a notch on two adjacent conductors. Circuit 4 was subject of two separate areas of arcing damage and this was the first arcing event - furthest area from the electrical source.

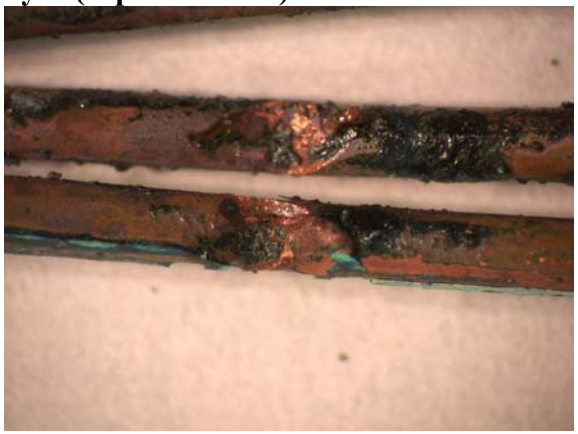

Figure 388 – 15x magnification of the two adjacent notches.

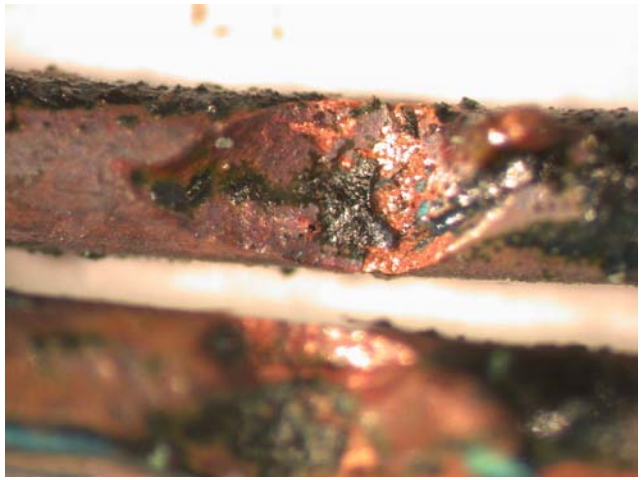

Figure 389 - Microscope image of the top notch at 40x magnification. The bottom notch is out of focus due to the limited field of view.

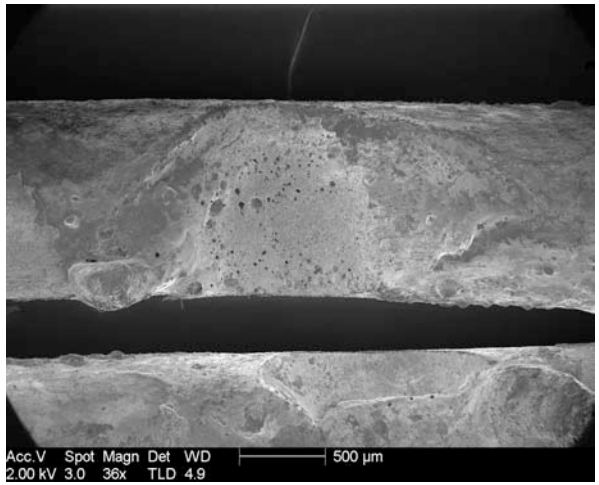

Figure 390 - SEM image detailing both notches. The notch edges show a clear demarcation.

Microscope and SEM images for exhibit 058A - arcing category H (experiment 17)

Figure 391 - Microscope image of exhibit 58A. This was the second area of arcing on the same circuit (No 4) that operated the circuit breaker.

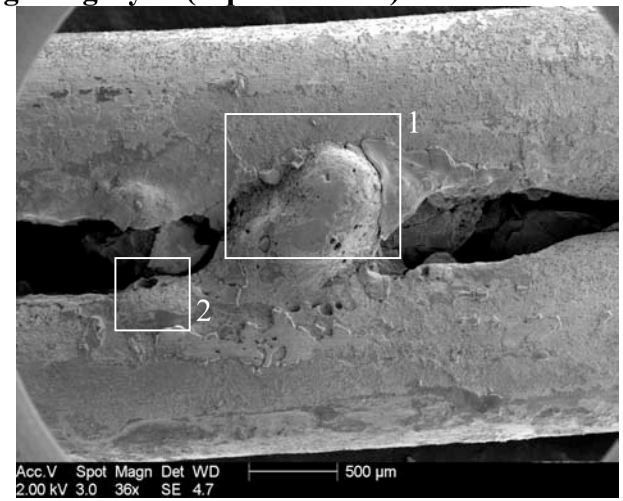

Figure 392 - SEM image of exhibit 58A. Higher magnified SEM images of areas 1 and 2 are detailed in figures 393 & 394 below.

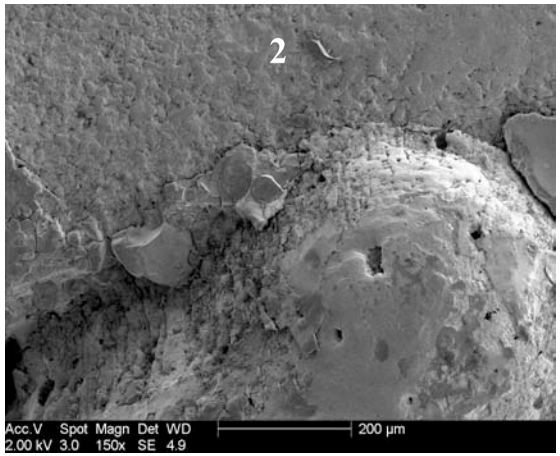

Figure 393 - SEM image at 150x magnification. This is a close-up of area 2 indicated by the square in figure 392.

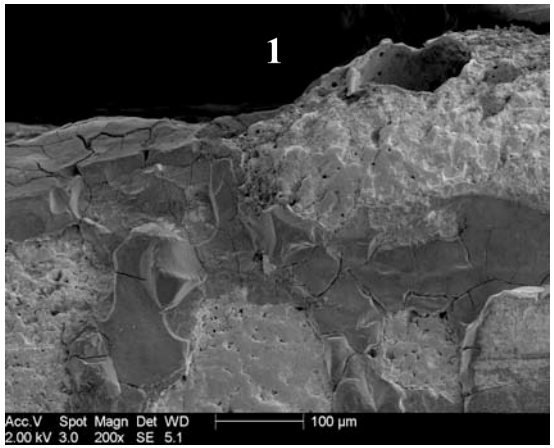

Figure 394 - SEM image at 200x magnification detailing the small bead on the lower conductor adjacent to the welded area.

Confocal laser scanning microscope images of exhibit 058 (arcing category E) and 58a (arcing category H) experiment 17

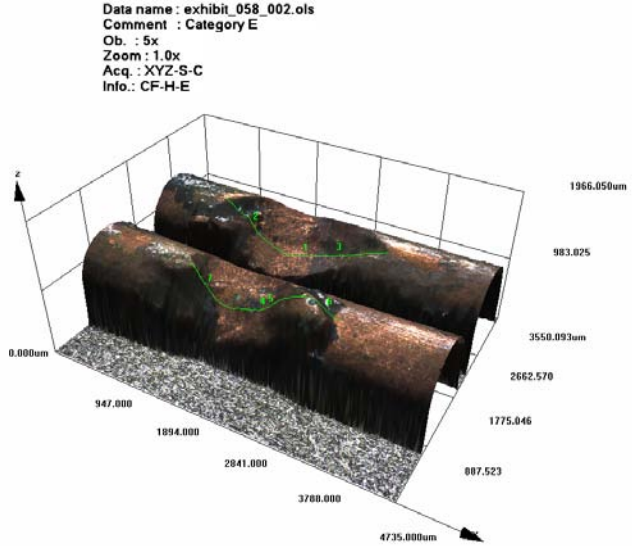

Figure 395 - LEXT image of exhibit 058 detailing the entire exhibit.

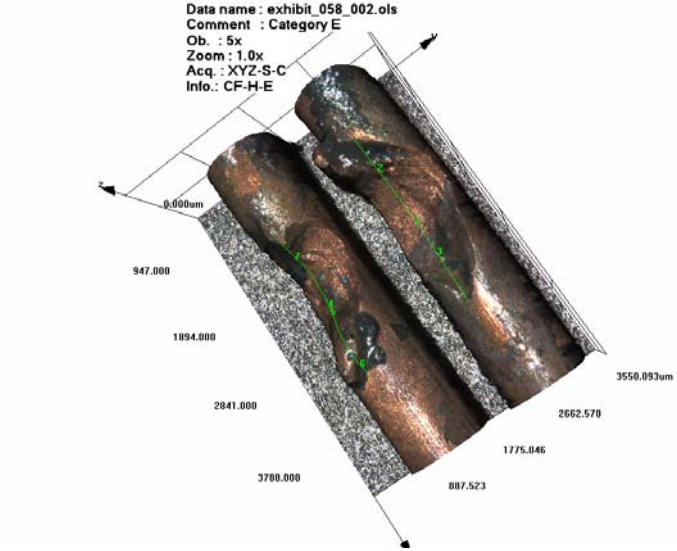

Figure 396 - LEXT image of exhibit 058 orientated in the software package.

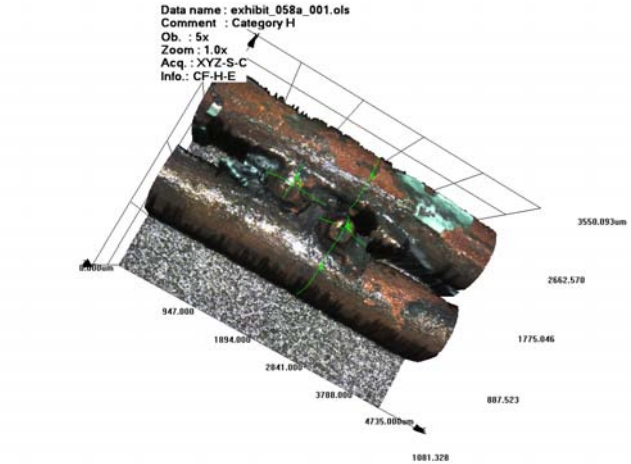

Figure 397 – Image captured in the LEXT software package.

Figure 398 – LEXT image captured during the orientation.

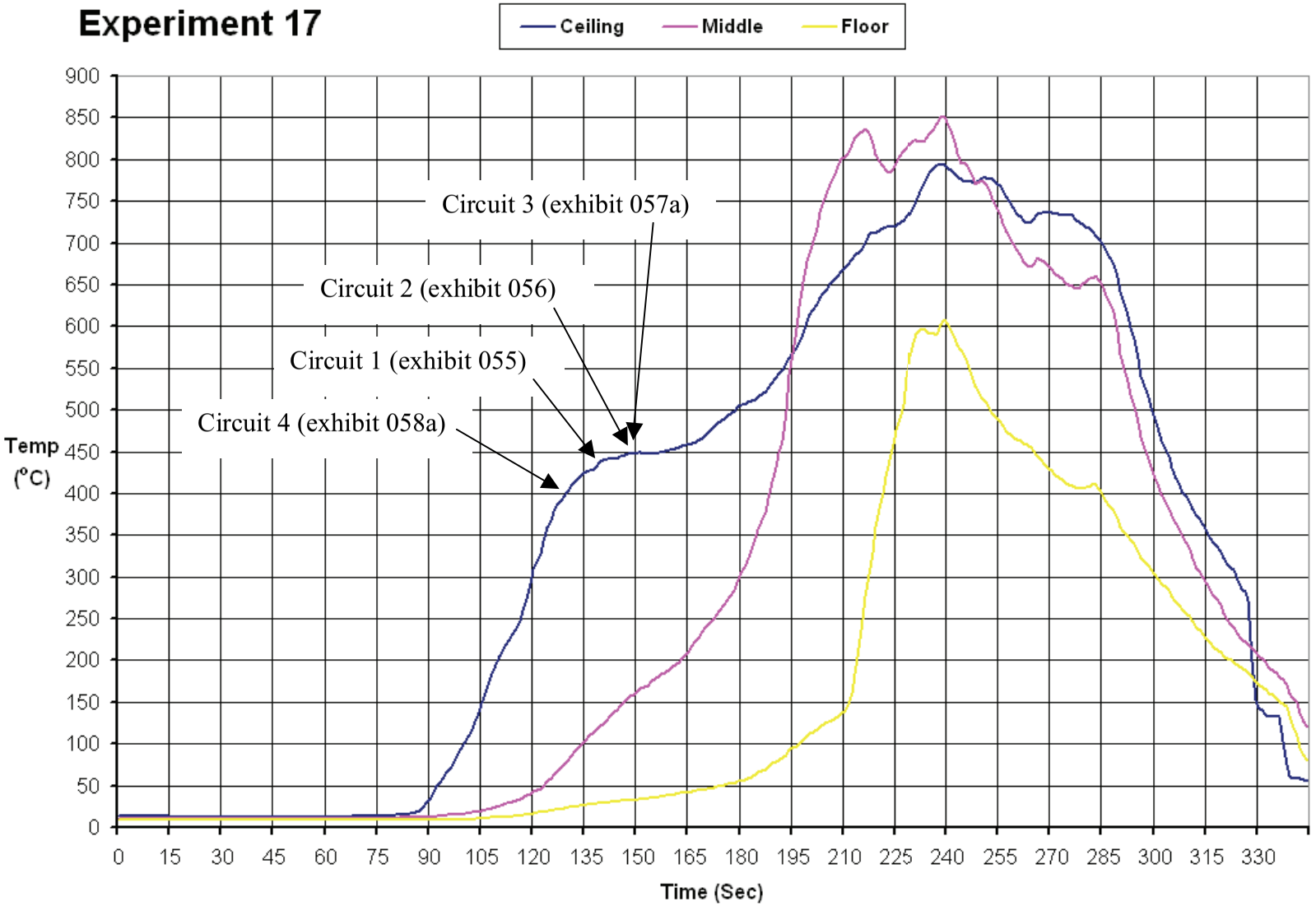

Figure 399 - Time temperature graph for experiment 17

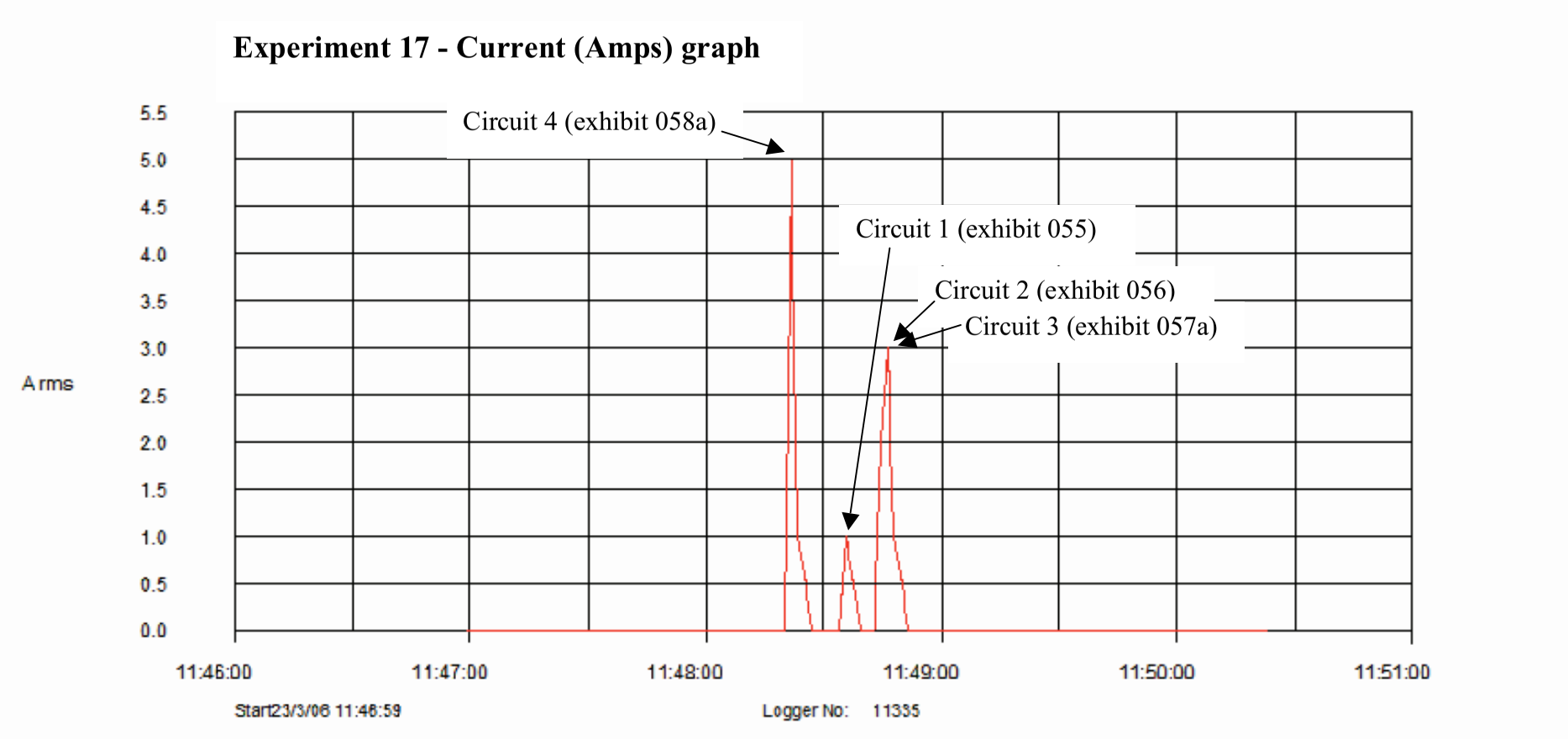

Figure 400 - Current (Amps) graph for experiment 17 detailing the operation of the circuit breakers and the fault current

Experiment 18

Figure 401 – “Scenario D” 23 March 2006

Circuit number	MCB operating time from ignition
4	0:54 minutes
1	1:03 minutes
2	1:11 minutes
3	1:16 minutes

Table 21 – circuit breaker operation data

The fire in experiment 18 (scenario D) originated in three separate areas at the rear of the compartment. They encompassed a total area of 2.2m wide and 1.2m deep (when linked together into one area). The dominant fire plume was from the right side of the three-seat settee.

Arcing damage was located on circuit 1 - adjacent to the left wall and 1450mm from the rear wall at ceiling level.

Arcing damage was located on circuits 2 and 3 – 860mm from the left wall and 1000mm from the front wall at the ceiling level (3.56m from the rear wall). The arcing occurred close to a fixing screw for both of the circuits. The ceiling height is 2.27 meters.

Arcing damage was located on circuit 4 in two separate areas – 850mm from the left wall and 1400mm from the left wall. Both points are 1000mm from the rear wall.

Pre-fire and post fire photographs of experiment 18

Figure 402 - Pre-fire photograph of experiment 18. The three areas of origin for this fire are detailed with black ovals.

Figure 403 - A photograph showing the fire in its early development – 1 minute after the left sofa was initially ignited with a flaming torch.

Figure 404 - Post-fire photograph with white ovals indicating the three points of origin. The right arrow locates the arcing damage to circuit 4. The middle arrow indicates the second area of arcing to circuit 4, the left arrow indicates the arcing damage to circuit 1.

Figure 405 - A post-fire photograph showing the three points of origin close to the rear wall. The points of origin in order were the sofa end, the television and the upholstered stool.

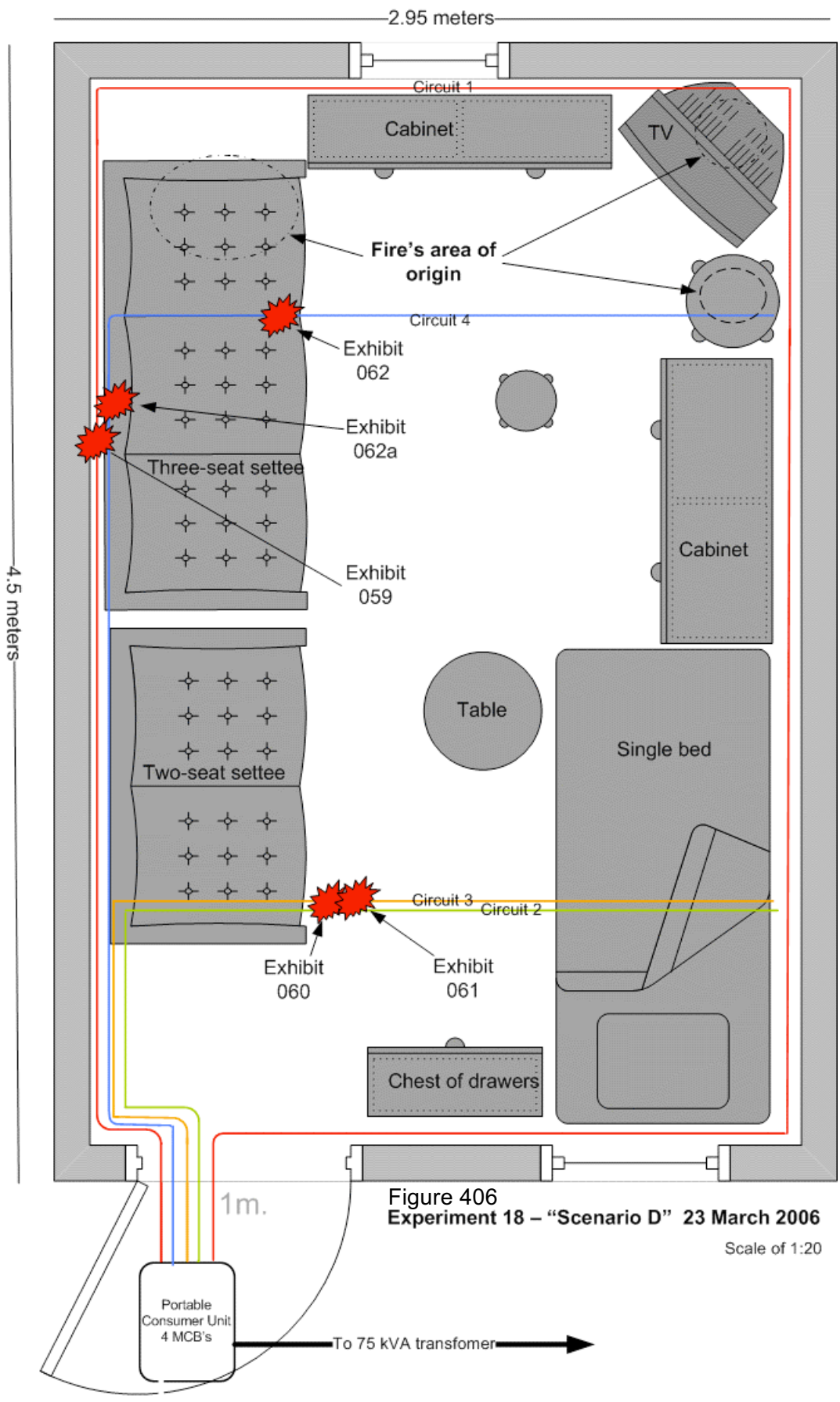

Figure 406
Experiment 18 – "Scenario D" 23 March 2006

Scale of 1:20

Microscope images for exhibit 059 - arcing category I (experiment 18)

Figure 407 - Microscope image of exhibit 059 at 6x magnification. The localised metallic damage is limited to one conductor with a surface bead.

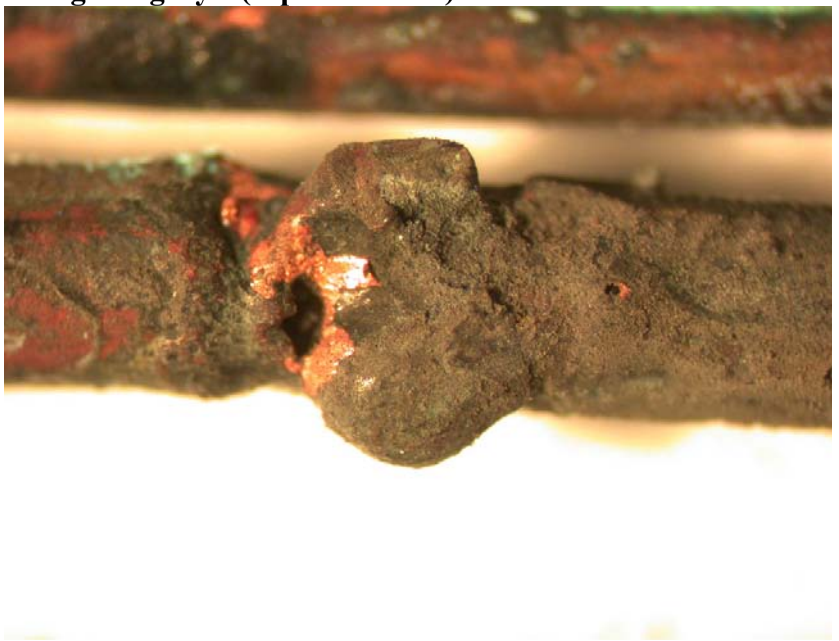

Figure 408 - Microscope image at 20x magnification of the area indicated in figure 407.

Microscope images for exhibit 060 - arcing category D (experiment 18)

Figure 409 - Microscope image of exhibit 060. The arcing damage affects one of the three conductors with a bead within a notch.

Figure 410 - Microscope image at 6x magnification of the area indicated in figure 409.

Figure 411 - Microscope image at 20x magnification of the localised melting pattern.

Microscope and SEM images for exhibit 061 - arcing category B (experiment 18)

Figure 412 - Microscope image of exhibit 061. One conductor has severed into two ends.

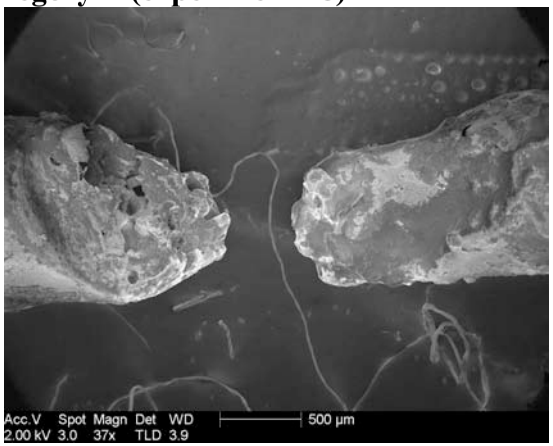

Figure 413 - SEM image detailing both of the severed ends of this conductor.

Figure 414 - SEM image at 65x magnification of the left end. The demarcation between the arcing damage and the undamaged conductor is clear in this image.

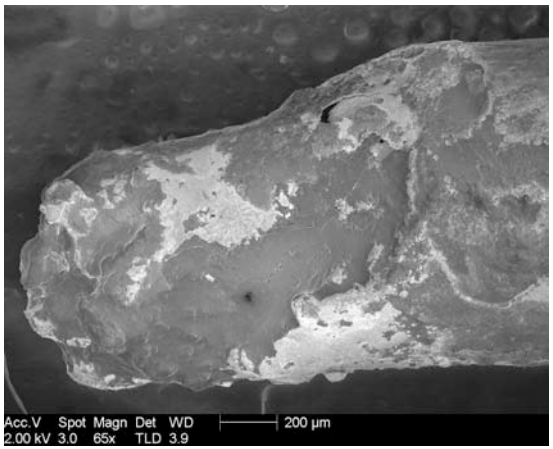

Figure 415 - SEM image of the right severed end at 65x magnification.

Microscope and SEM images for exhibit 062 - arcing category D (experiment 18)

Figure 416 - Microscope image of exhibit 062. The notch severed during packaging and the ends have been positioned together.

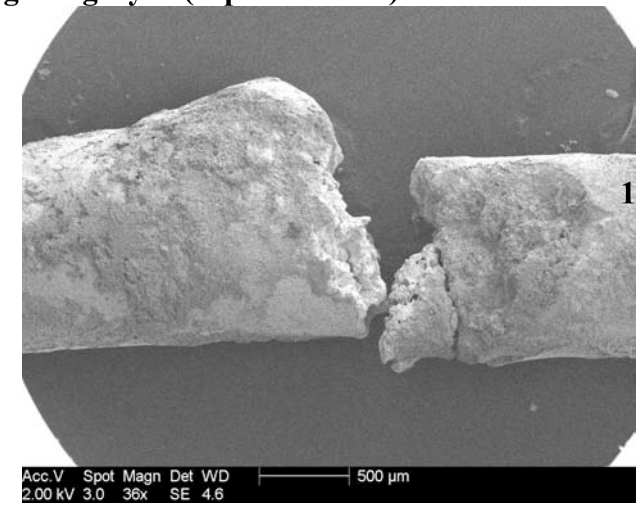

Figure 417 - SEM image of the two fractured ends. The left end has a bead at the top.

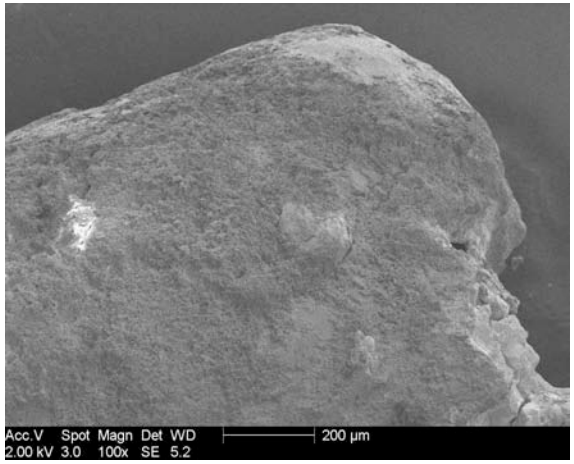

Figure 418 - SEM image at 100x magnification of the bead at the edge of the notch detailed in figure 417.

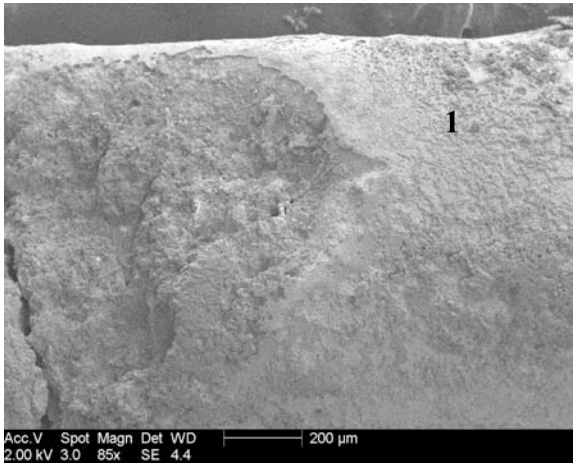

Figure 418 - The right edge of the notch indicating the demarcation of the edge of the arcing damage.

Microscope and SEM images for exhibit 062a - arcing category B (experiment 18)

Figure 420 - A microscope image of exhibit 062a, the second area of arcing on circuit 4. This event operated the circuit breaker.

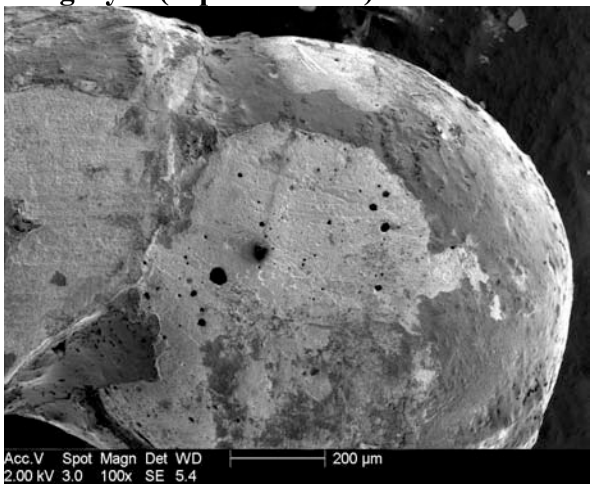

Figure 421 - SEM image of the right severed end detailed in figure 420 with a large bead.

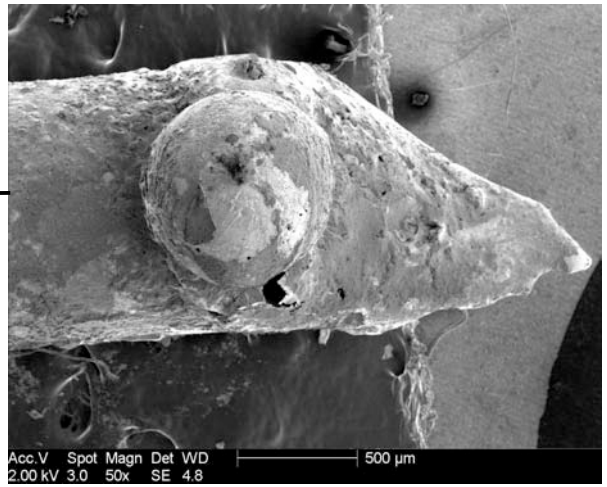

Figure 422 - SEM image of the notched severed end with a surface bead on the side on the conductor.

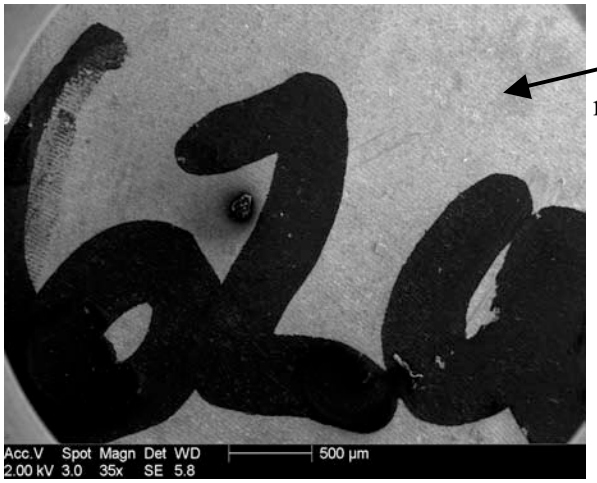

Figure 423 - Components in the marker ink used on the SEM mounting stub was unusually visible on the SEM scan.

Confocal laser scanning microscope images of exhibit 062 (arcing category D) and 62a (arcing category B) experiment 18

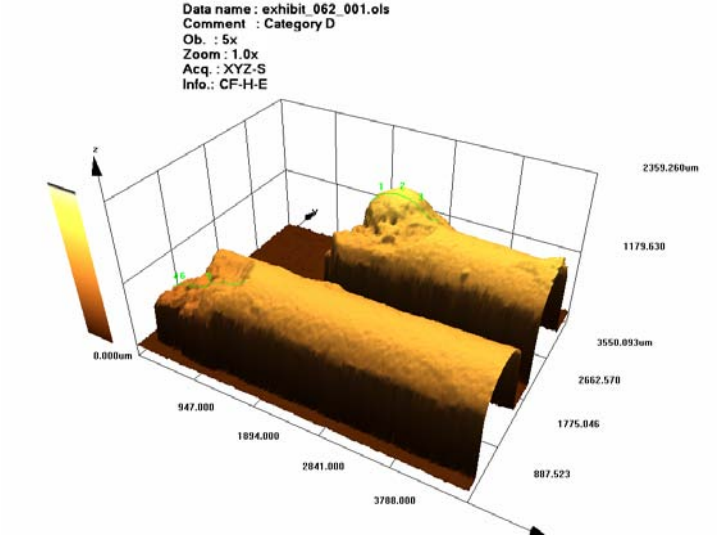

Figure 424 - LEXT image of exhibit 062 using the brown colour rendering.

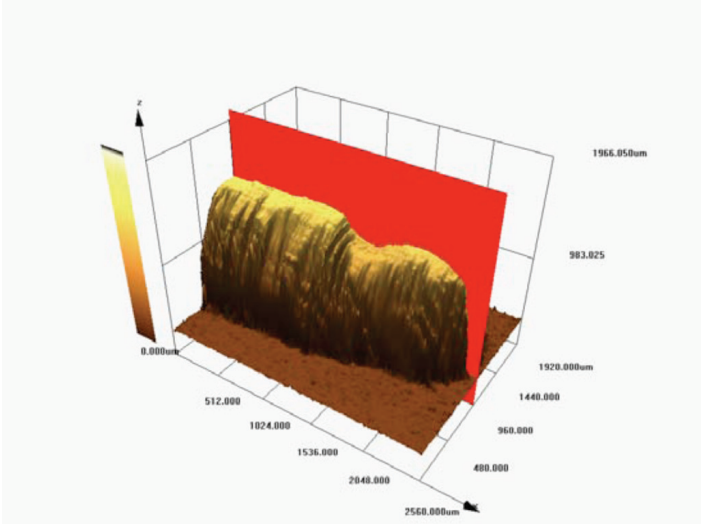

Figure 425 – The "slice tool" in use. Image source is LEXT report word document generated by the software.

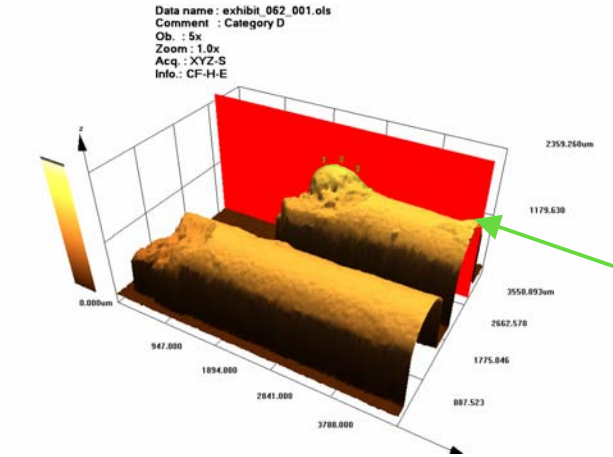

Figure 426 - LEXT image with the "slice tool" in use to create a profile.

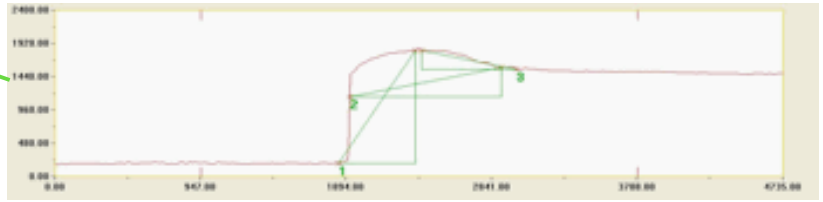

Figure 427 – A profile of the bead created with the LEXT software "slice tool" in figure 426.

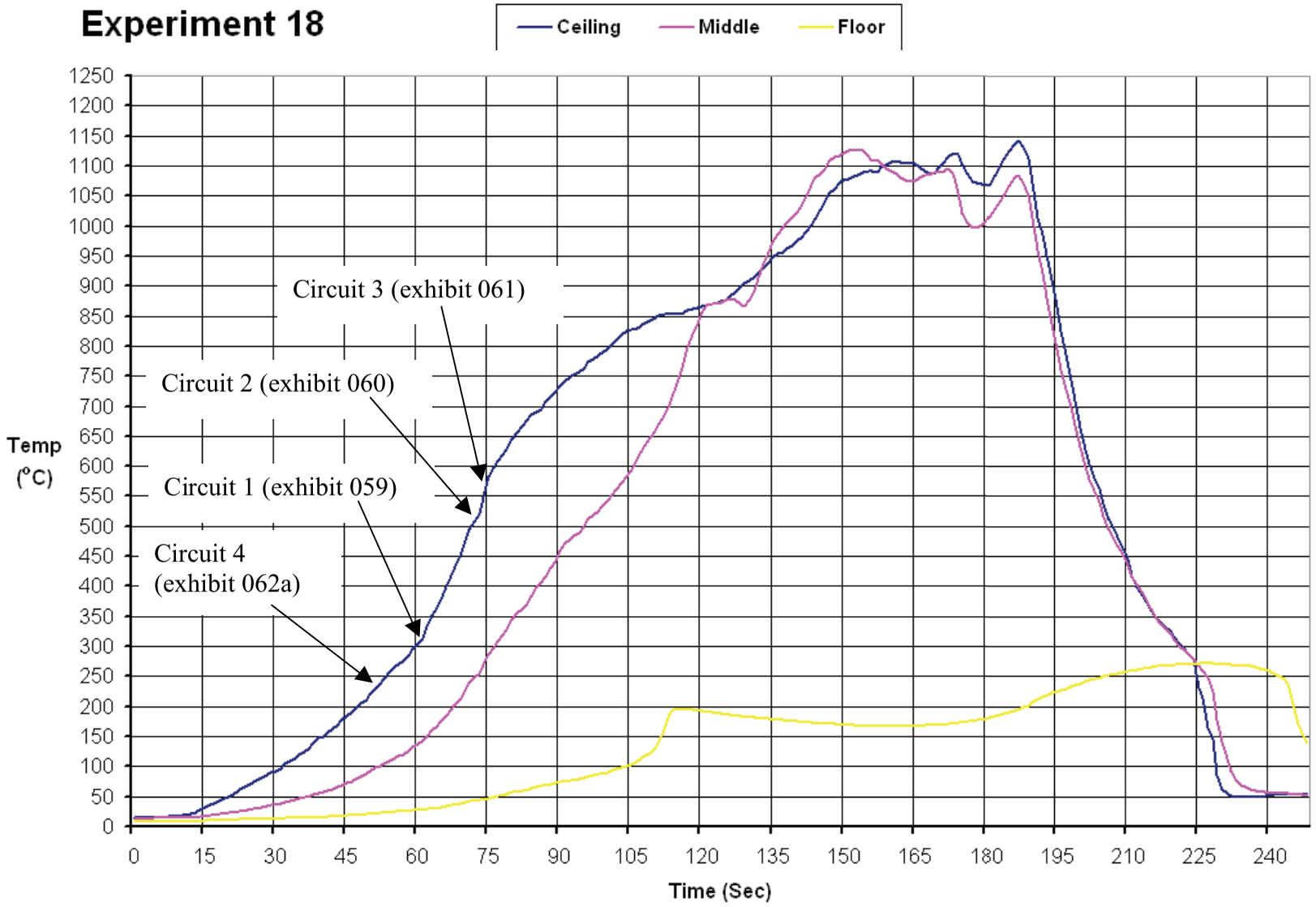

Figure 428 - Time temperature graph for experiment 18

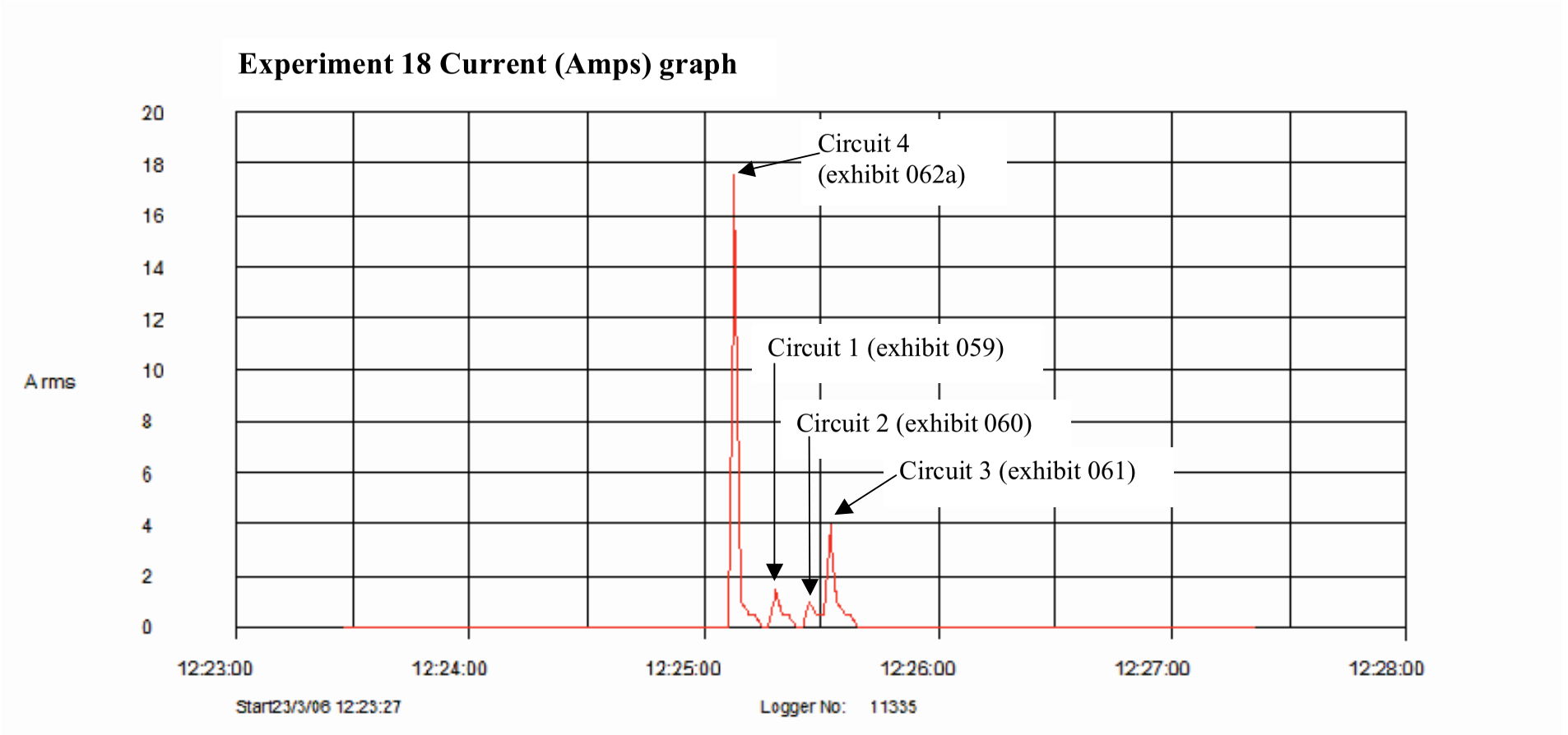

Figure 429 - Current (Amps) graph for experiment 18 detailing the operation of the circuit breakers and the fault current

Experiment 19

Figure 430 – “Scenario B” 23 March 2006

Circuit number	MCB operating time from ignition
4	4:48 minutes
1	5:22 minutes
2	5:22 minutes
3	5:22 minutes

Table 22 – circuit breaker operation data

The fire in experiment 19 (scenario B) involved a time delay where a white spirit was impregnated onto a polyurethane trail within the compartment. At 3:30 minutes (210 seconds) after the time of ignition, the fire was still confined to the trailers of polyurethane foam soaked with white spirit. The fire spread along to the trailer and spread into a wardrobe within the compartment first. The fire in the wardrobe appeared to restrict the development of the fire in the rear corners of the compartment.

Arcing damage was located on circuit 1 - no arcing damage located.

Arcing damage was located on circuit 2 – is 2120mm from the left wall and 3600mm from the rear wall.

Arcing damage was located on circuit 3 – 1650mm from the left wall and 3600mm from the rear wall.

Arcing damage was located on circuit 4 – 1000mm from the rear wall and 1880mm from the left wall.

Pre-fire and post-fire photographs of experiment 19

Figure 431 - Pre-fire photograph of experiment 19. Trails of white PU foam strips impregnated with ignitable liquid were used to start the fire. The wardrobe became the dominant fire plume in the compartment.

Figure 432 - Pre-fire photograph of the ceiling taken from the doorway. The image details the wiring installed on the ceiling.

Figure 433 - Post-fire photograph of the compartment. The white arrow indicates the dominant area of origin for this fire. Burn patterns on the right wall detailed a large “U” pattern with its base either side of the wardrobe.

Figure 434 - Post-fire photograph of the compartment with a white arrow indicating the arcing damage location on circuit 4 that was within 0.5m of the wardrobe edge.

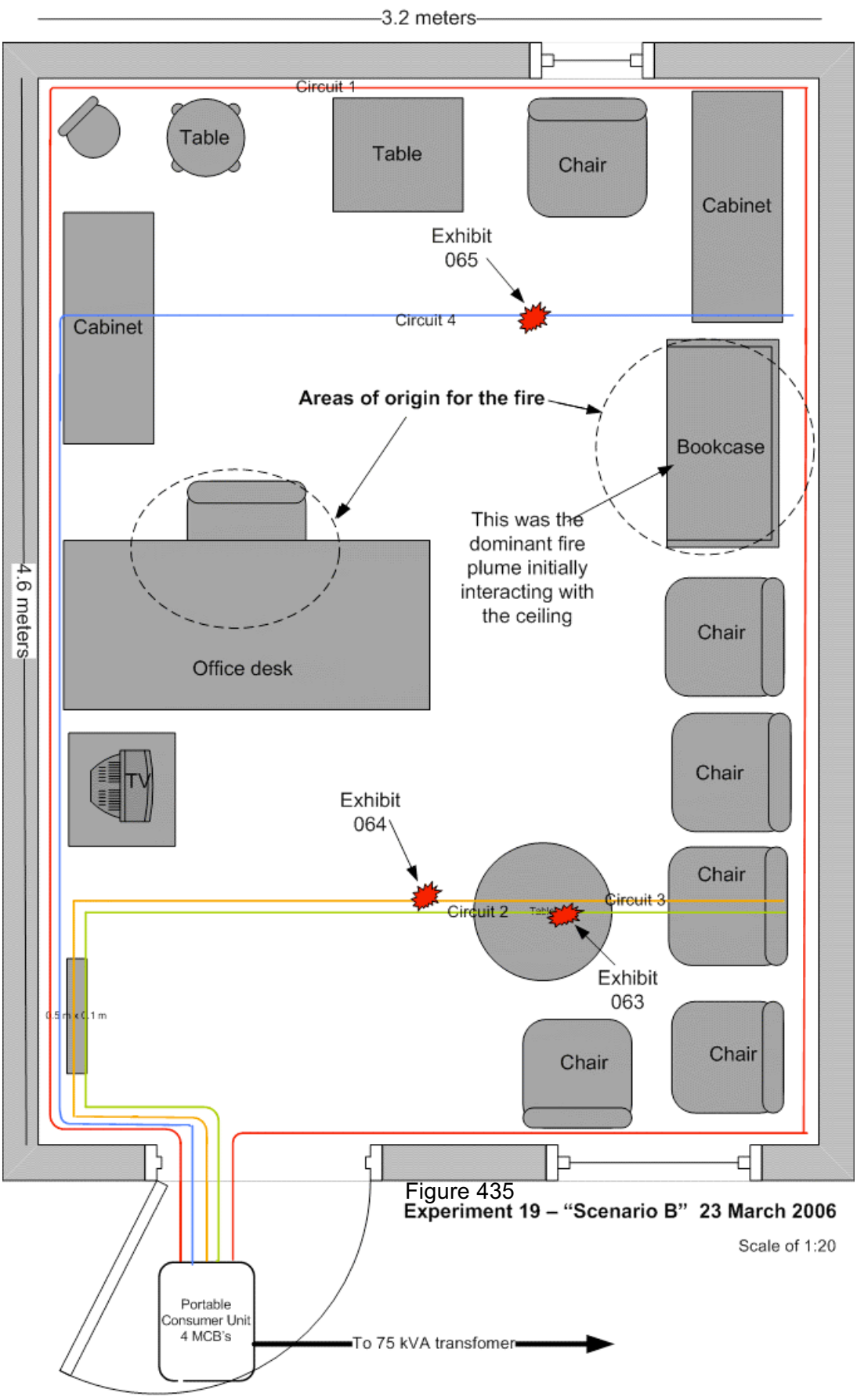

Figure 435
Experiment 19 – "Scenario B" 23 March 2006

Scale of 1:20

Microscope and SEM images for exhibit 063 - arcing category F (experiment 19)

Figure 436 - SEM image at 99x magnification detailing the demarcation area between the arcing damage and the undamaged conductor on the left edge of figure 437.

Figure 437 - Microscope image of exhibit 063. One of the three conductors had arcing damage consisting of a large notch.

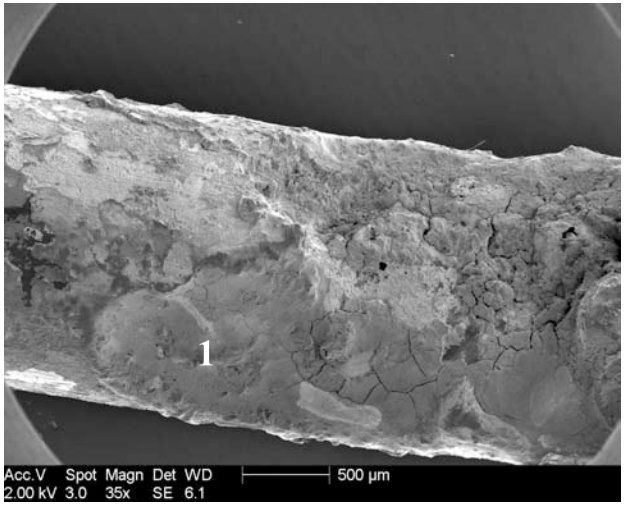

Figure 438 - SEM image of left side of the large notch in figure 437.

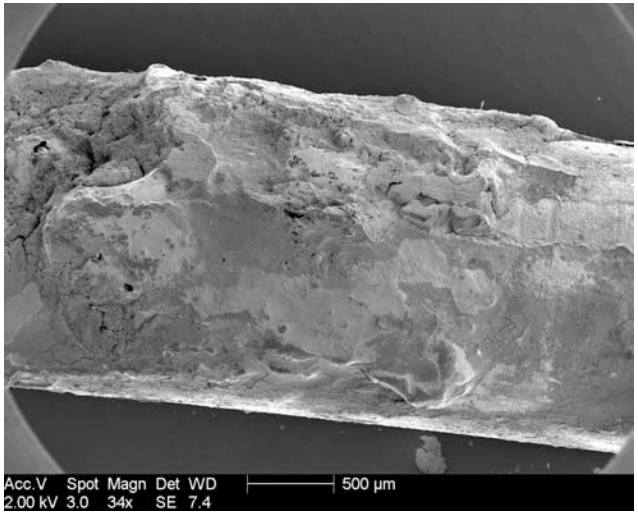

Figure 439 - Right side of the notch in figure 437.

Confocal laser scanning microscope images of exhibit 063 - arcing category F (experiment 19)

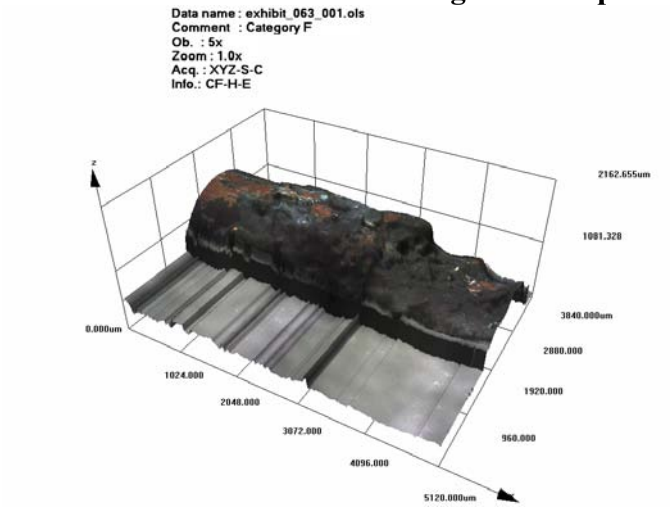

Figure 440 - LEXT image of exhibit 063.

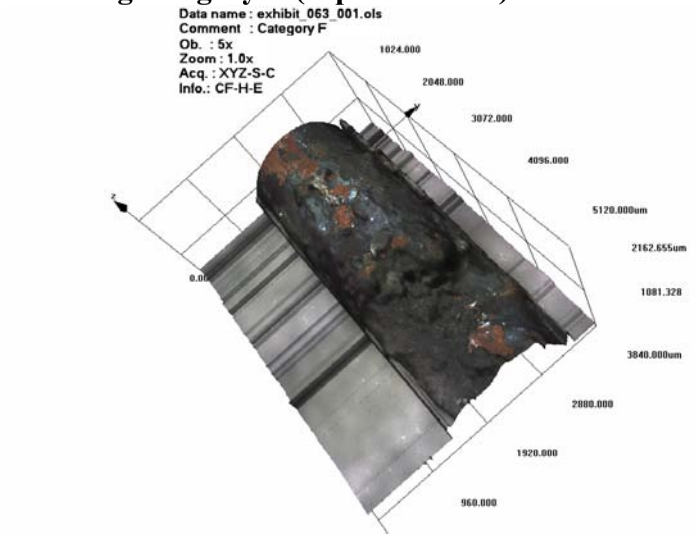

Figure 441 - LEXT image captured in the software.

The parameters of this confocal laser scanning microscope scan were incorrectly inputted during the set-up procedure of the scan. Therefore, only two-thirds of the arcing damage was scanned.

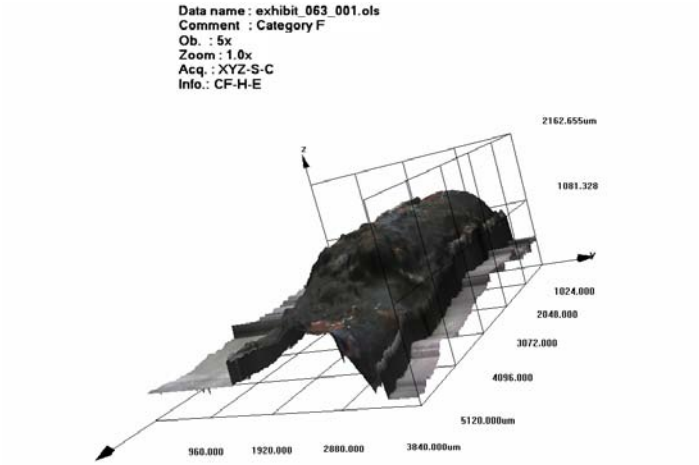

Figure 442 – Alternative view captured in the LEXT 3-D software.

Microscope and SEM images for exhibit 064 - arcing category E (experiment 19)

Figure 443 - Microscope image of exhibit 064. The top conductor is severed and there was a notch in the bottom conductor.

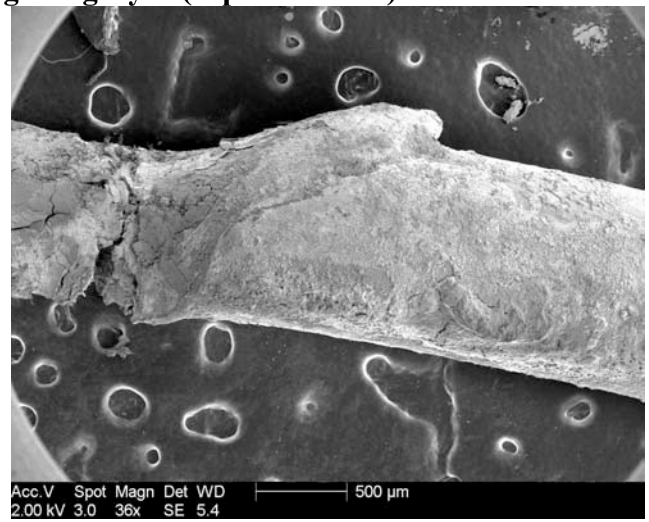

Figure 444 - SEM image of bottom conductor notch indicated in figure 443.

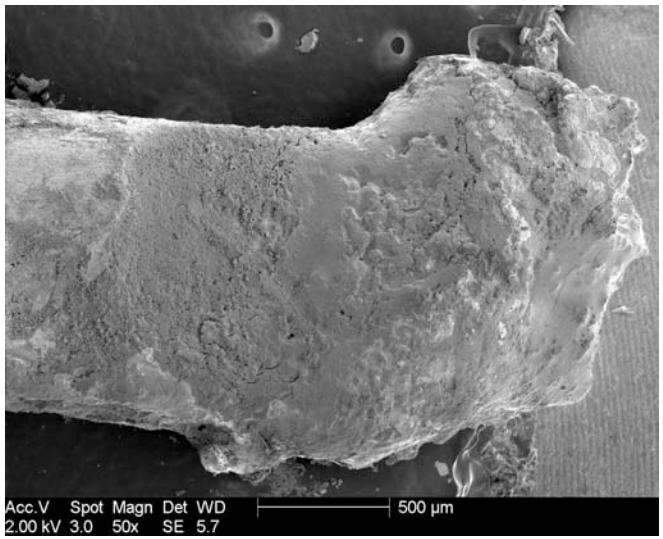

Figure 445 - SEM image of left severed end indicated in figure 443.

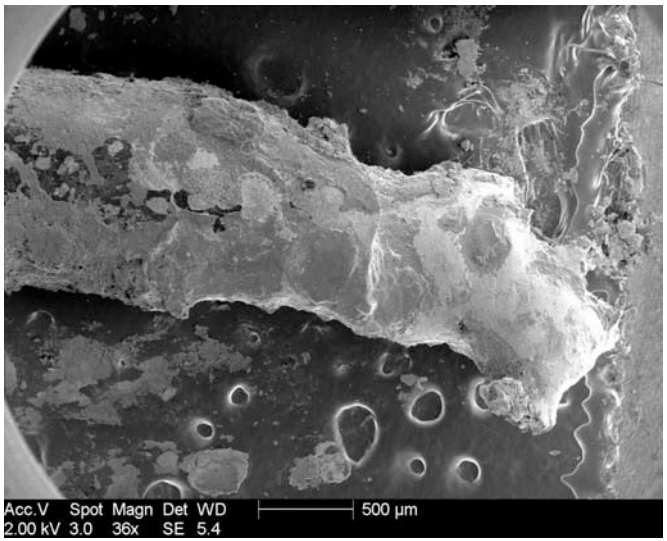

Figure 446 - SEM image of right severed end in figure 443.

Confocal laser scanning microscope images of exhibit 064 - arcing category B (experiment 19)

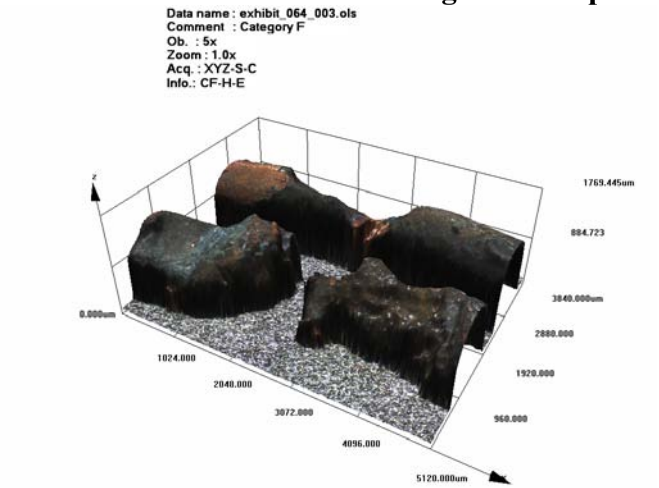

Figure 447 - LEXT image of the two conductors of exhibit 064.

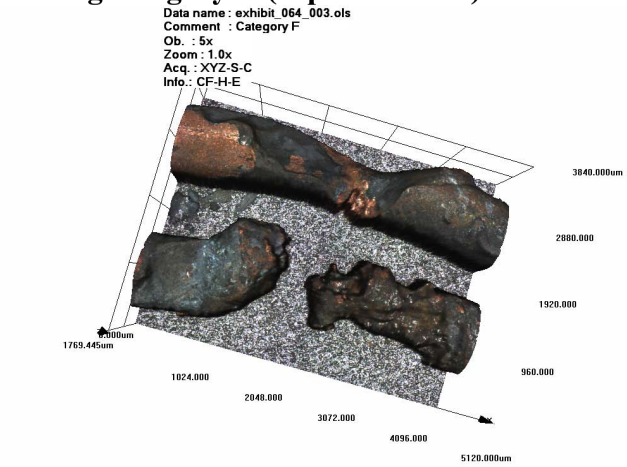

Figure 448 - LEXT image viewing the exhibit in plan view detailing the metallic damage. The shape of the two severed ends was very chaotic.

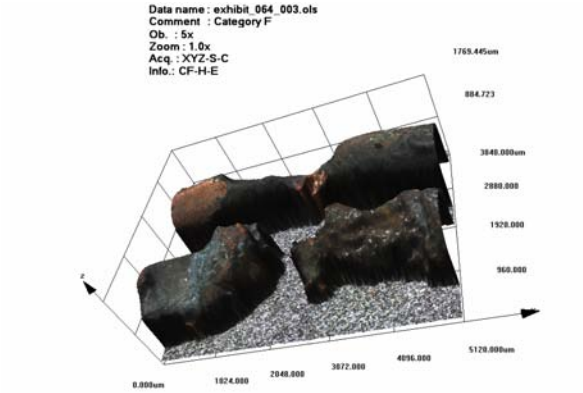

Figure 449 – Capture of 3-D image from the LEXT software package.

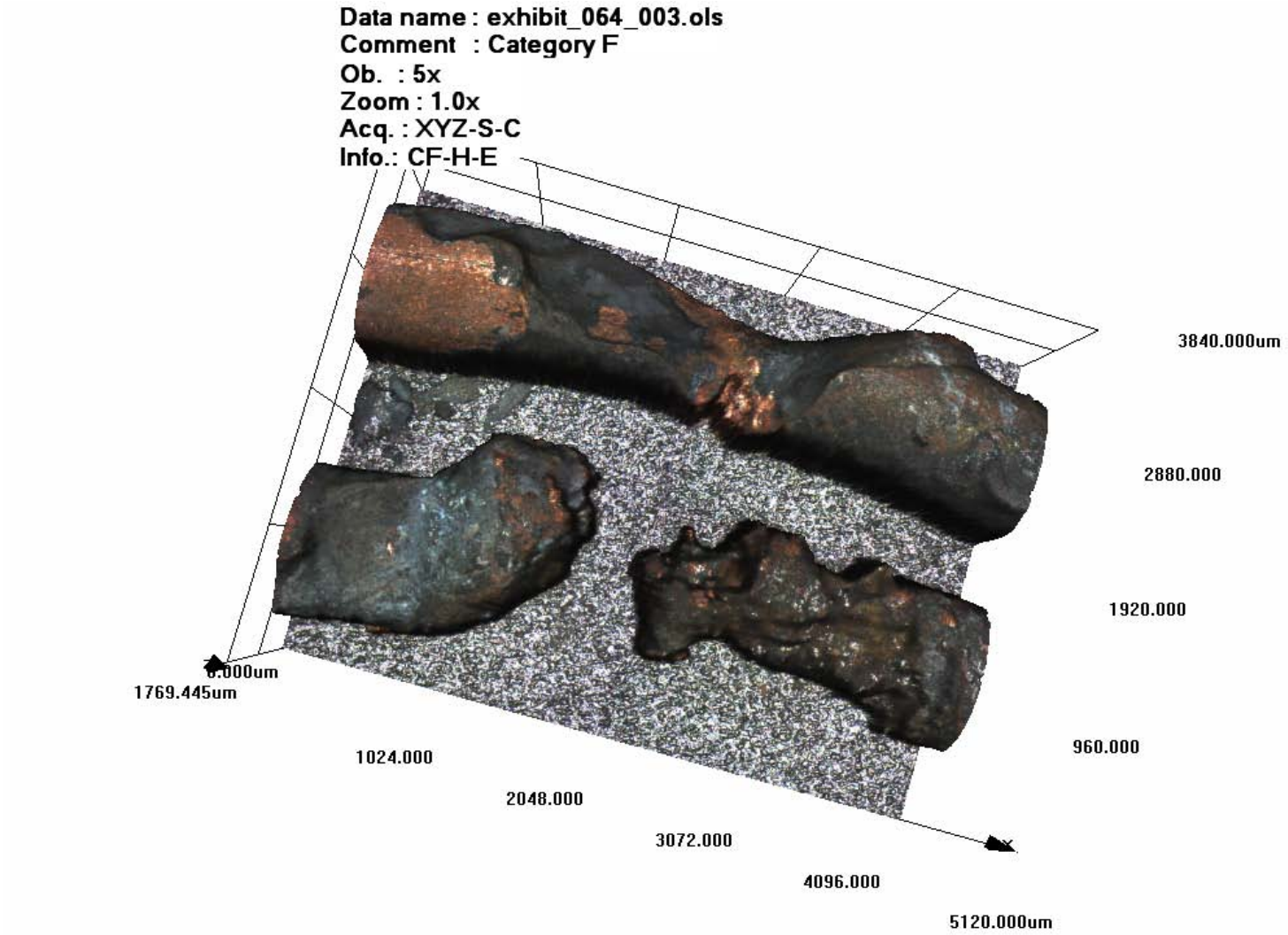

Figure 450 - Full-size LEXT image captured from the three-dimensional scan in the Olympus LEXT software

Microscope and SEM images for exhibit 065 - arcing category B (experiment 19)

Figure 451 - Microscope image of exhibit 065 that affected two conductors. The top was severed had the middle had a notch.

Figure 452 - 20x magnification of the right severed conductor end with a large bead detailed in figure 451.

Figure 453 - Microscope image of the notch arcing damage on the middle conductor of figure 451. Depth of field limitations rendered both edges of the notch out of focus.

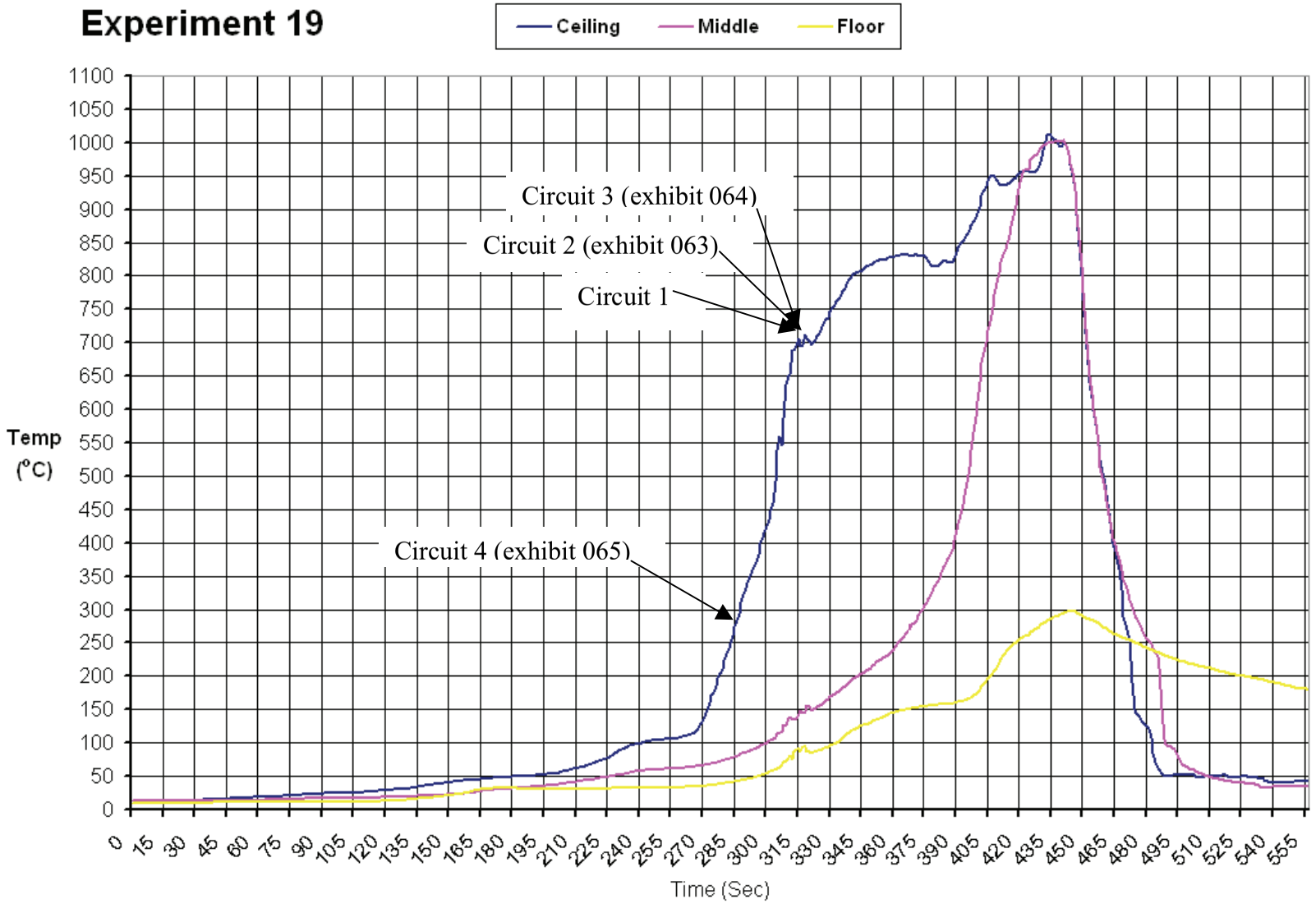

Figure 454 - Time temperature graph for experiment 19

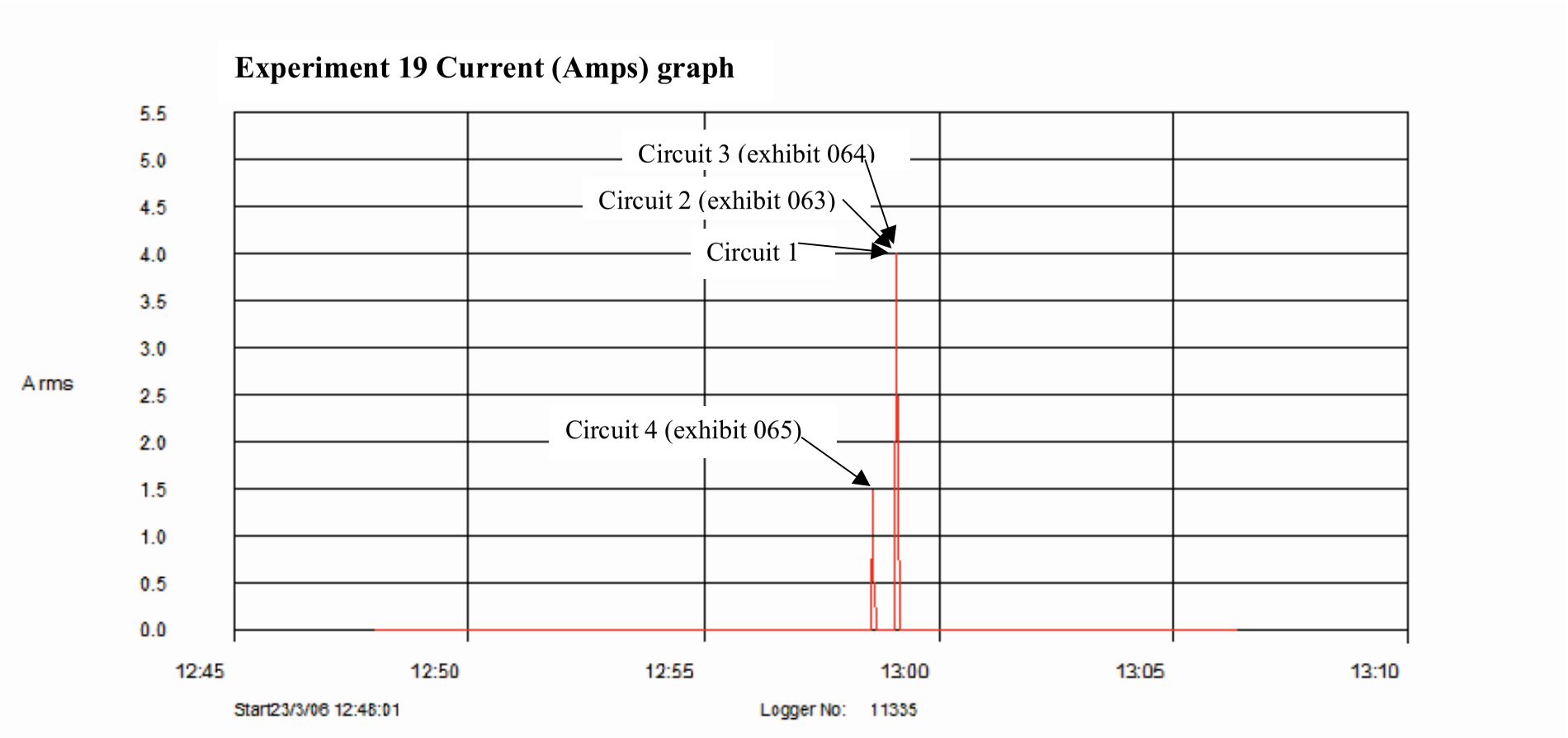

Figure 455 - Current (Amps) graph for experiment 19 detailing the operation of the circuit breakers and the fault current

Experiment 20

Figure 456 – "Scenario D" 20 April 2006

Circuit number	MCB operating time from ignition
4	1:32 minutes
1	2:13 minutes
3	2:36 minutes
2	3:00 minutes

Table 23 – circuit breaker operation data

The fire in experiment 20 (scenario D) originated in three separate areas of origin. They were all ignited almost simultaneously and were two armchairs and a sofa at the rear end of the compartment.

The fire developed rapidly with the ceiling and middle temperatures reaching 1050° C in 4.5 minutes. The floor temperature was 800° C at this point and the compartment had reached flashover conditions.

Arcing damage was located on circuit 1 – at a fixing screw 900mm from the rear wall (just above the window) on the left wall.

No arcing damage was located during the examination of circuit 2.

Arcing damage was located on circuit 3 – 2240mm from the left wall (almost at the centre of the window) and 1000mm from the front wall. A second area of arcing is adjacent to the entrance door where the cables are routed up the wall 1120mm from the ceiling.

Arcing damage was located on circuit 4 – 830mm from the left wall and 1000mm from the rear wall.

Pre-fire and post fire photographs of experiment 20

Figure 457 - Pre-fire photograph of experiment 20. The fire's areas of origin are the two arm chairs adjacent the rear wall and the edge of the settee on the left wall.

Figure 458 - Pre-fire photograph of the front of the room with the entrance door in the background and detailing the wiring for the experiments installed on the ceiling.

Figure 459 - Post-fire photograph of above. The fire's areas of origin are detailed with the white ovals.

Figure 460 - Post-fire photograph of the front area of the compartment adjacent to the entrance door.

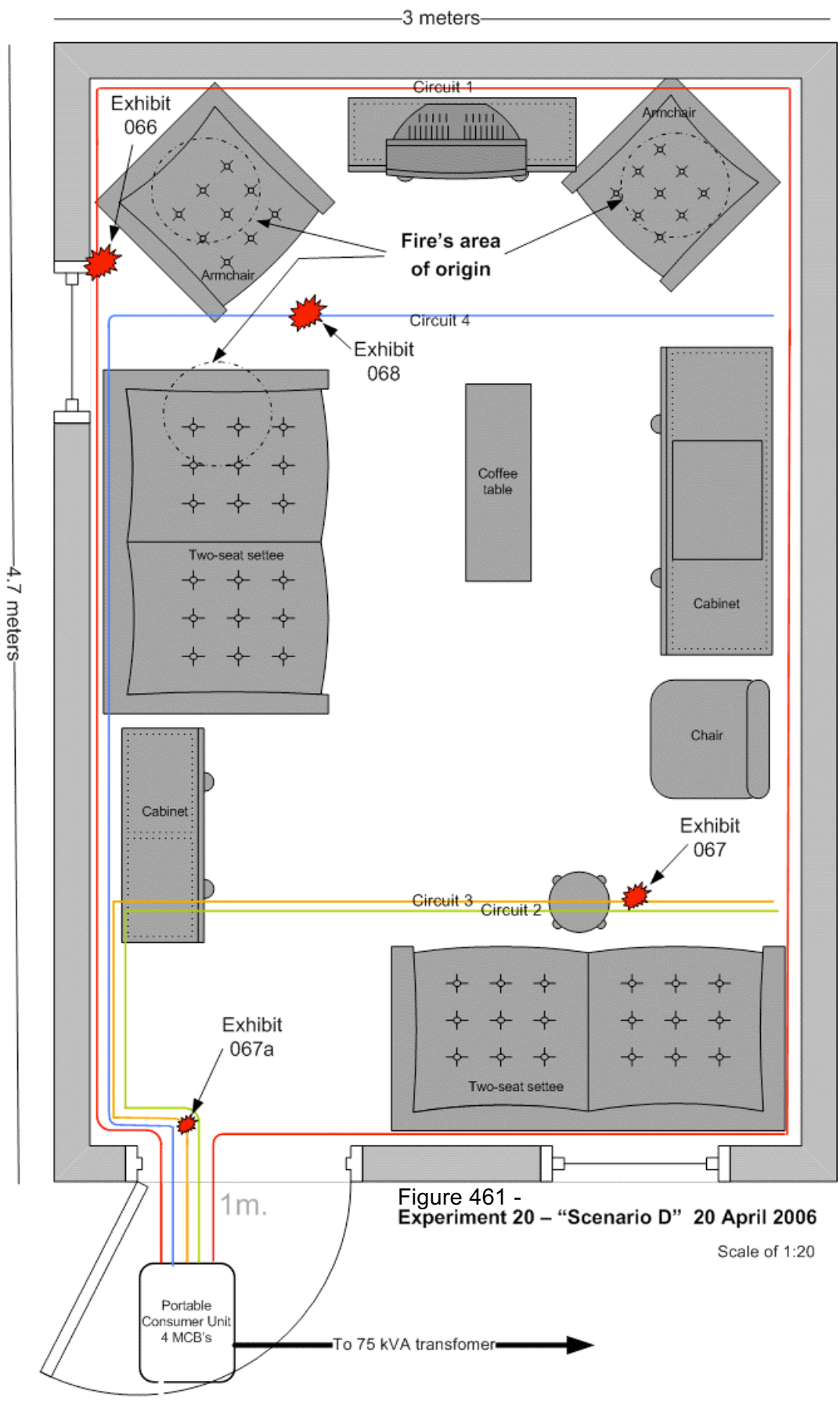

Figure 461 -
Experiment 20 – "Scenario D" 20 April 2006

Scale of 1:20

Microscope and SEM images for exhibit 066 - arcing category E (experiment 20)

Figure 462 - Microscope image of exhibit 066 with notch damage to all three conductors.

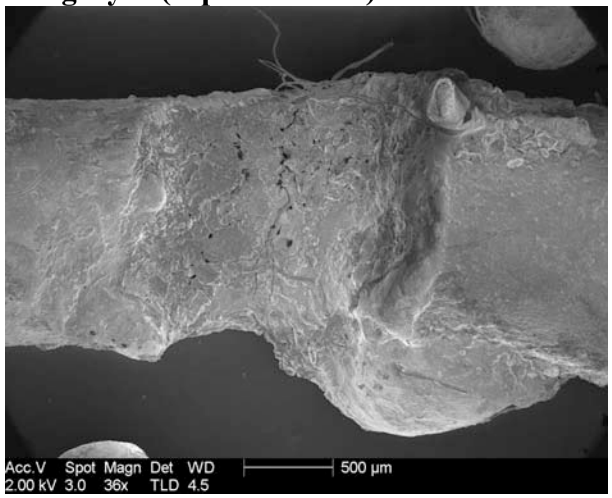

Figure 463 - SEM image of the centre conductor detailed in figure 462.

Figure 464 - SEM image of the bottom conductor detailed in figure 462.

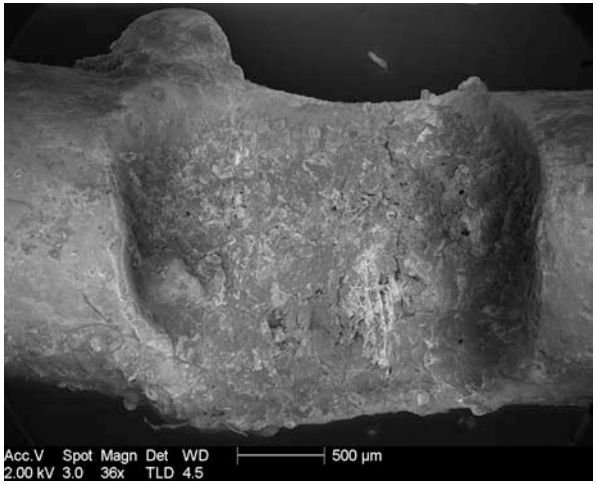

Figure 465 - SEM image of the top conductor in figure 462, this image details the clear demarcation between the arcing damage and the undamaged conductor.

Microscope and SEM images for exhibit 067 - arcing category B (experiment 20)

Figure 466 - Microscope image of exhibit 067 detailing the two severed ends of the one conductor with metallic damage.

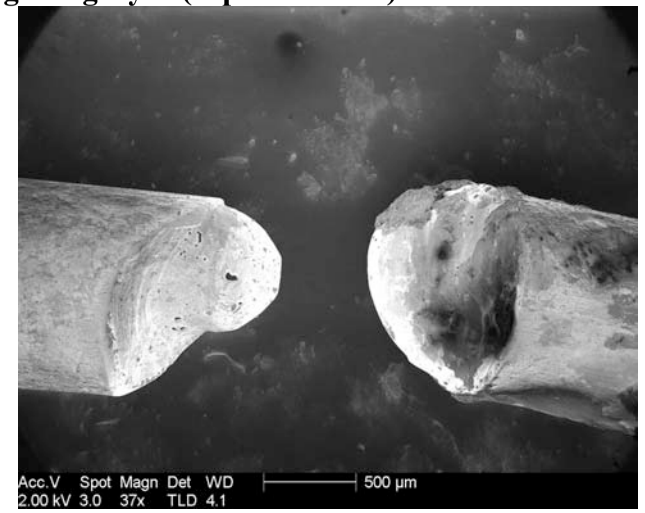

Figure 466 - SEM image of the two severed ends.

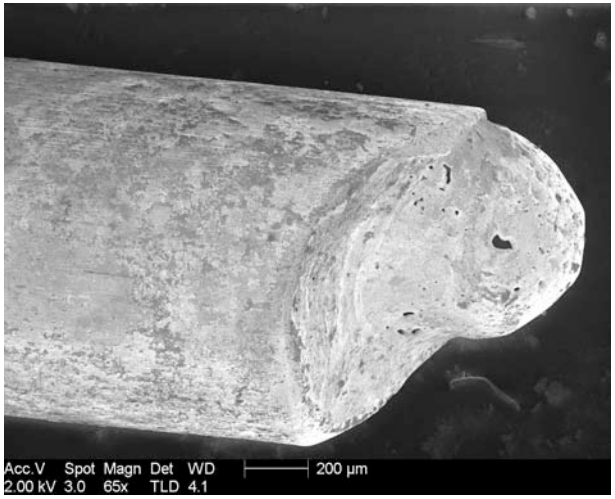

Figure 467 - SEM image of the left severed end at 65x magnification detailed in figure 466.

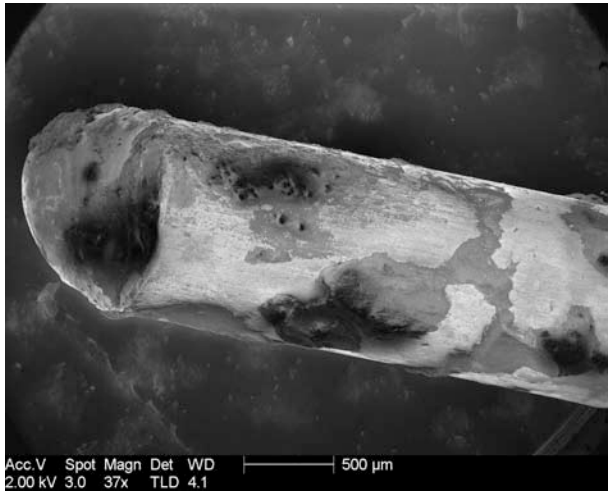

Figure 468 - SEM image of the right severed end at 37x magnification detailed in figure 466.

Microscope and SEM images for exhibit 067a - arcing category B (experiment 20)

Figure 470 - Microscope image for exhibit 067a. This is the second area of arcing for circuit 4 that is located closer to the electrical source It was located adjacent to the entrance door 1120mm from the ceiling.

Figure 471 - Microscope image at 20x magnification of exhibit 067a detailing the right severed end of this conductor.

Figure 472 – Microscope image detailing the left severed end of this conductor at 20x magnification.

Microscope and SEM images for exhibit 068 - arcing category D (experiment 20)

Figure 473 - Microscope image of exhibit 068 detailing all three conductors. The top and middle conductors have a notch with a large bead within each notch.

Figure 474 - SEM image of both conductors that are detailed in figure 473.

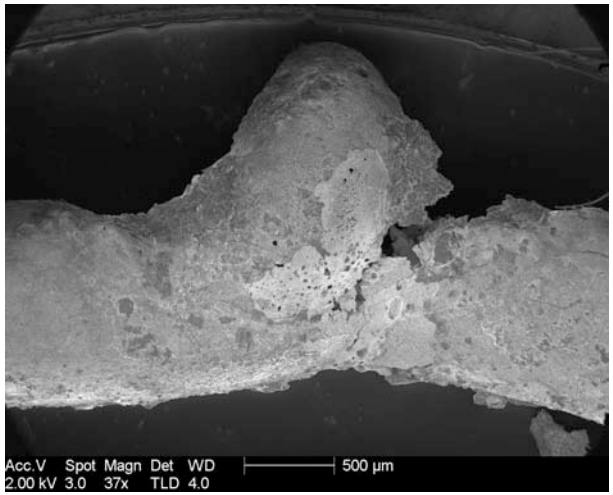

Figure 475 - SEM image of the top conductor detailed in figure 474.

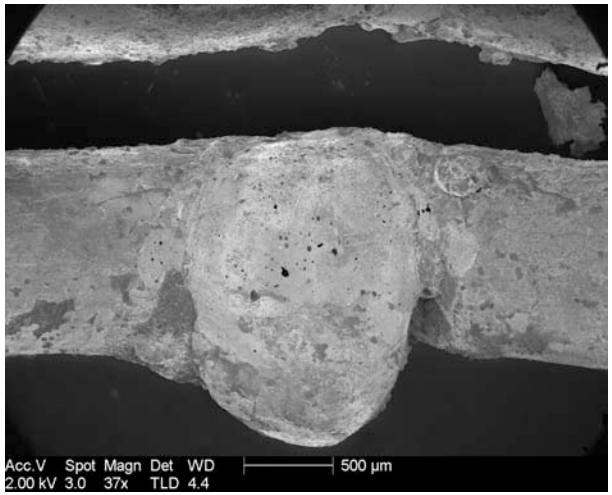

Figure 476 - SEM image detailing the bottom conductor's arcing damage detailed in figure 474.

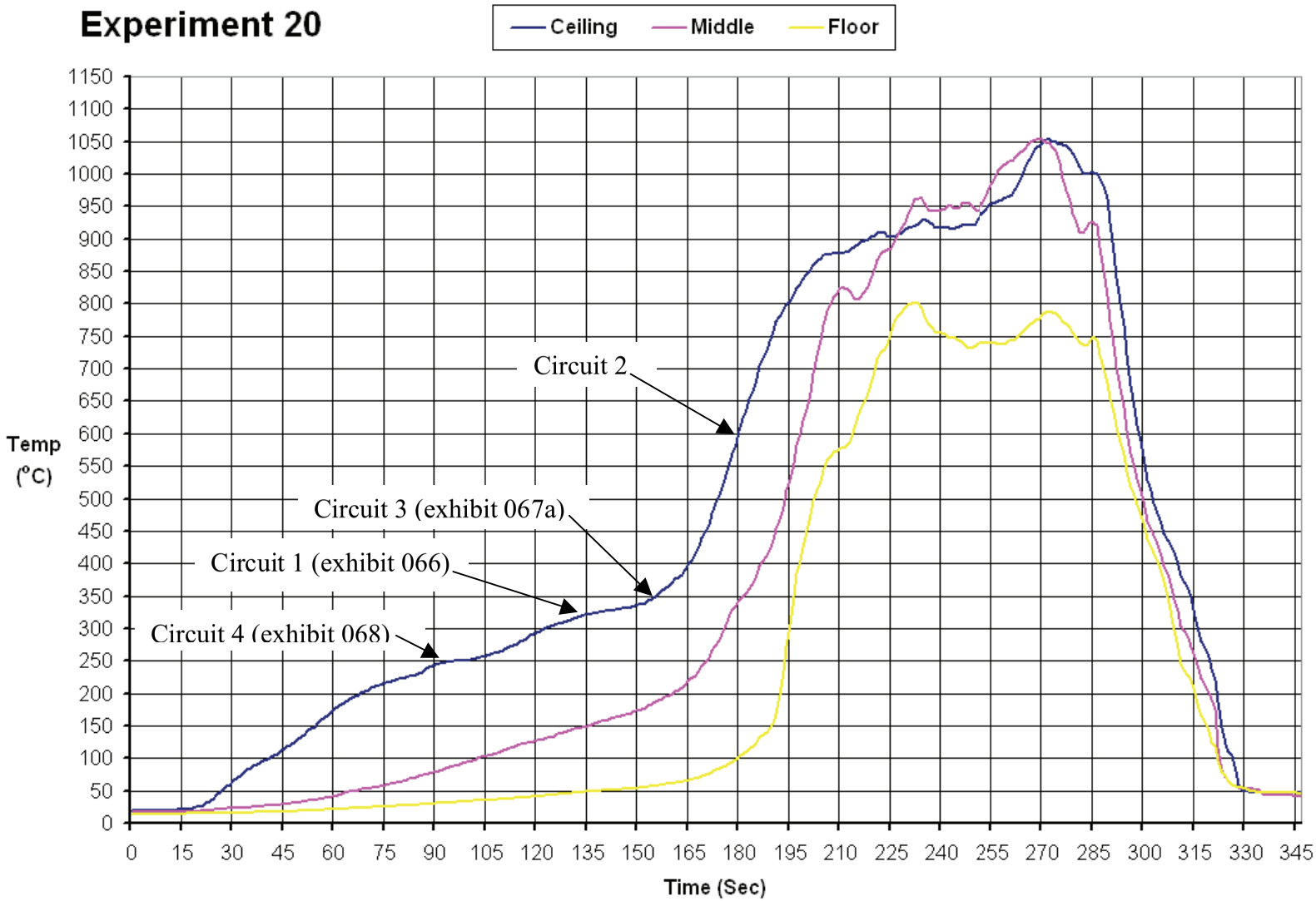

Figure 477 - Time temperature graph of experiment 20

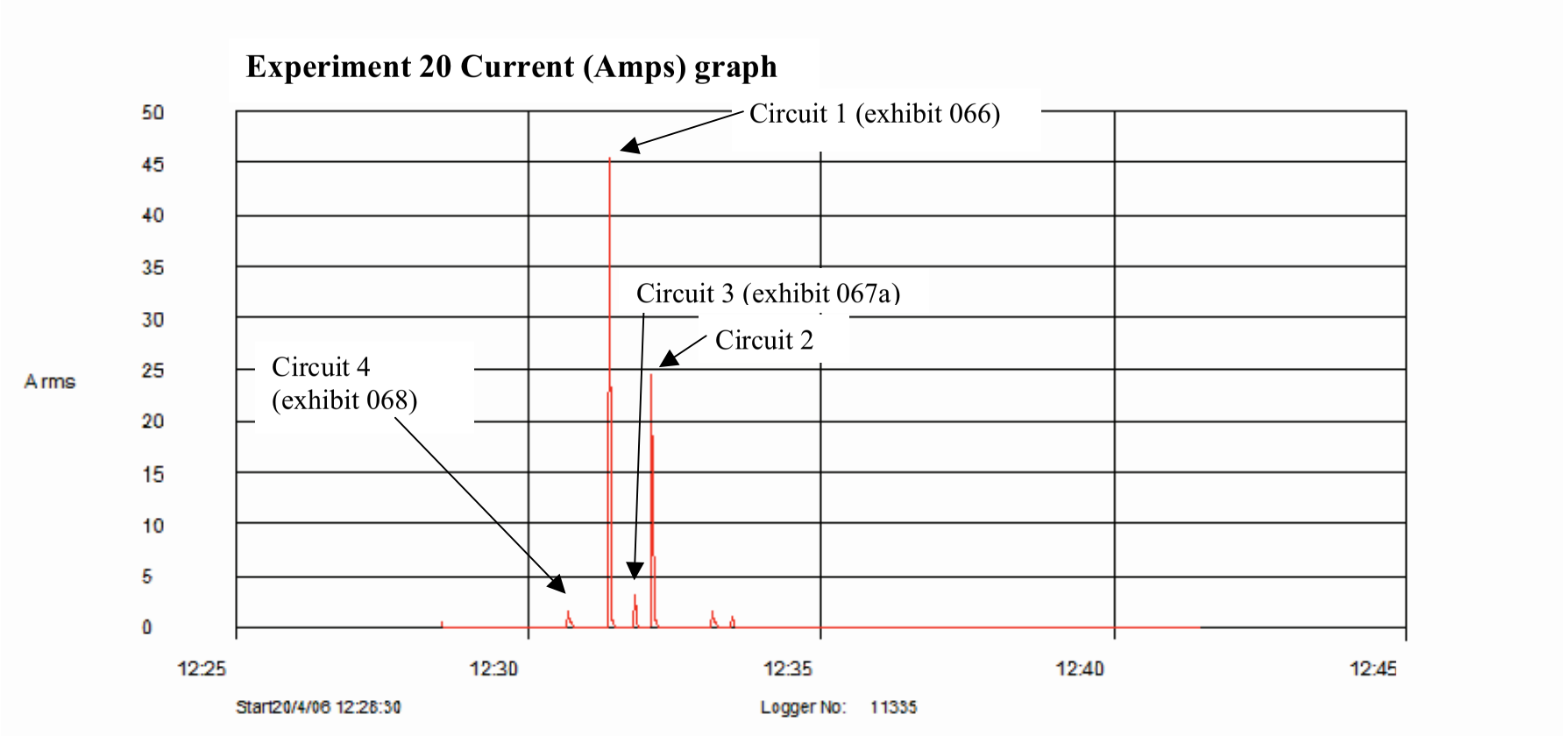

Figure 478 - Current (Amps) graph for experiment 20 detailing the operation of the circuit breakers and the fault current

Experiment 21

Figure 479 – “Scenario B” 20 April 2006

Circuit number	MCB operating time from ignition
4	9:45 minutes
1	9:59 minutes
3	10:15 minutes
2	10:24 minutes

Table 24 – circuit breaker operation data

The fire in experiment 21 (scenario B) was ignited with a trailer of polyurethane foam soaked with ignitable liquid. The foam was laid on the floor and divided to spread the fire to different areas of the room.

A vacuum cleaner in the rear left corner of the room was the first area to be ignited by the trailer. A display unit on the right wall close to the rear right corner was the second area to be ignited and became the dominant area of the fire’s development within the compartment.

Arcing damage was located on circuit 1 – on the right wall 2430mm from the rear wall.

Arcing damage was located on circuit 2 – 1340mm from the left wall on the ceiling and 1000mm from the front wall.

Pre-fire and post-fire photographs of experiment 21

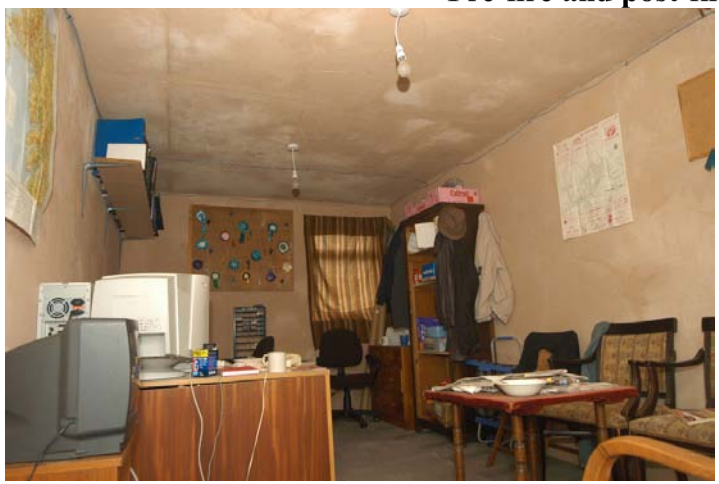

Figure 480 - Pre-fire photograph of experiment 21. The display unit on the right of the image created the dominant fire plume that interacted with the ceiling.

Figure 481 - A view of the trailer of the burning PU foam trailer soaked with ignitable liquid, taken from the doorway.

Figure 482 - Post-fire photograph of the compartment.

Figure 483 – Post-fire image of circuits 1 and 4 on the ceiling above the display unit.

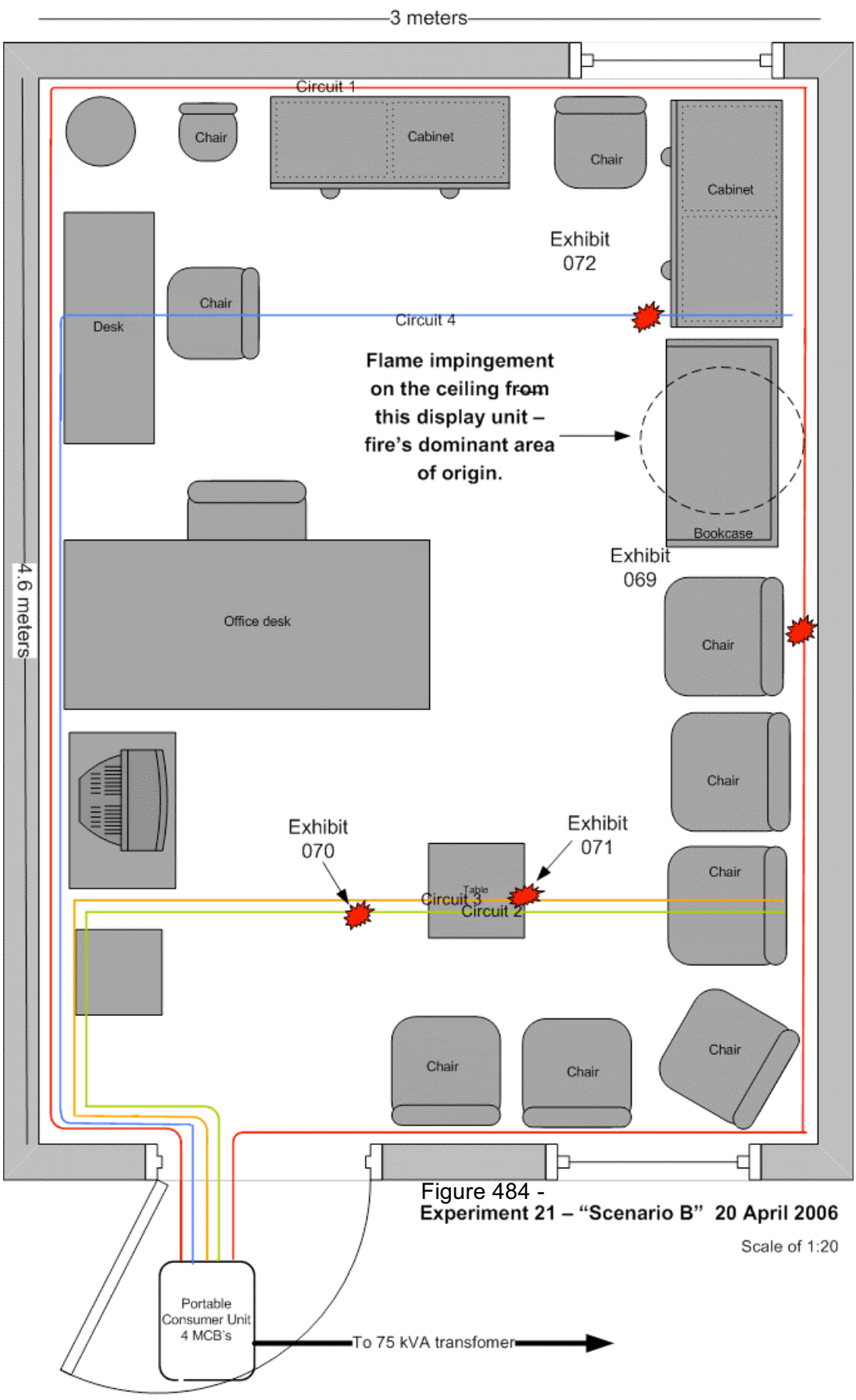

Figure 484 -
Experiment 21 – "Scenario B" 20 April 2006

Scale of 1:20

Microscope and SEM images for exhibit 069 - arcing category H (experiment 21)

Figure 485 - Microscope image of exhibit 069. The two conductors were originally welded together but they separated during the solvent and ultrasonic bath cleaning process.

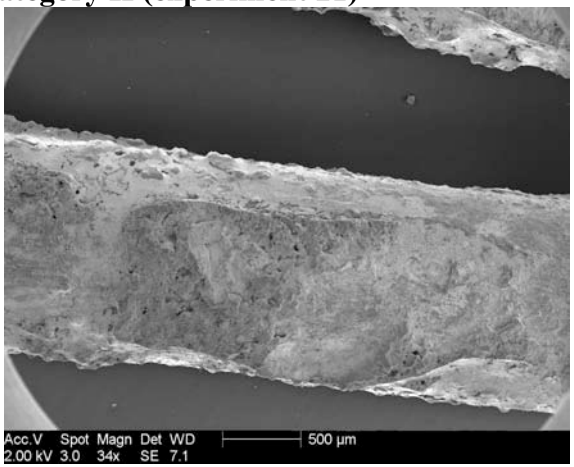

Figure 486 - SEM image of the top conductor in figure 485.

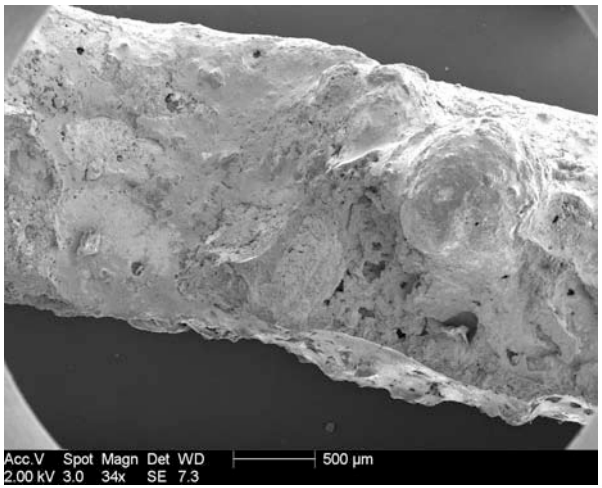

Figure 487 - SEM image of the bottom conductor in figure 485.

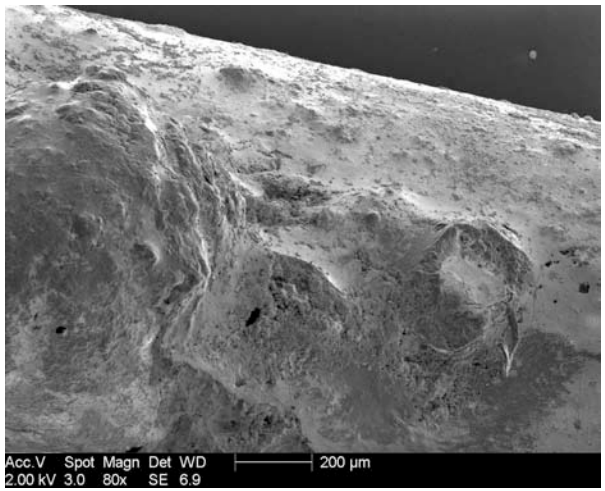

Figure 488 - SEM image at 80x magnification detailing the edge and demarcation of the arcing damage.

Microscope images for exhibit 070 - arcing category C (experiment 21)

Figure 489 - Microscope image of exhibit 070 with all three conductors for this circuit detailed.

Figure 490 - Image of the two conductors with arcing damage. Depth of field issues renders one conductor out of focus in this image.

Figure 491 - Close-up view of the bead for the top conductor in figure 489.

Figure 492 - Close-up view of the bottom conductor in figure 489 with a large notch with a bead on the edge of the notch.

Microscope and SEM images for exhibit 071 - arcing category C (experiment 21)

Figure 493 - Microscope image of one of the two conductors with arcing damage for circuit 3.

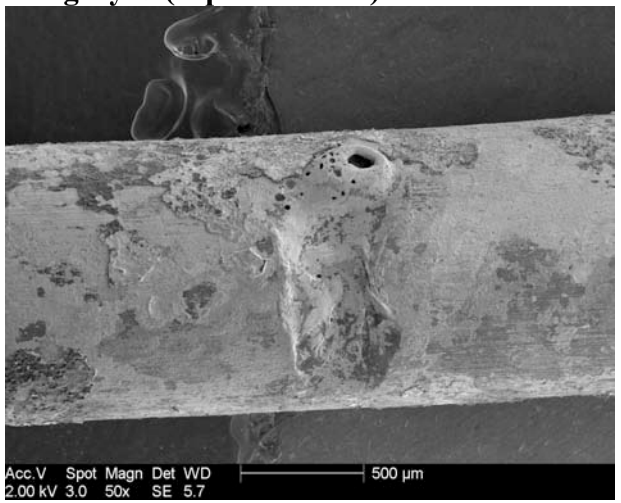

Figure 494 - SEM image of the bottom conductor (out of focus in figure 493) with a small notch.

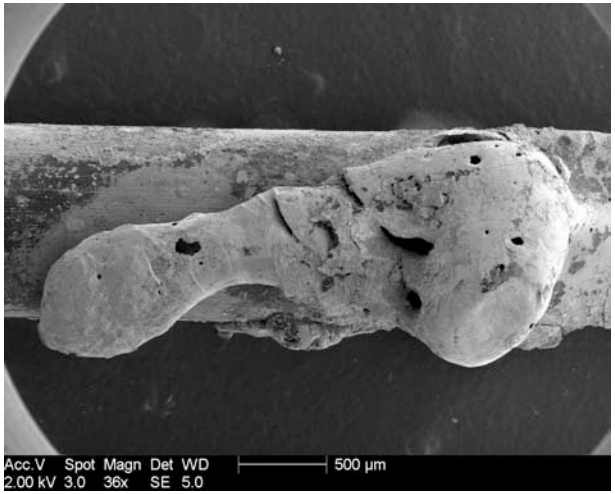

Figure 495 - SEM image of the conductor above detailing the large elongated bead at the side of the notch.

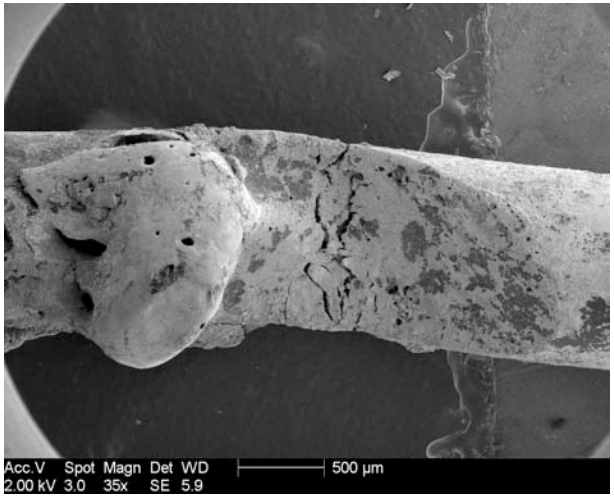

Figure 496 - SEM image of the large notch. This image is a continuation to the right of figure 495.

Confocal laser scanning microscope images for exhibit 071 – arcing category C (experiment 21)

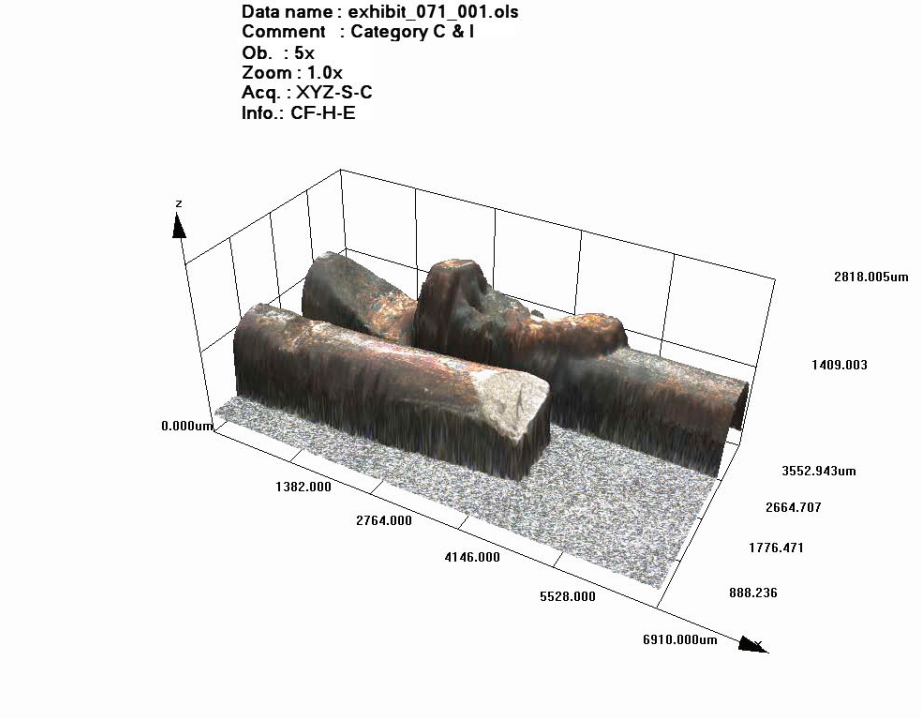

Figure 497 - LEXT image detailing both of the conductors side-by-side.

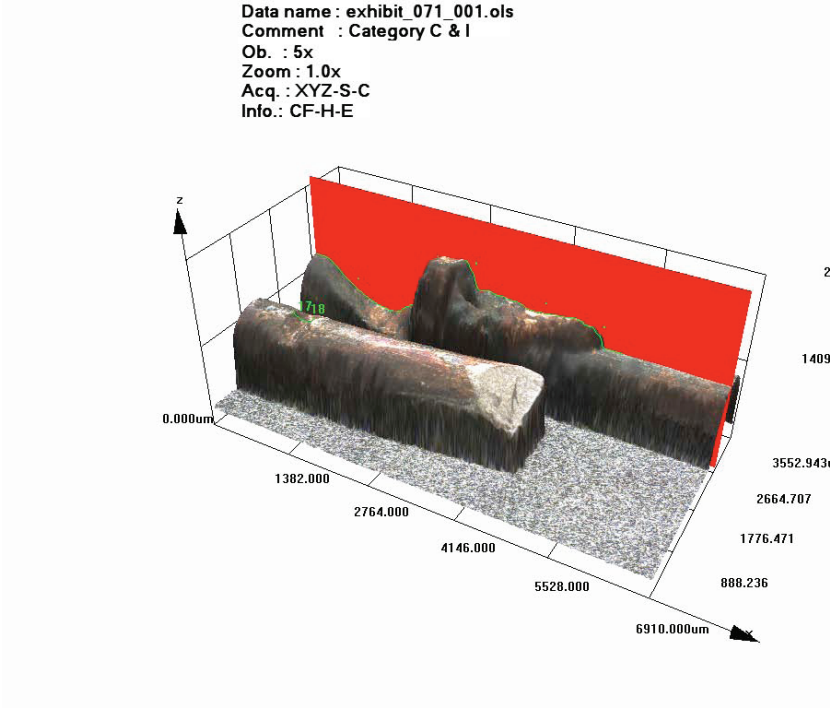

Figure 498 - LEXT image detailing the profile “slice tool” in use in the LEXT software.

Microscope images for exhibit 072 - arcing category E (experiment 21)

Figure 499 - Microscope image of exhibit 072 with arcing damage to two if the three conductors.

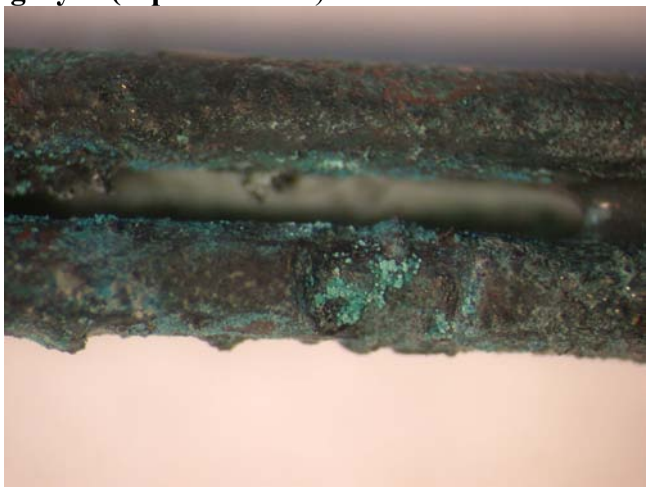

Figure 500 - 20x magnification of the bead within the notch of the top conductor.

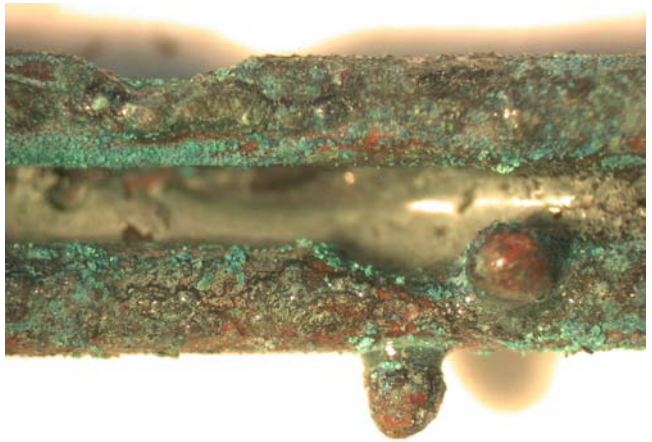

Figure 501 - 20x magnification of the notch with an adjacent bead. There is a lot of oxide corrosion on the surface of this exhibit.

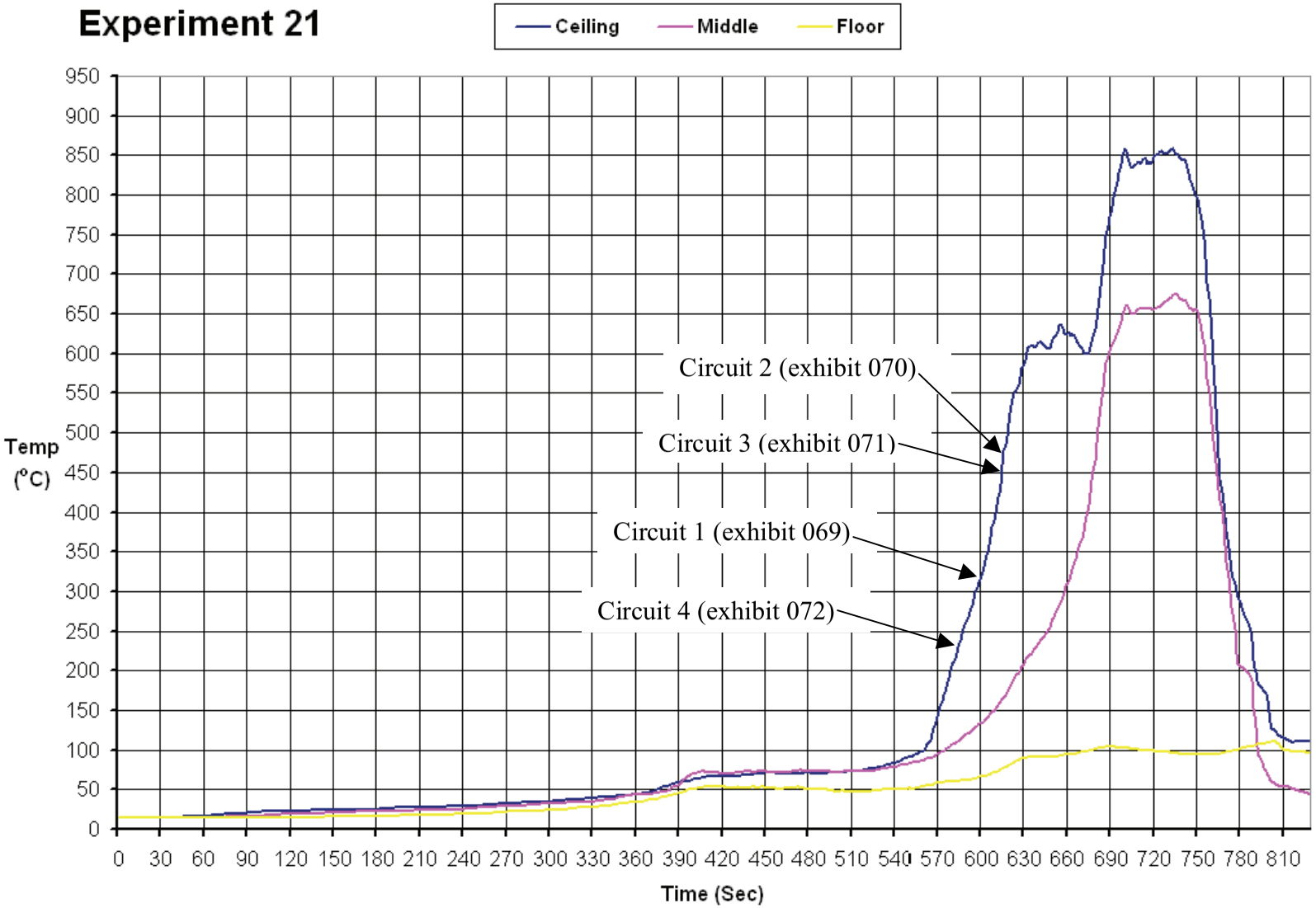

Figure 502 - Time temperature graph for experiment 21

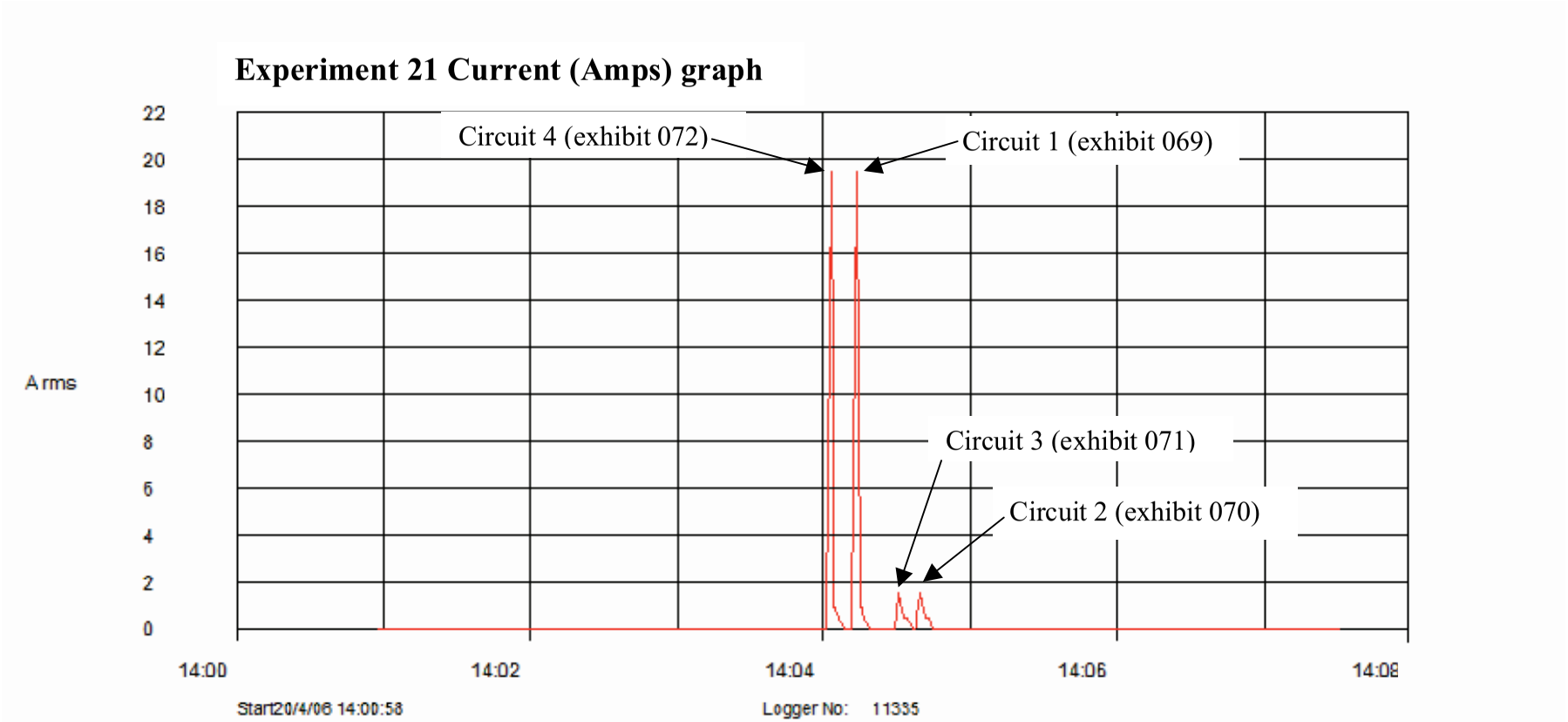

Figure 503 - Current (Amps) graph for experiment 21 detailing the operation of the circuit breakers and the fault current

Experiment 22

Figure 505 - “Scenario A” 20 April 2006

Circuit number	MCB operating time from ignition
1	3:00 minutes
4	3:00 minutes
3	3:30 minutes
2	3:50 minutes

Table 25 – circuit breaker operation data

The fire in experiment 22 (scenario A) originated on a clothing rail and the side of each adjacent bed at the far end of the room.

The fire developed rapidly with the ceiling temperature reaching 940° C in just under 7 minutes. The middle thermocouple temperature reached 900° C at this time with the floor thermocouple reaching 450° C. The fire reached flashover conditions just prior to being extinguished at 7 minutes from the time of ignition.

Arcing damage was located on circuit 1 – 1460mm from the right wall.

Arcing damage was located on circuits 2 and 3 – 730mm from the right wall on the ceiling and 1000mm from the front wall.

Arcing damage was located on circuit 4 – 1930mm from the right wall 1000mm from the rear wall.

Pre-fire and post-fire photographs of experiment 22

Figure 505 - Pre-fire photograph of experiment 22 The white oval details the fire's area of origin.

Figure 506 - Post-fire photograph of the ceiling above the fire's area of origin.

Figure 507 - Post-fire photograph detailing the fire's area of origin located adjacent to the rear wall and between the beds.

Figure 508 - Close-up photograph of the fire's area of origin. The fire was ignited with a flame to simulate a faulty fan heater below portable clothes rail full of clothing.

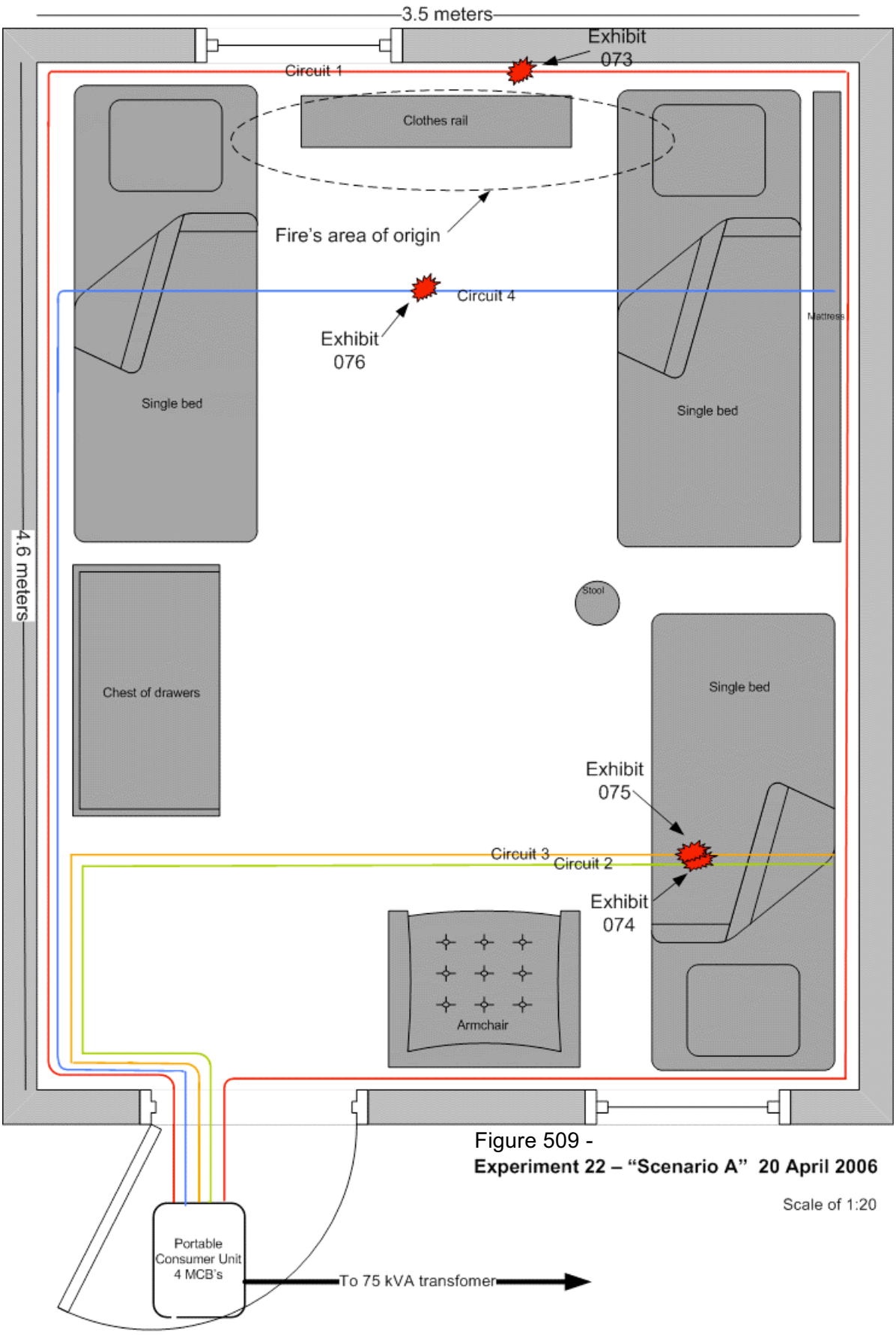

Figure 509 -
Experiment 22 – "Scenario A" 20 April 2006

Scale of 1:20

Microscope and SEM images for exhibit 073 - arcing category E (experiment 22)

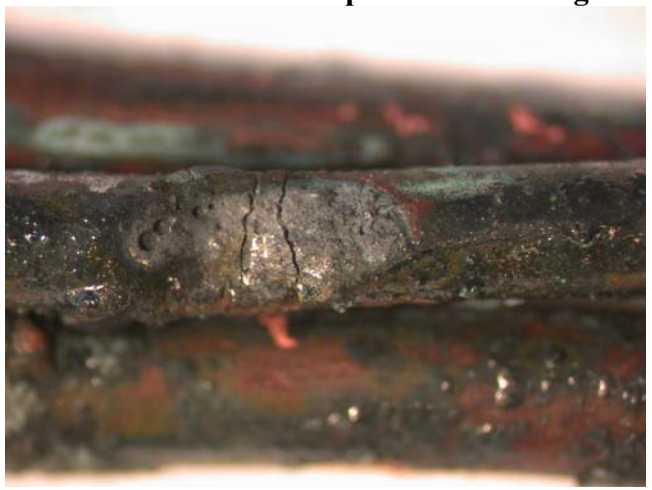

Figure 510 - Microscope image of the bottom conductor - exhibit 073.

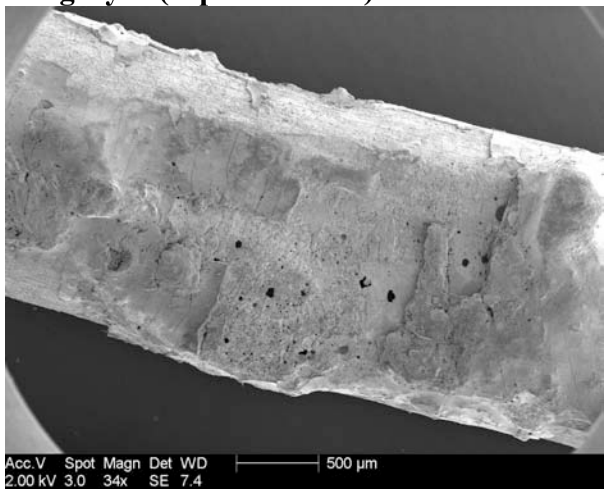

Figure 511 - SEM image of the top conductor.

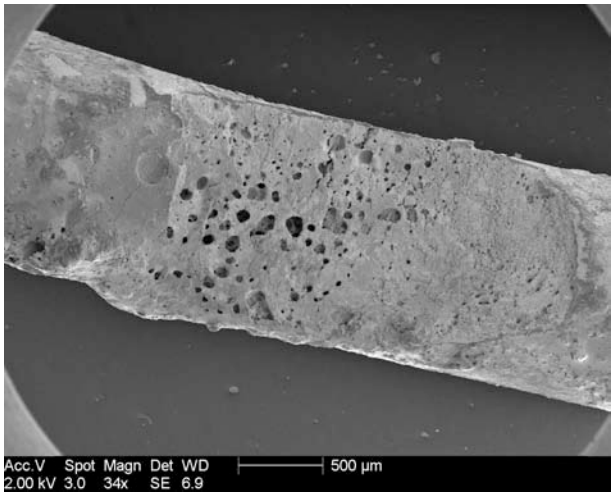

Figure 512 - SEM image of the bottom conductor detailed in figure 510.

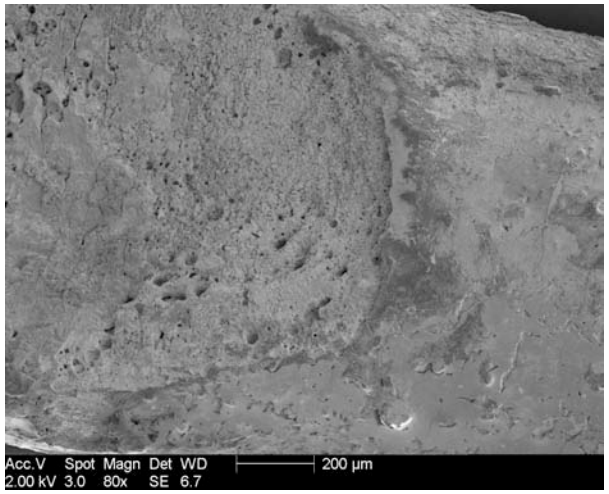

Figure 513 - SEM image of the right side of the notch for the bottom conductor in figure 512, detailing the clear demarcation between the arcing damage and the undamaged conductor.

Confocal laser scanning microscope images for exhibit 073 – arcing category E (experiment 22)

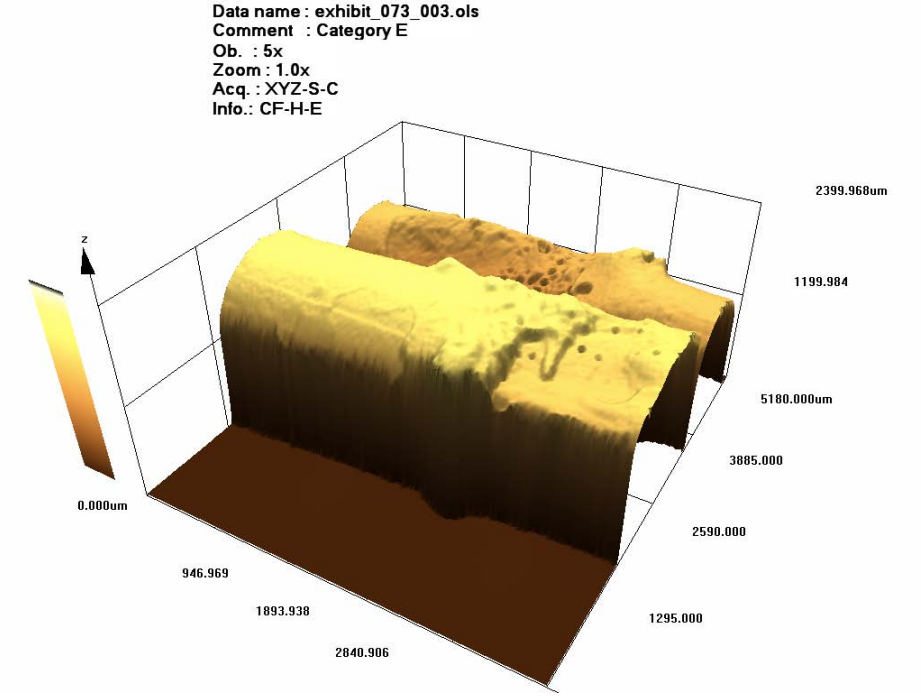

Figure 514 - LEXT image of exhibit 073 in the “brown” rendering mode.

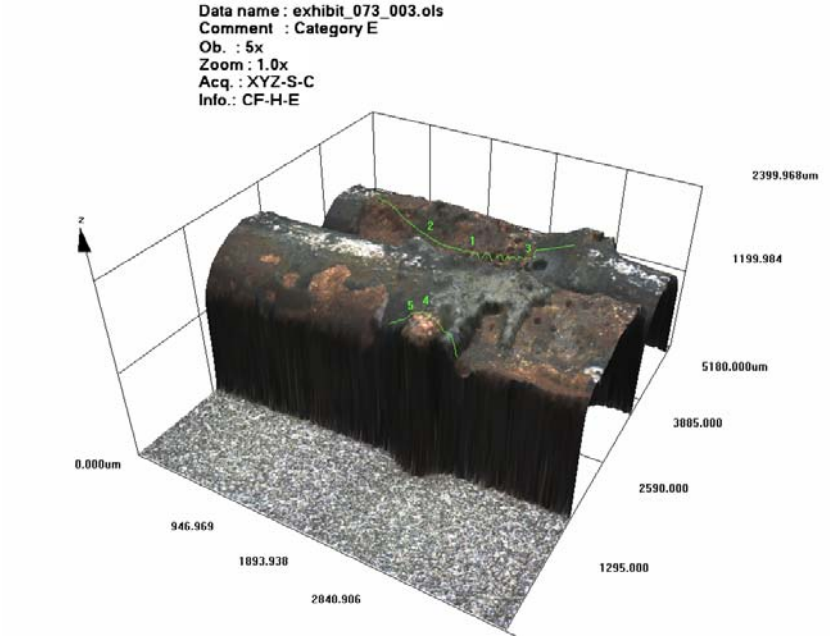

Figure 515 - LEXT image of exhibit 073 detailing both of the conductors involved with this exhibit, captured in the “real colour” rendering mode.

Microscope images for exhibit 074 - arcing category F (experiment 22)

Figure 516 - Microscope image of exhibit 074. This exhibit is linked to exhibit 075

Figure 517 - Close-up microscope image of the notch and adjacent bead.

Figure 518 - Image of a small bead attached to the surface of the copper conductor 6mm from the notch above.

Figure 519 – 40x magnification microscope image of the bead on the conductor surface detailed to the left.

Microscope images for exhibit 075 - arcing category H (experiment 22)

Figure 520 - Microscope image of exhibit 075. This is the fixing screw for circuits 2 and 3. It has a copper conductor welded to its surface. The conductor fractured during the recovery process.

Figure 521 - Close-up microscope image at 40x magnification of the copper conductor welded to the surface of the fixing screw.

Microscope images for exhibit 076 - arcing category B (experiment 22)

Figure 522 - Microscope image of exhibit 076. This comprises of two severed ends. The left end appears to be fractured and is linked to exhibit 075.

Figure 523 - Close-up microscope image at 20x magnification of the two severed ends.

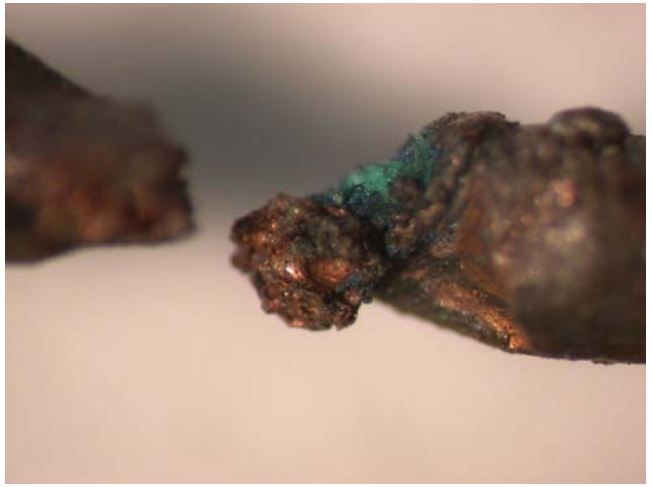

Figure 524 - Microscope image at 40x magnification of the right severed end with a bead attached to the tip.

Microscope and SEM images for exhibit 077 - arcing category B (experiment 22)

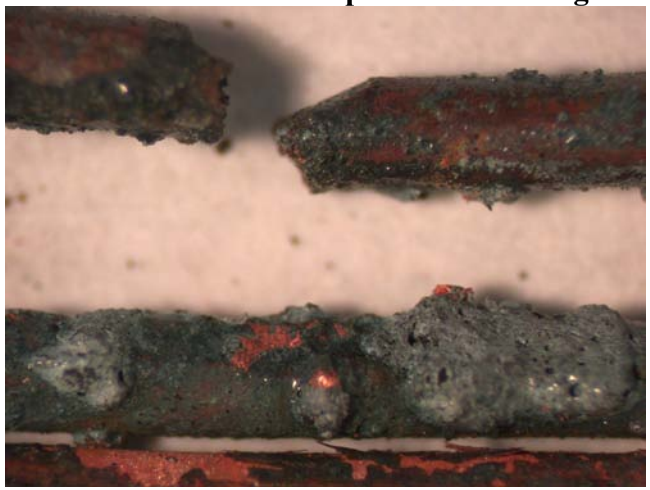

Figure 525 - Microscope image of exhibit 077. This exhibit comprises of two severed ends of one conductor and a large notch in a second conductor.

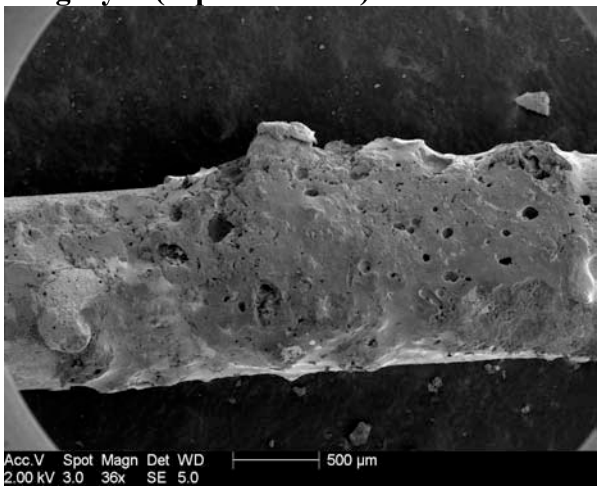

Figure 526 - SEM image of the large notch in the bottom conductor detailed to the left.

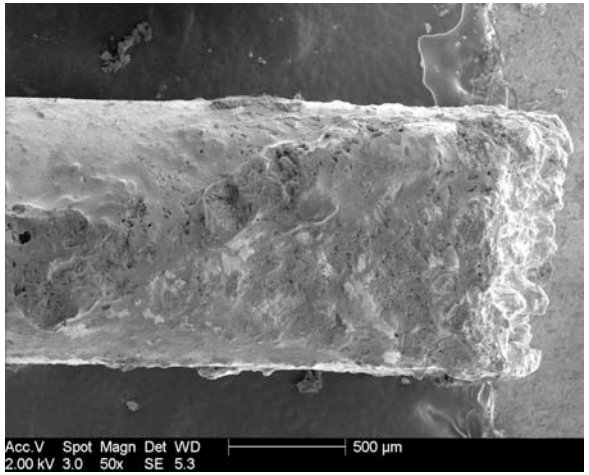

Figure 527 - SEM image of the right severed end detailed in figure 525. The demarcation is observed at the edge of the notch.

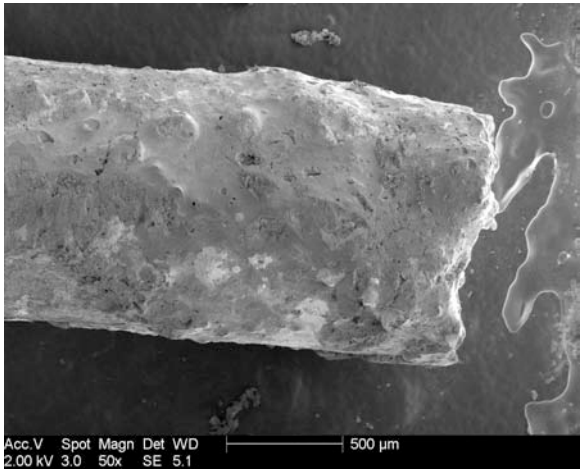

Figure 528 - SEM image of the left severed end in the microscope of figure 526.

Confocal laser scanning microscope images for exhibit 077 – arcing category B (experiment 22)

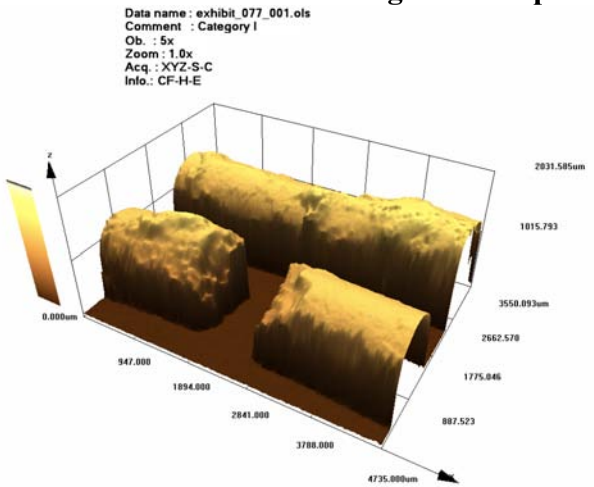

Figure 529 - LEXT image using “brown” rendering option in the LEXT software.

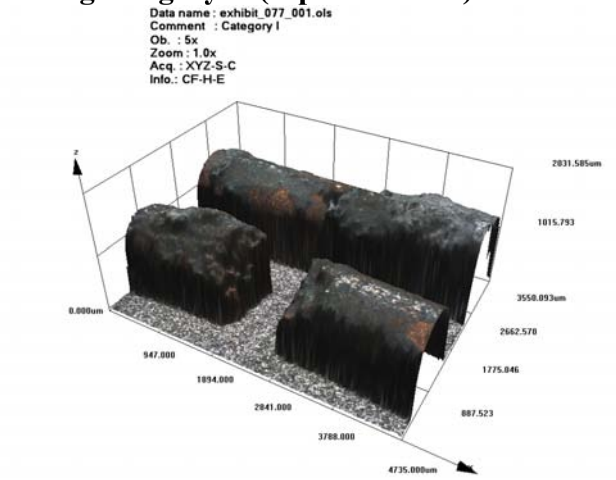

Figure 530 - LEXT image of all three conductor sections forming this exhibit using “real colour” rendering option.

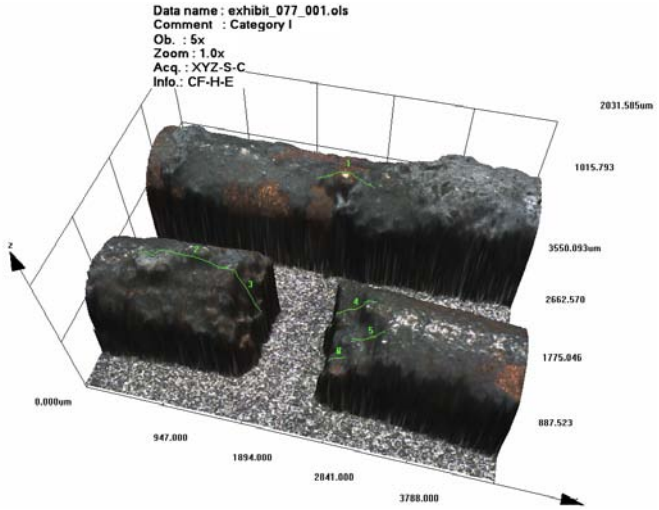

LEXT image using “real colour” rendering option re-orientated in the 3-D software.

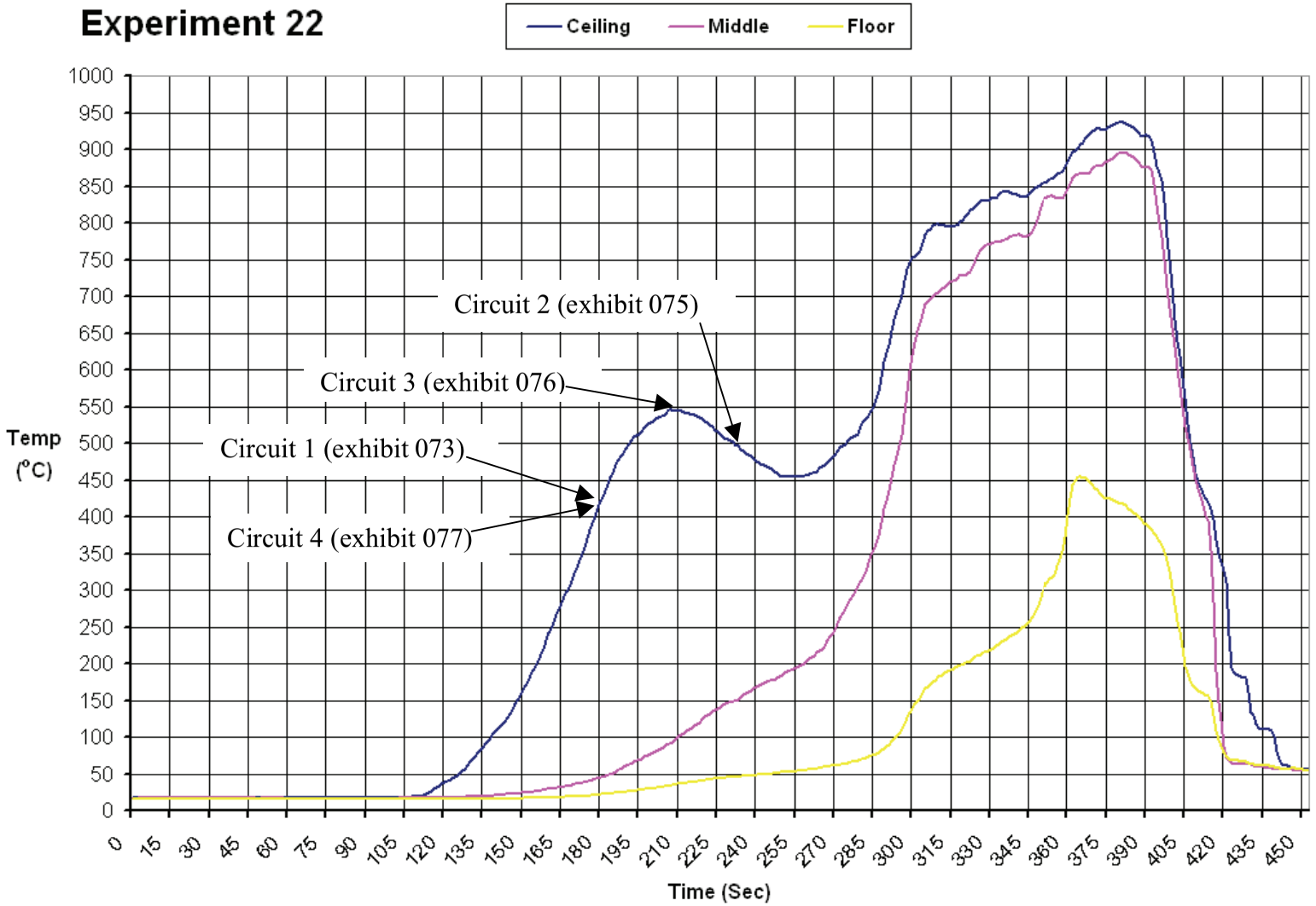

Figure 532 - Time temperature graph for experiment 22

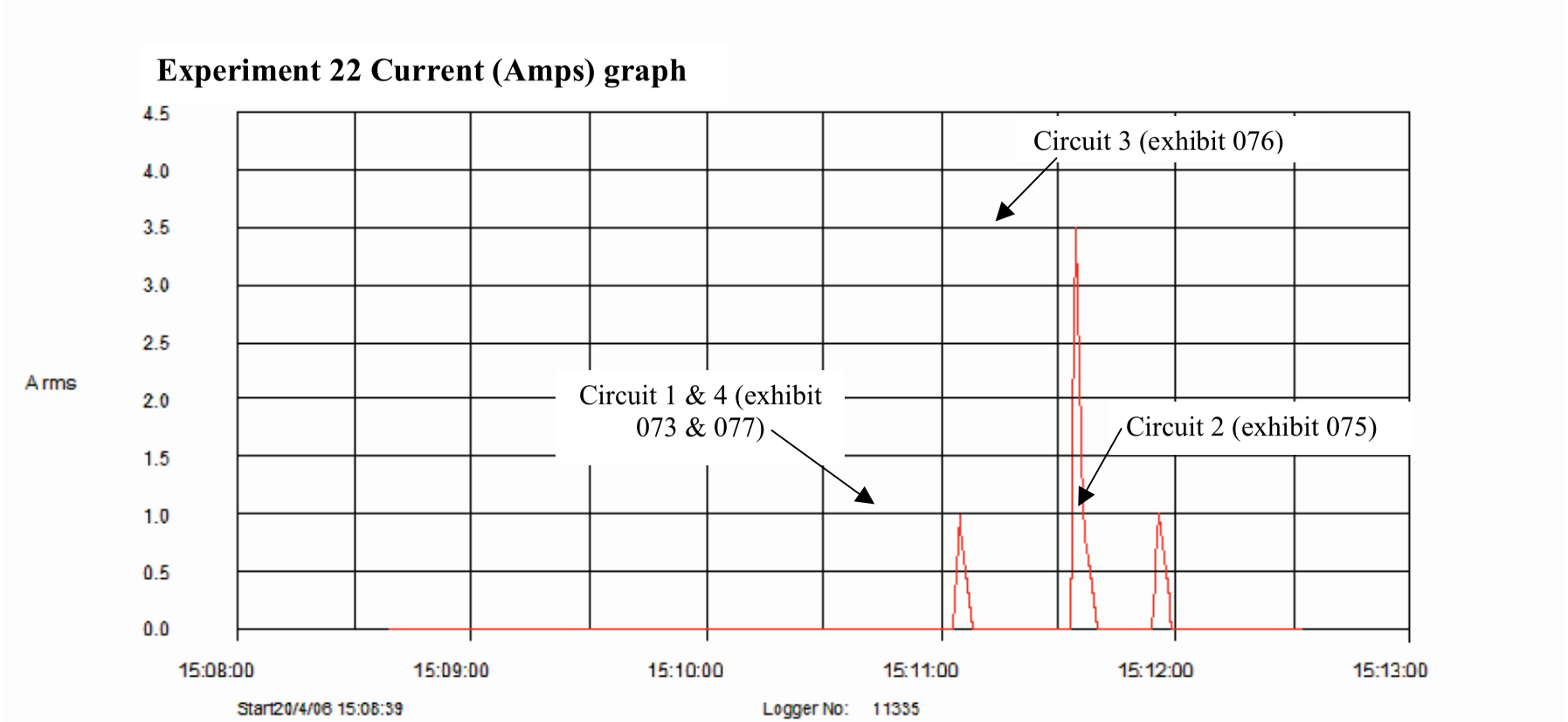

Figure 533 - Current (Amps) graph for experiment 22 detailing the operation of the circuit breakers and the fault current

Experiment 23

Figure 534 – “Scenario C” 20 April 2006

Circuit number	MCB operating time from ignition
4	2:35 minutes
1	3:35 minutes
2	4:00 minutes
3	4:09 minutes

Table 26 – circuit breaker operation data

The fire in experiment 23 (scenario C) originated in a toy box located in front of a Christmas tree at the back of the compartment.

The compartment reached flashover conditions at just under 8.5 minutes from the ignition time. The ceiling temperature reached 1030° C at this time, with the middle thermocouple recording 1100° C and the floor thermocouple recording 950° C.

Arcing damage was located on circuit 1 – 1400mm from the left wall.

Arcing damage was located on circuit 2 – 1500mm from the left wall on the ceiling and 1000mm from the front wall.

Arcing damage was located on circuit 3 – 2340mm from the left wall on the ceiling and 1000mm from the front wall.

Arcing damage was located at circuit 4 – 1600mm from the left wall 1000mm from the rear wall (almost directly above the point of origin).

Pre-fire and post-fire photographs of experiment 23

Figure 535 - Pre-fire photograph of experiment 23. The white oval indicates the fire's area of origin.

Figure 536 - Pre-fire photograph of the wiring fixed to the ceiling above the fire's area of origin.

Figure 537 - Post fire photograph detailing the fire's area of origin. The floor has failed just in front of the remains of the Christmas tree.

Figure 538 - Post-fire photograph of the rear left corner of the ceiling above the fire's area of origin. The arrow indicates circuit 4 that was routed across the ceiling.

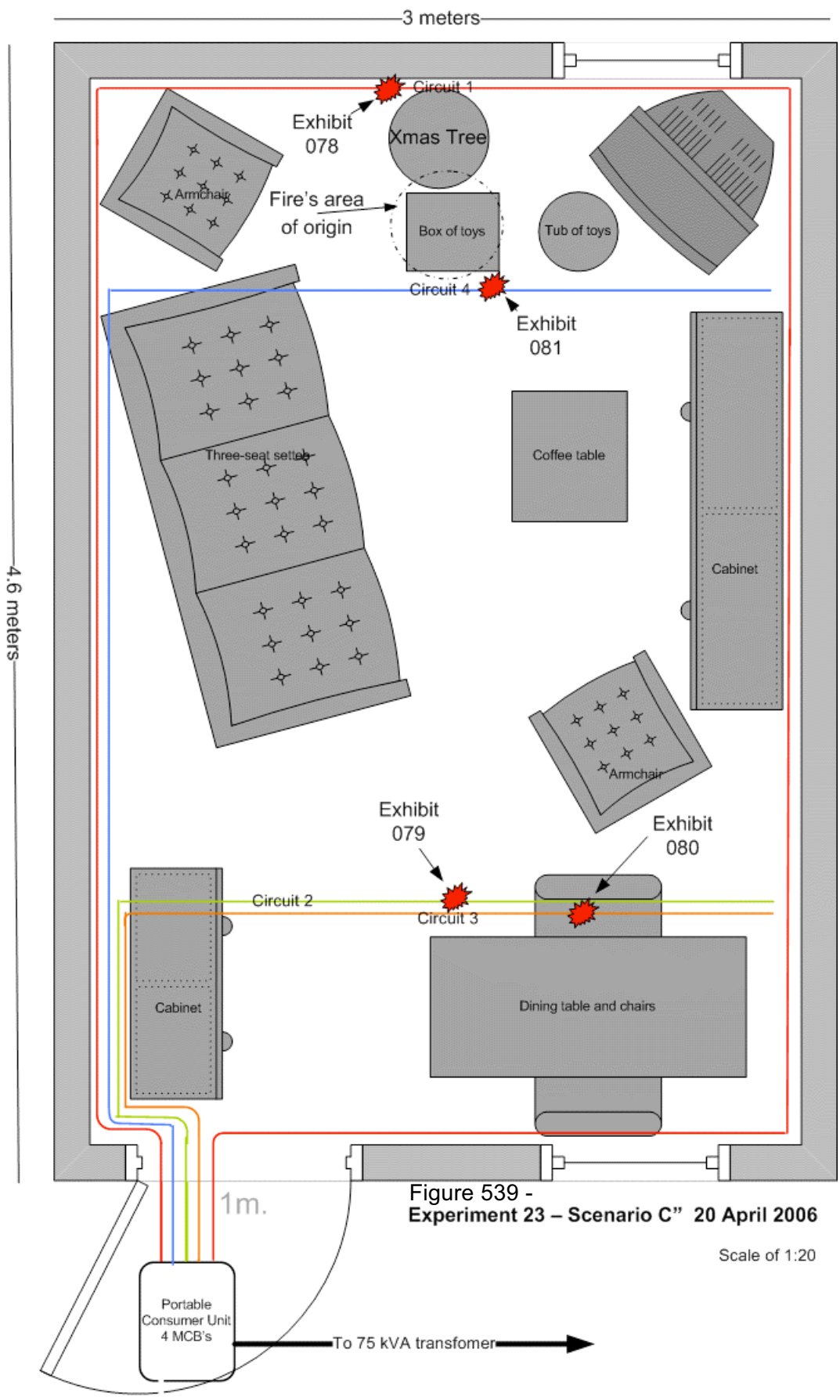

Figure 539 -
Experiment 23 – Scenario C" 20 April 2006

Scale of 1:20

Microscope and SEM images for exhibit 078 - arcing category B (experiment 23)

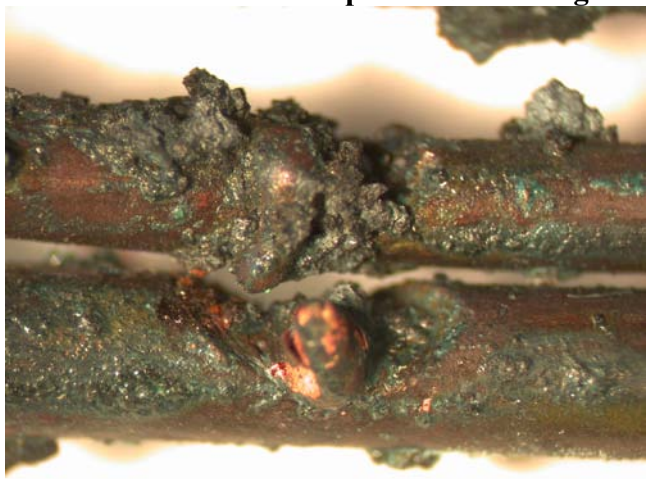

Figure 540 - Microscope image indicating two of the three conductors involved with this arcing location The limited depth of field has rendered the lower bead within a notch out of focus.

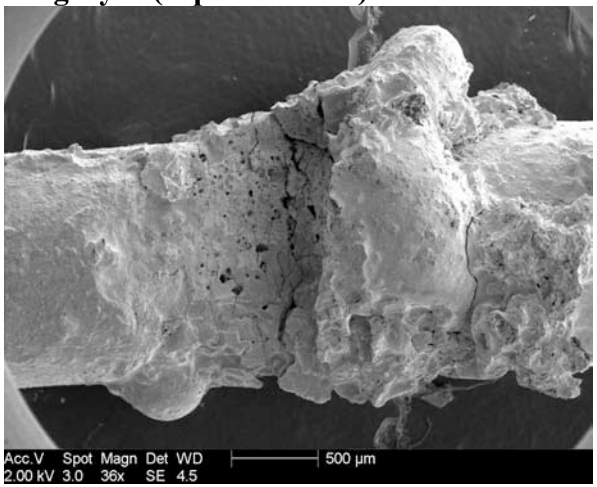

Figure 541 - SEM image if the top conductor in the microscope image. This is a large bead within a notch with a clear demarcation area at the edge of the notch.

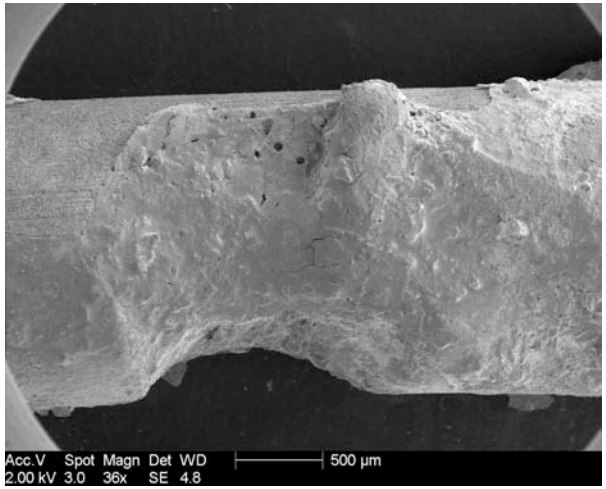

Figure 542 - SEM image of the notch not indicated in the microscope figure 540.

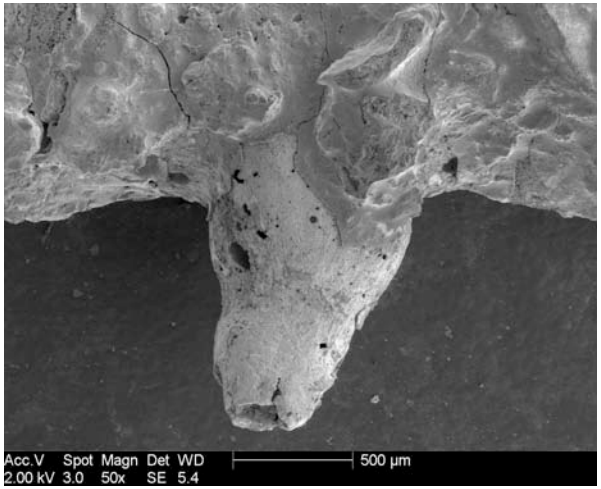

Figure 543 - SEM image magnifying the elongated bead that is out of focus in the microscope image of figure 540.

Confocal laser scanning microscope images for exhibit 078 – arcing category D (experiment 23)

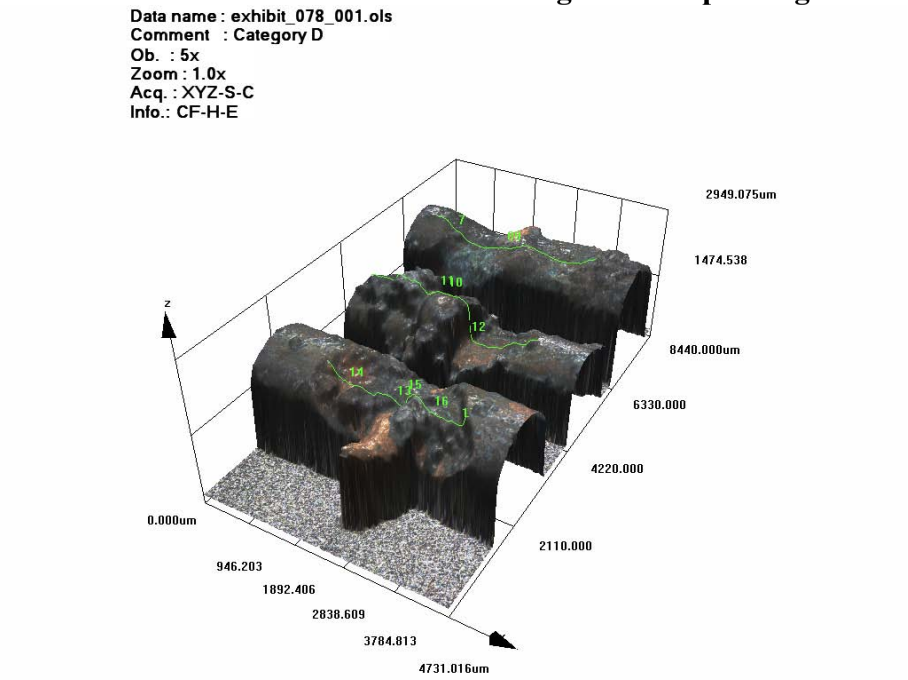

Figure 544 - LEXT image of exhibit 078 detailing all three of the conductors that form this exhibit.

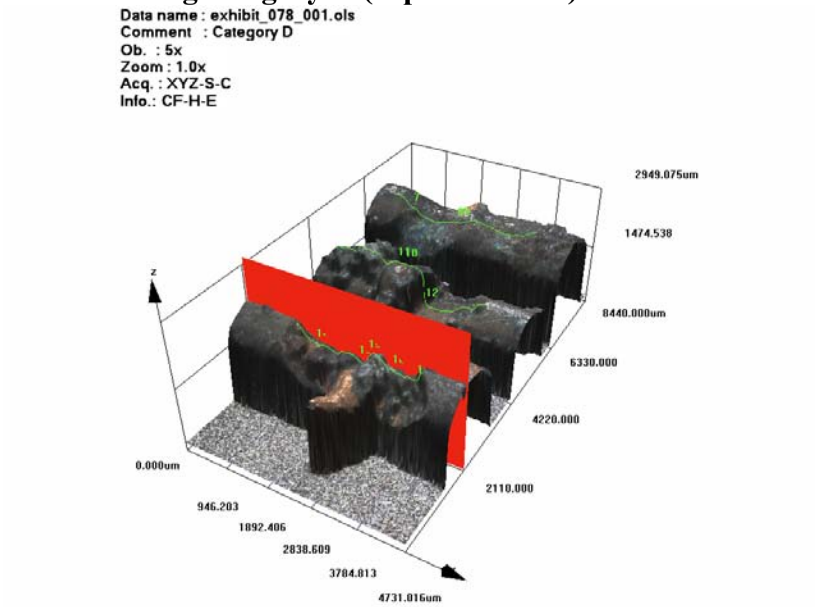

Figure 545 - LEXT image with the “slice tool” in use in the LEXT software that was used to create the profile in fig 546.

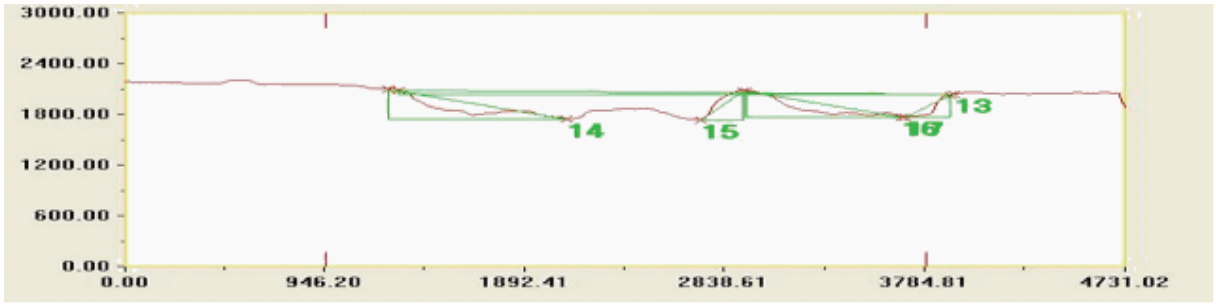

Figure 546 - LEXT profile and measurements (in microns) of the lower conductor detailed in figure 545.

Microscope images for exhibit 079 - arcing category D (experiment 23)

Figure 547 - Microscope images of exhibit 079. Overview of exhibit with damage to one of the three conductors, at 6x magnification.

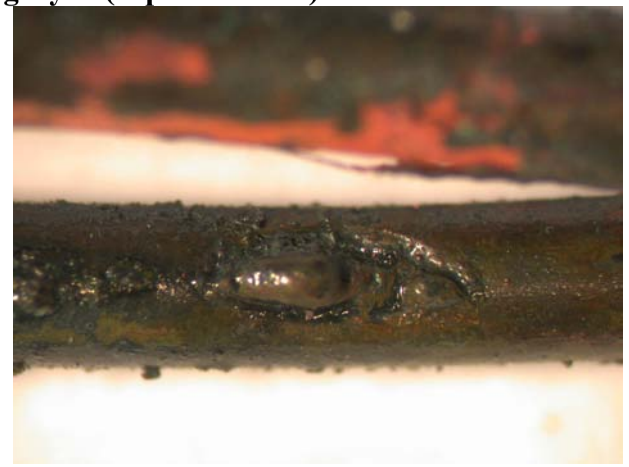

Figure 548 - Microscope image at 20 x magnification, detailing the bead within a small notch.

Figure 549 - Contrasting microscope view at 20x magnification detailing the bead's profile.

Figure 550 - 40x magnification microscope image of the bead and notch. This image details the demarcation between the localised metallic damage and the un-damaged conductor.

Microscope and SEM images for exhibit 080 - arcing category I (experiment 23)

Figure 551 - Microscope image of exhibit 080 detailing the shallow metallic damage to both conductors.

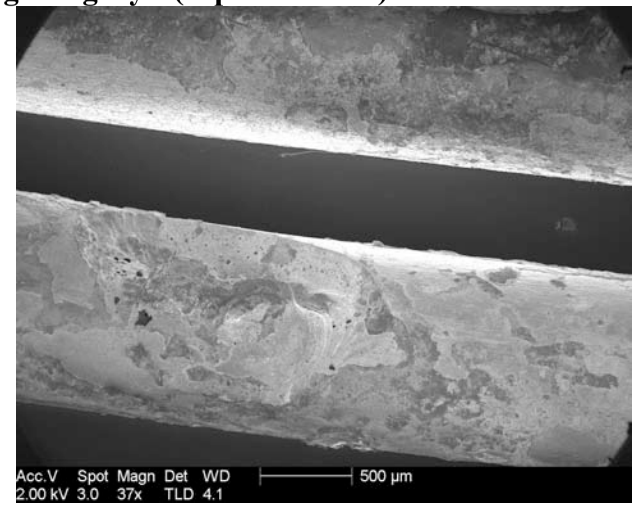

Figure 552 - SEM image highlighting the shallow notch damage of the bottom conductor in figure 551.

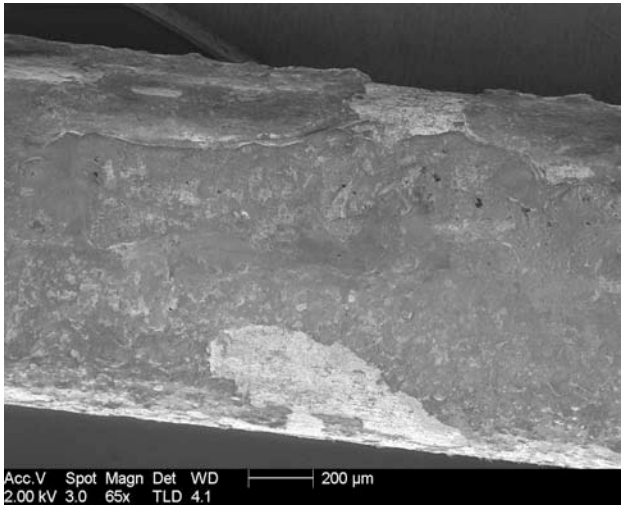

Figure 553 - SEM image of the minimal melting damage to the top conductor in figure 551.

Confocal laser scanning microscope images for exhibit 080 – arcing category I (experiment 23)

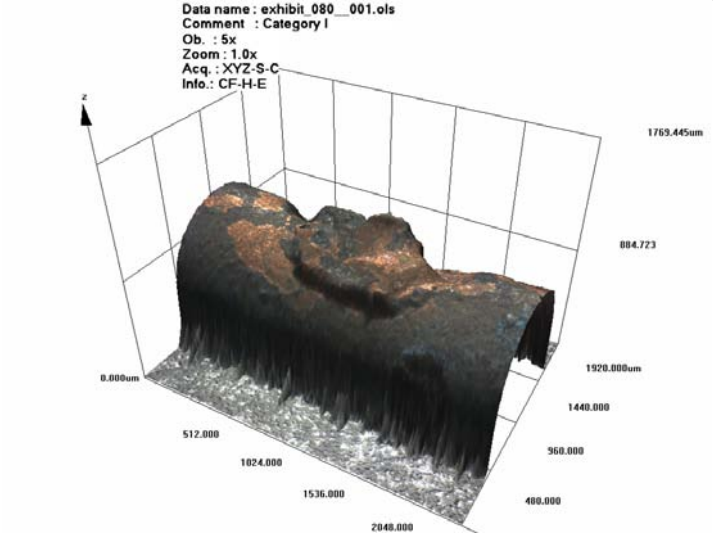

Figure 554 - LEXT image of exhibit 080, figure 552 is the comparison SEM image.

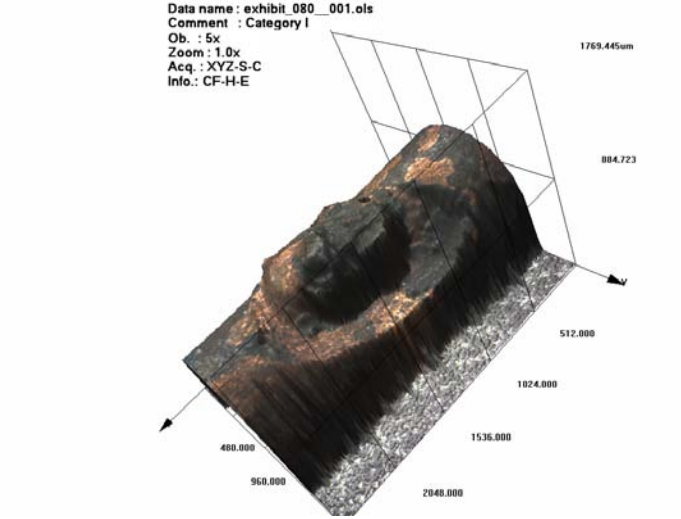

Figure 555 - LEXT image rotated 180 degrees in the 3-D software.

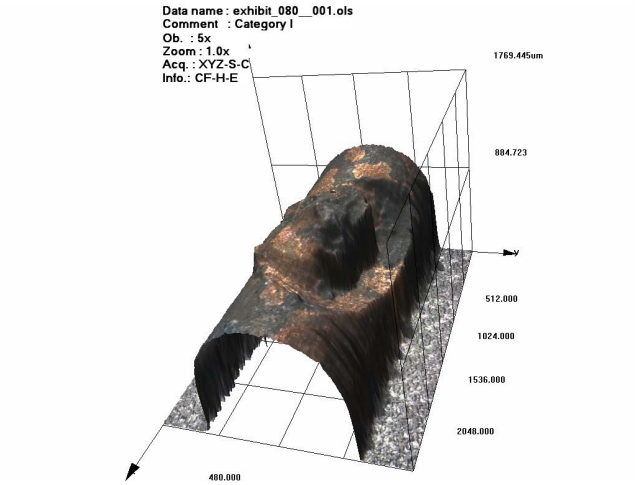

Figure 556 - LEXT image further rotated. A full-size version of this image is detailed in figure 558.

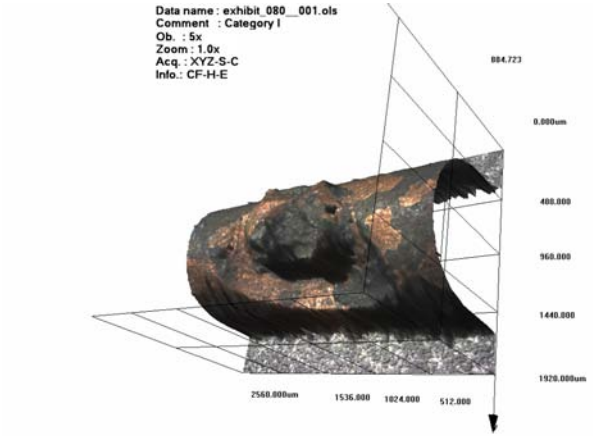

Figure 557 - LEXT image with the axis rotated for a contrasting view of the bead within a notch.

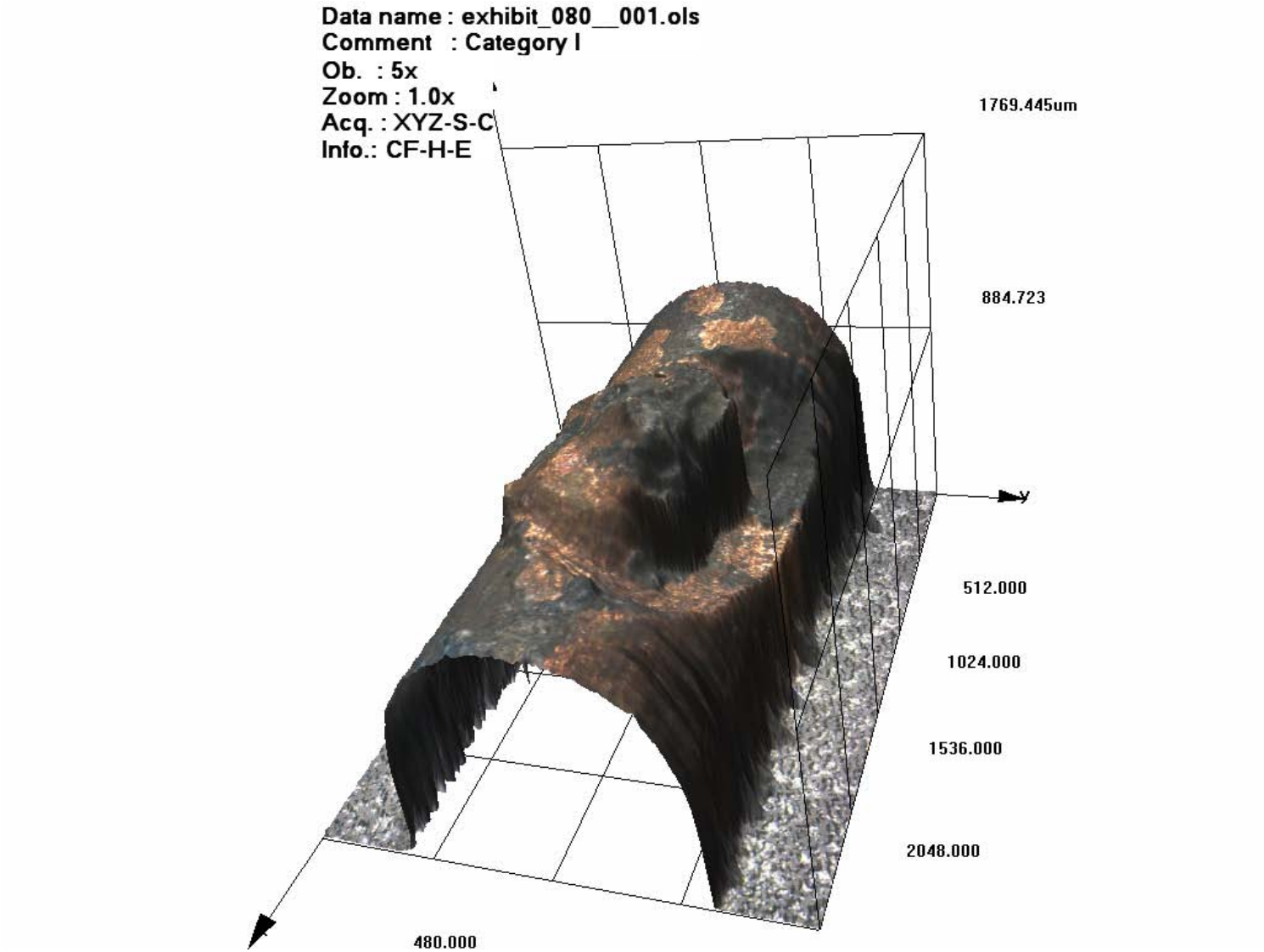

Figure 558 - Full-size LEXT image for exhibit 080 detailing the demarcation area between the localised metallic (arcing) damage to the conductor and the undamaged area.

Microscope and SEM images for exhibit 081 - arcing category E (experiment 23)

Figure 559 - Microscope image of exhibit 081 with large multiple beads to all three conductors.

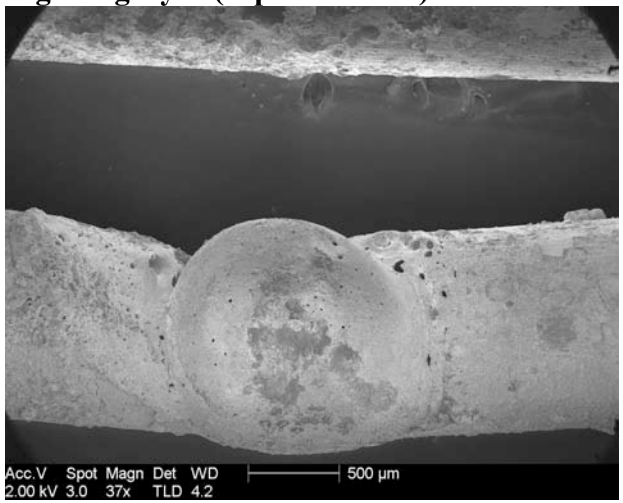

Figure 560 - SEM image of the top conductor of the three depicted in figure 559.

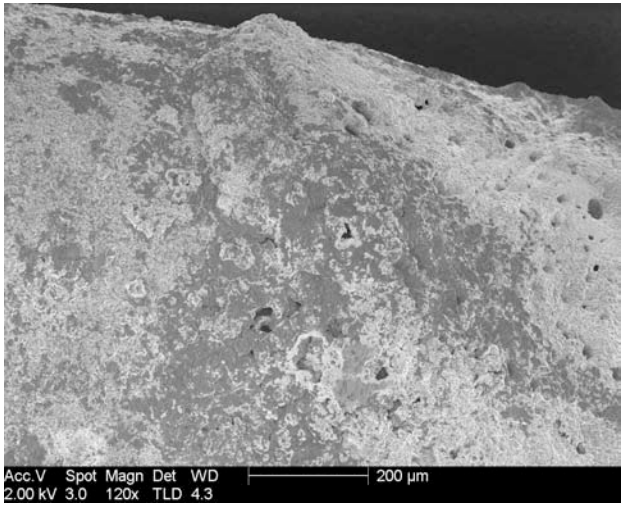

Figure 561 - SEM image at 120x magnification detailing the left edge of the notch in figure 560.

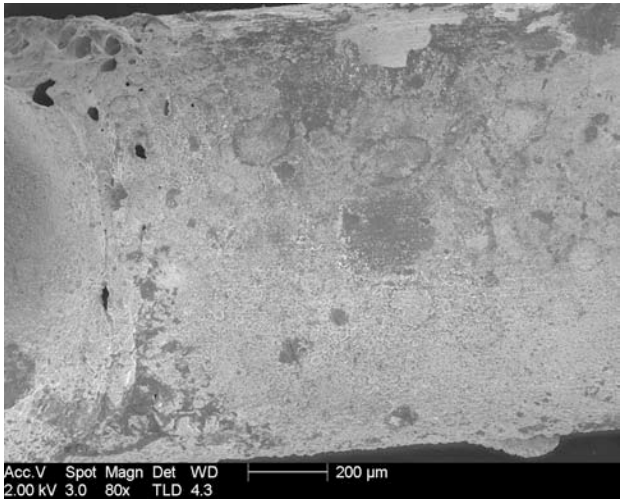

Figure 562 - SEM image at 80x magnification detailing the right edge of the notch and the clear demarcation in figure 560.

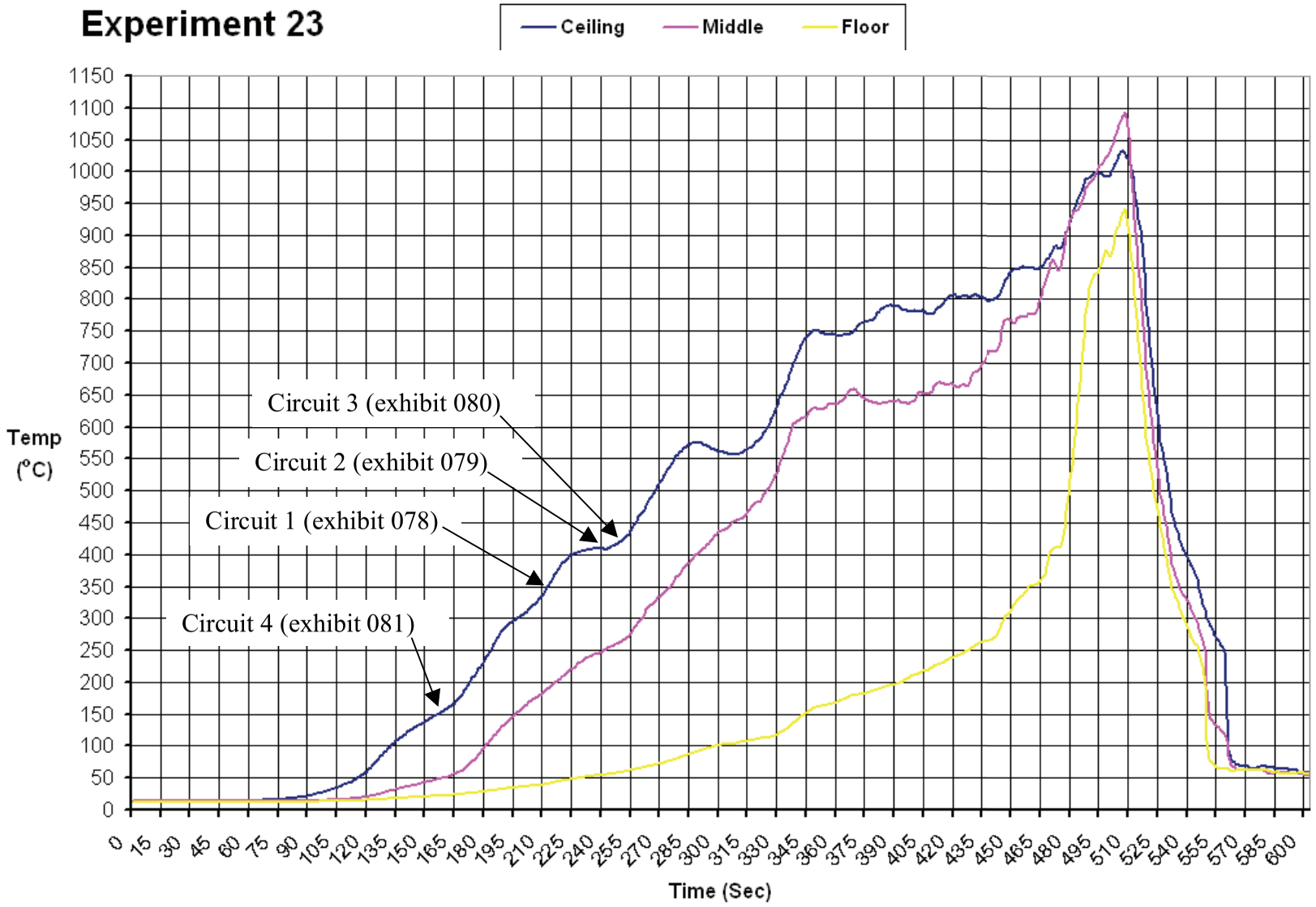

Figure 563 - Time temperature graph for experiment 23

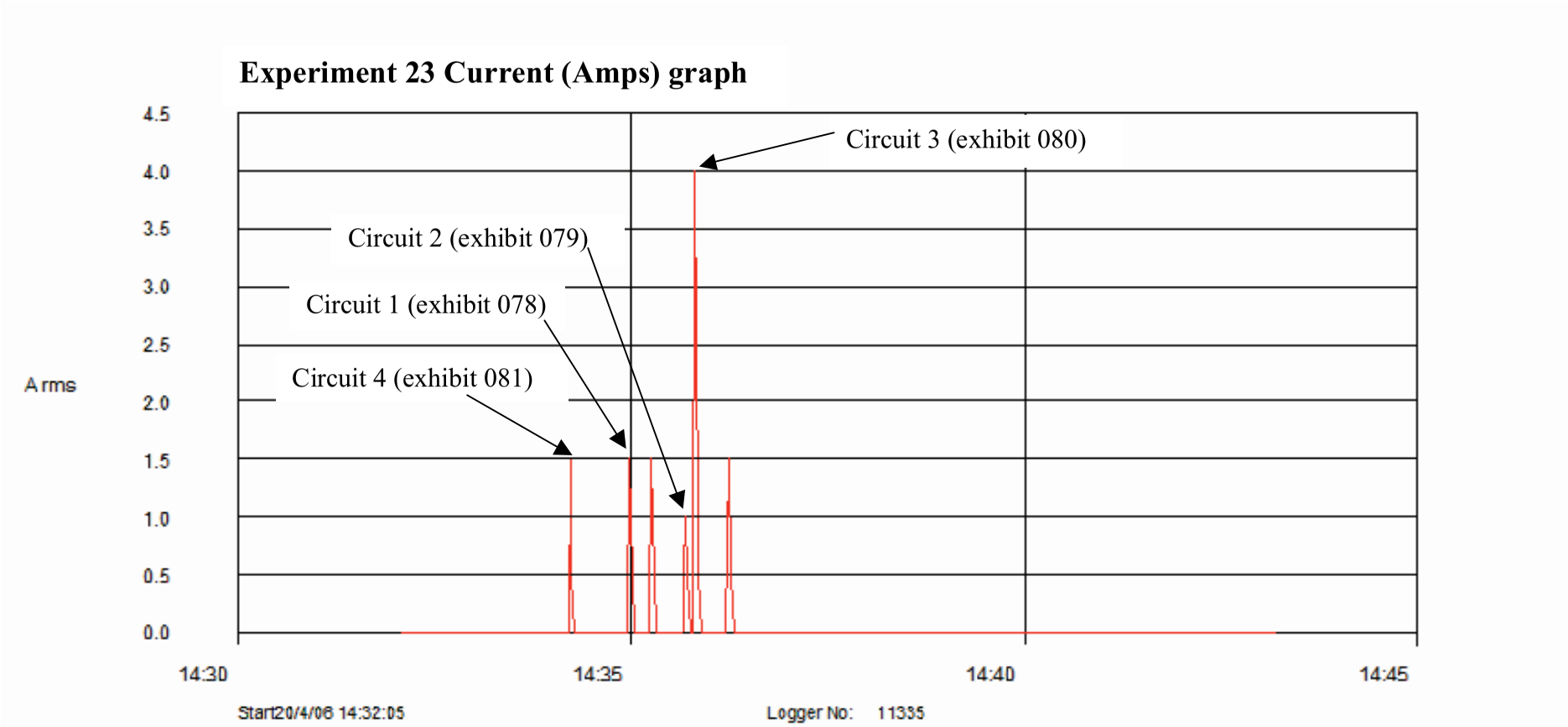

Figure 564 - Current (Amps) graph for experiment 23 detailing the operation of the circuit breakers and the fault current

Experiment 24

Figure 565 – “Scenario B” 11 May 2006

Circuit number	MCB operating time from ignition
4	4:38 minutes
1	4:57 minutes
3	5:32 minutes
2	5:32 minutes

Table 27 – circuit breaker operation data

The fire in experiment 24 (scenario B) originated in a refuse bin located in the rear left corner of the compartment (as viewed from the entrance door).

The ceiling temperature reached 850° C at 12 minutes, with the middle thermocouple recording 675° C at this time. The floor thermocouple recorded a maximum of 100° C. The burn patterns of the post-fire compartment suggested that it reached flashover conditions. The compartment configuration may have protected the floor thermocouple.

Arcing damage was located on circuit 1 – on the rear wall 500mm from the left wall.

Arcing damage was located on circuits 2 and 3 – 800mm from the left wall and also 1830mm from the left wall and 1000mm from the front wall.

Arcing damage was located on circuit 4 – 1140mm from the left wall and 1000mm from the rear wall.

Pre-fire and post-fire photographs of experiment 24

Figure 566 - Pre-fire photograph of experiment 24. The fire's area of origin is indicated with the black dashed line circle.

Figure 567 - Close-up view of the fire's area of origin – the rear left corner of the compartment.

Figure 568 - Post-fire view of the experiment. The white dashed line circle indicates the fire's area of origin.

Figure 569 - View of the fire damaged wiring above the fire's area of origin.

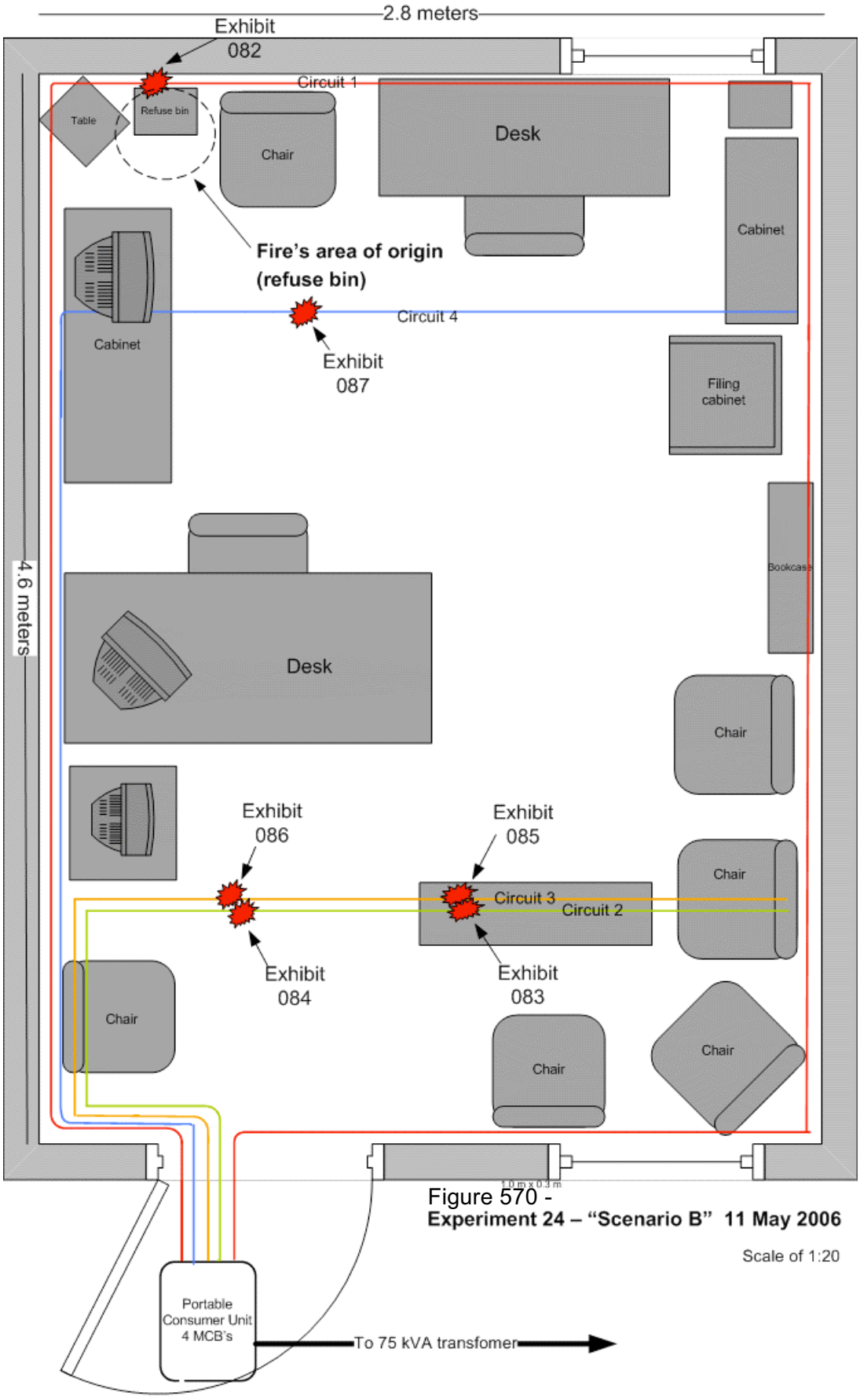

Figure 570 -
Experiment 24 – "Scenario B" 11 May 2006

Scale of 1:20

Microscope images for exhibit 082 - arcing category B (experiment 24)

Figure 571 - Microscope image of exhibit 082. The top conductor is the protective earth conductor.

Figure 572 - 20x magnification of the lower conductor with a bead located within a notch.

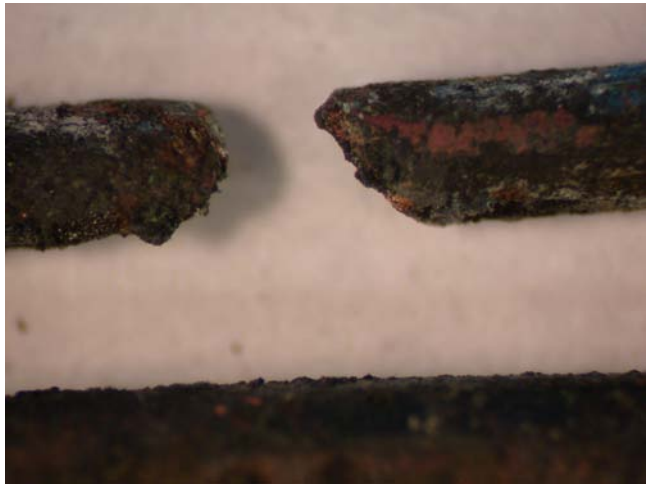

Figure 573 - 20x magnification image of the severed ends of the top conductor.

Figure 574 - A molten bead was attached to the fixing screw adjacent to the arcing damage for this exhibit.

Microscope and SEM images for exhibit 083 - arcing category D (experiment 24)

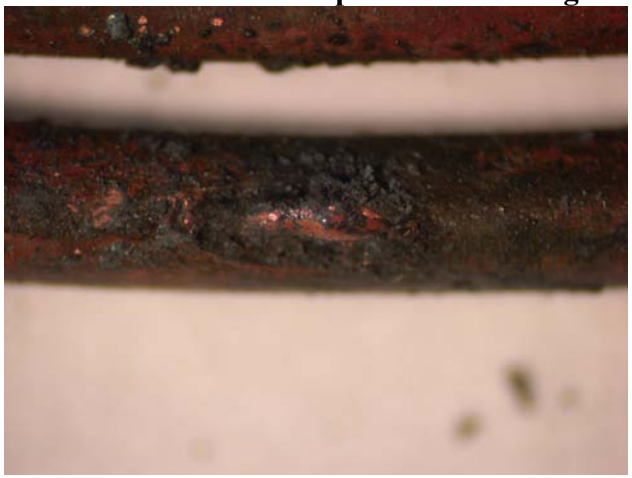

Figure 575 - Microscope image of exhibit 083. This arcing damage is one of two areas affecting this circuit. This exhibit was furthest away from the electrical source.

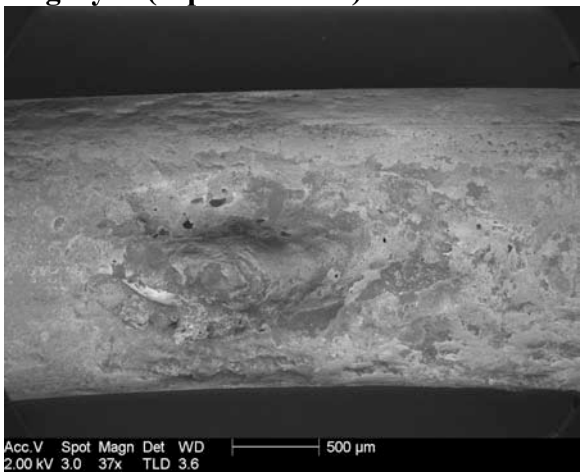

Figure 576 - SEM image of the small elongated bead located within the notch.

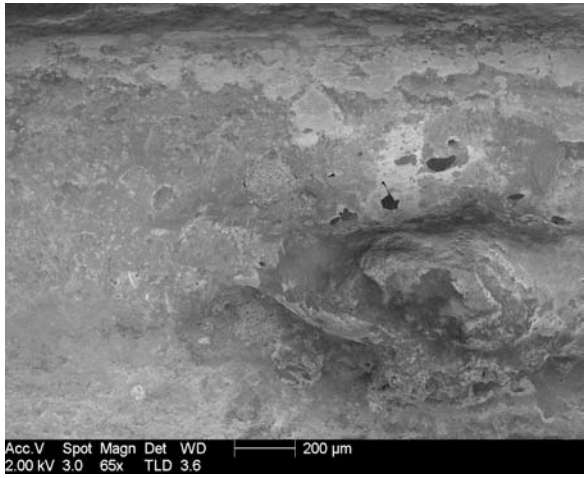

Figure 577 - SEM image at 65x magnification indicating the clear demarcation area between the edge of the notch and the undamaged conductor.

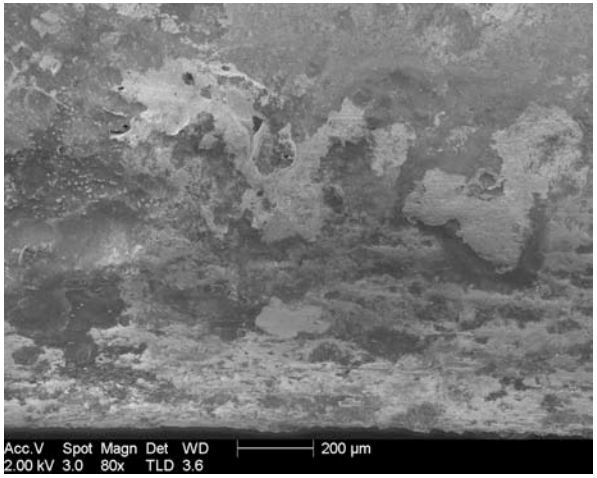

Figure 578 - SEM image at 80x magnification detailing the right edge of the notch.

Microscope and SEM images for exhibit 084 - arcing category C (experiment 24)

Figure 579 - Microscope image of exhibit 084. This is the second area of arcing on this circuit that was closest to the electrical source.

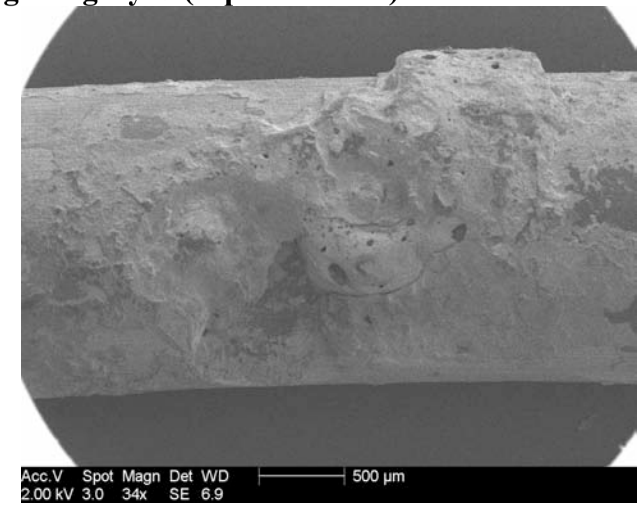

Figure 580 - SEM image at 34x magnification. The image contrast setting is lower than ideal.

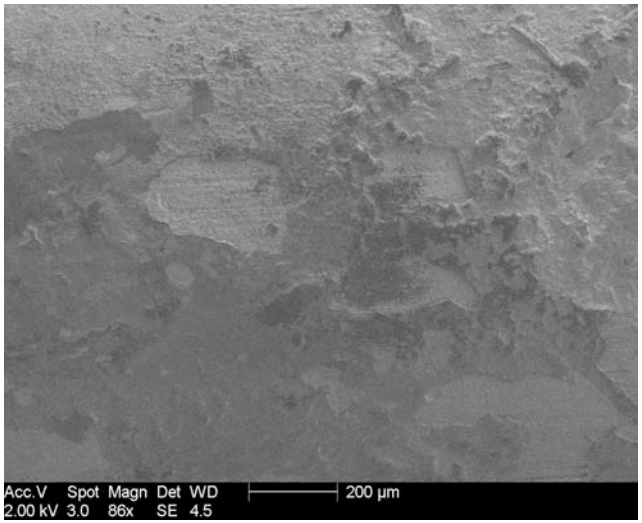

Figure 581 - SEM image at 86x magnification detailing the left area of the notch.

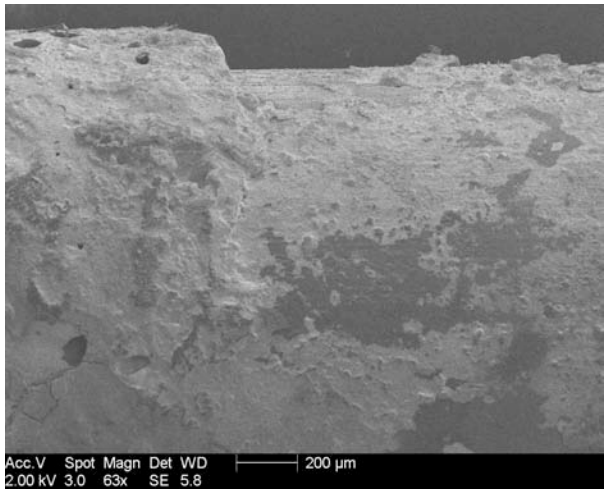

Figure 582 - SEM image at 63x magnification detailing the right edge of the arcing damage.

Confocal laser scanning microscope images for exhibit 084 – arcing category C (experiment 24)

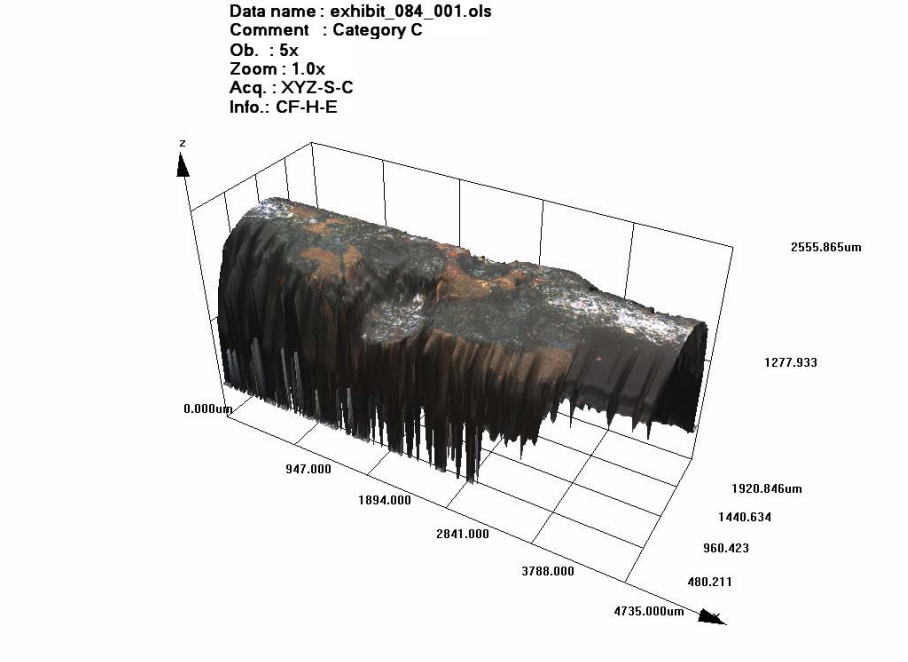

Figure 583 - LEXT image of exhibit 084 detailing the overall localised melting damage.

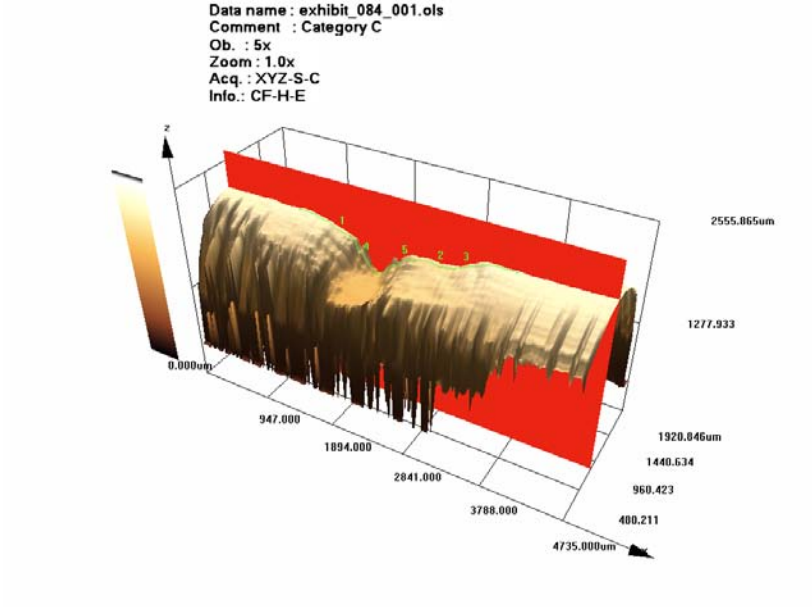

Figure 584 - LEXT image with the “slice tool” in use to create a profile and measurements.

Figure 585 - Profile of the notch in the location shown by the “slice tool” in figure 584.

Microscope images for exhibit 085 - arcing category B (experiment 24)

Figure 586 - Microscope image of exhibit 085 with one of the three conductors affected by localised melting.

Figure 587 - Microscope image of the left severed conductor at 20x magnification.

Figure 588 - Microscope image of the right severed conductor at 20x magnification.

Figure 589 - Left severed end detailing the demarcation area between the arcing damage and the un-damaged conductor.

Microscope images for exhibit 086 - arcing category D (experiment 24)

Figure 590 - Microscope image of exhibit 086 with localised melting affecting one of the three conductors.

Figure 591- Microscope image of the bead within the notch and the adjacent elongated bead at 20x magnification.

Figure 592 – The exhibit has been rotated 180 degrees detailing the opposite side of the arcing damage to figure 591.

Microscope images for exhibit 087 - arcing category D (experiment 24)

Figure 593 - Microscope image of exhibit 087. Two of the conductors are affected by this arcing damage.

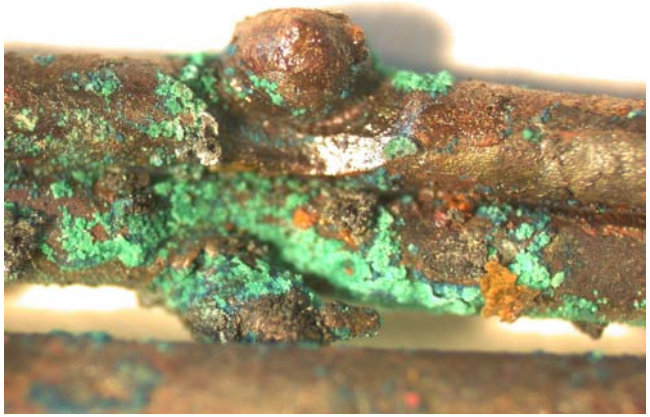

Figure 594 - Microscope image at 20x magnification of the top conductor in figure 593.

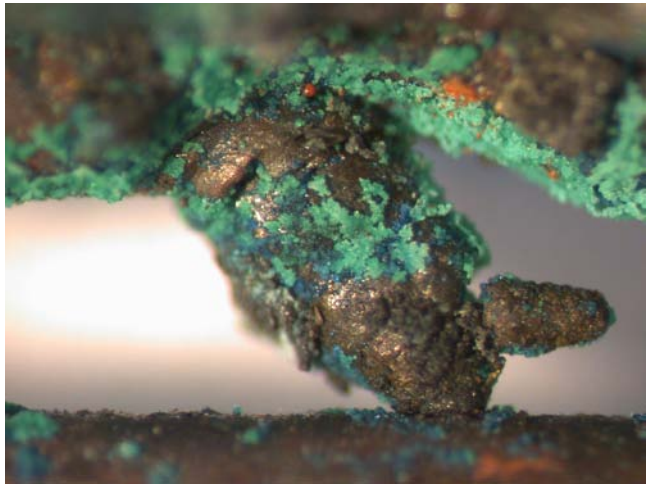

Figure 595 – A 60x magnification of the long bead in the middle conductor of figure 593.

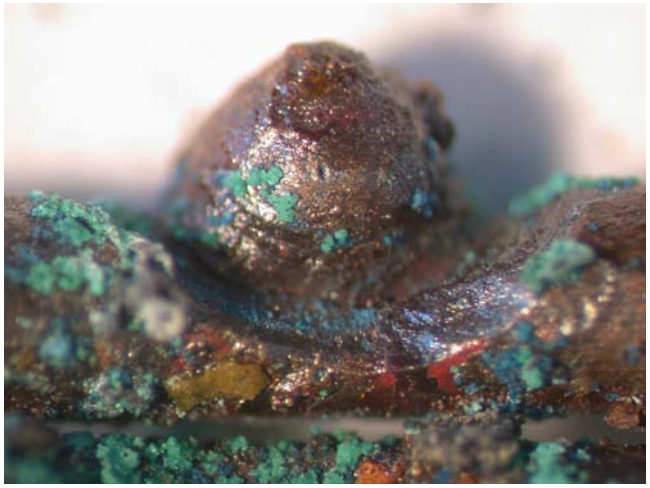

Figure 596 - 60x magnification of figure 594. This details the demarcation area at the edge of the notch

Figure 597 - Time temperature graph for experiment 24

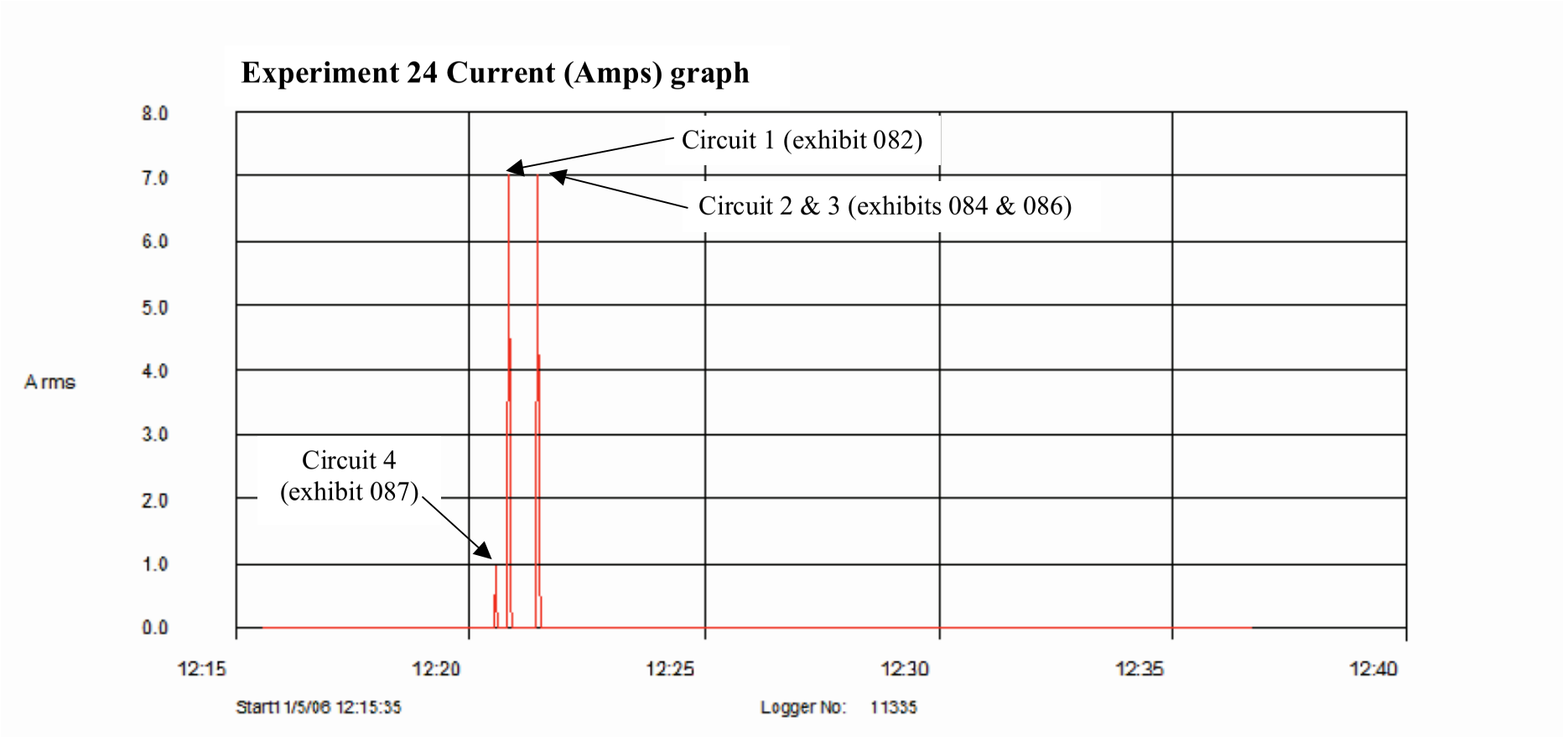

Figure 598 - Current (Amps) graph for experiment 24 detailing the operation of the circuit breakers and the fault current

Experiment 25

Figure 599 – “Scenario D” 11 May 2006

Circuit number	MCB operating time from ignition
4	0:58 minutes
1	1:14 minutes
3	1:14 minutes
2	1:20 minutes

Table 27 – circuit breaker operation data

The fire in experiment 25 (scenario D) originated in three separate areas. They were at a large armchair located against the centre of the rear wall, a two-seat settee adjacent to the left wall and a two-seat settee adjacent to the front wall under the window.

The fire developed very rapidly with the ceiling temperature reaching 1000° C in 2.5 minutes. The middle thermocouple recorded 975° C and the floor thermocouple recorded 625° C at this time. The compartment reached flashover conditions just before being extinguished at 2.5 minutes from the time of ignition.

Arcing damage was located on circuit 1 – on the rear wall 1500mm from the left wall.

Arcing damage was located on circuits 3 and 2 – 1900mm from the left wall on the ceiling and 1000mm from the front wall.

Arcing damage was located on circuit 4 – 770mm from the left wall and 1000mm from the rear wall.

Pre-fire and post-fire photographs of experiment 25

Figure 600 - Pre-fire photograph of experiment 25 indicating the three areas of origin for this fire.

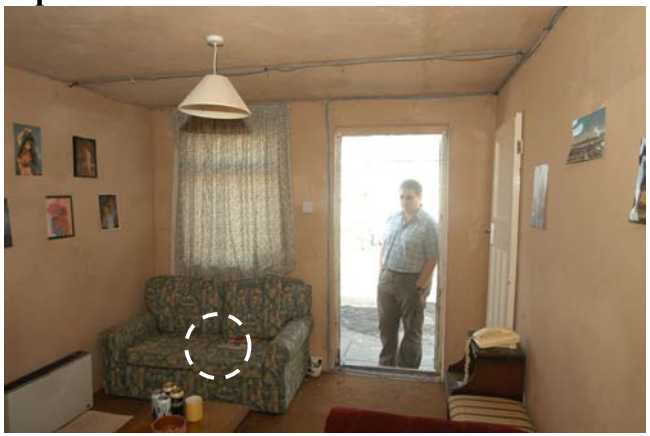

Figure 601 - Pre-fire photograph indicating the third area of origin for this fire on the settee adjacent to the entrance door.

Figure 602 - Post-fire photograph of the compartment. The circles indicate the fire's three areas of origin.

Figure 603 - Post-fire view of the front area of the compartment with the entrance door in the background.

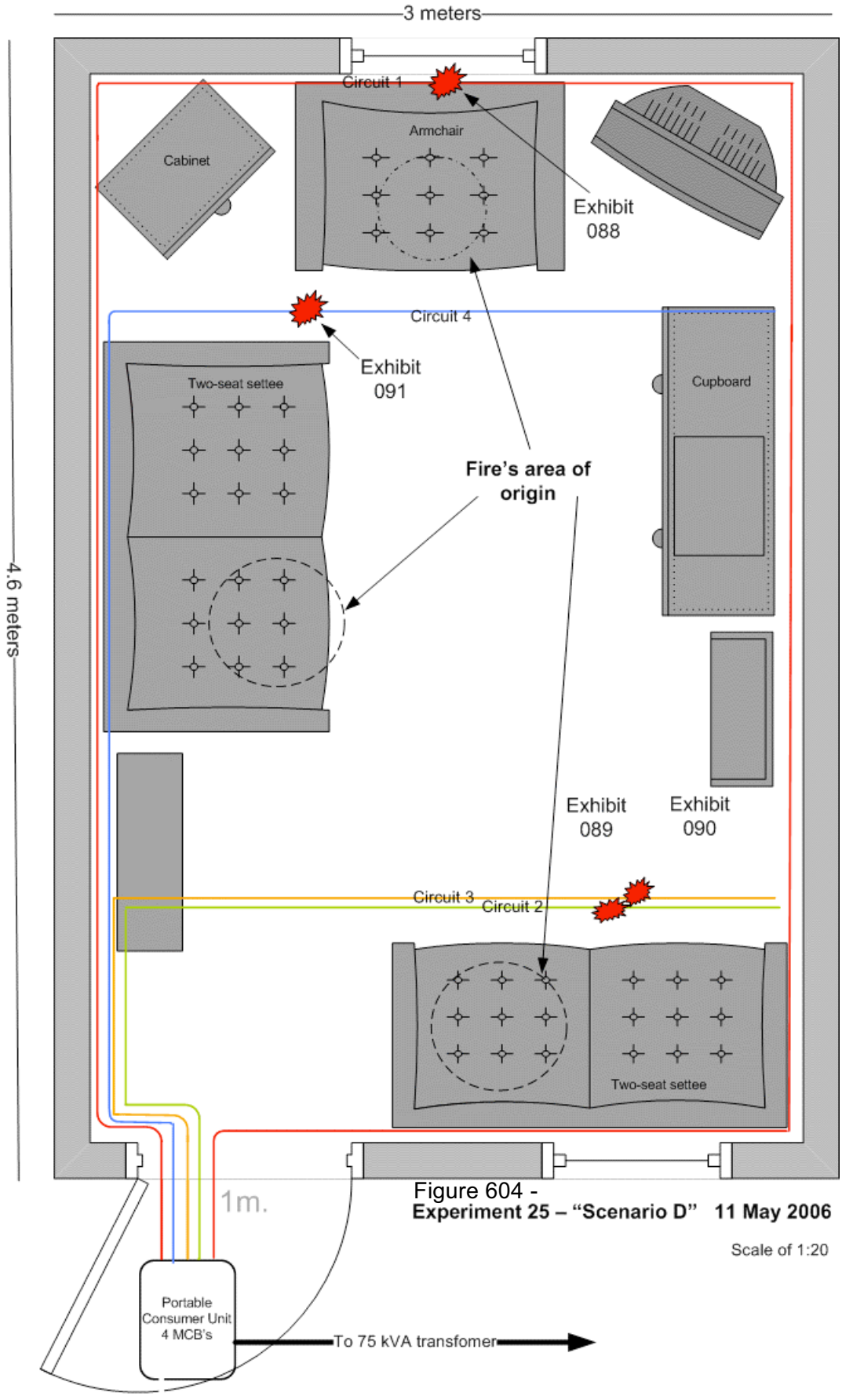

Figure 604 -
Experiment 25 – "Scenario D" 11 May 2006

Scale of 1:20

Microscope and SEM images for exhibit 088 - arcing category A (experiment 25)

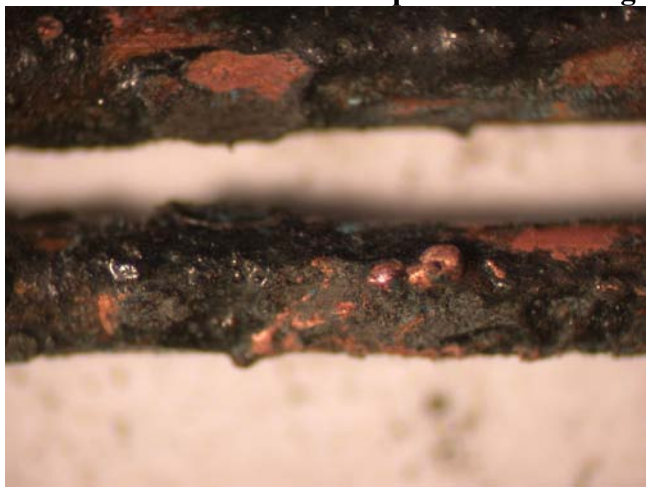

Figure 605 - Microscope image of one of the two conductors affected by the arcing damage.

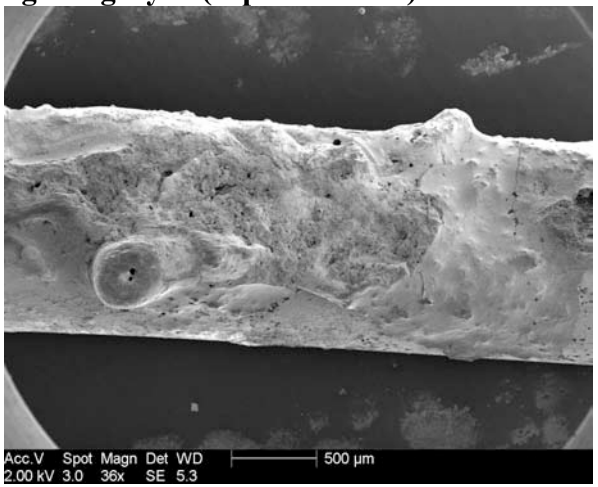

Figure 606 - SEM image of the conductor indicated in figure 605.

Figure 607 - Microscope image of the second conductor with arcing category A.

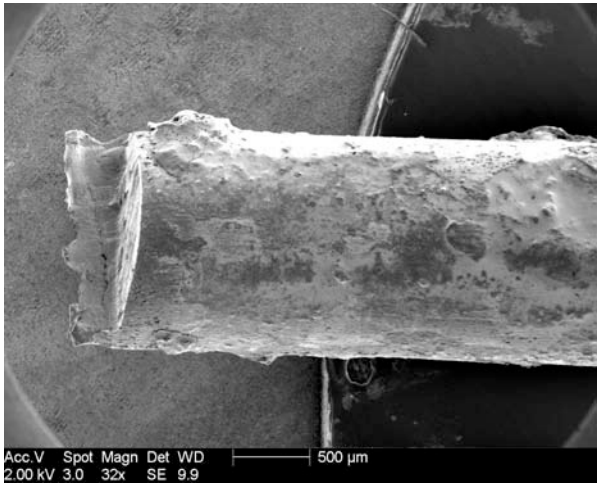

Figure 608 - The right side of this SEM image indicates the edge of the arcing damage in figure 606 and the demarcation. The left side is the cut end of the conductor.

Microscope images for exhibit 089 - arcing category B (experiment 25)

Figure 609 - Microscope image of exhibit 89 detailing all the conductors. The arcing damage is confined to the top conductor.

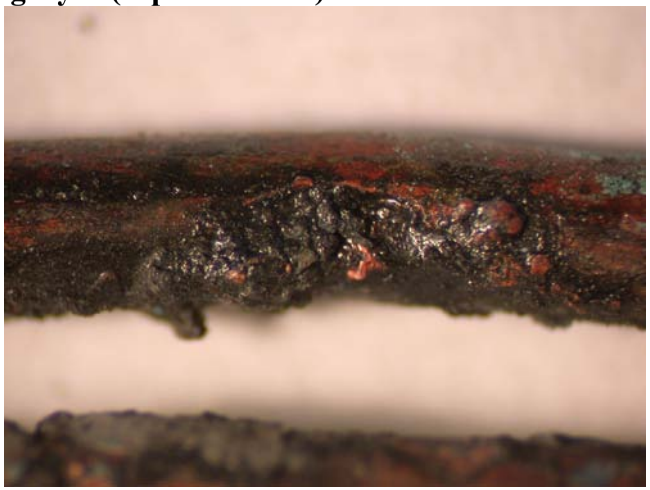

Figure 610 – A microscope image of the notch with beads attached to the edge of the notched area.

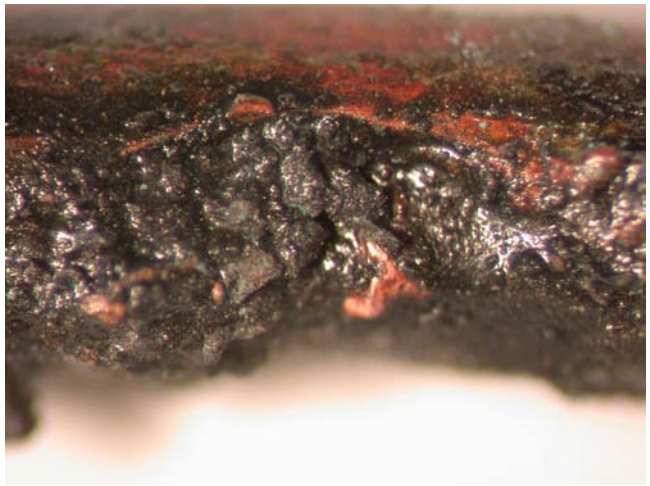

Figure 611 - Microscope image at 40x magnification detailing the PVC debris in the notch and the demarcation area at the top edge of the notch.

Microscope and SEM images for exhibit 090 - arcing category H (experiment 25)

Figure 612 - Microscope image of exhibit 090. The conductor was welded to the fixing screw when recovered at the experiment scene.

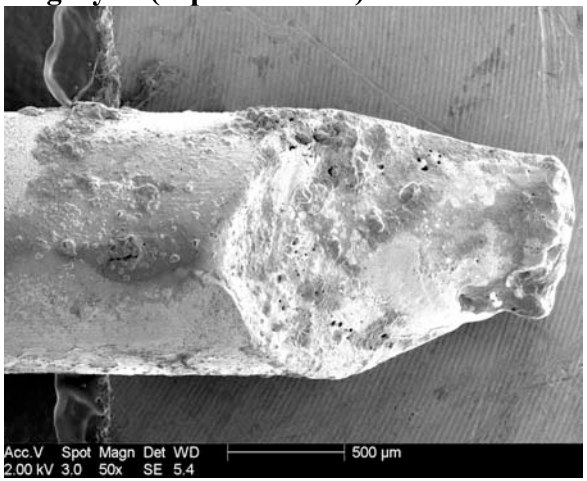

Figure 613 - SEM image of the conductor that was originally welded to the fixing screw until the ultrasonic cleaning.

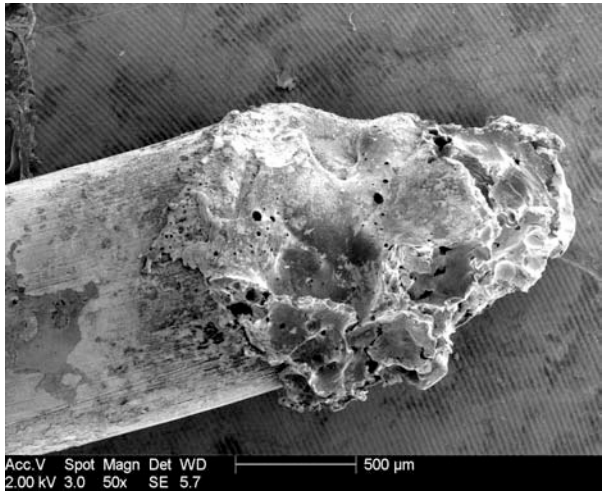

Figure 614 - SEM image of the right severed conductor detailed in figure 612.

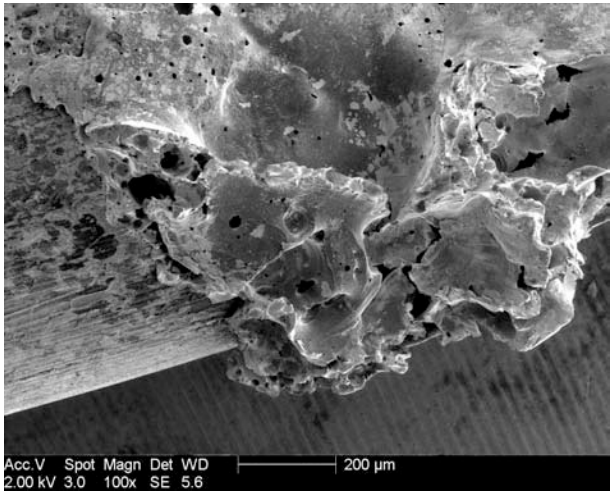

Figure 615 - SEM image at 100x magnification of the view in figure 614, detailing the demarcation area between the arcing damage and the undamaged conductor.

Confocal laser scanning microscope images for exhibit 090 – arcing category H (experiment 25)

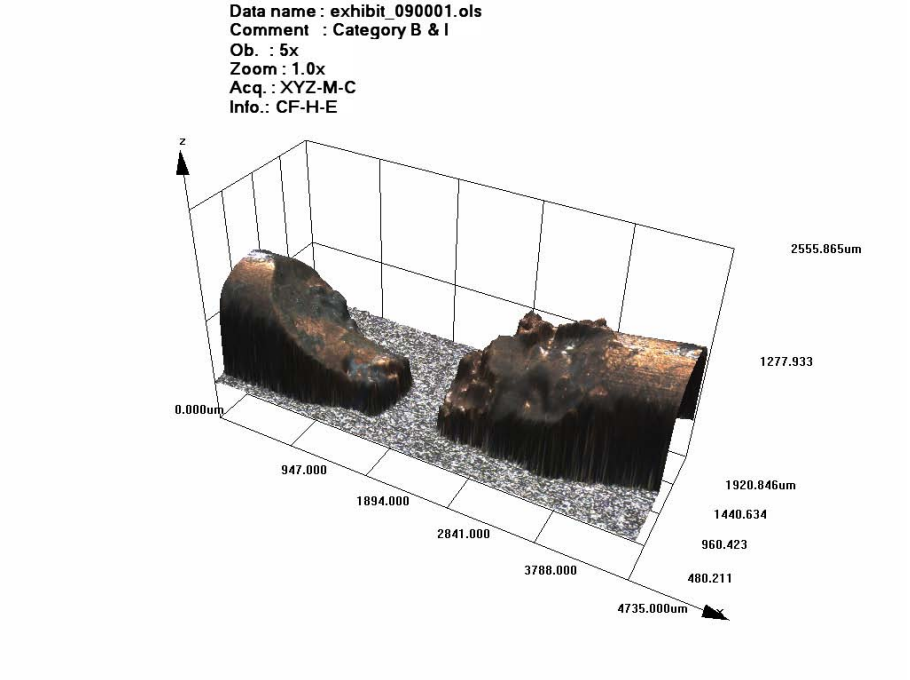

Figure 616 - LEXT image displaying both severed ends of the conductor that was originally welded to the fixing screw.

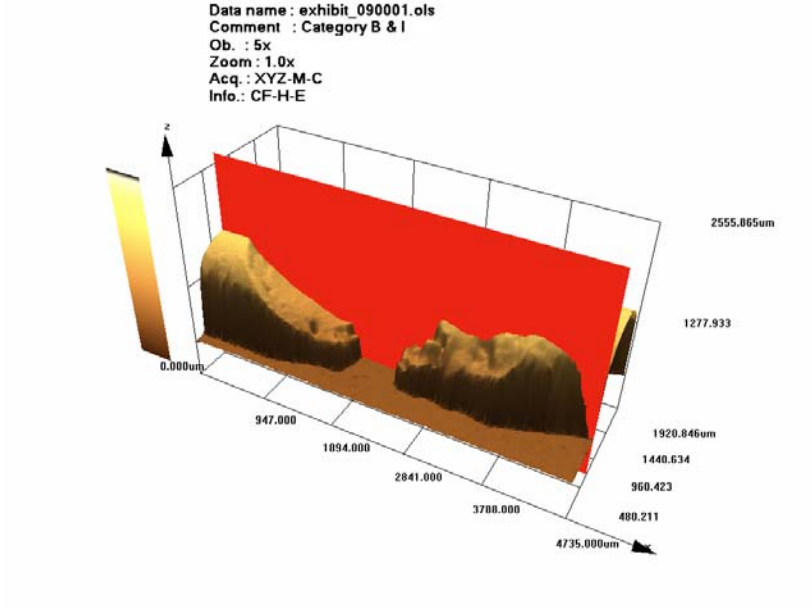

Figure 617 - LEXT image in “yellow” rendering mode with the software “slice tool” in use to create the profile in figure 618.

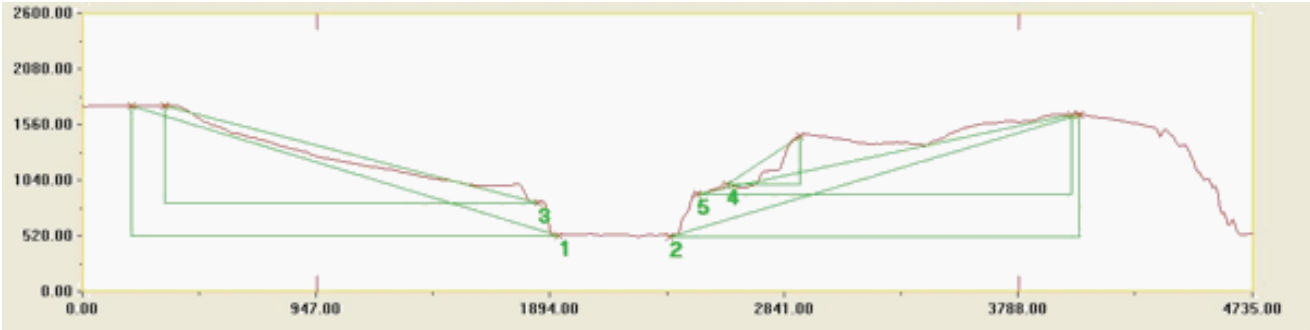

Figure 618 - LEXT profile produced including both severed ends using the LEXT software “slice tool” (all measurements are in microns)

Microscope images for exhibit 091 - arcing category B (experiment 25)

Figure 619 - Microscope image of exhibit 091. Two of the conductors are damaged and both have severed.

Figure 620 - The severed ends of the middle conductor detailed in figure 619.

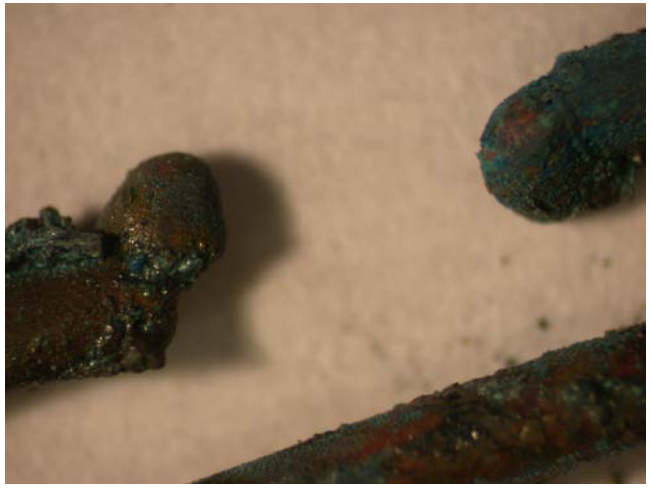

Figure 621 - The severed ends of the top conductor detailed in figure 619 at 20x magnification.

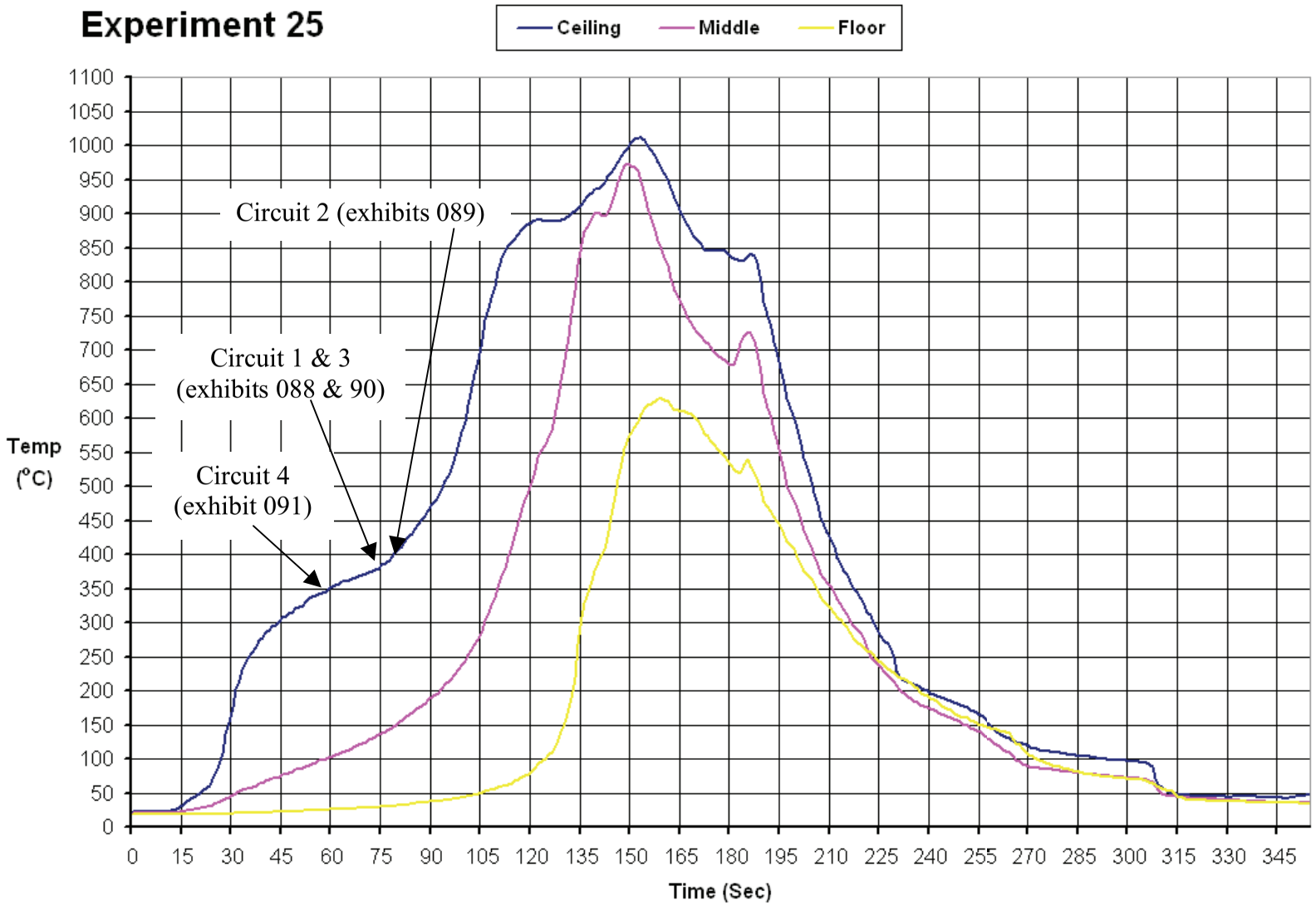

Figure 622 - Time temperature graph for experiment 25

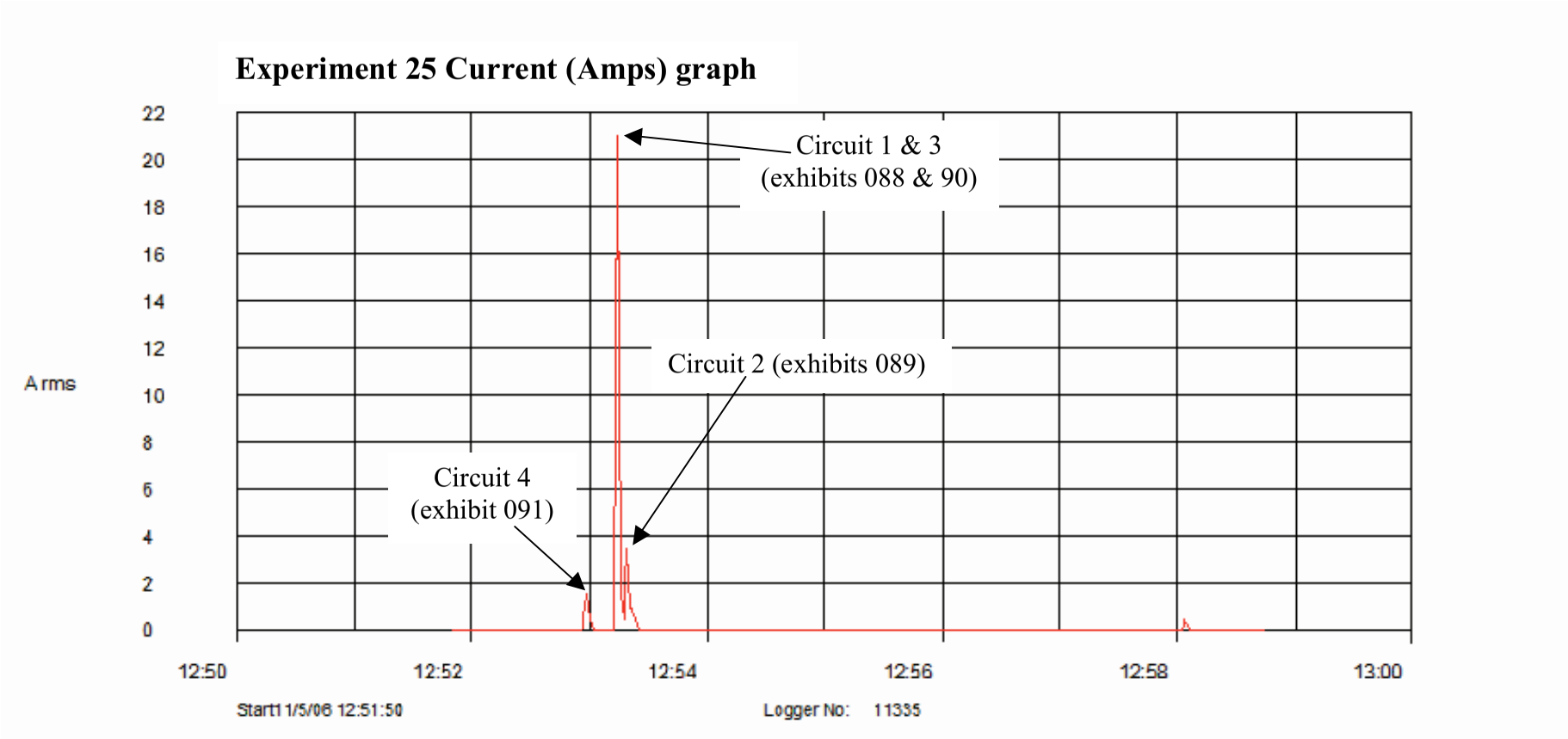

Figure 623 - Current (Amps) graph for experiment 25 detailing the operation of the circuit breakers and the fault current

Experiment 26

Figure 624 – “Scenario A” 11 May 2006

Circuit number	MCB operating time from ignition
4	1:40 minutes
1	1:43 minutes
3	2:00 minutes
2	2:02 minutes

Table 28 – circuit breaker operation data

The fire in experiment 26 (scenario A) originated in three separate areas. The areas of origin for this fire were located close to each other on the edge of the beds either side of the clothes rail and at the bottom of the clothes rail. The three points of origin create a zone 1.3m wide and 0.3m deep.

This fire developed rapidly with flashover conditions in the compartment attained at 3 minutes from the time of ignition. The ceiling temperature reached 900° C, with the middle thermocouple recording 820° C and the floor thermocouple recording 650° C.

Arcing damage was located on circuit 1 – on the rear wall 2370mm from the left wall.

No arcing damage was located on circuit number 2.

Arcing damage was located on circuit 3 – 870mm from the left wall on the ceiling and 1000mm from the front wall.

Arcing damage was located on circuit 4 – 960mm from the left wall and 1000mm from the rear wall.

Pre-fire and post-fire photographs of experiment 26

Figure 625 - Pre-fire photograph of experiment 26. The oval indicates the fire's area of origin between the singe beds.

Figure 626 - Pre-fire photograph detailing the electrical circuits fixed to the ceiling above the area of origin.

Figure 627 - Post-fire photograph, a 'U' shaped burn pattern was visible on the rear wall. Arcing damage was located above the area of origin on circuits 1 and 4 and is indicated by the white arrows.

Figure 628 - Post-fire view of the ceiling above the area of origin. The left arrow was the arcing location of circuit 4 and the right arrow was the location on circuit 1.

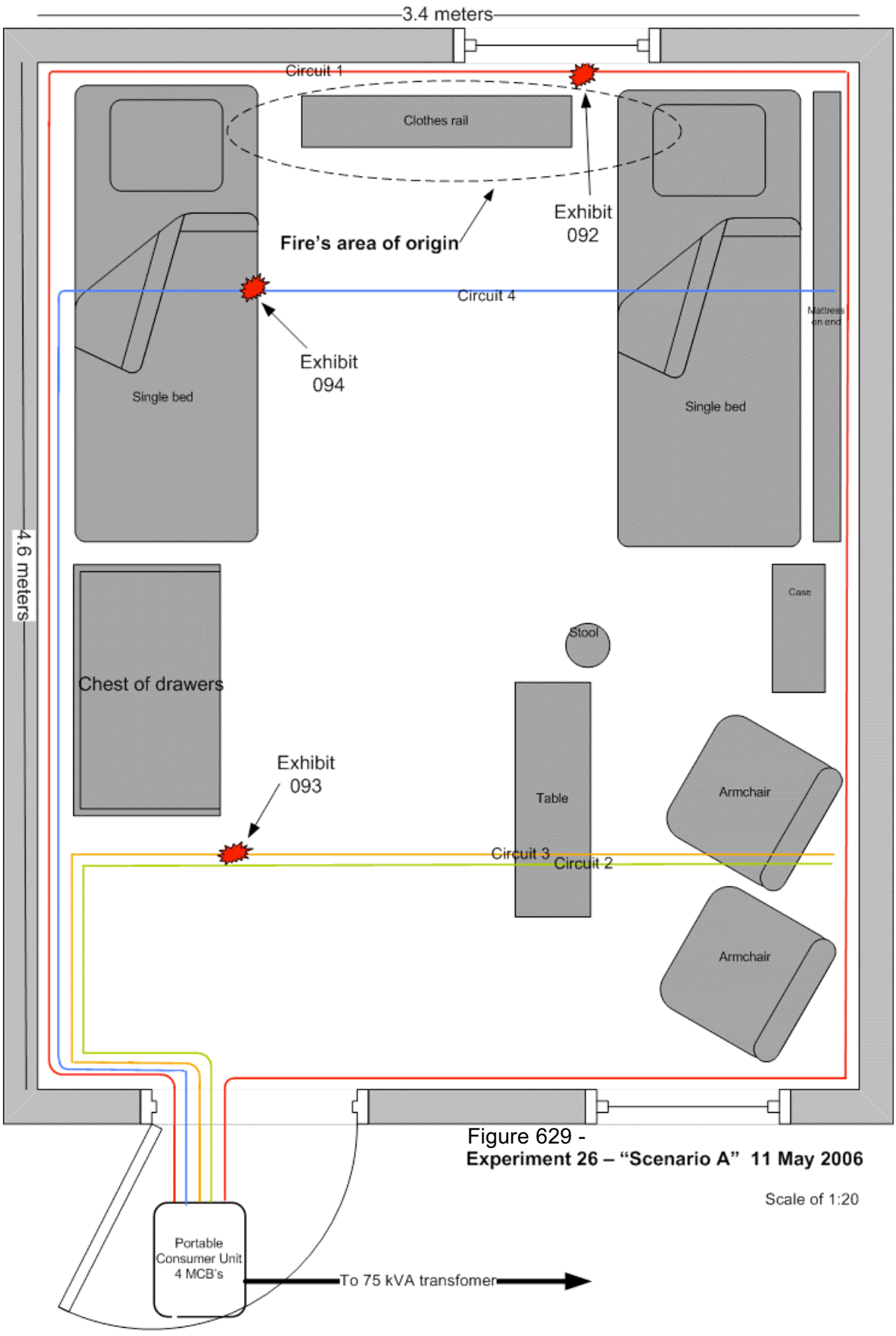

Figure 629 -
Experiment 26 – "Scenario A" 11 May 2006

Scale of 1:20

Microscope images for exhibit 092 - arcing category D (experiment 26)

Figure 630 - Microscope image of exhibit 092. The top and middle conductors are affected by arcing damage.

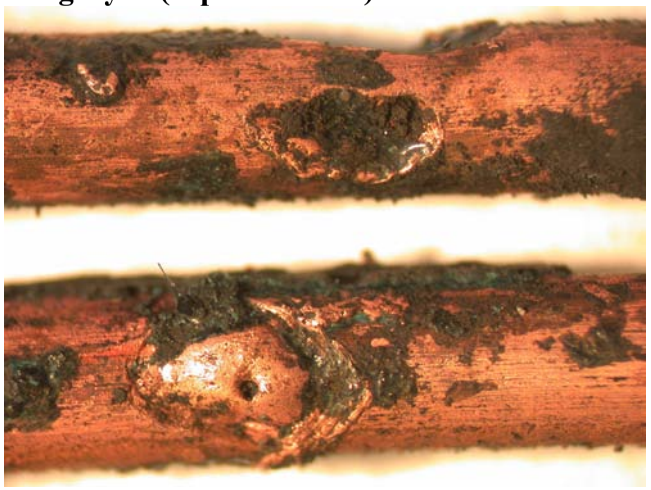

Figure 631 - View of both conductors and the notch damage on the conductors.

Figure 632 - View of the larger notch affecting the top conductor. The clear demarcation is indicated at the edge of the notch and the undamaged conductor.

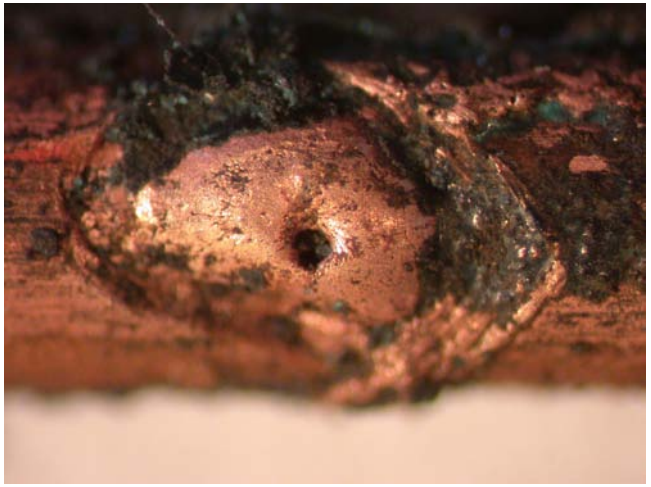

Figure 633 - 40x magnification microscope image of the lower conductor notch, with a bead within the notch.

Microscope and SEM images for exhibit 093 - arcing category B (experiment 26)

Figure 634 - Microscope image of exhibit 093. The middle and bottom conductors were severed.

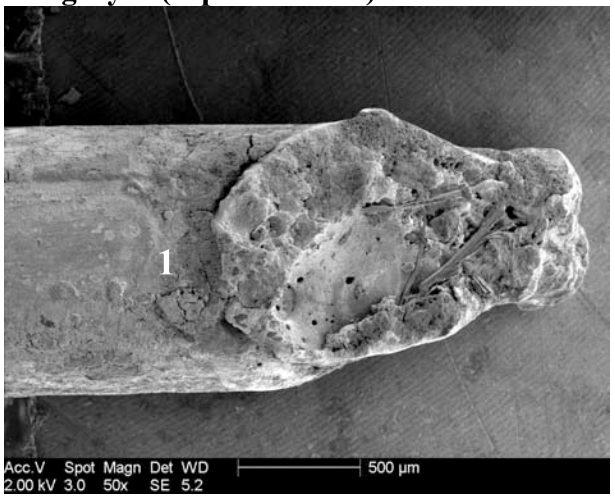

Figure 635 - SEM image of the right severed end of the middle conductor detailed in figure 634.

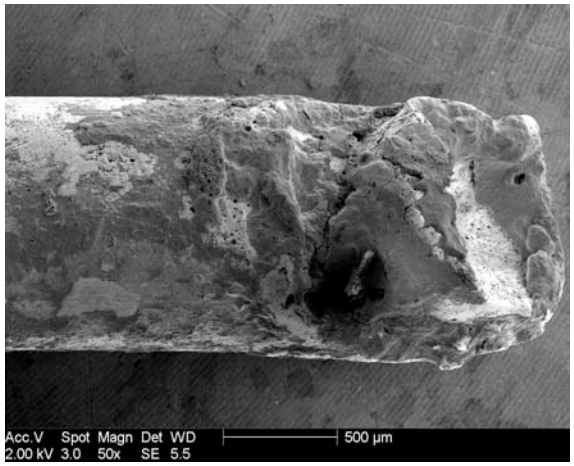

Figure 636 - SEM image of the left severed end of the middle conductor detailed in figure 634.

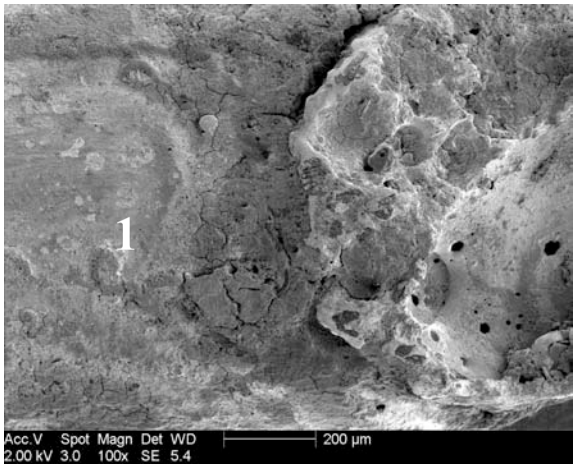

Figure 637 - SEM image of the demarcation area detailing the edge of the arcing damage in figure 635 above.

Confocal laser scanning microscope images for exhibit 093 – arcing category B (experiment 26)

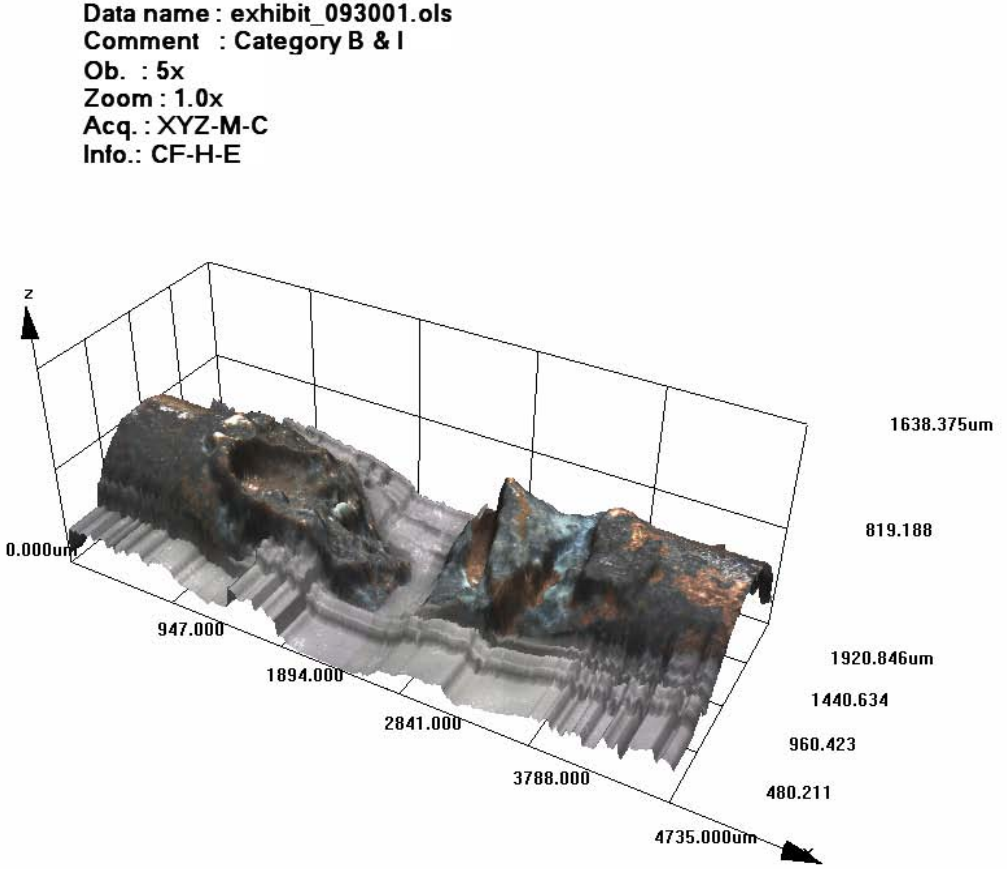

Figure 638 - LEXT image of exhibit 093. The laser scan was not set with sufficient layers to scan the entire exhibit; therefore the lower area of the conductors is not detailed. The resultant un-scanned edge effect appeared as a silver-grey colour texture.

Microscope images for exhibit 094 - arcing category C (experiment 26)

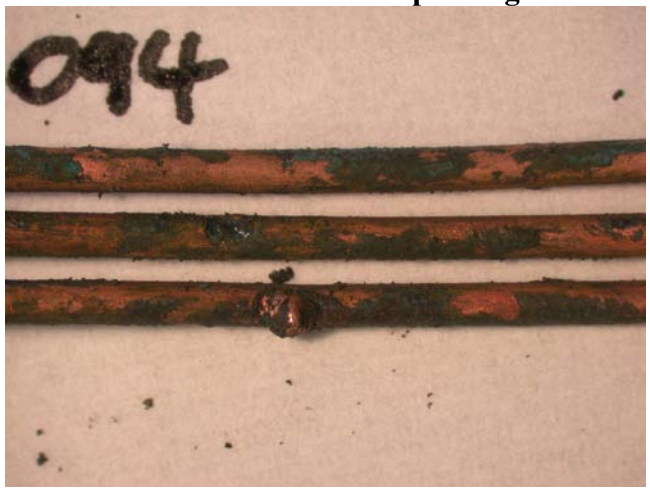

Figure 639 - Microscope image of exhibit 094. The middle and bottom conductors had localised metallic damage.

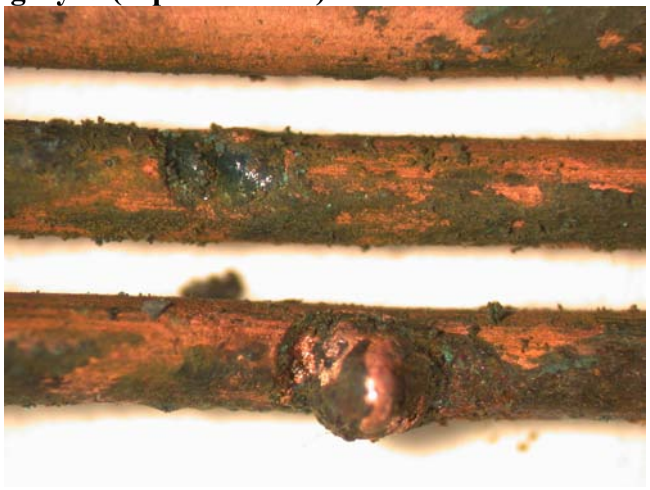

Figure 640 - 20x magnification detailing the localised melting to the middle and bottom conductors.

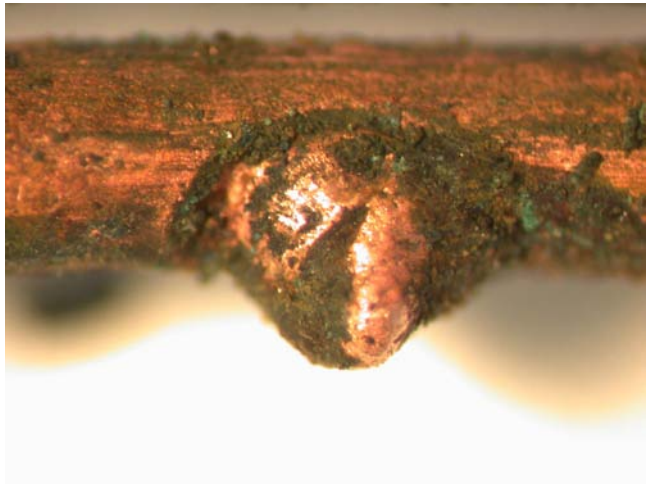

Figure 641 - 40x magnification of the notch with a bead within detailing the clear demarcation between the arcing damage and the undamaged conductor.

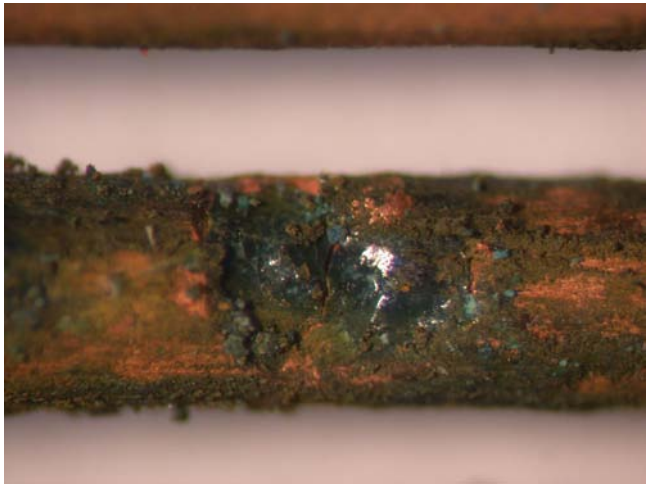

Figure 642 - 40x magnification of the notch affecting the middle conductor.

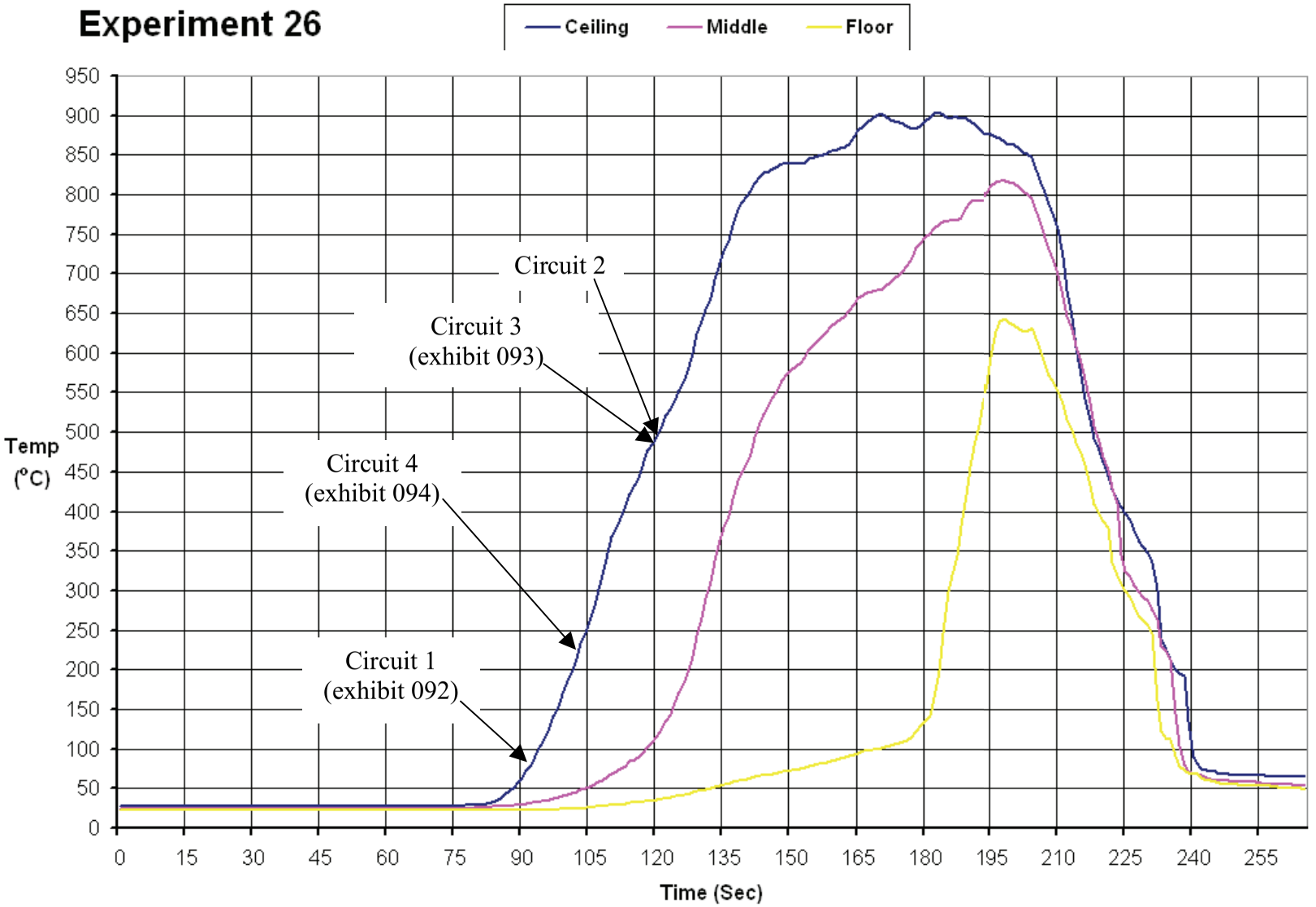

Figure 643 - Time temperature graph for experiment 26

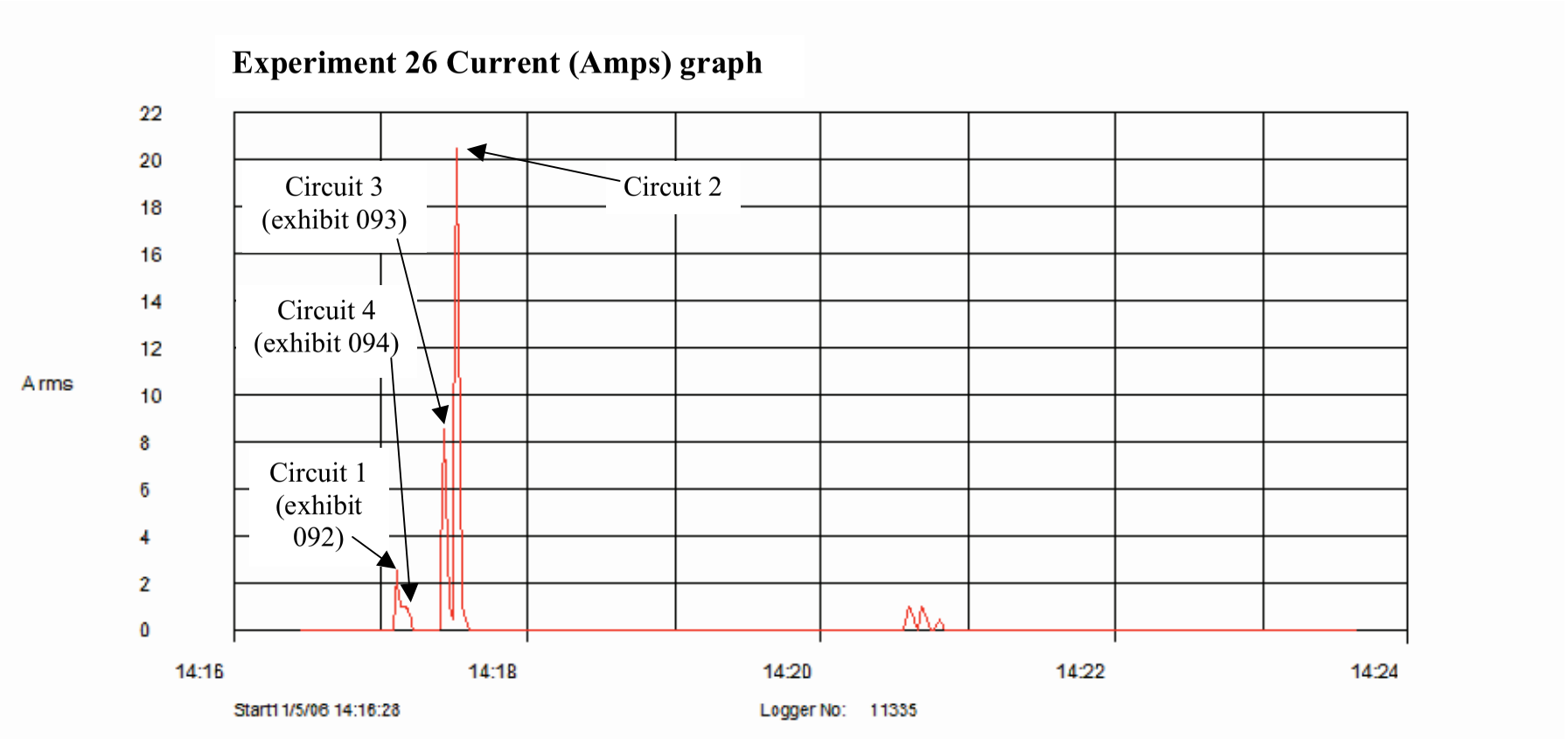

Figure 644 - Current (Amps) graph for experiment 26 detailing the operation of the circuit breakers and the fault current

Experiment 27

Figure 645 – “Scenario C” 11 May 2006

Circuit number	MCB operating time from ignition
4	5:16 minutes
3	5:39 minutes
2	5:55 minutes
1	5:58 minutes

Table 29 – circuit breaker operation data

The fire in experiment 27 (scenario C) originated in a box of toys located under a Christmas tree 1380mm from the left wall and 700mm from the rear wall.

The fire’s developed steadily to a maximum ceiling temperature of 1000° C reached at 8.5 minutes after ignition. The middle thermocouple also recorded a temperature of 1010° C at this point with the floor thermocouple recording a maximum temperature of 470° C. The compartment was at flashover conditions at 8 minutes until it was extinguished at 8.5 minutes from the time of ignition.

A voltage reading at the portable consumer unit located just outside the compartment recorded 261 Volts.

Arcing damage was not located on circuit number 1.

Arcing damage was located on circuits 2 and 3 – 1300mm from the left and 1000mm from the front wall.

Arcing damage was located on circuit 4 – 1440mm from the left wall and 1000mm from the rear wall.

Pre-fire and post-fire photographs of experiment 27

Figure 646 - Pre-fire photograph of experiment 27. The white circle details the fire's area of origin in a toy box.

Figure 647 - Pre-fire photograph of the ceiling area detailing the wiring located above the fire's area of origin.

Figure 648 - Post-fire photograph detailing the fire's area of origin. The black arrow was the location of the arcing damage to circuit 4 above the fire's area of origin.

Figure 649 - Post-fire photograph of the ceiling area above the fire's area of origin. The white arrow details the arcing damage location of circuit 4 - exhibit 097.

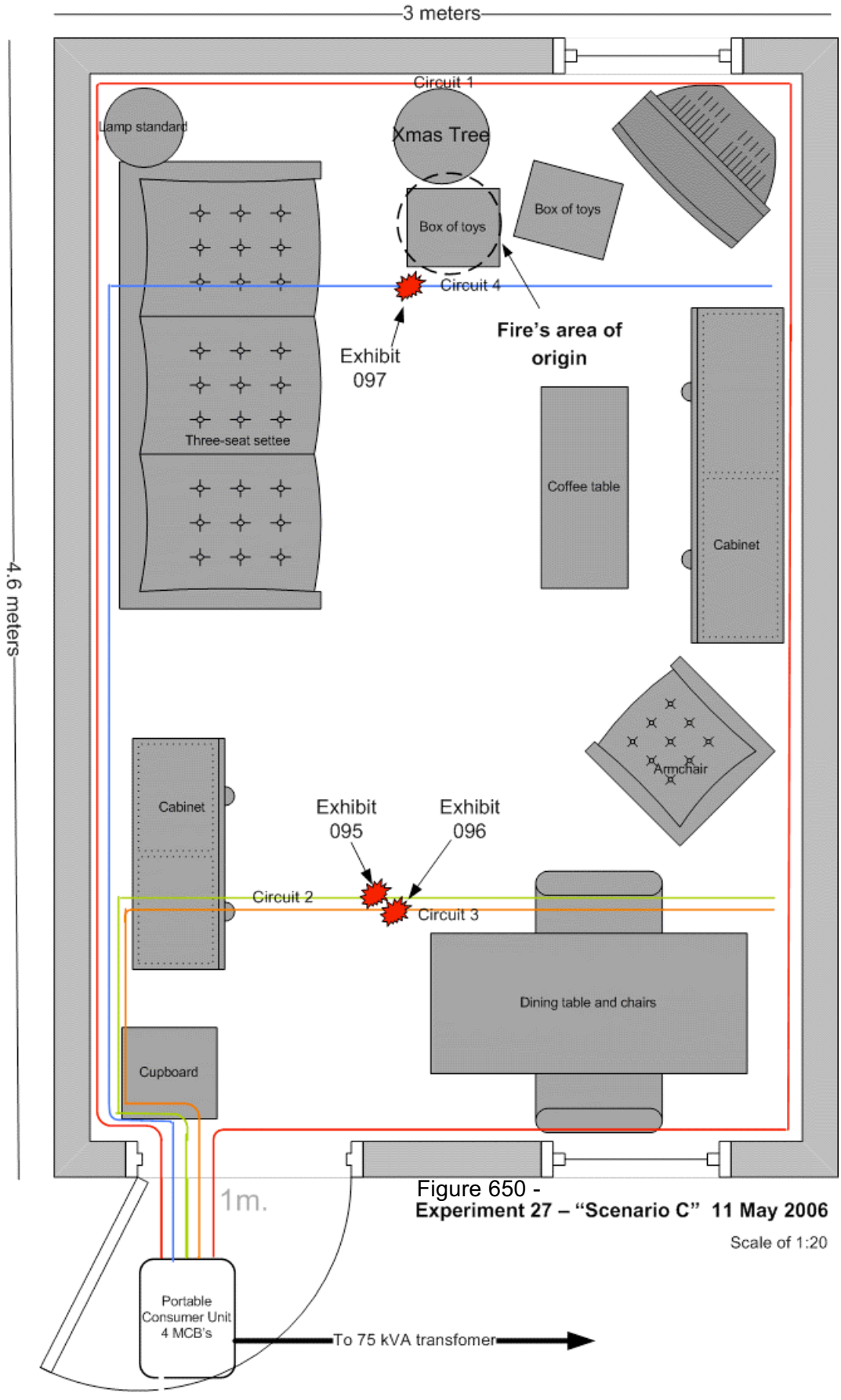

Figure 650 -
Experiment 27 – "Scenario C" 11 May 2006

Scale of 1:20

Microscope images for exhibit 095 - arcing category F (experiment 27)

Figure 651 - Microscope image for exhibit 095 detailing the notch damage to one of the three conductors.

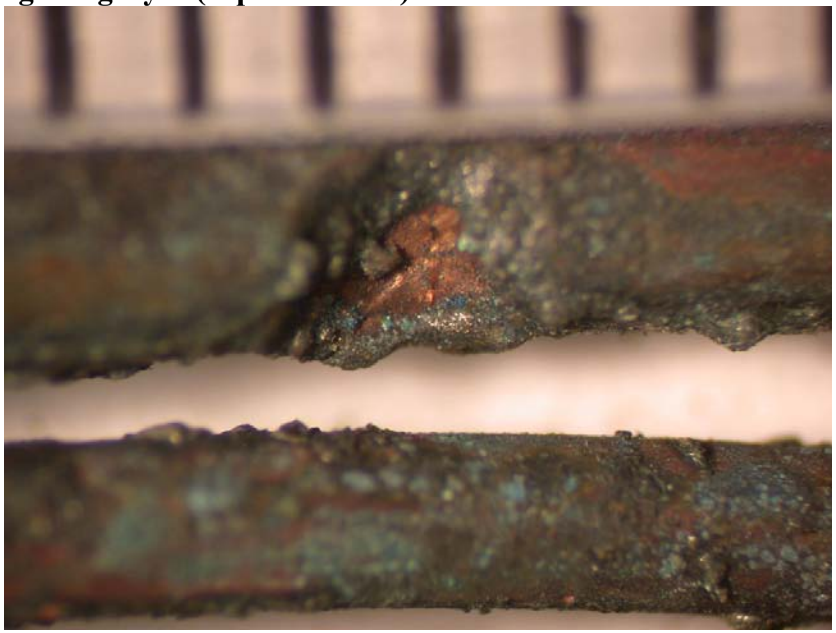

Figure 652 - 20x magnification of the notch on the top conductor detailed in figure 651. The notch is 2mm wide. A limited depth of field using the digital camera on the dedicated microscope coupler limited the area of this image that is in focus.

Microscope images for exhibit 096 - arcing category B (experiment 27)

Figure 653 - Microscope image of exhibit 096. The arcing damage has affected one of the three conductors.

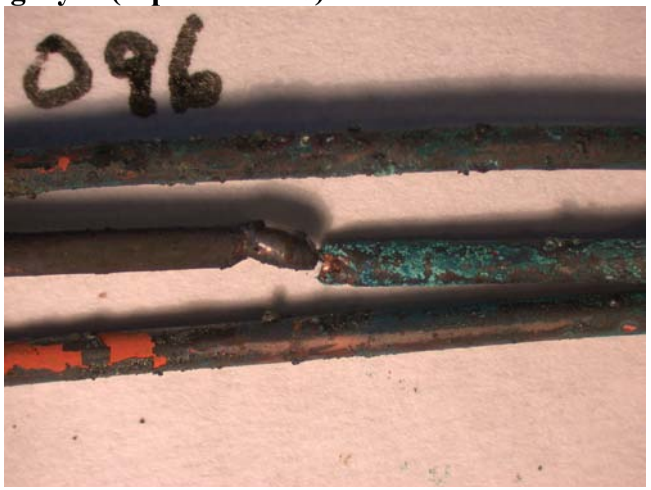

Figure 654 – The middle conductor is severed with a large bead on one end and a smaller bead on the other severed end.

Figure 655 - 20x magnification of the severed conductors. The demarcation area is clear on the left conductor.

Microscope images for exhibit 097 - arcing category B (experiment 27)

Figure 656 - Microscope image of exhibit 097. Two conductors have arcing damage. One is severed and the other is welded to a fixing screw.

Figure 657 - 20x magnification of the right severed end. There was a lot of oxide and corrosion on the surface of this conductor.

Figure 658 - 20x magnification of the conductor welded to the screw.

Figure 659 - 40x magnification of the welded conductor that details the severe oxidation of the steel screw.

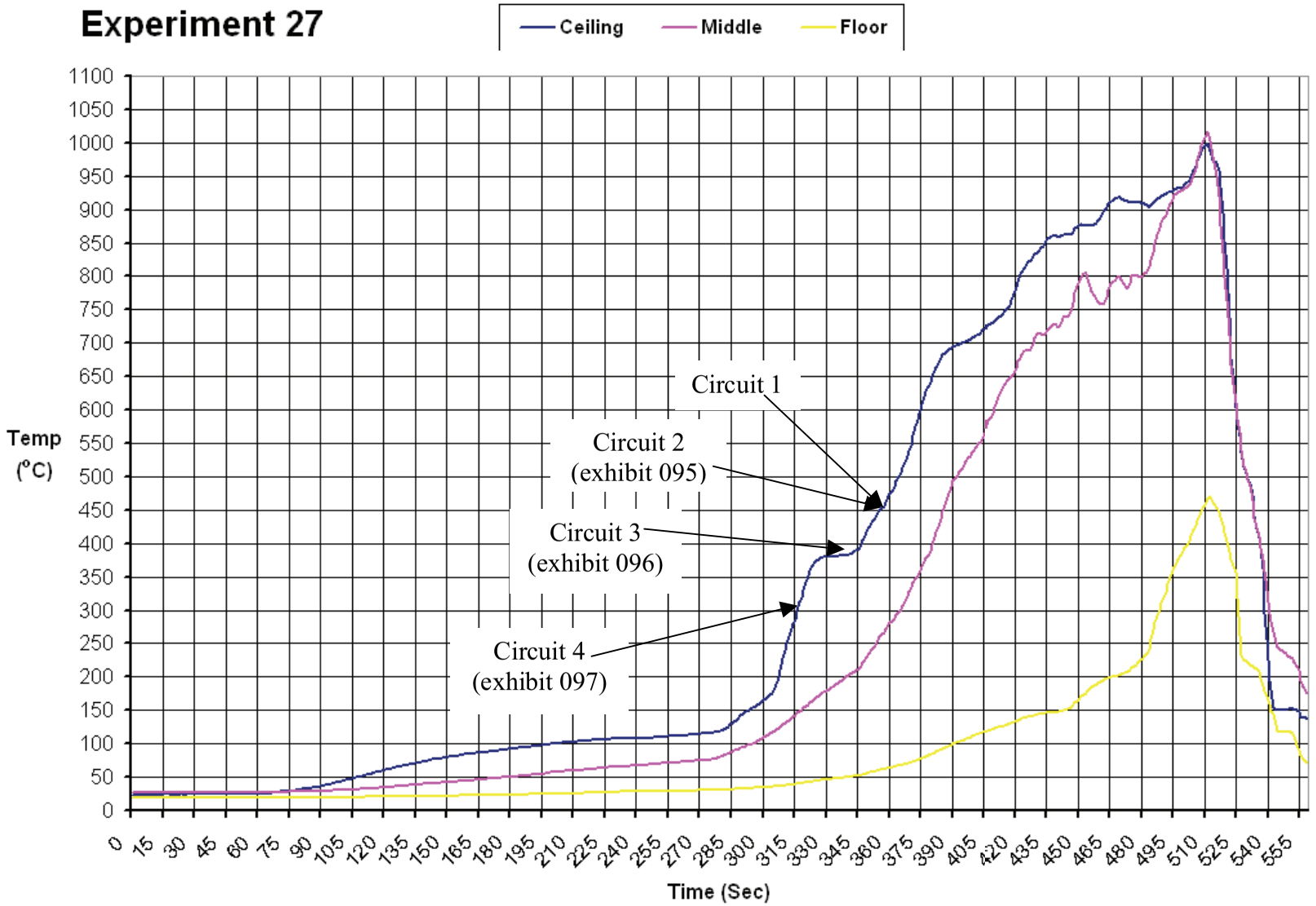

Figure 660 - Time temperature graph for experiment 27

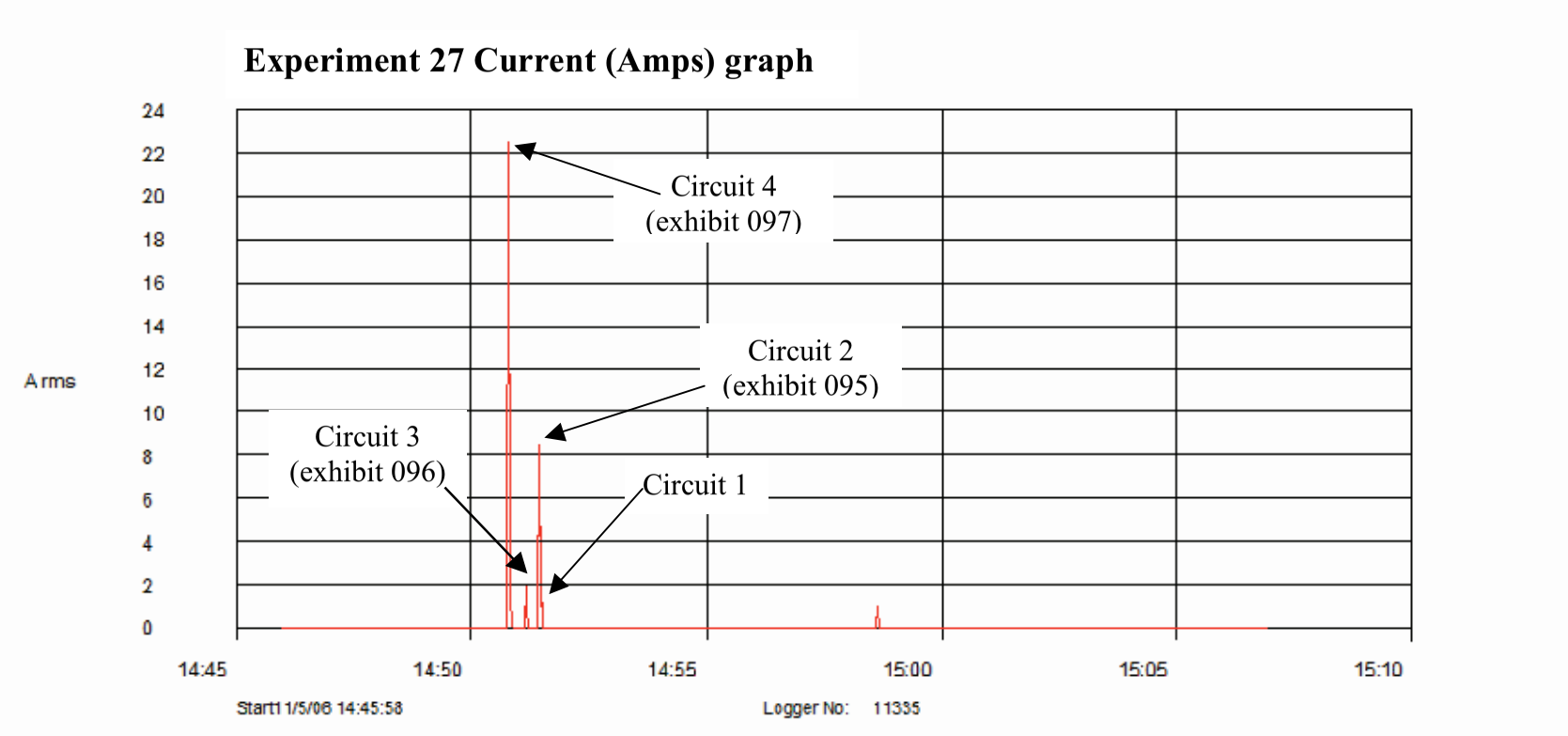

Current (Amps) graph for experiment 27 detailing the operation of the circuit breakers and the fault current

Experiment 28

Figure 662 – “Scenario D” 22 June 2006

Circuit number	MCB operating time from ignition
4	1:07 minutes
1	1:13 minutes
3	2:00 minutes
2	2:18 minutes

Table 30 – circuit breaker operation data

The fire in experiment 28 (scenario D) originated in three separate areas within the compartment. The first area was above an electric fire located on the rear wall. The second area of origin was on a seat of an armchair located in the rear left corner of the room (this was the fire’s main plume affecting the ceiling in the initial stages of the fire). The third area of origin was on the left armrest area of a two-seat sofa located on the left wall.

The fire developed rapidly with the ceiling and middle thermocouples recording 950° C in 4 minutes and 15 seconds. The floor thermocouple recorded a temperature of 425° C at this time. The compartment was reached flashover conditions at approximately 4 minutes.

Arcing was located on circuit 1 – adjacent to the rear wall and 550mm from the left wall.

Arcing was located on circuits 2 and 3 – 1250mm from the left wall on the ceiling and 1000mm from the front wall.

Arcing was located on circuit 4 – 120mm from the left wall and 1000mm from the rear wall.

Pre-fire and post-fire photographs of experiment 28

Figure 663 - Pre-fire photograph of experiment 28. The white circles indicate the fire's area of origin. The armchair adjacent to the rear left wall was the dominant fire plume.

Figure 664 - View of the ceiling above the rear left corner of the compartment. Circuit 1 is the ring routed along the top of the walls and circuit 4 crosses the ceiling.

Figure 665 - Post-fire photograph detailing the fire's areas of origin.

Figure 666 - Post-fire view of the ceiling above the fire's dominant plume. The left arrow details the arcing damage location of circuit 4 (exhibit 101). The right arrow details exhibit 098 (circuit 1).

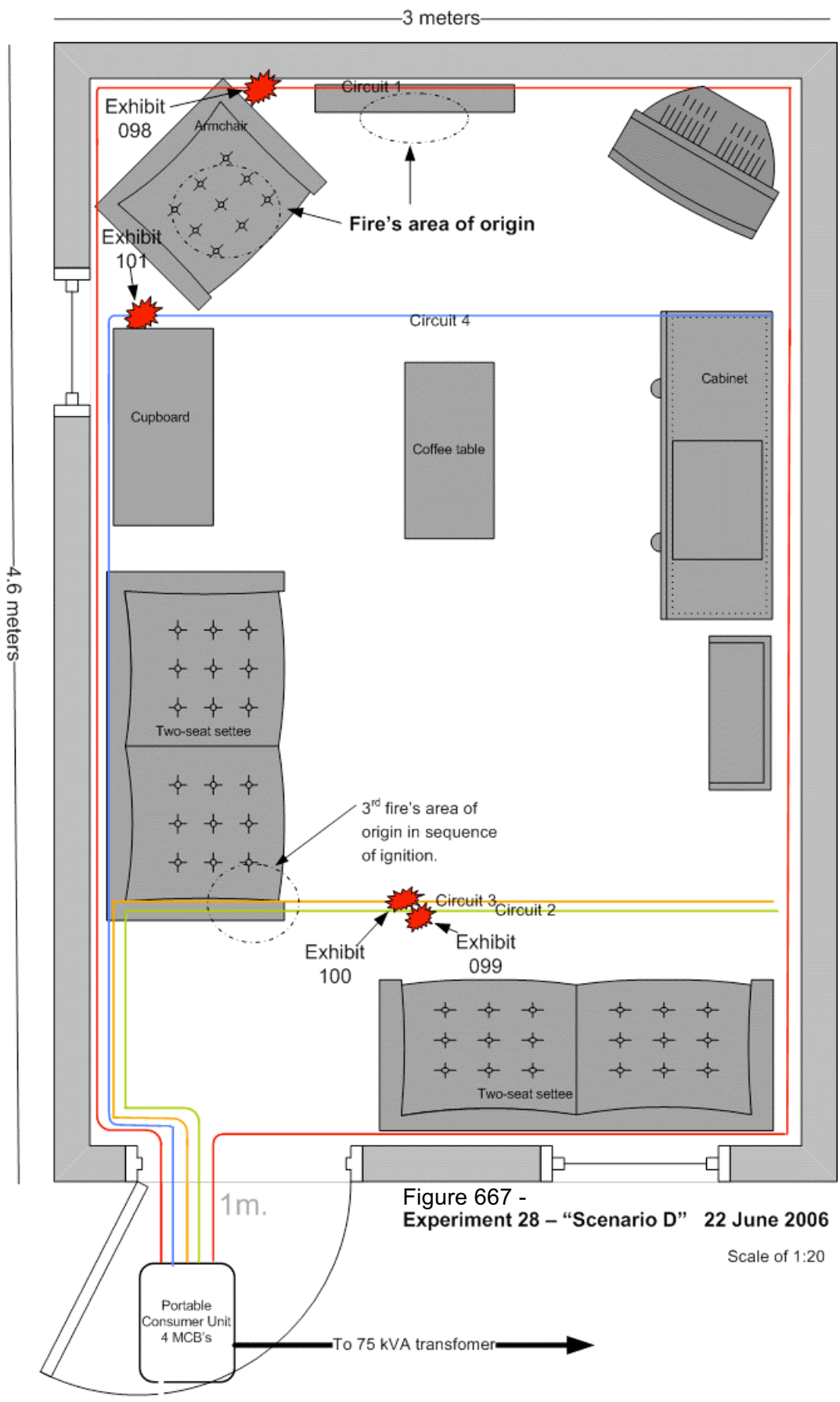

Figure 667 -
Experiment 28 – "Scenario D" 22 June 2006

Scale of 1:20

Microscope images for exhibit 098 - arcing category D (experiment 28)

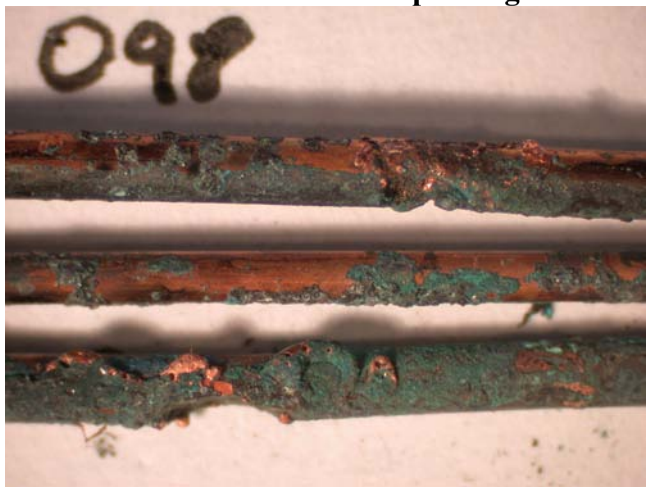

Figure 668 - Microscope image of exhibit 098.The live and neutral 2.5mm^2 conductors have arcing damage. Each one was a notch.

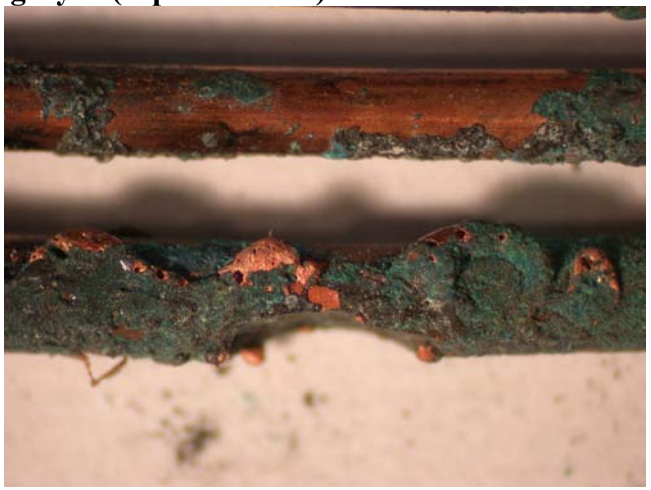

Figure 669 - 20x magnification of the lower conductor notch with adjacent beading splatter on the conductor surface.

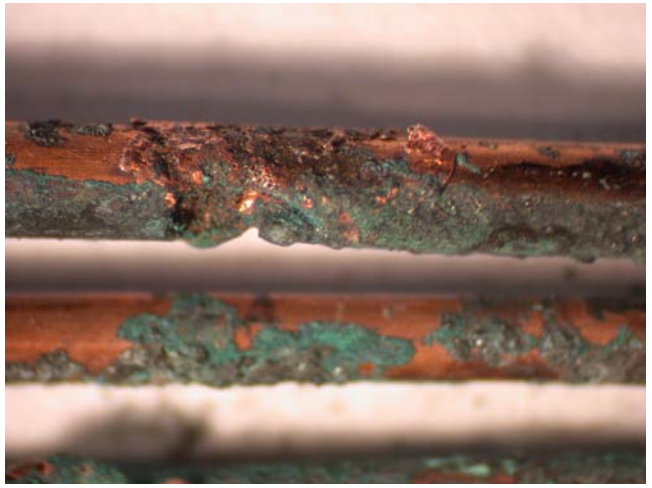

Figure 670 - 20x magnification of the top conductor detailing its notch damage.

Figure 671 - A similar view to figure 670, with the conductor positioned at a different angle.

Microscope and SEM images for exhibit 099 - arcing category F (experiment 28)

Figure 672 - Microscope image of exhibit 099. One of the three conductors had arcing damage.

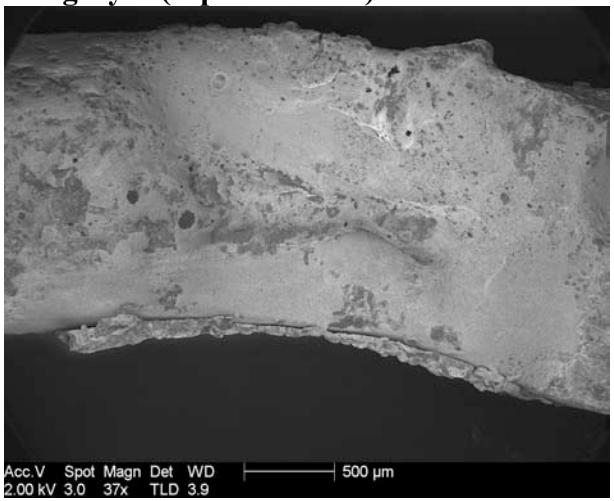

Figure 673 - SEM image of the exhibit detailing the large notch with copper splatter at the bottom of the image.

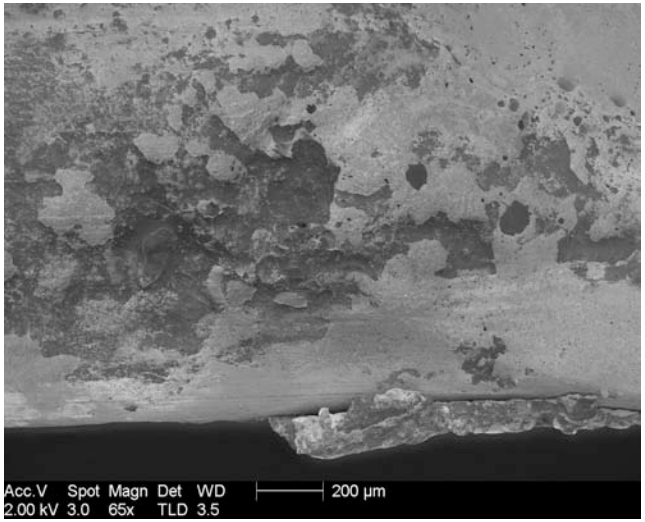

Figure 674 - SEM image at 65x magnification detailing the left edge of the copper splatter.

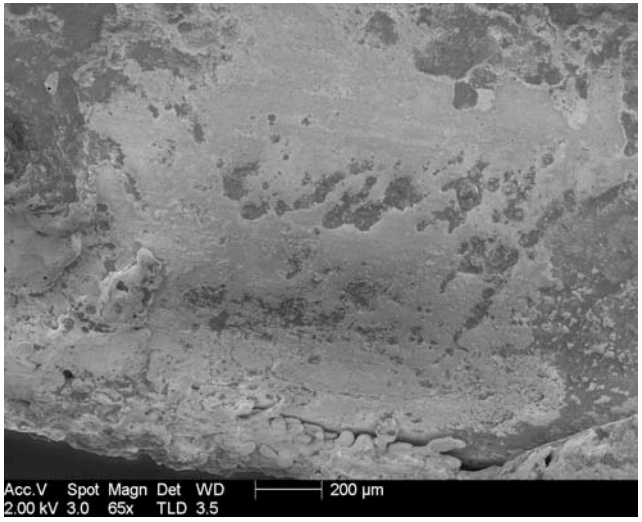

Figure 675 - SEM image of the copper splatter on the right side of the notch.

Microscope images for exhibit 100 - arcing category D (experiment 28)

Figure 676 - Microscope image of exhibit 100. One of the three conductors had arcing damage that consisted of a deep notch with a large bead within that protruded above the conductor.

Figure 677 - 20x magnification microscope image of the bead and notch.

Figure 678 - 40x magnification of the bead. Several smaller beads of the adjacent conductor surface were observed and are detailed in the right of this image.

Microscope images for exhibit 101 - arcing category D (experiment 28)

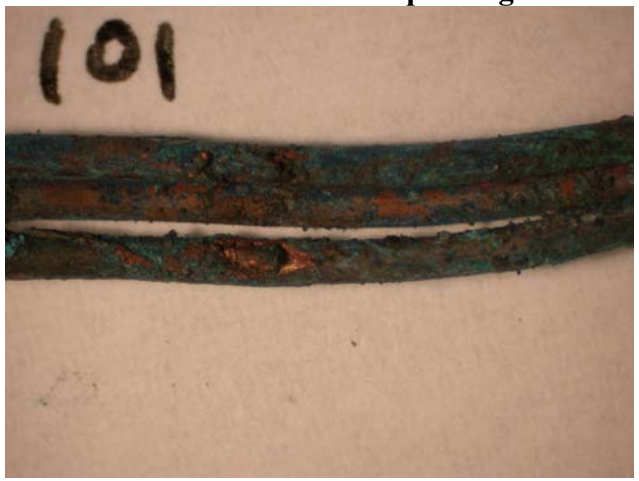

Figure 679 - Microscope image of exhibit 101. Two conductors (live and neutral) sustained arcing damage.

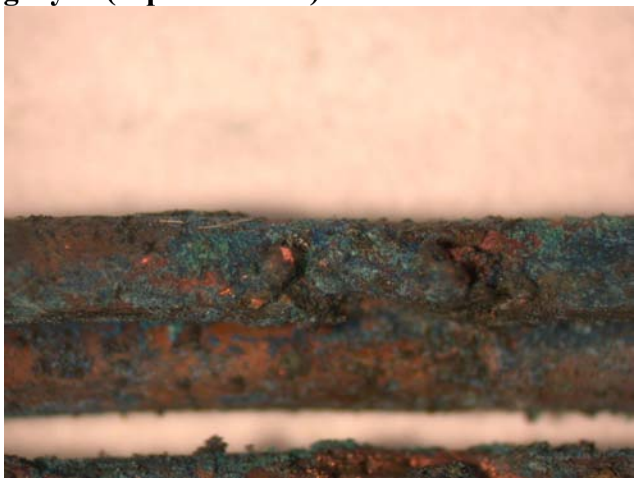

Figure 680 - 20x magnification of the top conductor detailed in figure 679 with a notch and small beads at the notch edge.

Figure 681 - 20x magnification of the bottom conductor detailed in figure 679. The conductor has a notch with a bead within it. This image details the demarcation between the arcing damage and the undamaged area.

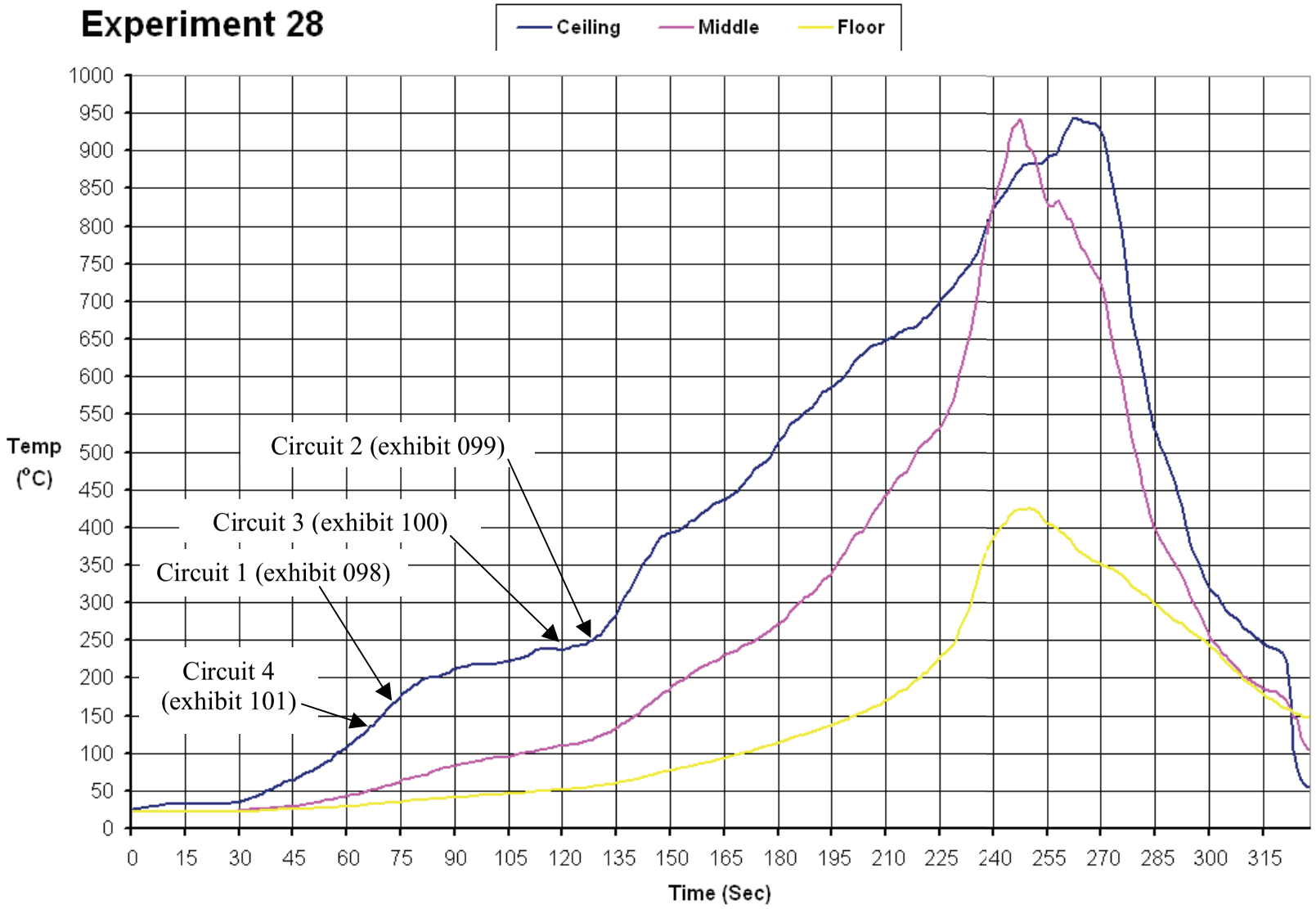

Figure 682 - Time temperature graph for experiment 28

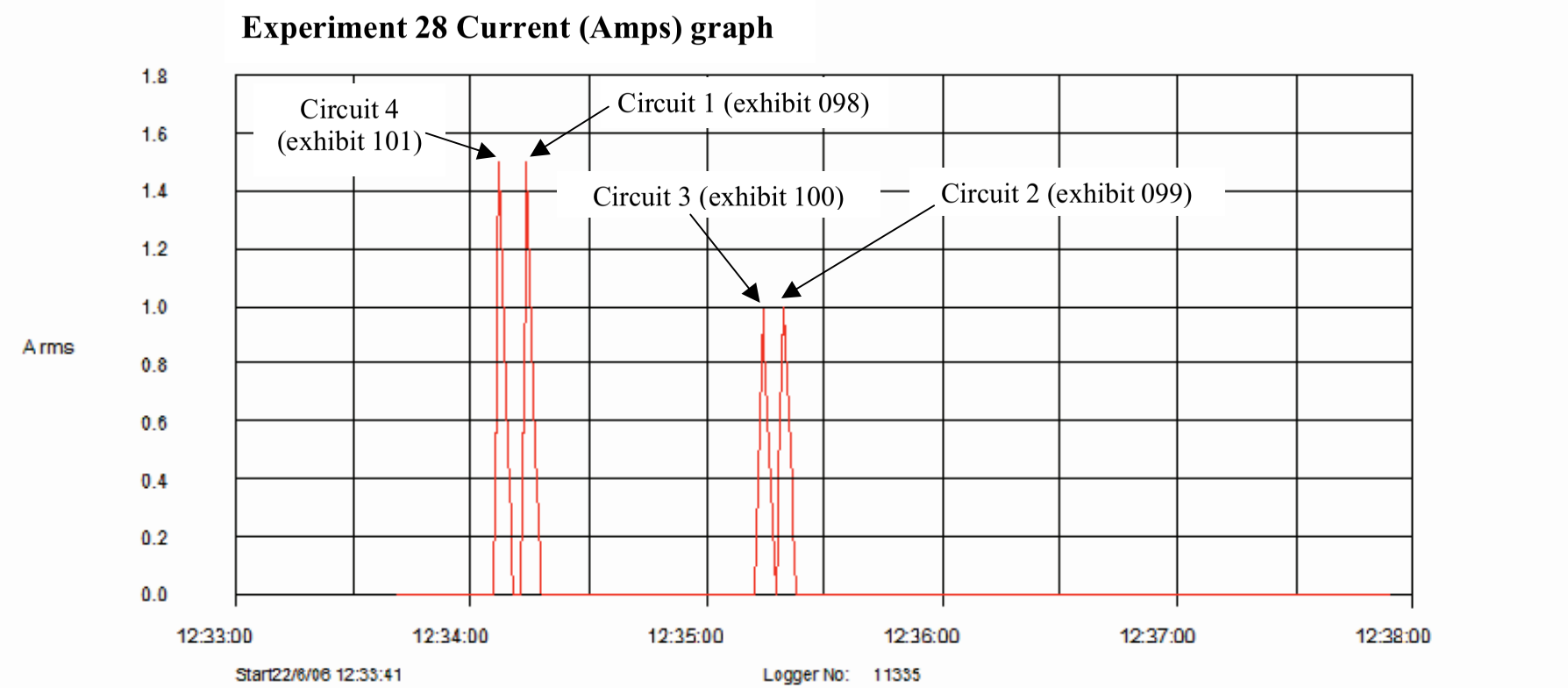

Figure 683 - Current (Amps) graph for experiment 28 detailing the operation of the circuit breakers and the fault current

Experiment 29

Figure 684 – “Scenario B” 22 June 2006

Circuit number	MCB operating time from ignition
4	8:08 minutes
1	9:09 minutes
3	9:36 minutes
2	9:37 minutes

Table 31 – circuit breaker operation data

The fire in experiment 29 (scenario B) originated in a refuse bin located in the rear left corner of the compartment.

There was a delay with the development of this fire as ignition was achieved using a trailer where the flame spread slowly along the trailer. At 7:00 minutes the temperature at the ceiling had reached only 125° C. The temperatures in the compartment increased rapidly at 10 minutes and at 13 minutes the compartment was at flashover conditions with all three thermocouples exceeding 900° C.

Arcing was located on circuit 1 – adjacent to the rear wall and 850mm from the left wall.

Arcing was located on circuit 2 - 600mm from the left wall on the ceiling and 1000mm from the front wall in the same location as the left area of arcing to circuit 3.

Arcing damage was located in two separate locations on circuit number 3 - 600mm and 1100mm from the left wall on the ceiling and 1000mm from the front wall.

Arcing damage was located on circuit 4 – 670mm from the left wall and 1000mm from the rear wall.

Pre-fire and post-fire photographs of experiment 29

Figure 685 - Pre-fire photograph of experiment 29. The fire's area of origin is the refuse bin in the rear left corner of the compartment indicated with the dashed line black circle.

Figure 686 - The incendiary device being set up in the refuse bin located adjacent to the rear left corner of the compartment.

Figure 687 - Post-fire photograph of the compartment. The fire's area of origin is detailed with the white circle.

Figure 688 - Post-fire view of the fire's area of origin. The black arrows indicate the arcing damage to circuit 1 (R) and circuit 4 (L).

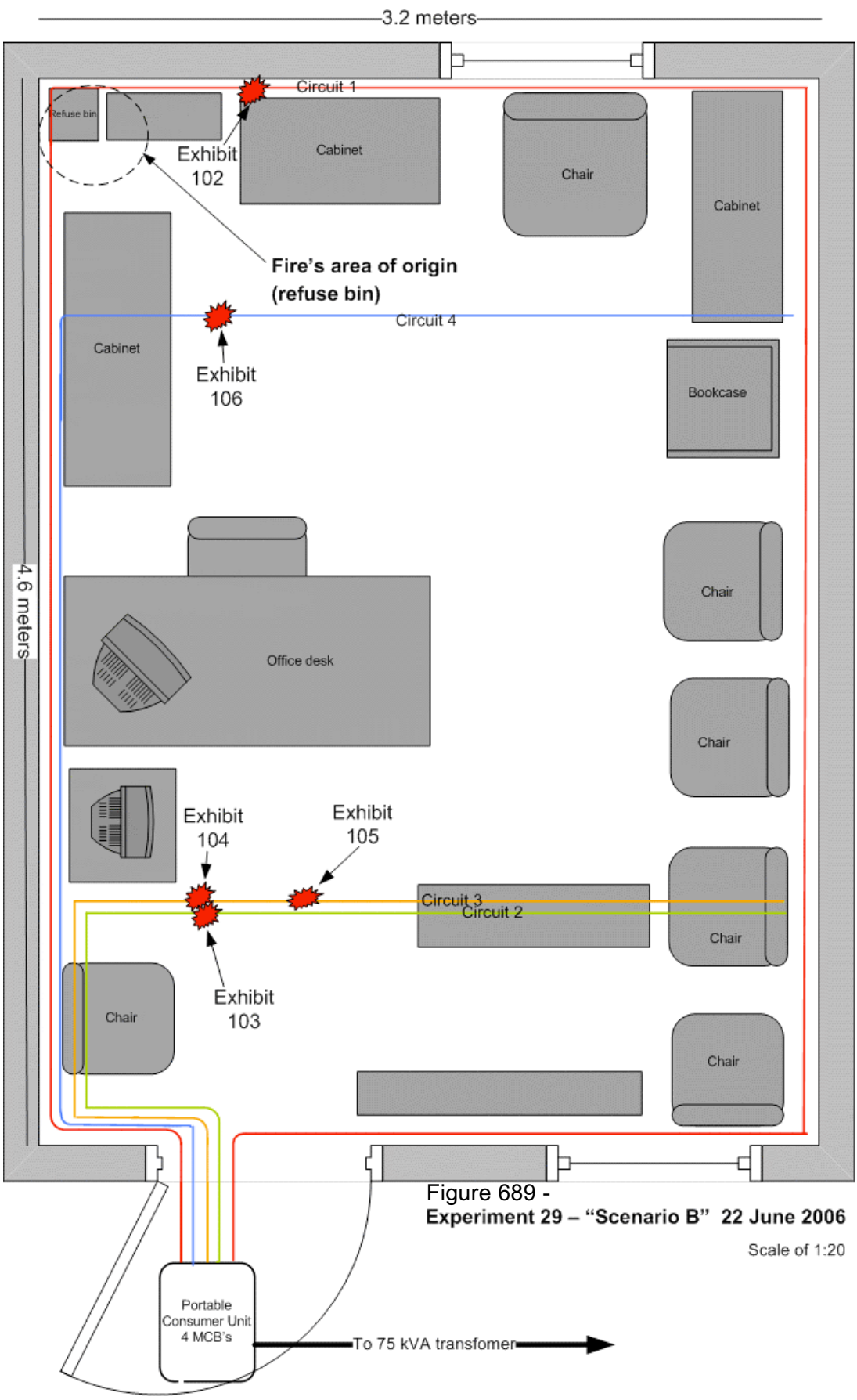

Figure 689 -
Experiment 29 – "Scenario B" 22 June 2006

Scale of 1:20

Microscope images for exhibit 102 - arcing category D (experiment 29)

Figure 690 - Microscope image of exhibit 102. The arcing damage affected the two 2.5mm^2 conductors (live & neutral). A fixing screw adjacent to this metallic damage had a small notch on the thread.

Figure 691 - 20x magnification of the top conductor. The notch has a bead with a chaotic surface.

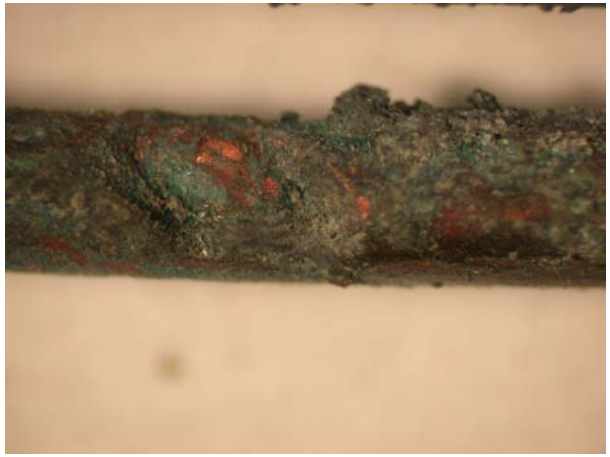

Figure 692 - The bottom conductor had a notch, with a bead within the notch. There is a lot of PVC debris still attached to the conductor surface. However the demarcation area is still clear.

Microscope images for exhibit 103 - arcing category F (experiment 29)

Figure 693 - Microscope image of exhibit 103. A small notch of one of the 2.5mm^2 conductors and a bead within a notch on the top conductor. A lot of PVC debris and oxide was attached to the conductor surface.

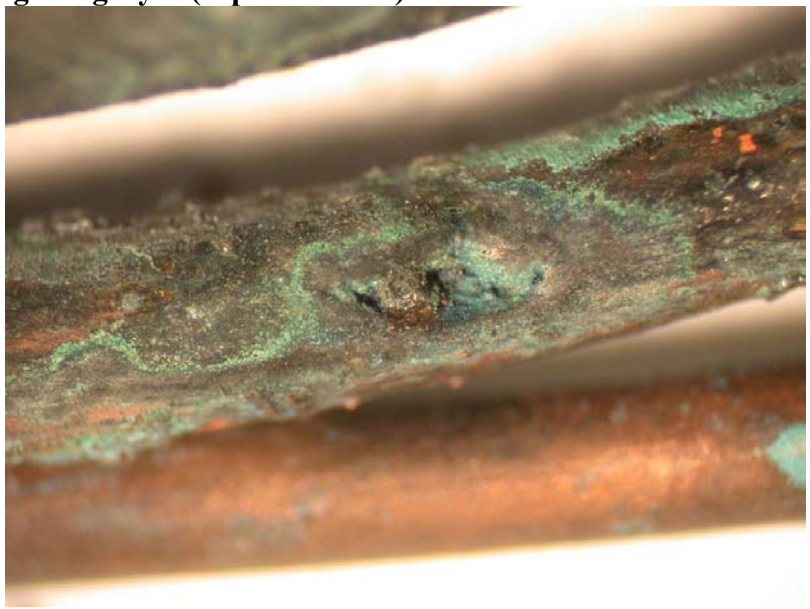

Figure 694 - A close-up of the arcing damage to this conductor, the middle conductor detailed in figure 693.

Microscope images for exhibit 104 - arcing category B (experiment 29)

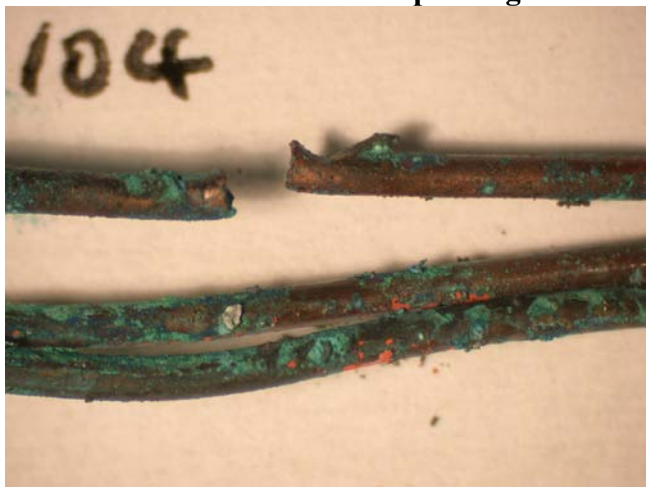

Figure 695 - Microscope image of exhibit 104. This arcing damage is closest to the electrical source

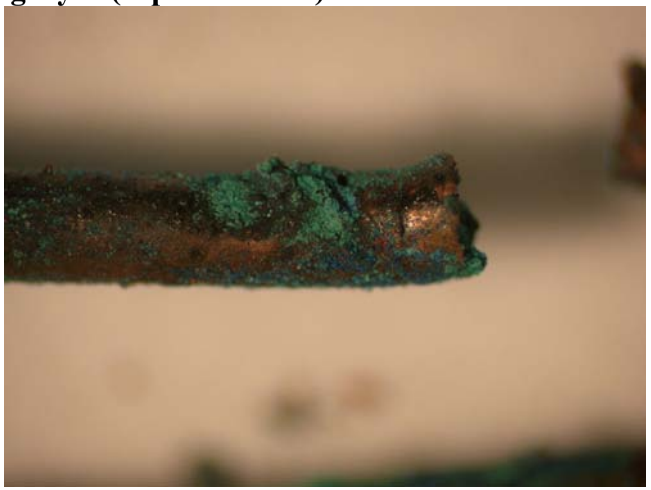

Figure 696 - The left severed conductor in figure 695. The severed edge appears to be fractured.

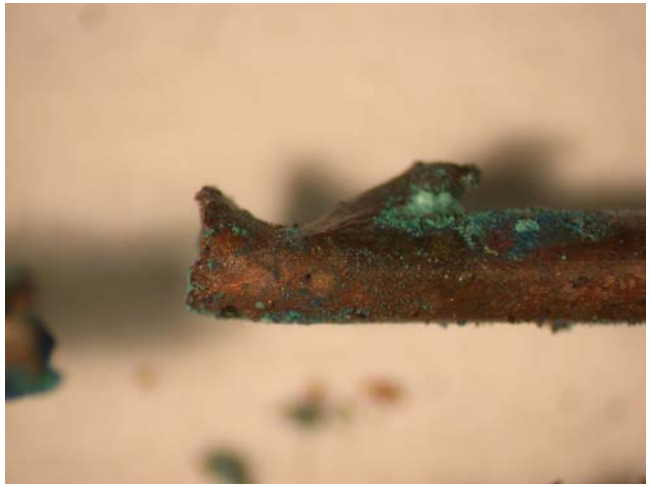

Figure 697 - The right severed conductor. The surface of the severed end appears to be a fracture at the edge of the notch.

Microscope images for exhibit 105 - arcing category B (experiment 29)

Figure 698 - Microscope image of exhibit 105. Two conductors are affected. The bottom one is severed and has a large bead protruding from the conductor surface.

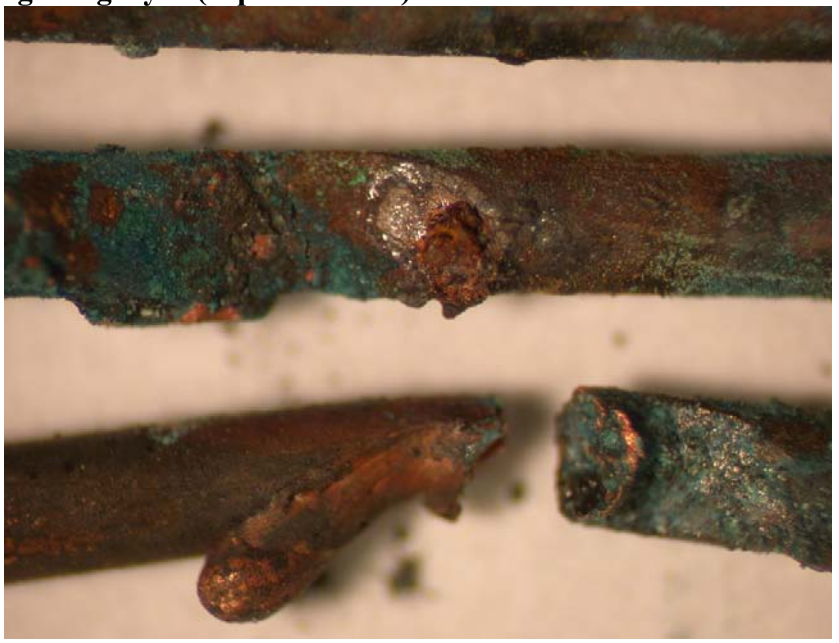

Figure 699 - 20x magnification of the two conductors detailing the top conductor with a large notch and the bottom conductor with severed ends.

Microscope images for exhibit 106 - arcing category B (experiment 29)

Figure 700 - Microscope image of exhibit 106. The arcing damage has only affected one conductor. It appears to be a large notch that has fractured after recovery at the scene.

Figure 701 - 20x magnification of the right severed end.

Figure 702 - The left severed end at 20x magnification. The demarcation between the edge of the notch and the undamaged conductor is clear.

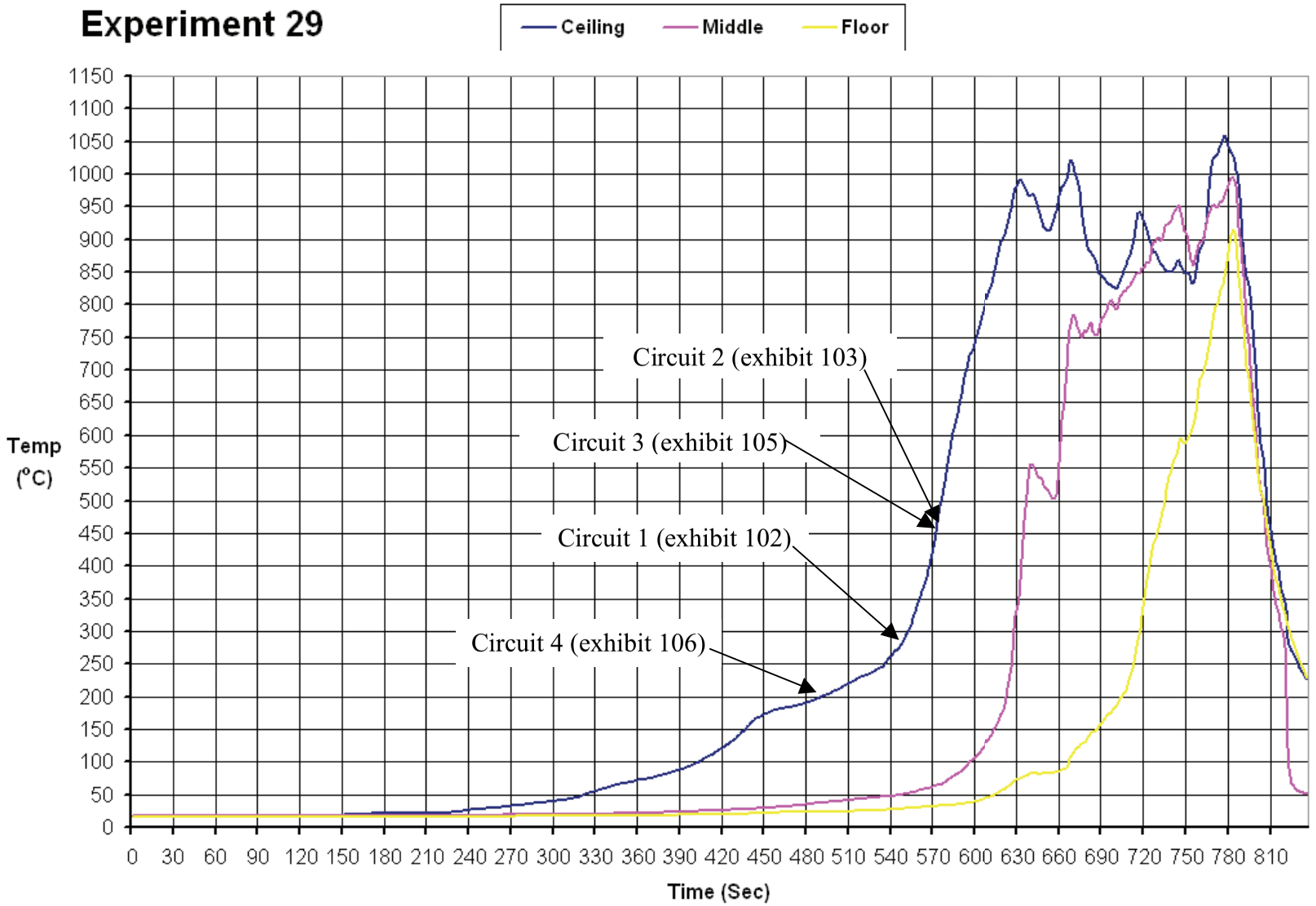

Figure 703 - Time temperature graph for experiment 29

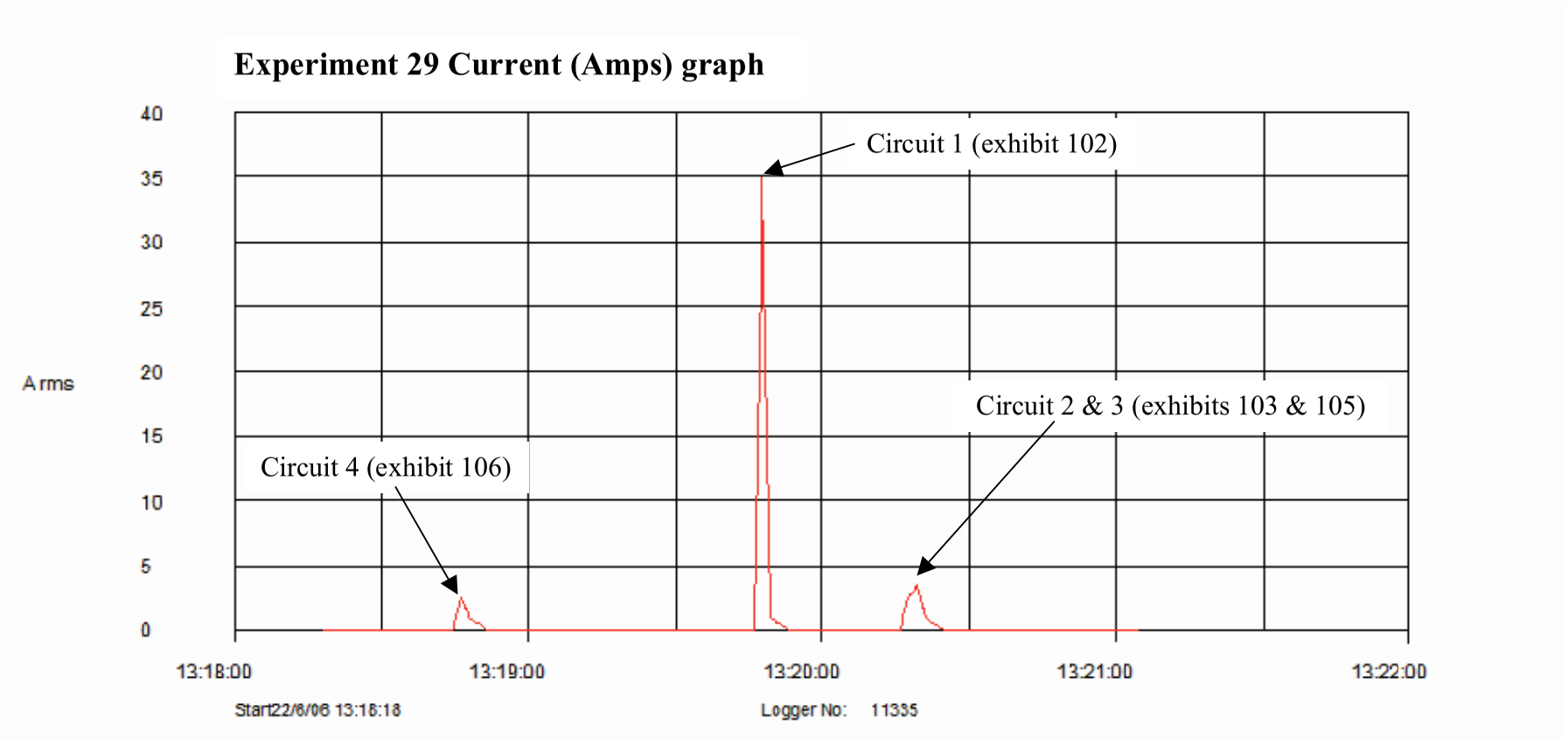

Figure 704 - Current (Amps) graph for experiment 29 detailing the operation of the circuit breakers and the fault current

Experiment 30

Figure 705 – “Scenario C” 22 June 2006

Circuit number	MCB operating time from ignition
4	3:24 minutes
1	4:06 minutes
3	4:15 minutes
2	4:24 minutes

Table 32 – circuit breaker operation data

The fire in experiment 30 (scenario C) originated in a toy box located in front of a Christmas tree located adjacent to the centre of the rear wall.

The fire developed rapidly with the ceiling temperature reaching 1050° C at 5.5 minutes. The middle thermocouple recorded 840° C at this point in the fire’s development. The floor thermocouple did not record a temperature above 80 degrees and the post-fire burn patterns in the compartment suggest that the fire did not reach flashover conditions prior to being extinguished.

Arcing was located on circuit 1 – adjacent to the rear wall and 2400mm from the left wall.

Arcing was located on circuit 2 - is 2300mm from the left wall and 1000mm from the front wall.

Arcing was located on circuit 3 – 520mm from the left wall on the ceiling and 1000mm from the front wall.

Arcing was located on circuit 4 – 1030mm from the left wall and 1000mm from the rear wall.

Pre-fire and post-fire photographs of experiment 30

Figure 706 - Pre-fire photograph of experiment 30. The fire's area of origin is detailed with a white circle.

Figure 707 - Post-fire photograph of the ceiling area above the fire's area of origin. The left arrow indicates the arcing damage to circuit 4. The right arrow indicates the arcing damage location to circuit 1.

Figure 708 - Post-fire photograph of the scene. The fire's are of origin is indicated with the white circle.

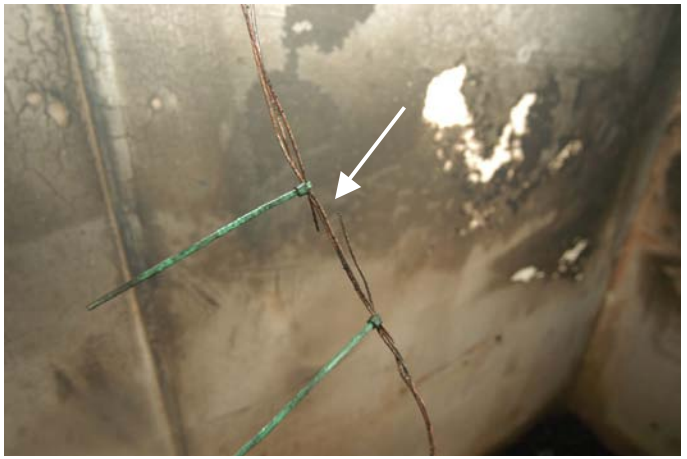

Figure 709 - A close-up photograph of the cable ties used during the electrical examination to identify the arcing damage to circuit 4.

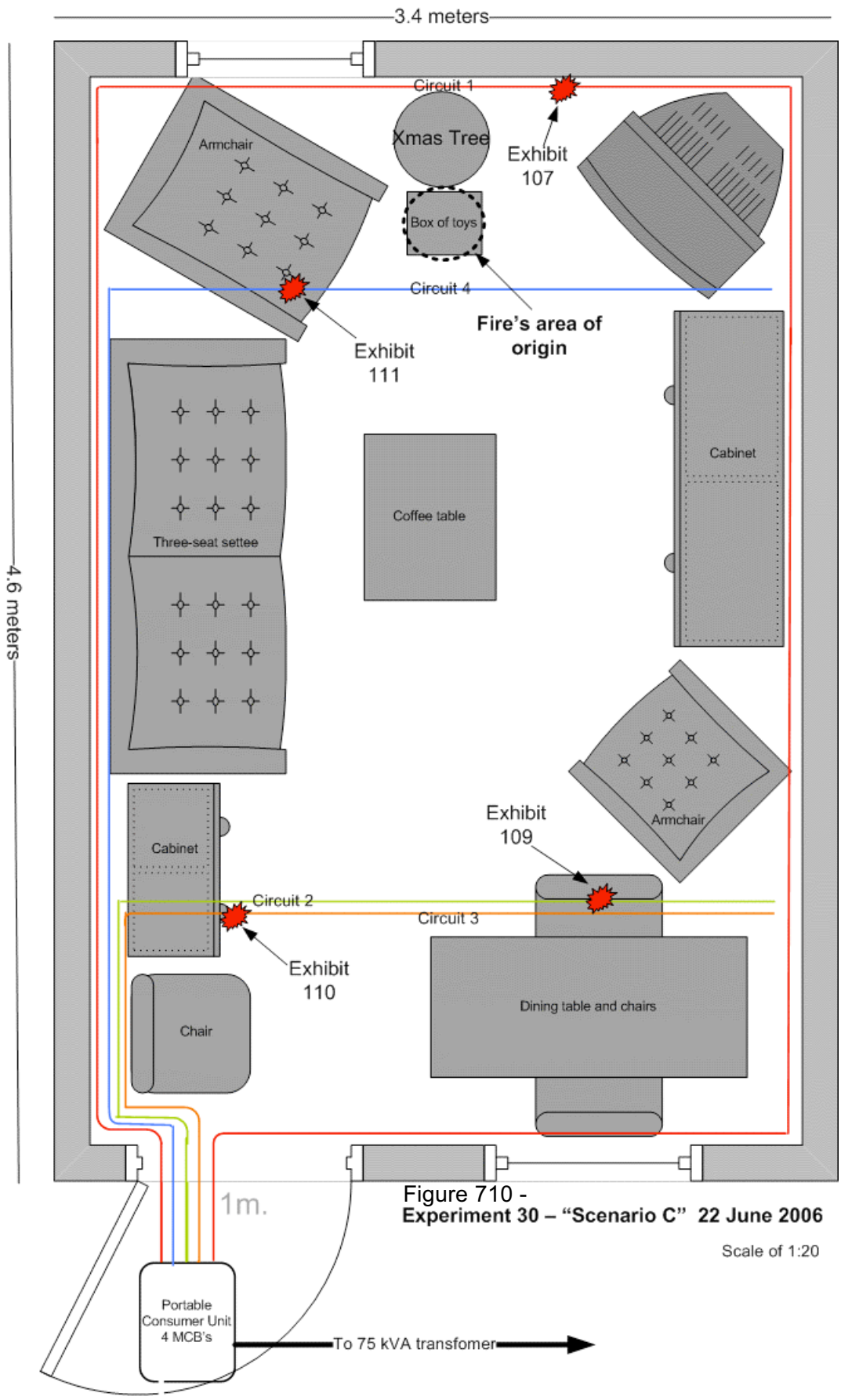

Figure 710 -
Experiment 30 – "Scenario C" 22 June 2006

Scale of 1:20

Microscope and SEM images for exhibit 107 - arcing category E (experiment 30)

Figure 711 - Microscope image of exhibit 107. Arcing between the live and earth conductors of this circuit. Each conductor has a notch. The 2.5mm^2 conductor also has a large bead at the side of the notch.

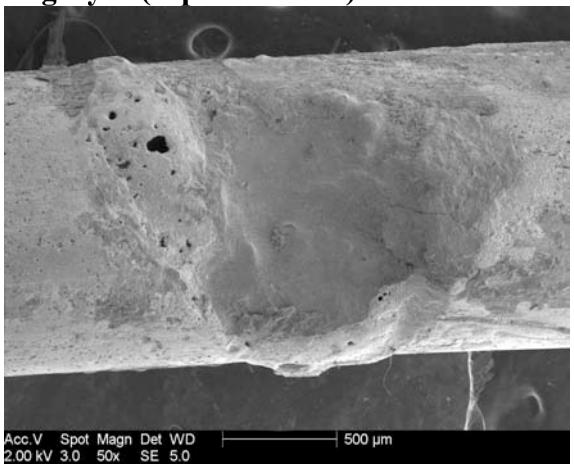

Figure 712 - SEM image of the top conductor detailed in figure 711. The large bead is also detailed in figures 715 -718, confocal laser scanning microscope images.

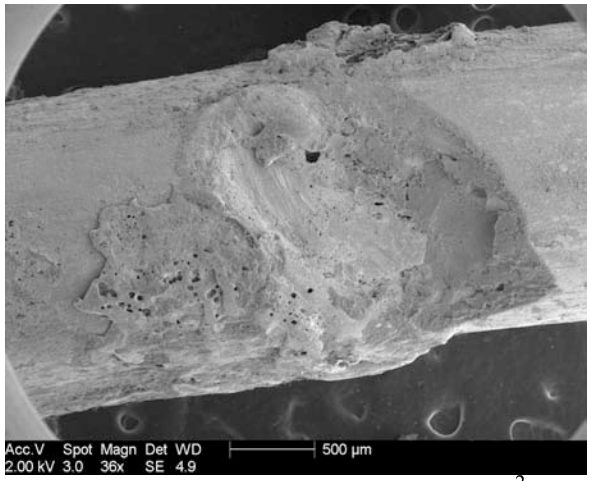

Figure 713 - SEM image of the notch in the 1.5mm^2 protective earth conductor.

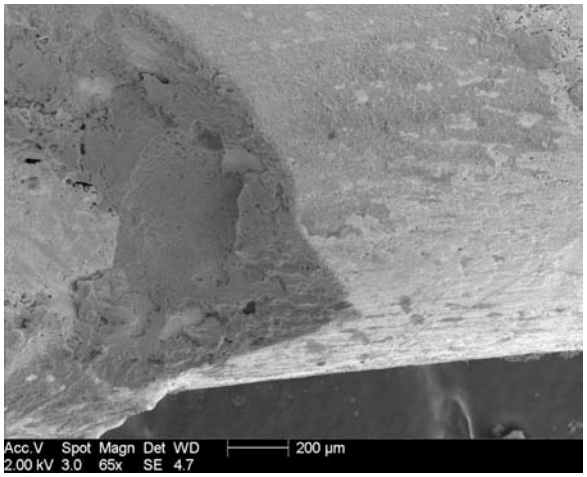

Figure 714 - SEM image at 65x magnification detailing the left of the notch in fig. 713 with a clear demarcation area between the arcing damage and the undamaged conductor surface.

Confocal laser scanning microscope images for exhibit 107 – arcing category E (experiment 30)

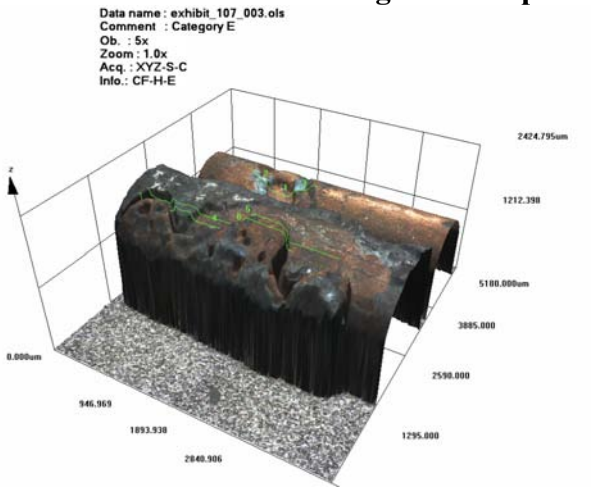

Figure 715 - LEXT image of exhibit 107.

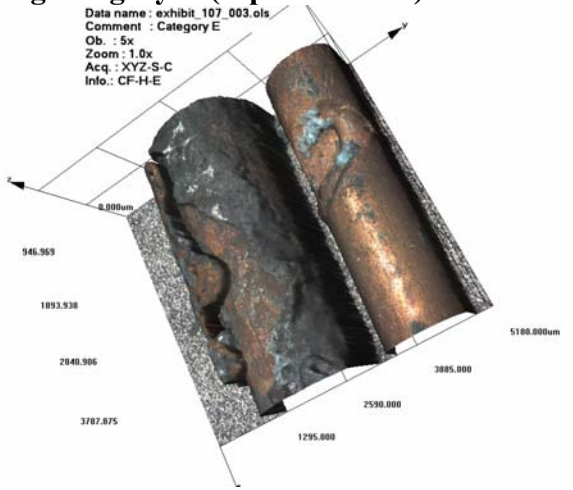

Figure 716 - LEXT image captured from the 3-D software.

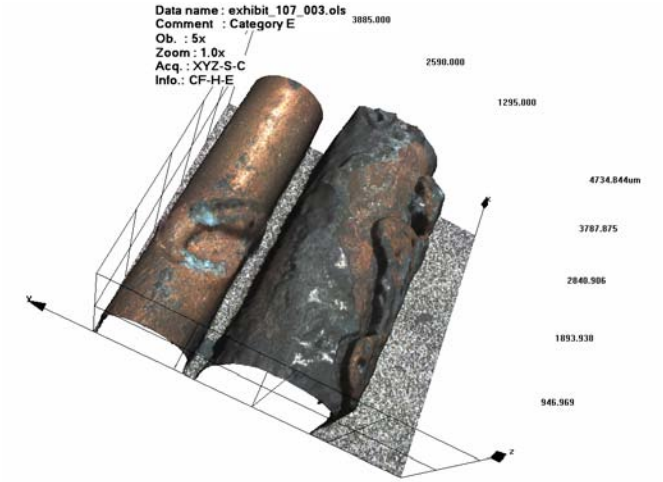

Figure 717 - LEXT image with the exhibit orientated within the LEXT software.

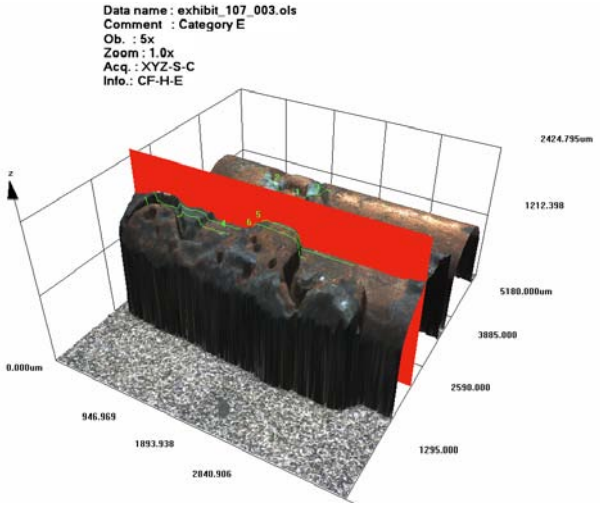

Figure 718 - LEXT image with the software slice tool in use to produce a profile of the conductor surface.

Microscope and SEM images for exhibit 109 - arcing category C (experiment 30)

Figure 719 - Microscope image of exhibit 109. One of the 2.5mm^2 conductors has a notch with an adjacent bead and copper splatter around the periphery of the notch.

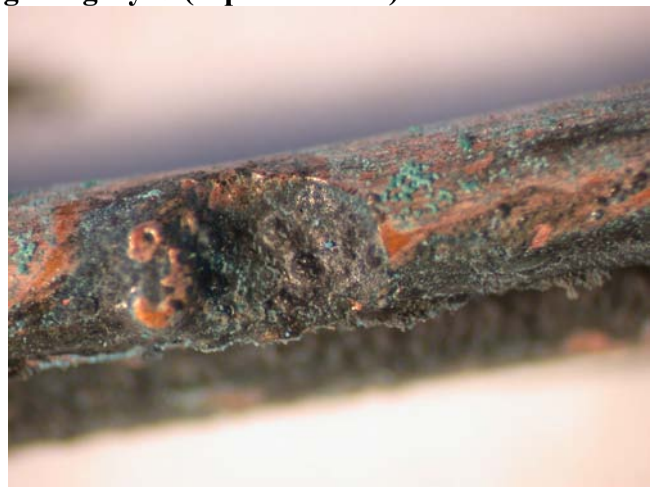

Figure 720 - 20x magnification of the notch detailed in figure 719. There was a lot of PVC debris still attached to the copper surface.

Figure 721 - 20x magnification side view of the notch.

Microscope and SEM images for exhibit 110 - arcing category E (experiment 30)

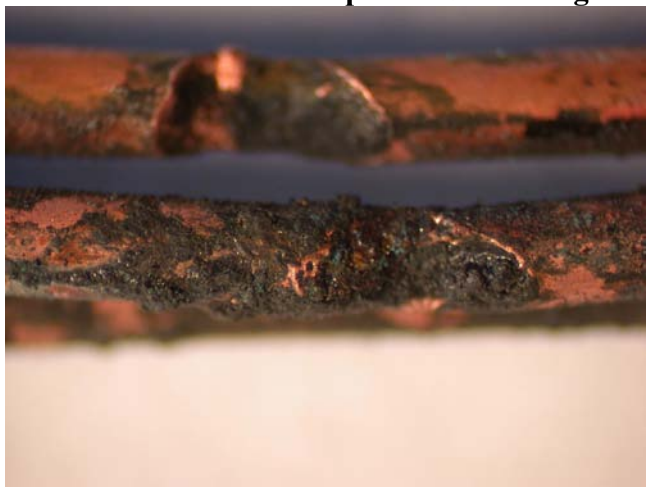

Figure 722 - Microscope image of exhibit 110. Two of the three conductors have arcing damage.

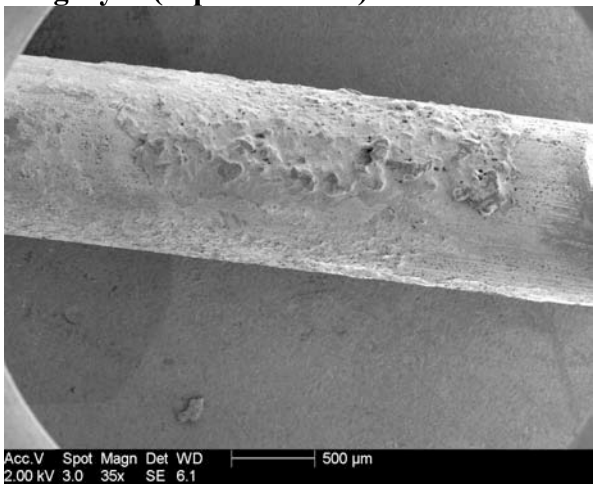

Figure 723 - SEM image of the bottom conductor detailed in figure 722.

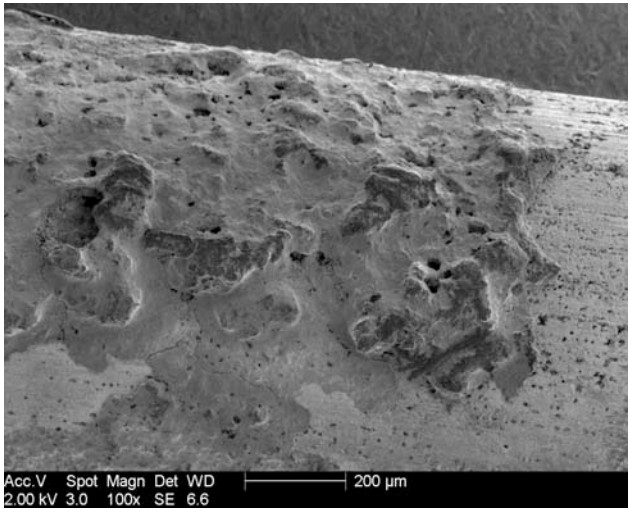

Figure 724 - SEM image of figure 723 at 100x magnification. The demarcation area at the edge of the arcing damage detailed.

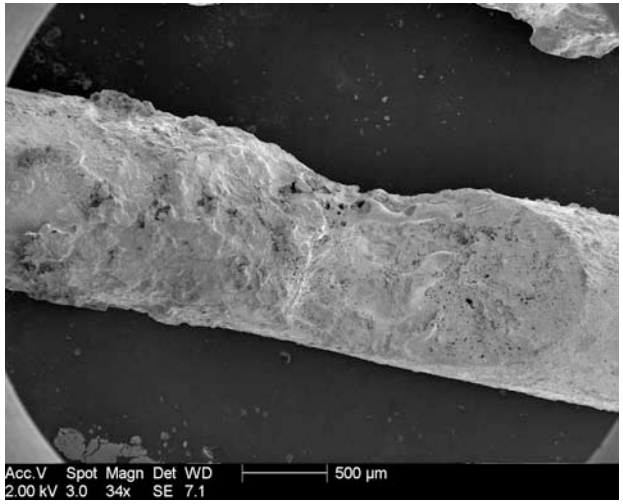

Figure 725 - SEM overview of the top conductor detailed in figure 722, with its large notch on the conductor surface.

Confocal laser scanning microscope images for exhibit 110 – arcing category E (experiment 30)

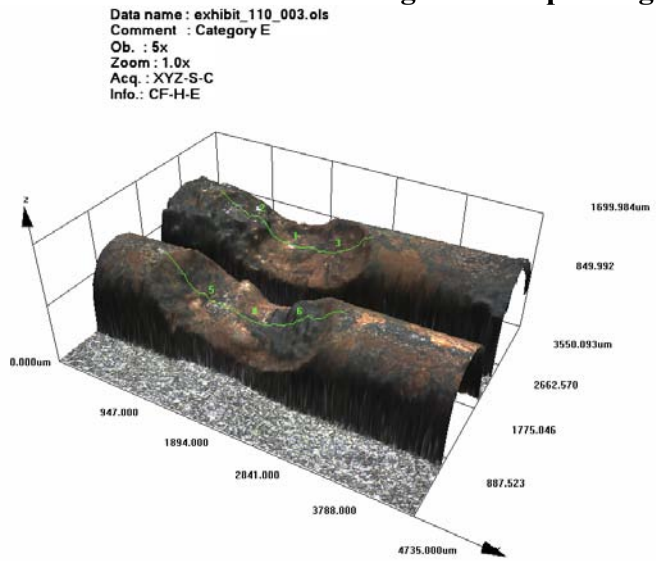

Figure 726 - LEXT image detailing both conductors side-by-side.

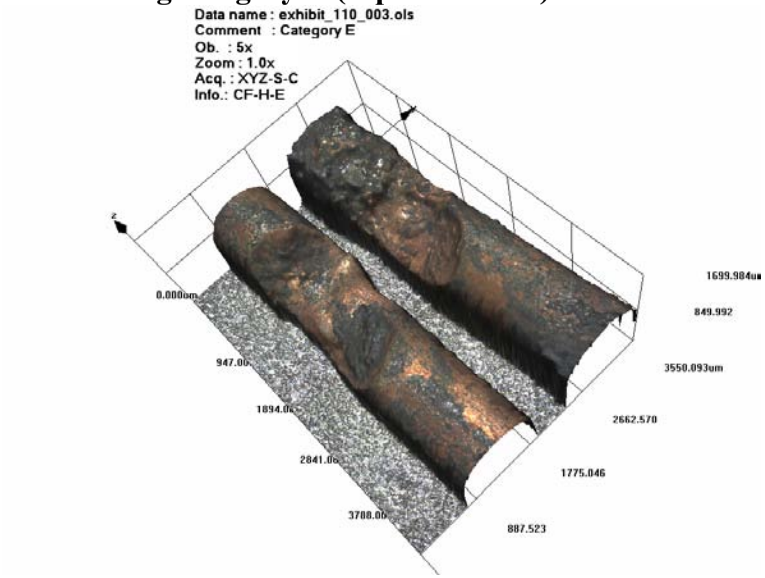

Figure 727 - Capture of LEXT 3-D software orientating the scanned image.

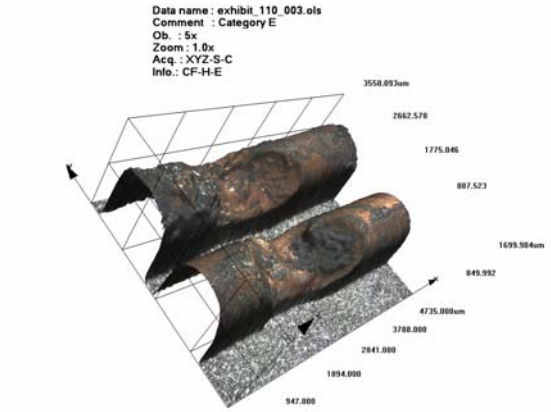

Figure 728 - Capture of the LEXT 3-D imaging software with a 180 degrees view compare to figure 726.

Microscope and SEM images for exhibit 111 - arcing category G (experiment 30)

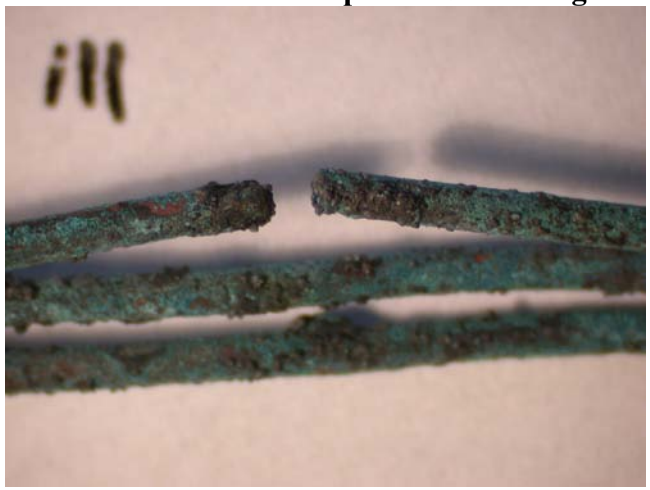

Figure 729 - Microscope image of exhibit 111. One conductor is severed and the adjacent conductor has a large bead on its surface.

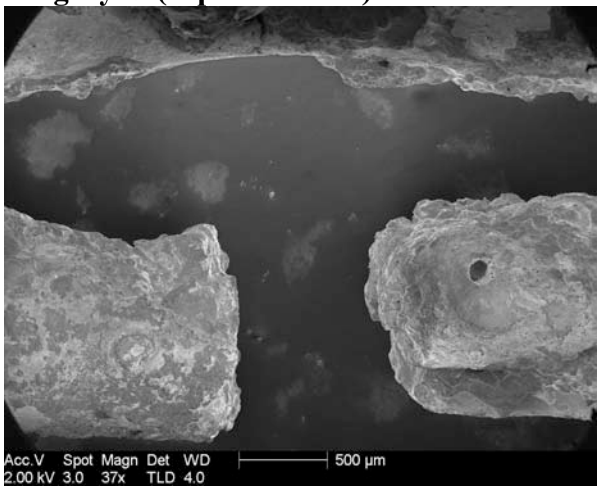

Figure 730 - SEM image of the severed ends.

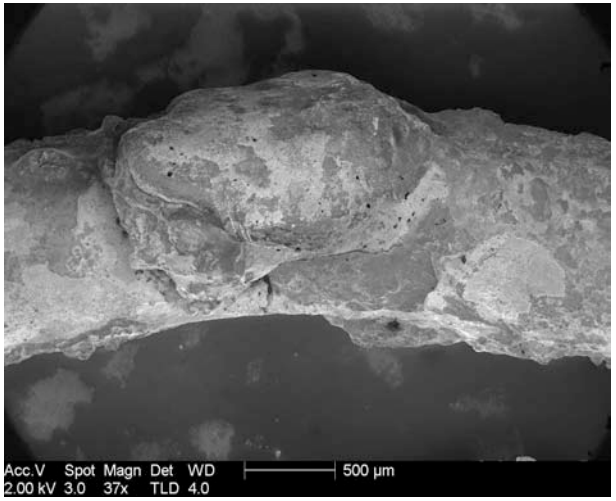

Figure 731 - SEM image of the large bead just visible in figure 729.

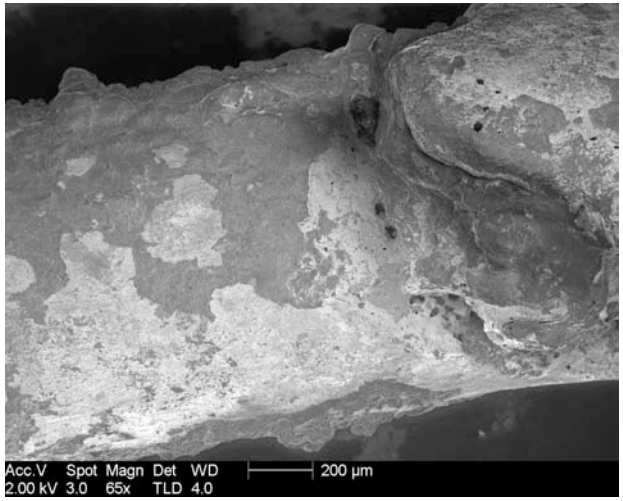

Figure 732 - SEM image of the left side of the bead detailed in figure 731, highlighting the demarcation area at the edge of the arcing damage.

Confocal laser scanning microscope images for exhibit 111 – arcing category G (experiment 30)

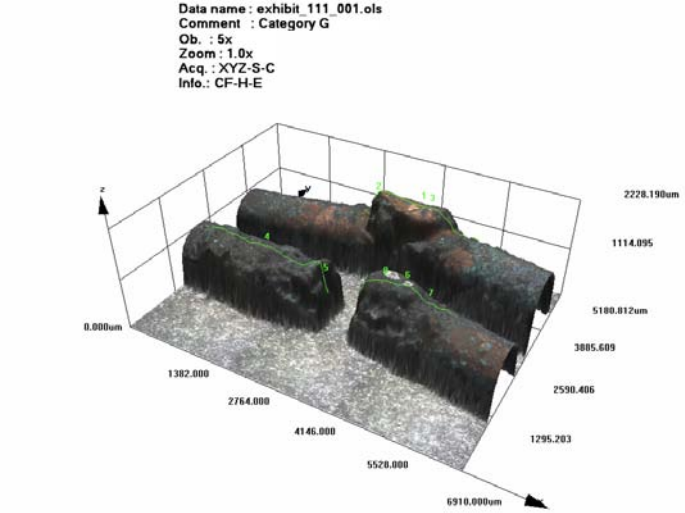

Figure 733 - LEXT image of both conductors viewed side-by-side.

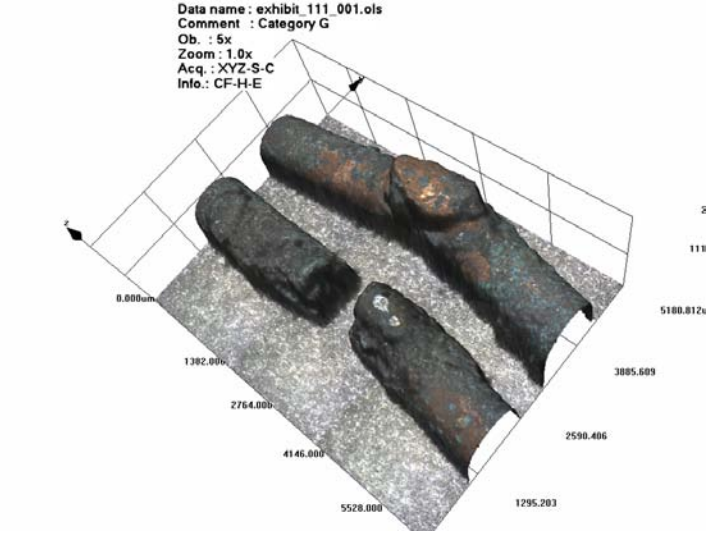

Figure 734 - LEXT image with the exhibit re-orientated in the LEXT 3-D software.

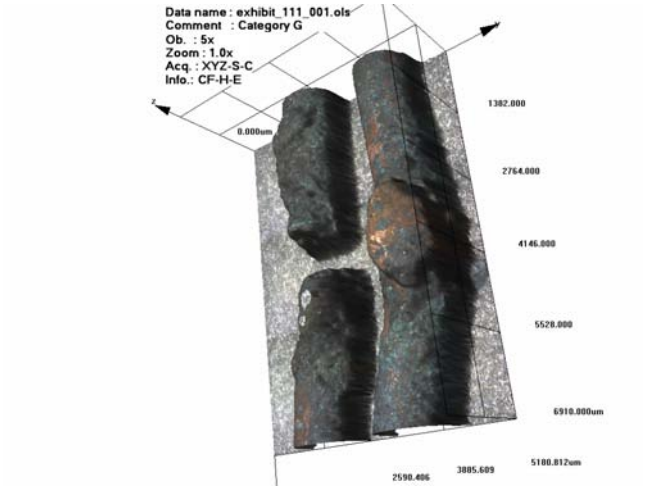

Figure 735 – Exhibit re-orientated in the LEXT software.

Figure 736 - Profile of the bead surface created with the LEXT software (scale in microns).

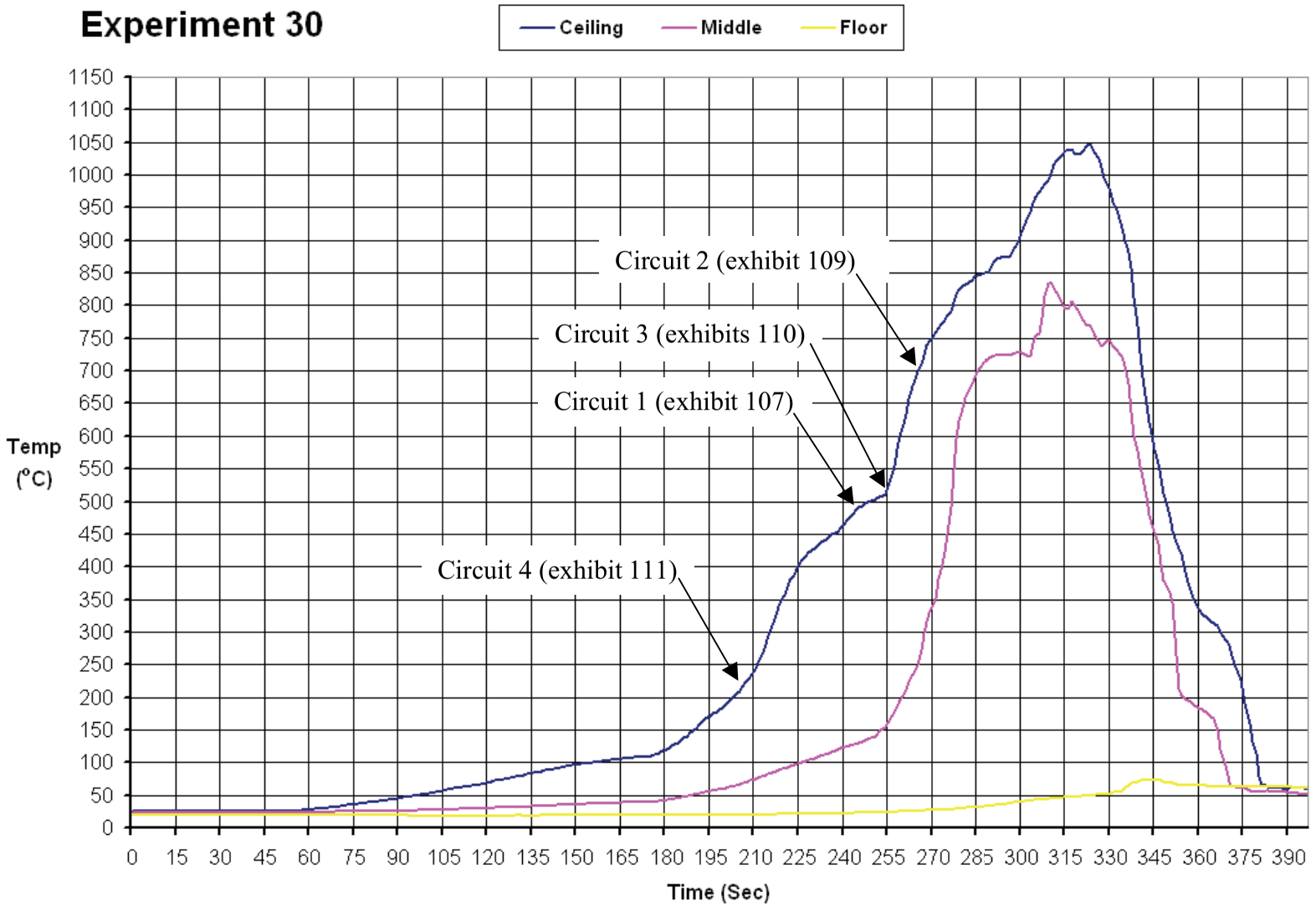

Figure 737 - Time temperature graph for experiment 30

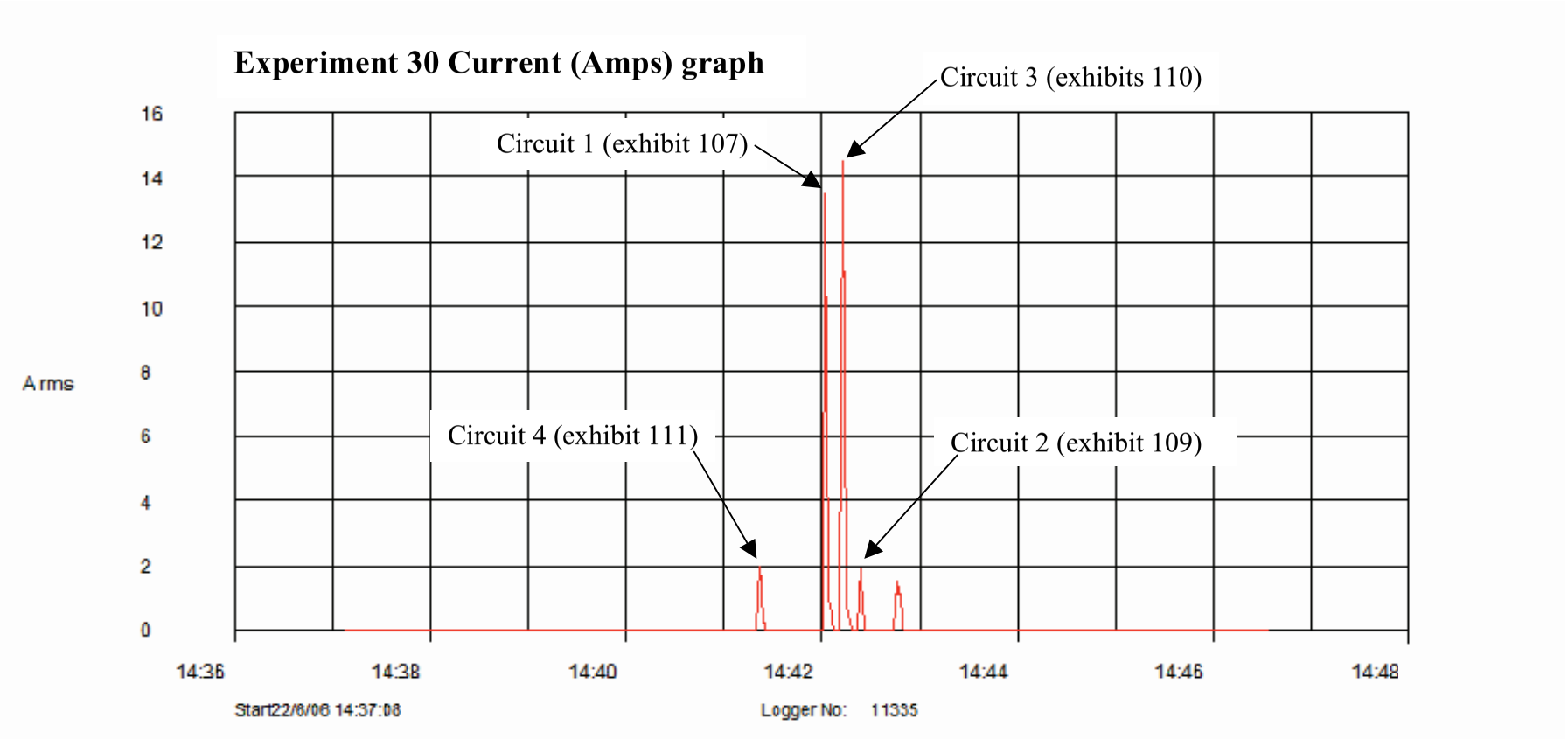

Figure 738 - Current (Amps) graph for experiment 30 detailing the operation of the circuit breakers and the fault current

Experiment 31

Figure 739 – “Scenario A” 22 June 2006

Circuit number	MCB operating time from ignition
1	1:37 minutes
4	1:38 minutes
3	1:52 minutes
2	1:52 minutes

Table 33 – circuit breaker operation data

The fire in experiment 31 (scenario A) originated within a clothes rail and the edge of two beds either side of the clothes rail. The clothes rail was located against the rear wall of the compartment.

The fire rapidly developed with the ceiling and middle thermocouples recording just over 1000° C at 3 minutes and 45 seconds. The floor thermocouple recorded a temperature of 250° C at this point. The compartment appeared to be at flashover conditions just prior to the fire being extinguished.

Arcing damage was located on circuit 1 – 2350mm from the left wall and on the rear wall.
Arcing damage was located on circuit 2 is 1180mm and 1800mm from the left wall and 1000mm from the front wall.
Arcing damage was located on circuit 3 – 1800mm from the left wall on the ceiling and 1000mm from the front wall.
Arcing damage was located on circuit 4 – 1850mm from the left wall and 1000mm from the rear wall.

Figure 740

Pre-fire and post-fire photographs of experiment 31

Figure 741 - Pre-fire photograph of experiment 31. The fire's area of origin is detailed with the white oval.

Figure 742 - Post-fire photograph of the ceiling detailing circuits 2 and 3.

Figure 743 - Post-fire photograph detailing the fire's area of origin between the two single beds.

Figure 744 - Close up image of exhibits 113 and 115 in position prior to recovery and packaging.

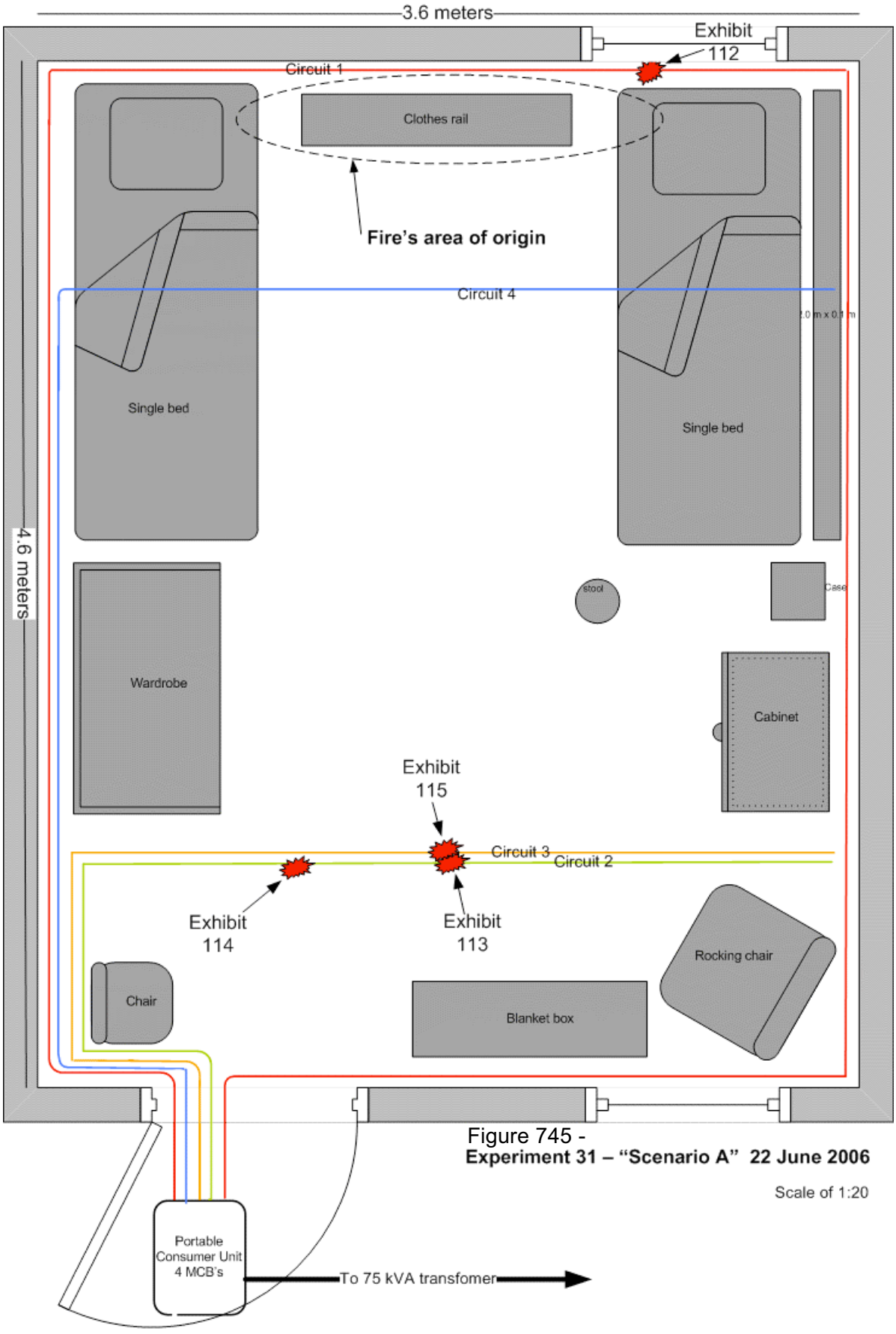

Figure 745 -
Experiment 31 – "Scenario A" 22 June 2006

Scale of 1:20

Microscope and SEM images for exhibit 112 – arcing category D (experiment 31)

Figure 746 - Microscope image of exhibit 112. Two conductors have arcing damage consisting of a notch with a bead within each notch.

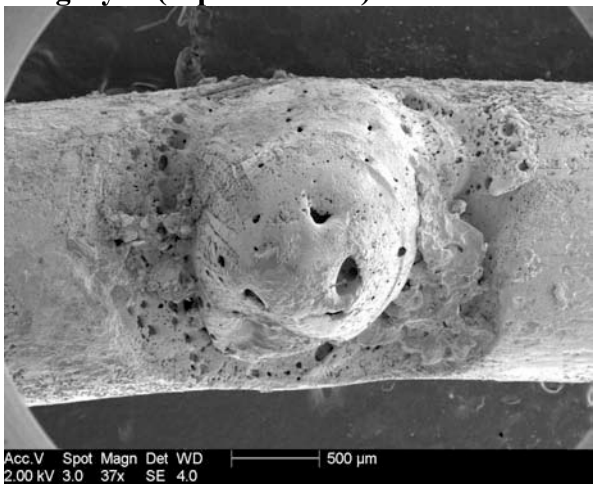

Figure 747 - SEM image of the middle conductor detailed in figure 746. The demarcation area is clear on this exhibit.

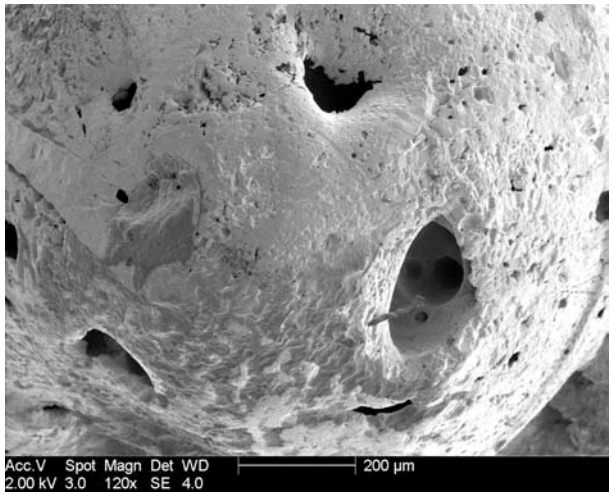

Figure 748 - SEM image at 120x magnification detailing the hollow areas of the bead known in the literature as the “Swiss cheese effect”.

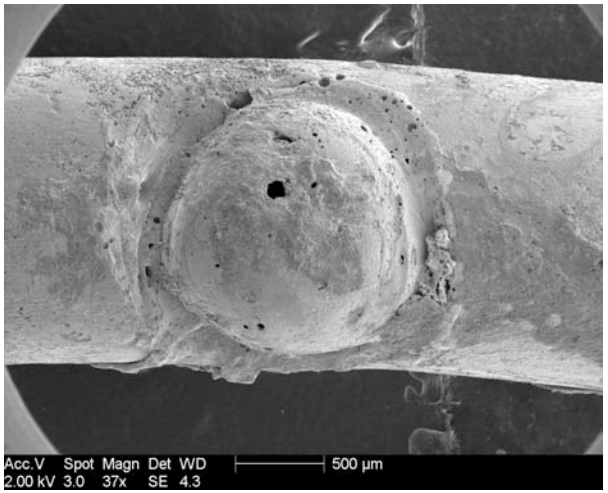

Figure 749 - SEM image of the bottom conductor detailed in figure 746. This image details the demarcation area at the edge of the notch.

Confocal laser scanning microscope images for exhibit 112 – arcing category D (experiment 31)

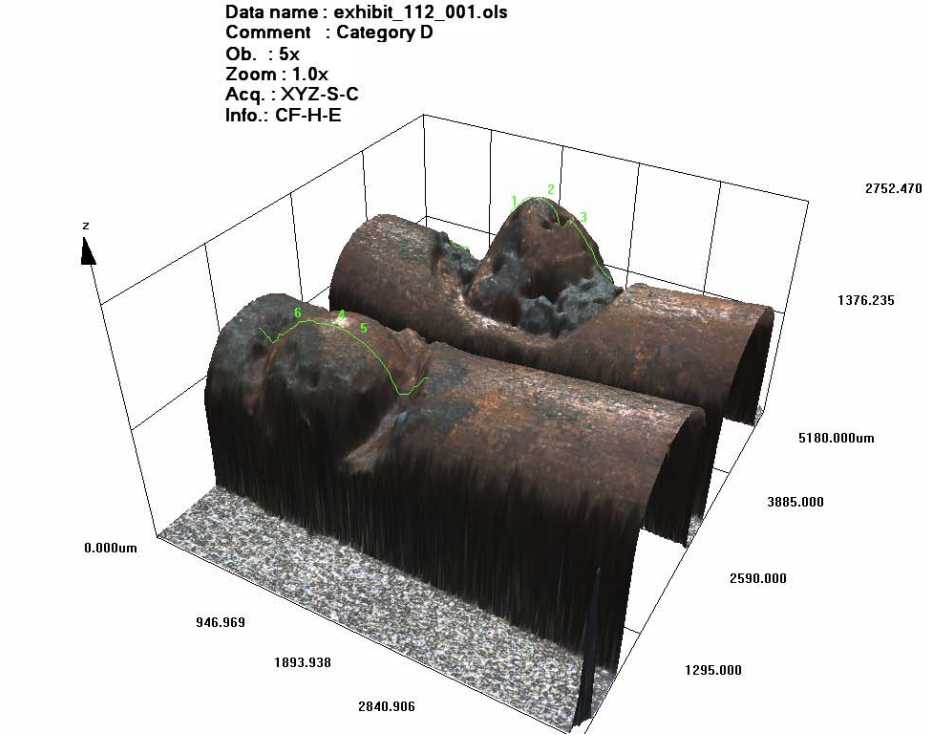

Figure 750 - LEXT image detailing both of the conductors side-by-side. The top conductor profile is detailed in figure 752.

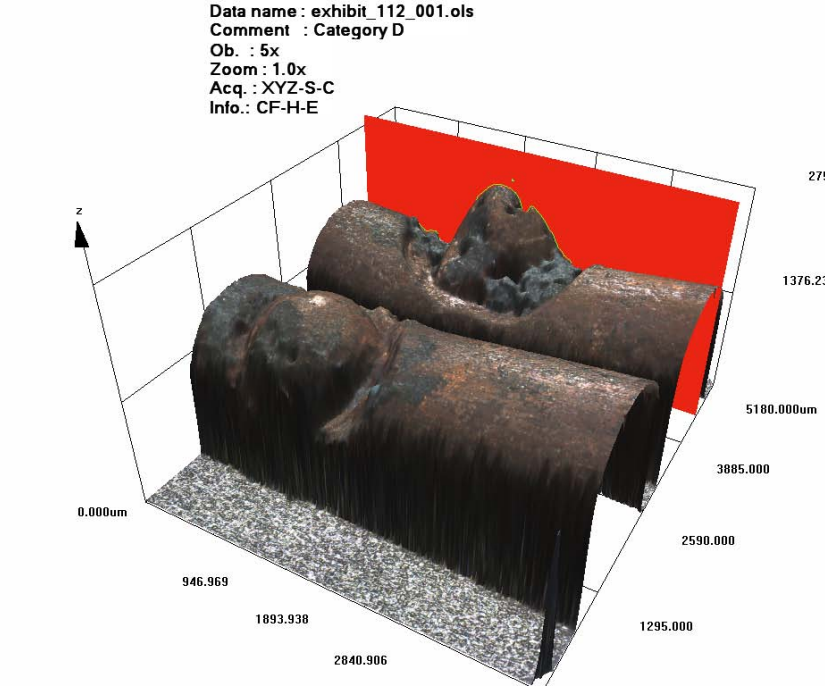

Figure 751 - LEXT image of the slice tool in use to obtain measurements and a profile.

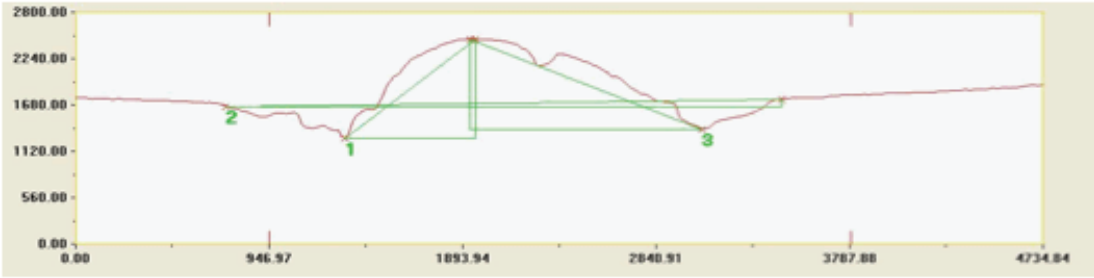

Figure 752 - Profile created in the LEXT software using the “slice tool”, measurements and scale detailed in microns.

Microscope images for exhibit 113 – arcing category F (experiment 31)

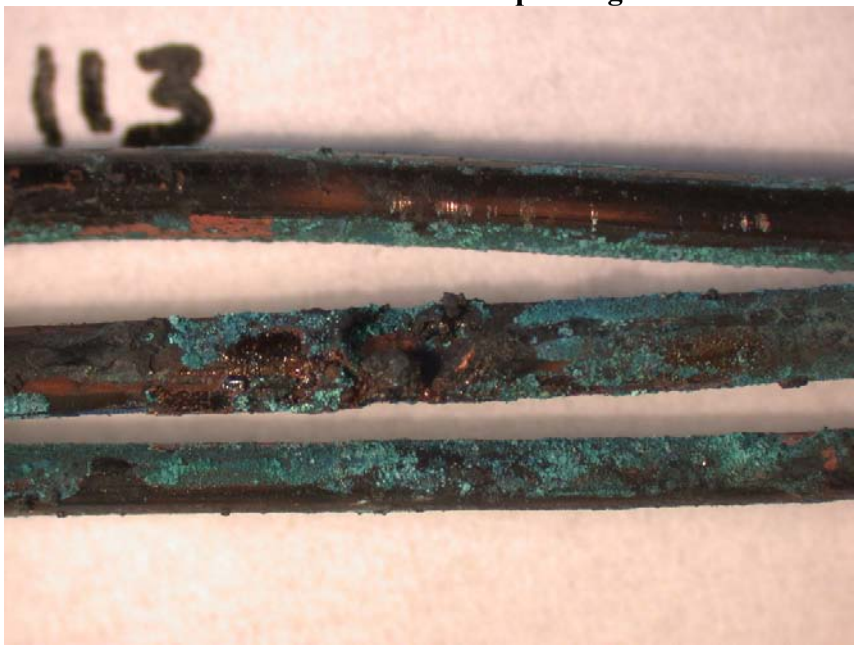

Figure 753 - Microscope image of exhibit 113. The arcing damage affected one conductor with a notch and copper splatter around the notch edge.

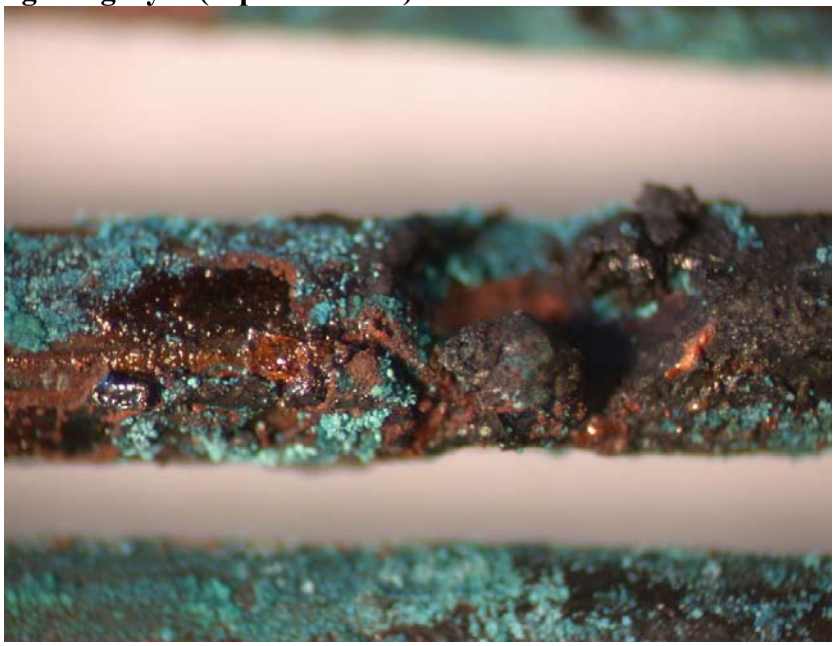

Figure 754 - 20x magnification microscope image of the notch. There was a lot of PVC debris and oxidation on the surface of this conductor.

Microscope and SEM images for exhibit 114 – arcing category E (experiment 31)

Figure 755 - Microscope image of exhibit 114. The arcing damage affected two of the three conductors. Each conductor has a notch with a bead at the edge.

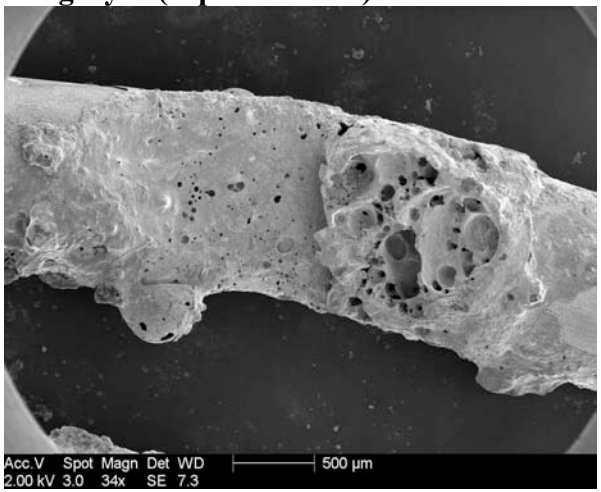

Figure 756 - SEM image of the top conductor detailed in figure 755.

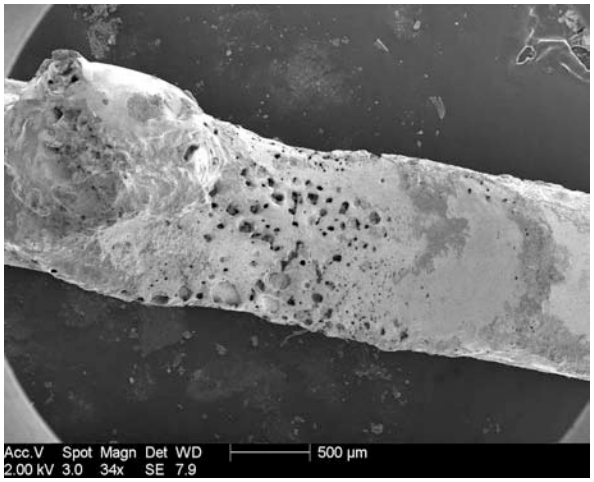

Figure 757 - SEM image of the bottom conductor detailed in figure 755.

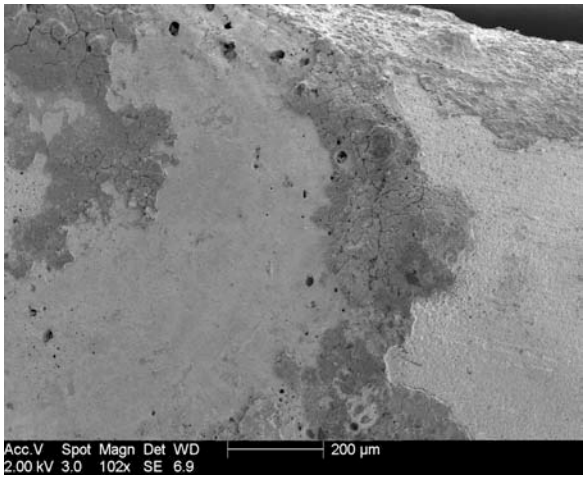

Figure 758 - SEM image at 102x magnification detailing the demarcation area at the edge of the notch.

Confocal laser scanning microscope images for exhibit 114 – arcing category E (experiment 31)

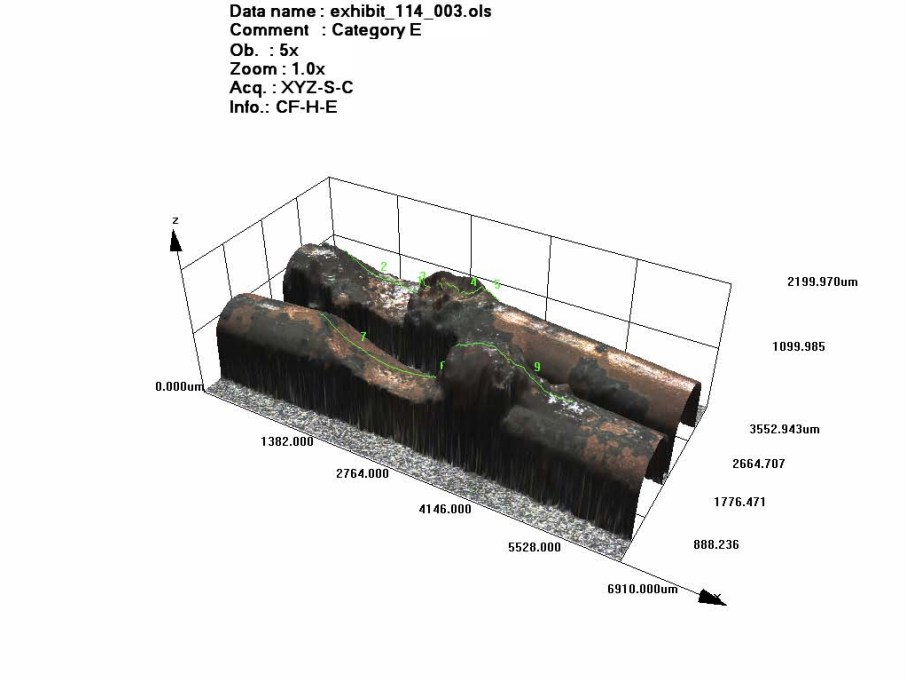

Figure 759 – LEXT image of both conductors side-by-side.

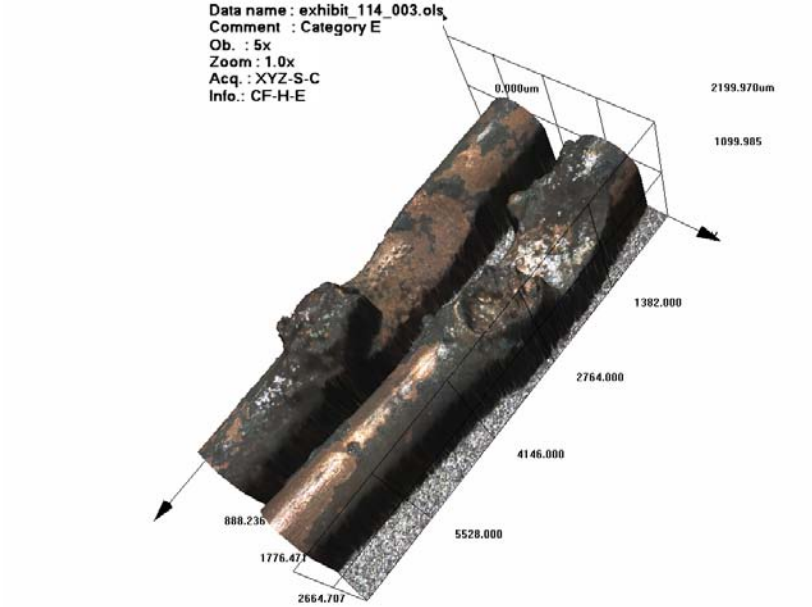

Figure 760 – The exhibit re-orientated in the LEXT software.

Figure 761 - Profile of the bottom conductor in the LEXT image above created with the “slice tool” option in the software.

Microscope images for exhibit 115 – arcing category D (experiment 31)

Figure 762 - Microscope image of exhibit 115. Two notches are located close to each other on the same conductor. The smaller notch arcing damage may have failed to operate the circuit breaker. The circuit breakers for circuits 2 and 3 operated simultaneously.

Figure 763 - 20x magnification of the smaller notch. There is a demarcation area at the edge of the notch between the arcing damage and the undamaged conductor.

Figure 764 - 30x magnification of the larger notch and associated bead at the notch edge.

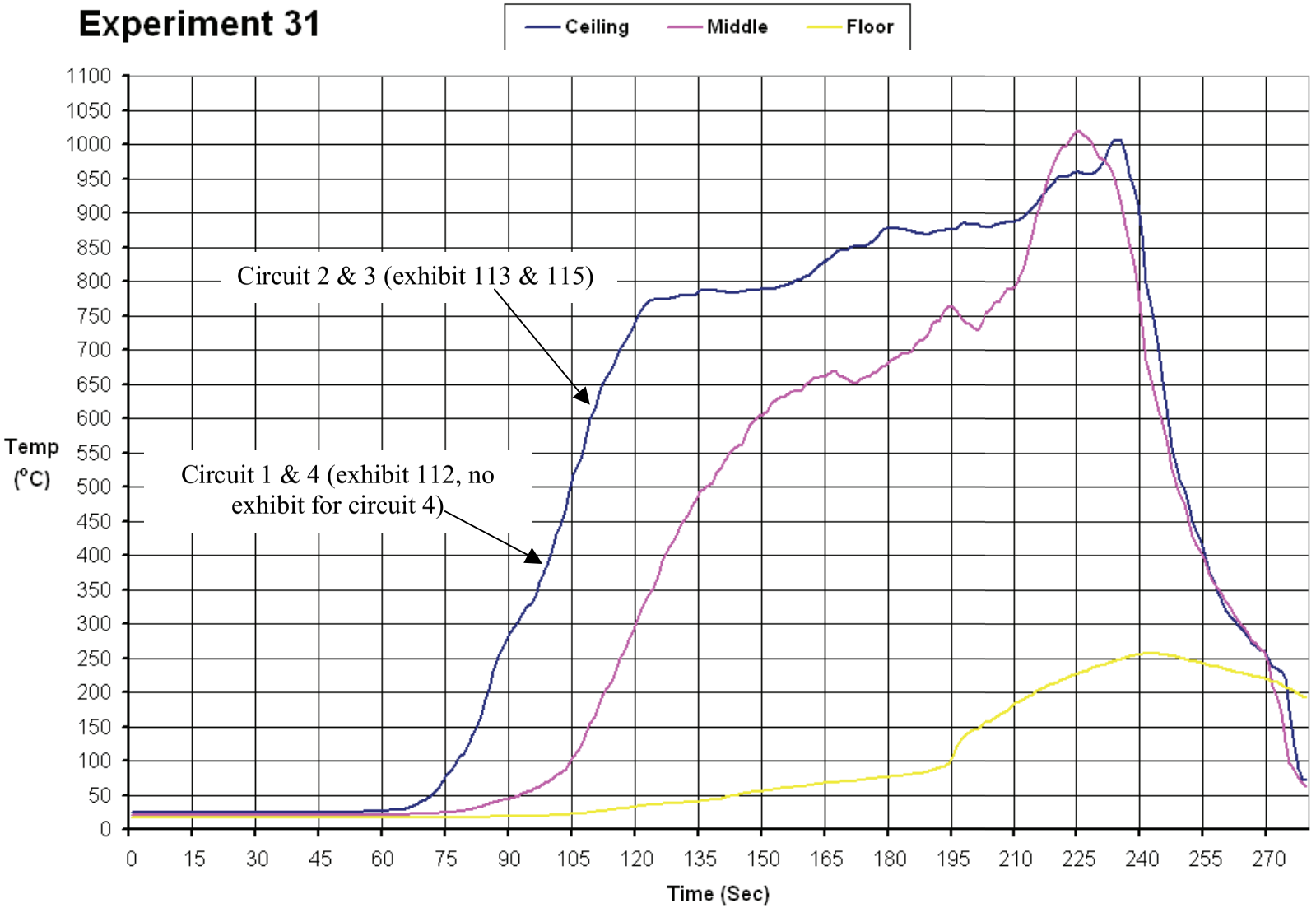

Figure 765 - Time temperature graph for experiment 31

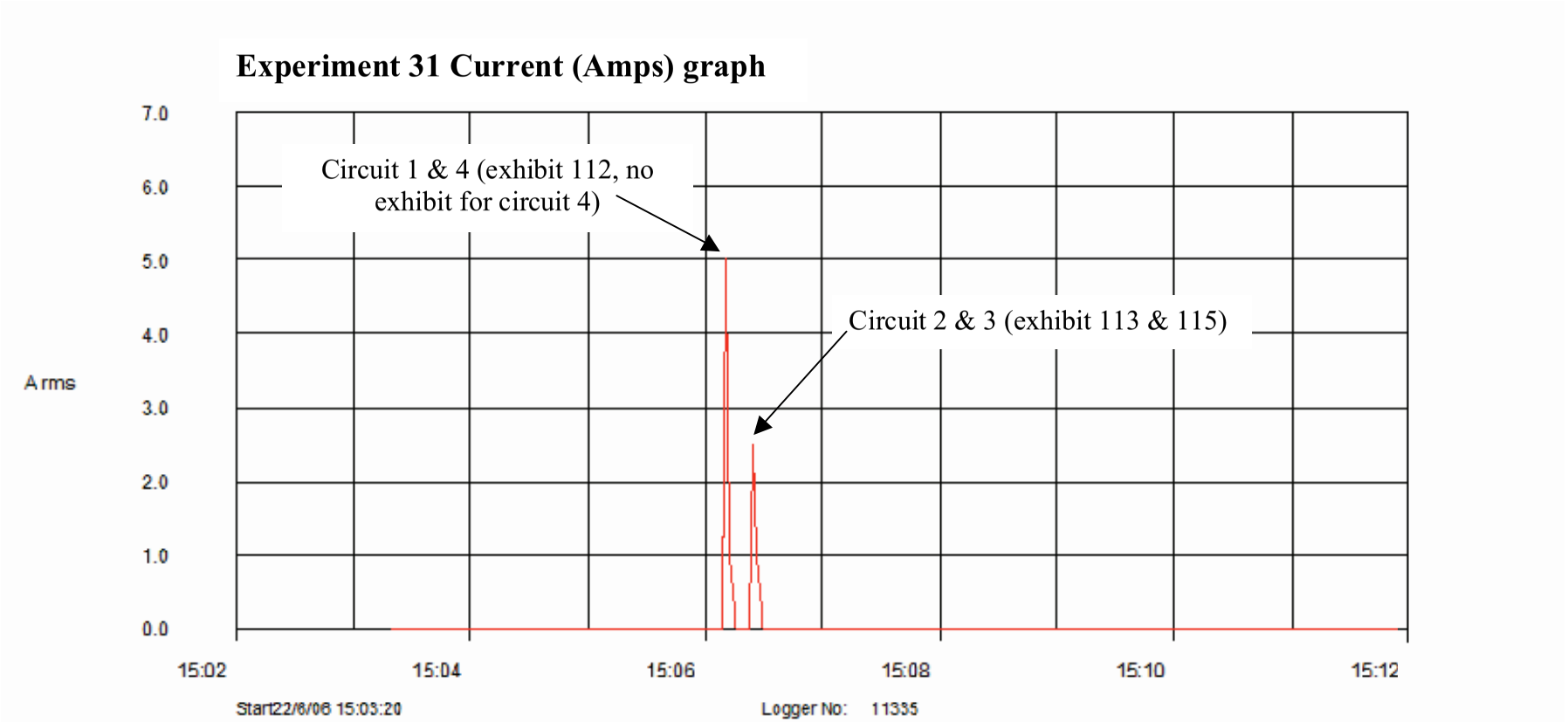

Figure 766 - Current (Amps) graph for experiment 31 detailing the operation of the circuit breakers and the fault current

Experiment 32

Figure 767 – “Scenario D” 7 September 2006.

Circuit number	MCB operating time from ignition
4	1:00 minutes
1	1:20 minutes
3	1:16 minutes
2	1:16 minutes

Table 34 – circuit breaker operation data

The fire in experiment 32 (scenario A) had three separate areas of origin. One was located on an armchair adjacent to the rear left corner of the compartment. The second area of origin was on a two-seat settee on the left wall. The third area of origin was on a three-seat settee located against the front wall of the compartment, this was the predominant fire plume in the early development of the fire with flames impinging on the ceiling before the other two areas. The fire developed rapidly and was at flashover conditions within 2.5 minutes.

Arcing damage was located on circuit 1 – 1520mm from the floor and 1200mm from the left wall.
Arcing damage was located on circuit 4 – 1240mm from the floor and 1200mm from the left wall.
Arcing damage was located on circuits 2 and 3 – 1970mm from the left wall on the ceiling and 1000mm from the front wall.

Figure 768 - Early fire development

Pre-fire and post-fire photographs of experiment 32

Figure 769 - Pre-fire photograph of experiment 32. The white circles indicate the fire's area of origin.

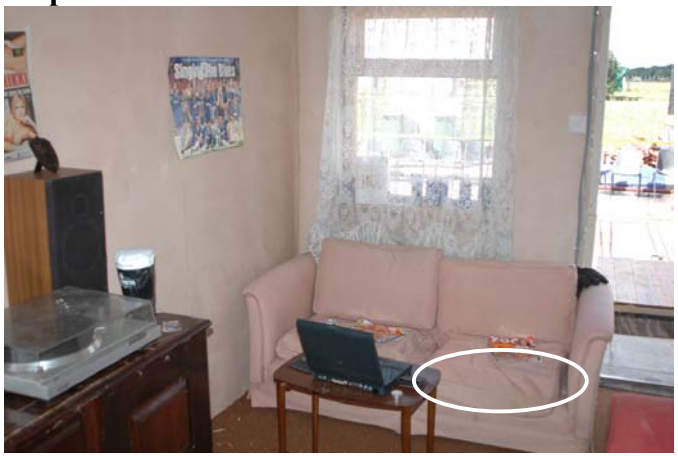

Figure 770 - The white circle indicates the fire's third and dominant area of origin.

Figure 771 - Post-fire photograph taken from the entrance door.

Figure 772 - Post-fire view of the three-seat settee next to the entrance door that was the dominant fire plume in the early development of this fire.

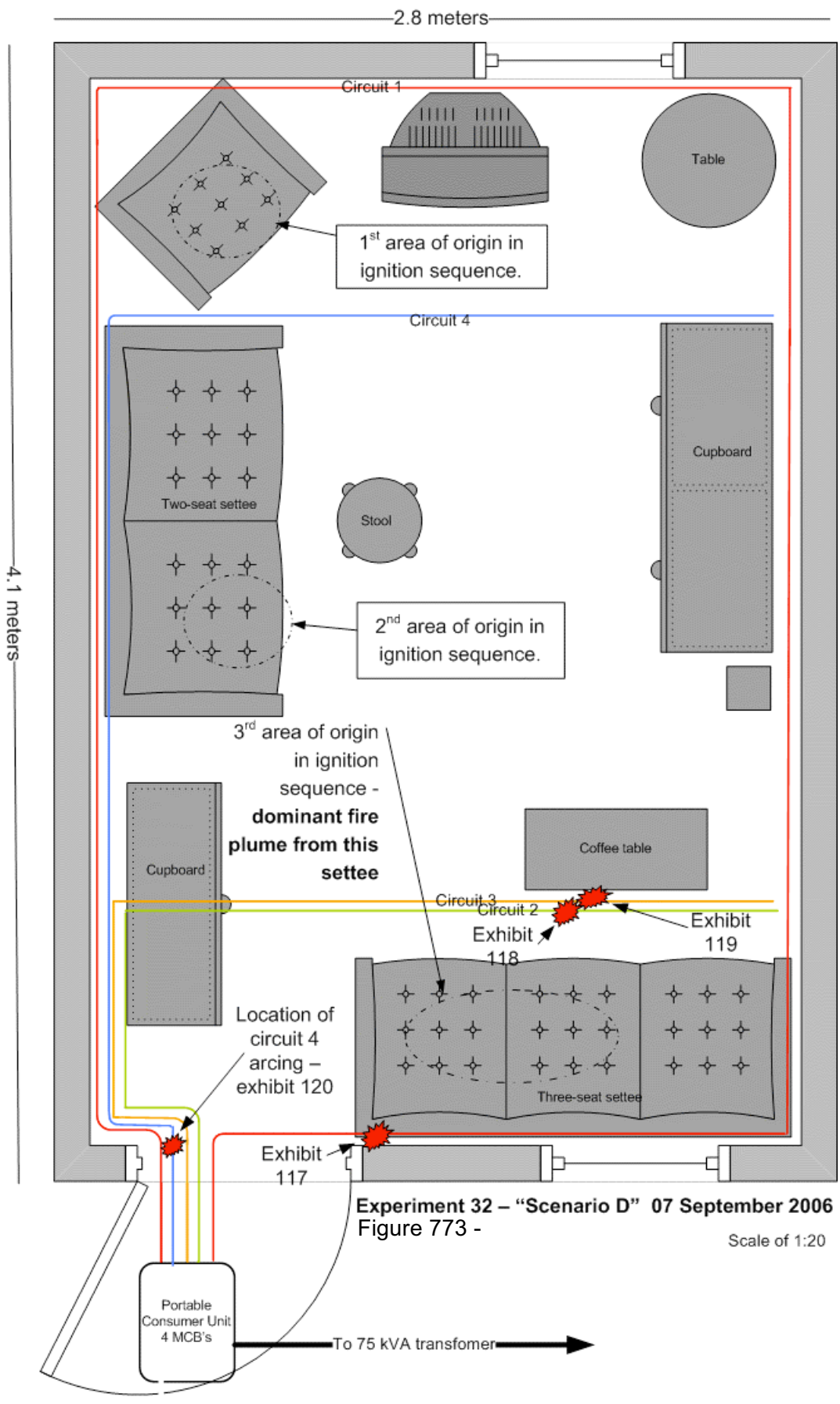

Experiment 32 – "Scenario D" 07 September 2006

Figure 773 -

Scale of 1:20

Microscope and SEM images for exhibit 117 – arcing category H (experiment 32)

Figure 774 - Microscope image of exhibit 117. The live and earth conductors are welded to a fixing screw.

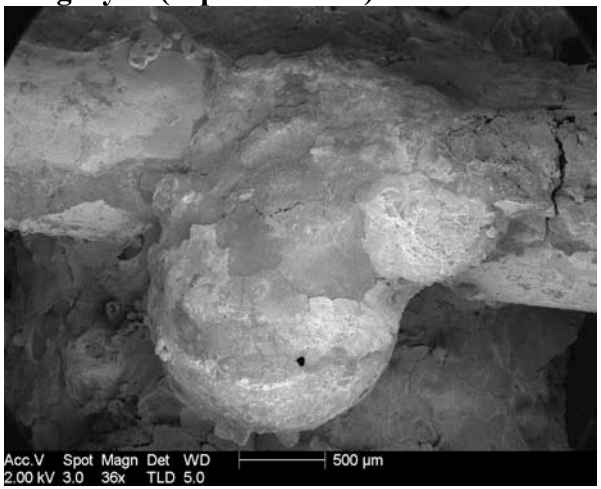

Figure 775 - SEM image of the lower conductor bead. It took two sessions of acetone an ultrasonic cleaning to remove the Fe oxide.

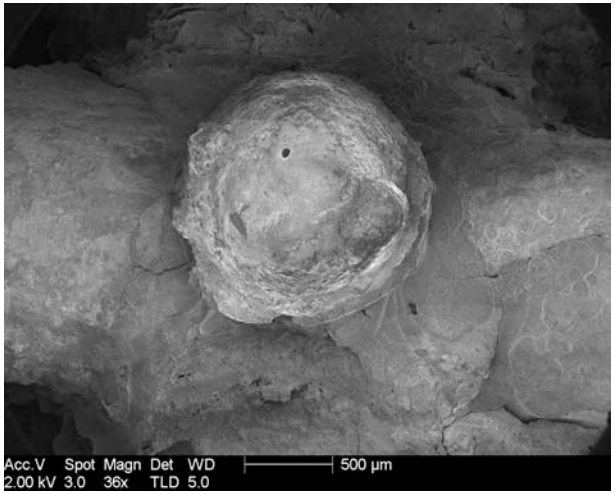

Figure 776 - SEM image of the top conductor in figure 774.

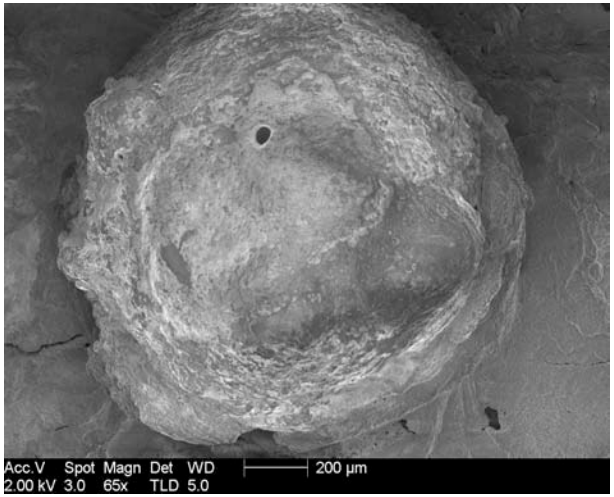

Figure 777 - 65x magnification SEM image of the bead surface detailed in figure 776.

Confocal laser scanning microscope images for exhibit 117 – arcing category H (experiment 32)

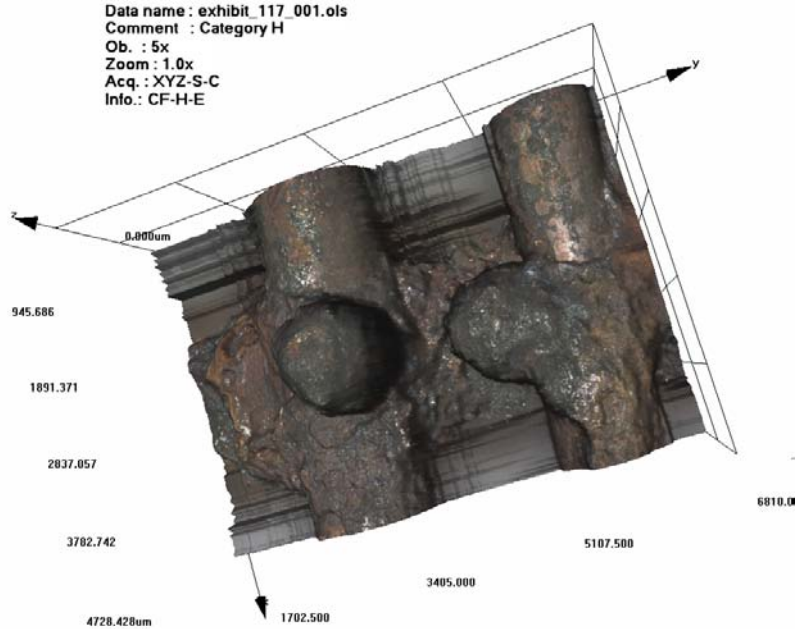

Figure 778 - LEXT image of both conductors welded to the fixing screw. The LEXT was much more practical to scan this exhibit due to its size and height. It was the only method that documented the entire exhibit clearly.

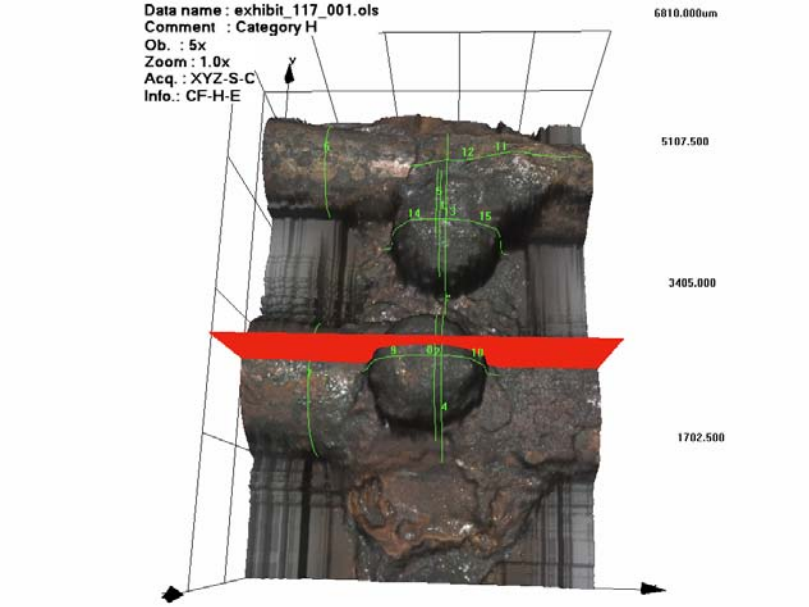

Figure 779 - LEXT image capturing the use of the "slice tool' in the software to obtain a profile and various measurements.

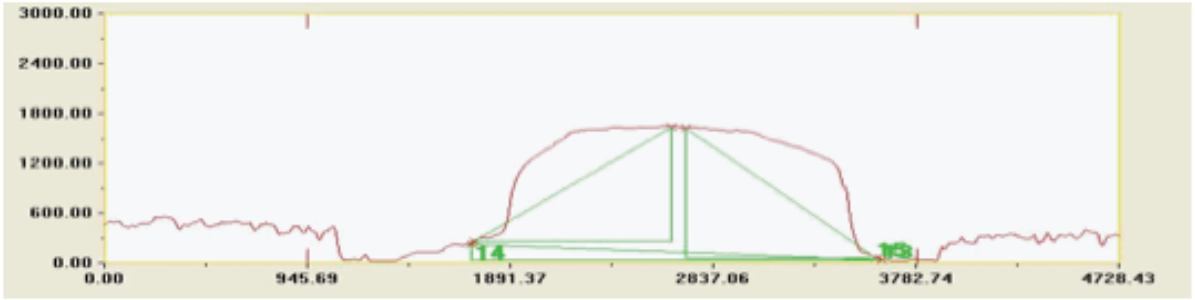

Figure 780 - Profile created with the "slice tool" option of the LEXT software detailed in figure 779, measurements are in microns.

Microscope and SEM images for exhibit 118 – arcing category H (experiment 32)

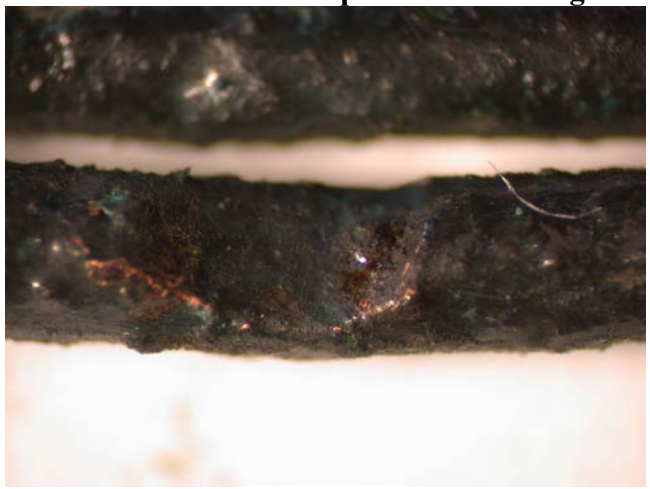

Figure 781 - Microscope image of exhibit 118. The arcing damage is confined to a large notch to one of the conductors.

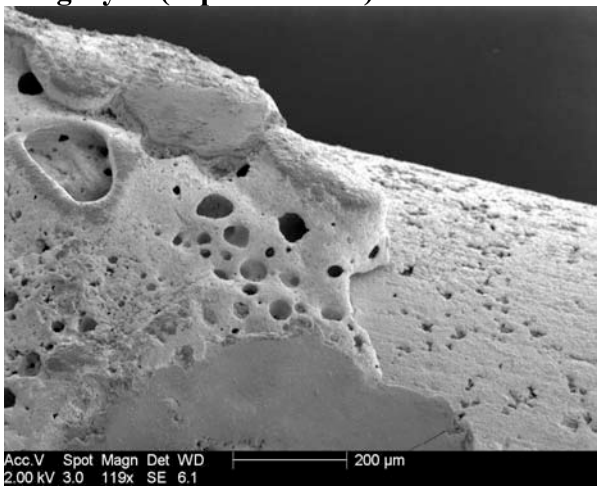

Figure 782 - An SEM image at 118x magnification of the top right edge of the notch with a clear demarcation area.

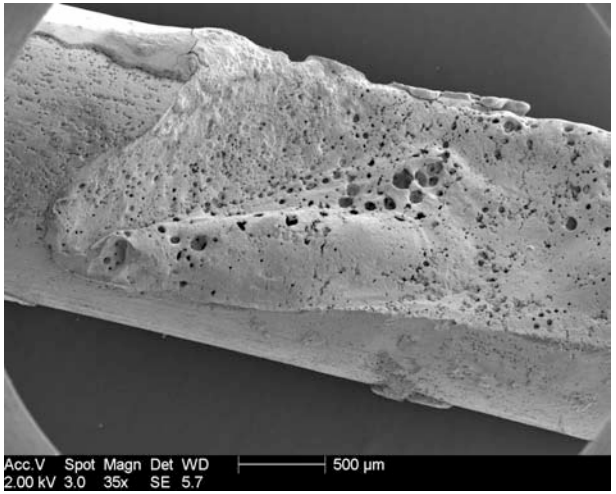

Figure 783 - SEM image of the left side of the notch. The demarcation area was on the left and bottom edge of the notch.

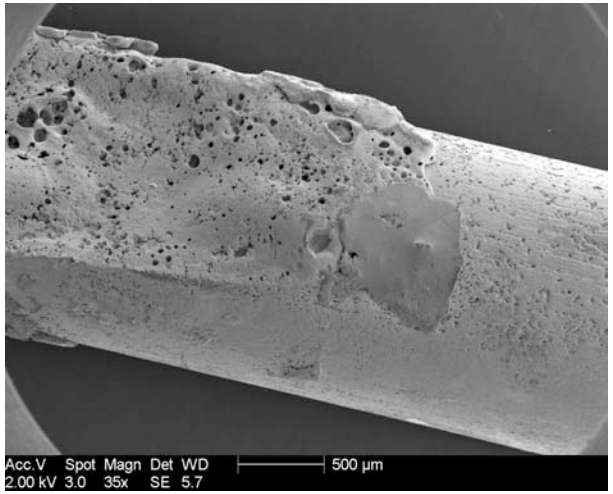

Figure 784 - SEM image of the right side of the notch. A close up image of the top right edge is detailed in figure 782.

Confocal laser scanning microscope images for exhibit 118 – arcing category H (experiment 32)

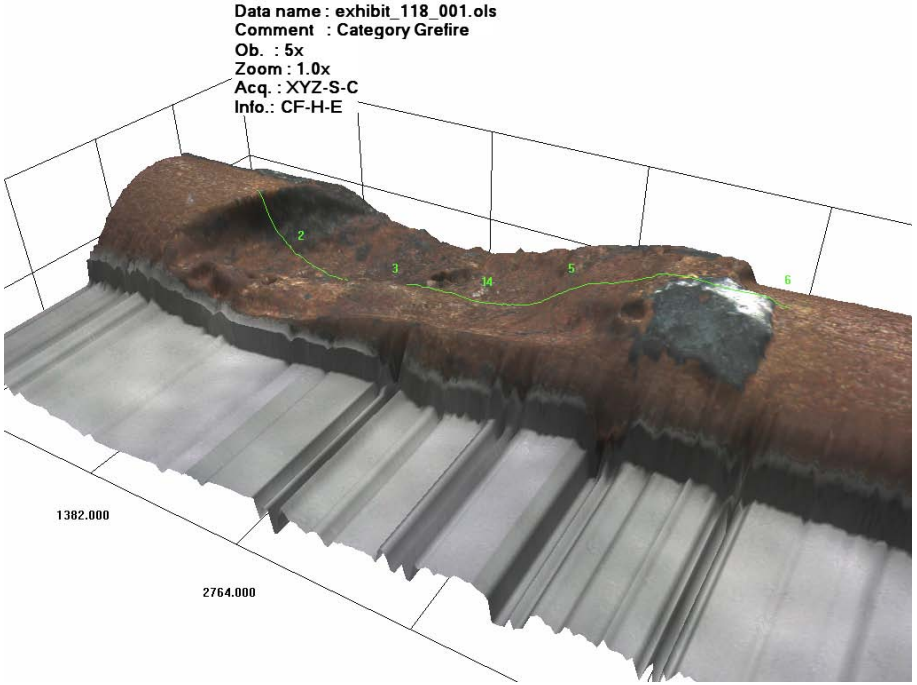

Figure 785 - LEXT image of figure 118. This notch is quite shallow and so the laser scan time was reduced. The green line profile is detailed in figure 787.

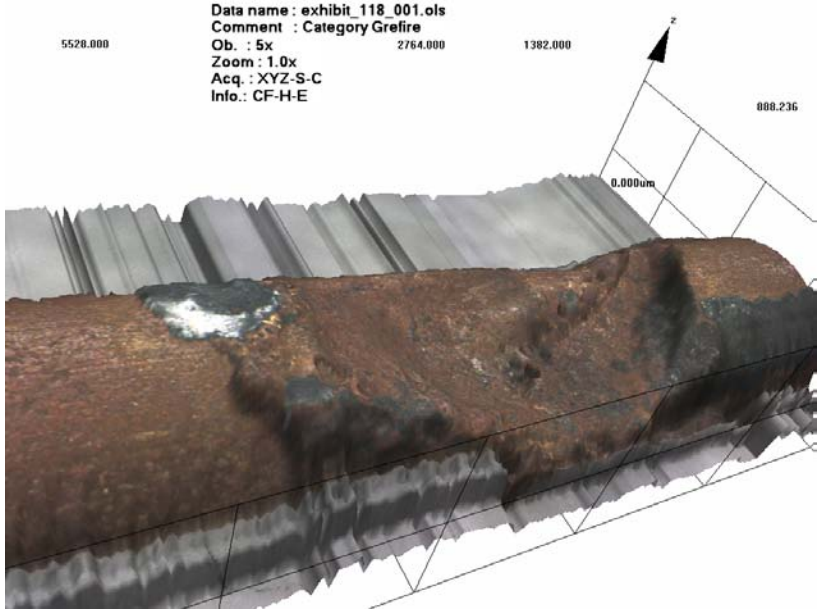

Figure 786 - LEXT image 180 degrees opposite view from figure 785.

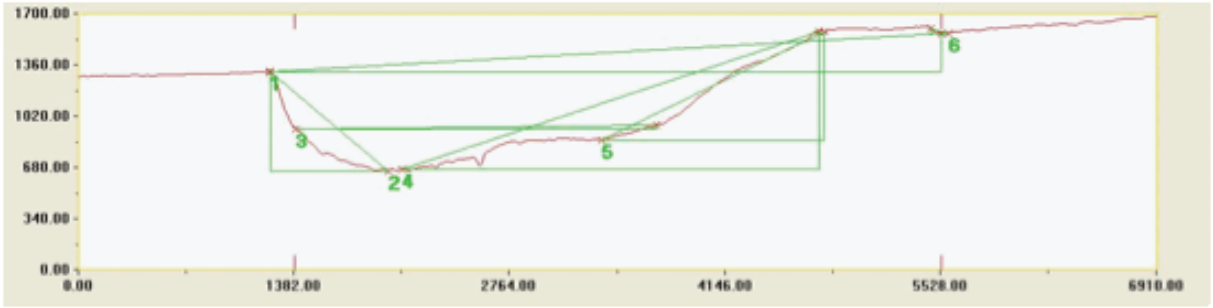

Figure 787 - Profile of the exhibit created by using the software's "slice tool", measurements are detailed in microns

Microscope images for exhibit 119 – arcing category D (experiment 32)

Figure 788 - Microscope image of exhibit 119. The arcing damage was restricted to one conductor with a notch and a bead within the notch. Some copper splatter was also observed on the conductor surface to the side of the notch.

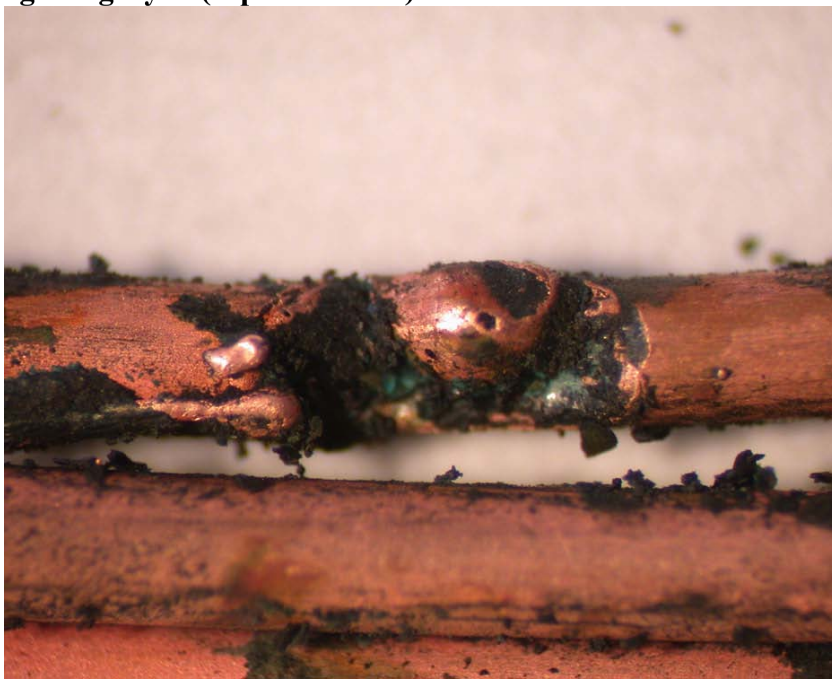

Figure 789 - 20x magnification of the arcing damage. The demarcation is clear in this image on the right and left sides of the notch.

Microscope and SEM images for exhibit 120 – arcing category F (experiment 32)

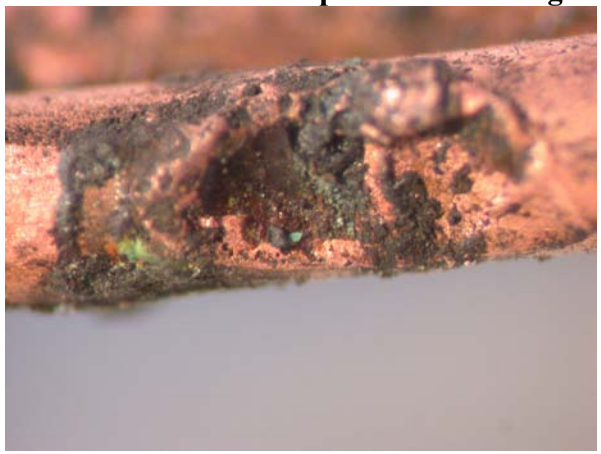

Figure 790 - Microscope image of exhibit 120. The arcing damage is limited to one conductor. The limited depth of field renders the edge of the notch out of focus.

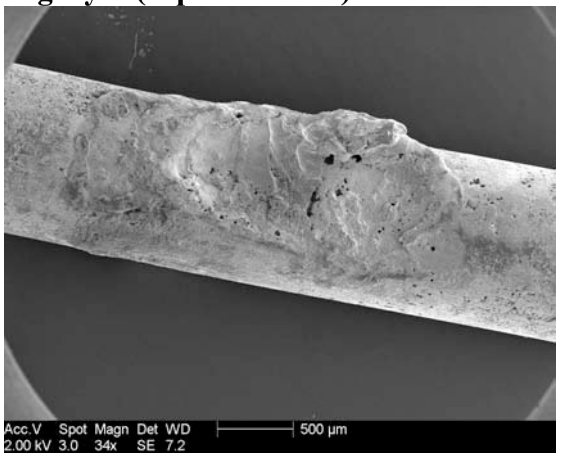

Figure 791 - SEM image of the notch. The demarcation at the edge of the notch is defined.

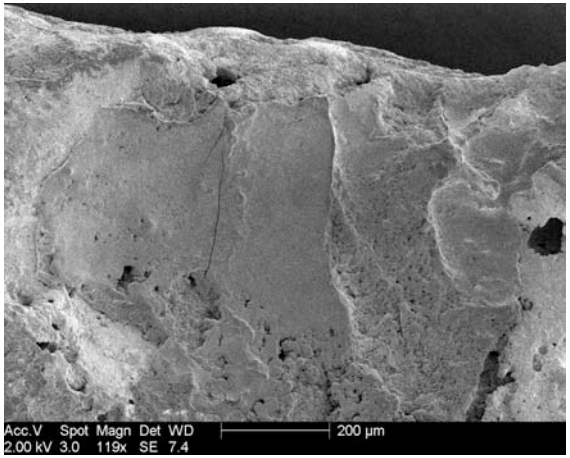

Figure 792 - SEM image of the left side of the notch. The ridge patterns in this image were observed on other exhibits and this could be an effect of alternating current during the arcing event.

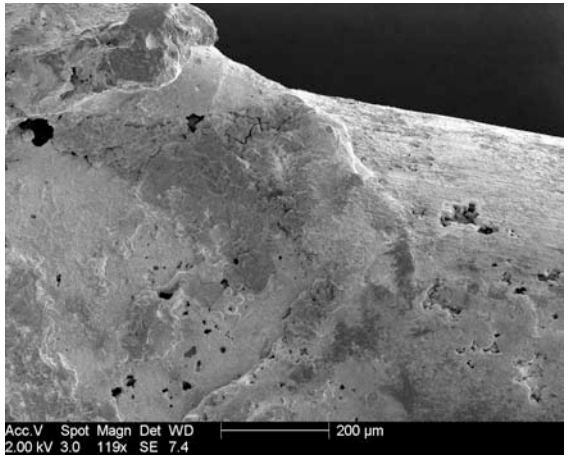

Figure 793 - SEM image of the right side of the notch. This image re-enforces the defined demarcation between the arcing damage and the undamaged conductor that is consistent with electrical localised metallic (arcing) damage to conductors.

Confocal laser scanning microscope images for exhibit 120 – arcing category F (experiment 32)

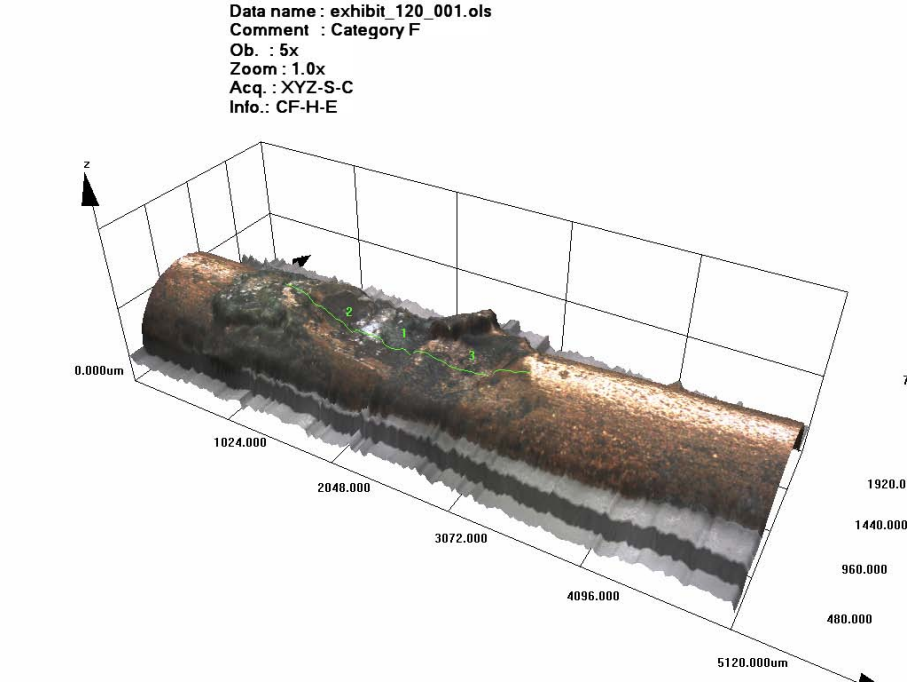

Figure 794 - LEXT image of exhibit120. The green line is the profile line detailed in figure 796.

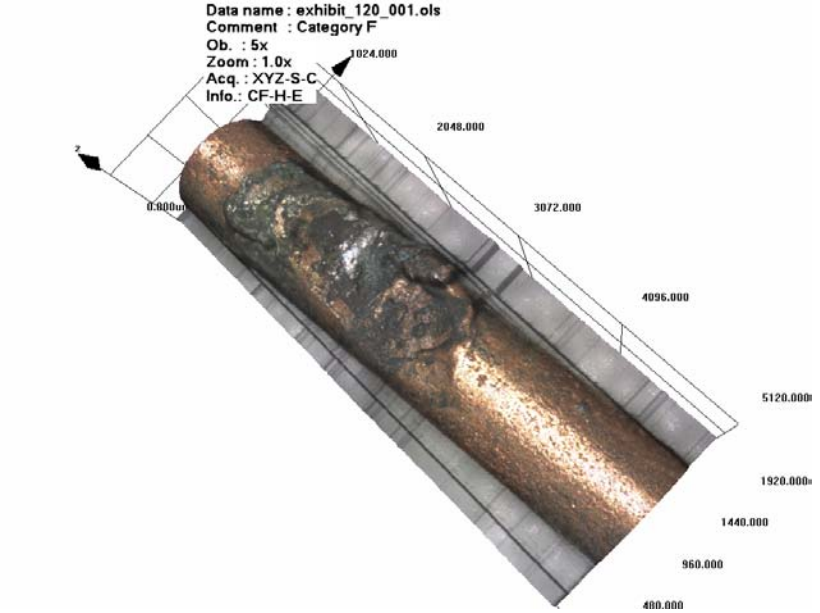

Figure 795 - LEXT image of the exhibit rotated and captured within the LEXT 3-D software.

Figure 796 - Profile of the notch detailed in figure 794, created by the LEFT software “slice tool”, measurements in microns.

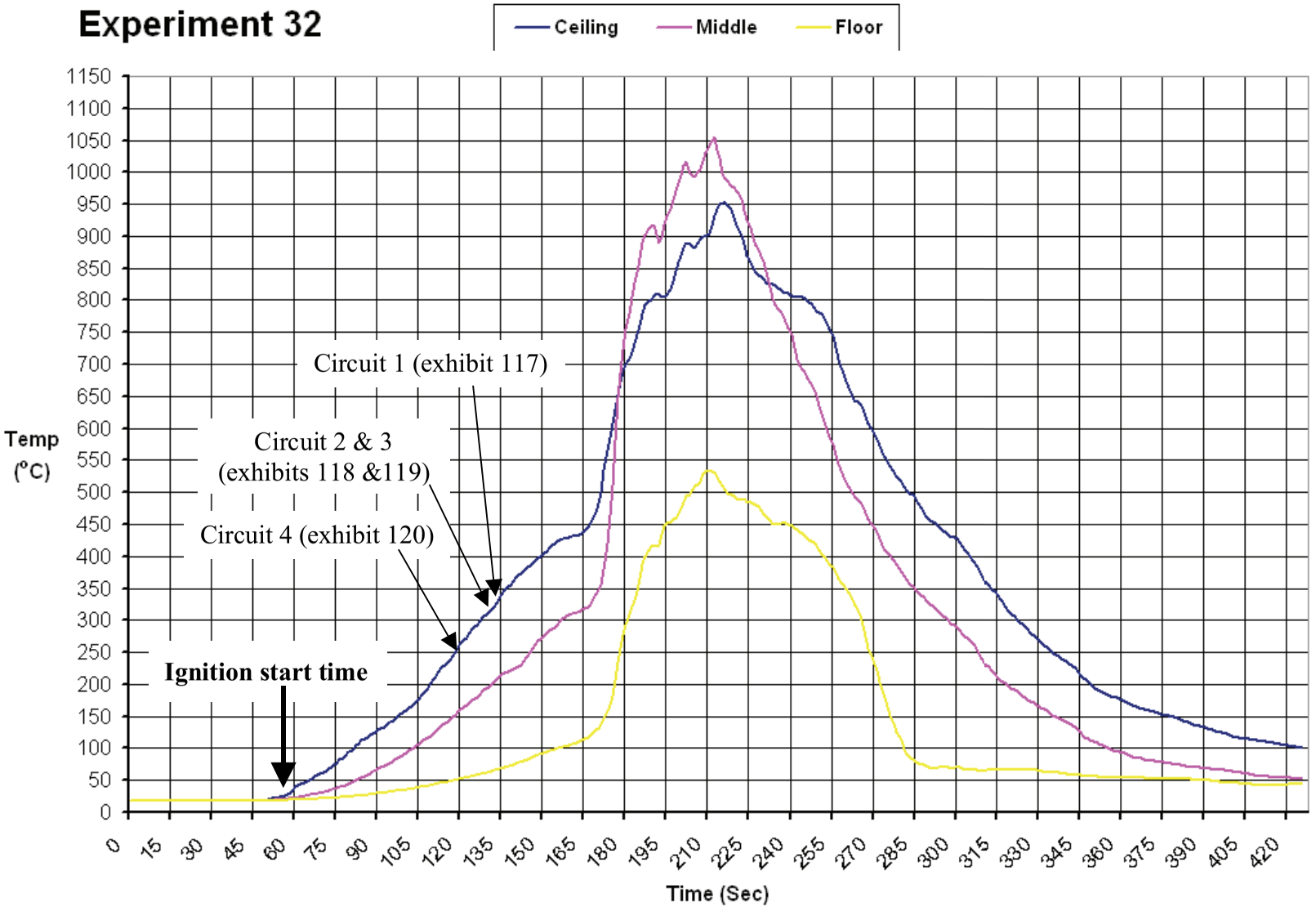

Figure 797 - Time temperature graph for experiment 32 (ignition start time adjusted following the review of the video recording).

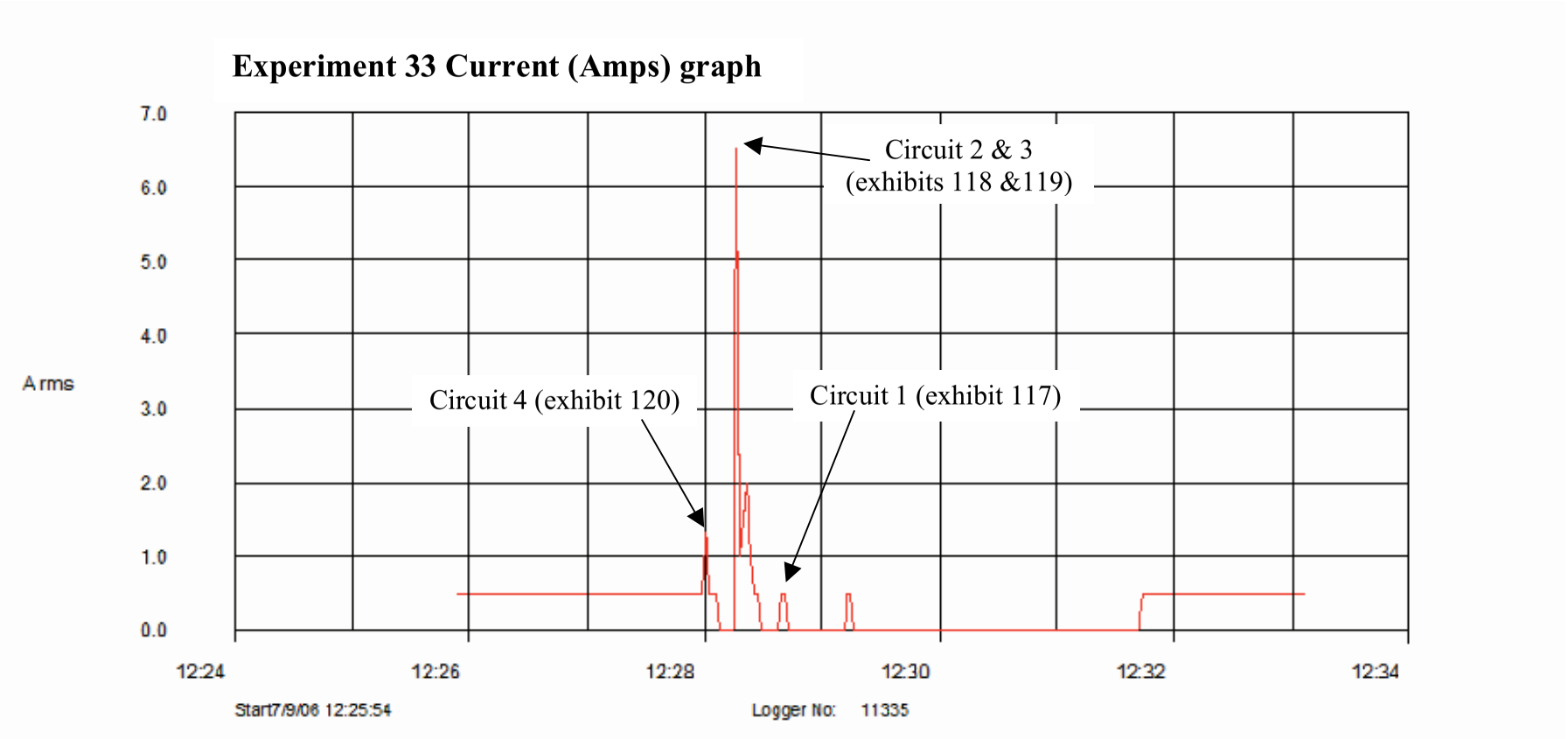

Figure 798 - Current (Amps) graph for experiment 32 detailing the operation of the circuit breakers and the fault current

Experiment 33

Figure 799 – "Scenario B" 7 September 2006.

Circuit number	MCB operating time from ignition
4	1:31 minutes
1	1:47 minutes
3	1:26 minutes
2	1:26 minutes

Table 35 – circuit breaker operation data

The fire in experiment 33 (scenario B) originated in a refuse bin located in the rear left corner of the compartment. The compartment fire developed to flashover conditions within 5 minutes from the ignition time. The ceiling temperature reached 975° C with the floor thermocouple recording 725° C at this time.

Arcing was located on circuit 1 – 1350mm from the left wall and adjacent to the rear wall.
Arcing was located on circuits 2 & 3 – 1690mm from the left wall on the ceiling and 1000mm from the front wall.
Arcing was located on circuit 4 – 100mm from the left wall and 1000mm from the rear wall.

Figure 800 - The refuse bin alight

Figure 801 – Initial flame impingement on the ceiling.

Pre-fire and post-fire photographs of experiment 33

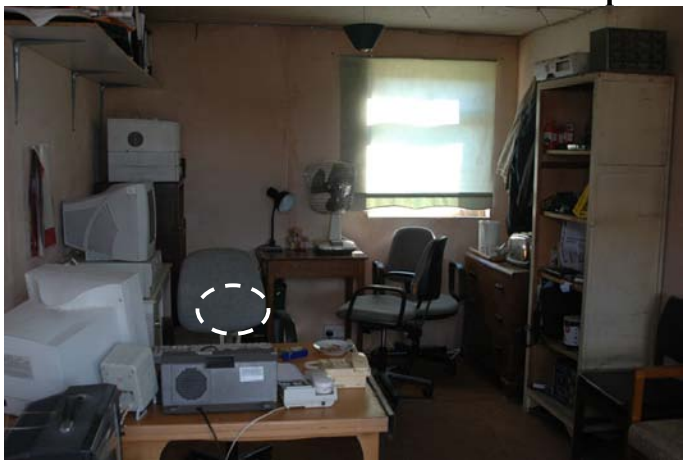

Figure 802 - Pre-fire view of experiment 33. The dashed white circle indicates the fire's area of origin, a refuse bin in the rear left corner of the compartment.

Figure 803 - Close-up view of the fire's area of origin – the green refuse bin located between the vacuum cleaner and the table.

Figure 804 - Post fire overview of the compartment with the white dashed line oval indicating the fire's area of origin.

Figure 805 - Post-fire view of the area of origin for this fire. The refuse bin and the vacuum cleaner have been severely damaged in the fire.

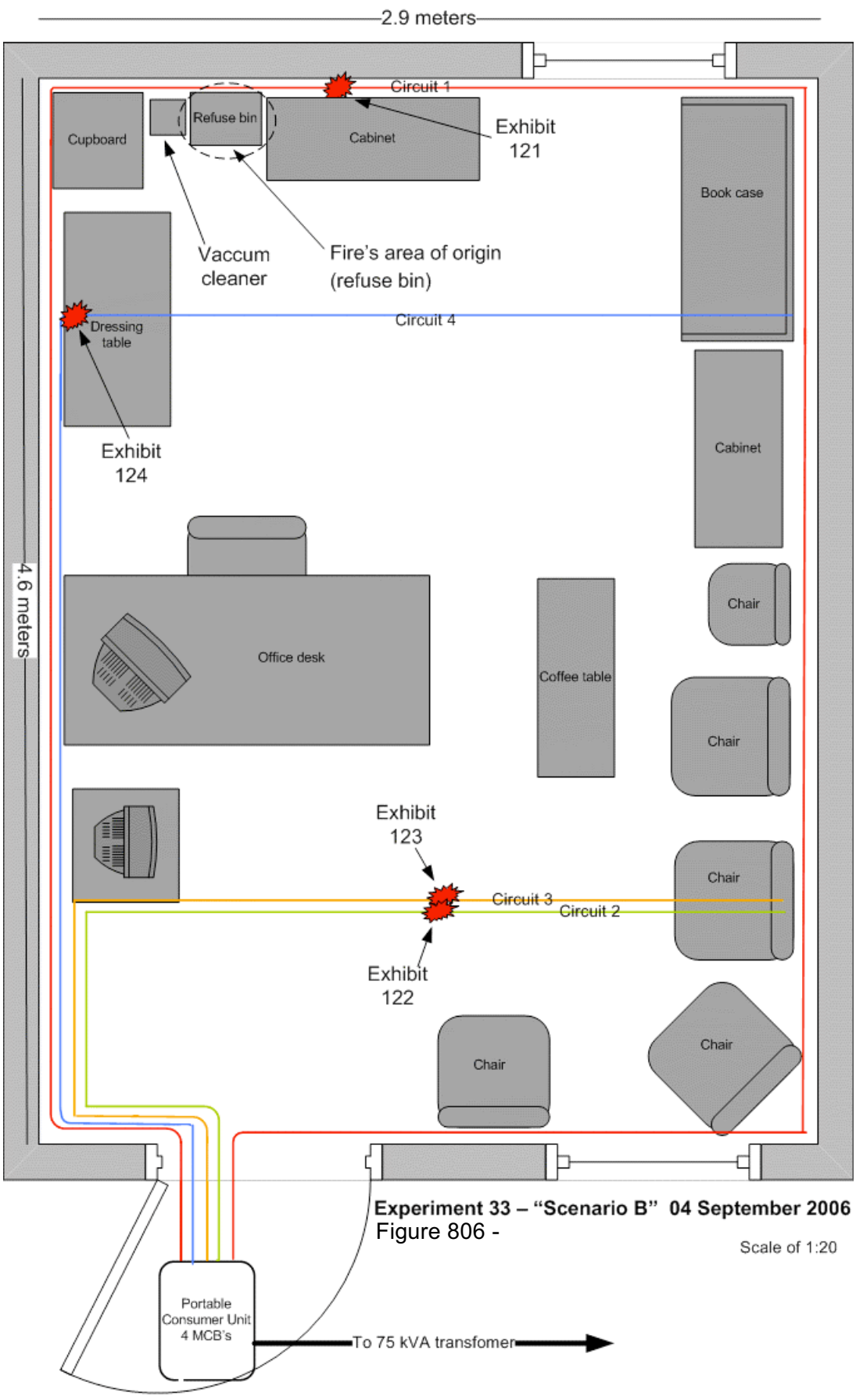

Experiment 33 – "Scenario B" 04 September 2006

Figure 806 -

Scale of 1:20

Microscope images for exhibit 121 – arcing category D (experiment 33)

Figure 807 - Microscope image of exhibit 121. The two 2.5mm^2 conductors (live & neutral) each have a notch with a bead within the notch. The top conductor's bead is protruding up from the surface.

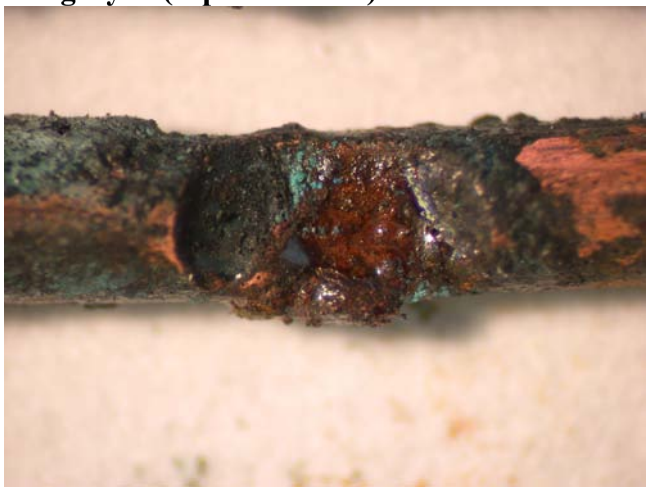

Figure 808 - 20x magnification image of the bottom conductor area of figure 807, detailing the notch.

Figure 809 - 20x magnification image of the top conductor with its large bead above the conductor surface.

Figure 810 - This is a 180 degree view of figure 809 detailing this large example of a bead.

Microscope images for exhibit 122 – arcing category D (experiment 33)

Figure 811 - One of the three conductors had arcing damage in the pattern of a notch. This circuit (number 2) appears to have faulted with circuit 3.

Figure 812 - 15x magnification of the notch with a small bead at the left edge if the notch.

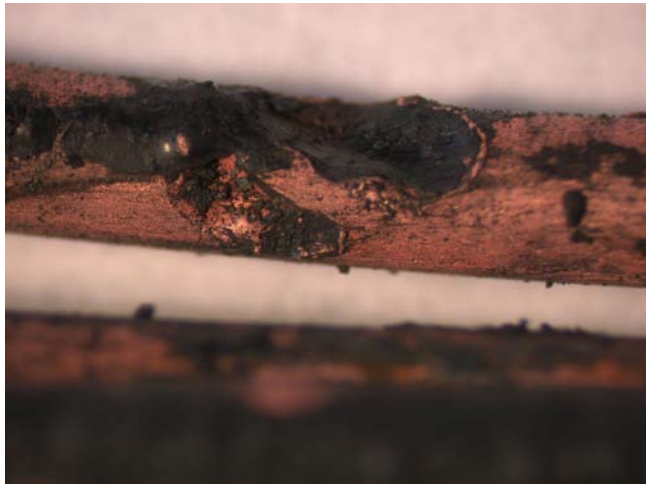

Figure 813 - An alternative view of figure 811 above.

Figure 814 - 20x magnification highlighting the demarcation at the edge of the notch and what appeared to be a copper ridge.

Microscope and SEM images for exhibit 123 – arcing category B (experiment 33)

Figure 815 - Microscope image of exhibit 123. Two conductors had arcing damage. The lower conductor has a bead with a large hole.

Figure 816 - SEM image of the lower conductor. The demarcation is clearly defined at the notch edge.

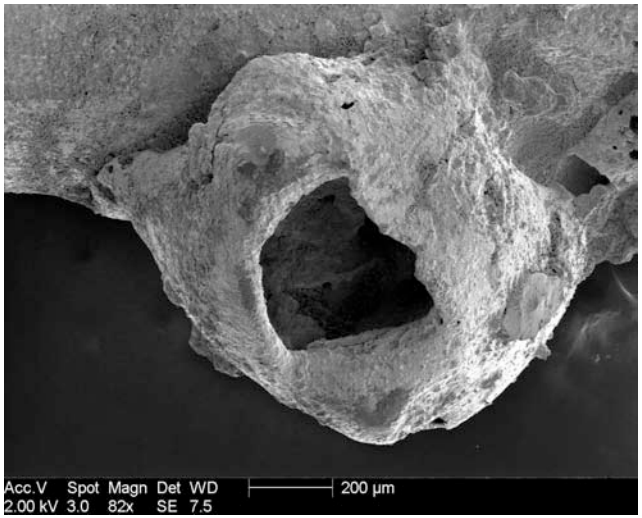

Figure 817 - SEM image at 82x magnification of the bead of the lower conductor.

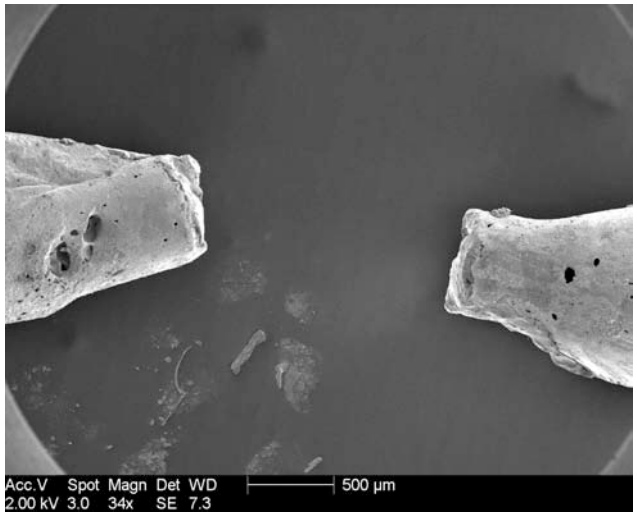

Figure 818 - SEM overview image of the severed ends of the top conductor in figure 815.

Confocal laser scanning microscope images for exhibit 123 – arcing category B (experiment 33)

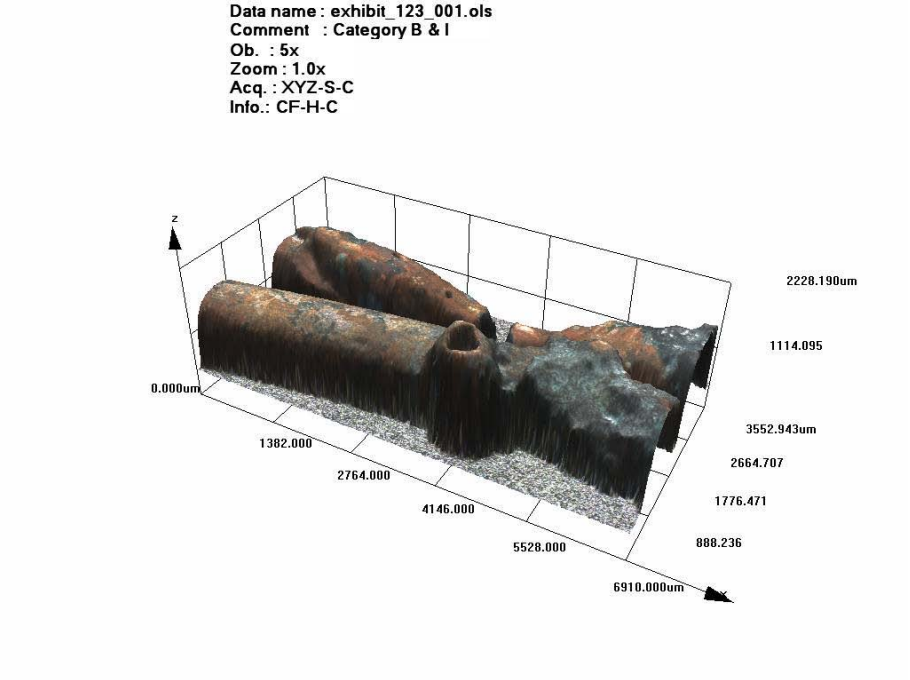

Figure 819 - LEXT image of exhibit 123 in real colour rendering mode. The scan has enabled the entire exhibit to be documented.

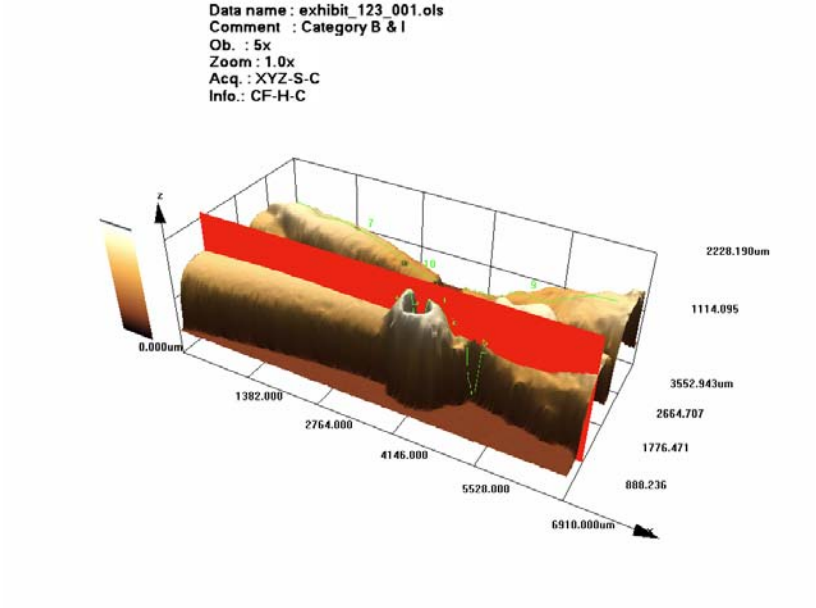

Figure 820 - A brown rendered view using the “slice tool” in the LEXT software to create a profile of the bead.

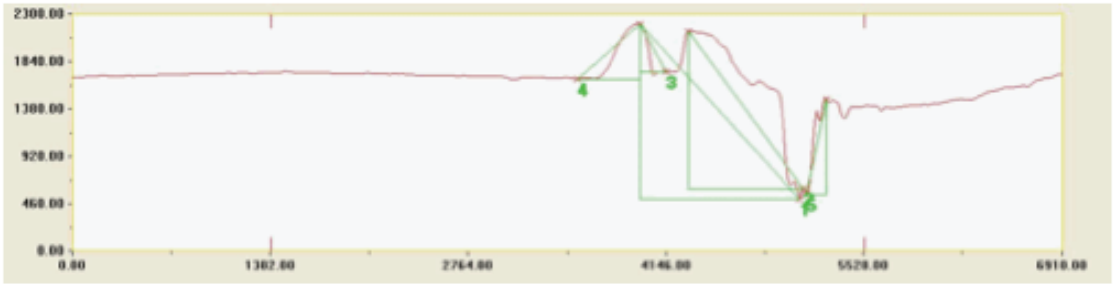

Figure 821 - Profile of the notch and bead using the “slice tool” detailed in figure 820, the scale is in microns

Microscope and SEM images for exhibit 124 – arcing category G (experiment 33)

Figure 822 - Microscope image of exhibit 124. The middle conductor has a notch with a large bead on the edge. The lower conductor has severed ends with a bead at the right severed end.

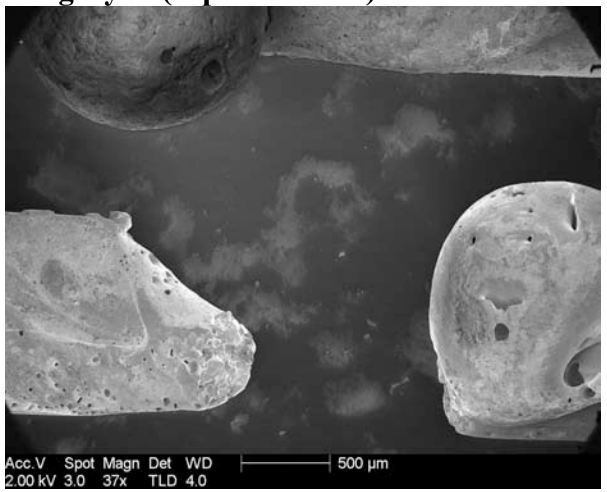

Figure 823 - SEM image of the lower conductor as detailed in figure 822 with an overview of the severed ends.

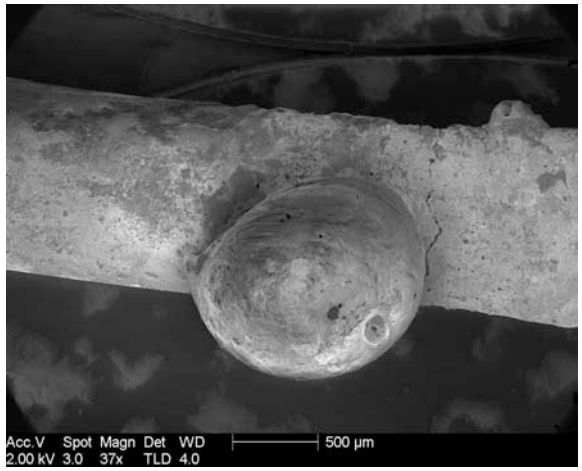

Figure 824 - SEM image of the notch with a bead on the surface. There was a crack in the conductor surface to the right of the bead.

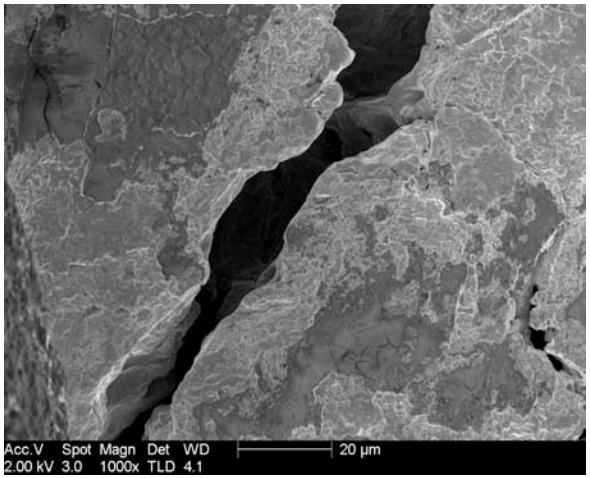

Figure 825 - SEM image at 1000x magnification documenting the crack in the conductor surface detailed in figure 824.

Confocal laser scanning microscope image for exhibit 124 – arcing category G (experiment 33)

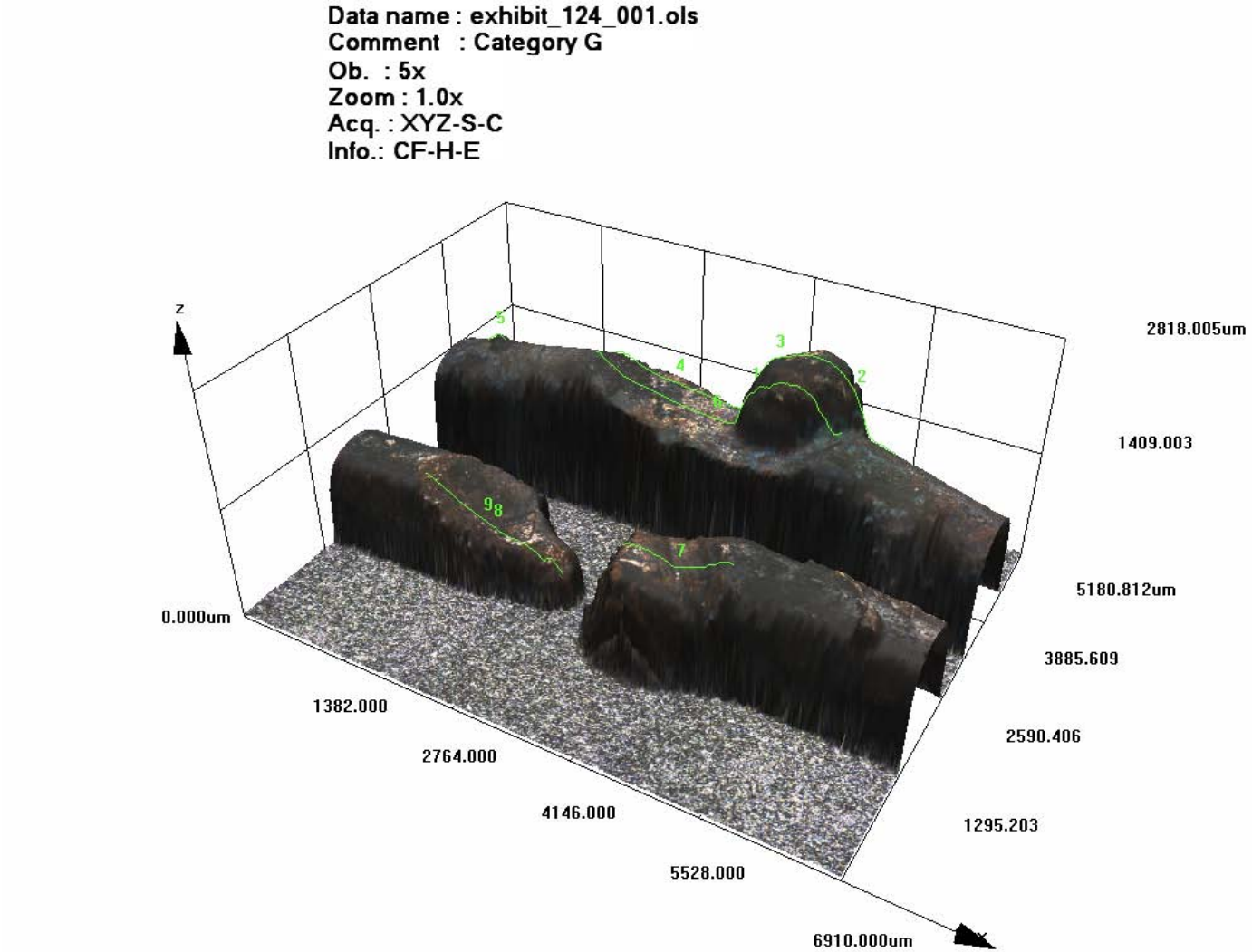

Figure 826 - LEXT image for exhibit 124. The Confocal laser scanning microscope enabled the entire to be documented in detail.

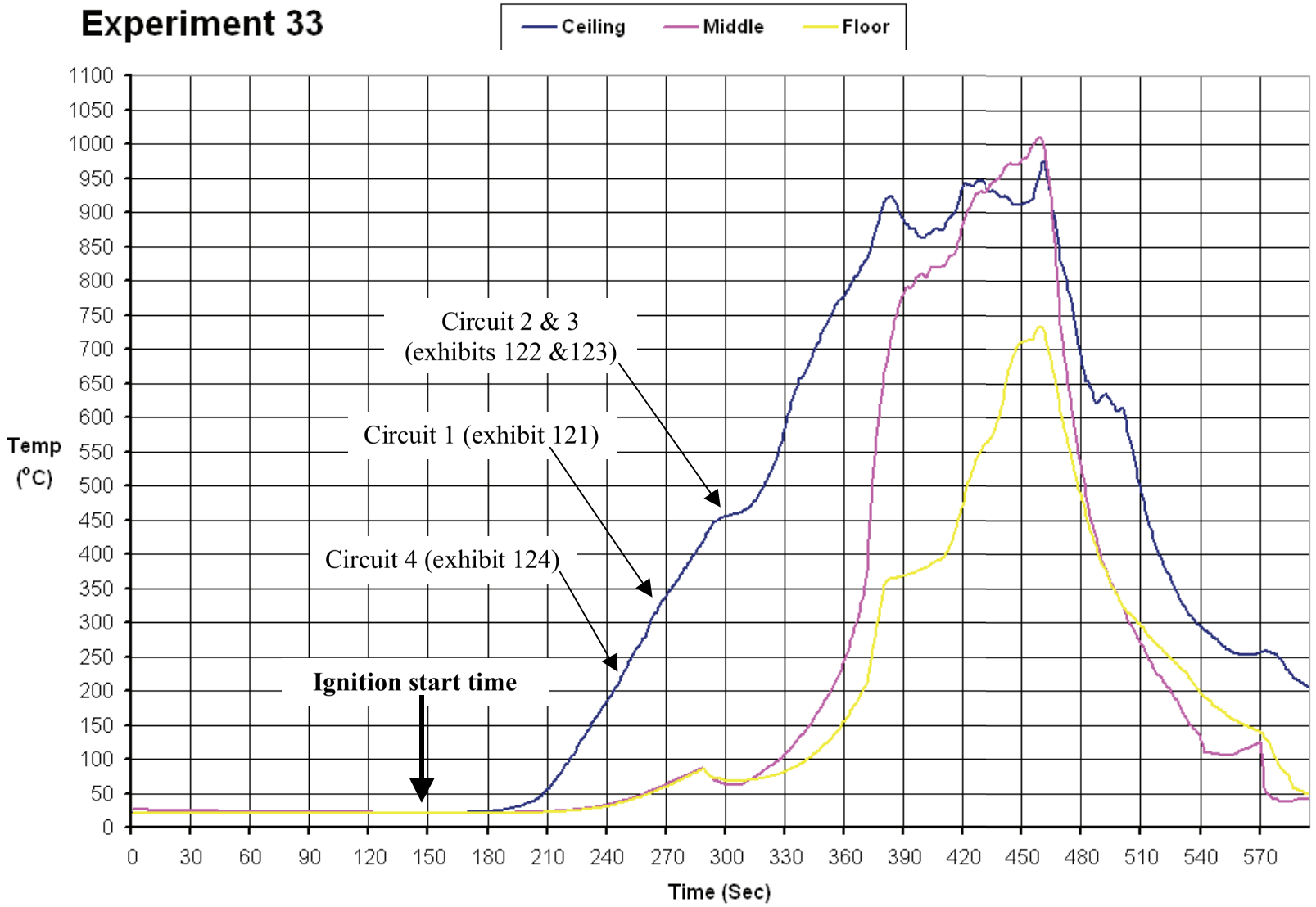

Figure 827 - Time temperature graph for experiment 33 (ignition start time adjusted following analysis of video recording).

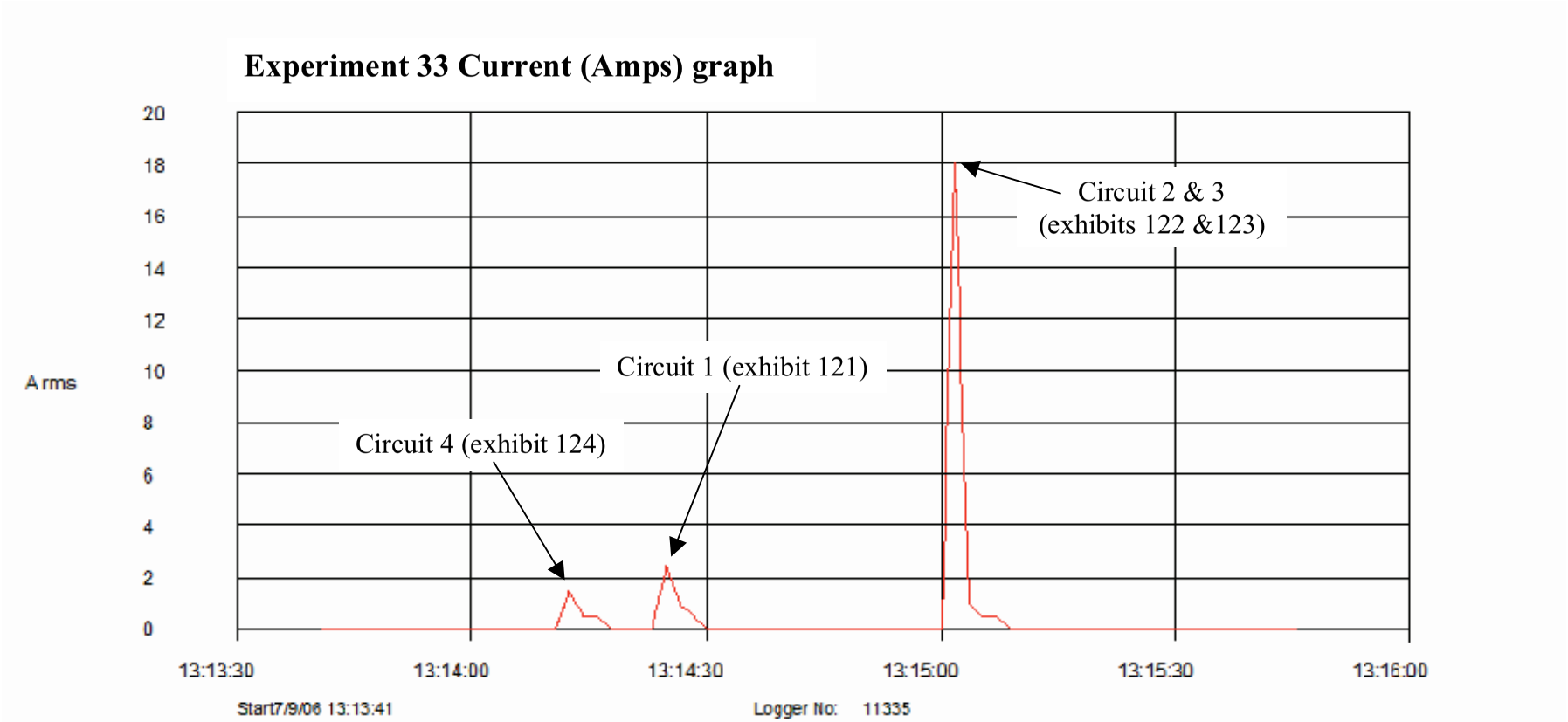

Figure 828 - Current (Amps) graph for experiment 33 detailing the operation of the circuit breakers and the fault current

Experiment 34

Figure 829 – “Scenario A” 7 September 2006.

Circuit number	MCB operating time from ignition
4	2:00 minutes
1	2:09 minutes
3	2:20 minutes
2	2:20 minutes

Table 36 – circuit breaker operation data

The fire in experiment 34 (scenario A) originated in a clothes rail located between two single beds and at the edge of each single bed. The fire developed rapidly with the compartment reaching flashover conditions within 3.5 minutes. The ceiling and middle thermocouples recorded a temperature of 1000° C. The floor thermocouple recorded 650° C at this time.

Arcing damage was located on circuit 1 – 2170mm from the left wall and adjacent to the rear wall.
Arcing damage was located on circuit 2 is 1300mm from the left wall and 1000mm from the front wall.
Arcing damage was located on circuit 3 – 2120mm from the left wall on the ceiling and 1000mm from the front wall.
Arcing damage was located on circuit 4 – 1000mm from the left wall and 1000mm from the rear wall.

Figure 830 - The clothes and beds ignited.

Figure 831 - Flame impingement on the ceiling.

Pre-fire and post-fire photographs of experiment 34

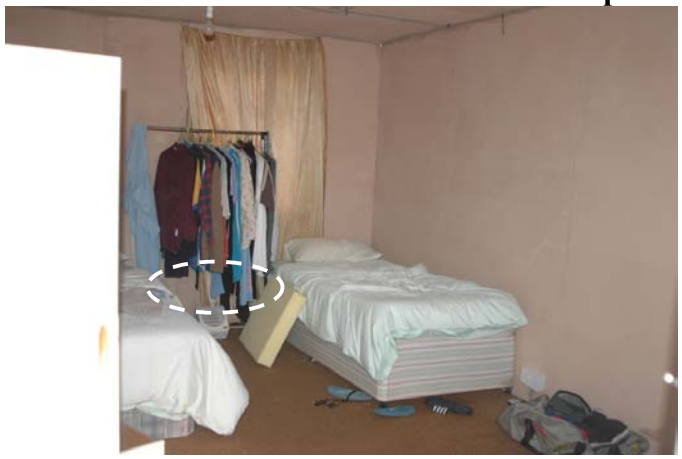

Figure 832 - Pre-fire photograph of experiment 34. The dashed line white oval indicated the fire's area of origin.

Figure 833 - View of the area of origin. The polyurethane foam slabs are used to ensure the fuel package is sufficient for this experiment scenario.

Figure 834 – Post-fire view of the experiment. There are burn patterns on the rear and right wall of the compartment.

Figure 835 - Close-up view of the fire's area of origin. Arcing damage to circuits 1 and 4 was located above this area on the ceiling.

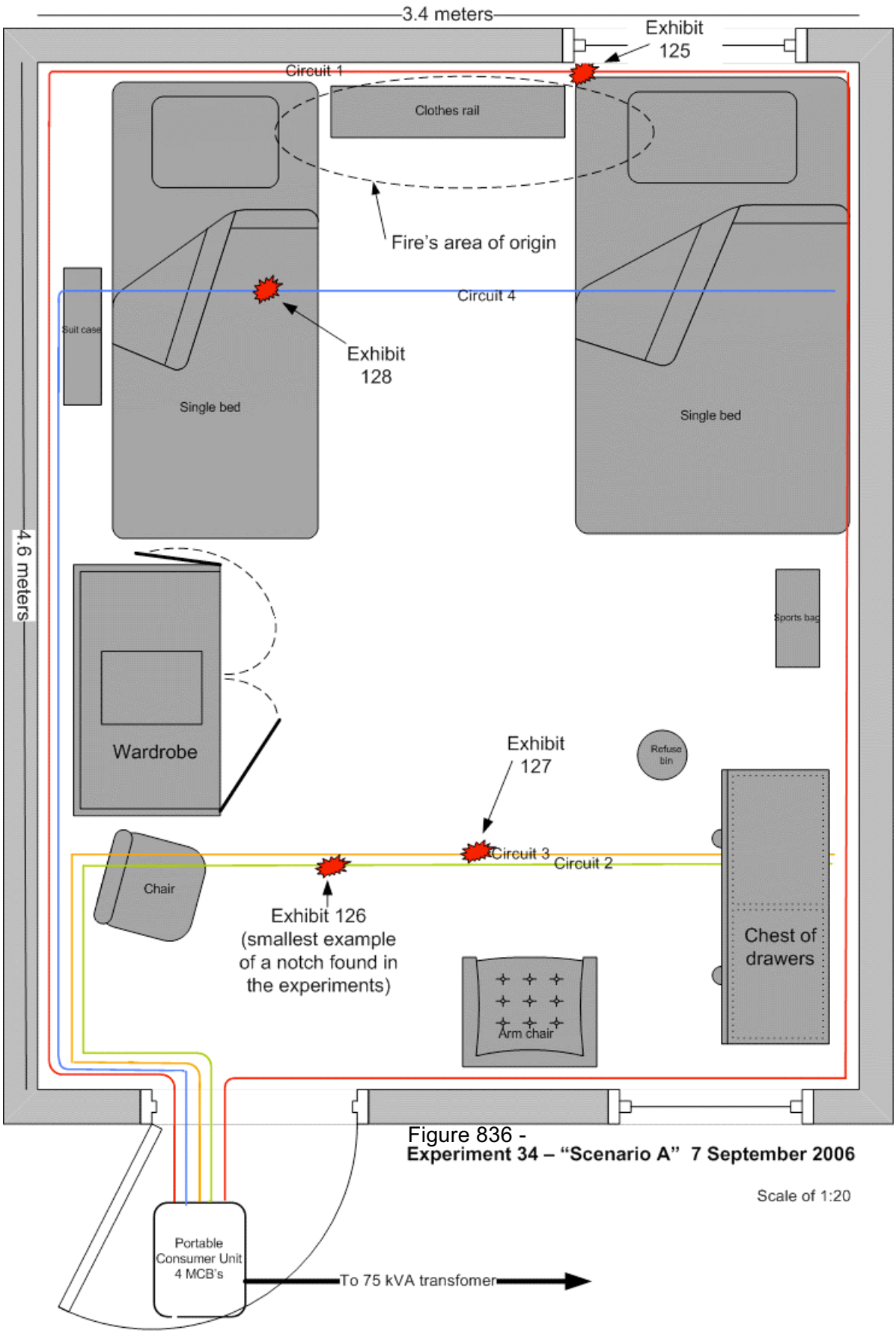

Figure 836 -
Experiment 34 – "Scenario A" 7 September 2006

Scale of 1:20

Microscope and SEM images for exhibit 125 – arcing category E & I (experiment 34)

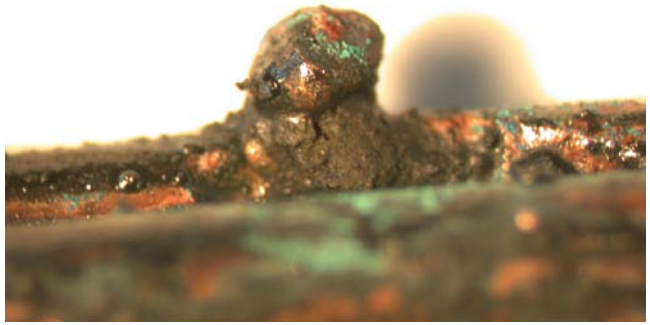

Figure 837 - Microscope image of exhibit 125. Two conductors had notch arcing damage. One had a large bead protruding from the surface and has a sub-category “I”.

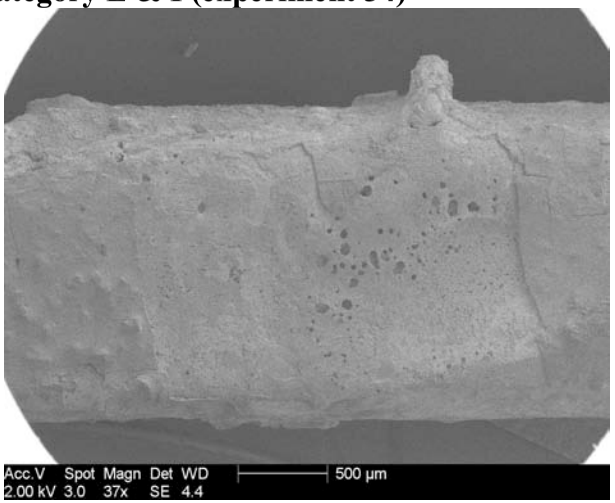

Figure 838 - SEM image of the lower conductor. The image quality is limited due to incorrect adjustment of the SEM.

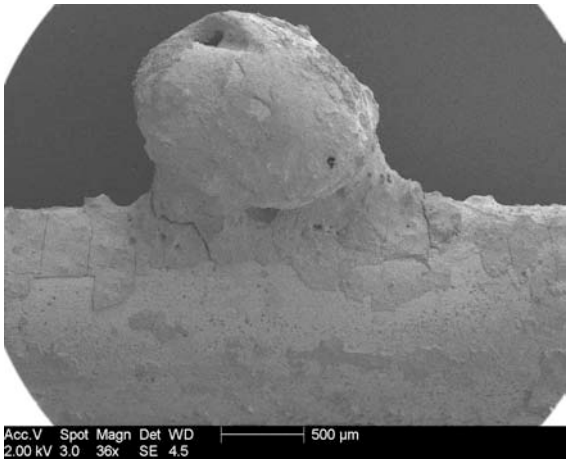

Figure 839 - SEM image of the top conductor with its tall bead. This is one of the best examples of arcing category I from the experiments.

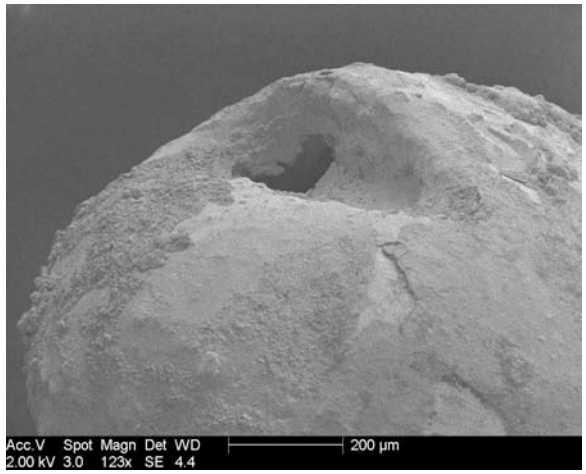

Figure 840 - SEM image at 123x magnification of the top of the bead surface with a hollow.

Confocal laser scanning microscope image for exhibit 125 – arcing category E (experiment 34)

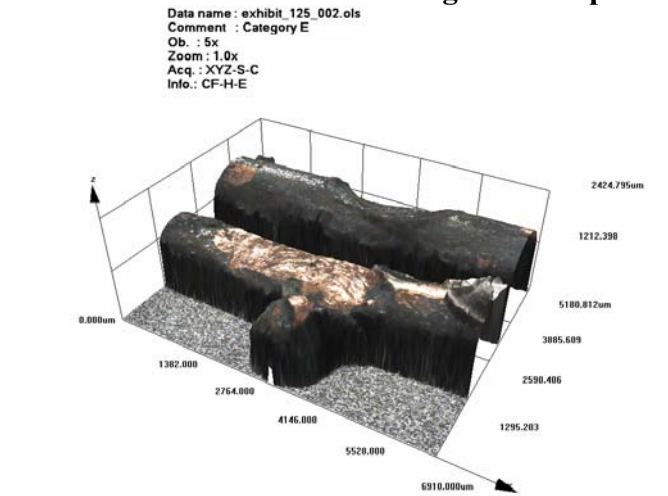

Figure 841 - LEXT image of exhibit 125. The 3-D scan enabled the whole exhibit to be documented in detail.

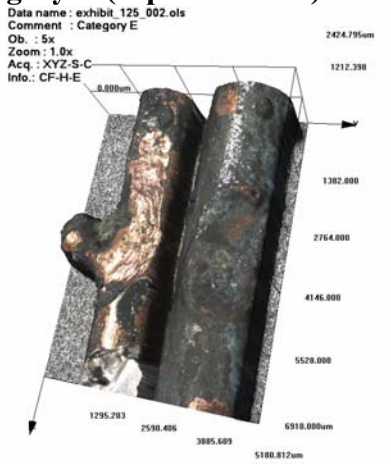

Figure 842 - An image captured when the exhibit was rotated within the LEXT software.

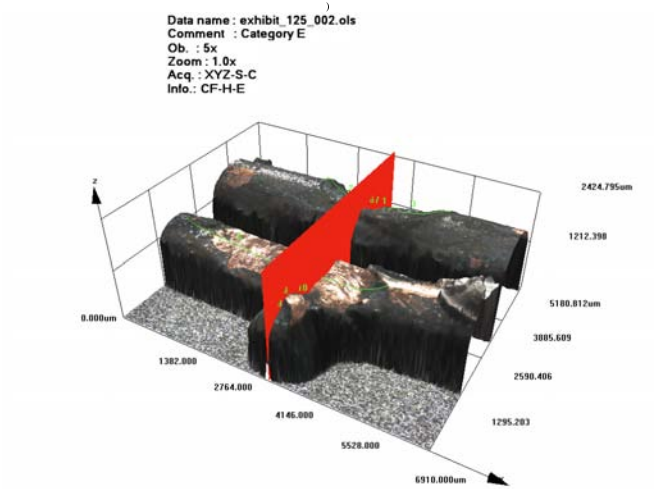

Figure 843 - “Slice tool” in operation to create the profile for both conductors detailed in figure 844.

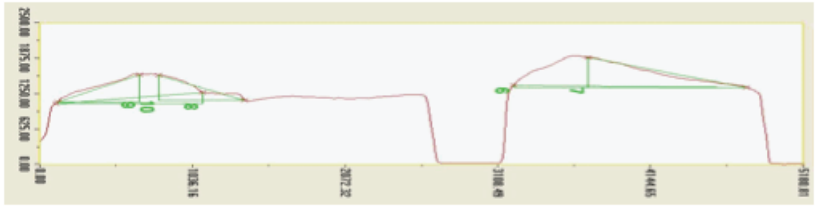

Figure 844 – The profile produced with the “slice tool” detailed in figure 843.

Microscope and SEM images for exhibit 126 – arcing category F (experiment 34)

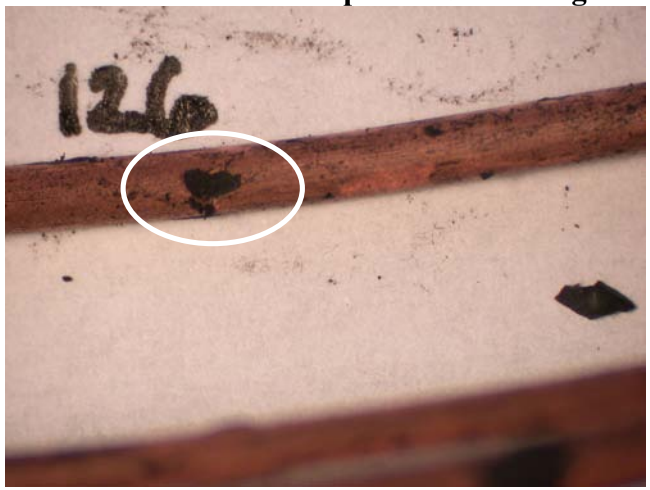

Figure 845 - Microscope image of exhibit 126. This was the smallest notch observed in the series of experiments

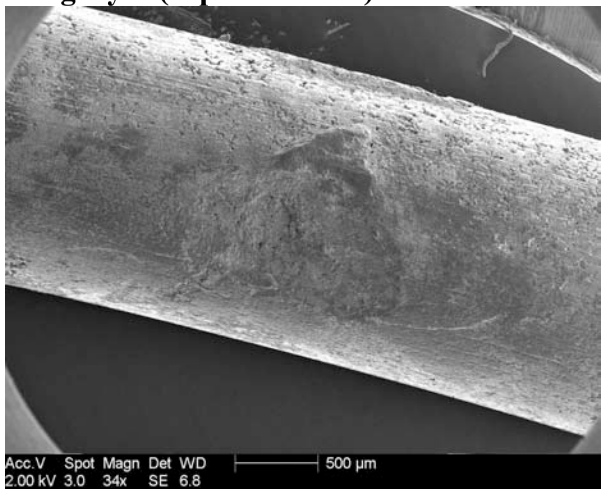

Figure 846 - SEM image of the small notch.

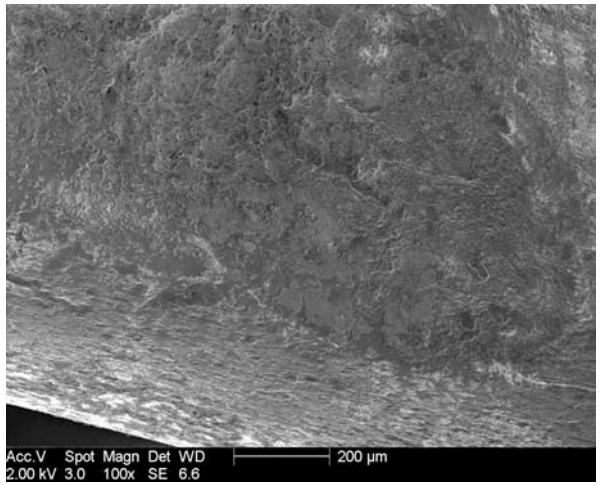

Figure 847 - SEM image of the lower area of the notch at 100x magnification. The notch is so shallow that at this angle it is difficult to recognise even at this 100x magnification.

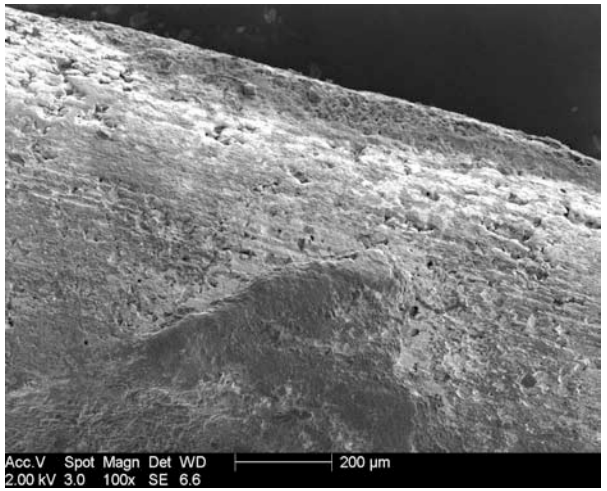

Figure 848 - The top edge of the notch at 100x magnification where the demarcation is clearer between the notch edge and the undamaged conductor surface.

Confocal laser scanning microscope image for exhibit 126 – arcing category F (experiment 34)

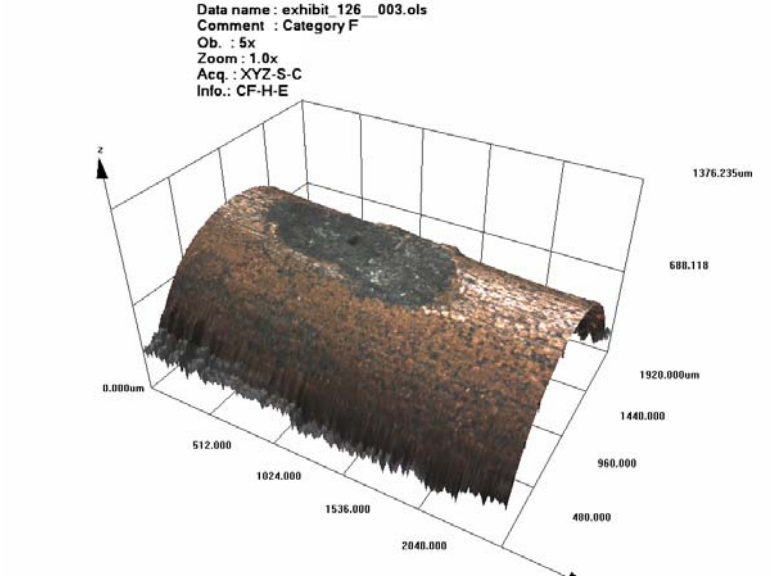

Figure 849 - LEXT image clearly detailing the shallow notch damage to this exhibit.

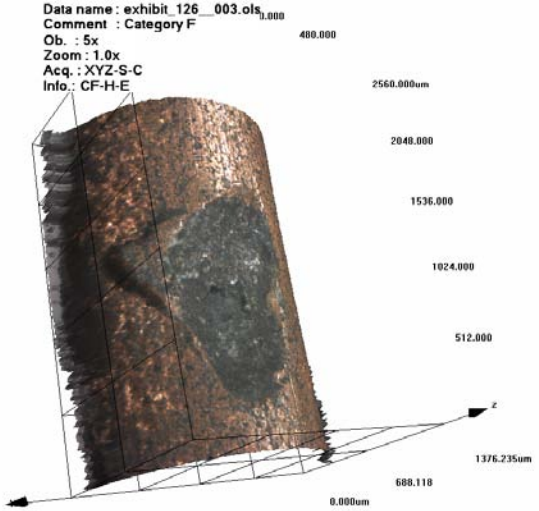

Figure 850 - The LEXT scan produced this new view of the exhibit detailing a small bead not observed prior to this scan.

Figure 851 - Profile of the notch using the “slice tool” option in the LEXT software. Measurement details for the smallest notch located in the series of 39 experiments: notch width=1345 microns, (1.34mm), notch height=173.9 microns (0.174mm)

Microscope images for exhibit 127 – arcing category D (experiment 34)

Figure 852 - Microscope image of exhibit 127. One conductor of the three is involved. This is a large notch with a small bead within the notch and a small bead on the notch edge.

Figure 853 - 20x magnification of the exhibit. The left edge of the notch displays a clear demarcation between the arcing damage and the undamaged conductor surface.

Figure 854 - A side view of the notch detailing its depth. There is a lot of PVC debris attached to the conductor surface.

Microscope and SEM images for exhibit 128 – arcing category D (experiment 34)

Figure 855 - Microscope image of exhibit 128. Two of the three conductors had arcing damage and one conductor produced some unusually shaped multiple beads.

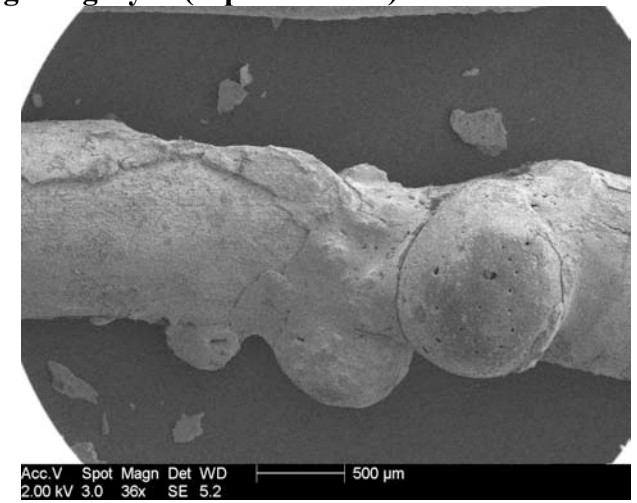

Figure 856 - SEM image of the bottom conductor. Incorrect adjustment of the SEM produced lower quality images than normal.

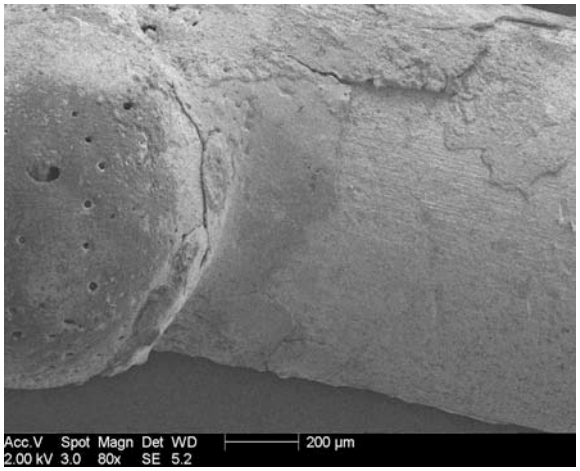

Figure 857 - SEM image at 80x magnification detailing the right side of the arcing damage and the demarcation area.

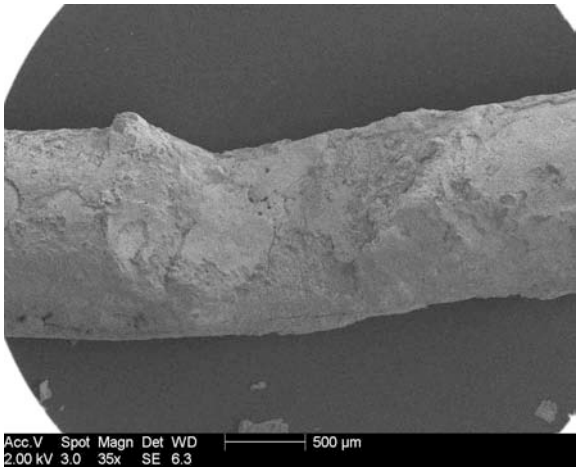

Figure 858 - SEM image of the top conductor detailing the notch damage and the demarcation area.

Confocal laser scanning microscope image for exhibit 128 – arcing category D (experiment 34)

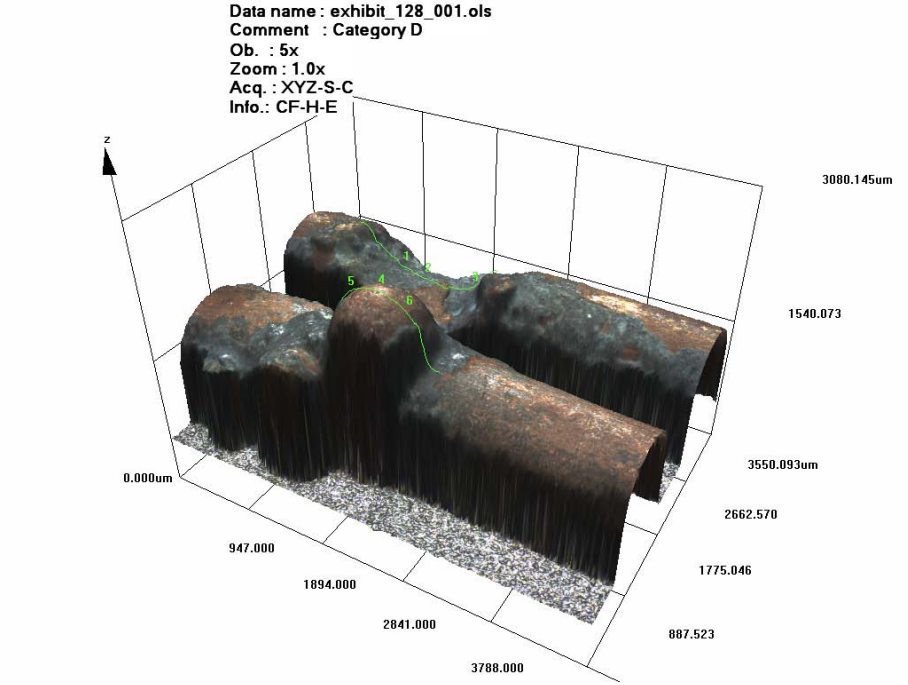

Figure 859 - LEXT image of exhibit 128. This scan enables the entire exhibit to be documented in detail.

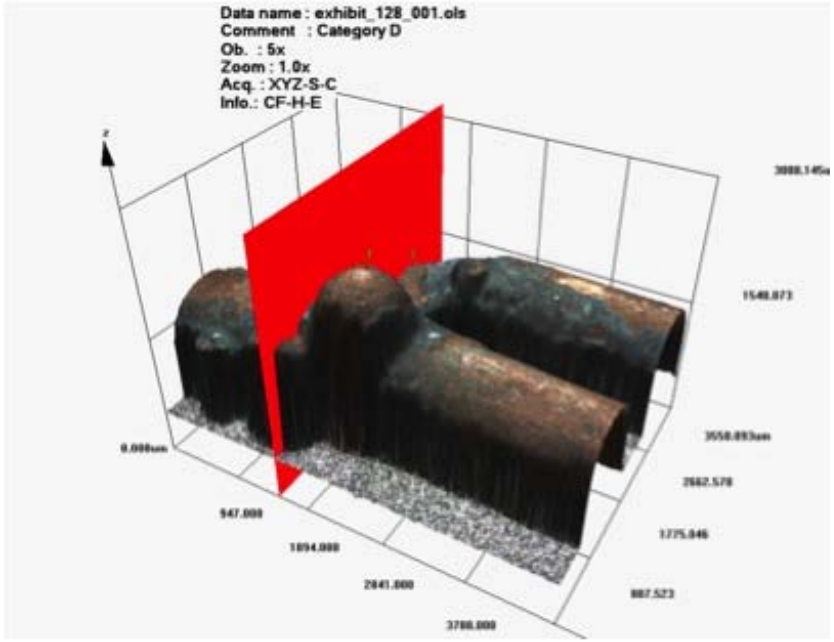

Figure 860 - The “slice tool” being used in the LEXT software across both conductors to create the profile in figure 861.

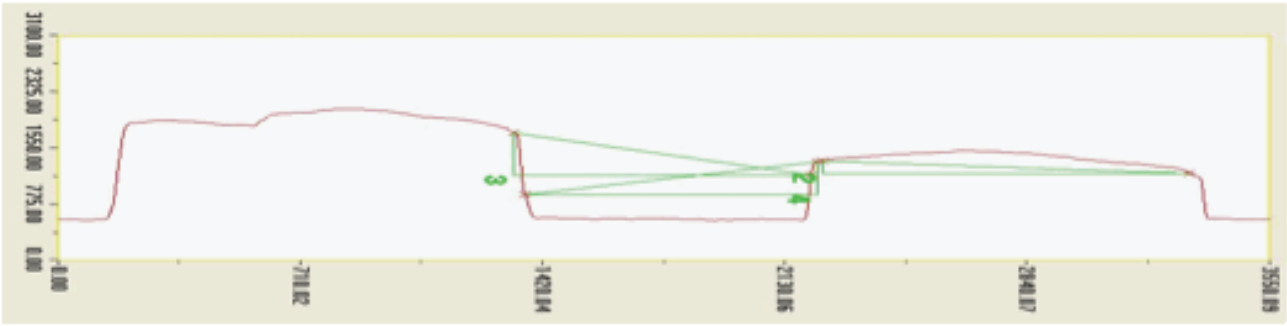

Figure 861 - Profile created using the “slice tool” in the LEXT software, measurement scales are detailed in microns

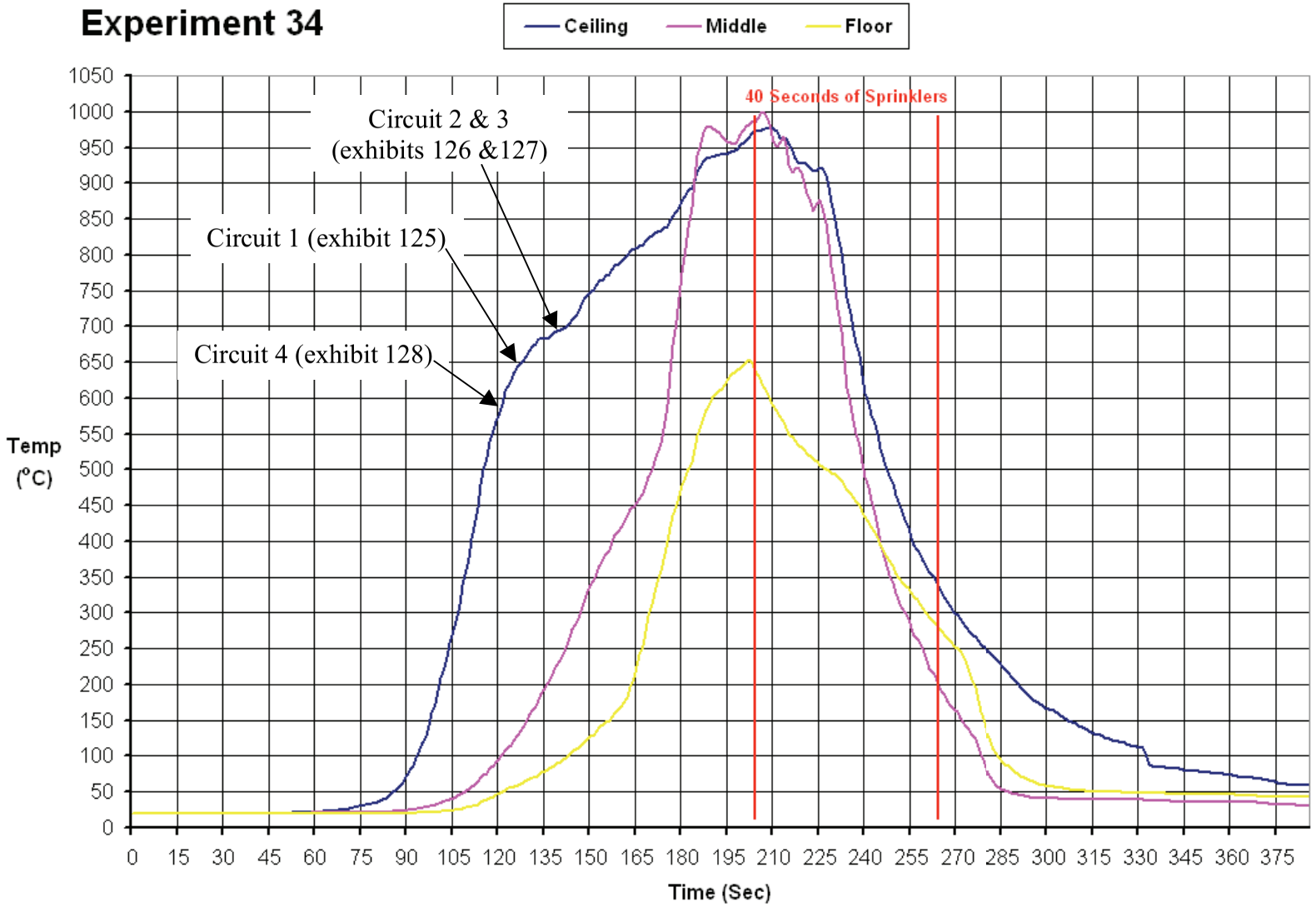

Figure 862 - Time temperature graph for experiment 34

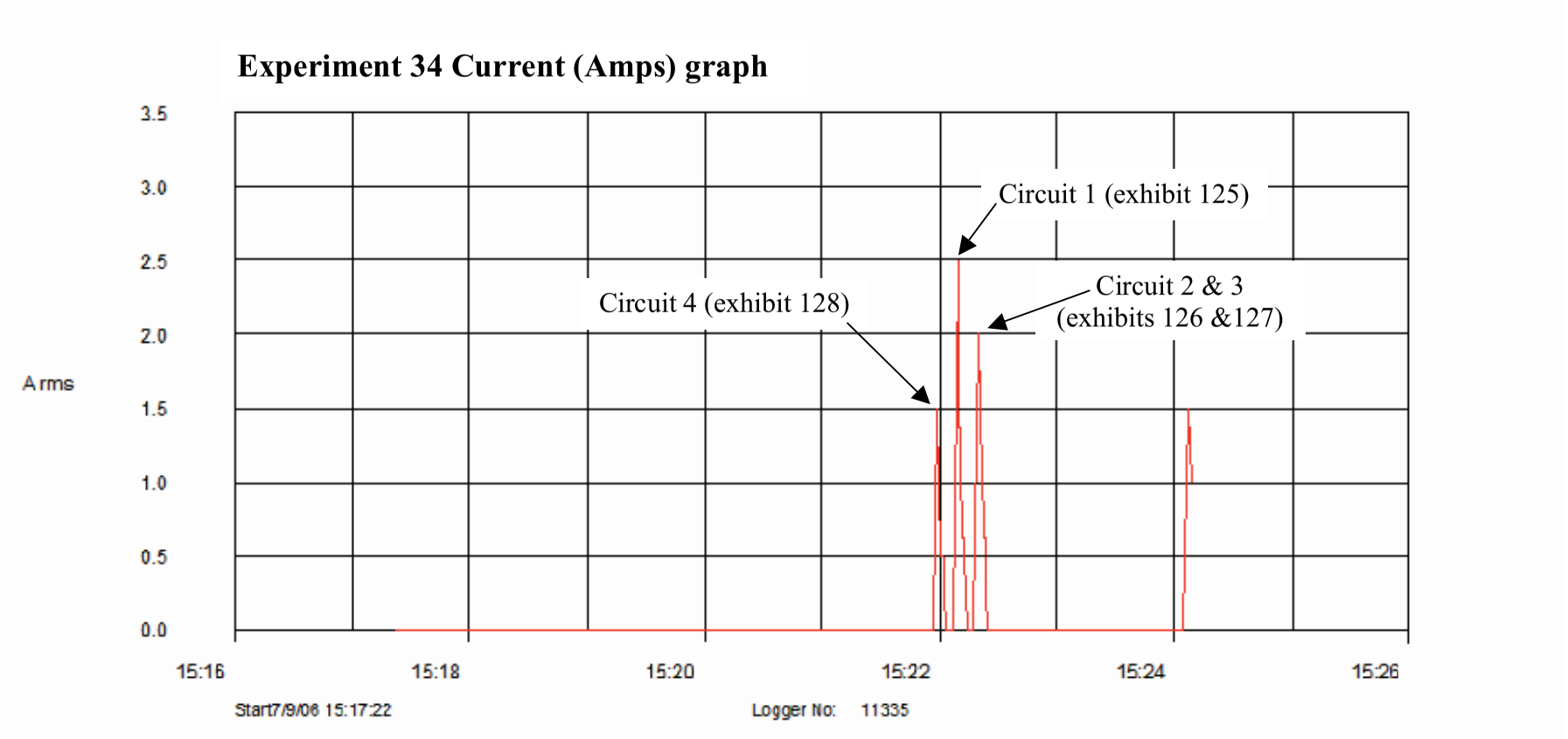

Figure 863 - Current (Amps) graph for experiment 34 detailing the operation of the circuit breakers and the fault current

Experiment 35

Figure 864 – "Scenario C" 7 September 2006.

Circuit number	MCB operating time from ignition
4	3:50 minutes
1	4:17 minutes
3	4:17 minutes
2	4:23 minutes

Table 37 – circuit breaker operation data

The fire in experiment 35 (scenario C) originated in a toy box located in front of a Christmas tree adjacent to the centre of the rear wall of the compartment. The fire developed steadily with a ceiling temperature of 825° C recorded at 6 minutes. The middle thermocouple recorded a temperature of 650° C and the floor thermocouple recorded 200° C at this time. The compartment did not appear to have reached flashover conditions prior to be being extinguished.

No arcing was located on circuit 1.
Arcing damage was located on circuit 2 - 2970mm from the left wall and 1000mm from the front wall.
Arcing damage was located on circuit 3 – 2370mm from the left wall on the ceiling and 1000mm from the front wall.
Arcing damage was located on circuit 4 – 1470mm, plus 2250mm from the left wall and 1000mm from the rear wall.

Figure 865 - The toy box ignited.

Figure 866 - The toy box and Christmas tree alight.

Pre-fire and post-fire photographs of experiment 35

Figure 867 - Pre-fire photograph of experiment 35. The dashed line white oval indicated the fire's area of origin.

Figure 868 - The ceiling and wiring above the area of origin.

Figure 869 - Post-fire photograph with the area of origin detailed with a white dashed line oval.

Figure 870 - Post-fire view of above. The arrows indicate the two arcing areas located on circuit 4.

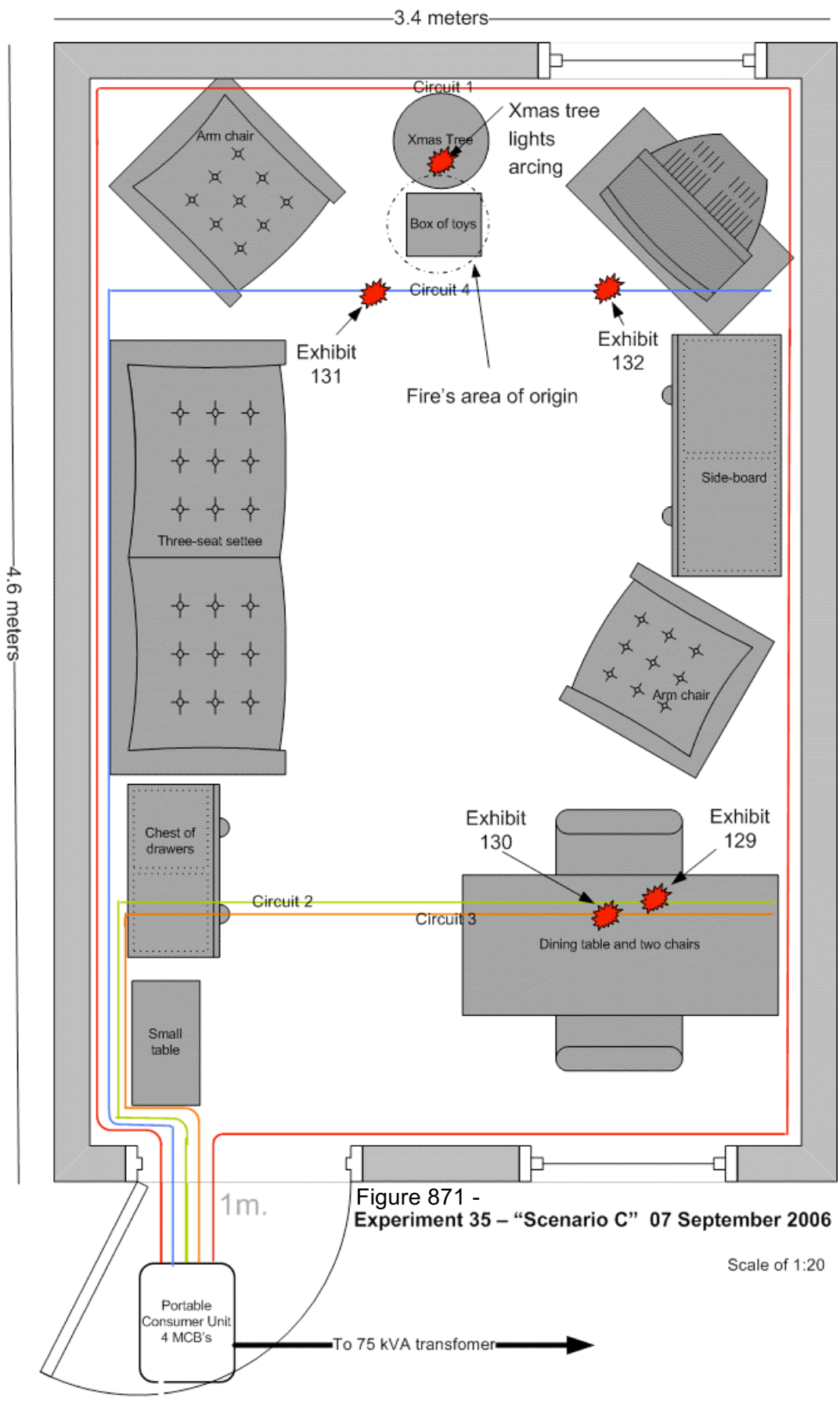

Figure 871 -
Experiment 35 – "Scenario C" 07 September 2006

Scale of 1:20

Microscope and SEM images for exhibit 129 – arcing category D (experiment 35)

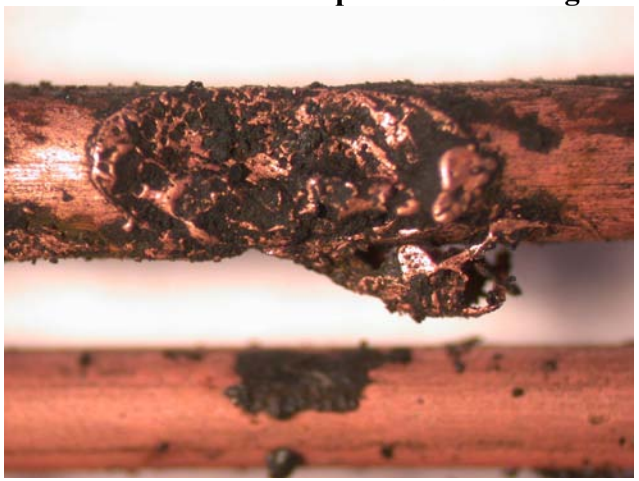

Figure 872 - Microscope image of exhibit 129. Arcing damage affected one conductor. The splatter attached to the lower area of the conductor came away during the subsequent cleaning process.

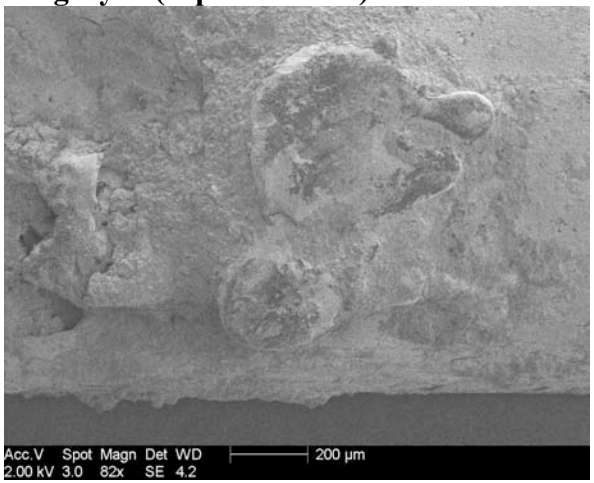

Figure 873 - SEM image at 82x magnification. This is the right side of the notch edge as detailed in figure 875.

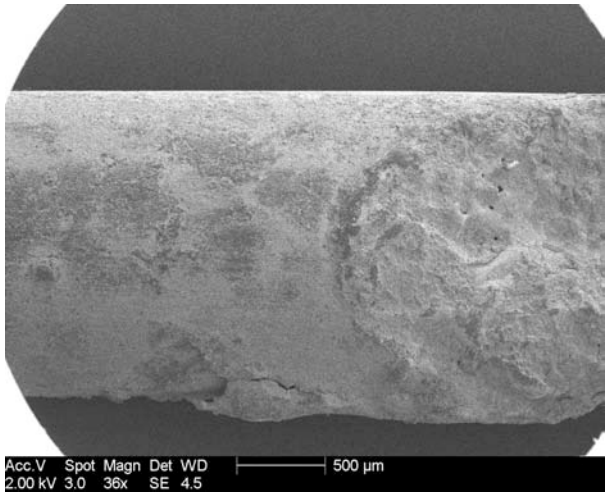

Figure 874 - SEM image of the left half of this large notch. The demarcation at the notch edge is defined.

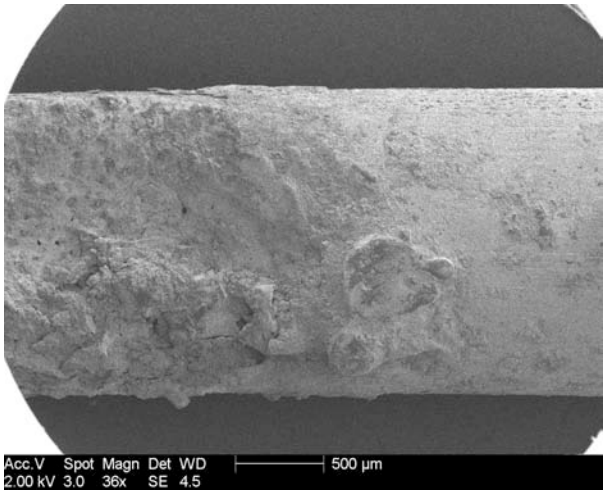

Figure 875 - SEM image of the right half of the notch. Figure 873 details a close-up image of the bead at the notch edge.

Confocal laser scanning microscope image for exhibit 129 – arcing category D (experiment 35)

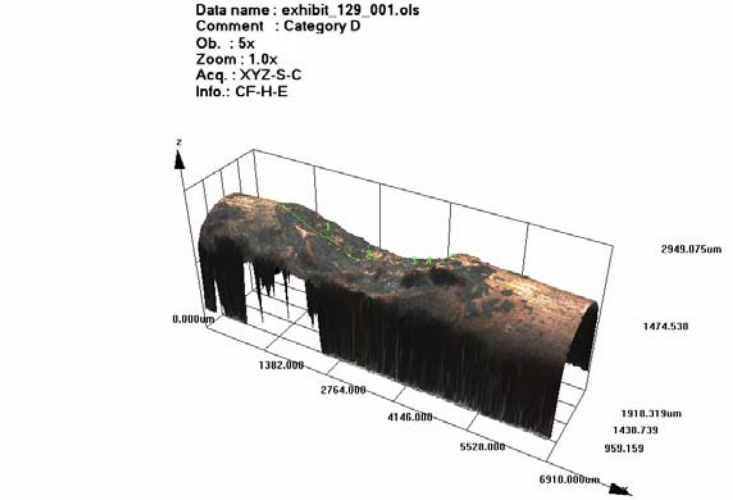

Figure 876 - LEXT image displaying the entire exhibit in detail

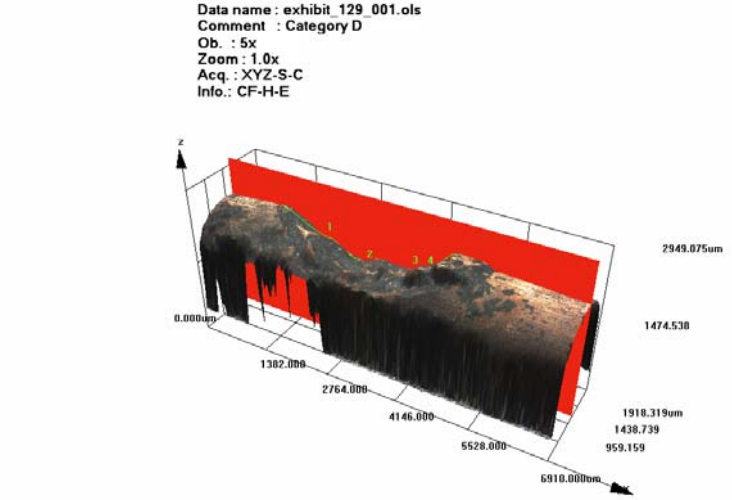

Figure 877 - LEXT image capturing the “slice tool” feature of the software obtaining a surface profile and measurements.

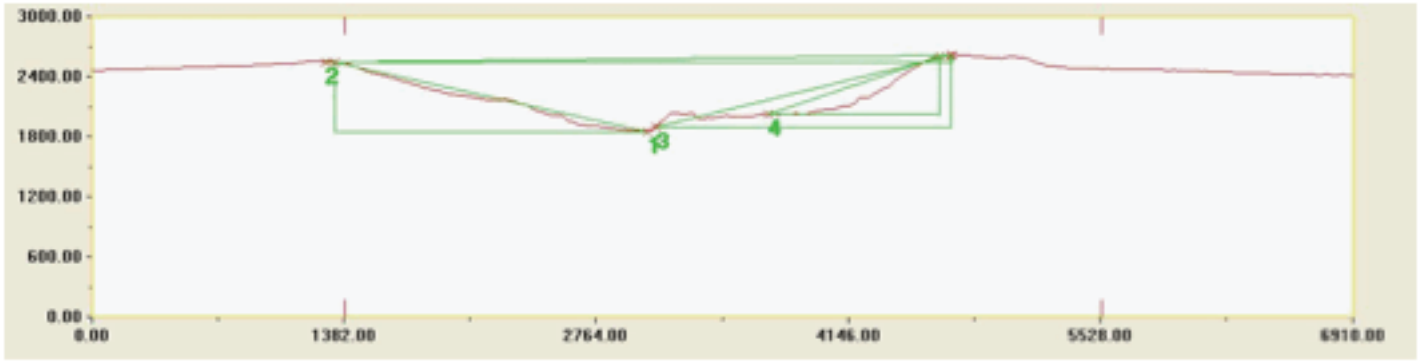

Figure 878 - Profile of the notch obtained using the “slice tool” detailed in figure 877.
The measurement scale is microns, the notch width = 3431 microns (3.43mm).

Microscope and SEM images for exhibit 130 – arcing category B (experiment 35)

Figure 879 - Microscope image of exhibit 130. One conductor was involved and it was severed into two sections.

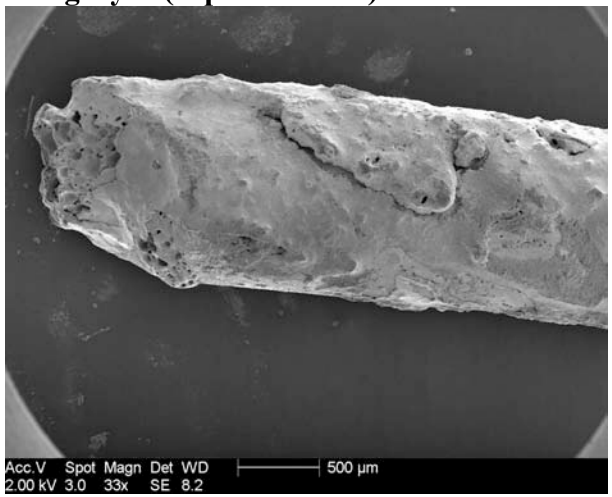

Figure 880 - SEM image of the left severed end detailed in figure 879.

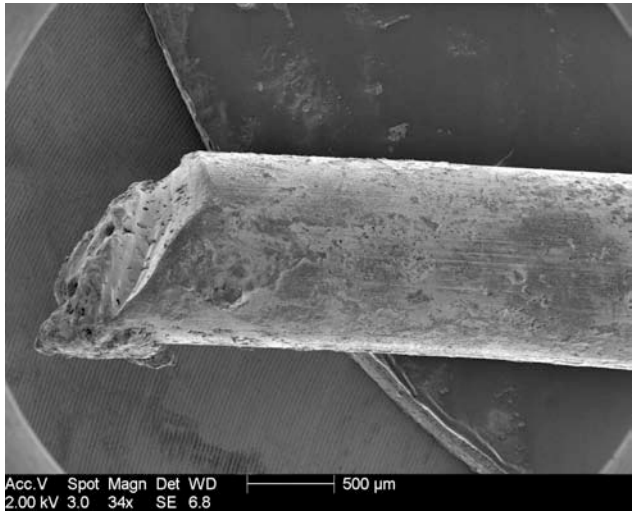

Figure 881 - SEM image of the right severed end detailed in figure 879.

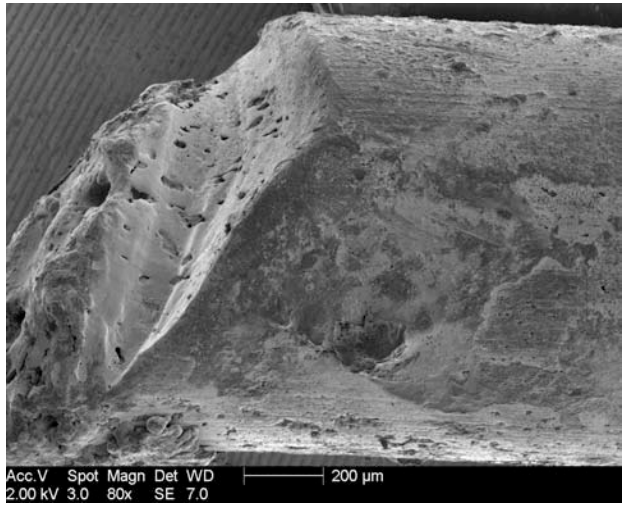

Figure 882 - SEM image at 80x magnification detailing the demarcation at the edge of the arcing damage.

Confocal laser scanning microscope image for exhibit 130 – arcing category B (experiment 35)

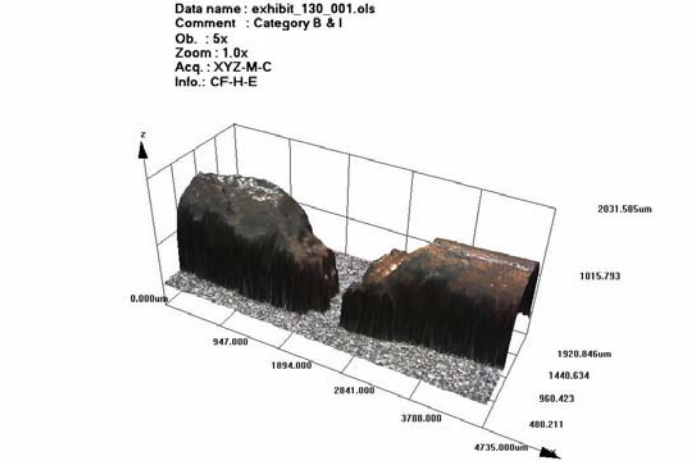

Figure 883 - LEXT image detailing the scan of both severed ends.

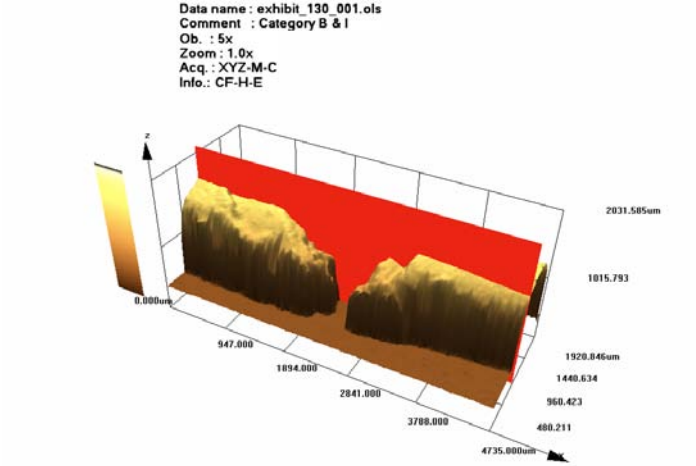

Figure 884 - LEXT image with the “slice tool” in use.

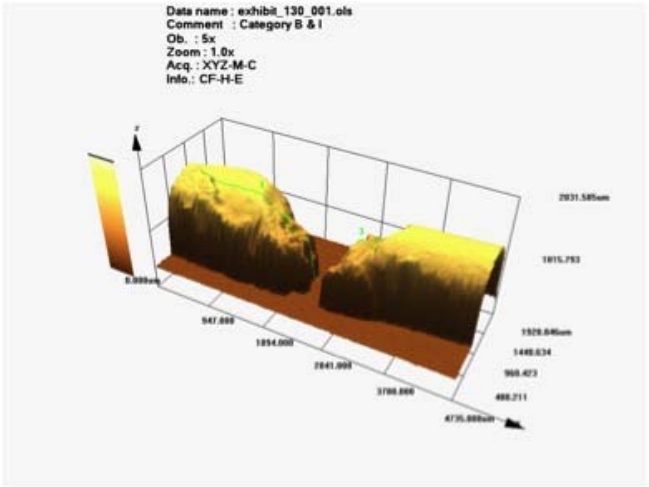

Figure 885 - LEXT image using the yellow colour rendering option in the software.

Microscope images for exhibit 131 – arcing category D (experiment 35)

Figure 886 - Microscope image of exhibit 131. This is the second area of arcing for circuit 4 closest to the electrical source. Two conductors have localised melting damage in the shape of a notch.

Figure 887 - 20x magnification of the bottom conductor. The notch has a bead on the right edge that protrudes above the surface of the undamaged conductor.

Figure 888 - 20x magnification of the top conductor detailed in figure 886. The edge of the notch and demarcation is visible.

Figure 889 - A view of the top conductor at a different angle to document the notch and bead profile with more accuracy.

Microscope and SEM images for exhibit 132 – arcing category B (experiment 35)

Figure 890 - Microscope image of exhibit 132. This is the first area of arcing on circuit 4. One conductor is involved with severed ends.

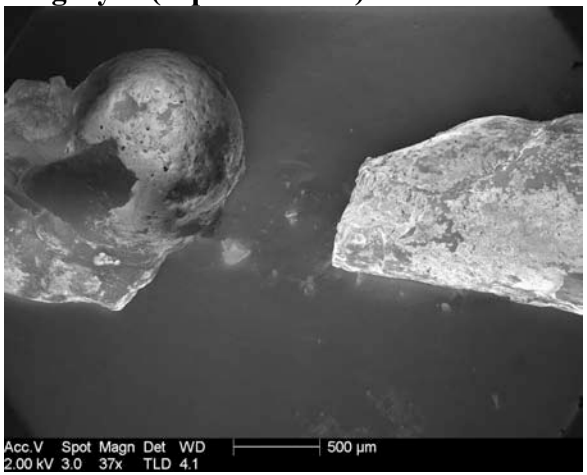

Figure 891 - SEM image of the two severed ends.

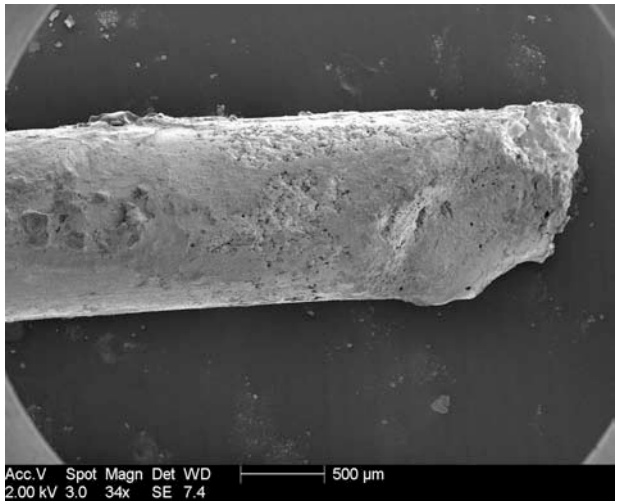

Figure 892 - SEM image of the right severed end detailed in figure 891.

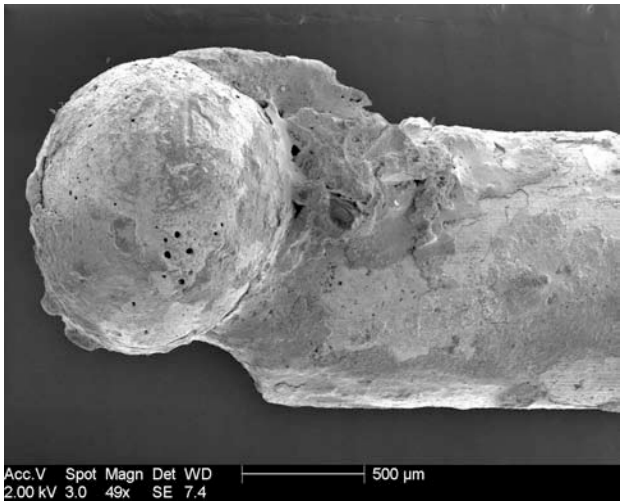

Figure 893 - SEM image of the left severed end detailed in figure 891. The demarcation at the edge of the bead and the undamaged conductor is defined.

Confocal laser scanning microscope image for exhibit 132 – arcing category B (experiment 35)

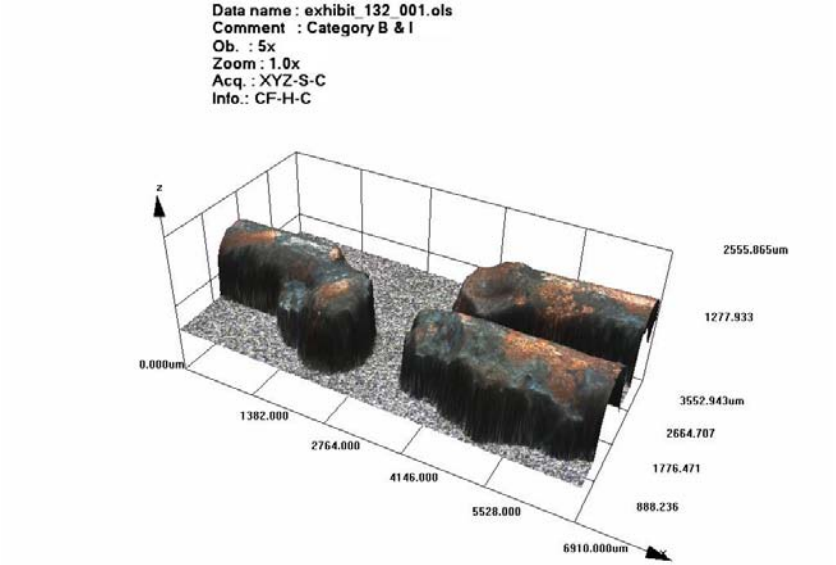

Figure 894 - LEXT image of exhibit 132.The exhibit consists of the two lower severed ends.

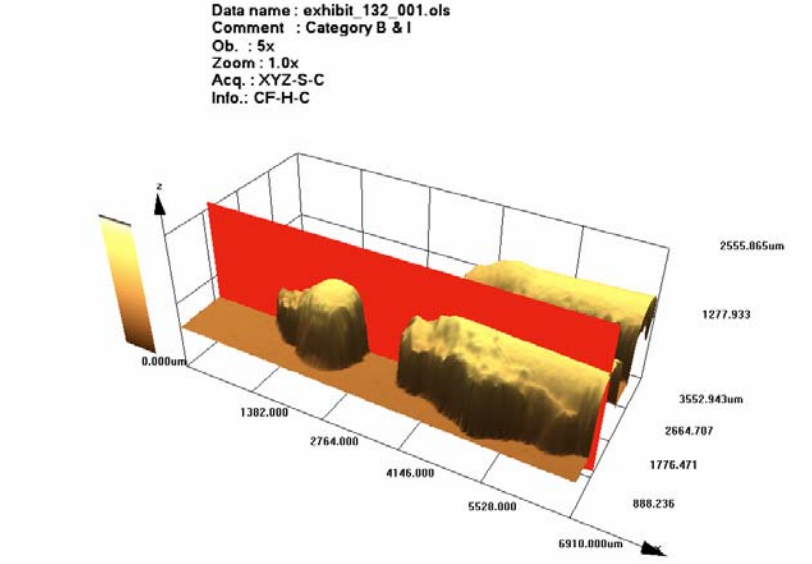

Figure 895 – A capture of the "slice tool" option in the LEXT software being used to obtain a profile and measurements.

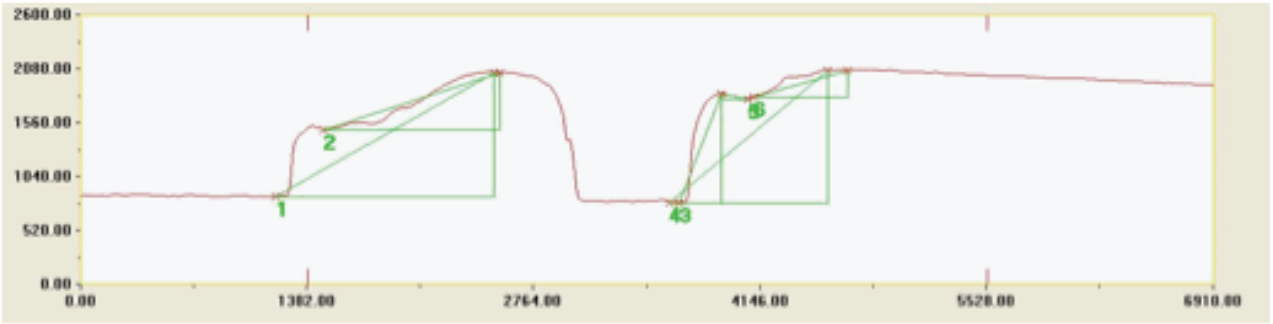

Figure 896 - Profile created with the "slice tool" as captured in the top right image above, the scale is detailed in microns. The green colour numeral "2" details the height of the left bead – 527 microns (0.52mm) above the conductor surface.

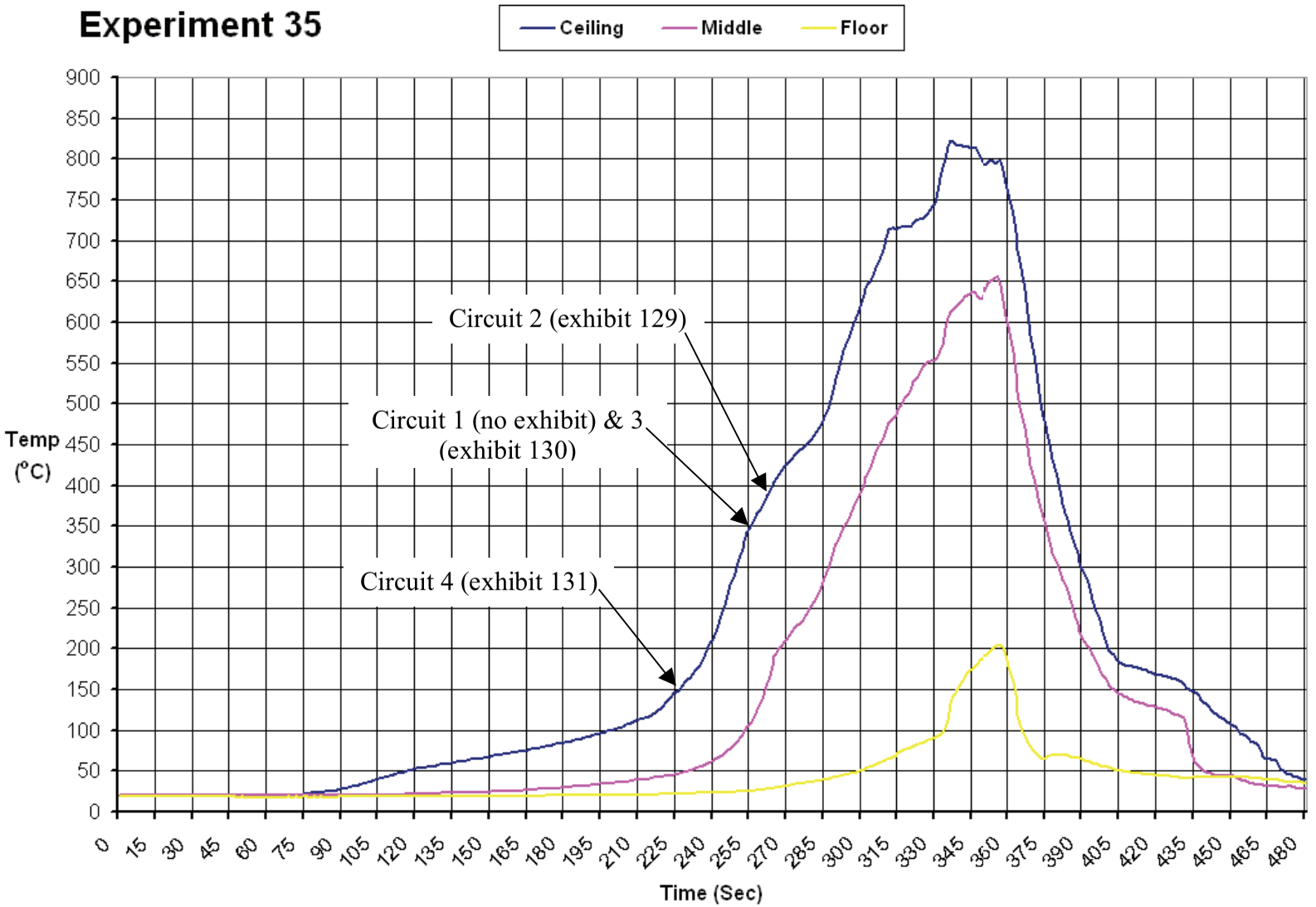

Figure 897 - Time temperature graph for experiment 35

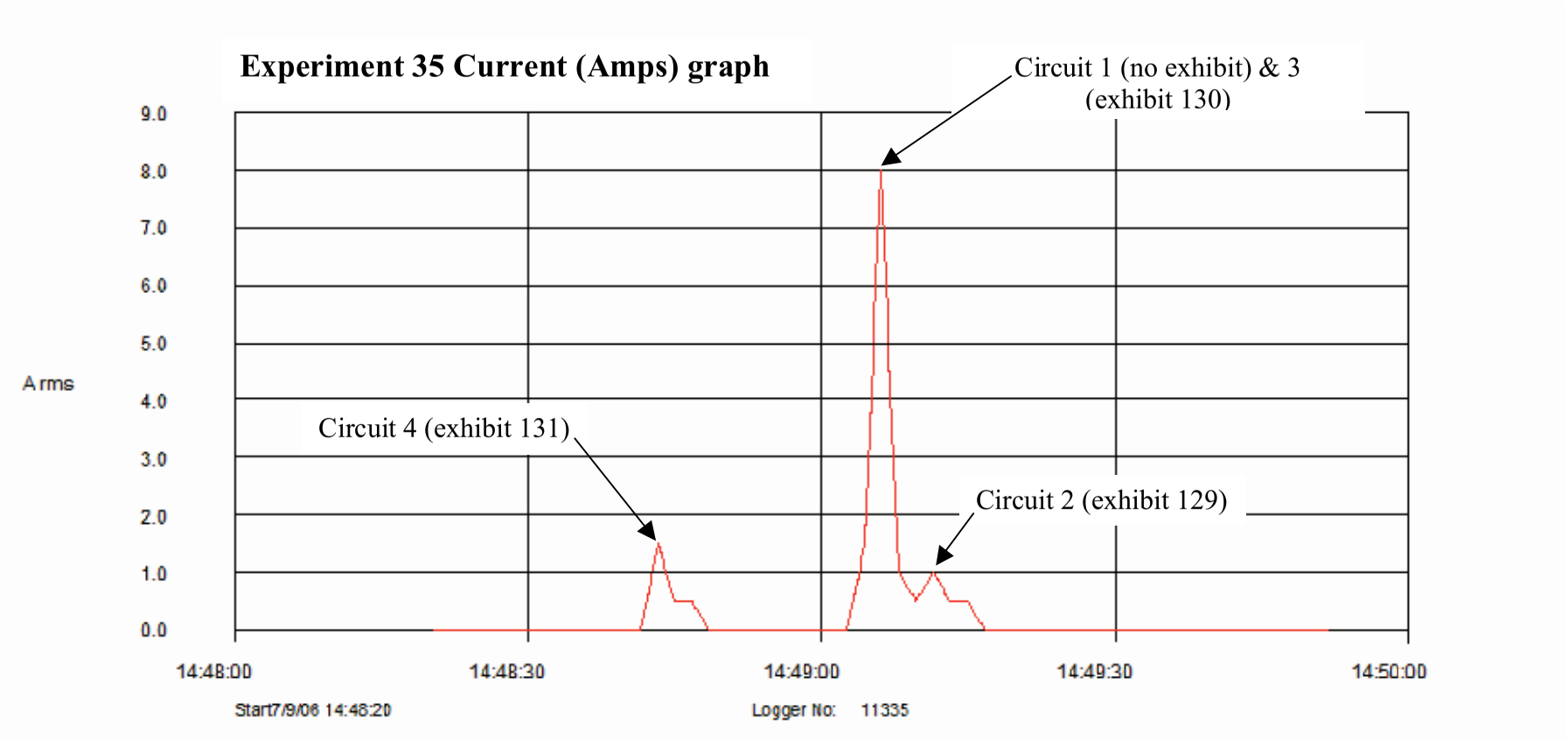

Figure 898 - Current (Amps) graph for experiment 35 detailing the operation of the circuit breakers and the fault current

Experiment 36

Figure 899 – "Scenario D" 28 September 2006

Circuit number	MCB operating time from ignition
4	1:13 minutes
1	1:24 minutes
3	1:51 minutes
2	1:51 minutes

Table 38 – circuit breaker operation data

The fire in experiment 36 (scenario D) originated in five separate areas. An armchair located in the left rear corner, (this was observed as the dominant fire plume in the fire's development). A television against the centre of the rear wall. On top of the cabinet located adjacent to the rear right corner. A three-seat settee adjacent to the left wall. A second three-seat settee adjacent to the front wall.

The fire developed rapidly with the ceiling temperature reaching 1000° C at 3.5 minutes and the middle thermocouple recording 1150° C at this point. The floor temperature reached just over 900° C confirming that the compartment was at flashover conditions.

Arcing damage was located on circuit 1 – 1070mm from the left wall and adjacent to the rear wall.

No arcing damage was located on circuit 2.

Arcing damage was located on circuit 3 – adjacent to the left wall on the ceiling and 1000mm from the front wall.

Arcing damage was located on circuit 4 – 180mm from the left wall and 1000mm from the rear wall.

Pre-fire and post-fire photographs of experiment 36

Figure 900 - Pre-fire photograph of experiment 36. This fire had 5 areas of origin that are documented on the scene diagram Figure 904. The dominant fire plume was the armchair in the rear left corner.

Figure 901 - Pre-fire photograph detailing the wiring installed on the ceiling using wooden blocks. The arrows indicate the arcing locations to circuit 4 (L) and circuit 1 (R).

Figure 902 - Post-fire photograph. The dominant fire plume is indicted with the white circle.

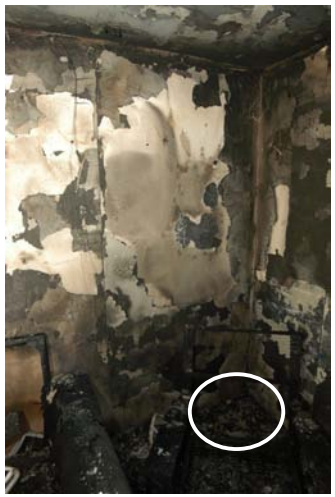

Figure 903 - Post-fire photograph of the dominant fire plume area – the rear left corner of the room.

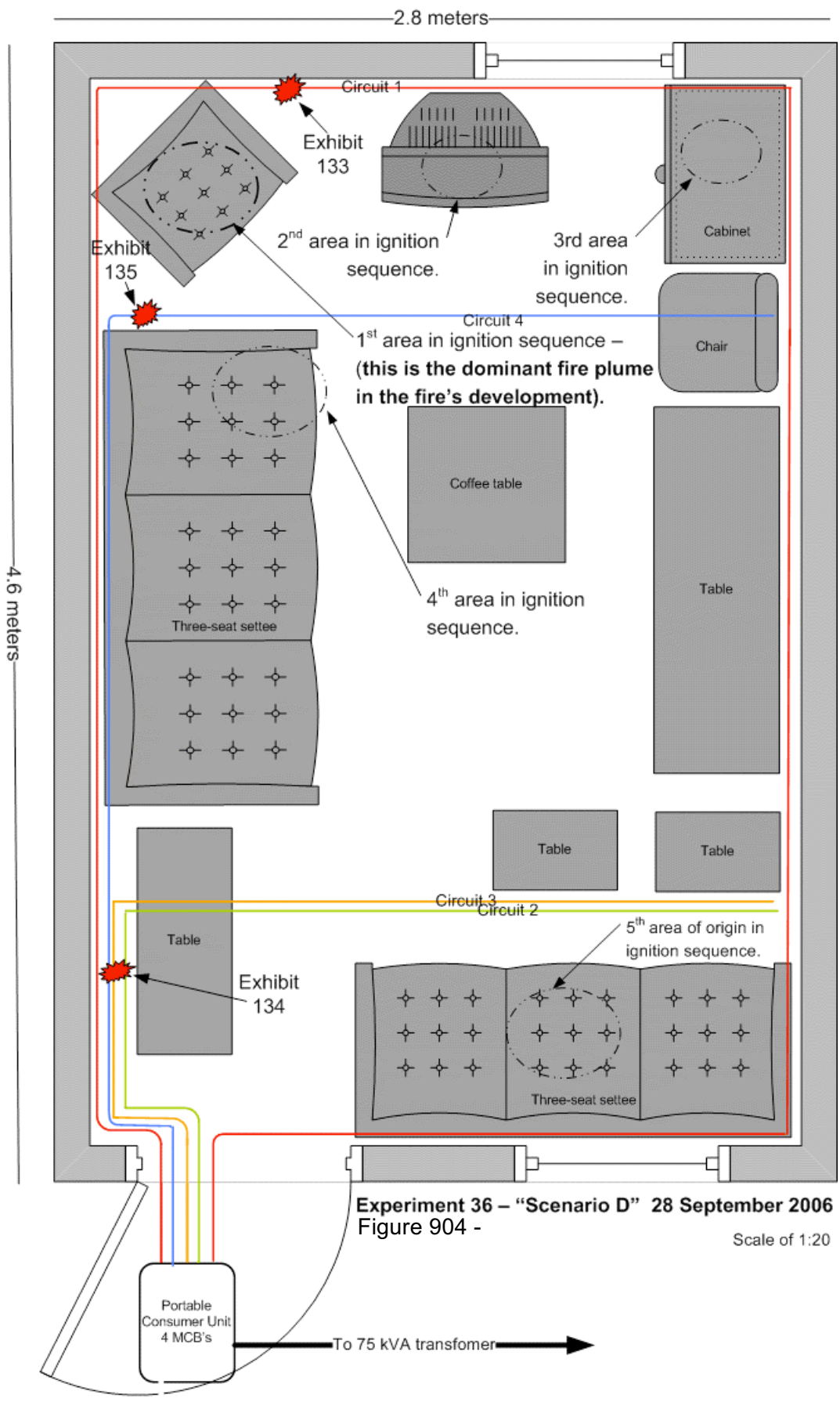

Experiment 36 – "Scenario D" 28 September 2006

Figure 904 -

Scale of 1:20

Microscope and SEM images for exhibit 133 – arcing category D (experiment 36)

Figure 905 - Microscope image of exhibit 133. The two 2.5mm^2 conductors (L&N) had arcing damage. The conductors had arced across the fixing screw.

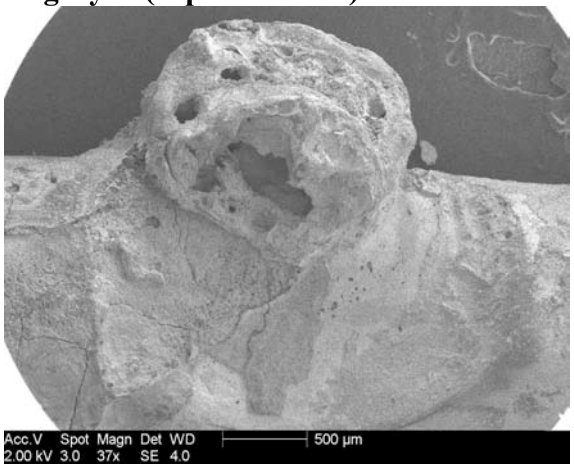

Figure 906 - SEM image of the top conductor in figure 905. The bead on the edge of the notch has a number of holes in the copper surface.

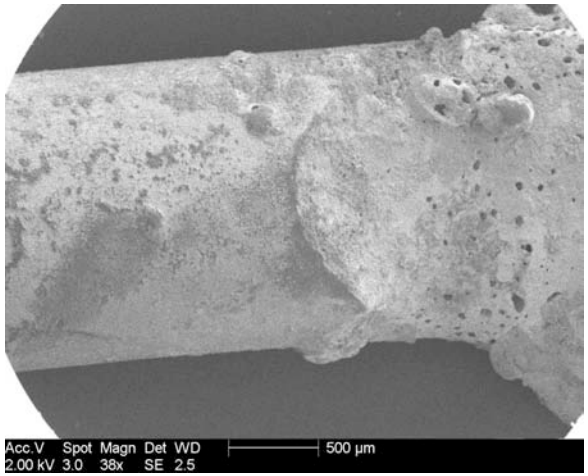

Figure 907 - SEM image of the bottom conductor detailed in figure 905. The notch is large with holes in the copper surface and clear edge demarcation.

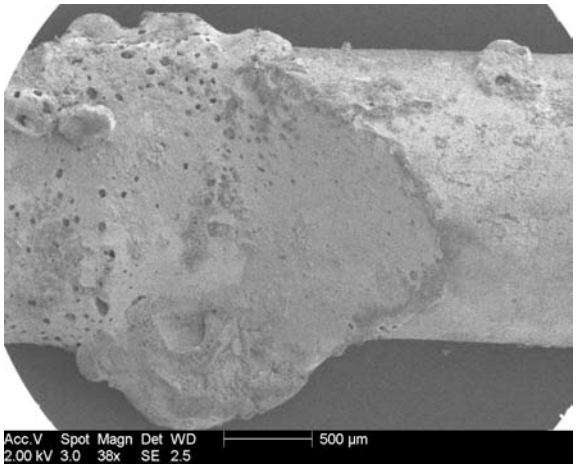

Figure 908 - SEM image displaying the majority of the notch and the right edge indicates a clear demarcation between the arcing damage and the undamaged metallic surface.

Confocal laser scanning microscope image for exhibit 133 – arcing category D (experiment 36)

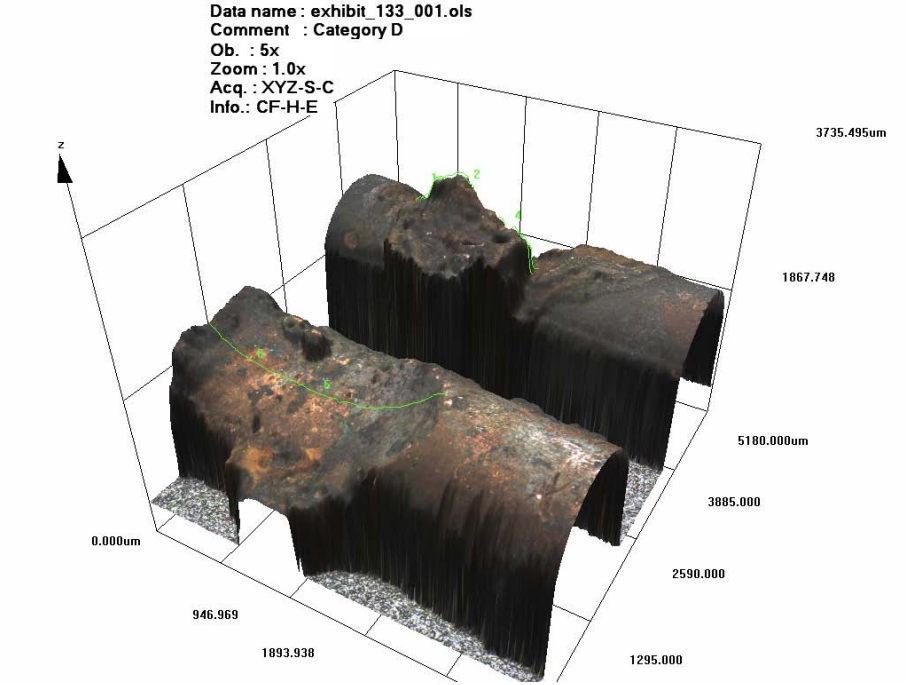

Figure 909 - LEXT image of exhibit 133. The LEXT scan enabled the entire exhibit to be displayed in detail.

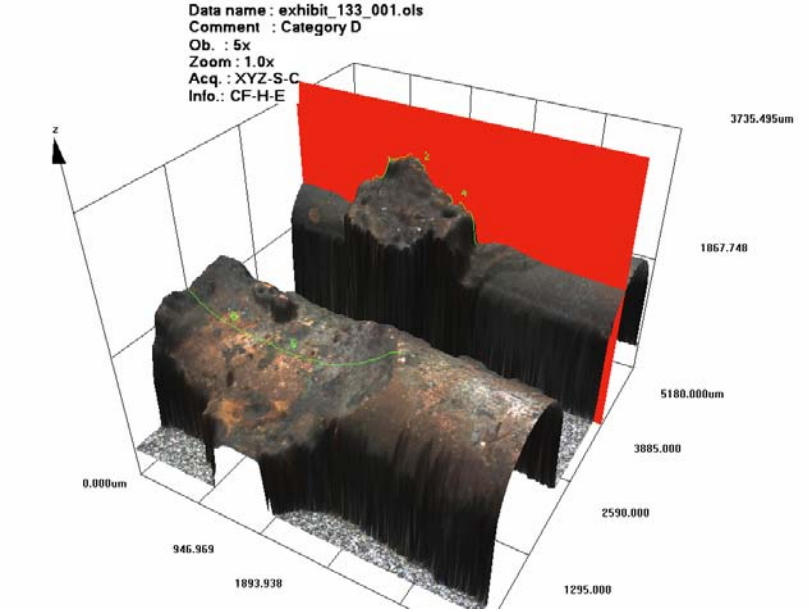

Figure 910 - LEXT image capturing the “slice tool” in the software in use. The profile is not available as the report “.rtf” document file is corrupted.

Microscope and SEM images for exhibit 134 – arcing category B (experiment 36)

Figure 911 - Microscope image of exhibit 134. The conductor is welded to the fixing screw. The conductor has fractured at the bead.

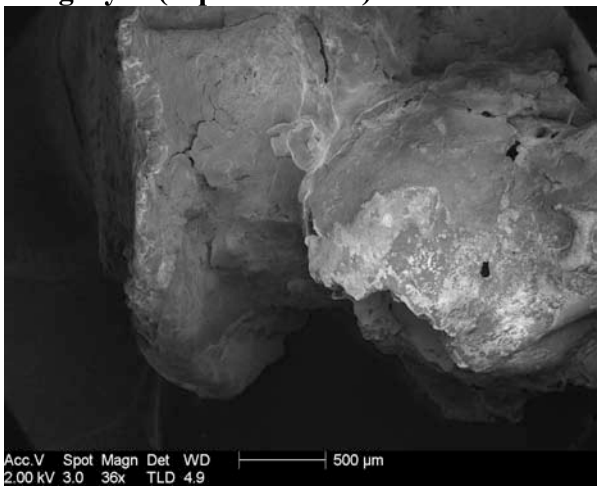

Figure 912 - SEM image of the read on the fixing screw. The edge of the screw thread is visible on the left side of the image.

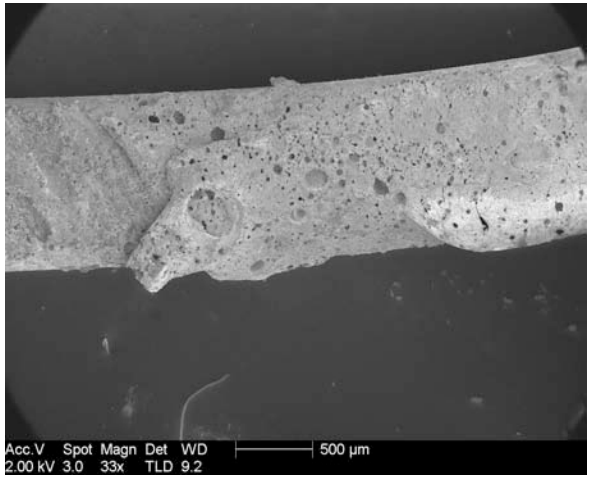

Figure 913 - SEM image of a notch on the conductor.

Figure 914 - SEM image of the fractured end of the conductor visible in the microscope image above.

Microscope and SEM images for exhibit 135 – arcing category H (experiment 36)

Figure 915 - Microscope image of exhibit 135. Two of the three conductors are welded together with a bead.

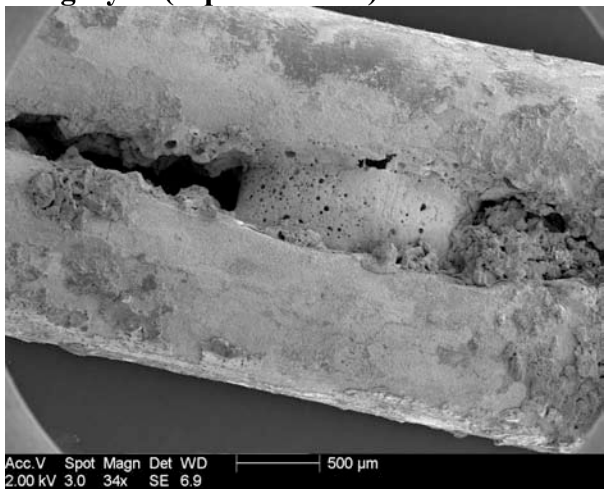

Figure 916 - An SEM image of the large bead that has welded the two 1mm^2 conductors together.

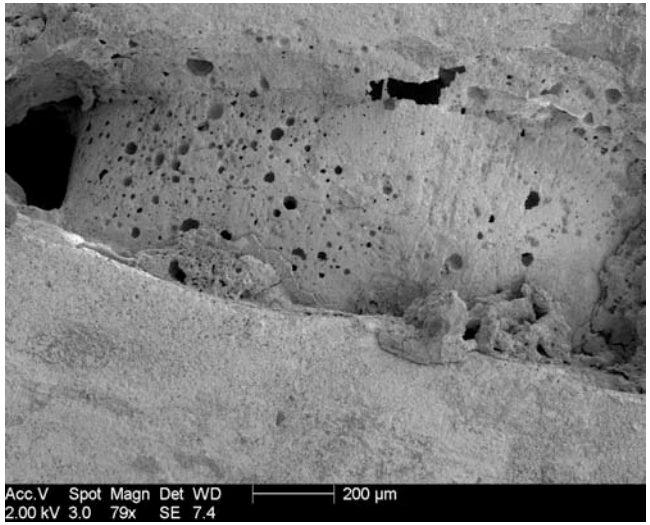

Figure 917 - SEM image of bead at 79x magnification.

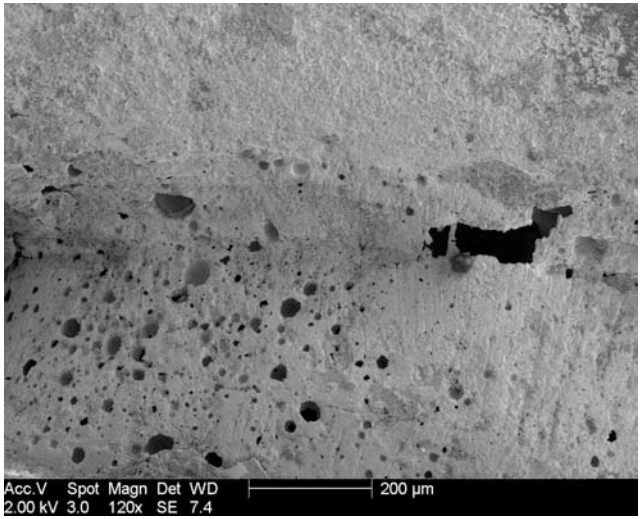

Figure 918 - SEM image at 120x magnification of the top area of the weld bead indicating the holes on the surface.

Confocal laser scanning microscope image for exhibit 135 – arcing category H (experiment 36)

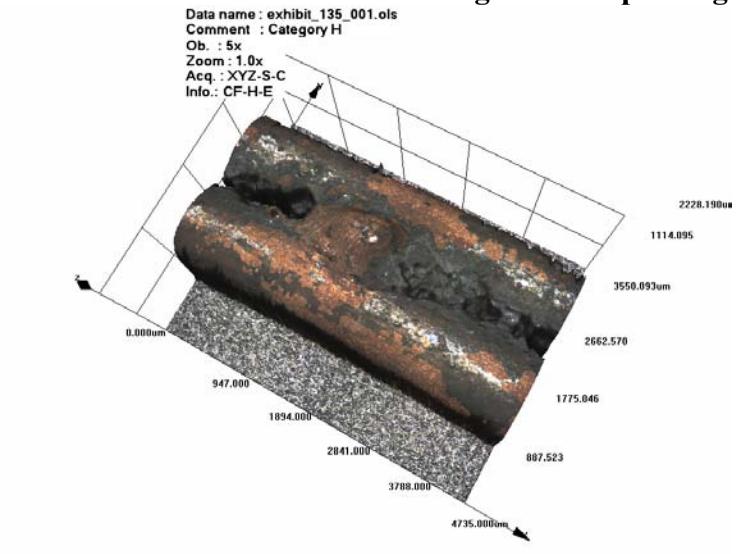

Figure 919 - LEXT image detailing the entire exhibit.

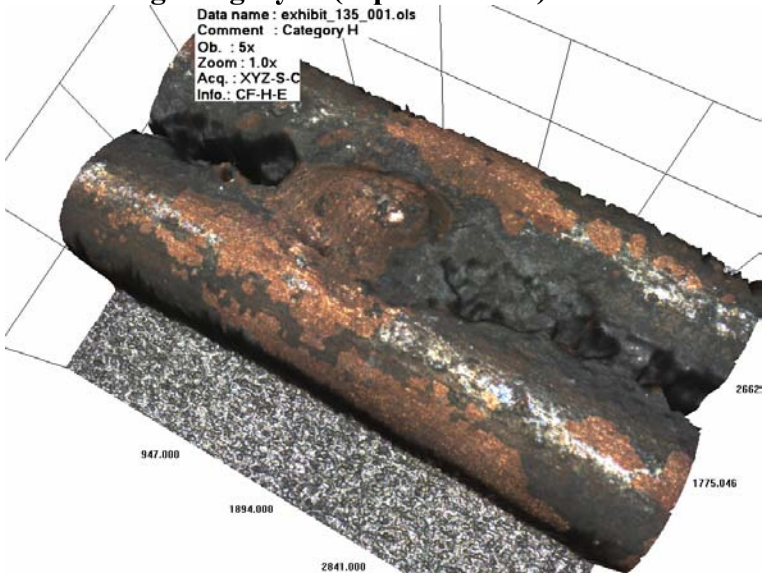

Figure 920 - LEXT image captured in the 3-D software.

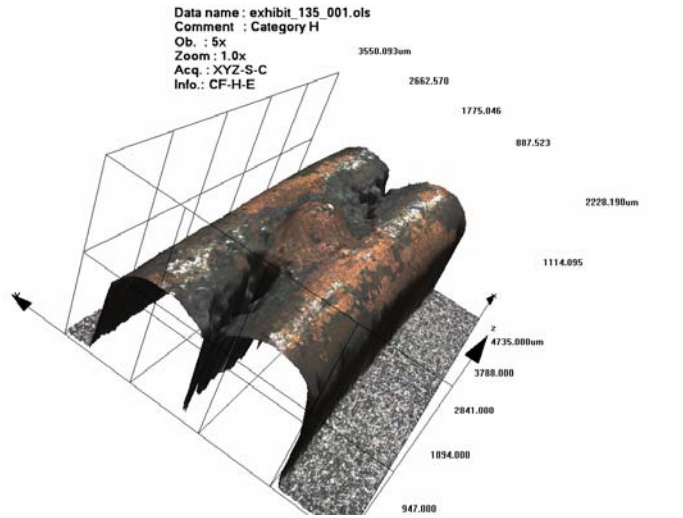

Figure 921 – re-orientation of the exhibit in the 3-D software.

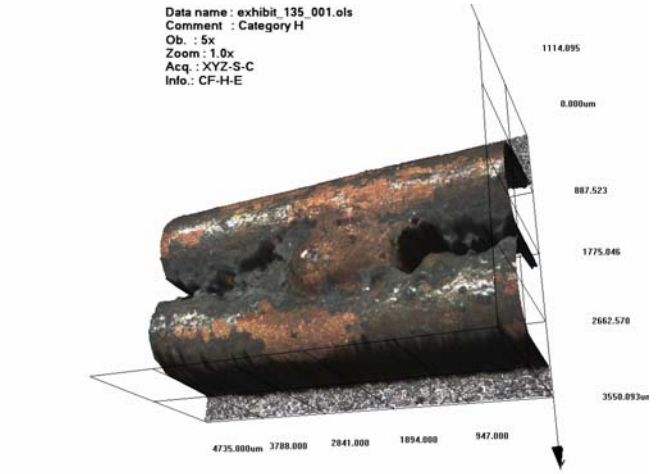

Figure 922 – re-orientation of the exhibit in the 3-D software.

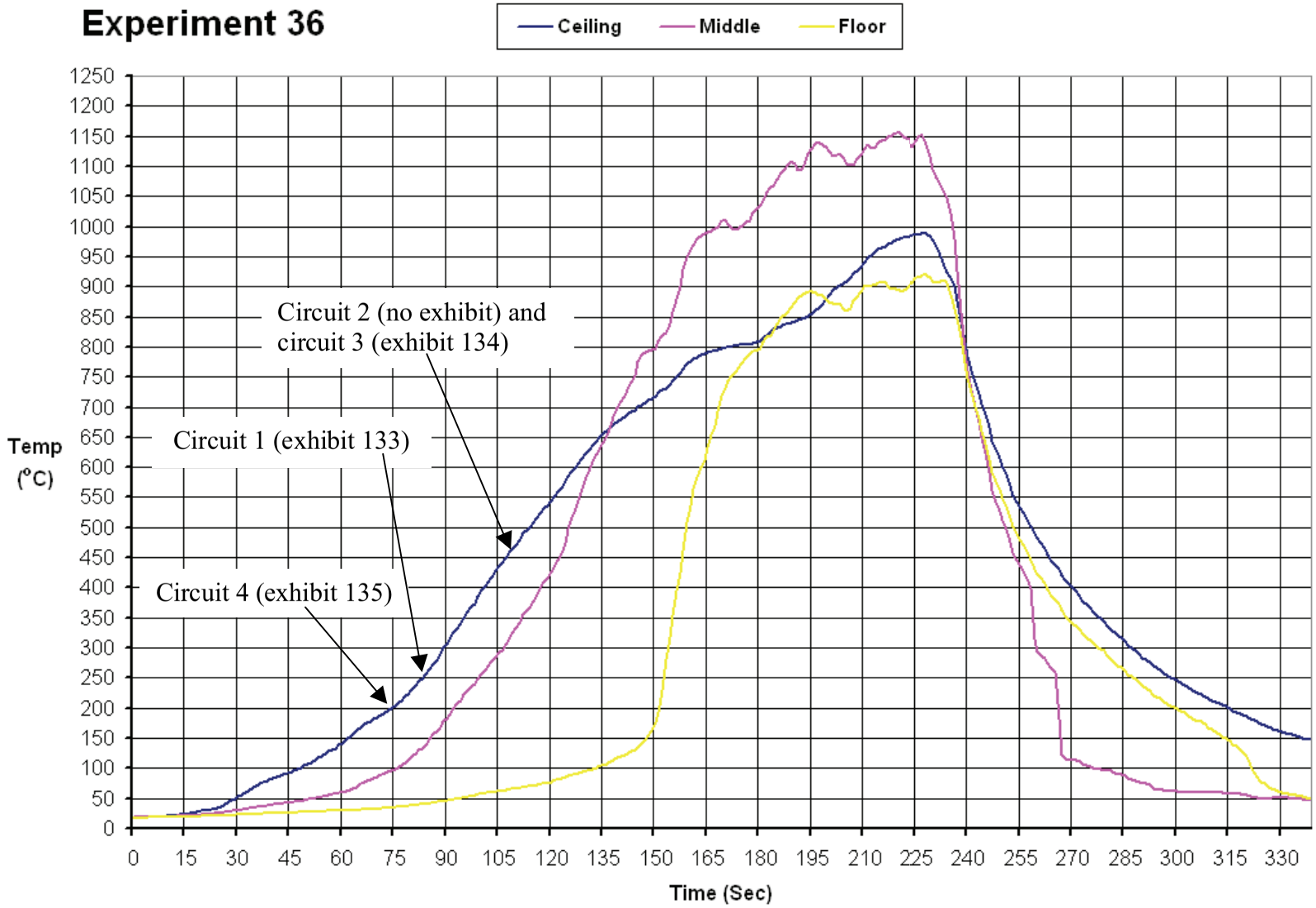

Figure 923 - Time temperature graph for experiment 36

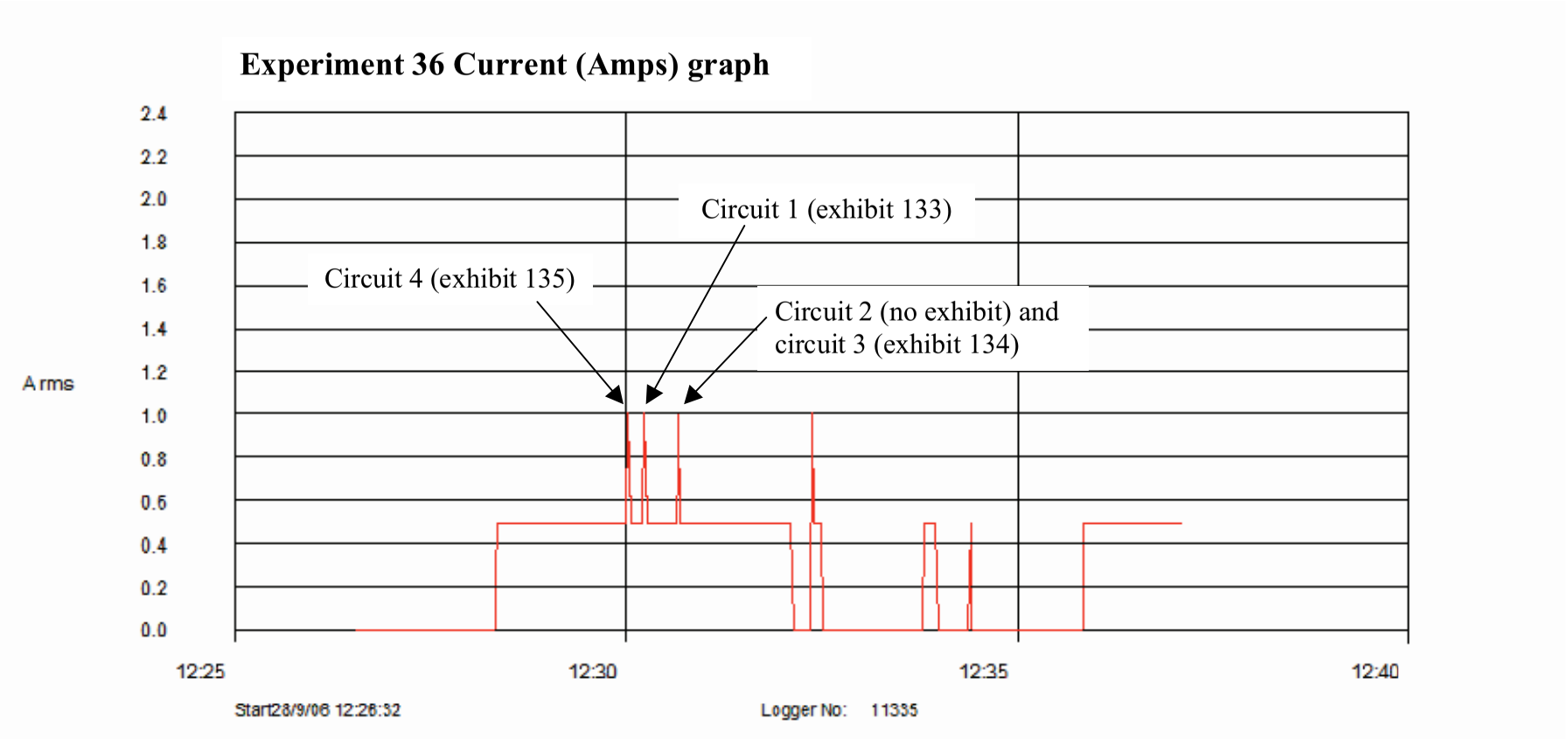

Figure 924 - Current (Amps) graph for experiment 36 detailing the operation of the circuit breakers and the fault current

Experiment 37

Figure 925 – “Scenario B” 28 September 2006

Circuit number	MCB operating time from ignition
4	2:25 minutes
1	2:36 minutes
2	2:54 minutes
3	2:55 minutes

Table 39 – circuit breaker operation data

The fire in experiment 37 (scenario B) originated in a wardrobe located adjacent to the right wall within the compartment. The fire steadily developed to flashover conditions within 5 minutes. The ceiling temperature thermocouple recorded 1050° C with the middle thermocouple recording 950° C and the floor reaching 900° C.

Arcing damage was located on circuit 1 – adjacent to the right wall and 1510mm from the front wall.
No arcing damage was located on circuit 2.
Arcing damage was located on circuit 3 - 795mm from the right wall and 1000mm from the front wall (conductors were welded together).
Arcing was damage located on circuit 4 – 380mm from the right wall and 1000mm from the rear wall (conductors were welded together).

Figure 926 - Early development of the fire in the bottom of the high display unit.

Pre-fire and post-fire photographs of experiment 37

Figure 927 - Pre-fire photograph of experiment 37. The area of origin for this fire was the bottom of the display unit on the right wall (indicated by the white arrow).

Figure 928 - Pre-fire photograph of circuit 4 detailing the installation method for the ceiling wiring of experiments 36-39, using wood blocks fixed to the ceiling.

Figure 929 - Post-fire photograph of the scene. The area of origin is indicated by the white oval.

Figure 930 - Close-up post-fire view of the wood blocks used to support the ceiling wiring.

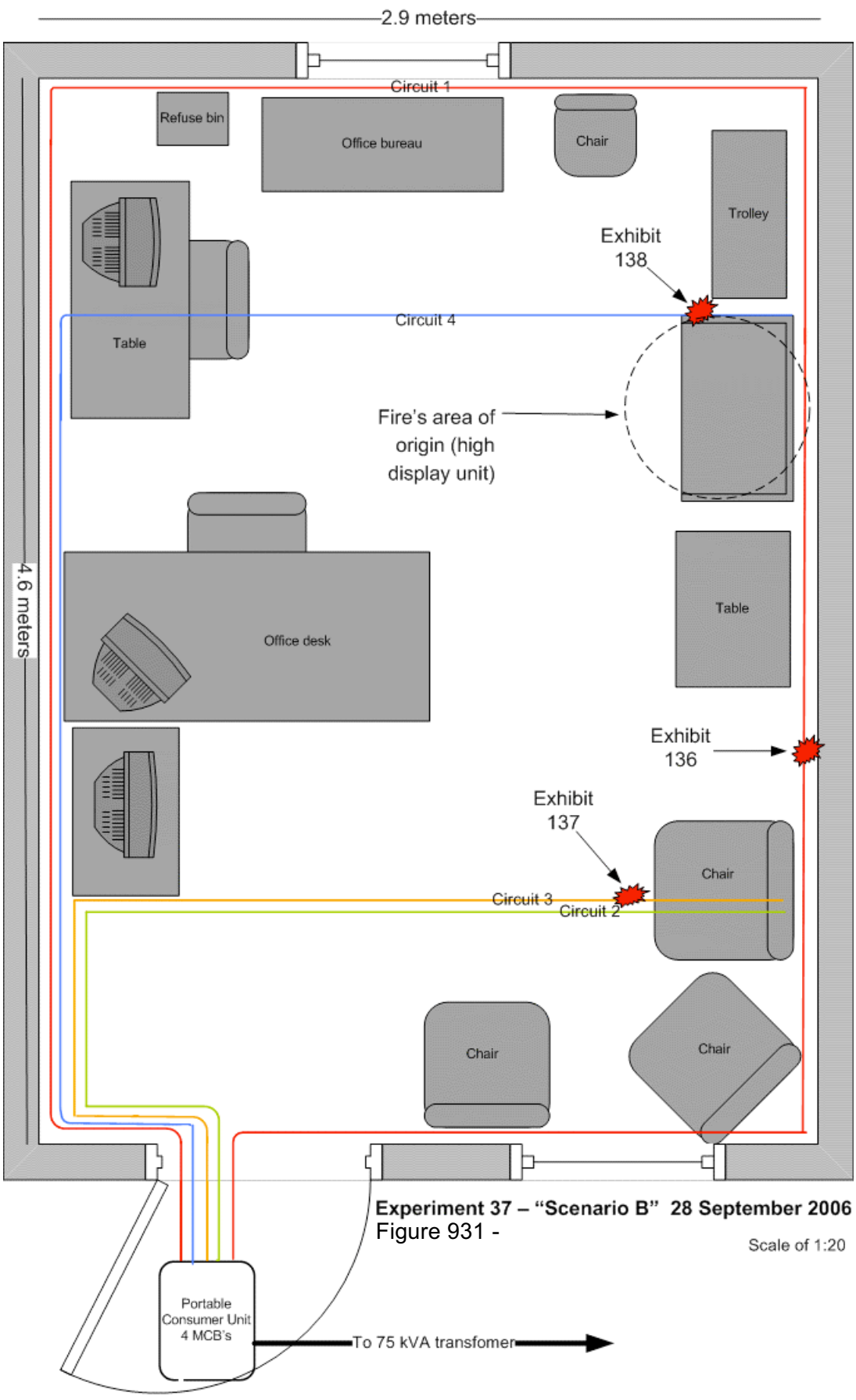

Experiment 37 – "Scenario B" 28 September 2006
Figure 931 -

Scale of 1:20

Microscope and SEM images for exhibit 136 – arcing category D (experiment 37)

Figure 932 - Microscope image of exhibit 136. The conductors have arced at a fixing screw and affected the two 2.5mm^2 L & N conductors. Each had a large notch with a bead within the notch.

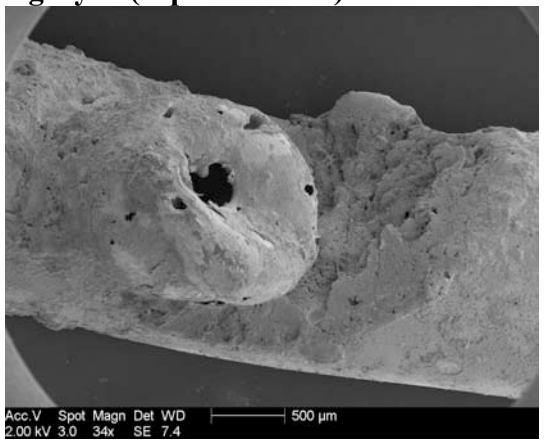

Figure 933 - SEM image of the lower conductor displayed on the left. The bead had a large hole in the metallic surface.

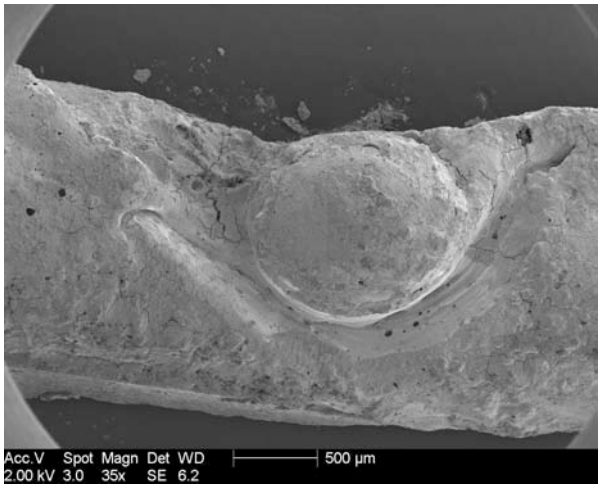

Figure 934 - SEM image of the top conductor detailed in figure 932.

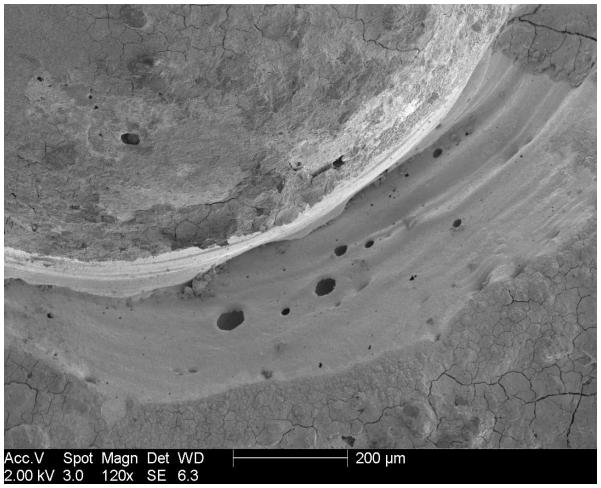

Figure 935 - SEM image at 120x magnification of the lower area of the notch. The notch had ridges on its surface and this may be an effect of alternating current.

Full-size SEM image of the upper conductor of exhibit 136 – detailing the ridge lines in the copper surface of the notch

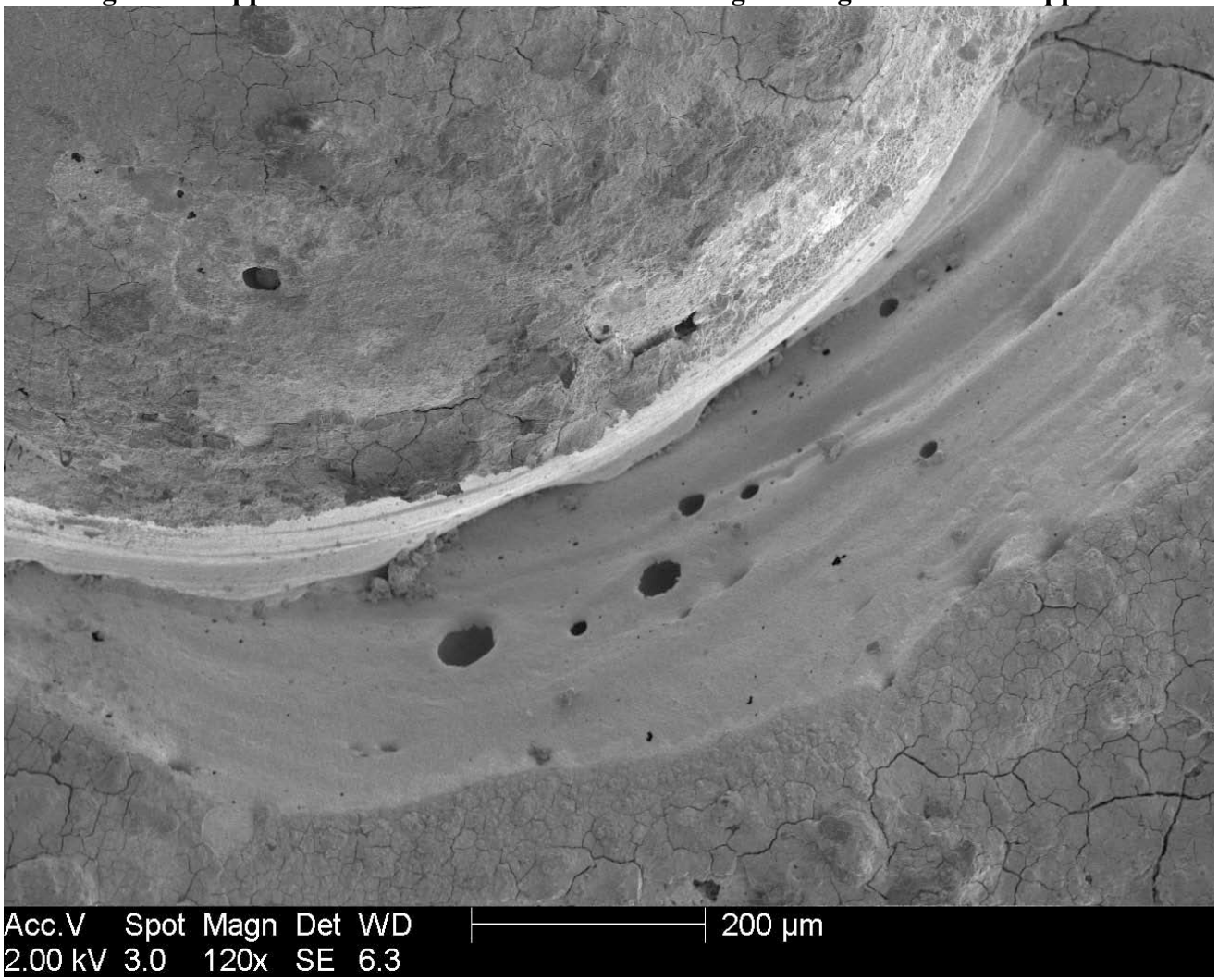

Figure 936 – Rib lines observed in the copper surface of the notch

Confocal laser scanning microscope image for exhibit 136 – arcing category D (experiment 37)

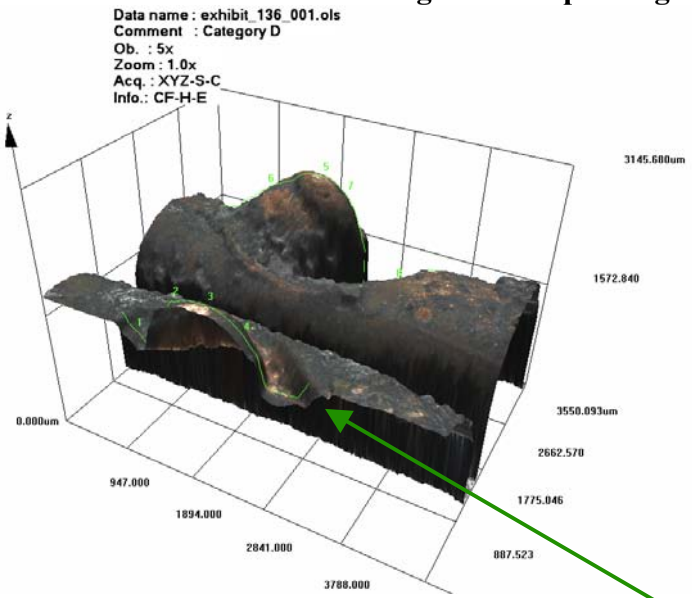

Figure 937 – LEXT image detailing exhibit 136.

Figure 938 – Image rotated in the 3-D software and captured.

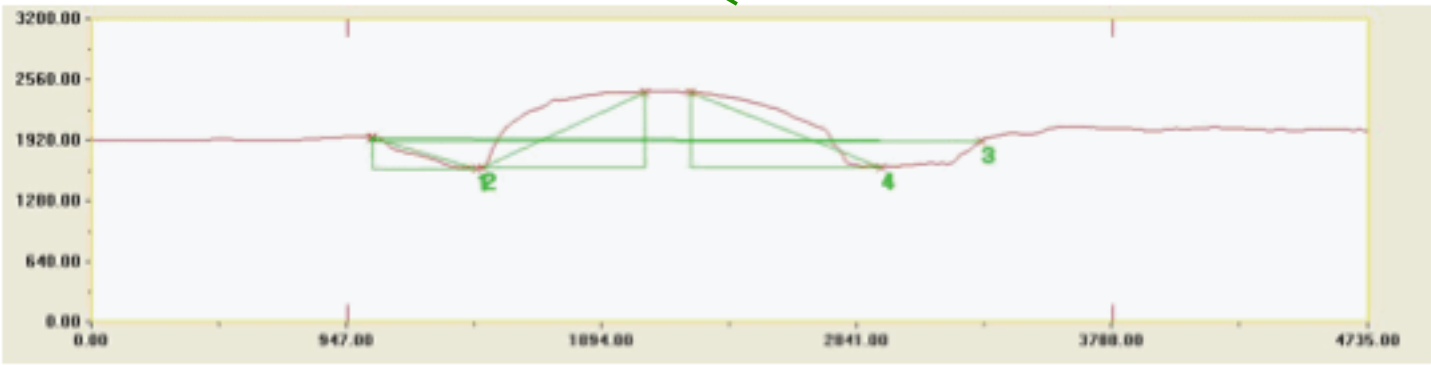

Figure 939 - Profile of the notch with the ridge lines, the notch is 2263 microns wide (2.26mm). The bead is 769 microns (0.76mm) high

Microscope images for exhibit 137 – arcing category D (experiment 37)

Figure 940 - Microscope image of exhibit 137. Arcing damage located on one of the three 1mm^2 conductors, a notch with a bead within the notch.

Figure 941 - 20x magnification of the notch and bead detailed in figure 940.

Microscope and SEM images for exhibit 138 – arcing category D (experiment 37)

Figure 942 - Microscope image detailing one of the two conductors for exhibit 138. Both conductors had notch damage. This top conductor notch was unusually large at 4mm wide.

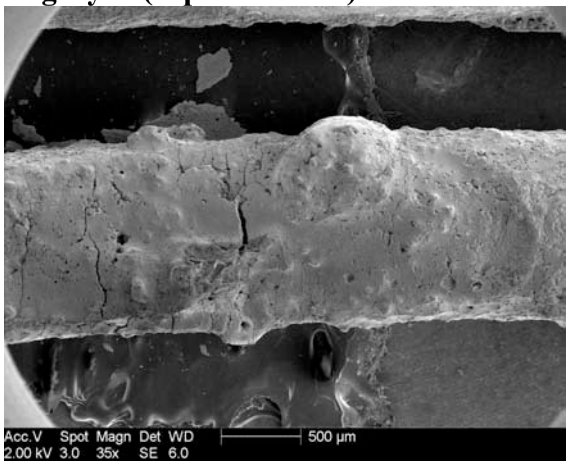

Figure 943 - SEM image of the bottom conductor. There was still a lot of PVC residue remaining following the cleaning process.

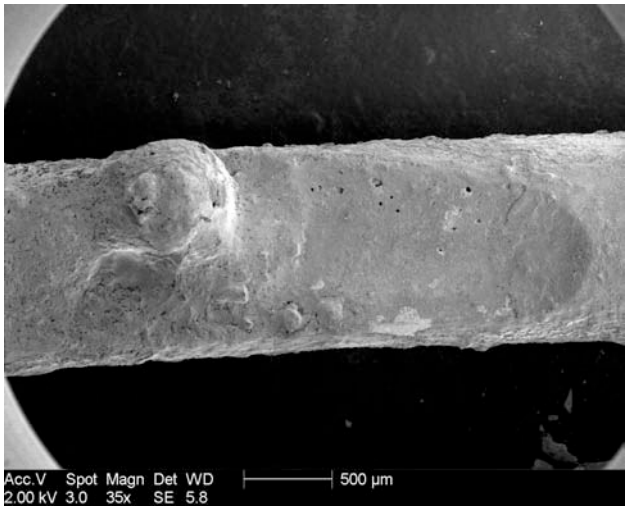

Figure 944 - SEM image of the top conductor as detailed in the microscope image, figure 942.

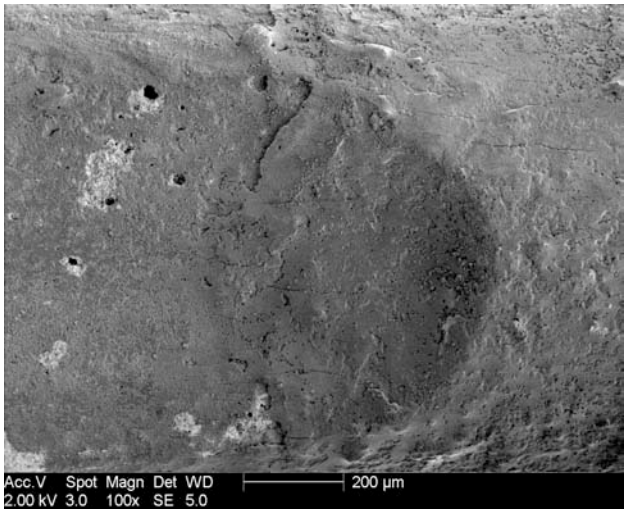

Figure 945 - SEM image at 100x magnification detailing the right edge of the notch and the demarcation area.

Full-size confocal laser scanning microscope image for exhibit 138 – arcing category D (experiment 37)

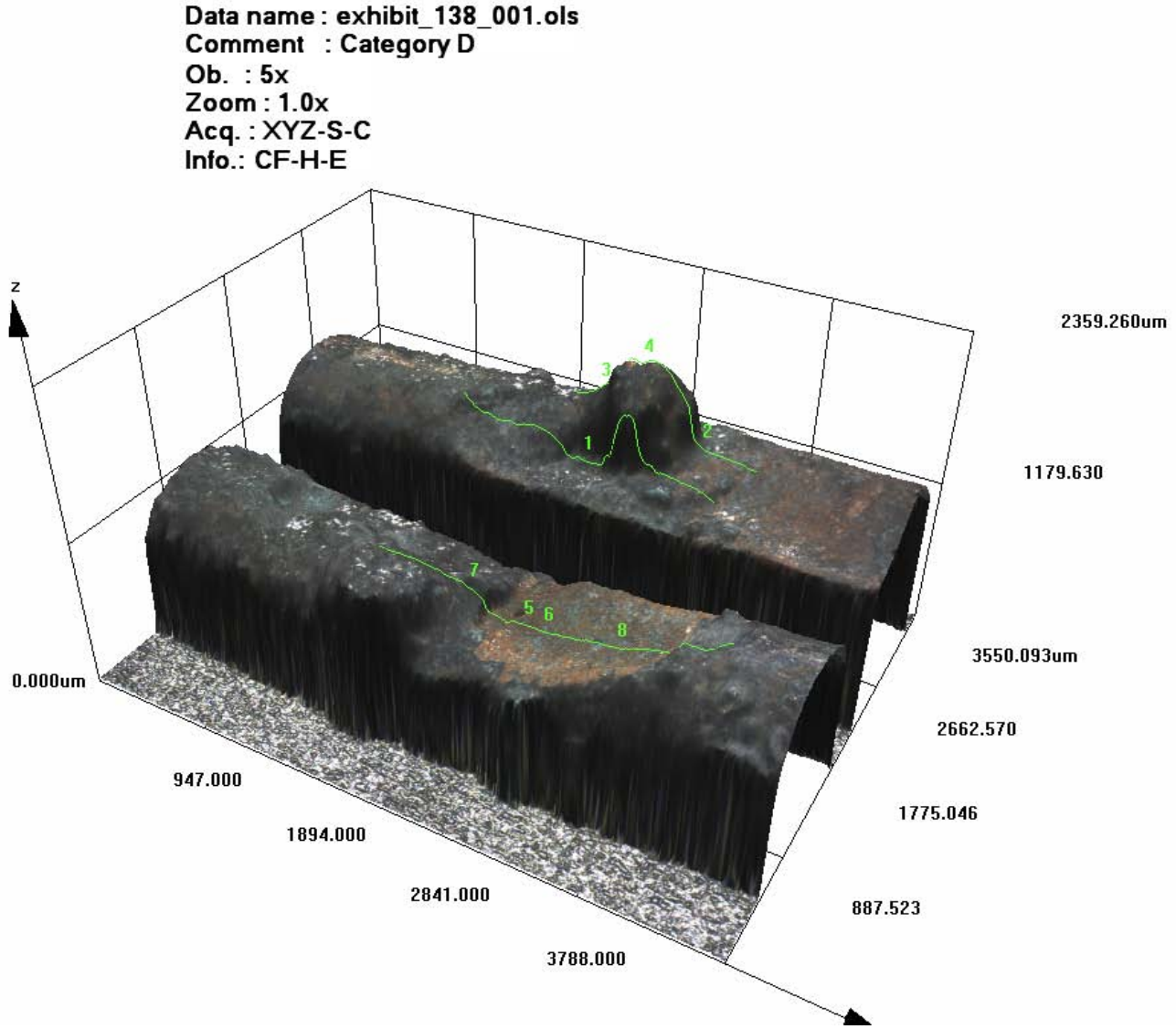

Figure 946 – Exhibit 138 LEXT image.

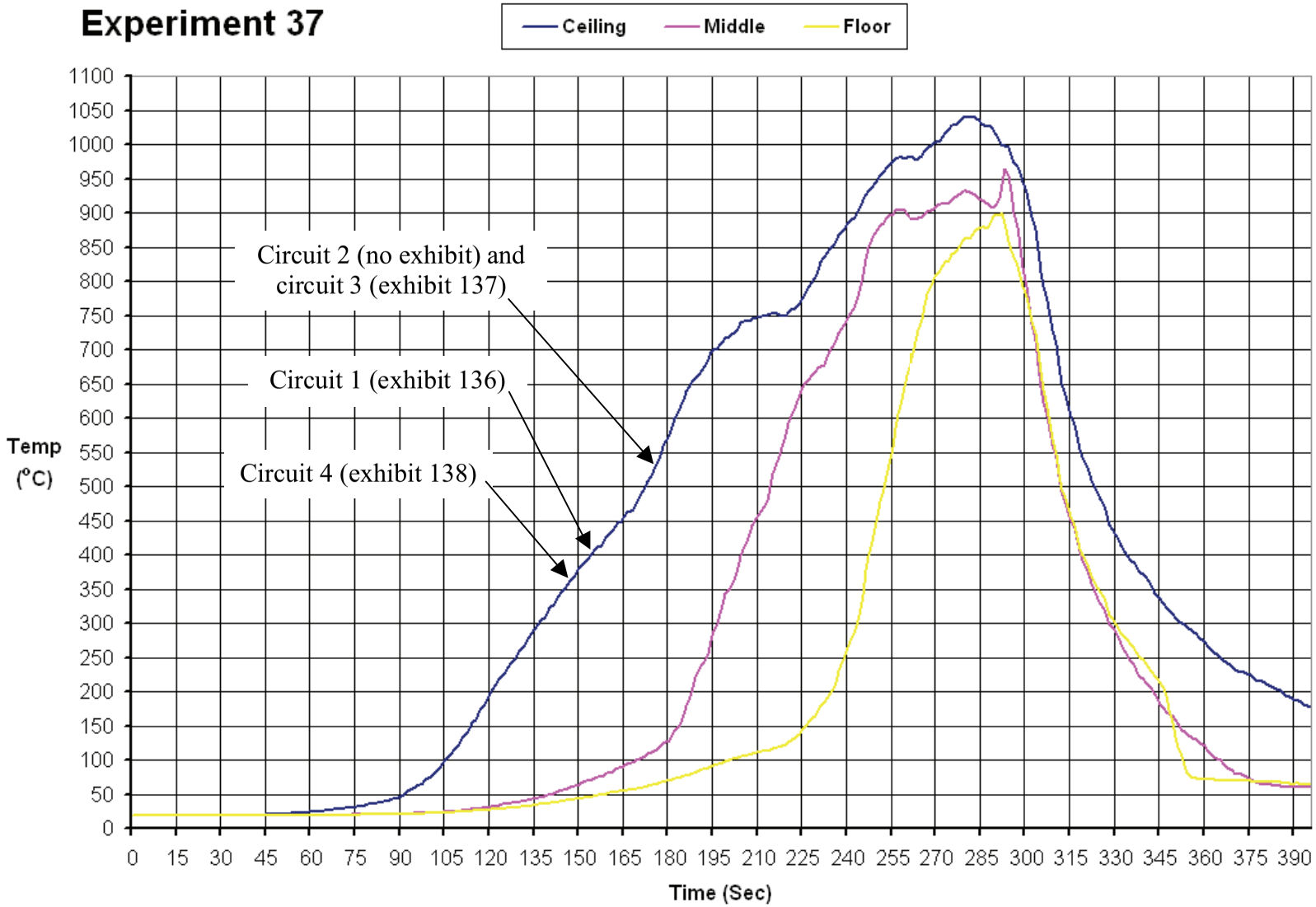

Figure 947 - Time temperature graph for experiment 37

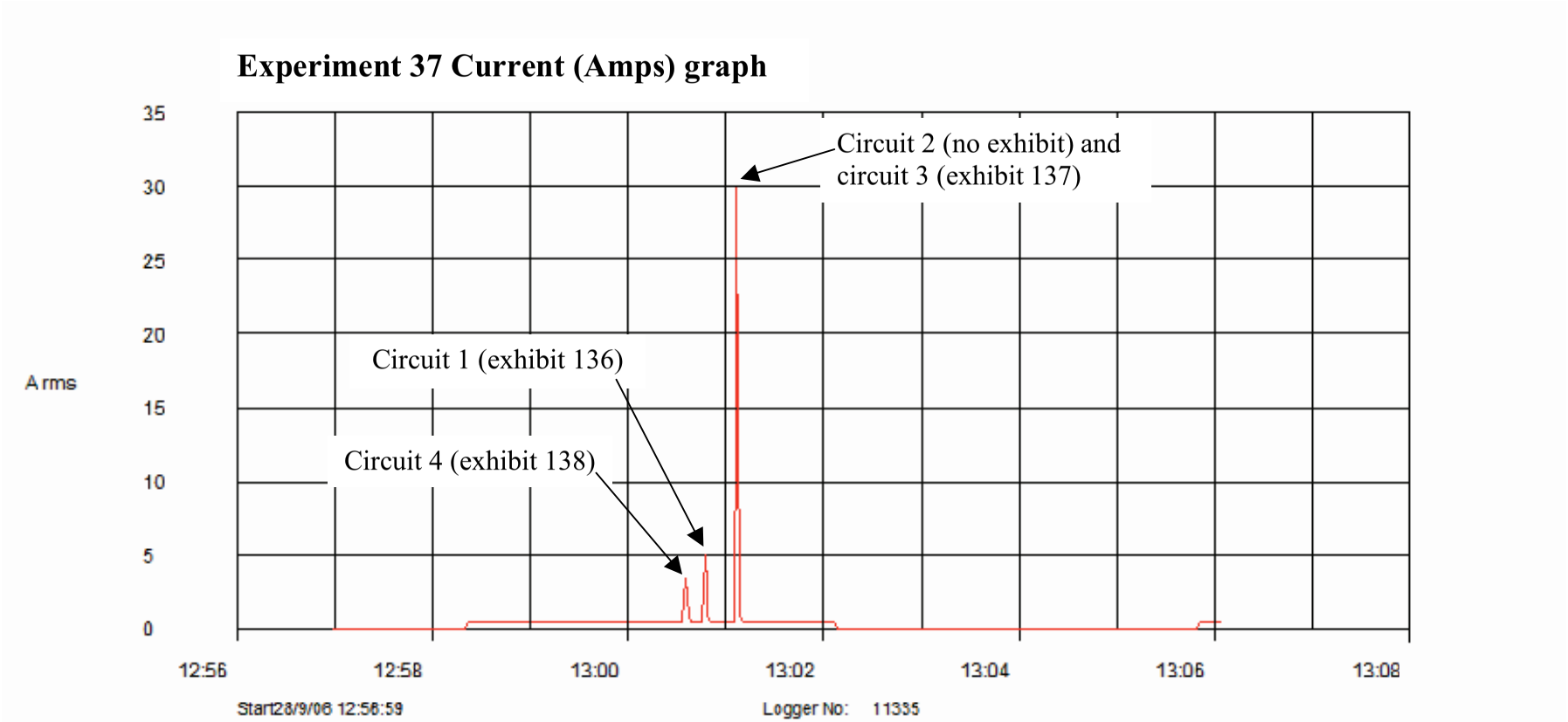

Figure 948 - Current (Amps) graph for experiment 37 detailing the operation of the circuit breakers and the fault current

Experiment 38

Figure 949 – "Scenario A" 28 September 2006

Circuit number	MCB operating time from ignition
4	1:56 minutes
1	1:58 minutes
3	2:16 minutes
2	2:56 minutes

Table 40 – circuit breaker operation data

The fire in experiment 38 (scenario A) originated in a clothes rail adjacent to the centre of the rear wall and the side of two single beds located either side of the clothes rail.

The fire developed rapidly in the first 2 minutes with the ceiling reaching a temperature of 500° C. The temperatures dropped for a short time before increasing again to reach a maximum ceiling temperature of 930° C recorded at 4.5 minutes. The middle thermocouple recorded 820° C at this point. The floor temperature did not exceed 130° C. The burn patterns suggest that this compartment fire did not reach flashover conditions.

Arcing was located on circuit 1 – 2800mm from the front wall and adjacent to the left wall.

Arcing was located on circuit 2 – 860mm from the left wall and 1000mm from the front wall.

No arcing damage was located on circuit 3.

Two separate areas of arcing damage were located on circuit 4 – 2010mm from the left wall and 1000mm from the rear wall. The second area of arcing damage was in the same location as circuit 1.

Pre-fire and post-fire photographs of experiment 38

Figure 950 - Pre-fire photograph of experiment 38. The fire's area of origin is indicated with the white oval.

Figure 951 - Pre-fire view of the cables installed to the ceiling using wood blocks.

Figure 952 - Post-fire photograph of the experiment. The arrows indicate the location of the arcing damage to circuit 1 & 4 (L) and the initial arcing damage to circuit 4 (R).

Figure 953 - Post-fire view of the ceiling detailing the fire damaged circuit 4, suspended by the charred timber blocks. The arcing damage to circuit 4 is out of view to the right.

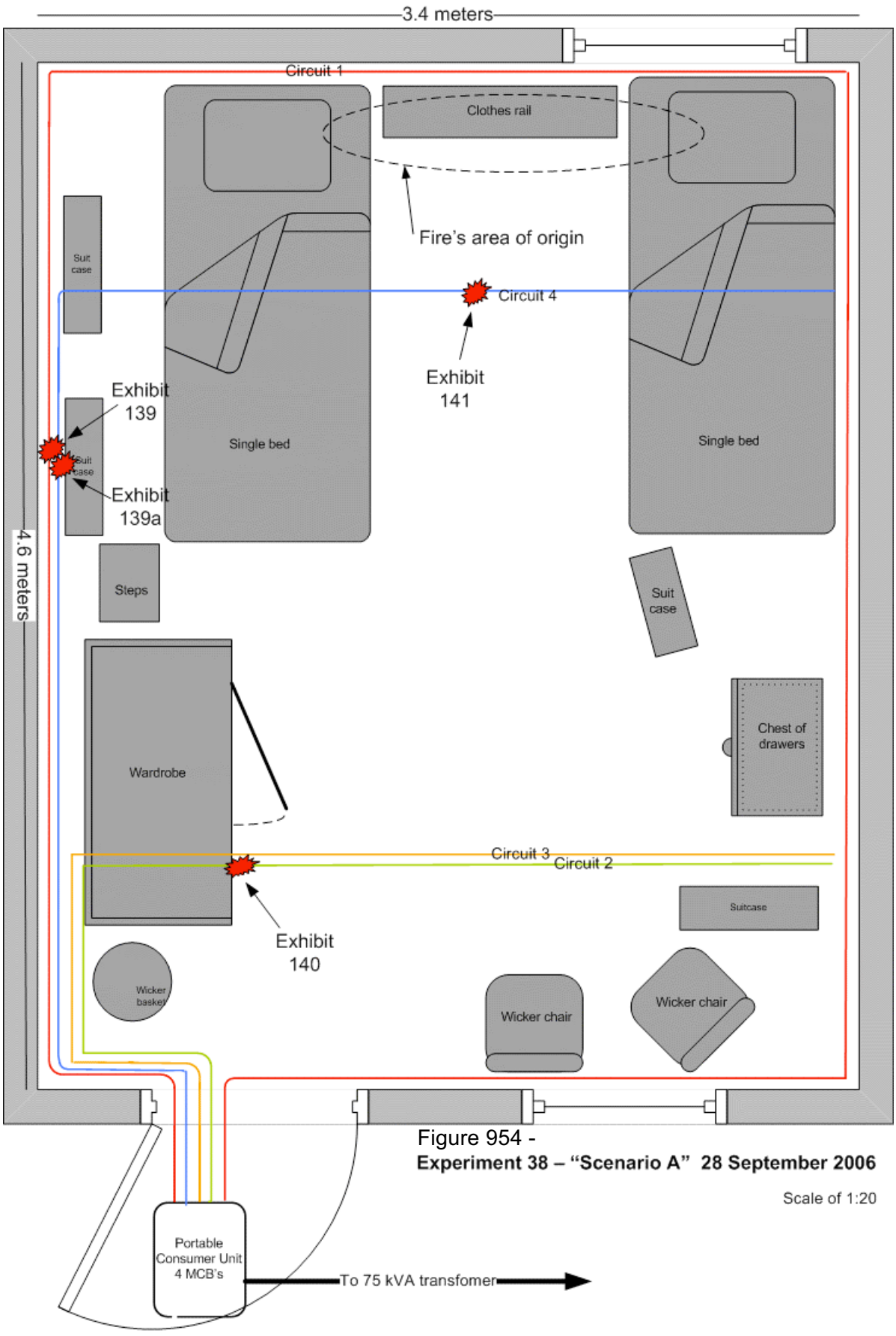

Figure 954 -
Experiment 38 – "Scenario A" 28 September 2006

Scale of 1:20

Microscope and SEM images for exhibit 139 – arcing category I (experiment 38)

Figure 955 - Microscope image of exhibit 139. This was a large notch with beads at the edge.

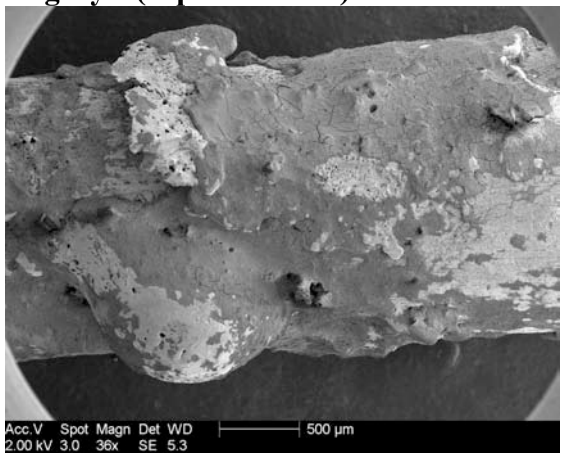

Figure 956 - SEM image of the notch with two beads on the left edge.

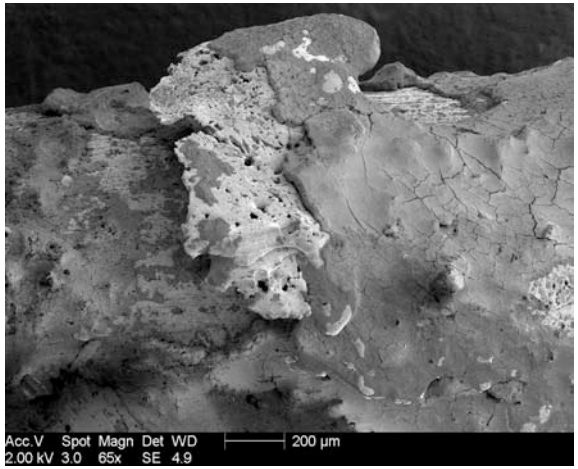

Figure 957 - SEM image at 65x magnification detailing the thin flat bead. The black material is PVC debris that still remained following the acetone & ultrasonic bath cleaning process.

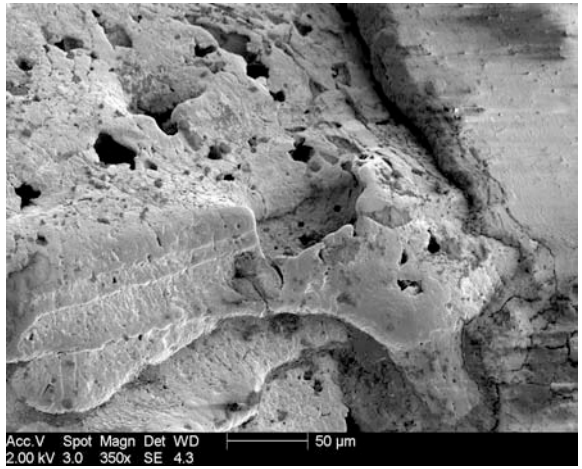

Figure 958 - SEM image at 350x magnification of the bottom edge of the thin flat bead. This image details the edge of the charred PVC debris as detailed in figure 957.

Full-size confocal laser scanning microscope image for exhibit 139 – arcing category I (experiment 38)

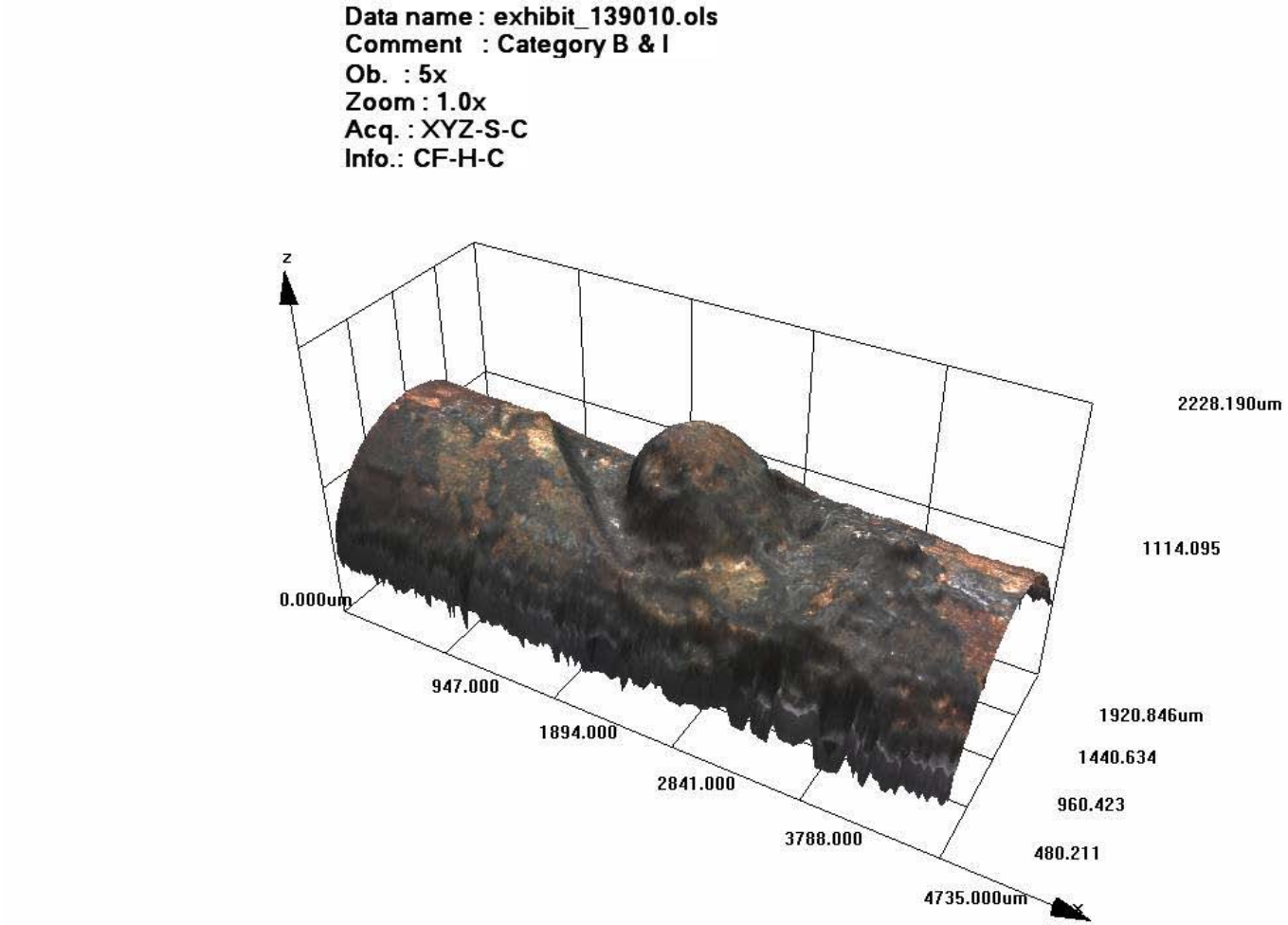

Figure 959 – LEXT image of exhibit 139.

Microscope and SEM images for exhibit 139a – arcing category B (experiment 38)

Figure 960 - Microscope image of exhibit 139a (circuit 4), The conductor had two severed ends with a large bead on the right.

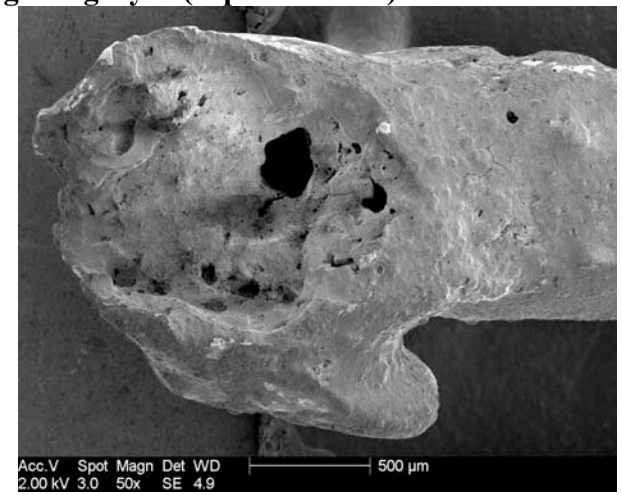

Figure 961 - SEM image of the tight bead, there are several holes in the bead.

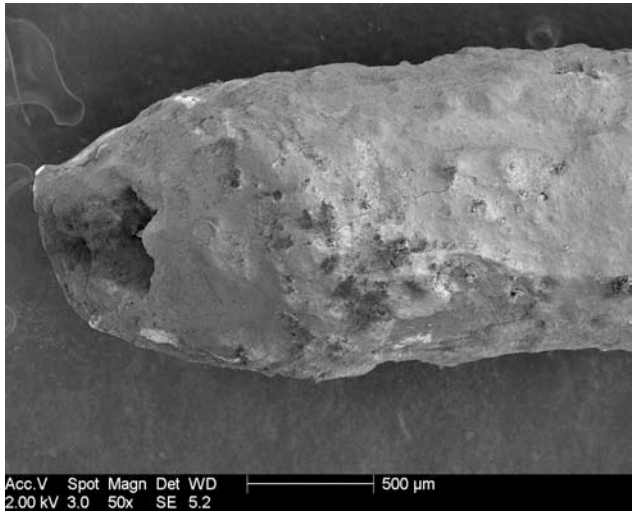

Figure 962 - SEM image of the left severed conductor end as detailed in figure 960.

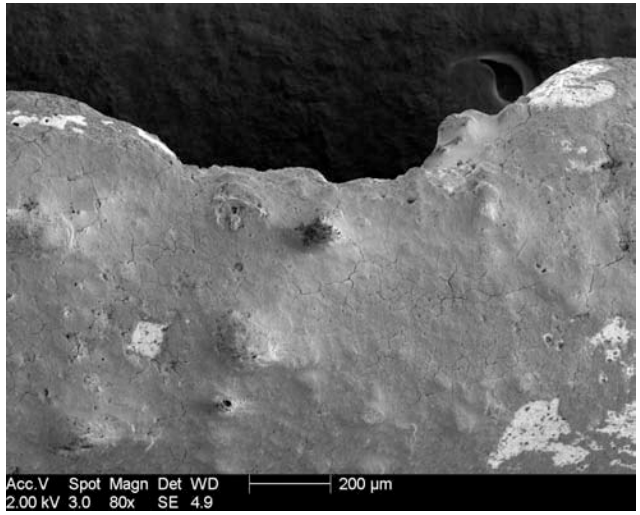

Figure 963 - SEM image of the notch adjacent to the right severed end detailed in figure 961.

Microscope and SEM images for exhibit 140 – arcing category A (experiment 38)

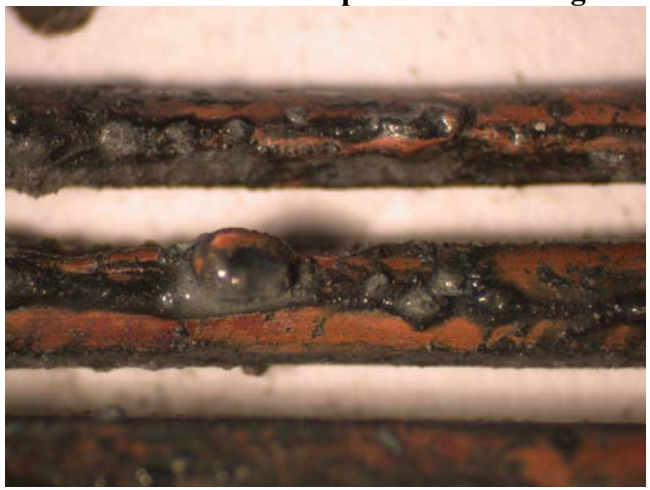

Figure 964 - Microscope image of exhibit 140. The arcing damage has affected the live and smaller earth conductor. The damage extends to 7mm in length and is a good example of arcing through char.

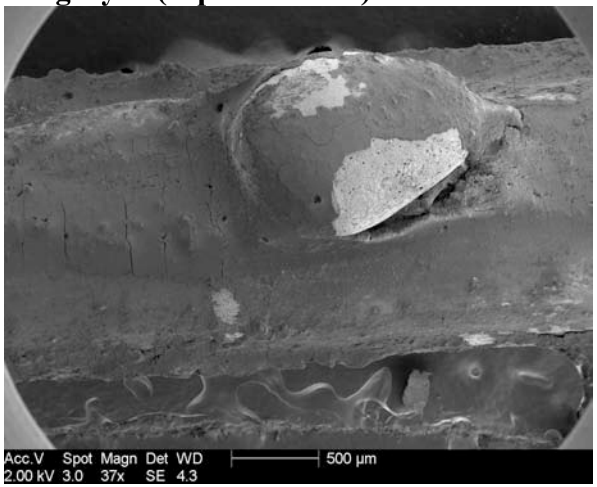

Figure 965 - SEM image detailing one of the beads on the lower conductor as detailed in figure 964.

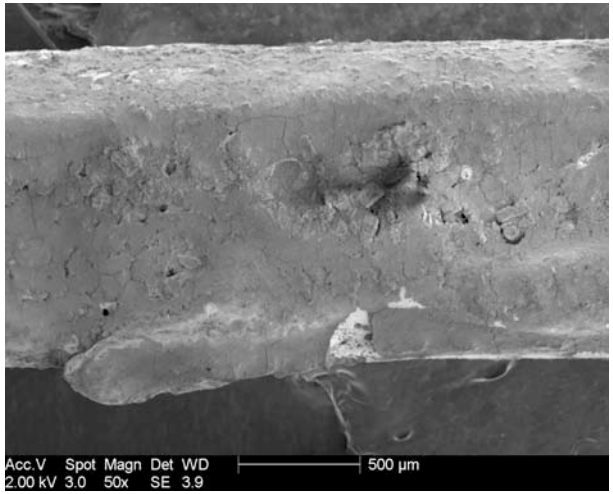

Figure 966 - SEM image detailing the left edge of the top conductor in figure 964.

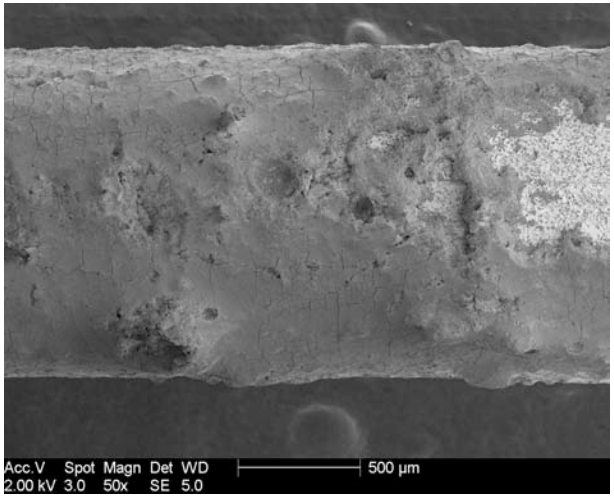

Figure 967 - SEM image detailing the right end of the top conductor in figure 964.

Full-size confocal laser scanning microscope image for exhibit 140 – arcing category A (experiment 38)

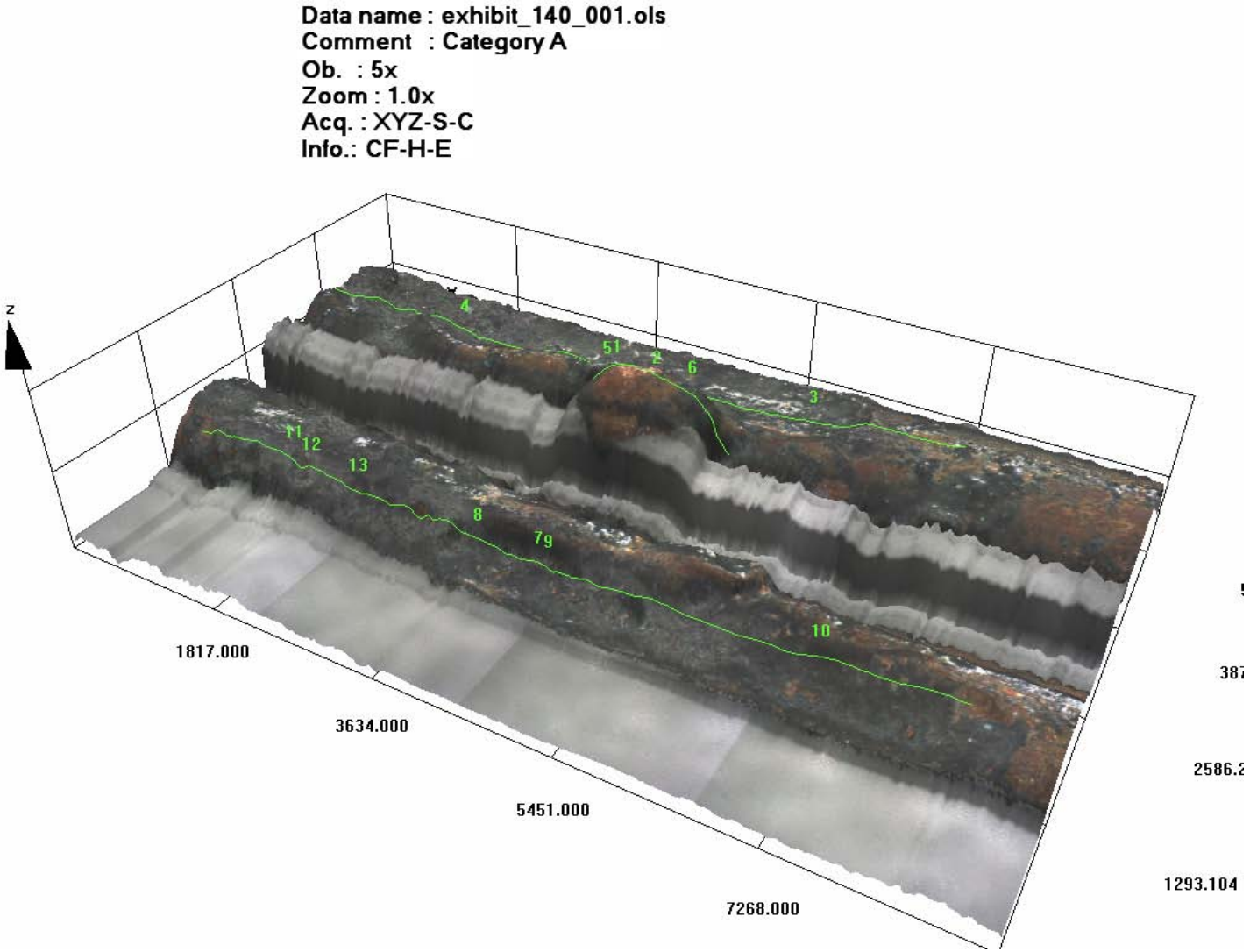

Figure 968 - LEXT image detailing both affected conductors of exhibit 140.

Microscope and SEM images for exhibit 141 – arcing category H (experiment 38)

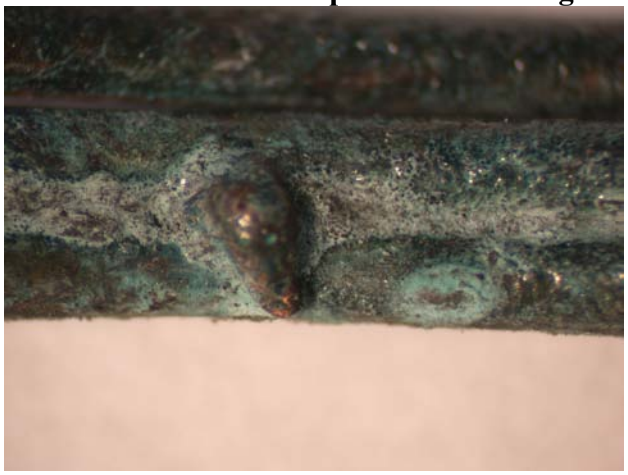

Figure 969 - Microscope image of exhibit 141. The arcing damage welded two conductors of circuit 4 together.

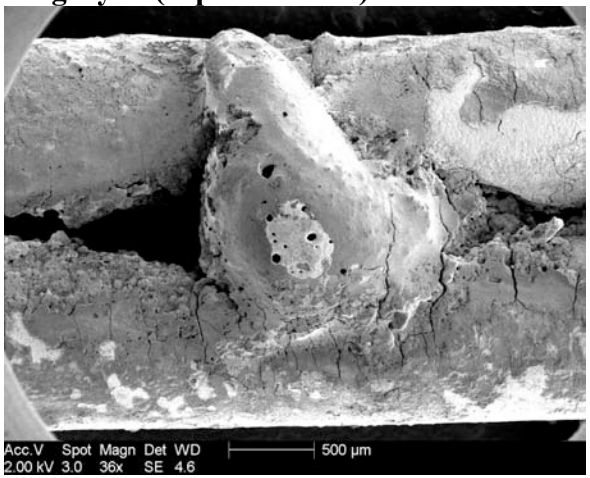

Figure 970 - SEM image of the bead forming the weld between the two conductors.

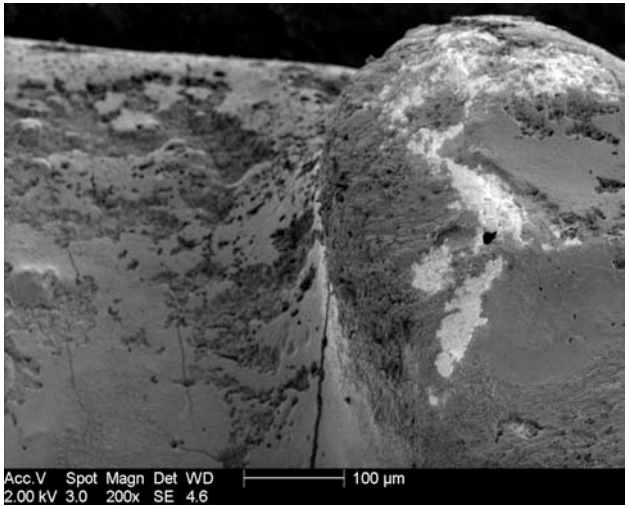

Figure 971 - SEM image at 200x magnification of the top left area of the bead.

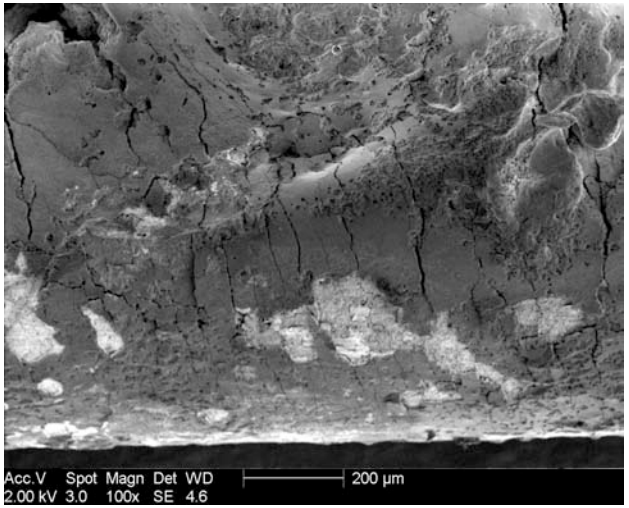

Figure 972 - SEM image at 100x magnification detailing the lower area of the bead where it is attached to the conductor.

Confocal laser scanning microscope image for exhibit 141 – arcing category H (experiment 38)

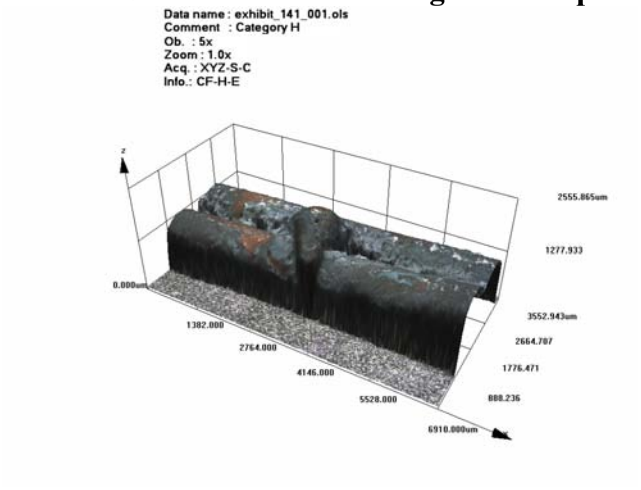

Figure 973 - LEXT image detailing the entire exhibit.

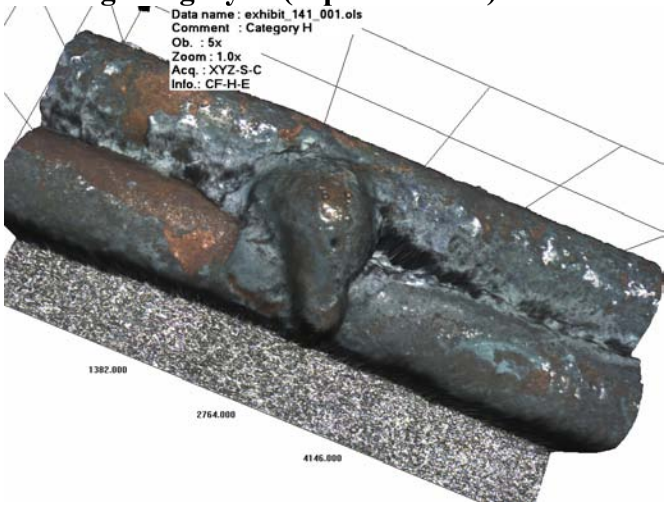

Figure 974 - LEXT image rotated in the 3-D software.

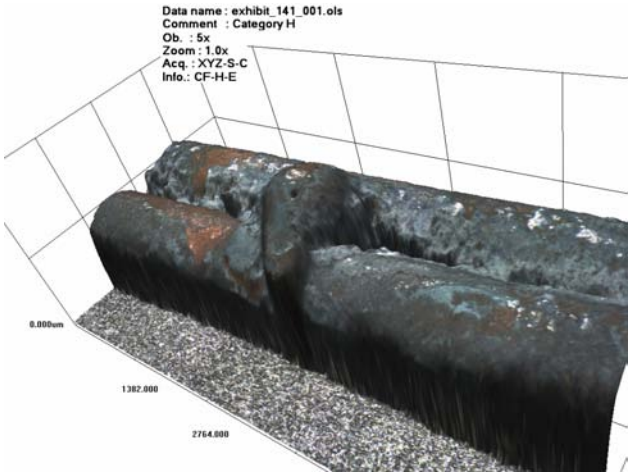

Figure 975 - LEXT image orientated in the 3-D software.

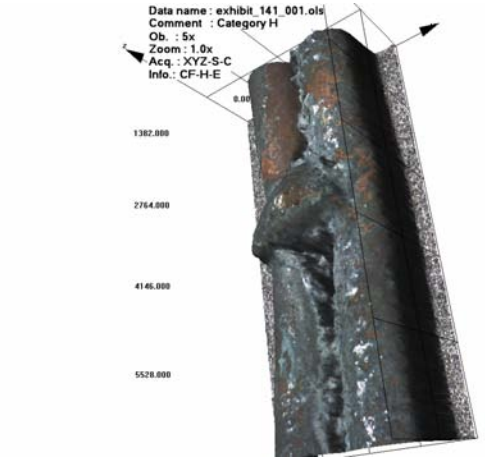

Figure 976 – LEXT image detailing the opposite view to figure 973.

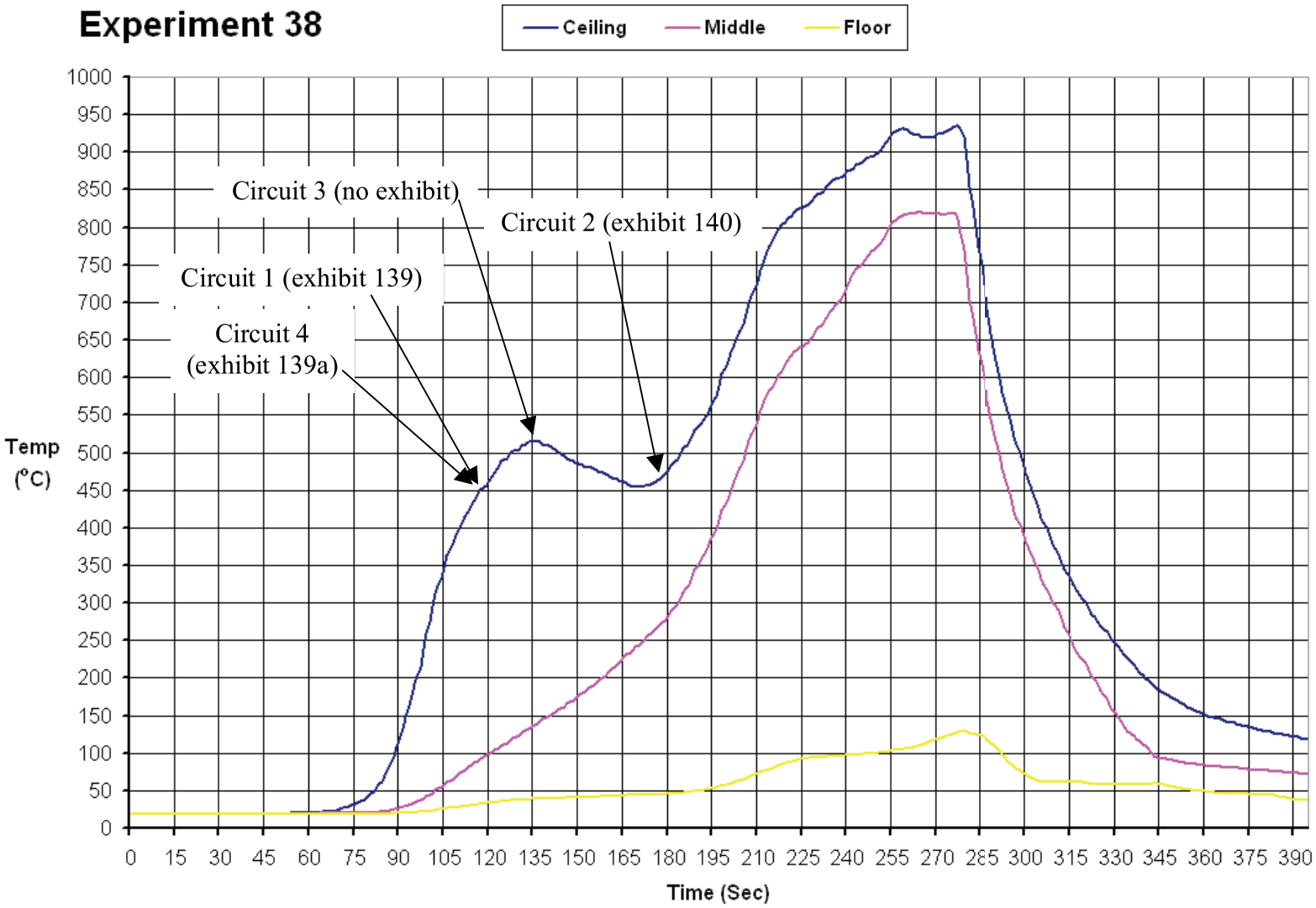

Figure 977 - Time temperature graph for experiment 38

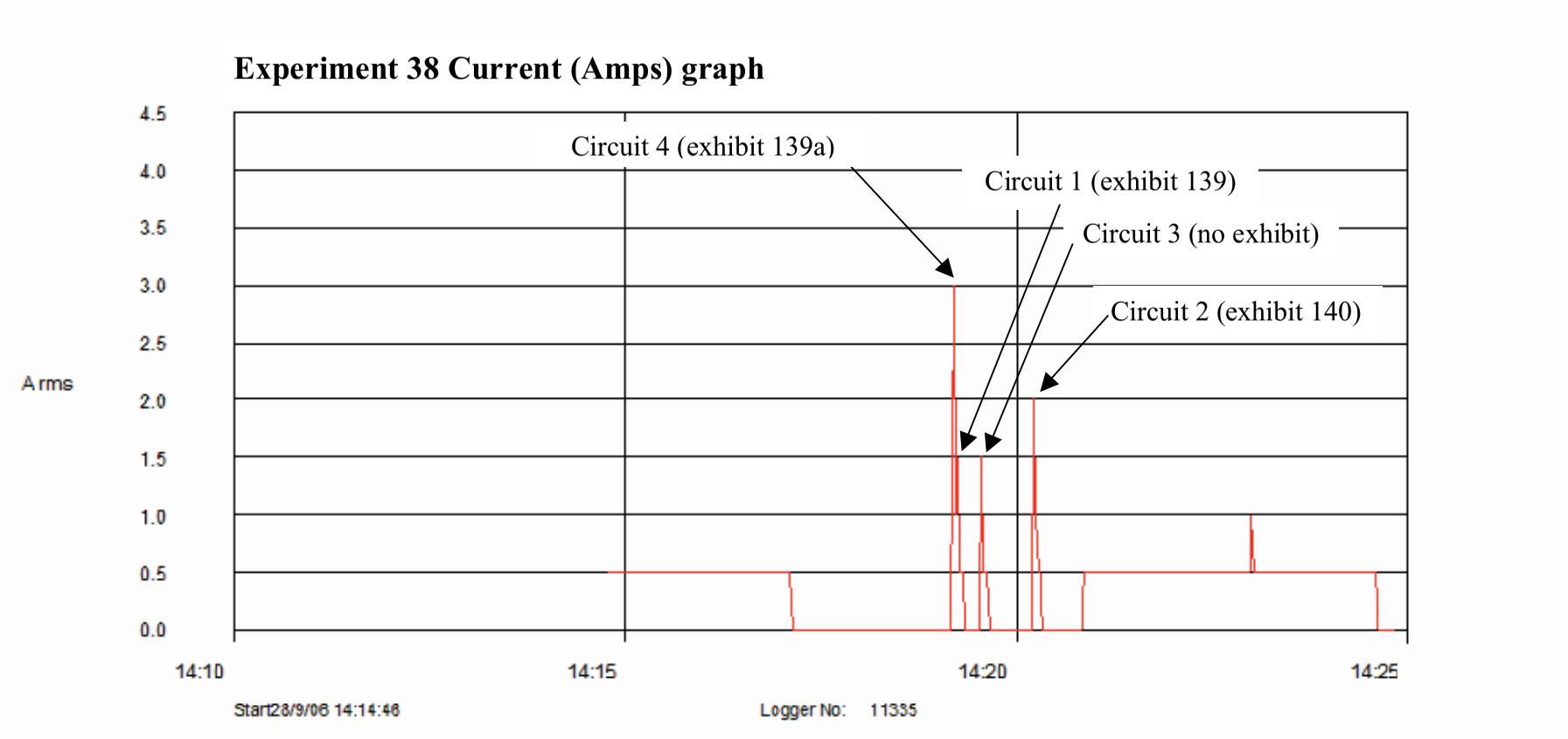

Figure 978 - Current (Amps) graph for experiment 38 detailing the operation of the circuit breakers and the fault current

Experiment 39

Figure 979 – "Scenario C" 28 September 2006

Circuit number	MCB operating time from ignition
4	4:57 minutes
1	5:07 minutes
3	7:30 minutes
2	7:45 minutes

Table 41 – circuit breaker operation data

The fire in experiment 39 (scenario C) originated in a toy box located between a Christmas tree and a television. They were both adjacent to the rear wall of the compartment.

This fire developed steadily until it reached flashover conditions at 10 minutes after ignition. The ceiling thermocouple recorded 900° C at this point with the middle and floor thermocouples recording 790° C.

Arcing damage was located on circuit 1 – is in the corner of the rear right wall.

Arcing damage was located on circuit 2 - is 180mm from the right wall and 1000mm from the front wall.

Arcing damage was located on circuit 3 - is 480mm from the right wall and 1000mm from the front wall.

Arcing damage was located on circuit 4 – 400mm from the right wall and 1000mm from the rear wall (two conductors were welded together).

Pre-fire and post-fire photographs of experiment 39

Figure 980 - Pre-fire view of experiment 39. The fire's area of origin is a toy box and it is indicated with a white circle. The Christmas tree fell over during the early development of the fire and ignited the TV. The television became the predominant fire plume.

Figure 981 - A close-up view of the fire's area of origin. Arcing damage was located on circuits 1 and 4 on the ceiling above the Christmas tree and television area.

Figure 982 - Post-fire view of the fire scene with the area of origin indicated with a white circle as above. The left arrow is arcing damage to circuit 1 and the right arrow is arcing damage to circuit 4.

Figure 983 - Post-fire view of the ceiling above the fire's area of origin and the armchair located in the left rear corner of the compartment.

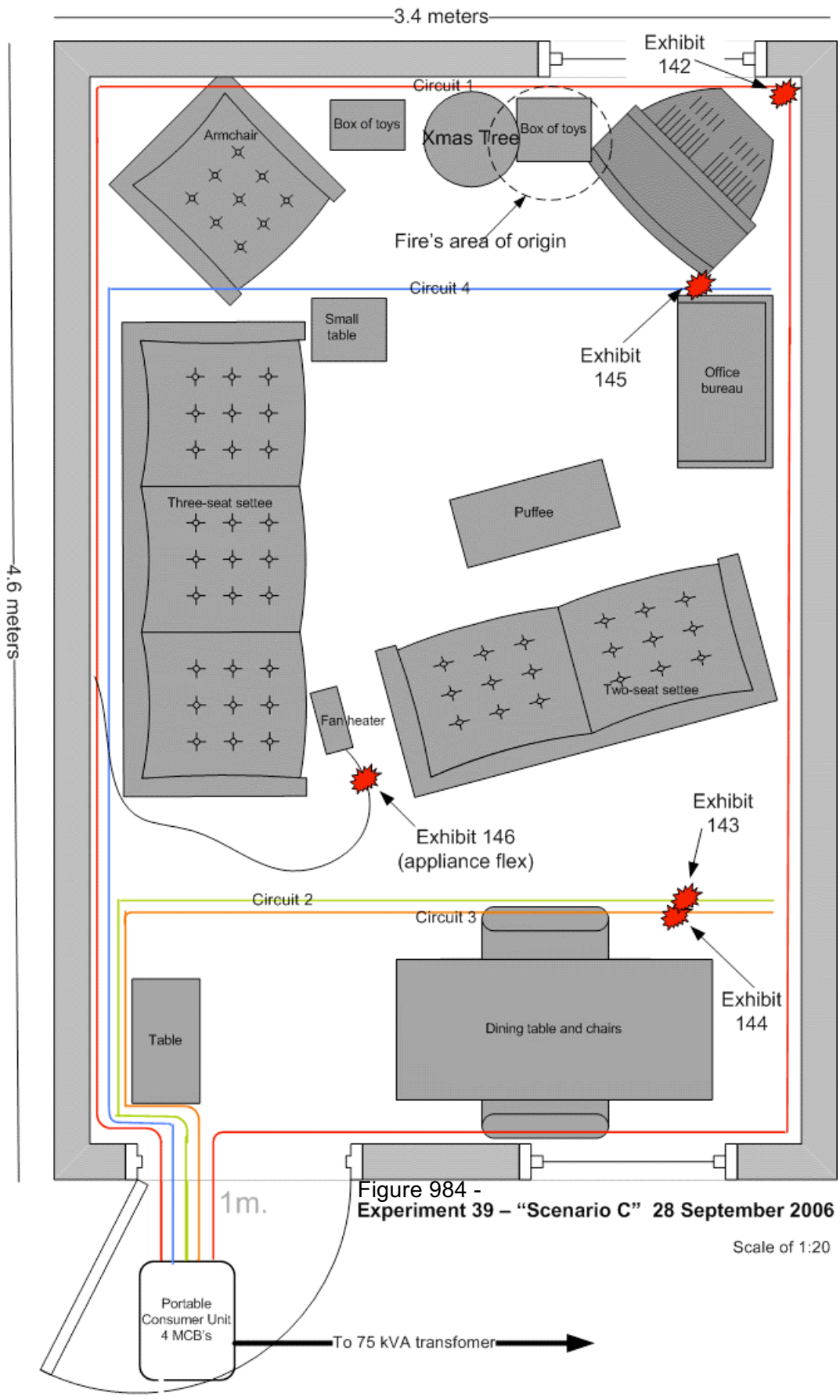

Figure 984 -
Experiment 39 – "Scenario C" 28 September 2006

Scale of 1:20

Microscope and SEM images for exhibit 142 – arcing category A (experiment 39)

Figure 985 - Microscope image of exhibit 142, this is an example of arcing through char with multiple small beads and notches.

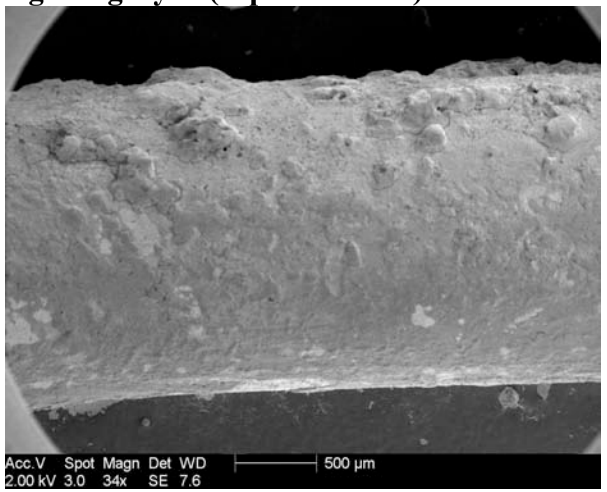

Figure 986 - SEM image of the left end of the lower conductor, just in view in figure 985.

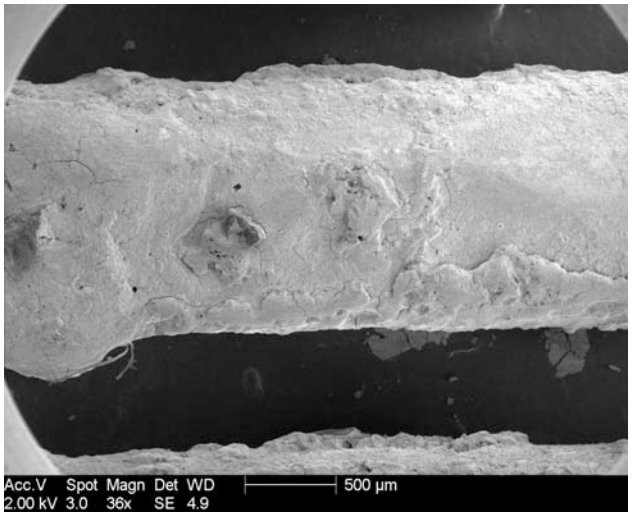

Figure 987 - SEM image of the central area of the middle conductor detailed in figure 985.

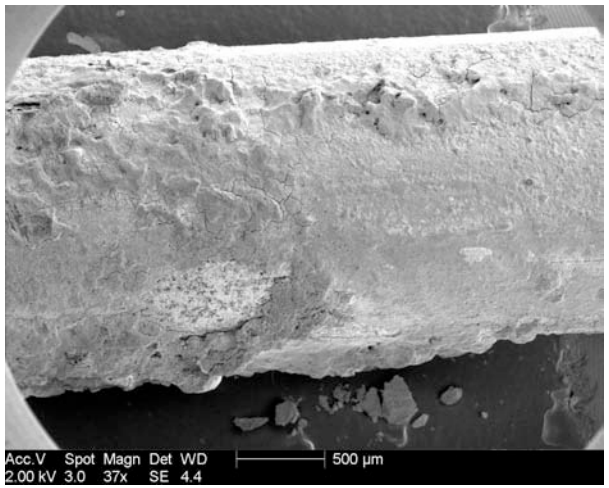

Figure 988 - SEM image of the right edge of the arcing damage to the top conductor detailed in figure 985.

Confocal laser scanning microscope image for exhibit 142 – arcing category A (experiment 39)

Figure 989 - LEXT image that displays the entire exhibit in detail.

Figure 990 - LEXT image rotated in the 3-D software.

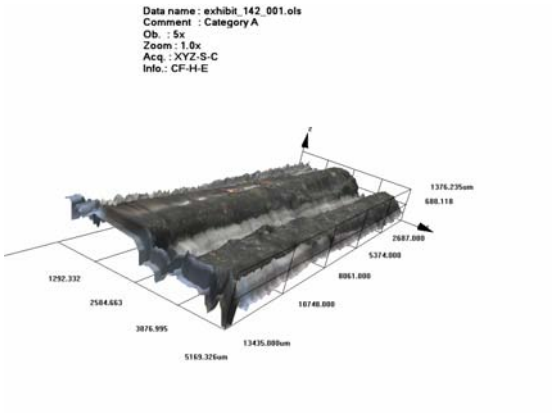

Figure 991 - LEXT image orientated in the software to show the opposite view to figure 989.

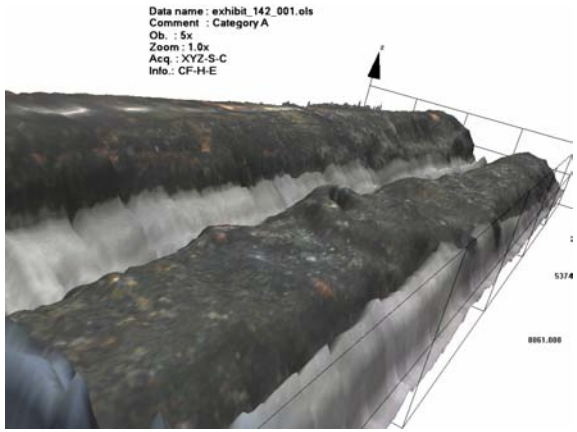

Figure 992 – A close-up LEXT image rotated in the 3-D software. This thoroughly details the “category A” surface.

Microscope and SEM images for exhibit 143 – arcing category D (experiment 39)

Figure 993 - Microscope image of exhibit 143. The two 2.5mm^2 conductors are involved with a notch and adjacent bead.

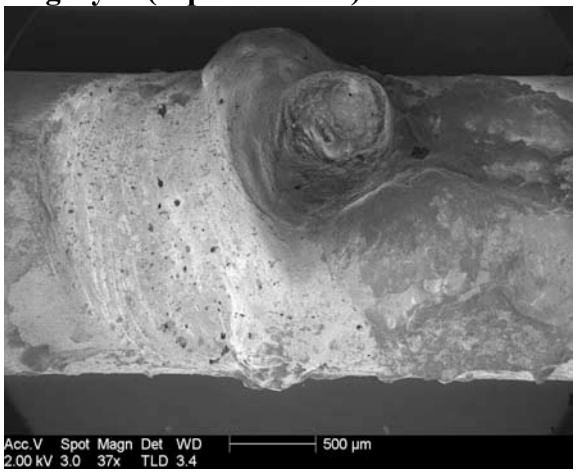

Figure 994 - SEM image of the bottom conductor displayed in figure 993. Rib lines in the notch surface were observed.

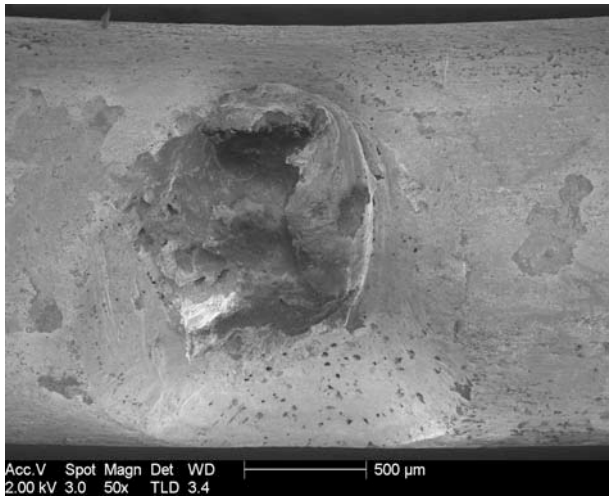

Figure 995 - SEM image of the notch and small bead for the top conductor in figure 993.

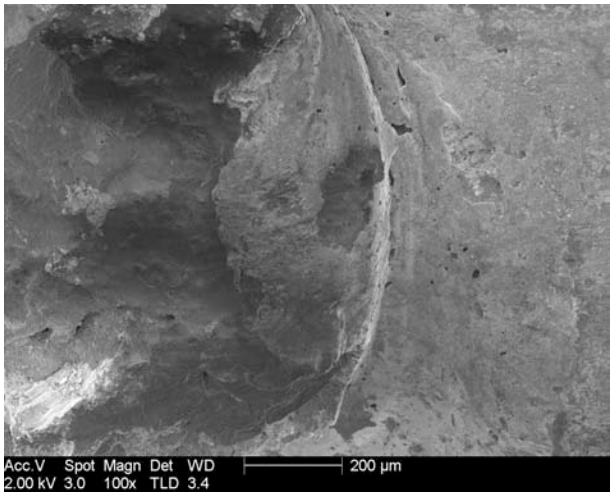

Figure 996 - SEM image at 100x magnification of the right side of the small notch detailed in figure 995.

Full-size confocal laser scanning microscope image for exhibit 143 – arcing category D (experiment 39)

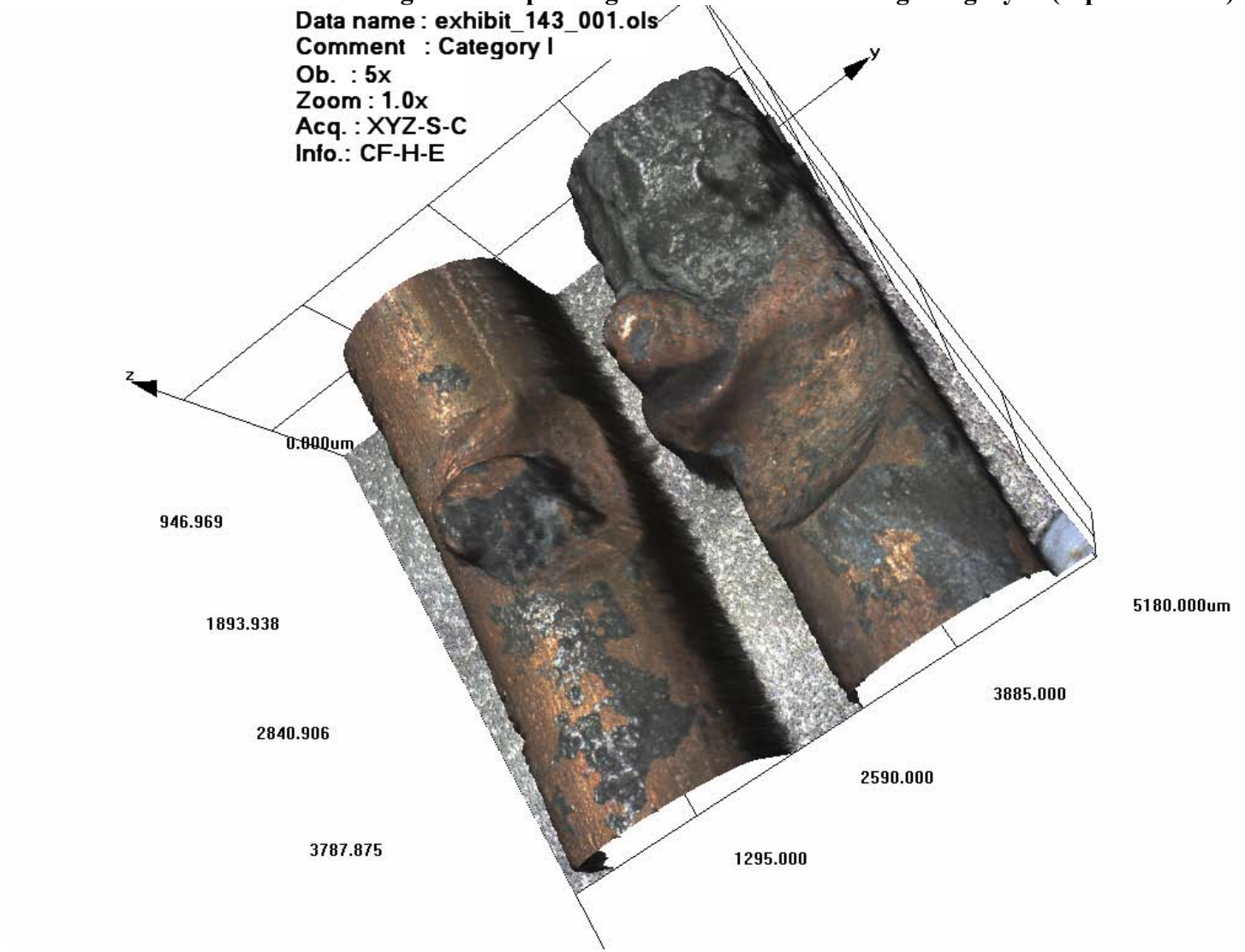

Figure 997 - LEXT image that effectively displays the arcing damage to both conductors in context and in detail.

Microscope and SEM images for exhibit 144 – arcing category D (experiment 39)

Figure 998 - Microscope image of exhibit 144. There is one conductor with arcing damage. The demarcation edge is very clear.

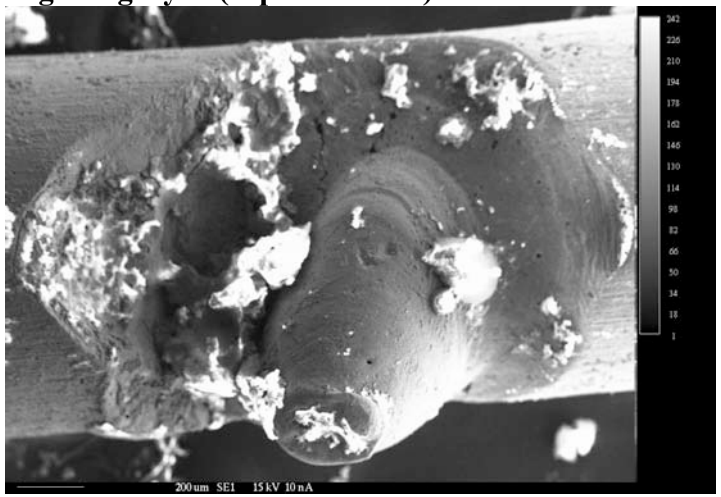

Figure 999 - Cameca SEM image of this exhibit.

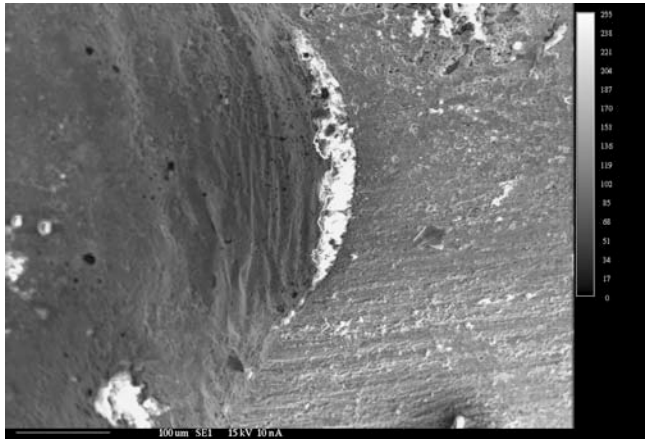

Figure 1000 - SEM image of the right edge of the notch detailed in figure 999. The conductor striation marks are visible on the undamaged conductor surface.

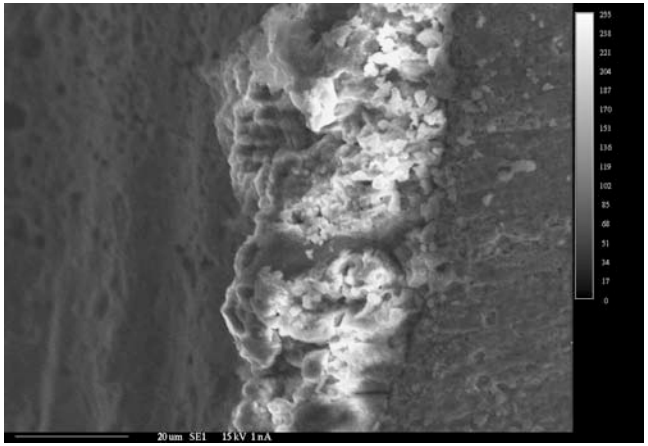

Figure 1001 - SEM image detailing the slight beading at the edge of the notch detailed in figure 1000.

Confocal laser scanning microscope image for exhibit 144 – arcing category D (experiment 39)

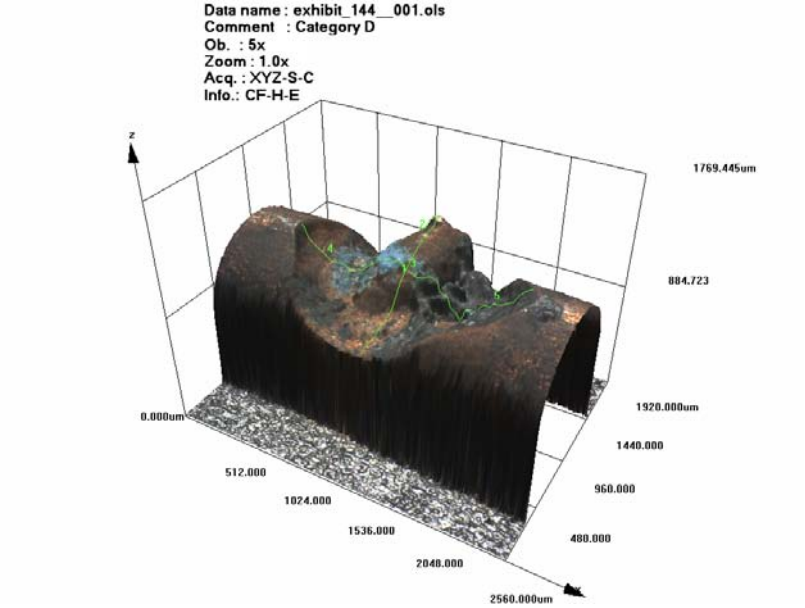

Figure 1002 - LEXT image enabling a three-dimensional aspect of this exhibit.

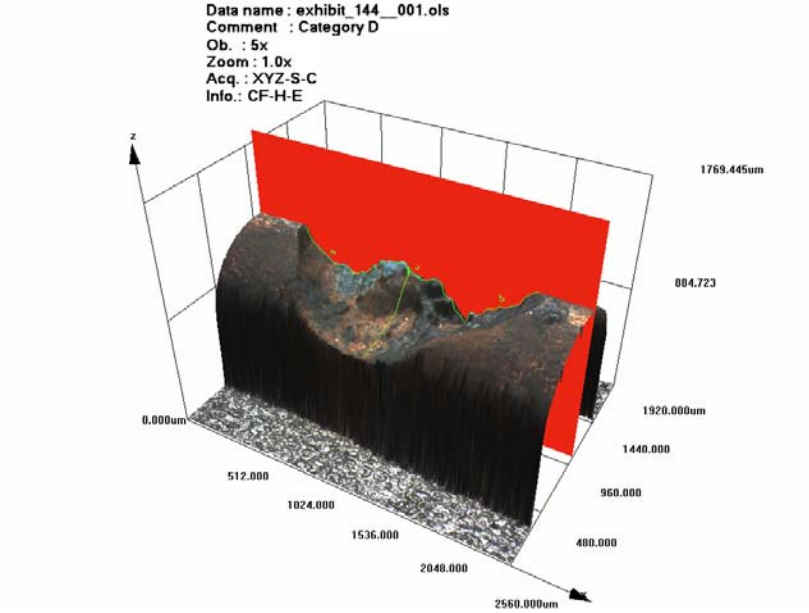

Figure 1003 - LEXT image capturing the "slice tool" option of the software in use to capture a profile and measurements.

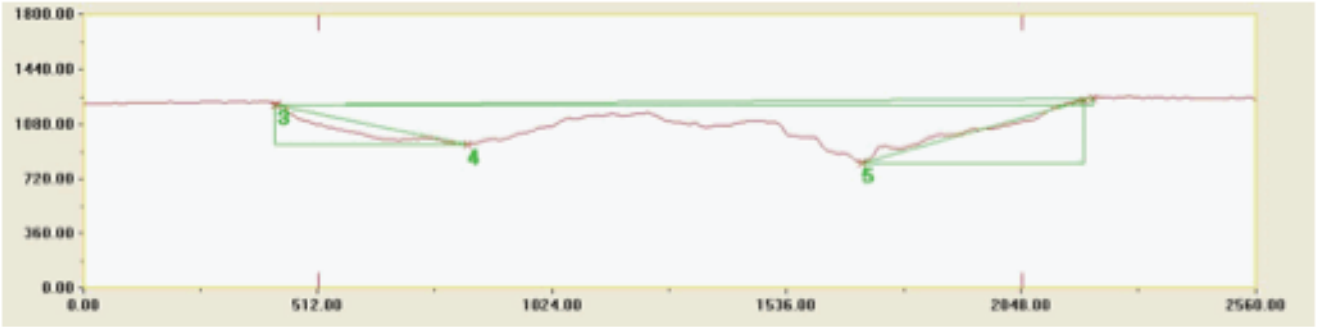

Figure 1004 - LEXT profile created with the software "slice tool" option. The notch width = 1780 microns (1.78mm), the height = 406 microns (0.4mm)

Microscope and SEM images for exhibit 145 – arcing category D (experiment 39)

Figure 1005 - Microscope image of exhibit 145. The arcing damage affected two conductors with shallow notches.

Figure 1006 - 20x magnification of the surface damage, a lot of PVC debris was attached to the conductor surface.

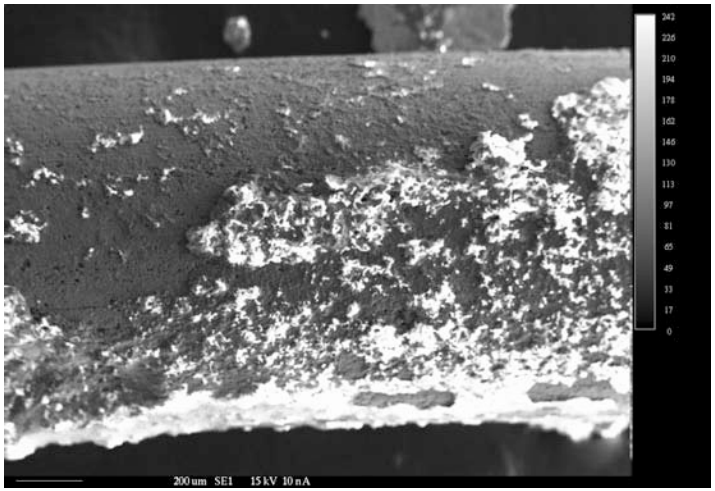

Figure 1007 - SEM image with the bottom of the conductor detailing the notch outline.

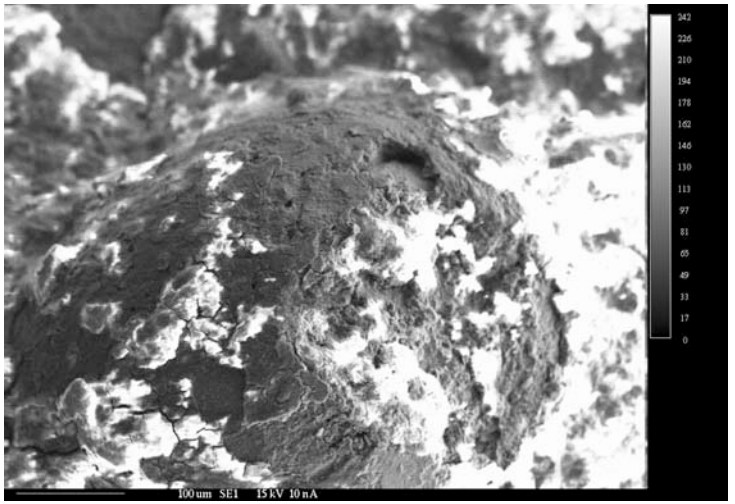

Figure 1008 - SEM image detailing a small surface bead on the top conductor surface detailed in figure 1005.

Confocal laser scanning microscope image for exhibit 145 – arcing category D (experiment 39)

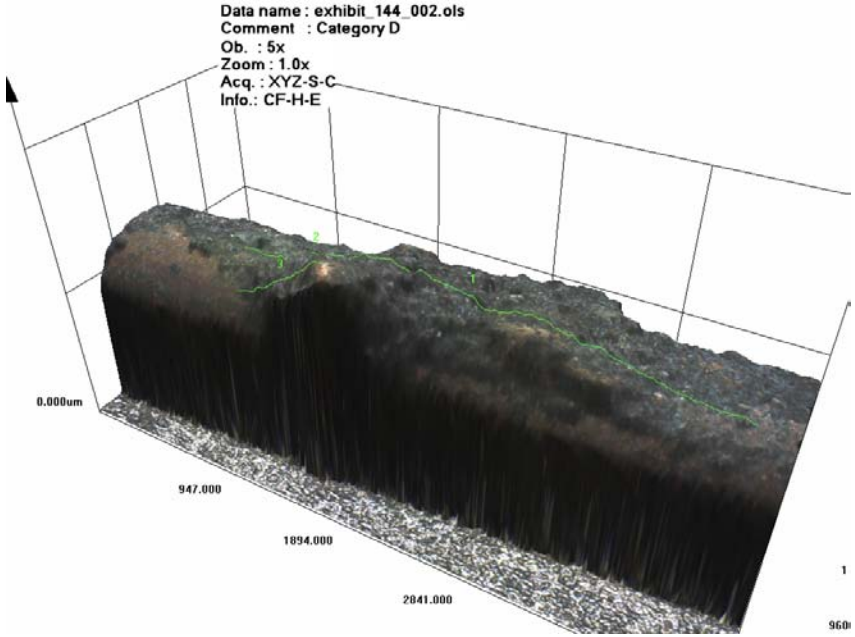

Figure 1009 - LEXT image that enables an overall perspective of the arcing damage to this conductor.

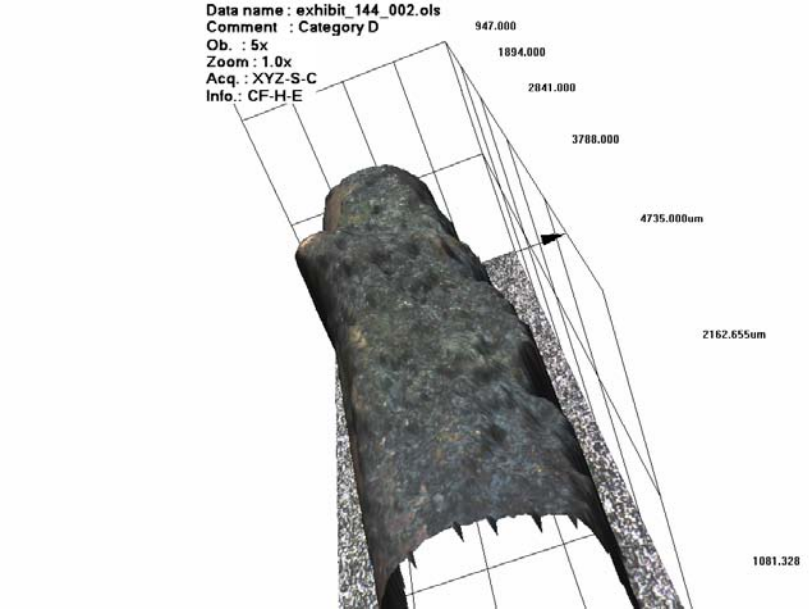

Figure 1010 - The image was rotated and captured in the LEXT software to enhance the surface view.

Figure 1011 - Profile of the conductor surface. Length of arcing damage = 3531 microns (3.53mm), height = 271 microns (0.27mm)

Microscope and SEM images for exhibit 146 – arcing category C (experiment 39 – fan heater flexible cable)

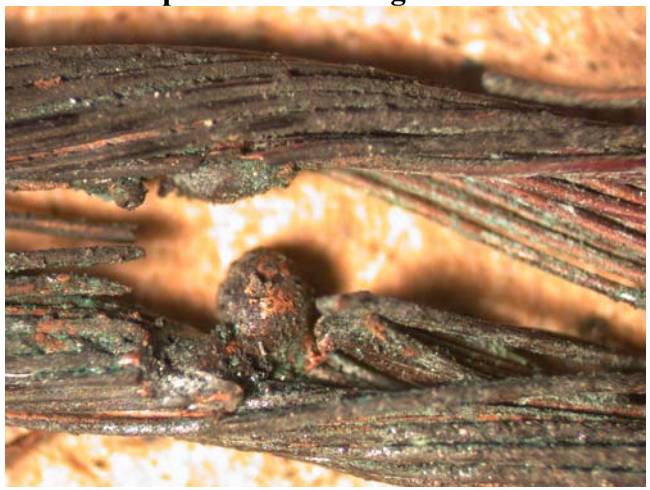

Figure 1012 - Microscope image of the arcing damage sustained to a fan heater appliance flexible cable during experiment 39.

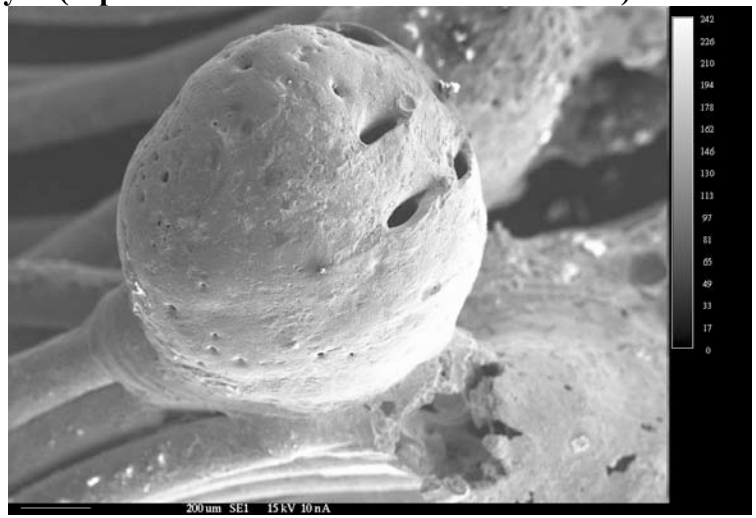

Figure 1013 - SEM image of the bead and adjacent notch with three holes in the bead surface.

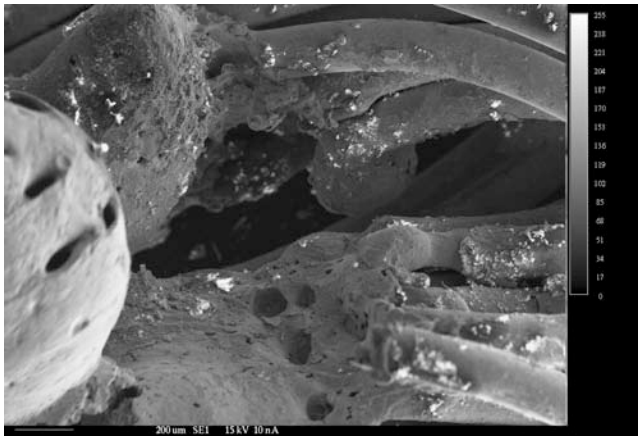

Figure 1014 - SEM image of the notch area. The localised melting appeared to be more pronounced due to the thin conductor strands when compared to a solid conductor.

Figure 1015 - SEM image of the holes in the bead.

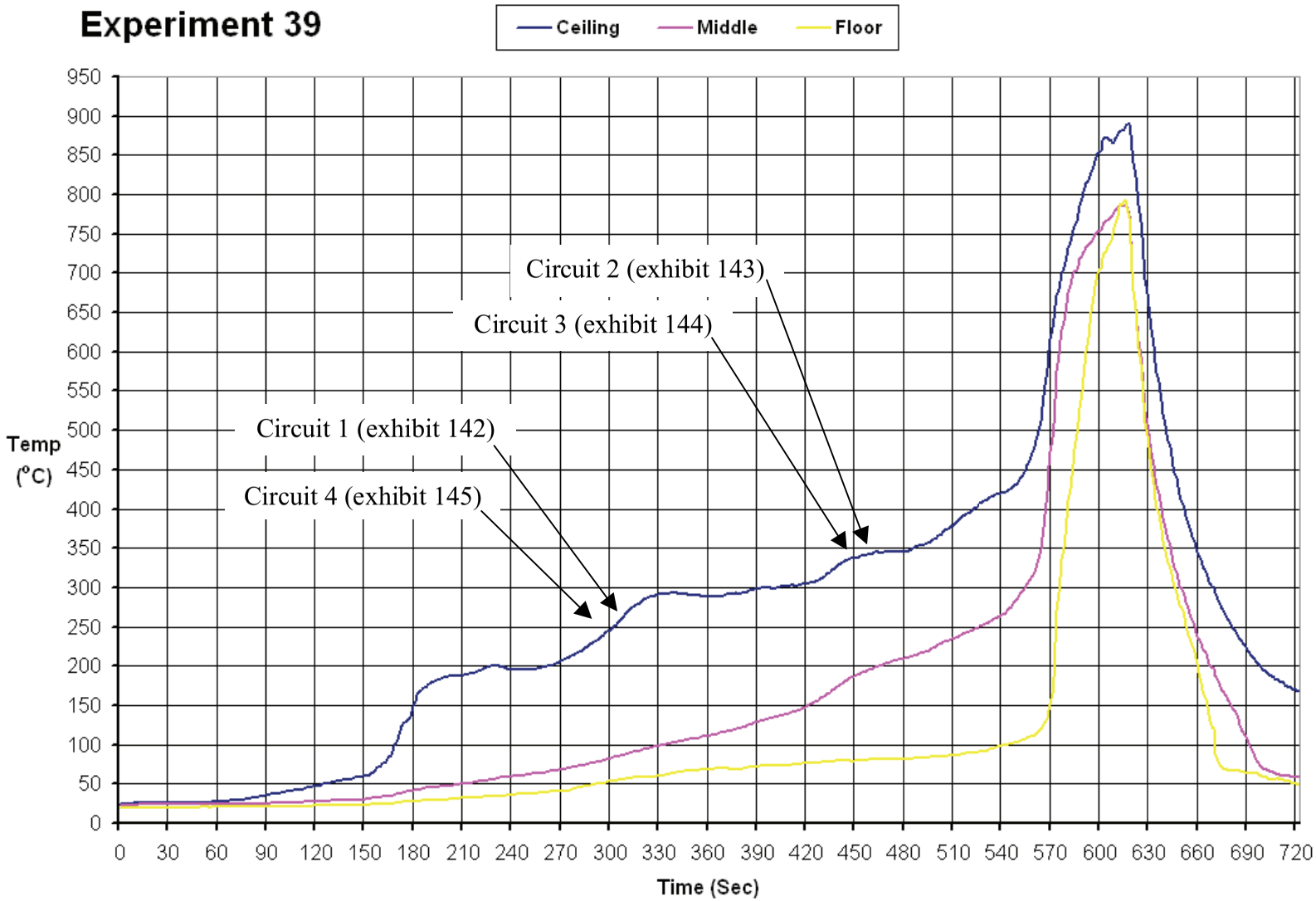

Figure 1016 - Time temperature graph for experiment 39

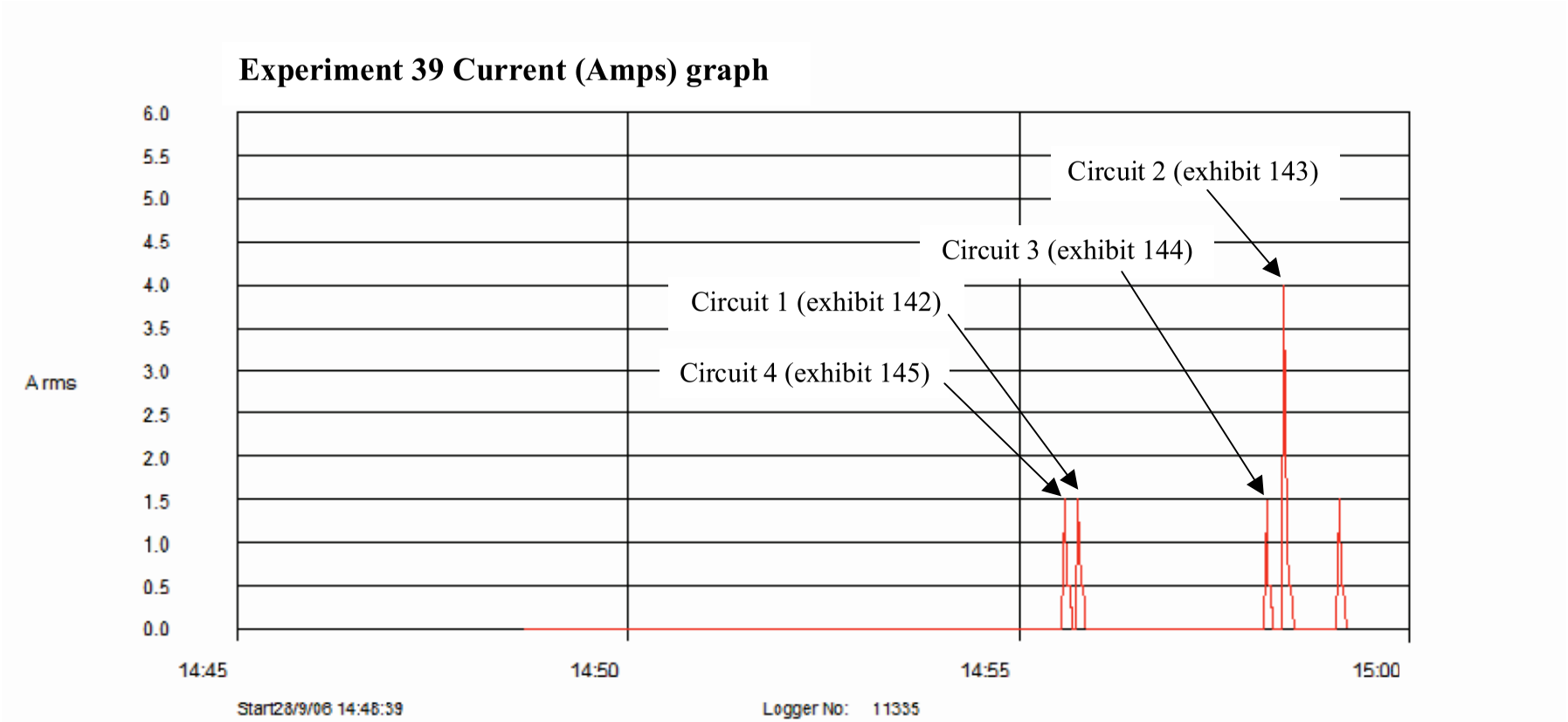

Figure 1017 - Current (Amps) graph for experiment 39 detailing the operation of the circuit breakers and the fault current

Page intentionally left blank